Biofortification and Plant Stress: the Role of Azospirillum brasilense Sp7

Sarah Boyd Lade Lee

Universitat de Lleida

TESI DOCTORAL

BIOFORTIFICATION AND PLANT STRESS: THE ROLE OF *Azospirillum brasilense* Sp7

Sarah Boyd Lade Lee

Memòria presentada per optar al grau de Doctor per la Universitat de Lleida
Programa de Doctorat en Ciència i Tecnologia Agrària i Alimentària

Directors

Vicente Medina Piles
Pilar Muñoz Odina

June 2019

Cover pages: *Azospirillum brasilense* Sp7 – inoculated (front) and non-inoculated (back) maize roots

Supervisors: **Vicente Medina Piles**

Pilar Muñoz Odina

Department of Plant Production and Forest Science

School of Agricultural and Forestry Engineering

University of Lleida

June 2019

Signatures

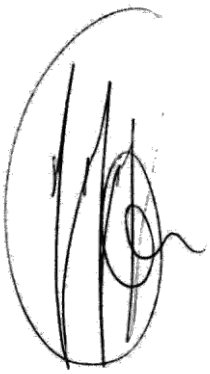

V. Medina

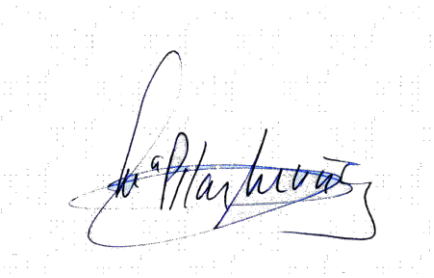

P. Muñoz

Dedication

For Adrian

Acknowledgments

Primarily, I would like to express my deepest gratitude for my supervisor and friend Dr. Vicente Medina. It has been an absolute pleasure to have your guidance, both in and out of the lab. This document is a testament to your countless hours of encouragement and revision. I wish you infinite joy in your next phase of life.

A very special thanks to my supervisor Dra. Pilar Muñoz for your unwavering and selfless support throughout this journey. You have been so wonderful always checking in and offering on-the-ground assistance when the going got rough.

Thank you Dr. Paul Christou and Dra. Teresa Capell, it has been such a privilege to have the opportunity to collaborate with you and your lab. I am so grateful for all the scientific knowledge and life lessons I will walk away with, and could not have asked for a richer experience.

Thank you Dr. Changfu Zhu and Dr. Ludovic Bassie for sharing your consistency, good nature and professionalism. To Can Baysal and Dra. Gemma Farré, for showing me the ropes of how to move in the APB lab, and for always answering my many questions. To Carla Román and Yasmine Piñuela, for being incomparable lab colleagues and friends, for always sharing, and always laughing. To Paula Betancur and Nathan Nicholson for working tireless hours, but forever with a smile. And to all other lab colleagues from then and now: Ana, Xin, Erika, Lucia, Gemma M, Gemma C, Ravi, Daniela, Edu, Andrew, Marco, Vicky, Pedro, Jose, Derry, Amaya, Sarai and Yi, thank you for all of the joyful moments and coffee breaks, I will miss you.

Many thanks to the professors who have altruistically enriched the quality of my work and depth of knowledge in various fields: Drs. Ignacio Romagosa, Jordi Voltas, Luis Serrano and Maria Ángeles Achón. Thanks to Dra. Isabel Sánchez from the UdL 'Servei de Genòmica i Proteòmica', Xavier Calomarde from the UdL 'Servei de Microscòpia Electrònica', Dr. Jordi Giné from IRTA, Dra. Ána Alvarez & Adrián Villaroyo from CSIC in Zaragoza and Dr. Alfonso Albacete from CSIC in Murcia for your willingness to collaborate and share your skills with us. To our colleagues Drs. Carlos Barassi and Laura Maneiro from ‘Universidad Nacional del Mar del Plata’ in Argentina, thank you for introducing us to *Azospirillum.*

This project's success is in part attributed to the work of Jaume Capell for keeping our plants alive and green, Nuria Gabernet for maintaining us organized and to Maria Josep Pau's hard work and persistence; thank you all immensely. To Teresa Estela and Dr. Alex Juarez for always going above and beyond in taking care of everyone in the department. You make PVCF and ETSEA feel like home.

I would like to thank the Spanish 'Ministerio de Economía y Competitividad' Project AGL2010-15691 and the University of Lleida JADE PLUS grant for the financial support.

To my Mom, Dad, Lizbee and Tripp, thank you for your love and encouragement from the beginning. You have taught me the importance of wonder and diligence. Gracias a Mila, Isma y toda la familia española por todo vuestro apoyo y siempre aceptándome.

Finally, thank you friends near and far for your depths of kindness, and for always checking in despite my disappearance over the last three years: Anscari, Lynne, Ana, Annika, Requena, Montse, Neus, Jess, Caitlin, Blakeley, Sarah A, Liz, Dafna, Conor, Isaac and Mel.

Last but certainly not least, I would like to thank Ruben, because none of this would have been possible without your support, patience, and genuine interest at every step of the way. Your love has kept me sane.

Thank you all a million times over. Gracias a todos. Gràcies a tots.

Abstract

The sustainable production of nutritious and safe food for human consumption is the ultimate goal of crop biofortification. However, I propose a fundamental shift in this dynamic: to biofortify crops so as to benefit the health of the plant and the population consuming them. In order to accomplish this, it is likely that multiple biofortification strategies must be employed simultaneously. In this doctoral thesis, I examine how various biofortification strategies affect the well-being of economically important crops, by focusing on the plant immune system during vegetative developmental stages.

Azospirillum brasilense Sp7 (Sp7) is a growth promoting rhizobacterium (PGPR) that agronomically biofortifies plants by solubilizing soil nutrients and moving them to plant parts. By doing so, Sp7 also increases plant growth and improves defense mechanisms in plants. In different experiments, I inoculated Sp7 to crops that had previously been bred to have superior agronomic traits or were transgenically, namely: various barley cultivars, carotenoid-fortified maize (HC) and iron (Fe)-fortified rice (RB92). In each case, seedlings were then exposed to biotic or abiotic stress conditions to study mechanisms of defense regulation in the plant. The analysis of physiological parameters was combined with proteomic, hormonal and/or transcriptomic data to elucidate macro- and microscopic variations in plant behavior at the cellular and molecular scale.

Preliminary trials were run to inform subsequent work. For this, I found that the individual components of different inoculation buffers engender specific interactions with Sp7 and the environment. I also determined that Sp7 interacts differently with plant primary metabolism depending on the species. Specifically, the influence that Sp7 has over maize plants (compared to tomato) is more effective because C_4 photosynthesis is more efficient and offsets stress, and Sp7 causes better maize seedling emergence and vigor. In two common pathosystems tested, maize/Maize dwarf mosaic virus (MDMV, AM110558) and potato/Potato virus X (PVX, KJ631111), Sp7 does not influence viral replication. Sp7 does, however, incite induced systemic resistance (ISR) in both plant species, thereby delaying the onset of MDMV in maize and increasing the tolerance of tomato seedlings to PVX.

Biofortification proved effective for increasing plant defenses against both biotic and abiotic stresses. Inoculating barley cultivars 'Barberousse' and 'Plaisant' with Sp7 positively and significantly affects seed germination and seedling growth. Then, under conditions of abiotic stress imposed by the *in vitro* system tested, Sp7 consistently increased 'Albacete' root development. HC maize plants inoculated with Sp7 shows greater resistance to the phytopathogenic fungus *Fusarium graminareum,* inciting simultaneous up-regulation of hormones representative of systemic acquired resistance (SAR) and ISR. Then, I identified ZmGAMYB as a candidate transcription factor (TF) coordinating the cellular redox response

and the two defense pathways. Finally, RB92 rice seedlings subjected to Fe-starvation and inoculated with Sp7 accumulate more Fe and Zn in leaf tissues, and up-regulate Fe-homeostasis gene expression. This response is accompanied by the increased expression of *OsIRO2*, a TF typically bound by ISR protein products.

The conclusions obtained in this doctoral thesis provide important insights into how Sp7 intervenes in plant molecular processes. Results collectively support the hypothesis that simultaneously using multiple biofortification strategies is effective for increasing plant health, drawing attention to the centrality of TF activation and coordinated hormone signaling in these responses.

Resumen

La producción sostenible de alimentos nutritivos y seguros para el consumo humano es el objetivo final de la biofortificación. Sin embargo, propongo un cambio fundamental en esta dinámica: biofortificar para beneficiar la salud de las plantas a la vez que la de la población que las consume. Para lograr esto, es probable que se vayan a utilizar múltiples estrategias de biofortificación simultáneamente. En esta tesis doctoral, examino como diversas estrategias de biofortificación afectan al bienestar de cultivos económicamente importantes, al centrarme en el sistema inmunológico de la planta durante las etapas de desarrollo vegetativo.

Azospirillum brasilense Sp7 (Sp7) es una rizobacteria promotora del crecimiento (PGPR) que biofortifica agronómicamente las plantas al solubilizar los nutrientes del suelo y así alcanzan diferentes partes de la planta. Al hacerlo, Sp7 también aumenta el crecimiento de las plantas y mejora los mecanismos de defensa de éstas. En diferentes experimentos, inoculé Sp7 en plantas de diferentes especies previamente mejoradas mediante genética clásica o biofortificadas mediante transgenia, en concreto: varios cultivares de cebada, maíz fortificado con carotenoides (HC) y arroz fortificado con hierro (Fe) (RB92). En cada caso, las plántulas fueron expuestas a condiciones de estrés biótico o abiótico para estudiar los mecanismos de regulación de defensa de la planta. El análisis de los parámetros fisiológicos se combinó con datos proteómicos, hormonales y/o transcriptómicos para dilucidar las variaciones macro y microscópicas en el comportamiento de las plantas a escala cel·lular y molecular

En unos ensayos iniciales para orientar el trabajo posterior, encontré que los componentes individuales de diferentes tampones de inoculación generan interacciones específicas con Sp7 y el medio ambiente. También determiné que Sp7 interactúa de manera diferente con el metabolismo primario de la planta dependiendo de la especie. Posteriormente, confirmé que la influencia que tiene Sp7 sobre las plantas de maíz (en comparación con el tomate) es más efectiva porque el mecanismo C_4 es más efectivo para contrarrestar el estrés, y que Sp7 causa una mejor emergencia y vigor en las plántulas de maíz. También comprobé que Sp7 no influye en la replicación viral en dos sistemas patológicos diferentes, maíz/Maize dwarf mosaic virus (MDMV, AM110558) y patata/Potato virus X (PVX, KJ631111). No obstante, Sp7 sí incitó la resistencia sistémica inducida (ISR) en ambas especies de plantas, lo que hizo que se retrasara la detección de MDMV en el maíz y aumentara la tolerancia de las plántulas de tomate a PVX.

La biofortificación resultó efectiva para aumentar las defensas de las plantas contra el estrés tanto biótico como abiótico. La inoculación con Sp7 afectó positiva y significativamente la germinación de las semillas y el crecimiento de las plántulas de los cultivares de cebada 'Barberousse' y 'Plaisant'. En cambio, bajo las condiciones de estrés abiótico impuesto por el sistema *in vitro* probado, fue el cultivar 'Albacete' el que se vió favorecido significativamente en

su volumen radicular con Sp7. Las plántulas de maíz HC cuyas semillas fueron inoculadas con Sp7 mostraron una mayor resistencia al hongo fitopatógeno *Fusarium graminareum*, pues en ellas aumentó la cantidad de hormonas representativas de la resistencia sistémica adquirida (SAR) y la ISR. En este caso, identifiqué a ZmGAMYB como un factor de transcripción (TF) candidato a coordinar la respuesta redox celular de las dos vías de defensa. Finalmente, las plántulas de arroz RB92 sometidas a inanición con Fe, e inoculadas con Sp7, acumularon más Fe y Zn en los tejidos de las hojas, y manifestaron una mayor expresión de genes de proteínas reguladores de la homeostasis del Fe. Esta respuesta estuvo acompañada por el aumento de la expresión de *OsIRO2*, un TF típicamente unido por productos de proteína ISR.

Las conclusiones obtenidas en esta tesis doctoral proporcionan información creo importante sobre cómo interviene Sp7 en los procesos moleculares de las plantes y apoyan la hipótesis de que varias estrategias de biofortificación se suman para aumentar la salud de las plantas, llamando la atención sobre la centralidad de la activación de TFs y la señalización coordinada de hormonas en estas respuestas.

Resum

La producció sostenible d'aliments nutritius i segurs per al consum humà és l'objectiu final de la biofortificació dels cultius. No obstant això, proposo un canvi fonamental en aquesta dinàmica: biofortificar els cultius per beneficiar al mateix temps la salut de les plantes. D'acord amb la complexitat de l'homeòstasi de la planta, és probable que es necessitin múltiples estratègies de biofortificació per aconseguir aquest objectiu. En aquesta tesi doctoral, examine diverses formes de biofortificació en cultius econòmicament importants i estudio la seva influència en el sistema immunològic de la planta durant les primeres etapes del seu desenvolupament vegetatiu.

Azospirillum brasilense Sp7 (Sp7) és una rizobacteria promotora del creixement (PGPR) que biofortifica agronòmicament augmentant el creixement i els mecanismes de defensa en les plantes. En diferents experiments, vaig inocular Sp7 en plantes de diferents espècies prèviament millorades mitjançant genètica clàsica o biofortificades per transgènia, en concret: diversos cultivars d'ordi, blat de moro fortificat amb més carotenoides (HC) i arròs fortificat amb més ferro (Fe) (RB92). En cada cas, les plàntules van ser exposades a condicions d'estrès biòtic o abiòtic per estudiar els mecanismes de regulació de defensa de la planta. L'anàlisi dels paràmetres fisiològics es va combinar amb dades proteòmiques, hormonals i/o transcriptòmiques per dilucidar les variacions macro i microscòpiques en el comportament de les plantes a escala cel·lular i molecular.

En uns assaigs inicials per orientar el treball posterior, vaig trobar que els components individuals de diferents tampons d'inoculació generen interaccions específiques amb Sp7 i el medi ambient. També vaig determinar que Sp7 interactua de manera diferent amb el metabolisme primari de la planta depenent de l'espècie. Posteriorment, vaig confirmar que la influència que té Sp7 sobre les plantes de blat de moro (en comparació amb el tomàquet) és més efectiva perquè el mecanisme C_4 contraresta l'estrès, i que Sp7 causa una millor emergència i vigor a les plàntules de blat de moro. També vaig comprovar en dos sistemes patològics diferents, blat de moro/Maize dwarf mosaic virus (MDMV, AM110558) i patata/Potato virus X (PVX, KJ631111) que Sp7 no influeix en la replicació viral. No obstant això, Sp7 si va incitar la resistència sistèmica induïda (ISR) en les dues espècies de plantes, el que va fer que es retardés la detecció de MDMV en el blat de moro i augmentés la tolerància de les plàntules de tomàquet a PVX.

La biofortificació amb Sp7 va resultar efectiva per augmentar les defenses de les plantes contra l'estrès tant biòtic com abiòtic. Sp7 va afectar positiva i significativament la germinació de les llavors i el creixement de les plàntules dels cultivars d'ordi 'Barberousse' i 'Plaisant'. En canvi, sota les condicions d'estrès abiòtic imposat pel sistema *in vitro* assaigat, va ser el cultivar 'Albacete' el que va veure afavorit el seu volum radicular amb Sp7. Les plàntules de blat de

moro HC les llavors de les quals van ser inoculades amb Sp7 van mostrar una major resistència al fong fitopatógeno *Fusarium graminareum*, ja que en elles va augmentar la quantitat d'hormones representatives de la resistència sistèmica adquirida (SAR) i la ISR. En aquest cas, vaig identificar a ZmGAMYB com un factor de transcripció (TF) candidat a coordinar la resposta redox cel·lular de les dues vies de defensa. Finalment, les plàntules d'arròs RB92 sotmeses a inanició amb Fe, i inoculades amb Sp7, van acumular més Fe i Zn en els teixits de les fulles, i van manifestar una major expressió de gens de proteïnes reguladors de l'homeòstasi del Fe. Aquesta resposta va estar acompanyada per l'augment de l'expressió de *OsIRO2*, un TF típicament unit per productes de proteïna ISR.

Les conclusions obtingudes en aquesta tesi doctoral proporcionen informació crec important sobre com intervé Sp7 en els processos moleculars de les plantes i donen suport a la hipòtesi que diverses estratègies de biofortificación se sumen per augmentar la salut de les plantes, cridant l'atenció sobre la centralitat de la activació de TFS i la senyalització coordinada d'hormones en aquestes respostes.

Table of Contents

Figure Index

CHAPTER 1

CHAPTER 3

CHAPTER 4

CHAPTER 5

CHAPTER 6

CHAPTER 7

CHAPTER 8

Table Index

List of Abbreviations

A	Photosynthesic rate
ABA	Abscisic acid
Ac	Acetylation
ACC	1-aminocyclopropane-1-carboxylic acid
ACN	Acetonitrile
ACO	1-aminocyclopropane-1-carboxylase oxygenase
AMF	Arbuscular mycorrhizal fungi
ANOVA	Analysis of variance
AP2/EREPB	APETALA2/ethylene-responsive element binding protein
AP2/ERF	AP2/ethylene responsive factor
APX	Ascorbate peroxidase
AREB/ABF	ABA-responsive element binding protein/ABRE-binding factor
ARF	Auxin response factor
ATCC	American type culture collection
ATPase	Adenosine 5'-triphosphatase
AUX	Auxin
BBCH	Biologische Bundesanstalt, Bundessortenamt und Chemische Industrie
BDM	Barley dwarf mosaic virus
BNF	Biological nitrogen fixation
BSA	Bovine serum albumin
bZIP	Basic Leucine Zipper
CB	Calvin-Benson
CECT	Colección Española de Cultivos Tipo
CDPK	Calcium-dependent protein kinase
CDSP	Chloroplastic drought-induced stress protein
cfu	Colony-forming unit
CHI	Chitinase
CIMMYT	Centro Internacional de Mejoramiento de Maíz y Trigo
CMV	Cucumber mosaic virus
CP	Coat protein
CR	Congo-red
CRISPR-Cas9	Clustered regularly interspaced short palindromic repeats- associated protein-9 nuclease
CSIC	Consejo Superior de Investigaciones Científicas
CSP41	Chloroplast stem-loop binding protein of 41 kDa
cv.	Cultivar
cyt b6	Cytochrome b6-f complex iron-sulfur subunit
DAMP	Damage-associated molecular pattern
DAS-ELISA	Double Antibody Sandwich-ELISA
DDT	Dithriothreitol
DIR1	Defective in induced resistance1
DLD	Dihydrolipoamide dehydrogenase precursor
DMA	2'-deoxymugineic acid
DNA	Deoxyribonucleic acid
DON	Deoxynivalenol
dpi	Days post-inoculation
DREB/CBF	Dehydration-responsive element binding/ C-repeat binding factor
DSMZ	Deutsche Sammlung vonMikroorganismen und Zellkulturen
DW	Dry weight
E	Transpiration
EDTA	Ethylenediaminetetraacetic acid
ELISA	Enzyme-like immunosorbent assay

EPS	Exopolysaccharides
ESI-TOF-MS	Electrospray ionization-time of flight-mass spectrometry
ET	Ethylene
ETI	Effector-triggered immunity
EtOH	Ethanol
ETSEA	Escola Tècnica Superior d'Enginyeria Agrària
FAO	United Nations Food and Agriculture Organization
FBA	Fructose-bisphosphate aldolase
FISH	Florescence *in situ* hybridization
Fus	*Fusarium graminearum*
GAE	Gallic acid equivalents
GAPDH	Glyceraldehyde-3-phosphate dehydrogenase
GDC-L	Glycine decarboxylase protein
GLDC	Glycine dehydrogenase
GLM	General Linear Model
GPX	Glutathione peroxidase
GRX	Glutaredoxin
GSH	Glutathione ascorbate
GST	Glutathione-S-transferase
HAMP	Herbivore-associated molecular pattern
HC	High-carotenoid
HDZ	Homeodomain leucine zipper
HESI	Heated electron-spray ionization
HPLC	High-performance liquid chromatography
HR	Hypersensitive response
HSD	Honest significant difference
HvNAATb	Barley nicotianamine amino transferase
IAA	Indole-3-acetic acid
ICA	Indole-3-carboxylic acid
ICM	Integrated Crop Management
ICP-MS	Inductively coupled plasma mass spectrometry
IEF	Isoelectric focusing
ISR	Induced systemic resistance
JA	Jasmonic acid
kDa	KiloDalton
LB	Luria-Bertani (broth)
LEA	Late embryogenesis abundant
LOX	Lipoxygenase
LSD	Least significant difference
MA	Mugineic acid
MALDI	Matrix-assisted laser desorption/ionization
MAMPs	Microbe-associated molecular patterns
MAPK	Mitogen-associated protein kinase
MAT	Methionine adenosyltransferase
MDAR	Monodehydroascorbate reductase-like
MDH	Malate dehydrogenase
MDMV	Maize dwarf mosaic virus
Me	Methylation
MHM	5-methyltetrahydropteroyltriglutamate-homocysteine methyltransferase-like
MS/MS	Tandem Mass Spectrometry
mRNA	Messenger RNA
MS	Murashige and Skoog media
MTI	MAMP-triggered immunity
MYB	Myeloblastosis

MYC	Mielocitomatosis
NA	Nicotianamine
NAAT	NA aminotransferase
NAC	NAN/ATAF/CUC
NADPH	Nicotinamide adenine dinucleotide phosphate
NADP-ME	NADP-dependent malic enzyme
NA	Nicotianamine
NAS	Nicotianamine synthase
NB-LRR	Nucleotide-binding-leucine-rich repeat
NCBI	National Center for Biotechnology Information
NCED	9-cis-epoxycarotenoid dioxygenase
Nfb	Nitrogen-free broth
NPR1	Non-expressor for pathogenesis-related genes 1
NTRC	NADPH-dependent thioredoxin reductase
NO	Nitric oxide
OD	Optical density
PacrtI	*Pantoea annatis* crtI
PAL	Phenylalanine ammonia lyase
PAMPs	Pathogen-associated molecular patterns
PBS	Phosphate buffered saline
PCA	Principle component analysis
PCD	Programmed cell death
PCR	Polymerase chain reaction
PDA	Potato dextrose agar
PEP	Phosphoenolpyruvate
PG	Phosphoglycerate
PGK	Phosphoglycerate kinase
PGPF	Plant growth-promoting fungi
PGPM	Plant growth-promoting microorganism
PGPR	Plant growth-promoting rhizobacteria
pI	Isoelectric point
PMF	Peptide mass fingerprint
PR	Pathogenesis-related
PRR	Pattern-recognition receptor
PRX	Peroxidase
PS	Phytosiderophores
PSII	Photosystem II
PTI	PAMP-triggered immunity
PVCF	Producció Vegetal i Ciència Forestal
PVX	Potato virus X
PVY	Potato virus Y
PYB	Peptone yeast broth
R	Resistance
RB92	Fe-biofortified rice seedlings (expressing NA and HvNAATb)
RBCS	Ribulose-1.5-bisphosphate carboxylase/oxygenase small subunit
RBSDV	Rice black-streaked dwarf virus
RLKs	Receptor-like kinases
RLPs	Receptor-like proteins
RNA	Ribonucleic acid
RNS	Reactive nitrogen species
ROS	Reactive oxygen species
RT	Reverse transcription
Rubisco	Ribulose 1,5-bisphosphate carboxylase/oxygenase
RYMV	Rice yellow mottle virus
SA	Salicylic acid

SAM	S-Adenosyl-L-methionine
SAR	Systemic Acquired Resistance
SCLM	Scanning confocal laser microscopy
SD	Standard deviation
SDS-PAGE	Sodium Dodecyl Sulfate Polyacrylamide Gel Electrophoresis
SDW	Sterile distilled water
SE	Standard error
SFA	Selective *Fusarium* agar
SM	Secondary metabolism
SODs	Superoxide dismutases
spp.	Multiple species
Sp7	*Azospirillum brasilense* Sp7
SPAD	Soil-plant analysis development (Chlorophyll content)
TCA	Trichloroacetic acid
TCA	Tricarboxylic acid (cycle)
TF	Transcription factor
TFA	Trifluoroacetic acid
THF1	Thylakoid formation 1
TKT	Transketolase
TMV	Tobacco mosaic virus
TOM	Transporter Of Mugineic acids
TPC	Total phenolic content
TRX	Thioredoxin
TYG	Tryptone yeast extract and glucose
tZ	Trans-zeatin
UdL	Universitat de Lleida
UHPLC-MS	Ultra-high performance liquid chromatography tandem mass spectrometry
VRCs	Viral replication complexes
WHO	World Health Organization
WT	Wild type
WUEi	Water-use efficiency
YSL	Yellow Stripe-Like
Zmpsy1	*Zea mays* phytoene synthase 1

CHAPTER 1

General Introduction

Chapter 1. General Introduction

1.1 Crop biofortification

1.1.1 Biofortification

According to the World Health Organization (WHO), the term biofortification refers to "the process by which the nutritional quality of food crops is improved through agronomic practices, conventional plant breeding, or modern biotechnology". As malnutrition plagues daily lives worldwide, disproportionally so in less developed countries in Asia, Central and South America, Sub-Saharan Africa, and more recently in the Middle East, crop biofortification is becoming increasingly critical. The United Nations Food and Agriculture Organization (FAO) has estimated that around 792.5 million people across the world are malnourished, 780 million of which live in developing countries (McGuire, 2015). Of these, two billion people suffer "hidden hunger", or inadequate intake of essential micronutrients (Muthayya et al., 2013; Hodge, 2016), despite increased food crop production (Gould 2017). These eminent numbers are a result of modern agriculture, which has mostly focused on the productivity of cash crops at the expense of the biodiversity of plants and soil, in addition to the nutritional value of food (Garg et al., 2018) (Figure 1). Producing nutritious and safe foods, sufficiently and sustainably, is the ultimate goal of biofortification (Saltzman et al., 2014).

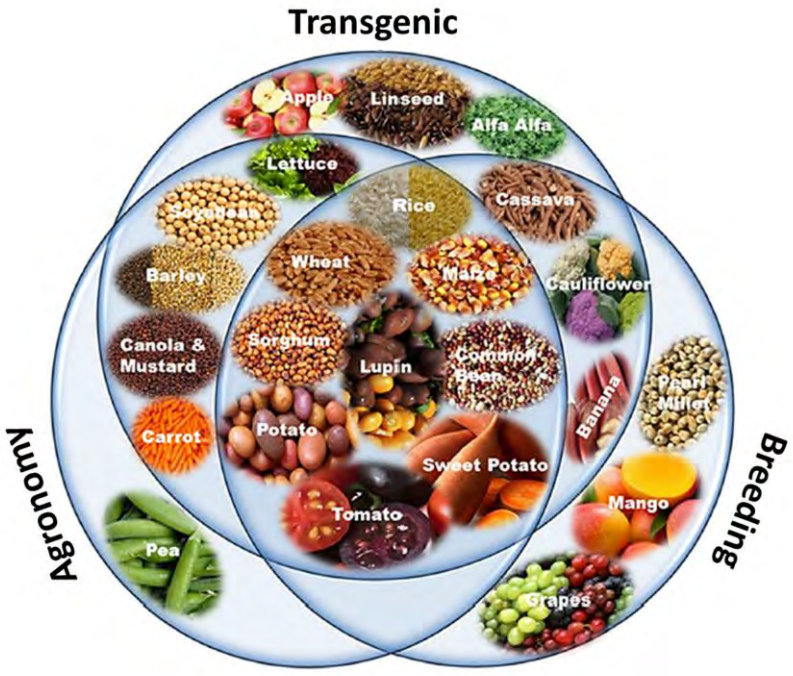

Figure 1. Biofortified crops generated by different approaches: transgenic, agronomic, and breeding (adapted from Garg et al., 2018)

Compared with the other approaches used to obtain biofortified crops, conventional **plant breeding** is the cost-effective. This method relies on the crossing of high nutrient parent lines with recipient lines possessing desirable agronomic traits over several generations to produce plants with desired nutrient and/or agronomic traits. The limitation is that breeding always relies on the limited genetic variation present in the gene pool (Garg et al., 2018).

Biofortification based on **transgenic** or modern **biotechnology** is a way to circumnavigate this limitation. The transgenic approach allows for the transfer and expression of genes from one species to another, independent of their evolutionary and taxonomic status (Zhu et al., 2007). As such, when a nutrient does not naturally exist in crops, transgenic approaches are the only feasible options to fortify these crops (Perez-Massot et al., 2013). The other advantage to using modern biotechnology is that the number of techniques available provides limitless options regarding gene modification to improve nutrient bioavailability, to decrease antinutrients, or to redirect nutrients to different tissues. Simultaneous genes can be incorporated at once via combinatorial nuclear transformation, genes can be edited and replaced via CRISPR-Cas9, or gene cassettes can be engineered and incorporated into a plant so as to synthetically overcome taxonomic barriers. These methods require a substantial investment at the onset, but are cost-effective and sustainable in the long run (Hefferon et al., 2016). The major limitation to transgenic methods in the mainstream is that they are not widely accepted politically, economically or socially. As a result, regulatory processes are very expensive, complicated and time consuming (Gómez-Galera et al., 2012).

Finally, there is **agronomic biofortification**, which is comparably most accessible for farmers. It employs targeted application of various organic and soluble inorganic fertilizers to enrich the soil environment, the health of the crop, and the accumulation and phytoavailability of minerals in the plant for human consumption (Rengel et al., 1999; Cakmak 2008). Since application is usually timed and repetitive, this type of biofortification is criticized for being less-cost effective and more time intensive. Furthermore, there are a number of drawbacks related to over-accumulation of nutrients in leaves and non-edible plant parts, or high variability due to differences in mobility of nutrients depending on plant species (Cakmak et al., 1999).

The agronomic practice of applying growth-promoting soil microorganisms is less utilized, but can have a number of beneficial effects on the development and mineral concentrations of plants (Garg et al., 2018). Plant growth-promoting rhizobacteria (PGPR) and mycorrhizal fungi are the two groups of plant growth-promoting microorganisms (PGPMs) that are most studied in this regard. They have been found to enhance nutrient mobility from the soil to edible plant parts, to increase phytoavailability of mineral elements, and to release siderophores, organic enzymes and acids into the rhizosphere that increase mineral concentrations in edible plant tissues (Hardarson and Broughton 2004; Smith and Read 2007; Cavagnaro 2008). Apart from improving crop status for human consumption, these

microorganisms also improve the health and resistibility of the plants under adversary environmental conditions and their associated stresses, or in the face of pathogen attack. This is an increasingly interesting outcome as climate change is marked by irregular rainfall patterns, warmer temperatures and other ideal conditions for microorganisms to flourish. Biofortification of crops through implications of PGPMs is a promising accompanying measure, which along with transgenic varieties, can lead to augmented micronutrient concentrations in food crop system, besides improving yield and soil fertility (Khan et al., 2019).

1.1.2 Staple crops

Apart from seriously affecting the well-being of the people directly concerned, micronutrient malnutrition negatively affects aggregate productivity and economic development (Zhu et al., 2007). Therefore, more nutritious crops have a positive impact on both the health and economy of the people in developing countries (Qaim et al., 2007). Currently, highly productive staple crops like barley, rice, maize and tomato are aims of these biofortification efforts (Table 1). In our study, we use rice, maize and tomato, which have been targeted by all three approaches, and barley, which has been biofortified transgenically and agronomically. As summarized in Table 1, great strides have been made to improve their nutritional value, and some lines have even been released to farmers. It should be highlighted that of these crops, only barley has been agronomically biofortified with a PGPR.

Minerals and nutrients are just as important for plants as they are for humans and animals. They play critical roles as enzyme co-factors (e.g., Fe) and structural components (e.g., Ca^{2+}), so plants have developed complex systems for managing their uptake and homeostasis (Gómez-Galera 2011). If then, crops were biofortified to benefit the health of the crop in addition to the population consuming them, the cost of production inputs, such as herbicides, pesticides and fertilizers, would drop significantly. In this way, there is a call for a fundamental shift in the dynamics of biofortification; to obtain plants with properties that benefit the plant and the consumer alike. As one example, plants are often bred or engineered to contain lower concentrations of antinutrients, which can block the bioavailability of nutrient acquisition for humans. However, antinutrients are major metabolites that play important roles in plant metabolism, in plant abiotic stress resistance, and in plant resistance to crop pests or pathogens (Graham et al., 2001). Finding ways to preserve these benefits for plants, or replacing them with other equally beneficial alternatives should be a priority.

Table 1. Tabulation of some biofortified crops, nutrients and research status (adapted from Garg et al., 2018; see for full list of references).

Crop	Type of Biofortification	Status	Method
Barley			
	Beta-glucan	Research	Transgenic
	Biofertilizers+NPK+Vermicompost	Research	Agronomic
	Human lactoferrin	Research	Transgenic
	Lysine	Research	Transgenic
	Phytase	Research	Transgenic
	Polyunsaturated fatty acids	Research	Transgenic
	Resistant starch	Research	Transgenic
	Zinc	Research	Transgenic
Maize			
	Anthocyanins	Research	Breeding
	Human lactoferrin	Research	Transgenic
	Lysine, Lysine and Tryptophan, Methionine	Research	Transgenic
		Released	Breeding
	Lysine	**Released**	Transgenic
	Multivitamin	Research	Transgenic
	PGPR and Cyanobacteria	Research	Agronomic
	Phytase, Ferritin	Research	Transgenic
	Phytate degradation	**Released**	Transgenic
	Provitamin A and Carotenoids	Research	Transgenic
		Released	Breeding
		Research	Breeding
	Se	Research	Agronomic
	Vitamin E	Research	Transgenic
		Research	Breeding
		Research	Breeding
	Vitamin C	Research	Transgenic
	Zinc	Research	Agronomic
Rice			
	Alpha-linolenic acid	Research	Transgenic
	Beta-carotene, Phytoene	Released	Transgenic
	Flavonoids and antioxidants	Research	Transgenic
	Folate	Research	Transgenic
	High amino acids and protein content	Research	Transgenic
	Human lactoferrin	Research	Transgenic
	Iron	Research	Transgenic
		Research	Agronomic
		Released	Breeding
		Research	Breeding
	Phytic acid	Research	Transgenic
	Resistant starch	Research	Transgenic
	Se	Research	Agronomic
	Zinc	Research	Transgenic
		Research	Agronomic
		Research	Breeding
Tomato			
	Antioxidant anthocyanins	Research	Transgenic
		Research	Breeding
	Ascorbate	Research	Transgenic
	Folate	Research	Transgenic
	Folate, phytoene, Beta-carotene, Lycopene, Provitamin A, Isoprenoids Carotenoid + Flavonoid	Research	Transgenic
	Iodine	Research	Agronomic

1.2 Stress in plants

Plants have evolved to endure two types of environmental stress: biotic and abiotic. Biotic stresses include bacteria and bacteria-like organisms (phytoplasma and rickettsia-like organisms), protozoa and parasitic flagellate, oomycetes and fungi, viruses and virus-like entities, nematodes and herbivores. Abiotic stresses, on the other hand, include salinity, drought, flood, extreme temperatures, heavy metals and radiation and they are the foremost cause of crop loss worldwide. To survive and combat the arsenal of both biotic and abiotic threats, plants have developed a multitude of mechanisms for adapting to stress.

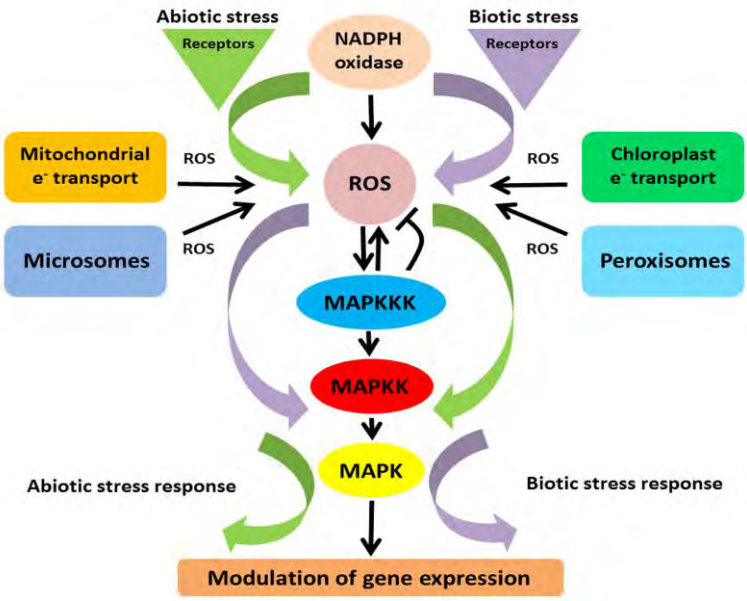

Figure 2. Schematic representation of reactive oxygen species (ROS) regulation of mitogen activated protein kinases (MAPK) signaling pathway in biotic and abiotic stress (adapted from Jalmi and Sinha 2015).

From the perception of stress to the final response in cells, plants use various signaling pathways depending on the challenge. Cellular responses work together to activate the signal transduction pathways located on the cell surface or in the cytoplasm to trigger the transcriptional machinery, which is situated in the nucleus (Rejeb et al., 2014). Resulting transcriptional changes help make the plant more tolerant to the stress. These signaling pathways play an indispensable role and act as a connecting link between sensing the stress in the environment and generating an appropriate physiological and biochemical response (Zhu, 2002). Other factors such as the plant species, the intensity of the stress, field conditions and developmental stage of the plant can also influence an interaction by changing the outcome of the plant defense response at the transcriptome, cellular or physiological level (Mittler and Blumwald 2010). Furthermore, plants respond in a specific manner when they have to face more than one stress simultaneously because they activate a specific program of gene expression relating to the exact environmental conditions encountered. Specificity in multiple

stress responses is further controlled by a range of molecular mechanisms that act together in a complex regulatory network. Transcription factors, kinase cascades, and reactive oxygen species are key components of this cross-talk, as are heat shock factors and small RNAs. This response is unique and cannot be predicted based on the plants' response to single individual stresses (Atkinson and Urwin 2012).

In general, callose accumulation, changes in ion fluxes, activation of mitogen-associated protein kinase (MAPK), reactive oxygen species (ROS) and phytohormone cross-talk are the first responses induced to combat the stress. The resulting signal transduction pathways trigger metabolic reprogramming towards defense (Yasuda et al., 2008; Bartoli et al., 2013). There are, however, some important differences between plant responses to biotic or abiotic stress (Figure 2).

1.2.1 The biotic stress-response

The first line of defense in plants is the recognition of conserved molecules characteristic of many microbes and pathogens. These elicitors are also known as microbe-associated molecular patterns (MAMPs) and pathogen-associated molecular patterns (PAMPs). Fungal or bacterial enzymes breaching the plant cell wall produce MAMPs (such as oligogalacturonides, or pectin fragments) that are typical and elicit defense responses (Ridley et al., 2001; Sanabria et al., 2008; Boller and Felix, 2009). Recognition of MAMPs and PAMPs by pattern recognition receptors (PRRs) that are plasma membrane localized receptor-like kinases (RLKs) or receptor-like proteins (RLPs) (Boutrot and Zipfel, 2017; Zhang et al., 2017) triggers MAMP- and PAMP-triggered immunity (MTI and PTI, respectively), thereby reinforcing the host defenses that halt infection before the pathogen gains a hold in the plant (Verma et al., 2013). Pathogenic microbes have, however, evolved the means to suppress MTI and PTI by secreting specialized proteins, called effectors, into the plant cell cytosol that alter resistance signaling or manifestation of resistance responses (Verma et al., 2013). Since pathogens acquired the capacity to suppress primary defenses, plants thereby developed a more specialized mechanism to detect microbes, called effector-triggered immunity (ETI). This serves as the second line of plant defense and involves the recognition of a given effector by a set of plant resistance (R) gene products (Jones and Dangl, 2006; Pel and Pieterse, 2013). MTI/PTI and ETI trigger down-stream signaling networks in coordination with MAPK cascades (Lanubile et al., 2017). MAPK ultimately phosphorylate and activate several downstream targets like transcription factors, other kinases, phosphatases, and cytoskeleton associated proteins (Hamel et al., 2006; Rodriguez et al., 2010; Sinha et al., 2011).

There is also Ca^{2+} signaling through the cell membrane, which is a result of the induction of calcium-dependent protein kinase (CDPK) gene expression after infection (Lanubile et al., 2014), and responsible for the activation of the redox state in the plant and early ROS production (Lanubile et al., 2017). ROS production is required for another component of

the response known as hypersensitive response (HR), a type of programmed cell death that limits the access of the pathogen to water and nutrients (Sato et al. 2010). The rapidly produced ROS affects the cellular oxidation state, inducing MAPK, as well as ascorbate peroxidase (APX), glutathione peroxidase (GPX), glutaredoxin (GRX), thioredoxin (TRX), peroxidase (PRX), and glutathione-S-transferase (GST) gene expression (Campo et al., 2004; Mohammadi et al., 2011). Hormones and hormone signaling genes orchestrate ROS signals until they reach the nucleus (Berens et al., 2017). Some of the key hormones involved are salicylic acid (SA), jasmonic acid (JA), ethylene (ET), abscisic acid (ABA) and auxin (AUX); and they are responsible for targeting various transcription factor families. For example, WRKY is typically associated with SA, myeloblastosis (MYB) with ABA, auxin response factor (ARF) for AUX and APETALA2/ethylene-responsive element binding protein (AP2/EREPB) and AP2/ethylene responsive factor (AP2/ERF) for ET (Campos-Bermudez et al., 2013; Lanubile et al., 2014; Wang et al., 2016; Lanubile et al., 2017) (Figure 3).

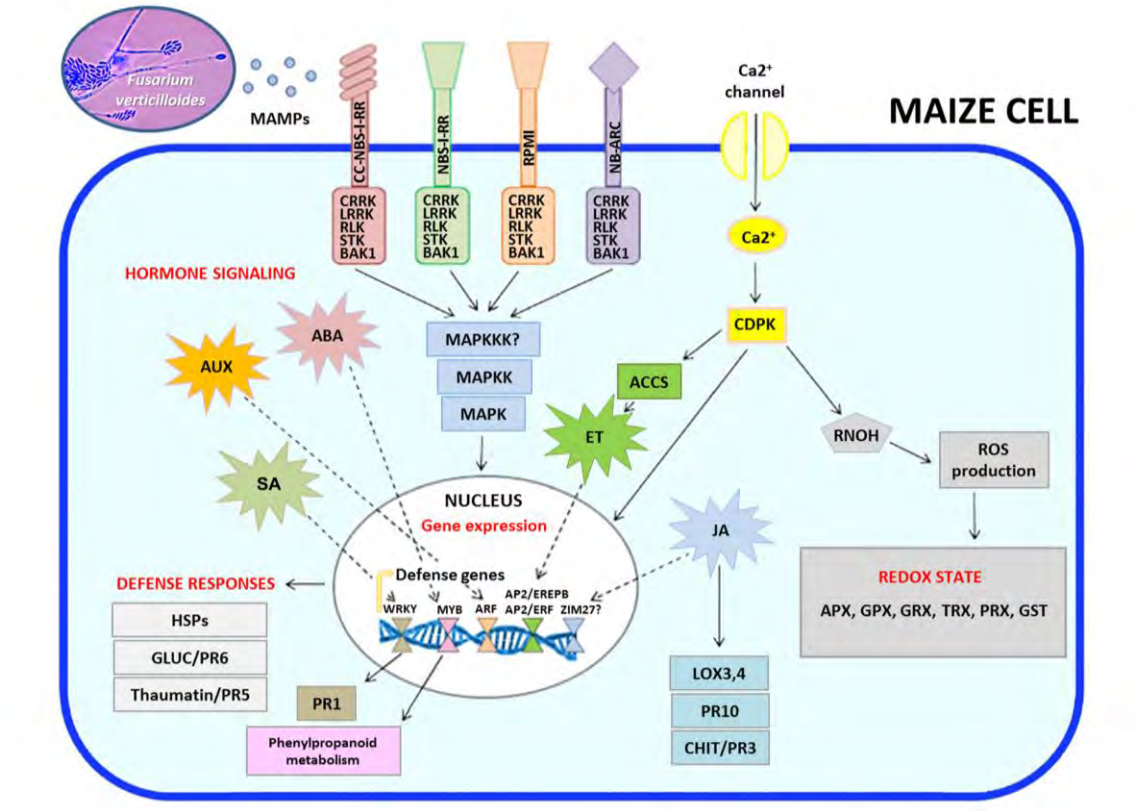

Figure 3. Schematic overview of maize defense gene activation in response to *Fusarium verticillioides* infection (adapted from Lanubile et al., 2017).

1.2.2 The abiotic stress-response

Responses to abiotic stress are very similar to those induced by biotic stress. At the cellular level, the stress response includes adjustments of the membrane system, modifications of cell wall architecture, changes in cell cycle and cell division. ROS and MAPK cascades are activated, and like in the biotic stress response, plants synthesize phytohormones to regulate the

protective responses (Fujita et al., 2006). At the molecular level, the abiotic response includes the expression of stress-inducible genes that can be divided into two major groups according to the functions of their products.

The first group consists of a large number of proteins: enzymatic and structural proteins, such as membrane proteins, enzymes for osmolyte biosynthesis, detoxification enzymes (GST, hydrolases, superoxide dismutases (SODs) and APX), and other proteins for macromolecular protection [such as the late embryogenesis abundant (LEA) proteins, chaperons and mRNA binding proteins] (Bohnert et al., 2001; Seki et al., 2001; Zhu et al., 2001; Agarwal et al., 2001). The second group comprises a variety of regulatory proteins (such as transcription factors, protein kinases, receptor protein kinases, ribosomal-protein kinases and transcription-regulation protein kinase) and signal transduction proteinases (phosphoesterases and phospholipase C) involved in the regulation of cascades of gene expression (Agarwal et al., 2001). Transcription factors that are more closely related with the abiotic response are basic leucine zipper (bZIP), dehydration-responsive element binding/ C-repeat binding factor (DREB/CBF), ABA-responsive element binding protein/ABRE-binding factor (AREB/ABF), myeloblastosis/mielocitomatosis (MYC/MYB), NAN/ATAF/CUC (NAC), homeodomain leucine zipper (HDZ) and WRKY (dos Reis et al., 2012).

1.3 Pathogen strategies

Plant pathogens are classified into three main groups based on the strategies they have devised to invade plant tissue, they are: **necrotrophic, biotrophic**, and **hemibiotrophic**. In all groups, phytohormones play a central role in the plant-pathogen interaction because they are fundamental to plant homeostasis (Muktar et al., 2016) (Figure 4).

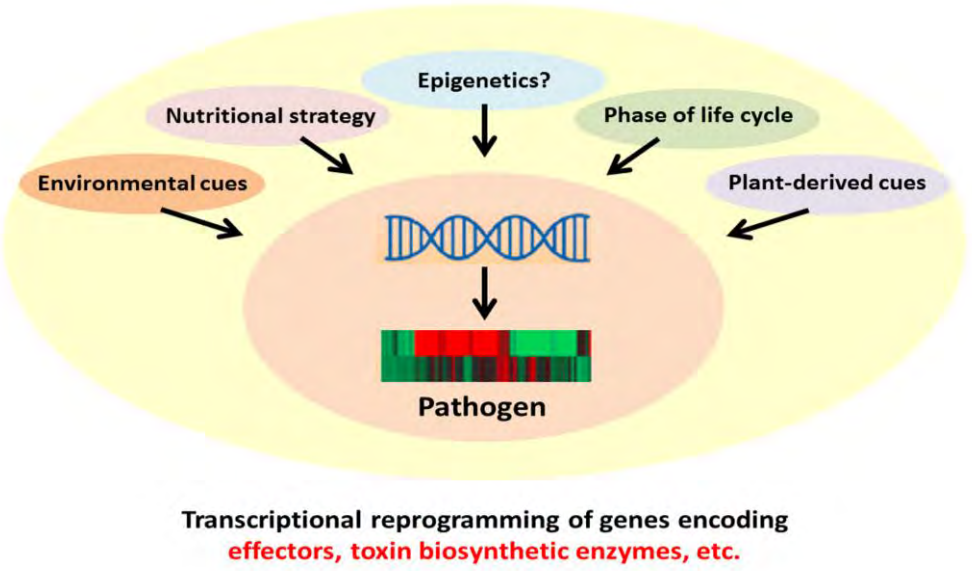

Figure 4. Transcriptional control of pathogen genes by external and internal cues and factors that temporally modulate gene expression (adapted from Muktar et al., 2016).

The activation of SA is typical to biotrophic pathogens, while JA/ET is more characteristic of necrotrophic and hemibiotrophic pathogens (Glazebrook 2005). As transcription data is becoming more common, pathogens that previously went undetected at incipient stages can now be perceived. Consequently, many necrotrophic pathogens are now being re-classified as hemibiotrophic. In our work, we have chosen to focus on biotrophic and hemibiotrophic groups.

Pathogen attack first initiates a series of rapid changes resulting in a decline in photosynthesis and an increase in respiration, photorespiration, and invertase enzyme activity (Berger et al., 2007). Then, the down-regulation of photosynthesis and the simultaneous increased demand for assimilates often leads to a transition of source tissue into sink tissue during plant–pathogen interactions. All of these changes are accompanied by the reactions typical to biotic stress, including transcriptional reprogramming of the plant. Studying the plant proteome has proven to be one of the most effective methods of gauging reactions associated with stress. Proteomic studies have been used to model the defense response related to hormones (for examples, see: Komatsu et al., 1999; Rakwal and Komatsu 2000). Other similar (proteomic) studies have characterized the nodular membrane caused by symbiosis with nitrogen-fixing bacteria in legumes (Panter et al., 2000), observed the outcomes of ozone in rice (Agrawal et al., 2002), and seen the effects of cold in flax (Tafforeau et al., 2002). Proteomics has revealed the effects of fungal elicitors on the extracellular proteins of *Arabidopsis* cell suspensions (Ndimba et al., 2003), and has facilitated a 'global analysis' of the rice/Rice yellow mottle virus (RYMV) interactome (Brizard et al., 2006).

1.3.1 Necrotrophic pathogens

The lifestyle of necrotrophic pathogens is unique in that they kill host tissue and feed on the remains to derive their nutrients (McDowell and Dangl 2000). To do so, the pathogens produce a variety of phytotoxins that likely promote host cell death (MacKinnon et al., 1999; Otani et al., 1998; Colmenares et al., 2002). The host also often employs programmed cell death to retain necrotrophic pathogens from spreading, which makes life easier for the pathogen by providing easier access to dead tissue (Glazebrook 2005). In general, necrotrophic pathogens are restricted by JA/ET-dependent defenses (Glazebrook 2005).

1.3.2 Biotrophic pathogens

Biotrophic pathogens thrive on living plant tissue for growth and reproduction and constitute the most investigated type of plant-pathogen interaction. Viruses and virus-like, nematodes and herbivores are usually classified as biotrophic since they need living tissue for nutrition, while bacteria and fungi often form a part of this group as well. The phytohormone SA is essential for this interaction (Thomma et al., 2001).

1.3.3 Hemibiotrophic pathogens

Hemibiotrophic pathogens incorporate mechanisms utilized by both biotrophic and necrotrophic pathogens. They require living plant tissue for growth and reproduction (biotrophic phase), but will cause the tissue to die at late stages of the infection. The pathogens are then able to feed on the dead tissue for survival (necrotrophic phase). Generally, bacteria and fungi are hemibiotrophic pathogens. The JA/ET hormone response pathway is crucial in the defense response against hemibiotrophic pathogens (Thomma et al., 2001).

1.4 The Plant Immune System: SAR and ISR

When plants are under attack or stressed by biotic and abiotic factors, they employ both constitutive and induced defense strategies to obviate damage. Constitutive defense mechanisms passively help the plant resist stressors. These are structural components and preformed barriers, such as cell walls and waxy epidermal cuticles (Freeman and Beattie, 2008). Inducible defenses are activated when plants detect that they are susceptible to damage or under attack by a compatible pathogen and lead to the production of toxic chemicals and secondary metabolites with antimicrobial activity, pathogen-degrading enzymes, phytohormones, defense-related proteins, hydrolytic enzymes and cell suicide to stop the spread of the damage (Madriz-Ordeñana, 2002). Inducible defenses, or 'induced resistance', protect the plant at the site of infection, as well as in non-exposed plant parts. In this way, plant parts are protected against future attack by pathogenic microbes and herbivorous insects (Kuc 1982).

Plant phytohormones assume a particularly pivotal role in inducible defenses because their activation depends upon the specific interaction, and the plant will activate either SA or JA/ET hormone signal transduction to promote resistance. Typically, noxious pathogens activate SA and beneficial microbes are associated with JA/ET (Pieterse et al., 2014) (Figure 5). The implications of eliciting one hormone pathway or another extend to downstream gene expression, proteins and other factors, so a term has been devised for each mode of resistance: systemic acquired resistance (SAR), representing the pathogenic induction of SA and PR proteins, and induced systemic resistance (ISR) referring to reactions caused by beneficial microbes and JA/ET induction.

1.4.1 Systemic acquired resistance (SAR)

SAR refers to pathogen-induced resistance that confers enhanced resistance against a broad spectrum of pathogens (including the initial one) (Ross 1961). At its core is the activation of PTI and ETI in infected plant cells. These mechanisms help the plant battle the pathogen at the site of infection, but also trigger long-distance signaling that induces resistance in tissues distal from the site of infection (Mishina and Zeier 2007). Accumulation of the hormone SA plays a central role in SAR signaling (Vernooj et al., 1994), as well as the activation of

pathogenesis-related (PR) genes. PR genes in turn encode PR proteins that have antimicrobial activity (Van Loon et al., 2006). SA accumulates in the phloem sap of SAR-expressing plants, but the long-distance signaling cascade is carried by a lipid-transfer protein chaperone known as defective in induced resistance1 (DIR1) (Champigny et al., 2011).The control hub of the SA response is the NONEXPRESSOR OF *PR* GENES1 (NPR1) transcriptional co-regulator, located in the nucleus. It interacts with TGA and WRKY transcription factors in SA-activated cells to bind to the promoters of and activate SA-responsive (PR) defense genes (Spoel et al., 2009).

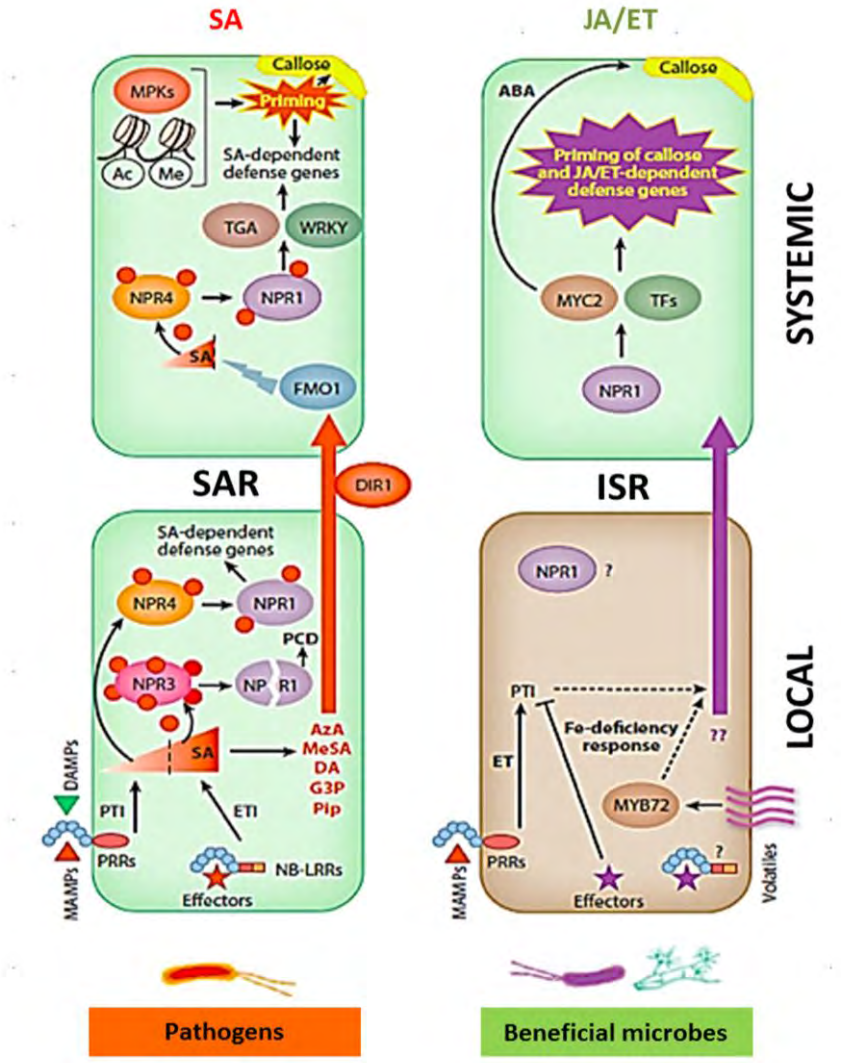

Figure 5. Schematic representation of molecular components and mechanisms involved in pathogen-induced systemic acquired resistance (SAR) and induced systemic resistance (ISR) triggered by beneficial soil-borne microbes. Solid black lines indicate established interactions; dashed black lines indicate hypothetical interactions. Colored arrows indicate systemic translocation of long-distance molecular or electric signals (indicated in the same color at the base of the arrows). Abbreviations: ABA, abscisic acid; Ac,acetylation; DAMP, damage-associated molecular pattern; ET, ethylene; ETI, effector-triggered immunity; Fe, iron; HAMP; herbivore-associated molecular pattern; JA, jasmonic acid; MAMP, microbe-associated molecular pattern; Me, methylation; NB-LRR, nucleotide-binding–leucine-rich repeat; PCD, programmed cell death; PRR, pattern-recognition receptor; PTI, PAMP-triggered immunity; SA, salicylic acid; TF, transcription factor (adapted from Pieterse et al., 2014).

1.4.2 Induced systemic resistance (ISR)

ISR is a systemic defense strategy triggered by a plant's association with beneficial (non-pathogenic) microbes (Alström 1991) in the rhizosphere that sensitizes distal plant parts (leaves) for enhanced pathogen defense (Van Peer et al., 1991). It is an interesting phenomenon in that it is SA and PR independent, relying on JA/ET signal transduction pathways instead (Verhagen et al., 2004). Accordingly, it has been shown to be most effective against necrotrophic and hemibiotrophic pathogens, which are sensitive to the up-regulation of these hormones. The beneficial microbes fall into two main categories: plant growth-promoting rhizobacteria (PGPR) and fungi (PGPF) (Lugtenberg and Kamilova 2009). Evidence suggests that both plants and beneficial microbes have evolved mechanisms to promote specific relationships leading to ISR. For example, plants have been shown to enrich their microbiome with root exudates to elicit and promote the proliferation of certain beneficial microbes (and not others), while PGPR/PGPF can locally suppress root immune responses to facilitate root colonization (Berendsen et al., 2012).

When ISR is induced, the plant undergoes 'priming', by which the plant is made more sensitive to up-regulation of the JA/ET defense response. In this way, priming prepares the plant so when it is invaded by a noxious pathogen or insect, activation of its cellular defenses is induced to a higher degree, thereby enhancing plant resistance (Conrath et al., 2006). At the onset, priming is rather elusive because it does not involve direct activation of resistance, so is nearly invisible at the protein or transcriptome level. As a result, ISR is normally studied in combination with pathogen attack, which is when changes in JA and ET up-regulation are made perceivable (Verhagen et al., 200; Wang et al., 2005). A primed plant exhibits several other physiological changes that help delay disease progression, such as enhanced callose deposition (Ton et al., 2005) and more rapid stomatal closure (Kumar et al., 2012).

One of the most important molecular mechanisms involved in priming is the up-regulation of NPR1. This gene is required for JA/ET hormone up-regulation and subsequent ISR activation, but it does not activate PR defense genes (as in the SAR response) (Dong, 2004; Pieterse et al., 1998). Although it has been determined that the ISR-related NPR1 is cytosolic (not nuclear like SAR NPR1), it is unknown whether NPR1 is an important TF shared by both induced resistance responses. TFs that have been specifically associated with ISR are AP2/ERF (Van der Ent et al., 2009) and MYC2 (Memelink 2009), both of which are also closely related with the regulation of JA- and ET-dependent defenses. MYC2 binds to *cis*-acting G-box-like motifs, which are enhanced substantially in the promoters of ISR primed genes as well (Memelink 2009). MYB72 has also been highlighted as a root-specific TF that is essential for the onset of ISR by various PGPR and PGPF alike (Verhagen et al., 2004). Its over-expression alone does not enhance resistance to foliar pathogens (Van der Ent et al., 2008), suggesting that MYB72 acts together with one or more other signaling components (Pieterse et al., 2014).

Identifying long-distance signaling molecules is, however, still an elusive aspect to the ISR response. Ethylene is considered to be a key in unravelling this mystery since its expression in roots is required for ISR expression in leaves (Knoester et al., 1999).

Despite the unique intricacies of SAR and ISR, there is speculation regarding their interconnectedness. It still remains in question as to why they share signaling components, or how simultaneous activation of both SAR and ISR leads to an additively enhanced defense capacity in the plant (Van Wees et al., 2000).

1.5 Plant growth-promoting rhizobacteria (PGPR) and plant health

The term "rhizobacteria" and "PGPR" was coined in the late 1970s by Kloepper and Schroth (1978), referring to the community of soil bacteria that competitively colonizes plant roots, stimulates plant growth and reduces the incidence of plant diseases. Since then, PGPR have been studied at length, having been found to stimulate plant growth both directly and indirectly. Direct mechanisms include the synthesis of stimulatory bacterial volatiles, exopolysaccharides (EPS) and phytohormones (like ABA, gibberellic acid, auxin, ET, cytokinins, and indole-3-acetic acid (IAA)), lowering plant ET levels, fixing nitrogen, and promoting plant nutrition via phosphate and mineral solubilization (Persello-Cartieaux et al. 2003; Van Loon 2007; Solano et al., 2008) (Figure 6).

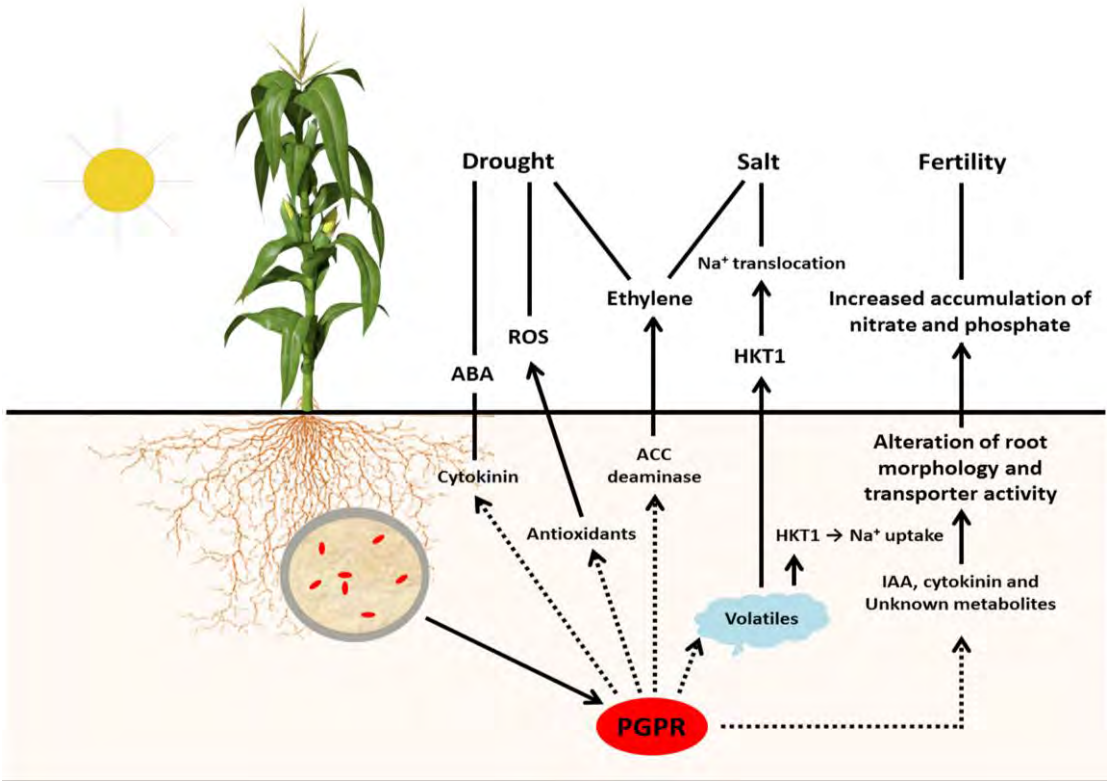

Figure 6. Plant growth-promoting rhizobacteria (PGPR) above- and below-ground influence on the plant and rhizosphere (adapted from Prasad et al., 2015).

In turn, PGPR stimulate plant growth indirectly by protecting against soilborne fungal pathogens or deleterious bacteria. This is done by suppressing antagonistic organisms through competition for iron and antibiotic secretion (Bloemberg & Lugtenberg 2001), or by inducing resistance (ISR) in plants (Jetiyanon & Kloepper 2002).

Plant–PGPR associations are mediated through an exchange of metabolites. Root exudates provide energy-rich organic acids, sugars, and amino acids that are metabolized by PGPR, while the PGPR generate an array of biologically active compounds that elicit plant growth promotion. Many free-living PGPR actively respond to root exudates by adjusting their transcriptional program toward traits involved in chemotaxis, root colonization, and energy metabolism (Fan et al., 2012; Neal et al., 2012). Once established on the root epidermis, PGPR typically form biofilms in which multicellular communities are enclosed within an extracellular matrix of self-produced polymeric substances, mainly EPS, and mucilage (Rudrappa et al., 2008). PGPR have even been shown to suppress activation of root defense genes that are triggered by MAMP, to protect the microbes and their colonization events from MAMP-triggered production of antimicrobial compounds (Millet et al., 2010; Pieterse et al., 2014). A summary of effects induced by PGPR is shown in Figure 7.

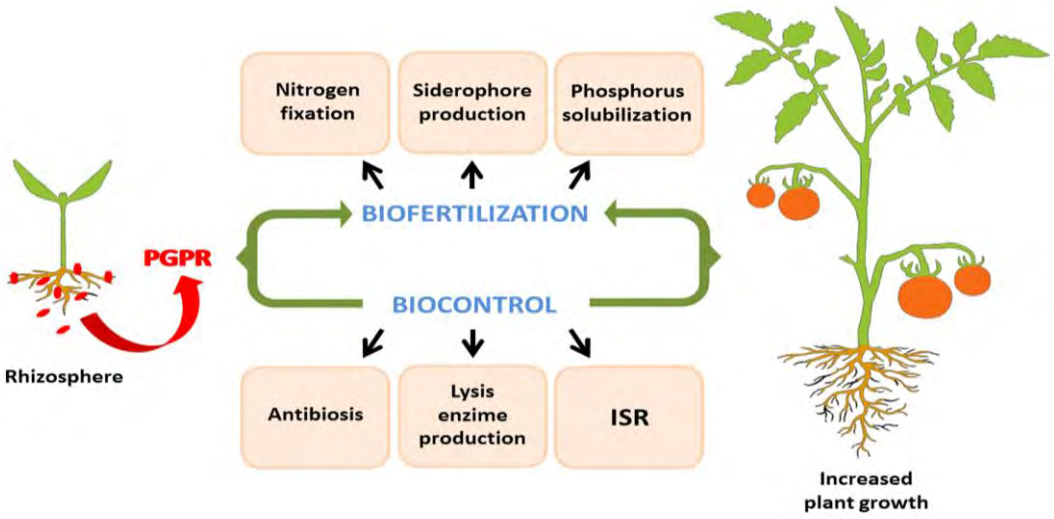

Figure 7. Schematic illustration of key mechanisms employed by PGPR to increase plant growth. Mechanisms are broadly classified as biofertilization and biocontrol of pathogens. Biofertilization encompasses: N_2 fixation, siderophore production, and phosphate solubilization by rhizobacteria. Biocontrol involves: antibiosis, enzyme secretion, and causing induced systemic resistance (ISR) in the host plant (adapted from Kumar et al. 2011).

The use of biological approaches is becoming more popular both as an additive to chemical fertilizers for improving crop yield in an integrated plant nutrient management system, and alone, for farmers to assume the pedigree of certified 'bio'/'organic' products. Depending on the activities of the PGPR, they have been classified as biofertilizer, phytostimulators,

rhizoremediators, and biopesticides (Somers and Vanderleyden, 2004). Main parameters affecting activity and determining how the PGPR will interact with the plant and surrounding environment are whether it is endophytic or epiphytic, symbiotic or free-living. Some of the more common genera of symbiotic PGPR are *Rhizobium*, *Bradyrhizobium*, *Azorhizobium*, *Allorhizobium*, *Sinorhizobium* and *Mesorhizobium*, while some 'free-living nitrogen-fixing bacteria' or 'associative nitrogen fixers' are *Azospirillum*, *Azotobacter*, *terobacter*, *Klebsiella*, and *Pseudomonas* (Cocking 2003). Of these, *Azospirillum* spp. is one of the most widely studied due to its ability to significantly improve the growth, development and yield of numerous species of agricultural interest worldwide (Bashan et al., 2004).

1.6 *Azospirillum* spp.

Azospirillum spp. was first discovered in the 1920s after significantly increasing the nitrogen content of garden soil (Beijerinck 1925). At the time, it was named *Spirillum lipoferum* due to its spirillum-like structure and spirilloid movement. Little more attention was given to it until it was then re-discovered on the roots of *Digitaria* sp. in Brazil and re-classified in 1978 by Tarrand et al. Based on DNA homology and taxonomic study of various isolates, it was then classified into two main species, *A. lipoferum* and *A. brasilense*.

Now, *Azospirillum* is one of the most well characterized and commercially employed genera of PGPR, with 20 N-fixing and non-N-fixing species (Leibniz Institute DSMZ, 2018). It is gram-negative and a member of the α-subclass of proteobacteria. It is easily isolated, and has been found in many parts of the world, including Argentina, Peru, Colombia, Sweden, Nigeria, Senegal and the USA (Reis et al., 2015). Most notably, *Azospirillum* spp. is free-living, which increases its versatility by giving it the ability to associate with the roots of an array of plants like grasses, legumes, cereals, fruits and vegetables.

For *Azospirillum* spp. to be applied to soil in large-scale operations, it must be delivered in a carrier that will protect the bacterial population physically, and provide a suitable microenvironment for it to thrive. In the absence of a proper carrier or plants, the bacterial population declines rapidly and disappears after 15 days (Bashan 1999). Peat and synthetic alginate are the only efficacious soil inoculants for *Azospirillum* spp. to date (Bashan et al., 2002; Deaker et al., 2011). These inoculants allow the bacteria to remain in the soil at concentrations high enough to keep them viable and competitive, and 'to slow release' until seeds are ready to germinate. Current research is exploring the possibility of delivering *Azospirillum* spp. to plants in cysts, but there is the caveat that it has been difficult to entice vegetative *A. brasilense* cultures to produce cysts at yields high enough to use as a seed inoculum (Malinich and Bauer 2018). Otherwise, seed-coating with *Azospirillum* spp. and peat is the most reliable way of delivering it to a cropping system (Bashan and de-Bashan 2015). Every year, three million doses of *Azospirillum* spp. inoculants are applied on a commercial

scale to mostly cereals and legumes throughout the world; mainly in Argentina, Brazil, Mexico, South Africa, Australia, India and Europe (Díaz-Zorita and Fernández-Canigia 2009; Hartmann and Bashan 2009; Fukami et al., 2018).

The mode of action by which *Azospirillum* spp. increases plant growth was initially thought to be its biological nitrogen-fixing abilities, but review of contemporary research has led to the "theory of multiple mechanisms" in which the bacterium acts in a cumulative or sequential pattern of effects, resulting from mechanisms occurring simultaneously or consecutively (Bashan and de-Bashan, 2010). Some examples of these mechanisms are the production or metabolism of plant hormone-like compounds including auxins, cytokinins, gibberellins, abscisic acid, ethylene and salicylic acid; solubilization of inorganic phosphorous; siderophore synthesis; and altering plant metabolism and production of secondary metabolites (Fukami et al., 2018).

1.7 *Azospirillum brasilense* Sp7

Of all *Azospirillum* species*, A. brasilense* is the most studied. This is because it is very common, and because endophytic *A. brasilense* strains are highly invasive (Khammas et al., 1989). Such strains, such as *A. brasilense* Sp245 (Sp245), normally enter the inner part of the plant via disrupted cortical tissues, lysed root hairs or natural cracks in the plant tissue (Steenhoudt and Vanderleyden 2000). Epiphytic strains, like *A. brasilense* Sp7 (Sp7), remain on the root epidermis and in the rhizosphere, but respond strongly to the soil environment, sensing stress and contaminants more acutely (Kamnev et al., 2012) (Figure 8).

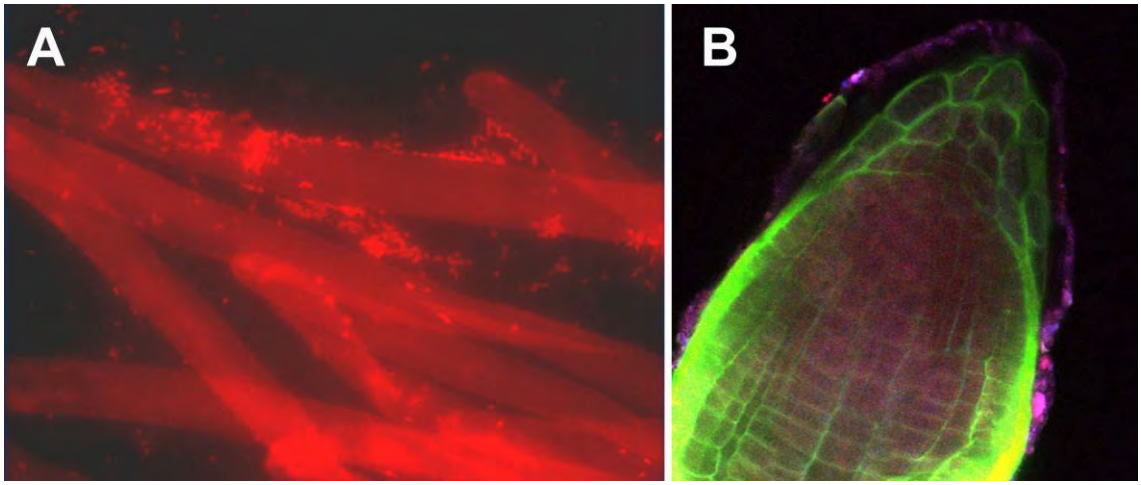

Figure 8. A. Root colonization by *Azospirillum brasilense,* visualized by florescence *in situ* hybridization (FISH). Brilliant dots are the bacterial cells. B. Root colonization of *Sorghum* plants by *A. brasilense,* visualized by scanning confocal laser microscopy (SCLM). Bacterial cells are glowing purple (From de-Bashan and Bashan, 2016).

Therefore, Sp7 has more potential to protect plants from soil pathogens since it blocks rhizospheric pathogen-plant interaction zones (Pereg, 2015). Sp7 is also valued for its ability to produce siderophores, especially since not all strains of *A. brasilense* are able to do so (Bachhawat and Ghosh 1987; Tortora et al., 2011). Fittingly, most of the existing literature regarding siderophore production by Sp7 relates to its role as a biocontrol agent used to limit the growth of soil-borne phytopathogens (Tortora et al., 2011).

Sp245 is the neotype strain for the species *A. brasilense* (Baldani et al., 1986), though Sp7 was previously considered the type strain (Tarrand et al., 1978). Sp7 is diazotrophic and has a positive effect on plant and root development, but also mitigates the effects biotic and abiotic stress on plants. Sp7 is known to have genotype-specific interaction (Correa et al., 2007; Drogue et al., 2014).

1.8 The current state of *Azospirillum* spp.

Current work with *Azospirillum* spp. still remains broad in nature. There are many unanswered questions regarding its relationship with N-metabolism in the plant, as well as the impact that it has in field-based application programs and crop yield. It is well established that *A. brasilense* helps plant growth and yield, though it does not replace the effect of N fertilization (Schaefer et al., 2019). Similarly, metabolomic analyses of inoculated plants grown in field trials has revealed that *A. lipoferum* CRT1 affects plant sugar metabolism, but not N and P assimilation. Mineral N feeding increases yield, yet not yield enhancement by the bacterial partner (Rozier et al., 2017). Instead, bacterial inoculation restores seed-to-adult plant ratio, thereby securing mature plant density, which is hypothesized as being the primary driver of *A. lipoferum* CRT1-mediated yield enhancement in maize fields (Rozier et al., 2017). It was also recently found that *Azospirillum* spp. affects the N balance in plants by supplying them with ammonium (NH^{4+}). In this way, *Azospirillum* spp. counteracts the plant response to nitrate induction, without compromising plant N nutrition (Pii et al., 2019). Finally, in cadmium (Cd)-contaminated soils, *A. brasilense* was found to reduce Cd levels in plants via an IRT1-dependent ABA-mediated mechanism (Xu et al., 2018). Together, all of these findings suggest that the agricultural application of *Azospirillum* spp. requires fine-tuning of external fertilizer inputs (Pii et al., 2019).

Work is also ongoing to better understand interactions between *Azospirillum* spp., and other microorganisms and plants. In tests with rhizobacteria *Rhizobium pisi* and *A. brasilense,* co-inoculation synergistically and significantly increased wheat grain yield, leaf epicuticular wax and relative water content (Zaheer et al., 2019). In sorghum, mycorrhiza and *A. brasilense* increased plant biomass, nutrient uptake and up-regulated metabolic pathways (Dhawi et al., 2015). Likewise, the symbiotic co-culture of microalgae (*Scenedesmus* spp.) with *A. brasilense*

was effectively performed on N-deficient media, demonstrating the potential to enhance microalgae colony size and fatty acid content of biomass for biofuels (Contreras-Angulo et al., 2019). Then just last year, quinoa, vetch and brachiaria plants all favorably responded to *A. brasilense* inoculation in terms of seed germination or fresh weight accumulation (Brito et al., 2018).

Effective root surface colonization is a prerequisite for the beneficial effects of *Azospirillum* spp. on plant growth, but the fundamental behavior of the bacteria in regards to biofilm formation, rhizosphere navigation and how it moves throughout the plant is poorly understood. In this regard, recent work identified TyrR as the putative transcriptional regulator involved in biofilm production and regulating the utilization of D-alanine as carbon source for *A. brasilense* Sp7 (Jijón-Moreno et al., 2019). Similarly, a third (of 51) chemotaxis receptor (Aer) was recently characterized in wheat (O'Neal et al., 2019). Norms governing *A. brasilense* movement inside the plant have been updated too, as it has been determined that the bacteria is broadly disseminated throughout plant tissue - well beyond plant roots (Malinich and Bauer 2018). It is a common inhabitant of plant seeds and appears to selectively migrate vertically from roots to developing seeds (Malinich and Bauer 2018).

Existing studies addressing the efficacy of *Azospirillum* spp. in plant biofortification largely focus on improving plant yield and nutritive value (of grains, proteins, oils, etc.) by facilitating nutrient uptake and altering the metabolic profile of associated plants (i.e.; Dhawi et al., 2015). These studies have examined the singular and combined effects of inoculation with arbuscular mycorrhizal fungi (AMF), other phosphate-solubilizing bacteria, and/or chemical fertilizers (Patidar and Mali, 2006; Nosheen et al., 2011; Garg et al., 2018).

1.9 References

Agrawal GK, Rakwal R, Yonekura M, Kubo A, Saji H (2002) Proteome analysis of differentially displayed proteins as a tool for investigating ozone stress in rice (*Oryza sativa* L.) seedlings. *Proteomics* 2:947-959.

Alström S (1991) Induction of disease resistance in common bean susceptible to halo blight bacterial pathogen after seed bacterization with rhizosphere pseudomonads. *Journal of General Applied Microbiology* 37:495–501.

Atkinson N, Urwin P-E (2012) The interaction of plant biotic and abiotic stresses: From genes to the field. *Journal of Experimental Botany* 63:3523–3544.

Bachhawat AK, Ghosh S (1987) Iron transport in *Azospirillum brasilense*: role of the siderophore, *spirilobactin*. *Journal of General Microbiology* 133:1759-1765.

Baldani VLD, Alvarez MAB, Baldani JI, Dobereiner J (1986) Establishment of inoculated *Azospirillum* spp in the rhizosphere and in root of field-grown wheat and sorghum. *Plant Soil* 90:35–46.

Bartoli CG, Casalongué CA, Simontacchi M, Marquez-Garcia B, Foyer CH (2013) Interactions between hormone and redox signaling pathways in the control of growth and cross-tolerance to stress. *Environmental and Experimental Botany* 94:73–88.

Bashan Y (1999) Interactions of *Azospirillum* spp. in soils: a review. *Biology and Fertility of Soils* 29:246-256.

Bashan Y, de-Bashan LE (2010) Chapter 2: How the plant growth-promoting bacterium *Azospirillum* promotes plant growth- a critical assessment. In: Sparks DL (ed) *Advances in Agronomy*, Volume 108. Academic Press, pp 77-136.

Bashan Y, Hernandez J-P, Leyva LA, Bacilio M (2002) Alginate microbeads as inoculant carrier for plant growth-promoting bacteria. *Biology and Fertility of Soils* 35:359-368.

Bashan Y, Holguin G, de-Bashan LE (2004) *Azospirillum*–plant relationships: Physiological, molecular, agricultural, and environmental advances (1997–2003). *Canadian Journal of Microbiology* 50:521–577.

Beijerinck M (1925) Uber ein *Spirillum*, welches freien Stickstoff binden kann? *Zentrablatt fur Bakteriologie, Parasitenkunde, Infektionskrankheiten und Hygiene Abt* 2 (63):353-359.

Berendsen RL, Pieterse CMJ, Bakker PAHM (2012) The rhizosphere microbiome and plant health. *Trends in Plant Science* 17:478–86.

Berens ML, Berry HM, Mine A, Arguesco CT, Tsuda K (2017) Evolution of hormone signaling networks in plant defense. *Annual Review of Phytopathology* 55:401–425.

Berger S, Sinha AK, Roitsch T (2007) Plant physiology meets phytopathology: plant primary metabolism and plant-pathogen interactions. *Journal of Experimental Botany* 58 (15/16):4019-4026.

Bloemberg GV, Lugtenberg BJ (2001) Molecular basis of plant growth promotion and biocontrol by rhizobacteria. *Current Opinion in Plant Biology* 4:343.

Bohnert HJ, Ayoubi P, Borchert C, Bressan RA, Burnap RL, Cushman JC, Cushman MA, Deyholos M, Fisher R, Galbraith DW, Hasegawa PM, Jenks M, Kawasaki S, Koiwa H, Kore-eda S, Lee B-H, Michalowski CB, Misawa E, Nomura M, Ozturk N, Postier B, Prade R, Song C-P, Tanaka Y, Wang H, Zhu JK (2001) A genomic approach towards salt stress tolerance. *Plant Physiology and Biochemistry* 39:295–311.

Boller T, Felix G (2009) A renaissance of elicitors: perception of microbe associated molecular patterns and danger signals by pattern-recognition receptors. *Annual Review of Plant Biology* 60:379–406.

Boutrot F, Zipfel C (2017) Function, discovery, and exploitation of plant pattern recognition receptors for broad-spectrum disease resistance. *Annual Review of Phytopathology* 55:257–286.

Brito TS, Schons DC, Ritter G, Netto LA, Eberling T, Pan R, Guimarã s VF (2018) Growth Promotion by *Azospirillum brasilense* in the Germination of Rice, Oat, Brachiaria and Quinoa. *Journal of Experimental Agriculture International* 22(1):1-9.

Brizard JP, Carapito C, Delalande F, Van Dorsselaer A, Brugidou C (2006) Proteome analysis of plant-virus interactome: comprehensive data for virus multiplication inside their hosts. *Molecular and Cellular Proteomics* 5:2279–2297.

Cakmak I (2008) Enrichment of cereal grains with zinc: agronomic or genetic biofortification. *Plant Soil* 302:1–17.

Cakmak I, Kalaycı M, Ekiz H, Braun HJ, Kılınç Y, Yılmaz A (1999) Zinc deficiency as a practical problem in plant and human nutrition in Turkey: a NATO- science for stability project. *Field Crops Research* 60:175–88.

Campo S, Carrascar M, Coca M, Abian J, San Segundo B (2004) The defense response of germinating maize embryos against fungal infection: proteomics approach. *Proteomics* 4:383–396.

Campos-Bermudez VA, Fauguel CM, Tronconi MA, Casati P, Presello DA, Andreo CS (2013) Transcriptional and metabolic changes associated to the infection by *Fusarium verticillioides* in maize inbreds with contrasting ear rot resistance. *PLOS ONE* 8:e61580.

Champigny M, Shearer H, Mohammad A, Haines K, Neumann M, Thilmony R, He SY, Fobert P, Denglar N, Cameron RK (2011) Localization of DIR1 at the tissue, cellular and subcellular levels during systemic acquired resistance in *Arabidopsis* using DIR1:GUS and DIR1:EGFP reporters. *BMC Plant Biology* 11:125

Cocking EC (2003) Endophytic colonization of plant roots by nitrogen-fixing bacteria. *Plant Soil* 252:169–175.

Colmenares AJ, Aleu J, Duran-Patron R, Collado IG, Hernandez-Galan R (2002) The putative role of botrydial and related metabolites in the infection mechanism of *Botrytis cinerea*. *Journal of Chemical Ecology* 28:997–1005.

Conrath U, Beckers GJM, Flors V, García-Agustín P, Jakab G, Mauch F, Newman MA, Pieterse CM, Poinssot B, Pozo MJ, Pugin A, Schaffrath U, Ton J, Wendehenne D, Zimmerli L, Mauch-Mani B (2006) Priming: getting ready for battle. *Molecular Plant-Microbe Interactions* 19:1062–1071.

Contreras-Angulo JR, Mata TM, Cuellar-Bermudez SP, Caetano NS, Chandra R, Garcia-Perez JS, Muylaert K, Parra-Saldivar R (2019) Symbiotic Co-Culture of *Scenedesmus* sp. and *Azospirillum brasilense* on N-Deficient Media with Biomass Production for Biofuels. *Sustainability* 11(3):707.

Correa OS, Romero AM, Montecchia MS, Soria MA (2007) Tomato genotype and *Azospirillum* inoculation modulate the changes in bacterial communities associated with roots and leaves. *Journal of Applied Microbiology* 102:781–786.

Deaker R, Kecskés ML, Rose MT, Amprayn K, Ganisan K, Tran TK C, Vu TN, Phan TC, Nguyen T Hein, Kennedy IR (2011) *Practical methods for the quality control of inoculant biofertilisers*. ACIAR monograph series no. 147. Canberra, Australia, pp 101.

de-Bashan L, Bashan Y (2016) Genetic manipulation and molecular detection and monitoring of plant growth-promoting bacteria (basic studies).
http://www.bashanfoundation.org/gmaweb/proyectos2/ilin8.html. Accessed 15 January, 2019.

Dhawi F, Datta R, Ramakrishna W (2015) Mycorrhiza and PGPB modulate maize biomass, nutrient uptake and metabolic pathways in maize grown in mining-impacted soil. *Plant Physiology and Biochemistry* 97:390–9.

Díaz-Zorita M, Fernández-Canigia MV (2009) Field performance of a liquid formulation of *Azospirillum brasilense* on dryland wheat productivity. *European Journal of Soil Biology* 45:3-11.

Dong X (2004) NPR1, all things considered. *Current Opinion in Plant Biology* 7:547–552.

dos Reis SP, Lima AM, Batista de Souza R (2012) Recent molecular advances in downstream plan responses to abiotic stress. *International Journal of Molecular Sciences* 13:8628-8647.

Drogue B, Sanguin H, Chamam A, Mozar M, Llauro C, Panaud O, Prigent-Combaret C, Picault N, Wisniewski-Dyé. Plant root transcriptome profiling reveals a strain-dependent response during *Azospirillum*-rice cooperation. *Frontiers in Plant Science* 5(607):1-14.

Fan B, Carvalhais L, Becker A, Fedoseyenko D, Von Wiren N, Borriss R (2012) Transcriptomic profiling of *Bacillus amyloliquefaciens* FZB42 in response to maize root exudates. *BMC Microbiology* 12:116.

Freeman BC, Beattie GA (2008) An Overview of Plant Defenses against Pathogens and Herbivores. *The Plant Health Instructor*. Iowa State University. Digital Repository. DOI: 10.1094/PHH-2008-0226-01.

Fujita M, Fujita Y, Noutoshi Y, Takahashi F, Narusaka Y, Yamaguchi-Shinozaki K, Shinozaki K (2006) Crosstalk between abiotic and biotic stress responses: A current view from the points of convergence in the stress signaling networks. *Current Opinion in Plant Biology* 9:436–442.

Fukami J, Cerezini P, Hungria M (2018) *Azospirillum*: benefits that go far beyond biological nitrogen fixation. *AMB Express* 8 (73):1-12.

Garg M, Sharma N, Sharma S, Kapoor P, Kumar A, Chunduri V, Arora P (2018) Biofortified crops generated by breeding, agronomy and transgenic approaches are improving lives of millions of people around the world. *Frontiers in Nutrition* 5:12.

Glazebrook J (2005) Contrasting mechanisms of defense against biotrophic and necrotrophic pathogens. *Annual Review of Phytopathology* 43:205-27.

Gómez-Galera SG (2001) *Towards the mineral biofortification of rice for food security*. PhD Dissertation, University of Lleida. 346pp.

Gómez-Galera SG, Twyman RM, Sparrow PA, Van Droogenbroeck B, Custers R, Capell T, Christou P (2012) Field trials and tribulations—making sense of the regulations for experimental field trials of transgenic crops in Europe. *Plant Biotechnology Journal* 10(5):511-23.

Gould J (2017) Nutrition: a world of insecurity. *Nature Outlook* 544:S7.

Graham RD, Welch RM, Bouis HE (2001) Addressing micronutrient malnutrition through enhancing the nutritional quality of staple foods: Principles, perspectives and knowledge gaps. *Advances in Agronomy* 70:77–142.

Hamel LP, Nicole MC, Sritubtim S, Morency MJ, Ellis M, Ehlting J, Beaudoin N, Barbazuk B, Klessig D, Lee J, Martin G, Mundy J, Ohashi Y, Scheel D, Sheen J, Xing T, Zhang S, Seguin A, Ellis BE (2006) Ancient signals: comparative genomics of plant MAPK and MAPKK gene families. *Trends in Plant Science* 11:192–198.

Hartmann A and Bashan Y (2009) Ecology and application of *Azospirillum* and other plant growth-promoting bacteria (PGPB)-special issue. *European Journal of Soil Biology* 45:1-2.

Hefferon KL (2016) Can biofortified crops help attain food security? *Current Molecular Biology Reports* 2(4):180–5.

Hodge J (2016) Hidden hunger: approaches to tackling micronutrient deficiencies. In: Gillespie S, Hodge J, Yosef S, Pandya-Lorch R (eds.) *Nourishing Millions: Stories of Change in Nutrition*. Washington: International Food Policy Research Institute (IFPRI), pp 35–43.

Jalmi SK, Sinha AK (2015) ROS mediated MAPK signaling in abiotic and biotic stress-striking similarities and differences. *Frontiers in Plant Science* 6:769.

Jetiyanon K, Kloepper JW (2002) Mixtures of plant growth-promoting rhizobacteria for induction of systemic resistance against multiple plant diseases. *Biological Control* 24: 285.

Jijón-Moreno S, Baca BE, Castro-Fernández DC, Ramírez-Mata A (2019) TyrR is involved in the transcriptional regulation of biofilm formation and D-alanine catabolism in *Azospirillum brasilense* Sp7. *PLOS ONE*. 14;14(2):e0211904.

Jones JDG, Dangl JL (2006) The plant immune system. *Nature* 444:323–329.

Kamnev AA, Tugarova AV, Tarantilis PA, Gardiner PHE, Polissiou MG (2012) Comparing poly-3-hydroxybutyrate accumulation in *Azospirillum brasilense* strains Sp7 and Sp245: the effects of copper(II). *Applied Soil Ecology* 61:213–216.

Khammas K, Ageron E, Grimont P, Kaiser P (1989) *Azospirillum irakense* sp. nov., a nitrogen-fixing bacterium associated with rice roots and rhizosphere soil. *Research in Microbiology* 140:679-693.

Khan A, Singh J, Upadhayay VK, Singh AV, Shah S (2019) Chapter 13: Microbial biofortification: a green technology through plant growth-promoting microorganisms. In: Shah S et al. (eds.) *Sustainable Green Technologies for Environmental Management*. Springer Nature, Singapore, pp.261.

Kloepper JW, Schroth MN (1978) Plant growth-promoting rhizobacteria on radishes. In: Clarey G (ed) *Proceedings of the 4th international conference on plant pathogenic bacteria*. pp 879–882.

Knoester M, Pieterse CMJ, Bol JF, Van Loon LC (1999) Systemic resistance in *Arabidopsis* induced by rhizobacteria requires ethylene-dependent signaling at the site of application. *Molecular Plant-Microbe Interactions* 12:720–27.

Komatsu S, Muhamad A, Rakwal R (1999) Separation and characterization of proteins from green and etiolated shorts of rice (*Oryza sativa* L.) towards a rice proteome. *Electrophoresis* 20:630-636.

Kuc J (1982) Induced immunity to plant disease. *Bioscience* 32:854–60.

Kumar AS, Prakash A, Johri BN (2011) *Bacillus* as PGPR in crop ecosystem. In: Maheshwari DK (ed.) *Bacteria in agrobiology: crop ecosystems*, 1st edn. Springer, New York, NY, pp 37–59.

Kumar AS, Lakshmanan V, Caplan JL, Powell D, Czymmek KJ, Levia DF, Bais HP (2012) Rhizobacteria *Bacillus subtilis* restricts foliar pathogen entry through stomata. *The Plant Journal* 72:694–706.

Lanubile A, Maschietto V, Borrelli VM, Stagnati L, Logrieco AF, Marocco A (2017) Molecular basis of resistance to fusarium ear rot in maize. *Frontiers in Plant Science* 8:1774.s

Lanubile A, Maschietto V, Marocco A (2014) Breeding maize for resistance to mycotoxins. In: Leslie JF, Logrieco AF (eds) *Mycotoxin Reduction in Grain Chains*. JohnWiley & Sons, Ltd, Chichester.

Leibniz Institute DSMZ-German Collection of Microorganisms and Cell Cultures, Germany, Prokaryotic Nomenclature Up-to-Date. https://www.dsmz.de/bacterial-diversity/prokaryotic-nomenclature-up-to-date/prokaryoticnomenclature-up-to-date.html. Accessed 25 Apr 2018.

Lugtenberg B, Kamilova F (2009) Plant-growth-promoting rhizobacteria. *Annual Review of Microbiology* 63:541–56.

MacKinnon SL, Keifer P, Ayer WA (1999) Components from the phytotoxic extract of *Alternaria brassicicola*, a black spot pathogen of canola. *Phytochemistry* 51:215–21.

Madriz-Ordeñana K (2002) Mecanismos de defensa en las interacciones planta-patógeno. *Manejo Integrado de Plagas (Costa Rica)* 63:22-32.

Malinich EA, Bauer CE (2018) Transcriptome analysis of *Azospirillum brasilense* vegetative and cyst states reveals large-scale alterations in metabolic and replicative gene expression. *Microbial Genomics* 4. Doi:10.1099/mgen.0.000200.

Malinich EA, Bauer CE (2018) The plant growth promoting bacterium *Azospirillum brasilense* is vertically transmitted in *Phaseolus vulgaris* (common bean). *Symbiosis* 76(2):97-108.

McDowell JM, Dangl JL (2000) Signal transduction in the plant immune response. *Trends in Biochemical Science* 25:79–82.

McGuire S. FAO, IFAD, WFP (2015) The state of food insecurity in the world 2015: meeting the 2015 international hunger targets: taking stock of uneven progress. Rome: FAO. *Advances in Nutrition* 6(5):623–4.

Memelink J (2009) Regulation of gene expression by jasmonate hormones. *Phytochemistry* 70:1560–70.

Millet YA, Danna CH, Clay NK, Songnuan W, Simon MD, Werck-Reichhart D, Ausubel FM (2010) Innate immune responses activated in *Arabidopsis* roots by microbe-associated molecular patterns. *Plant Cell* 22:973–90.

Mishina TE, Zeier J (2007) Pathogen-associated molecular pattern recognition rather than development of tissue necrosis contributes to bacterial induction of systemic acquired resistance in *Arabidopsis*. *The Plant Journal* 50:500–13.

Mittler R, Blumwald E (2010) Genetic engineering for modern agriculture: Challenges and perspectives. *Annual Review of Plant Biology* 61:443–462.

Mohammadi M, Anoop V, Gleddie S, Harris, LJ (2011) Proteomic profiling of two maize inbreds during early Gibberella ear rot infection. *Proteomics* 11:3675–3684.

Muktar MS, McCormack ME, Argueso CT, Pajerowska-Muktar KM (2016) Pathogen tactics to manipulate plant cell death. *Current Biology* 26:R608-R619.

Muthayya A, Rah JH, Sugimoto JD, Roos FF, Kraemer K, Black RE (2013) The global hidden hunger indices and maps: an advocacy tool for action. *PLOS ONE* 8(6):e67860.

Ndimba BK, Chivasa S, Hamilton JM, Simon WJ, Slabas AR (2003) Proteomic analysis of changes in the extracellular matrix of Arabidopsis cell suspension cultures induced by fungal elicitors. *Proteomics* 3:1047–1059.

Neal AL, Ahmad S, Gordon-Weeks R, Ton J (2012) Benzoxazinoids in root exudates of maize attract *Pseudomonas putida* to the rhizosphere. *PLOS ONE* 7:e35498.

Nosheen A, Bano A, Ullah F (2011) Nutritive value of canola (*Brassica napus* L.) as affected by plant growth promoting rhizobacteria. *European Journal of Lipid Science and Technology* 113(11):1342–6.

O'Neal L, Akhter S, Alexandre G (2019) A PilZ-Containing Chemotaxis Receptor Mediates Oxygen and Wheat Root Sensing in *Azospirillum brasilense*. *Frontiers in Microbiology* 10:312.

Otani H, Kohnobe A, Kodama M, Kohmoto K (1998) Production of a host-specific toxin by germinating spores of *Alternaria brassicicola*. *Physiological and Molecular Plant Pathology* 52:285–95.

Panter S, Thomson R, de Bruxelles G, Laver D, Trevaskis B, Udvardi M (2000) Identification with proteomics of novel proteins associated with the peribacteroid membrane of soybean root nodules. *Molecular Plant Microbe Interactions* 13, 325–333.

Patidar M, Mali AL (2004) Effect of farmyard manure, fertility levels and biofertilizers on growth, yield and quality of *Sorghum* (*Sorghum bicolor*). *Indian Journal of Agronomy* 2(49):117–20.

Pel MJ, Pieterse CM (2013) Microbial recognition and evasion of host immunity. *Journal of Experimental Botany* 64:1237–1248.

Pereg L (2015) Chapter 10 - *Azospirillum* cell aggregation, attachment, and plant interaction. In: Cassán FD, Okon Y, Creus CM (eds) *Handbook for Azospirillum*. Springer International Publishing, Switzerland, pp 186–187.

Persello-Cartieaux F, Nussaume L, Robaglia C (2003) Tales from the underground: Molecular plant-rhizobacteria interactions. *Plant Cell & Environment* 26:189.

Pieterse CMJ, Van Wees SCM, Van Pelt JA, Knoester M, Laan R, Gerrits H, Weisbeek PJ, van Loon LC (1998) A novel signaling pathway controlling induced systemic resistance in *Arabidopsis*. *Plant Cell* 10:1571–80.

Pieterse CMJ, Zamioudis C, Berendsen RL, Weller DM, Van Wees SCM, Bakker PAHM (2014) Induced systemic resistance by beneficial microbes. *Annual Review of Phytopathology* 52:347-375.

Pii Y, Aldrighetti A, Valentinuzzi F, Mimmo T, Cesco S (2019) *Azospirillum brasilense* inoculation counteracts the induction of nitrate uptake in maize plants. *Journal of Experimental Botany* 70(4):1313–1324.

Prasad R, Kumar M, Varma A (2015) Chapter 12: Role of PGPR in soil fertility and plant health. In: Egamberdieva D. et al. (eds.), *Plant-growth-promoting rhizobacteria (PGPR) and Medicinal plants, Soil Biology 42*. Springer International Publishing, Switzerland, p 247.

Qaim M, Stein AJ, Meenakshi JV (2007) Economics of biofortification. *Agricultural Economics* 37(s1):119-133.

Rakwal R, Komatsu S (2000) Role of jasmonate in the rice (*Oryza sativa* L.) self-defense mechanism using proteome analysis. *Electrophoresis* 21(12):2492-500.

Reis VM, Baldani VLD, Baldani JI (2015) Chapter 1: Isolation, identification and biochemical characterization of *Azospirillum* spp. and other nitrogen-fixing bacteria. In: Cassán FD, Okon Y, Creus CM (eds) *Handbook for Azospirillum.* Springer International Publishing, Switzerland, pp. 3.

Rejeb IB, Pastor V, Mauch-Mani B (2014) Plant responses to simultaneous biotic and abiotic stress: molecular mechanisms. *Plants* 3:458-475.

Rengel Z, Batten GD, Crowley DE (1999) Agronomic approaches for improving the micronutrient density in edible portions of field crops. *Field Crops Research* 60:27–40.

Ridley BL, O'Neill MA, Mohnen D (2001) Pectins: structure, biosynthesis, and oligogalacturonide-related signaling. *Phytochemistry* 57:929–967.

Rodriguez MC, Petersen M, Mundy J (2010) Mitogen-activated protein kinase signaling in plants. *Annual Review of Plant Biology* 61:621–649.

Ross AF (1961) Systemic acquired resistance induced by localized virus infections in plants. *Virology* 14:340–58.

Rozier C, Hamzaoui J, Lemoine D, Czarnes S, Legendre L (2017) Field-based assessment of the mechanism of maize yield enhancement by *Azospirillum lipoferum* CRT1. *Scientific Reports* 7:7416.

Rudrappa T, Czymmek KJ, Paré PW, Bais HP (2008) Root-secreted malic acid recruits beneficial soil bacteria. *Plant Physiology* 148:1547–56.

Saltzman A, Birol E, Bouis HE, Boy E, De Moura FF, Islam Y, Pfeiffer WH (2014) Biofortification: progress toward a more nourishing future. *Global Food Security* 2(1):9–17.

Sanabria N, Goring D, Nurnberger T, Dubery I (2008) Self/nonself perception and recognition mechanisms in plants: a comparison of self in compatibility and innate immunity. *New Phytologist* 178:503–513.

Sato M, Tsuda K, Wang L, Coller J, Watanabe Y, Glazebrook J, Katagiri F (2010) Network modeling reveals prevalent negative regulatory relationships between signaling sectors in *Arabidopsis* immune signaling. *PLOS Pathogens* 6:e1001011.

Schaefer PE, Martin TN, Pizzani R, Schaefer EL (2019) Inoculation with *Azospirillum brasilense* on corn yield and yield components in an integrated crop-livestock system. *Acta Scientiarum. Agronomy* 41: e39481.

Seki M, Narusaka M, Abe H, Kasuga M, Yamaguchi-Shinozaki K, Carninci P, Hayashizaki Y, Shinozaki K (2001) Monitoring the expression pattern of 1300 *Arabidopsis* genes under drought and cold stresses by using a full-length cDNA microarray. *Plant Cell* 13:61–72.

Sinha AK, Jaggi M, Raghuram B, Tuteja N (2011) Mitogen-activated protein kinase signaling in plants under abiotic stress. *Plant Signaling & Behavior* 6:196–203.

Solano BR, Maicas JB, Gutierrez Manero FJ (2008) Physiological and molecular mechanisms of plant growth promoting rhizobacteria (PGPR). In: Ahmad I, Pichtel J, Hayat S (eds) *Plant bacteria interactions, strategies and techniques to promote plant growth.* Wiley, Weinheim.

Somers E, Vanderleyden J, Srinivasan M (2004) Rhizosphere bacterial signalling: a love parade beneath our feet. *Critical Reviews in Microbiology* 30:205–240.

Steenhoudt O, Vanderleyden J (2000) *Azospirillum*, a free-living nitrogen-fixing bacterium closely associated with grasses: genetic, biochemical and ecological aspects. *FEMS Microbiology Reviews* 24:487-506.

Tafforeau M, Verdus MC, Charlionet R, Cabin-Flaman A, Ripoll C (2002) Two-dimensional electrophoresis investigation of short-term response of flax seedlings to a cold shock. *Electrophoresis* 23:2534–2540.

Tarrand J, Krieg N, Döbereiner J (1978) A taxonomic study of the *Spirillum lipoferum* group, with descriptions of new genus, *Azospirillum* gen. nov., and two species, *Azospirillum lipoferum* (Beijerinck) comb. nov. and *Azospirillum brasilense* sp. nov. *Canadian Journal of Microbiology* 24:967–980.

Thomma BPHJ, Penninckx IA, Broekaert WF, Cammue BP (2001) The complexity of disease signaling in *Arabidopsis*. *Current Opinion in Immunology* 13:63–68.

Ton J, Jakab G, Toquin V, Flors V, Iavicoli A, Maeder MN, Métraux JP, Mauch-Mani B (2005) Dissecting the β-aminobutyric acid–induced priming phenomenon in *Arabidopsis*. *Plant Cell* 17:987–99.

Tortora ML, Díaz-Ricci JC, Pedraza RO (2011) *Azospirillum brasilense* siderophores with antifungal activity against *Colletotrichum acutatum*. *Archives of Microbiology* 193 (4):275-286.

Van der Ent S, Van Hulten MHA, Pozo MJ, Czechowski T, Udvardi MK, Pieterse CMJ, Ton J (2009) Priming of plant innate immunity by rhizobacteria and β-aminobutyric acid: differences and similarities in regulation. *New Phytologist* 183:419–31.

Van der Ent S, Verhagen BWM,Van Doorn R, Bakker D,Verlaan MG, Pel MJ, Joosten RG, Proveniers MC, Van Loon LC, Ton J, Pieterse CMJ (2008) MYB72 is required in early signaling steps of rhizobacteria-induced systemic resistance in *Arabidopsis*. *Plant Physiology* 146:1293–304.

Van Loon LC (2007) Plant response to plant growth-promoting rhizobacteria. *European Journal of Plant Pathology* 119:243–254.

Van Loon LC, Rep M, Pieterse CMJ (2006) Significance of inducible defense-related proteins in infected plants. *Annual Review of Phytopathology* 44:135–62.

Van Peer R, Niemann GJ, Schippers B (1991) Induced resistance and phytoalexin accumulation in biological control of Fusarium wilt of carnation by *Pseudomonas* sp. strain WCS417r. *Phytopathology* 81:728–34.

Van Wees SCM, De Swart EAM, Van Pelt JA, Van Loon LC, Pieterse CMJ (2000) Enhancement of induced disease resistance by simultaneous activation of salicylate- and jasmonate-dependent defense pathways in *Arabidopsis thaliana*. *Proceedings of the National Academy of Sciences of the USA* 97:8711–8716.

Verhagen BWM, Glazebrook J, Zhu T, Chang H-S, Van Loon LC, Pieterse CMJ (2004) The transcriptome of rhizobacteria-induced systemic resistance in *Arabidopsis*. *Molecular Plant-Microbe Interactions* 17:895–908.

Verma S, Nizam S, Verma PK (2013) Chapter 2: Biotic and abiotic stress signaling in plants. In: Sarwat M, Ahmed A, Abdin MZ (eds) *Stress Signaling in Plants: Genomics and Proteomics Perspective*, Vol 1. Springer Science, New York, USA.

Wang YQ, Ohara Y, Nakayashiki H, Tosa Y, Mayama S (2005) Microarray analysis of the gene expression profile induced by the endophytic plant growth–promoting rhizobacteria, *Pseudomonas fluorescens* FPT9601-T5 in *Arabidopsis*. *Molecular Plant-Microbe Interactions* 18:385–96.

Wang Y, Zhou Z, Gao J, Wu Y, Xia Z, Zhang H, Wu J (2016) The mechanisms of maize resistance to *Fusarium verticillioides* by comprehensive analysis of RNA-seq data. *Frontiers in Plant Science* 7:1654.

Xu Q, Pan W, Zhang R, Lu Q, Xue W, Wu C, Song B, Du S (2018) Inoculation with *Bacillus subtilis* and *Azospirillum brasilense* Produces Abscisic Acid That Reduces Irt1-Mediated Cadmium Uptake of Roots. *Journal of Agricultural and Food Chemistry* 66(20):5229–5236.

Yasuda M, Ishikawa A, Jikumaru Y, Seki M, Umezawa T, Asami T, Maruyama- Nakashita A, Kudo T, Shinozaki K, Yoshida S, Nakashita H (2008) Antagonistic interaction between systemic acquired resistance and the abscisic acid-mediated abiotic stress response in *Arabidopsis*. *Plant Cell* 20:1678–1692.

Zaheer MS, Raza MAS, Saleem MF, Khan IH, Ahmad S, Iqbal R, Manevski K (2019) Investigating the effect of *Azospirillum brasilense* and *Rhizobium pisi* on agronomic traits of wheat (*Triticum aestivum* L.). *Archives of Agronomy and Soil Science*: 1–11.

Zhang X, Valdés-López O, Arellano C, Stacey G, Balint-Kurti P (2017) Genetic dissection of the maize (*Zea mays* L.) MAMP response. *Theoretical and Applied Genetics* 130:1155–1168.

Zhu C, Naqvi S, Gomez-Galera S, Pelacho AM, Capell T, Christou P (2007) Transgenic strategies for the nutritional enhancement of plants. *Trends in Plant Science* 12:548–55.

Zhu JK (2002) Salt and drought stress signal transduction in plants. *Annual Review of Plant Biology* 53:247–273.

Zhu T, Budworth P, Han B, Brown D, Chang HS, Zou G. Wang X (2001) Toward elucidating the global expression patterns of developing *Arabidopsis*: Parallel analysis of 8300 genes by a high-density oligonucleotide probe array. *Plant Physiology and Biochemistry* 39:221–242.

CHAPTER 2

Aims & Objectives

Chapter 2. Aims & Objectives

Aims

The overarching aim of my dissertation was to test how *Azospirillum brasilense* Sp7 affects generic mechanisms of defense regulation in plant-stress interactions of economically important crops. A further aim was to gauge if plant defense is positively modulated by the simultaneous use of transgenic and agronomic biofortification. Within this scope, the main objectives were the following:

Objectives

1. Determine how *Azospirillum brasilense* Sp7 inoculation modulates the defense response among cultivars of the same species, between bioengineered and wild-type plants of the same species, and between species

2. Relate ways in which *Azospirillum brasilense* Sp7 affects the defense response by analyzing plant hormone signaling and transcription factors

3. Ascertain how transgenically biofortified plants interact with *Azospirillum brasilense* Sp7 by assessing the fitness of plants subjected to biotic or abiotic stress

4. Identify mechanisms that may be essential for coordinating the defense response induced by *Azospirillum brasilense* Sp7

CHAPTER 3

Preliminary study

PBS and $MgSO_4$ buffers differentially affect the response of maize (*Zea Mays L. Mill* cv. B73) seedlings to *Azospirillum brasilense* Sp7

(Re-submitted to Cereal Research Communications, 2019. Annex 1)

Chapter 3. PBS and $MgSO_4$ buffers differentially affect the response of maize (*Zea Mays* L. Mill cv. B73) seedlings to *Azospirillum brasilense* Sp7

3.0 Abstract

The effect of *Azospirillum brasilense* Sp7 (Sp7) on maize (*Zea mays*, Mill cv. B73) seedlings was examined using phosphate buffered saline (PBS) or magnesium sulfate ($MgSO_4$) as the inoculation buffer. Maize seeds were inoculated, then seedling height, leaf chlorophyll levels, and root parameters were analyzed with WinRHIZO® at an early vegetative stage of plant development. Scanning and transmission electron microscope (SEM & TEM) analysis was conducted to evaluate bacterial binding to plant roots. $MgSO_4$+Sp7 caused a significant increase in the abundance of thick lateral roots, but rendered plants stunted compared to other treatment groups. Relative chlorophyll contents significantly increased in seedlings inoculated with PBS+Sp7. SEM & TEM elucidated that buffer choice does not interfere with bacterial binding to roots. Both inoculation buffers yield distinct benefits for plant growth, but also evidently promote stress that is mitigated by Sp7. These results form the basis of a narrative considering that Sp7 differentially affects an associated plant depending upon buffer choice.

3.1 Introduction

Fertilizer is one of the most important components for increasing crop growth rates. Nonetheless, chemical fertilizers pose the risk of eutrophication due to excessive nutrient enrichment of water systems from farm runoff (Carpenter et al., 1998). Plant-growth promoting rhizobacteria (PGPRs) have been found to offer the same benefits to crops as chemical fertilizers, which is why they have been examined extensively as a viable replacement option (Barassi et al., 2007).

Azospirillum brasilense Tarrand et al., 1979 is a well-studied PGPR that helps the host plant fix nitrogen (Bashan and Holguin 1996), increases plant growth by inciting root hair proliferation, facilitates water and nutrient uptake (Barassi et al., 2007), influences phytohormone production (Perrig et al., 2007), and reduces biotic and abiotic stresses (Bashan and Holguin 1997; Lugtenberg and Kamilova 2009). In this regard, *A. brasilense* provokes the defense mechanism *induced systemic resistance* (ISR) in plants upon association (Alström 1991). ISR relies on jasmonic acid (JA) and ethylene (ET) phytohormone signal transduction pathways to 'prime', or sensitize distal plant parts for enhanced pathogen defense (Van Peer et al., 1991). At the onset, priming is rather elusive because it does not involve direct activation of resistance, so is nearly invisible at the protein or transcriptome level. As a result, ISR is normally studied in combination with stress factors, which is when changes in JA and ET up-regulation are made perceivable (Verhagen et al., 200; Wang et al., 2005). A primed plant exhibits several other physiological changes that help delay disease progression, such as enhanced callose deposition (Ton et al., 2005) and more rapid stomatal closure (Kumar et al., 2012).

The conditions in which *A. brasilense* grows can also greatly influence some of its plant growth-promoting properties (Bashan and Bashan 2011). A number of studies have been carried out to weigh the impact of various culture media on the growth of *Azospirillum* spp., both in small-scale operations and commercially. Typically, a nitrogen free broth (Nfb) is the standard growth media. It has ammonium chloride (NH_4Cl) serving as the nitrogen (N) source and organic acids, such as malate, succinate, gluconate or glycerol as carbon (C) sources (Bashan and Bashan 2011). Carbon sources have been optimized since supplying them is fundamental for promoting efficient C metabolism in *Azospirillum* spp. (Hartmann and Zimmer 1994). Considering this, the most effective culture media identified and utilized to date are OAB (Okon, Albrecht and Burris 1977), and tryptone yeast extract & glucose (TYG) (Bashan et al., 2011).

Once cultured, the next step in manual delivery of the PGPR to the plant or seed is the inoculation buffer. There is no universal carrier for PGPRs, and choosing the proper formula has been identified as a strain-specific process (Rivera et al., 2014). Even still, there is little literature that makes distinction between the buffers, or classifies them by strain. A number of

solid, liquid, oil and gel-based formulas have been developed; liquid inoculants being the most economical for small-scale use (Mugilan et al., 2011). In the case of *Azospirillum* spp., liquid inoculant buffer options include PBS (Cohen et al., 2009), magnesium sulfate ($MgSO_4$) (Mangmang et al., 2015), 0.9% sodium chloride (NaCl) (Bashan and Levanony 1985), 66mM phosphate buffer (Creus et al., 1997) and Lauria-Bertani (LB)-broth (Khalid et al. 2017). Most studies with *A. brasilense* Sp7 (Sp7) in particular use PBS, though $MgSO_4$ has appeared in more contemporary works.

Azospirillum brasilense has been repeatedly studied for mitigating salinity stress in the rhizosphere because it accumulates amino acids such as proline and glutamate (Bashan and Holguin 1997), which act as osmoprotectants (Casanovas et al., 2002, 2003). Glutamate is central to N-metabolism in plants, and most assimilated N passes through this step before it is re-distributed to major N metabolites (Forde et al., 2007). Furthermore, the exopolysaccharides produced by A. *brasilense* restrict sodium (Na^{+1}) influx into roots (Ashraf et al., 2004). In this way, studies addressing the efficacy of *A. brasilense* in the control of salinity conveniently use phosphate or LB buffers, probably because both magnesium (Mg^{+2}) and Na^{+1} ions can disrupt the binding of rhizobacteria to roots (Gafny et al., 1985). It is not, however, known to what extent the Na^{+1} concentration in PBS disrupts bacterial binding compared to that of Mg^{+2} in $MgSO_4$. Study has shown that increasing $MgSO_4$ supply increased the concentration of total Mg and decreased the concentration of Ca in both roots and shoots irrespective of anion form supplied with Mg, such as sulfur (S). There is no significant difference in S concentration in the roots in *Arabidopsis* grown in the medium containing SO_4^{2-} concentration ranging from 250 to 10250μM. This is maybe an alternative explanation on why S has relatively little influence on the morphology of the root (Niu et al., 2014).

Based on previous research, we hypothesize that inoculation buffer components in PBS and $MgSO_4$ distinctly alter the way in which Sp7 interacts with seedlings, affecting plant growth overall.

3.2 Aims

- Investigate the effects of two common buffers on the phenotype of Sp7-inoculated maize seedlings
- Establish basic procedures related to Sp7 inoculation: create an imbibition curve, prepare inoculum, analyze roots bioinformatically (WinRHIZO®) and microscopically
- Determine if and how Sp7 binding and activity is modulated by two common buffers

3.3 Material and Methods

3.3.1 Experimental design and general information

The experiment consisted of 4 seed treatments 1) PBS, 2) PBS+Sp7, 3) $MgSO_4$, 4) $MgSO_4$+Sp7) with ten biological replicas each, and arranged in a completely randomized design. Maize seeds were sown in 0.3L pots filled with autoclaved commercial substrate (Traysubstrat®, Klasmann-Deilmann, Gmbh, Geeste, Germany) characterized by having an extra fine structure and pH of 6, which was sufficient for this study since ranges for N-fixation by *Azospirillum* spp. are between 5.5 and 9 (Day and Döbereiner 1976). Both inoculated and non-inoculated (control) maize seeds were maintained in a greenhouse on the ETSEA Campus at the University of Lleida, in Catalonia, Spain. They were maintained at 70-80% humidity, 25-30ºC, and protected from insect attack by an anti-aphid mesh. Automatic drip irrigation was administered in the morning and evening every day for an hour.

3.3.2 Imbibition curve preparation

A water imbibition curve was defined for maize. Initially, groups of ten maize (*Zea mays* L. Mill cv. B73) seeds (with five replicates) were disinfected with 70% ethanol (EtOH) for 2min. Seeds were then disinfected with 4% sodium hypochlorite (NaClO) for 15min (under constant agitation) and subsequently rinsed six times with sterile distilled water (SDW). Finally, seeds were dried on sterile paper.

The seeds, prepared as above, were weighed and moved to 50mL Falcon tubes containing SDW and maintained at 30ºC for 30min. The seeds were removed from the SDW and briefly allowed to dry on sterile distilled paper. Group seed weight was recorded. This process was repeated until the seeds stopped water uptake. A linear regression model was calculated from the curve and it was estimated that to imbibe 70% of its potential, the seeds should be left for 156min to absorb 0.05mL.

3.3.3 *Azospirillum brasilense* Sp7 inoculum preparation and inoculation

The *Azospirillum brasilense* Sp7 strain was kindly provided by the *Colección Española de Cultivos Tipo* (acc. CECT 590) at the Polytechnic University of Valencia (Spain). The material arrived freeze-dried and was cultivated in Petri® dishes containing sterile nitrogen free broth medium (Nfb) supplemented with 15mL/L of 1:400 aqueous solution of Congo-red (CR) (Bashan et al., 1993) for 48h.

To prepare the Sp7 suspension, OAB liquid media [per liter for Solution A: (g/L)DL-malic acid, 5; NaOH, 3; $MgSO_4 \cdot 7H_2O$, 0.2; $CaCl_2$, 0.02; NaCl, 0.1; NH_4Cl, 1; yeast extract, 0.1; $FeCl_3$, 0.01; (mg/1) $NaMoO_4 \cdot 2H_2O$, 2; $MnSO_4$, 2.1; H_3BO_3, 2.8; $Cu(NO_3)_2 \cdot 3H_2O$, 0.04; $ZnSO_4 \cdot 7H_2O$, 0.24 – per 100mL for Solution B: (g/L) K_2HPO_4, 6; KH_2PO_4, 4 - Solution A+B

post-autoclaving, pH 6.8] was prepared as described by Okon et al. (1977), inoculated with a single Sp7 colony selected from the CR medium and incubated at 32°C in constant agitation (100rpm) for 48 hours. The bacterial suspension was allowed to reach its late-log growth phase with an absorbance of 0.399nm at OD_{600} (using an Amersham Biosciences Ultraspec 3100 Pro spectrophotometer); a concentration yielding approximately $1.16x10^8 cfu \cdot mL^{-1}$ based on a previously established bacterial curve.

All seeds were disinfected with 4% NaClO for 15min (under constant agitation) and washed six times with SDW in the laminar flow hood. They were laid out to dry on sterile autoclaved paper until all water had evaporated. Seeds were then inoculated with the rhizobacteria via soaking at approximately $1.16x10^8 cfu \cdot mL^{-1}$ per seed. To do so, 10mL of the bacterial suspension was aliquoted for each inoculated seed group of ten and pelleted by centrifuging at 5000rpm for 10min. When PBS was used as inoculation buffer, the supernatant was poured off and the bacterial pellet was washed twice with 1xPBS adjusted to a pH of 7.4 (per L for 10xPBS: 80g NaCl, 2g KH_2PO_4, 29g Na_2HPO_4 12 H_2O, 2g KCl, 2g NaN_3). Then 0.056 mL 1X PBS was added to the tube together with ten sterile maize seeds and vortexed. In the case of $MgSO_4$, the bacterial pellet was washed twice with autoclaved 30mM $MgSO_4$, and then resuspended in the same volume of buffer solution as for PBS (Mangmang et al., 2015). For control groups, ten sterile seeds were placed in tubes with buffer only. All treatments and controls were left in horizontal agitation at 100rpm to imbibe as previously described.

3.3.4 Plant measurements

Maize leaf arch height and chlorophyll contents (SPAD 502Plus, Konica Minolta) were recorded four weeks after planting. Arch height was measured from the soil surface to the arch of the uppermost leaf that was at least 50% emerged from the whorl.

3.3.5 Root structure analysis

Plant roots from all treatments were washed, extended on glass and photographed. Photographs were scanned and analyzed with WinRHIZO® (version 2009; Regent Instruments Inc., Quebec, ON, Canada).

3.3.6 Electron microscopy

3.3.6.1 Transmission electron microscopy (TEM)

To visualize the *Azospirillum* polar flagella, a drop of bacterial suspension in OAB was applied onto a Formvar©-covered electron microscope 200mesh copper grid for 1min. The liquid was absorbed by filter paper, then a drop of the staining solution (1% uranyl acetate in

water) was applied to the grid and allowed to absorb for 30s. After drying, the specimen was ready to be introduced into the electron beam of an EM 910 Transmission Electron Microscope (Zeiss, Oberkochen, Germany). A minimum of two grids per treatment were analysed (Borisov et al., 2009).

3.3.5.2 Scanning electron microscopy (SEM)

To visualize the biofilm formed by bacterial root colonization with scanning electron microscopy (SEM), root pieces were excised for both treatment groups and controls, and fixed in 3% (v/v) glutaraldehyde solution buffered with 0.1M phosphate buffer (pH 7.4) for 3h at room temperature. They were then postfixed in 1% (v/v) osmium tetraoxide in the same buffer. Specimens were washed three times in sterile distilled water and treated with aqueous solution of uranyl acetate 2% (w/v) for 40min. After fixation, samples were dehydrated through a graded ethanol series (30–100%) followed with acetone (100%), critical-point dried, mounted on aluminum stubs, coated with gold and examined with a Jeold JSM-6300 scanning electron microscope (Guerrero-Molina et al., 2012).

3.3.6 Statistical analysis

Statistical analyses were conducted for all the obtained data for each treatment group by using a one-way ANOVA test and Tukey's HSD test. Analyses were processed with JMP® 12.1 (SAS Institute Inc.), while software and graphics were created with Microsoft Excel 2016. The F-ratio of 0.05 for a One-way ANOVA was used to evaluate the difference between averages.

3.4 Results

Chlorophyll contents (SPAD) was significantly higher in treatments with PBS+Sp7 ($p<0.05$) than other treatment groups (Figure 9). Scanned images of the washed roots reflected qualitative differences between root systems (Figure 10).

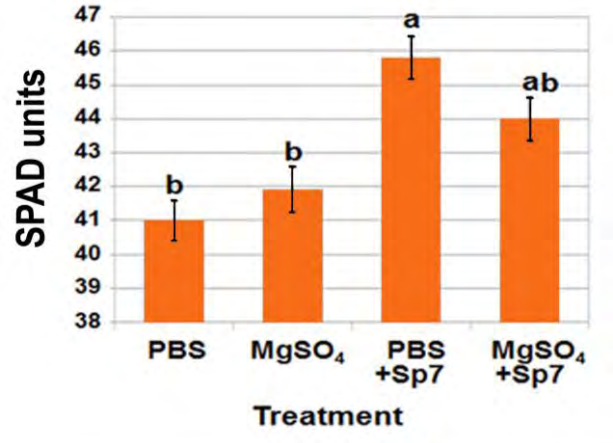

Figure 9. Relative chlorophyll contents of maize seedlings subjected to four inoculation treatments. Statistical differences ($p<0.05$) are denoted by different letters and error bars represent a 5% standard error (SE).

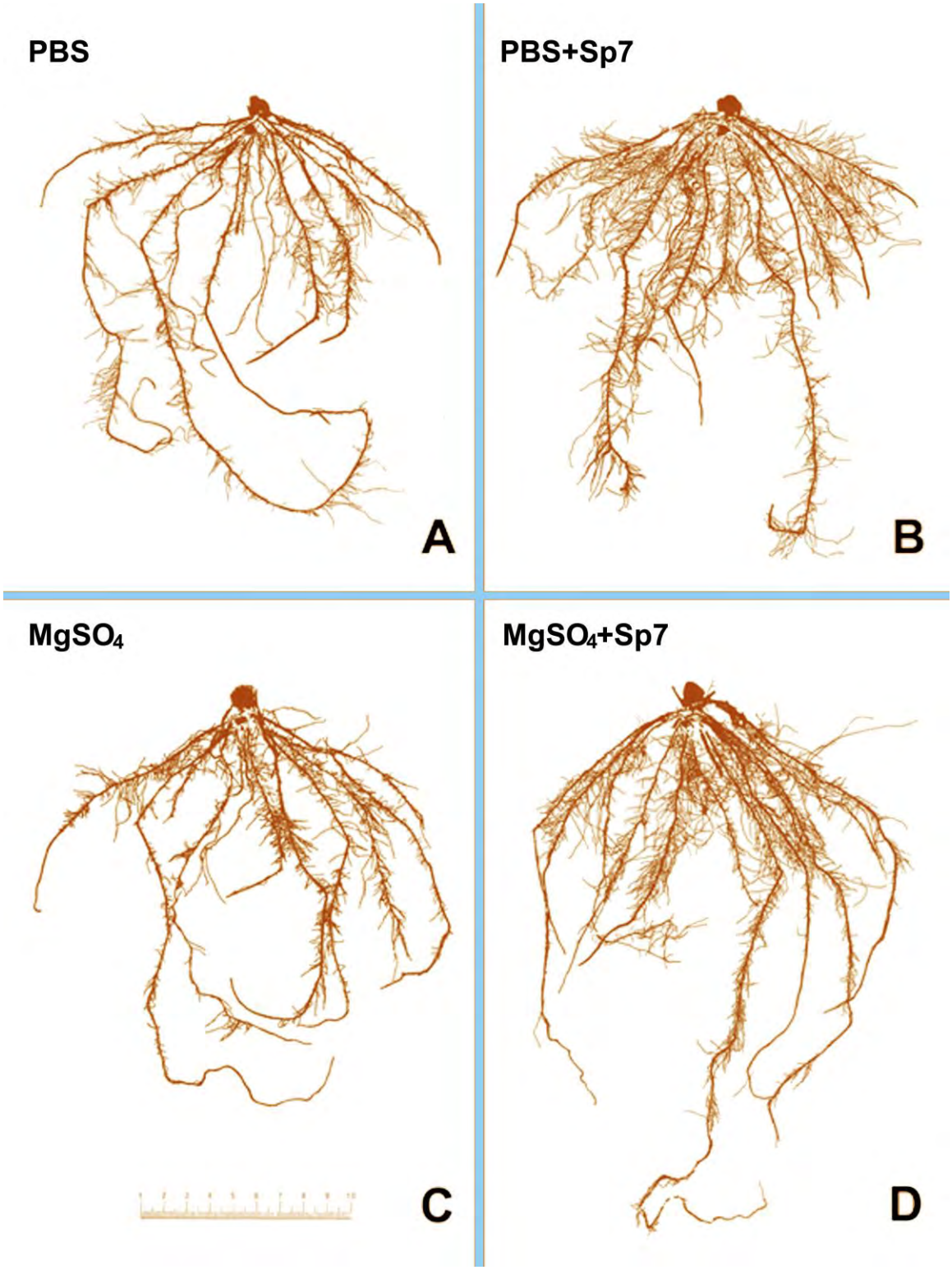

Figure 10. Representative images of maize seedling root systems with four inoculation treatments: PBS, $MgSO_4$, PBS+Sp7 and $MgSO_4$+Sp7. Images are the most representative example from sample groups of five (per treatment). C.) bar = 10cm.

WinRHIZO® analysis evidenced the efficacy of Sp7, detailing value increases in all root parameters over treatments without Sp7 (Tables 2 and 3). Then, subjecting the WinRHIZO® data to a one-way ANOVA statistical analysis revealed the abundance of certain root diameters to be significant between treatment groups. $MgSO_4$+Sp7 inoculated seedlings had significantly more abundance of roots measuring 2.0-2.5mm and 4.5-5.0mm than other treatment groups (Table 3).

Table 2. WinRHIZO® root values for four inoculation treatments in maize seedlings.

	PBS	**$MgSO_4$**	**PBS+Sp7**	**$MgSO_4$+Sp7**
Total length (cm)	245.50	265.06	336.23	346.81
Average diameter (cm)	0.76	0.49	0.80	0.86
Total surface area (cm^2)	61.10	68.79	85.06	92.36
Total projected area (cm^2)	19.41	21.88	28.73	29.39
Total volume (cm^3)	1.23	1.42	1.71	1.96

Table 3. Total root area (cm^2) in function of diameter class (mm) for four inoculation treatments in maize seedlings.

Root diameter class (mm)	**Inoculation treatment and total root area (cm^2) in function of root diameter class**			
	PBS	**$MgSO_4$**	**PBS+Sp7**	**$MgSO_4$+Sp7**
0.1-0.5	133	144	198	196
0.5-1.0	71	73.8	77	91.8
1.5-2.0	8.76	9.25	10.40	14.40
2.0-2.5	3.0	4.3	3.62	6.0*
2.5-3.0	5.34	2.0	1.44	2.95
3.0-3.5	0.6	0.86	2.75	1.80
3.5-4.0	0.32	0.61	0.55	1.12
4.0-4.5	0.17	0.02	0.32	0.68
4.5-5.0	0.11	0.69	0.32	1.07*

Data was subjected to a one-way ANOVA test and values with an asterisk (*) denote significant differences between treatments ($p<0.05$).

Plant arch height (Figure 11) was significantly shorter for $MgSO_4$+Sp7 seedlings compared to other groups. This finding was disproportional to increased root hair proliferation in $MgSO_4$+Sp7 seedlings (Table 2).

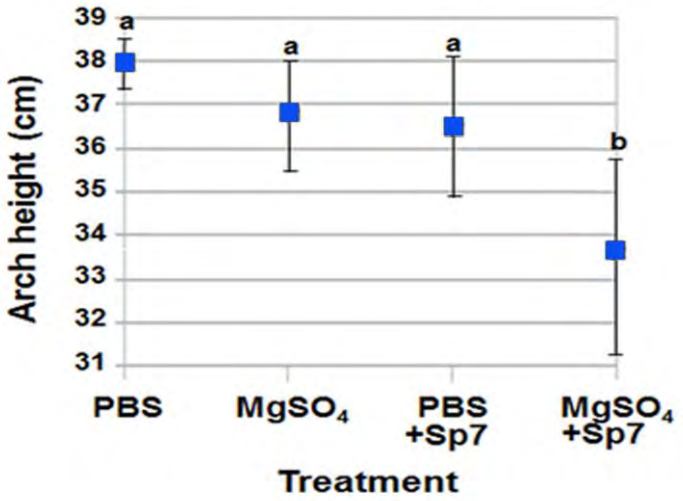

Figure 11. Average highest leaf arch height (cm). Statistical differences ($p<0.05$) are denoted by different letters and error bars represent a 5% SE.

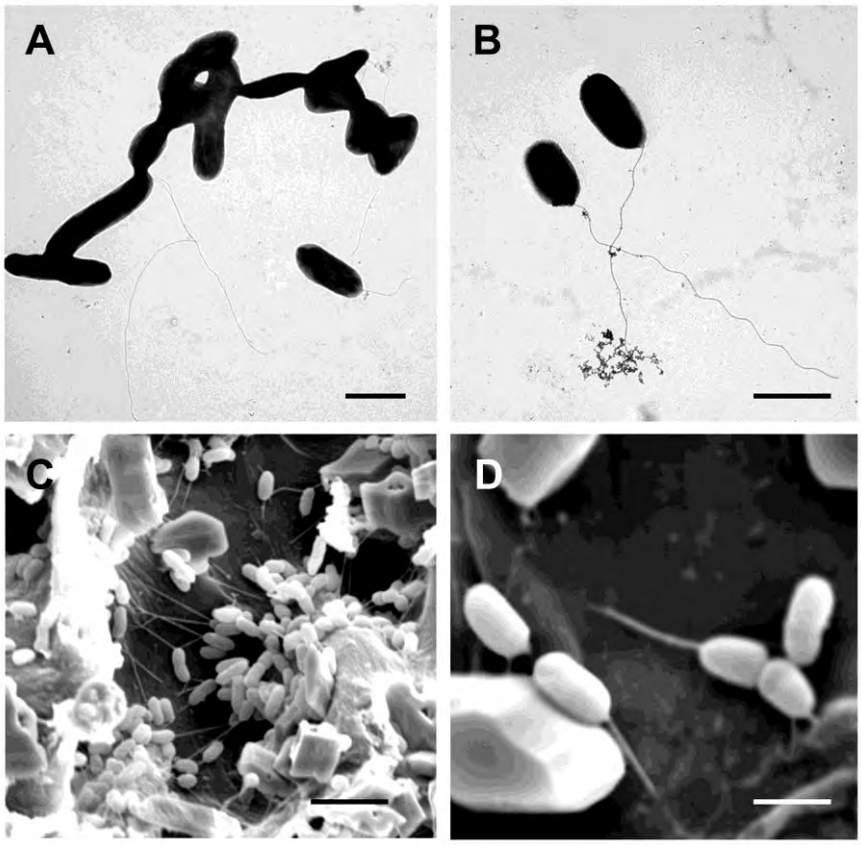

Figure 12. Electron microscopy (EM) images of *Azospirillum brasilense* (Sp7). **A-B.** Transmission electron microscopy (TEM) images of Sp7. **C-D.** Scanning electron micrographs (SEM) of Sp7-treated maize roots (bars: A & B = 2.5µm, C = 2µm, D = 6µm).

TEM examination of root microorganisms confirmed that the size of Sp7 bacterial cells is variable in general. There were some spiral shaped cells (typical to the *Azospirillum* genus) (Figure 12A), but the most abundant Sp7 phenotype was smaller (1.2x2-3µm) exhibiting a polar flagella (Figure 12B). All inoculated plants revealed different degrees of bacterial colonization and biofilm formation on the root surfaces, but from these figures, there was not a clear pattern or influence based on buffer (Figure 12C). The higher magnification in Figure 12D shows the Sp7 adherence to the root.

3.5 Discussion

Azospirillum brasilense Sp7 inoculation has repeatedly been shown to enhance plant growth (Bashan et al., 2006; Fukami et al., 2016). Our work expands upon these findings by demonstrating the specific ways in which Sp7 modulates plant growth depending upon buffer choice. When Sp7 is inoculated with PBS or $MgSO_4$ buffers, plant root diameter, height and leaf chlorophyll contents are differentially affected. Furthermore, we have found that these differences are not attributed to variations in bacterial binding to roots.

Plants inoculated with $MgSO_4$+Sp7 had a higher frequency of thick root hairs, but plant height was stunted relative to other treatment groups. This combination of events is unusual since Sp7 priming typically enhances plant growth overall, both above and below ground (Correa et al., 2007). A similar study reporting stunting in the presence of PGPR attributed it to other sources of unforeseen stress. Pathogenesis-related (PR) proteins were also detected, implying the activation of systemic acquired resistance (SAR) (Maurhofer et al., 1994). Proteomic analysis would enhance our findings, and help to understand this affect.

The $MgSO_4$ buffer augments the abundance of thicker root hairs compared to PBS in inoculated plants. There are several possible explanations for this: a) Sp7 potentiates the interaction of the buffer elements with early Mg-responsive genes in root hairs (Guo et al. 2016); b) Mg^{+2} in the buffer improves N_2 fixation by Sp7, thereby increasing plant root growth (Peng et al., 2018); c) high Mg-supply decreases starch and sucrose accumulation in leaves, but increases root concentrations, enhancing carbohydrate import into associated rhizobia (Peng et al., 2018). In the case of Sp7, enhanced carbohydrate supply would potentiate its hormone production, which stimulates plant root hair development.

Finally, PBS+Sp7 inoculation causes significant increases in chlorophyll production. Increased chlorophyll contents reflects C gain in the C-assimilation process through photosynthesis; and higher C absorption is often a byproduct of stress (Hernández-González et al. 2010). Work carried out with a similar PGPR, *Bacillus thuringiensis*, revealed that the bacteria was instrumental in reducing salt-stress in the plant by targeting the up-regulation of chloroplast proteins (Subramanian et al., 2016). Accordingly, the NaCl present in the PBS

buffer may exert stress on the plant, but Sp7 works to positively counterbalance this reaction by increasing chloroplast activity.

Our findings suggest that both common buffers tested interact with the plant to stimulate small stress reactions that are mitigated by Sp7.

3.6 Conclusions

- Sp7 increases plant growth regardless of inoculation buffer, PBS and $MgSO_4$
- Sp7 root binding is not affected by either of the buffers tested
- PBS is the most suitable buffer to use because plants inoculated with PBS+Sp7 exhibit higher carbon adsorption in leaf tissues, while $MgSO_4$+Sp7 presents a distress element that leads to stunted plant height

3.7 References

Alström S (1991) Induction of disease resistance in common bean susceptible to halo blight bacterial pathogen after seed bacterization with rhizosphere pseudomonads. *Journal of General Applied Microbiology* 37:495–501.

Ashraf M, Hasnain S, Berge O, Mahmood T (2004) Inoculating wheat seedlings with exopolysaccharide-producing bacteria restricts sodium uptake and stimulates plant growth under salt stress. *Biology and Fertility of Soils* 40:157–162.

Barassi CA, Sueldo RJ, Creus CM, Carrozzi LE, Casanovas EM, Pereyra MA (2007) *Azospirillum* spp., a dynamic soil bacterium favourable to vegetable crop production. *Dynamic Soil, Dynamic Plant* 1:68–82.

Barassi C, Fasciglione G, Casanovas E (2015) *Azospirillum* spp. and Related PGPRs Inocula Use in Intensive Agriculture. In: Cassán FD, Okon Y, Creus CM (eds) *Handbook for Azospirillum*. Springer International Publishing, Switzerland, pp 447-466.

Bashan Y, Levanony H (1985) An improved selection technique and medium for the isolation and enumeration of *Azospirillum brasilense. Canadian Journal of Microbiology* 31:947-952.

Bashan Y, Holguin G, Lifshitz R (1993) Isolation and characterization of plant growth-promoting rhizobacteria. In: Glick BR, Thompson JE (eds) *Methods in Plant Molecular Biology and Biotechnology*. CRC Press, Boca Raton, FL, USA.

Bashan Y, Holguin G (1996) Nitrogen-fixation by *Azospirillum brasilense* Cd is promoted when co-cultured with a mangrove rhizosphere bacterium (*Staphilococus sp.*). *Soil Biology and Biochemistry* 28(12):1651-1660.

Bashan Y, Holguin G (1997) *Azospirillum*-plant relationships: environmental and physiological advances (1990–1996). *Canadian Journal of Microbiology* 43:103–121.

Bashan Y, Bustillos JJ, Leyva LA, Hernandez JP., Bacilio M (2006) Increase in auxiliary photoprotective photosynthetic pigments in wheat seedlings induced by *Azospirillum brasilense*. *Biology and Fertility of Soils* 42(4):279-285.

Bashan Y, Trejo A, de-Bashan LE (2011) Development of two culture media for mass cultivation of *Azospirillum* sp. and for production of inoculants to enhance plant growth. *Biology and Fertility of Soils* 47:963–969.

Borisov IV, Schelud'ko AV, Petrova LP, Katsy EI (2009) Changes in *Azospirillum brasilense* motility and the effect of wheat seedling exudates. *Microbiological Research* 164:578—587.

Carpenter SR, Caraco NF, Correll DL, Howarth RW, Sharpley AN, Smith VH (1998) Nonpoint Pollution of Surface Waters with Phosphorous and Nitrogen. *Ecological Applications* 8(3):559-568.

Casanovas EM, Barassi CA, Sueldo RJ (2002) *Azospirillum* inoculation mitigates water stress effects in maize seedlings. *Cereal Research Communications* 30:343–350.

Casanovas EM, Barassi CA, Andrade FH, Sueldo RJ (2003) *Azospirillum*- inoculated maize plant responses to irrigation restraints imposed during flowering. *Cereal Research Communications* 31:395–402.

Cohen AC, Travaglia CN, Bottini R, Piccoli PN (2009) Participation of abscisic acid and gibberellins produced by endophytic *Azospirillum* in the alleviation of drought effects in maize. *Botany* 87:455-462.

Correa OS, Romero AM, Montecchia MS, Soria MA (2007) Tomato genotype and *Azospirillum* inoculation modulate the changes in bacterial communities associated with roots and leaves. *Journal of Applied Microbiology* 102:781–786.

Creus CM, Sueldo RJ, Barassi CA (1997) Shoot growth and water status in *Azospirillum*-inoculated wheat seedling grown under osmotic and salt stresses. *Plant Physiology and Biochemistry* 35(12):939-944.

Day DM, Döbereiner J (1976) Physiological aspects of N_2-fixation by a *Spirillum* from *Digitaria* roots. *Soil Biology and Biochemistry* 8:45-50.

Forde BG, Lea PJ (2007) Glutamate in plants: metabolism, regulation, and signaling. *Journal of Experimental Botany* 58:2339–2358.

Fukami J, Nogueira MA, Araujo RS, Hungria M (2016) Accessing inoculation methods of maize and wheat with *Azospirillum brasilense*. *AMB Express* 6 (3).

Gafny R, Okon Y, Kapulnik Y (1985) Adsorption of *Azospirillum brasilense* to corn roots. *Soil Biology and Biochemistry* 18 (1):69-75.

Guerrero-Molina MF, Winik BC, Pedraza RO (2012) More than rhizosphere colonization of strawberry plants by *Azospirillum brasilense*. *Applied Soil Ecology* 61:205-212.

Guo WL, Nazim H, Liang Z, Yang D (2016) Magnesium deficiency in plants: an urgent problem. *Crop Journal* 4:83-91.

Hartmann A, Zimmer W (1994) Physiology of *Azospirillum*. In: Okon Y (ed) *Azospirillum/plant associations*. CRC Press, Boca Raton, pp 15-39.

Hernández-González O, Yoisura SV, Larqué-Saavedra A (2010) Photosynthesis, transpiration, stomatal conductance, chlorophyll fluorescence and chlorophyll content in *Brosimum alicastrum*. *Bothalia Journal* 44(6):165-176.

Khalid M, Bilal M, Hassani D, Iqbal HMN, Wang H, Huang D (2017) Mitigation of salt stress in white clover (*Trifolium repens*) by *Azospirillum brasilense* and its inoculation effect. *Botanical Studies* 58 (1):5.

Kumar AS, Lakshmanan V, Caplan JL, Powell D, Czymmek KJ, Levia DF, Bais HP (2012) Rhizobacteria *Bacillus subtilis* restricts foliar pathogen entry through stomata. *The Plant Journal* 72:694–706.

Li P, Cao W, Fang H, Xu S, Yin S, Zhang Y, Lin D, Wang J, Chen Y, Xu C, Yang Z (2017) Transcriptomic Profiling of the Maize (*Zea mays* L.) Leaf Response to Abiotic Stresses at the Seedling Stage. *Frontiers in Plant Science* 8:290.

Lugtenberg B, Kamilova F (2009) Plant-Growth-Promoting Rhizobacteria. *Annual Review of Microbiology* 63:541-556.

Mangmang JS, Deaker R, Rogers I (2015) Early seedling growth response of lettuce, tomato and cucumber to *Azospirillum brasilense* inoculated by soaking and drenching. *Journal of Horticultural Science* 42 (1):37-46.

Maurhofer M, Hase C, Meuwly P, Métraux JP and Défago G (1994) Induction of systemic resistance of tobacco to tobacco necrosis virus by the root-colonizing *Pseudomonas fluorescens* strain CHA0: Influence of the *gacA* gene and of pyoverdine production. *Phytopathology* 84: 139–146.

Mugilan I, Gayathri P, Elumalai EK, Elango R (2011) Studies on improve survivability and shelf life of carrier using liquid inoculation of *Pseudomonas striata*. *International Journal of Pharma and Bio Sciences* 2 (4):1271-1275.

Niu YF, Jin GL, Zhang YS (2014) Root development under control of magnesium availability. *Plant Signaling & Behavior* 9:e29720.

Okon Y, Albrecht SL, Burris RH (1977) Methods for growing *Spirillum lipoferum* and for counting it in pure culture and in association with plants. *Applied and Environmental Microbiology* 33:85-88.

Perrig D, Boiero ML, Masciarelli OA, Penna C, Ruiz OA, Cassan FD, Luna MV (2007) Plant-growth-promoting compounds produced by two agronomically important strains of *Azospirillum brasilense*, and implications for inoculant formulation. *Applied Microbiology and Biotechnology* 75:1143–1150.

Rivera D, Obando M, Barbosa H, Rojas Tapias D, Bonilla R (2014) Evaluation of polymers for the liquid rhizobial formulation and their influence in the Rhizobium-Cowpea interaction. *Universitas Scientiarum* 19 (3):265-275.

Subramanian S, Souleimanov A, Smith DL (2016) Proteomic studies on the effects of lipo-chitooligosaccharide and thuricin 17 under unstressed and salt stressed conditions in *Arabidopsis thaliana*. *Frontiers in Plant Science* 7:1314.

Ton J, Jakab G, Toquin V, Flors V, Iavicoli A, Maeder MN, Métraux JP, Mauch-Mani B (2005) Dissecting the β-aminobutyric acid–induced priming phenomenon in *Arabidopsis*. *Plant Cell* 17:987–99.

Van Peer R, Niemann GJ, Schippers B (1991) Induced resistance and phytoalexin accumulation in biological control of Fusarium wilt of carnation by *Pseudomonas* sp. strain WCS417r. *Phytopathology* 81:728–34.

Verhagen BWM, Glazebrook J, Zhu T, Chang H-S, Van Loon LC, Pieterse CMJ (2004) The transcriptome of rhizobacteria-induced systemic resistance in *Arabidopsis*. *Molecular Plant-Microbe Interactions* 17:895–908.

Wang YQ, Ohara Y, Nakayashiki H, Tosa Y, Mayama S (2005) Microarray analysis of the gene expression profile induced by the endophytic plant growth–promoting rhizobacteria, *Pseudomonas fluorescens* FPT9601-T5 in *Arabidopsis*. *Molecular Plant-Microbe Interactions* 18:385–96.

Venable JH and Coggeshall R (1965) A simplified lead citrate stain for use in electron microscopy. *Journal of Cell Biology* 25:407–408.

CHAPTER 4

Root development in agronomically distinct six-rowed barley (*Hordeum vulgare*) cultivars inoculated with *Azospirillum brasilense* Sp7

(Published in Plant Breeding. 2018; 137:338–345. Annex 2)

Chapter 4. Root development in agronomically distinct six-rowed barley (*Hordeum vulgare*) cultivars inoculated with *Azospirillum brasilense* Sp7

4.0 Abstract

The growth-promoting rhizobacteria *Azospirillum brasilense* Sp7 positively affects many crops, but its influence on barley remains to be fully investigated. The aim of this study was to track early root growth of four barley cultivars that are widely used in Spanish breeding programs under different growing scenarios. Different growth conditions are hypothesized to affect the response of young plants to *A. brasilense* Sp7, so seeds were inoculated with *A. brasilense* Sp7 and directly sown in the growth chamber, or planted *in vitro*. Plant height was measured and root structure analyzed with the WinRHIZO® program. *Azospirillum brasilense* Sp7 inoculation increased the length, surface area and number of root tips in both systems and in most cultivars in a similar way. Cultivars 'Barberousse' and 'Plaisant' were the most responsive to *A. brasilense* Sp7 treatment, while 'Albacete' was especially interesting in terms of its physiological interaction with *A. brasilense* Sp7 under abiotic stress imposed by the *in vitro* system. The utility of the *in vitro* system is criticized.

4.1 Introduction

Barley (*Hordeum vulgare* L.) is especially important in the Mediterranean area, where the yield of certain crops is evaluated by their adaptability or tolerance to abiotic stress, mainly drought (López-Castañeda and Richards, 1994; Teulat et al., 2001). Among the agronomic practices that favor the adaptation of barley to unfavorable environments, the use of plant growth promoting rhizobacteria (PGPR), such as *Azospirillum brasilense* Tarrand et al., 1979 is increasingly popular. Its ability to increase auxin production in host plants leads to greater root surface area (Spaepen and Vanderleyden, 2011), which in turn alleviates adaptive stress to drought by increasing the absorption of water and minerals (Vacheron et al., 2013). *Azospirillum brasilense* inoculation has been shown to induce early vigorous growth, which is important in providing assimilates for grain filling when drought or any other kind of stress occurs post-anthesis (Siddique et al., 1989).

The most influential theory regarding the precise mode of action of A. brasilense in plants against abiotic stress suggests cross-talk between two stress-signaling pathways by means of priming and initiating induced systemic response (ISR) in the plant (Omar et al., 2009; Vacheron et al., 2015). Regardless of this overarching mechanism, *A. brasilense*-induced processes observed in plants are tightly intertwined with and influenced by the host plant's genetic makeup (Correa et al., 2007). In this way, understanding the genotype-by-environment (GxE) interaction, or barley cultivar x *A. brasilense* treatment interaction (CxT), can help elucidate genotype-inoculum specificities, which can be harnessed to ensure the ontogenesis of a relationship that imparts a positive plant response. Investigation into this relationship can complement breeders' goals by optimizing economically important traits, substantiating that they are not diminished by the inoculum in the environment (Rashid, 2014).

The possible relationship between *A. brasilense* and barley has been confirmed in previous studies (Zawoznik et al., 2014), and it has been observed that different genotypes indeed influence the activity of rhizobacteria differently; leading to distinct root architecture and/or exudation profiles (Comas and Eissenstat, 2009). As such, four six-rowed, winter-type barley cultivars characterized for their contrasting agronomic performance in the Mediterranean area have been chosen as subjects herein, viz., 'Albacete', 'Barberousse', 'Plaisant' and 'Orria'. These cultivars are traditionally classified and distinguished primarily by their vulnerability to drought (Voltas et al., 1999). Likewise, the genotype of the bacterial strain also influences the plant-bacterial interaction. In this work, the *Azospirillum* Sp7 strain has been selected because it responds more acutely to exogenously induced abiotic stress factors. Sp7 is an epiphyte, only colonizing plant root surfaces and thus remaining more closely connected to the outer environment (Kamnev et al., 2011).

In general, field performance of the bacteria in the rhizosphere is affected by soil-related factors as well, such as nitrogen content (Muthukumarasamy et al., 1999; 2002), soil type (de

Oliveira et al., 2006), soil sterility or any support system (or lack thereof) (Bueno dos Reis Junior et al., 2000). So in order to investigate this relationship, we have selected two distinct growing scenarios: 1) direct sowing in sterile soil under growth chamber conditions, and 2) a media-less *in vitro* premise, fit for sterile laboratory conditions. This work explores the two distinct environments held under constant experimental conditions in order to analyze the effects of *A. brasilense* Sp7 on barley root systems. To best summarize the overall effect of the CxT interaction, a two-way ANOVA is conducted to understand each studied parameter. Findings can help uncover mechanisms underlying the barley/*A. brasilense* Sp7 interaction in different scenarios for each of these cultivars.

4.2 Aims

- Elucidate genotype-Sp7 specificities of four six-rowed winter-type barley cultivars: 'Albacete', 'Barberousse', 'Plaisant' and 'Orria'
- Explore the efficacy of a media-less *in vitro* growing system for seedlings

4.3 Materials and methods

4.3.1 Barley cultivars

The seeds of the four selected cultivars of barley (Albacete, Barberousse, Plaisant and Orria) were obtained from the Aula Dei Experimental Station of the CSIC of Zaragoza. 'Albacete' is an inbred line that was first cultivated in the middle of the 20th century, within a local heterogeneous population of landowners in the Spanish province of Albacete. It is drought tolerant and with a stable grain yield, which is why it has been cultivated across vast expanses in dry zones for decades. 'Barberousse' was released in France in 1980. It was obtained from the cross [259 711 / (Hatif de Grignon/ Ares)/Ager] and is sensitive to drought. However, it is known for its high productivity and adaptability (Farré et al., 2011). 'Plaisant' is another French cultivar that was obtained in 1982. It has a strong vernalization requirement, causing late heading and slow maturing, so it often performs poorly in Mediterranean environments. It is grown for malt and originates from a rather narrow genetic base (Yau, 2016). Finally, 'Orria' is a productive Spanish cultivar of CIMMYT origin, well-adapted to fertile, rain-fed environments. It was released in 1993 and is commonly used as a parental line for crossing with other cultivars (Muñoz et al., 1998). 'Barberousse', 'Orria' and 'Plaisant' have been found to suffer acutely from the effect of terminal heat and drought stresses on grain growth, whereas 'Albacete' is rather insensitive to these climatic factors, but performs poorly in environments favoring a high grain weight due to its susceptibility to lodging (Voltas et al., 1999).

4.3.2 *Azospirillum brasilense* inoculum preparation and inoculation

The *Azospirillum brasilense* Sp7 strain (ATCC 29145) was kindly provided by the "Colección Española de Cultivos Tipo" (CECT) of the Polytechnic University of Valencia (Spain). For the *A. brasilense* Sp7 suspension, a peptone yeast broth (PYB) liquid medium amended with $CaCl_2$ 0.04% was prepared, as described by Döbereiner et al. (1976), and incubated at 32°C under constant agitation at 100rpm for 20h. At this point, the bacterial suspension had reached its late log-growth phase, with an absorbance of 1.0 at OD_{600}nm (determined via an Amersham Biosciences Ultraspec 3100 Pro spectrophotometer). This yielded an ideal bacterial density of $1x10^8$cfu·mL^{-1}.

The seeds of the four above-mentioned cultivars were disinfected with 70% ethanol for 2min, soaked in 1% sodium hypochlorite for 10min under constant agitation (100rpm), and washed six times with sterile distilled water. Seeds were dried on sterile autoclaved paper until all water had evaporated. They were then inoculated with the rhizobacteria via the seed-coat contamination method at $1x10^8$cfu per mL. To do so, 1mL of the bacterial suspension was aliquoted for each of the four seed groups and centrifuged at 5000rpm for 10min. The supernatant was poured out and the pellet was re-suspended in 1mL of 1X PBS and adjusted to a pH of 7.4 (per L for 10X PBS: 80g NaCl, 2g KH_2PO_4, 29g Na_2HPO_4 12 H_2O, and 2g KCl). Then, the inoculum was vortexed, and between 0.21 and 0.24mL of the inoculum was added to each tube of 30 seeds, depending on the cultivar (see Table 4). The tubes were put into horizontal agitation for 30min to 1h 15min, depending on the previously defined imbibition time for each cultivar (Table 4). Non-inoculated (control) seeds of each cultivar served as the controls and were 'inoculated' with PBS only. Note that only a total of 18 inoculated seeds were needed per cultivar (nine for direct sowing and nine *in vitro*), but inoculation was conducted in groups of 30 according to the imbibition curve so as to select and plant the most homogenous seeds post-inoculation.

Table 4. Time and volume of inoculum solution (mL) required to achieve 70% seed imbibition in 30 seeds for four barley cultivars: 'Albacete,' 'Barberousse,' 'Plaisant' and 'Orria'.

Cultivar	70% imbibition absorbance (mL)	Time (hr:min)
Albacete	0.21	00:30
Barberousse	0.24	01:15
Plaisant	0.18	01:05
Orria	0.22	01:00

4.3.3 Direct sowing (under growth chamber conditions)

For direct sowing (Figure 13), the treatments were defined as *A. brasilense* inoculated seeds, or non-inoculated seeds that were treated solely with PBS buffer and served as the controls. Each treatment was replicated nine times per cultivar in a completely randomized design. The seeds were planted in 0.3L pots filled with autoclaved commercial substrate (Traysubstrat®, Klasmann-Deilmann, Gmbh, Geeste, Germany) characterized by having an extra fine structure and pH of 6. Both inoculated and non-inoculated (control) barley seeds were sown and maintained in a growth chamber (1282 X 687 X 1487mm) at 23-25°C with a photoperiod of 16h light/8h dark cycle under 10,000lux fluorescent bulbs. Relative humidity was regulated at 90-95% and emerged plants were watered twice a week by flooding. Forty-five days after sowing, when the seedlings started to tiller and had reached a phenological growth stage of 21 according to the BBCH scale (Lancashire et al., 1991), root-development analysis was done. Roots were gently washed with distilled water, extended on glass and scanned with an Epson Perfection V700 modified flatbed scanner at an optical resolution of 4800 dots per inch.

4.3.4 *In vitro* procedure

For the *in vitro* assay (Figure 14), the experimental units for inoculated and non-inoculated (controls) were adjusted to the *in vitro* model. Three barley seeds were arranged linearly on a piece of sterile cardboard humidified with sterile distilled water and placed in a sterile transparent plastic bag (55-oz. 19 x 30cm, Nasco Whirl-Pak® sampling bag, Sigma Aldrich). Each bag of three seeds served as a randomization unit and was replicated three times per treatment and per cultivar in a completely randomized design. Closed bags were maintained at 23-25°C in the dark for five days, and then moved into the growth chamber (conditions described above) for 10 more days. After 15 days, which was enough time for all seeds to germinate and reach stage 09-10 according the BBCH scale; images of the plastic bags with germinated seeds were obtained with a scanner, as done at the end of the previous assay.

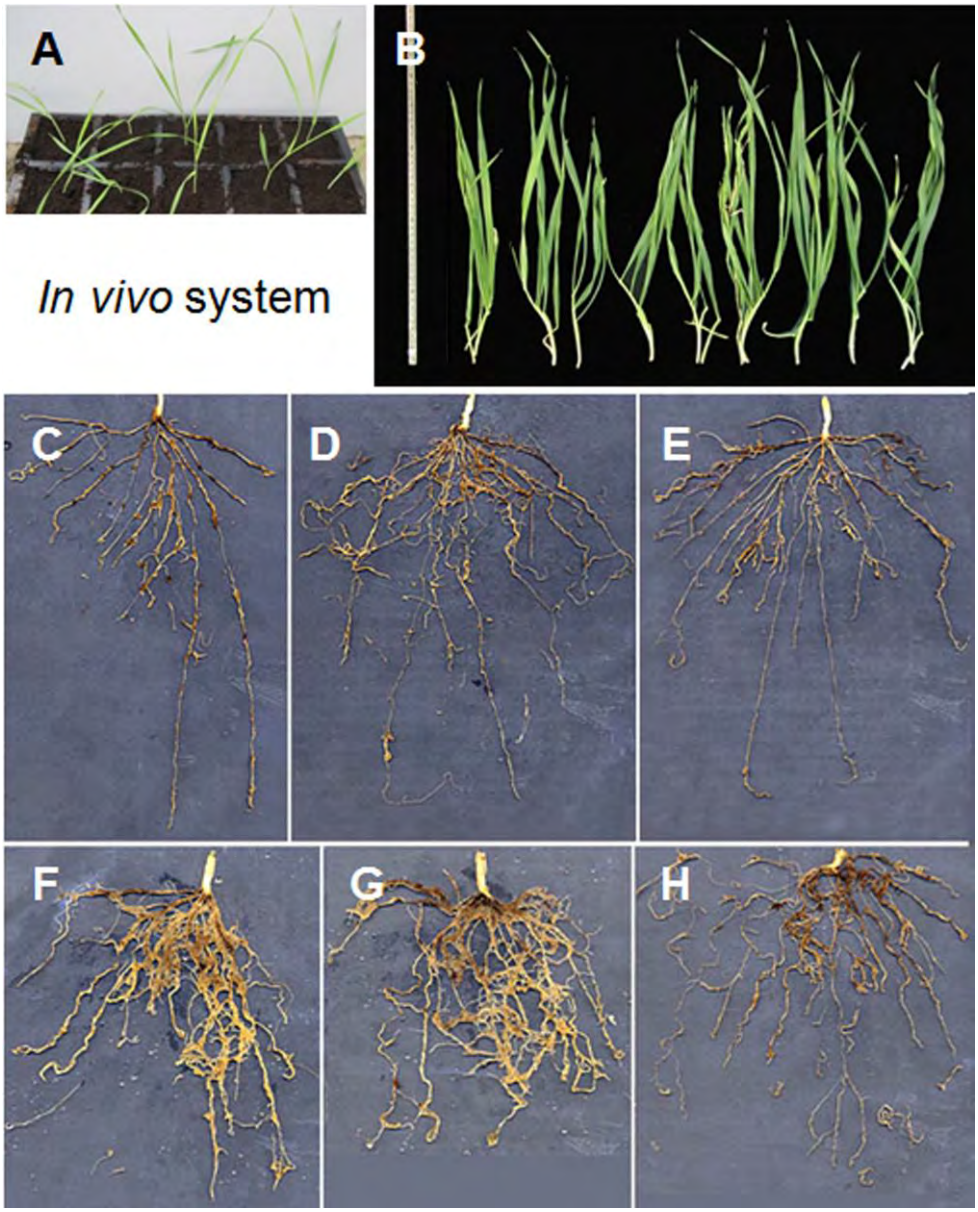

Figure 13. General view of the direct sowing system. (A) Barley seedlings (cv. Albacete) in pots. (B) Aerial parts of barley plants (cv. Albacete) that were measured. (C-E) Roots of non-inoculated plants. (F-H) Roots of plants inoculated with *Azospirillum brasilense* Sp7.

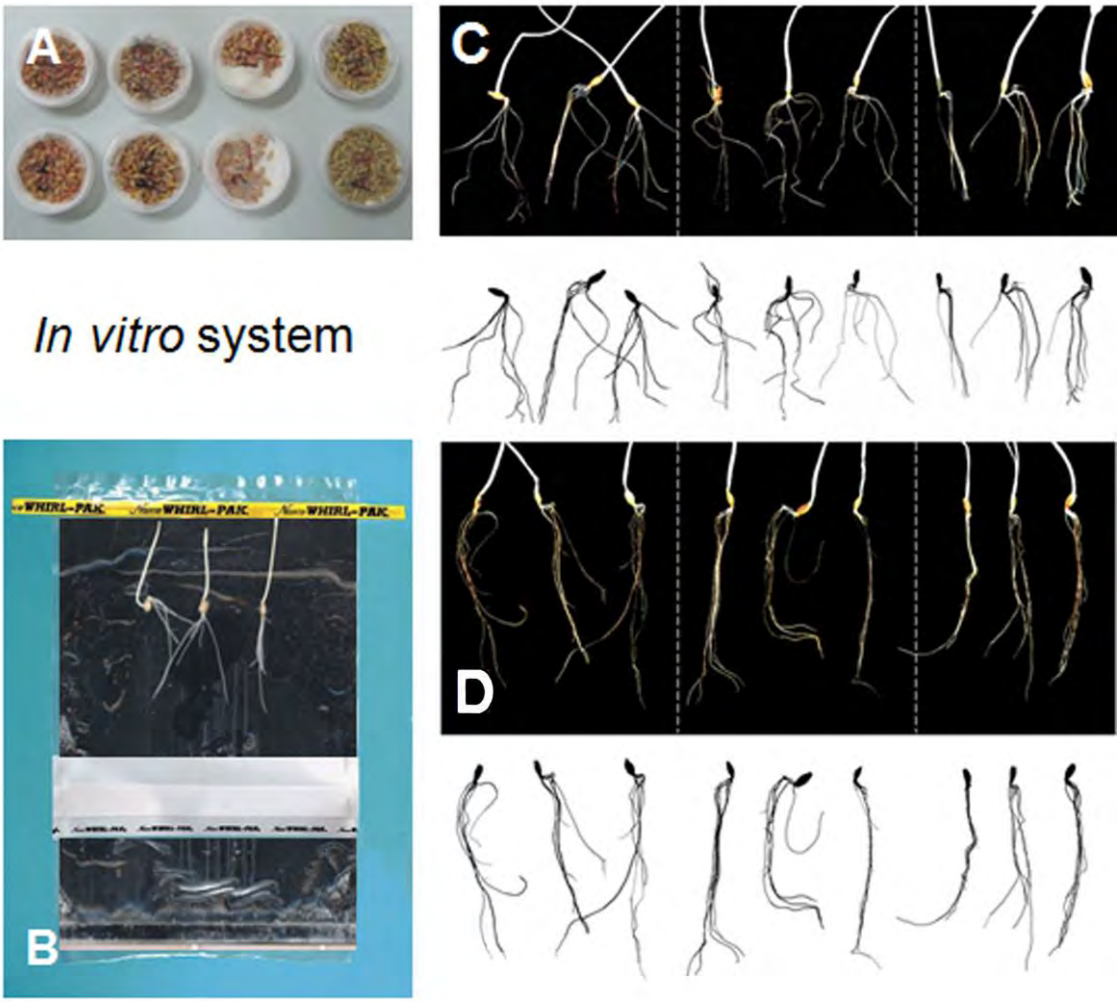

Figure 14. General view of the *in vitro* system. (A) Seed inoculation. (B) Root development in sterile plastic bags. (C) Germination of non-inoculated barley seeds ('Albacete'). Seedlings on the black background are the original photos, which were transposed to have a white background for WinRHIZO analysis. (D) Germination of barley seeds ('Albacete') inoculated with *Azospirillum brasilense* Sp7.

4.3.5 Plant growth analysis

For both direct sowing and *in vitro* assays, root-development analysis was performed to evaluate length (cm), surface area (cm^2) and number of root tips using WinRHIZO® software (version 2009; Regent Instruments Inc., Quebec, ON, Canada). Root imaging tools, such as WinRHIZO®, use a skeletonization method to generate root representation and to count root tips by counting endpoints of the root skeleton. Via user-defined average root thickness of primary roots, it is then possible to obtain an estimate of the number of primary roots and the number of lateral roots contained in that image (Cai et al., 2015). Directly sown samples were also analyzed for plant height at 45 days after planting. Effects of the treatment, growth characteristics, cultivars and their interactions were determined using the General Linear Model (GLM) in the case of direct sowing and the General Linear Mixed Model (GLMM) for *in vitro*, whereby bag was held as the random factor. Both direct sowing and *in vitro* growing scenarios

called for a two-way analysis of variance (ANOVA) to quantify the overall effect of the anticipated G×E interaction (in this case defined as cultivar × treatment interaction, or C×T) and the related effects. Least significant difference (LSD) was used for mean separation, and an individual error rate of 95% was considered in all tests. JMP® software version Pro 11.0.0 was used for all analyses (SAS Institute, Cary, NC, USA).

To clarify how each cultivar specifically reacts to Sp7 inoculation compared to the control, and irrespective of the other cultivars, one-way ANOVAs were run for each cultivar. The cultivar was held as the dependent factor and root growth parameters as independent. In the case of *in vitro* growth, the bag was an additional random factor, just as in the two-way ANOVA.

4.4 Results

The cultivar rank order for overall plant performance according to the parameters studied was: 'Plaisant', 'Barberousse', 'Orria' and, 'Albacete'. That is to say, barley cv. 'Plaisant' had the most positive growth for both treatments in nearly all parameters measured under both growing scenarios (Table 5).

Table 5. Relative overall growth of each barley cultivar (‘Albacete,’ ‘Barberousse,’ ‘Orria’ and ‘Plaisant’) SE, regardless of treatment: direct sowing vs. *in vitro.*

Method	Cultivar	Length (cm)	Area (cm2)	Tips (#)
Direct sowing	Plaisant	508 ± 53	496 ± 52	50 ± 8
	Orria	377 ± 26	362 ± 22	26 ± 3
	Barberousse	333 ± 22	325 ± 20	28 ± 6
	Albacete	238 ± 24	244 ± 24	15 ± 1
In vitro	Plaisant	45 ± 4	162 ± 16	36 ± 7
	Orria	46 ± 2	122 ± 9	22 ± 3
	Barberousse	47 ± 4	109 ± 8	22 ± 4
	Albacete	43 ± 3	86 ± 7	19 ± 2

Two-way ANOVA did not reveal any significant C×T interactions; though it was clear that *A. brasilense* Sp7 had an overall positive effect on plant growth. Specifically, 'Barberousse', 'Plaisant' and 'Albacete' were significantly and positively affected by *A. brasilense* in the direct sowing assay, whereas 'Albacete' was the only cultivar significantly affected by *A. brasilense* treatment *in vitro*. Effect tests revealed the random factor 'bag' to indeed be significant for all *in vitro* growth parameters.

Table 6. Effect tests of two-way analysis of variance (ANOVA). Mean squares for the terms of the two-way analyses of variance for variables measured at the two experimental set-ups.

		Length	Surface Area	Number of tips	Plant height
Direct sowing					
Cultivar	3	19854247***	199668***	3849***	266.64***
Treatment	1	6337490*	48996*	2201**	1.97
CxT	3	96897	1297	487	9.79
Residual	64	1132884	10280	277	36.07
In vitro					
Cultivar	3	43.2	1672.4**	1006*	
Treatment	1	483.01	562.7	675	
CxT	3	83.06	13.1	169	
Bag (CxT)	16	189.35*	205.5*	251	
Residual	48	76.72	75.2	150	

*,**,*** significant F value for P <0.05, <0.01, and <0.001, respectively.

For direct sowing under growth chamber conditions, the cultivar (C) effect was highly significant for all root parameters analyzed: length (cm), surface area (cm^2) and number of tips (Table 6). The effect of *Azospirillum brasilense* Sp7-treatment (T) on all root parameters was also significant, especially for the number of tips.

For all radicular parameters in which the T effect was significant under direct sowing, inoculated plants with *Azospirillum* Sp7 had larger values than their non-inoculated counterparts of the same cultivar. Overall, root length increased proportionally for each inoculated cultivar over its non-inoculated counterpart, though one way ANOVA revealed that 'Barberousse' was the only cultivar to exhibit significantly longer inoculated roots (p=0.034) (Figure 15a). Similarly, 'Barberousse' was also the only cultivar to exhibit significantly more root surface area in inoculated plants compared with non-inoculated ones (p=0.028) (Figure 15b). The number of root tips was significantly higher for inoculated 'Albacete' (p=0.037) and 'Plaisant' cultivars (p=0.057) over their non-inoculated controls (Figure 15c).

Inoculated and non-inoculated plants of the same cultivar showed a mixed trend for plant height. Inoculated 'Barberousse' and 'Plaisant' plants were slightly taller than their control counterparts, whereas those of 'Albacete' and 'Orria' were shorter (Figure 15d).

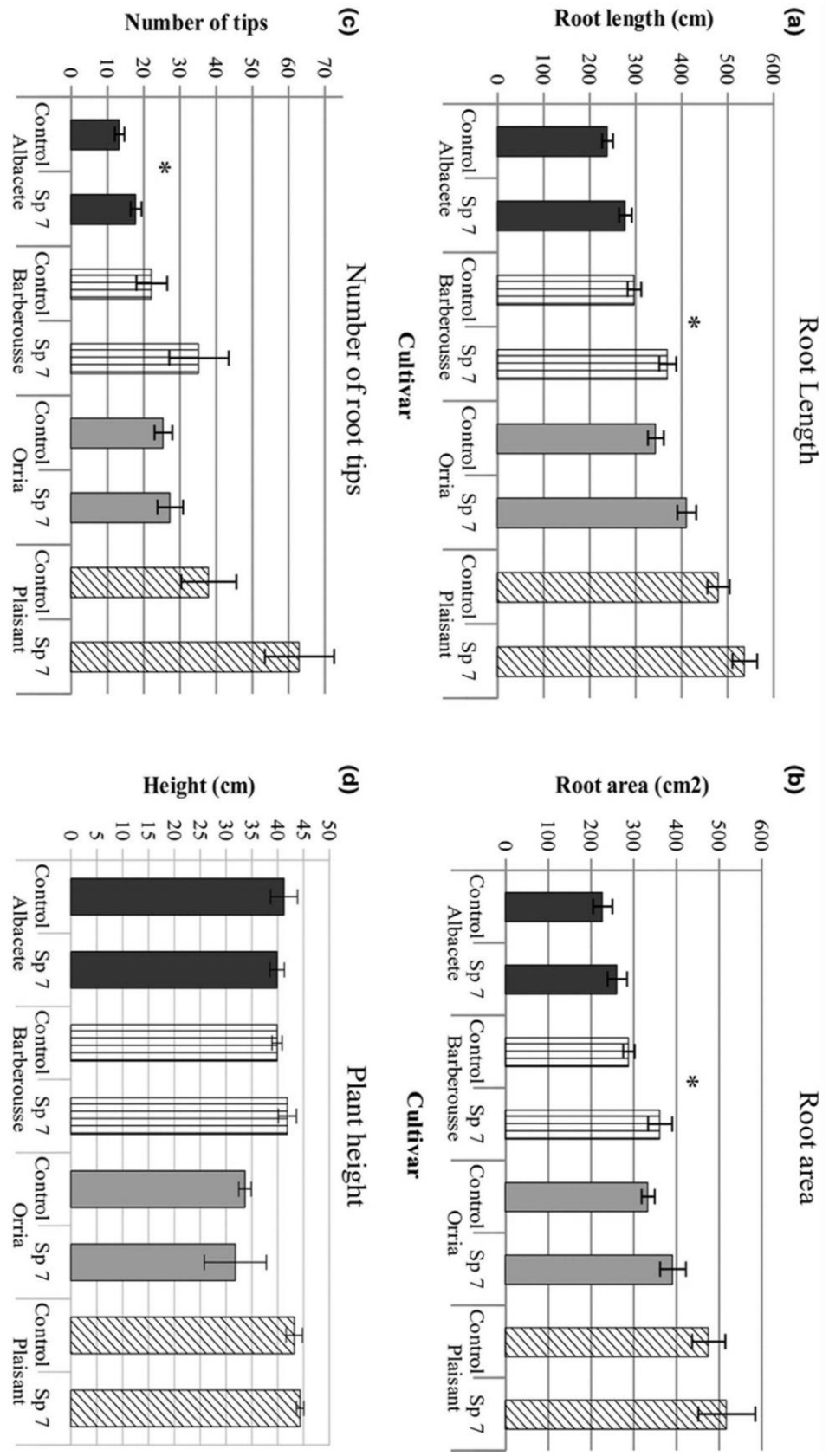

Figure 15. Direct sowing: *Azospirillum brasilense* Sp7 vs. control. Four barley cultivars ('Albacete', 'Barberousse', 'Orria' and 'Plaisant') treated with *Azospirillum brasilense* Sp7, or untreated (control), were evaluated for (a) root length (cm), (b) root area (cm^2), (c) number of root tips and (d) height (cm), 45 days after sowing in pots. Error bars indicate the mean standard error (SE) (Student's t test, $p<.05$) between treatments for each cultivar, individually. Significant differences between treatments are indicated with an asterisk (*).

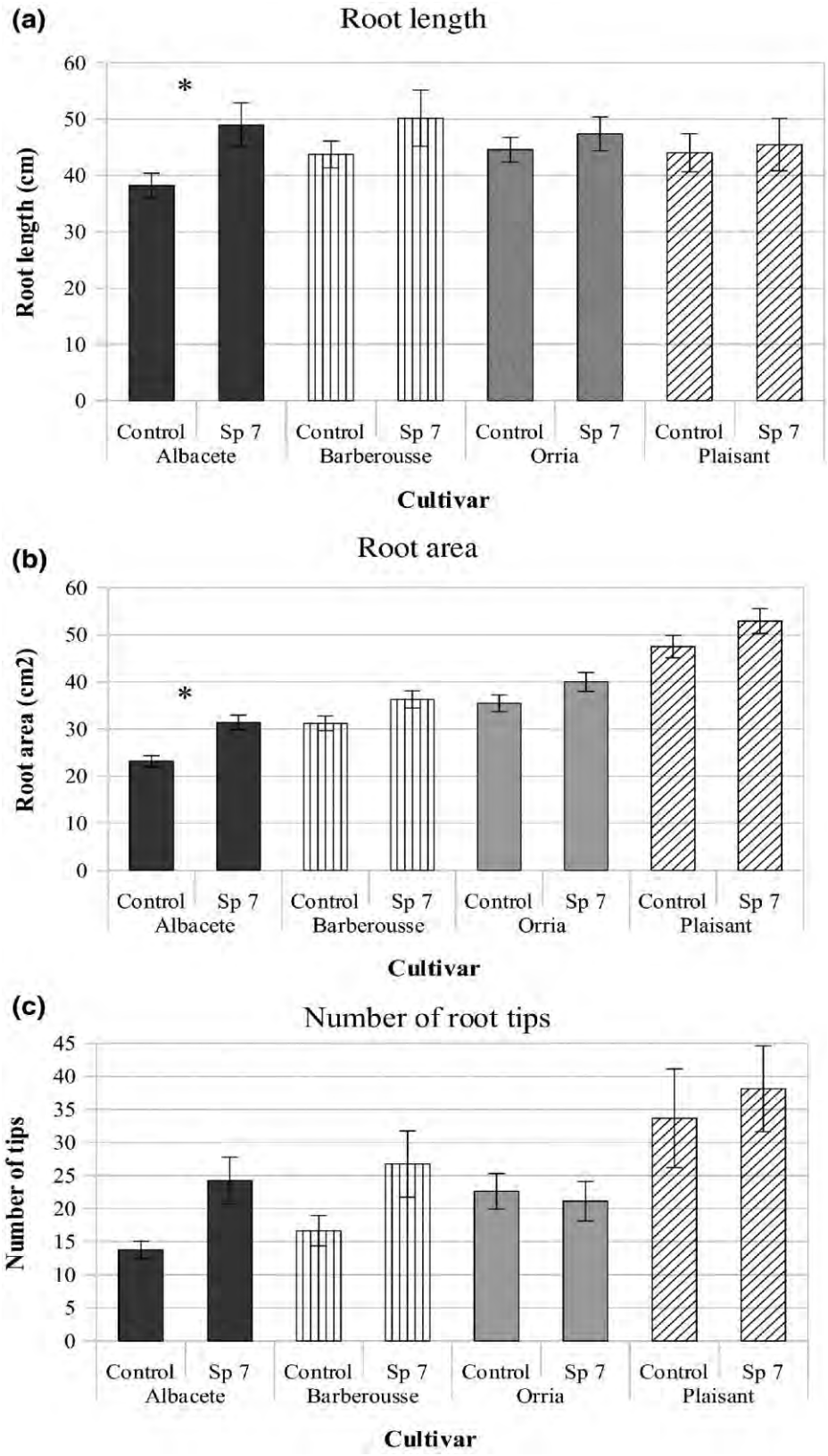

Figure 16. *In vitro* growth: *Azospirillum brasilense* Sp7 *versus* control. Four barley cultivars ('Albacete', 'Barberousse', 'Orria' and 'Plaisant') treated with *Azospirillum brasilense* Sp7 or untreated (control) were evaluated for (a) root length (cm), (b) root area (cm^2) and (c) number of root tips, 15 days after sowing in Nasco Whirl-Pak sampling bags. Error bars indicate the mean standard error (Student's t test, $p<.05$) between treatments for each cultivar, individually. Significant differences between treatments are indicated with an asterisk (*).

For the *in vitro*-grown plants, the C effect was significant for root area and number of tips; but not for root length. Neither the T effect nor the C×T interaction was not significant for any of the parameters studied.

In vitro one way analysis revealed that 'Albacete' was the only cultivar to exhibit significantly longer roots (p=0.029) (Figure 16a) and a significantly larger root surface area (p=0.025) (Figure 16b) when inoculated. Interestingly, there were quantifiable differences in the root surface area of non-inoculated cultivars, suggesting rooting capacity to be intrinsic for each cultivar in this growing scenario. Figure 16c depicts the mean number of root tips; a trend towards more root tips was observed in *A. brasilense* Sp7-inoculated seedlings of 'Albacete', 'Plaisant' and 'Barberousse', compared with their untreated counterparts.

4.5 Discussion

On the whole, this study concurs with literature in that *A. brasilense* Sp7-inoculated root systems display a significant increase in the number and length of root tips, and root surface area (Dobbelaere et al., 1999; Creus et al., 2005), adding that such effects take hold irrespective of growing conditions. Though isolated effects (C and T) are significant, there is not any significant interaction between the barley cultivars and *A. brasilense* treatments (CxT) under either growing environment tested.

Seedlings that were directly sown under growth chamber conditions have significantly different growth among inoculated cultivars, indicating an intrinsic variation in cultivar performance. Particularly, 'Barberousse' is the only cultivar to exhibit increased root length and significantly greater root surface area in inoculated plants over non-inoculated ones when directly sown. Historically, 'Barberousse' is the 'least drought-tolerant' and most stress-prone cultivar of those studied, lying grounds for the precedent that it has a different degree of responsiveness to *A. brasilense* Sp7 inoculation. Previous studies suggest two different reasons for these varying degrees of reactivity. For one, Cao et al. (2017) found that unique barley varieties have different giberellic acid 4 (GA_4)-dependent growth mechanisms and ICA (auxin phytohormone) differentials when under (salinity) stress, reiterating the intrinsic variation of various cultivars' hormonal responses to stressful situations. It still remains in question as to how exactly *A. brasilense* induces ISR and the hormonal cross-talk, connecting stress-signaling pathways that play into the unique biology of each cultivar.

Secondly, various studies relating PGPRs to increased drought tolerance attribute increased root surface area to the production of bacterial exopolysaccharides, which in turn provide additional proteins and soluble sugars to enhance plant growth, maintain soil-moisture and content and increase drought tolerance of plants (Freitas et al., 2011; Naseem and Bano, 2014). Since the cultivars in our study have different degrees of drought tolerance, it is hypothesized that they would in turn require different amounts of bacterial exopolysaccharides

to produce a uniform response. The concentration of inoculated bacteria was uniform for all cultivars, which is probably why we see a variety of responses between cultivars.

'Albacete' exhibits a significant up-regulation of number of tips in directly sown inoculated plants, though it has the lowest number of root tips. Comparatively, 'Albacete' is historically the more drought-tolerant cultivar, and while it has the least number of intrinsic root tips, they are the most sensitive to proliferation after inoculation. 'Albacete' also exhibited significantly longer roots for inoculated *in vitro* grown plants.

Longer roots of *A. brasilense*-treated plants grown *in vitro* have also been observed in other species, such as lettuce (Mangmang et al., 2015) and tomato (Botta et al., 2013). In cereals (e.g. sorghum and wheat), on the other hand, inoculation of high concentration of *Azospirillum* was documented to inhibit root elongation (Okon and Kapulnik 1986; Harari et al., 1988), and the effects on root elongation at various bacterial concentrations are recognized to be regulated by phytohormones (Hartmann and Baldani 2006; Cassán et al., 2009). More specifically, Harari et al. (1988) reported that the inconsistency of the effects of *Azospirillum* on root elongation could be the result of the antagonistic actions of IAA and other growth regulators produced by bacteria in any particular condition. Several studies have shown that the beneficial effects of PGPRs are dependent on matching specific strains of PGPR with crop species, specific cultivars, soils, inoculation methods and growing conditions (Chanway et al., 1988; Nowak 1998; Zahir et al., 2003). As such, we can conclude that the interaction between 'Albacete', the concentration of Sp7 and the *in vitro* growing conditions used herein do not induce antagonistic growth regulators, and in fact cause the opposite effect.

The *in vitro* method utilized is specific in that it does not involve nutrient-rich solid or semi-solid media. This situation was elected to circumvent a common side-effect of *in vitro* growth in agar, which has been referenced to have a limited supply of oxygen (O_2), causing poorly formed root hairs and tips (Maene and Dehbergh, 1985; Pierik, 2012). Such growth conditions would have contributed an additional factor affecting root tip number and overall surface area, which is why the bags were employed. In practice, using an agar-free *in vitro* environment was not ideal either, since the bag effect was significant too.

Even still, the treatment effect revealed *in vitro* inoculation of *A. brasilense* Sp7 to significantly augment root surface area and cause a trend for a greater number of tips over controls. Treatment therefore relieves the stress caused by the bags to some extent. The Whirl-pak® bags were sealed and without any oxygen intake or escape, thus creating the possibility for an environment with decreased O_2 concentrations. Situations of low O_2 concentrations *in vitro* are often the catalyst for a number of other disorders, such as excessive ethylene gas accumulation (Hazarika, 2006) and in more serious cases, hyperhydricity, by which the plants suffer decreased protein and chlorophyll contents (Phan and Letouze, 1983; Franck et al., 2004), low phenolics (Perry et al., 1999), increased water content (Bottcher et al., 1988) and altered ion

composition (Kevers and Gaspar, 1986). Ethylene is a plant growth regulator produced by plants under stress, and when it accumulates excessively around roots, this can lead to less hairy root formation (Adkins, 1992)

Finally, if inoculant imbibition were considered a potential factor influencing growth, it is worth mentioning that the cultivar 'Albacete' imbibed the inoculant twice as fast as any other cultivar (Table 1). The attachment of *A. brasilense* to roots is divided into two steps: a weak, reversible and unspecified binding governed by bacterial surface proteins, capsular polysaccharides and flagella; followed by an irreversible attachment phase that happens up to 16h after inoculation, and is mediated by bacterial surface polysaccharides (Zhu et al., 2002). Extracellular polysaccharide production has also been related to the process of flocculation of *Azospirillum* cells (Burdman et al., 1998). *In vitro* growth conditions lack a crucial component in anchoring kinetics (soil), so in the case of 'Albacete,' our results suggest that faster absorption leads to firmer anchoring, regardless of the growing environment. Anchoring may also be more efficient because of the specific chemistry of 'Albacete' seed secretions and the dynamics of extracellular polysaccharides required for *A. brasilense* Sp7 adhesion (Michiels et al., 1991). This precedence is further substantiated by a related study, in which the change in sugar metabolism was found to vary among different barley varieties; and when looking at the main monosaccharides in plant roots, like fructose and glucose, it was apparent that different cultivars had different metabolic sugar adaptations when subjected to stress (Cao et al., 2017). Henceforth, *Azospirillum brasilense* Sp7 colonization of barley cultivars based on sugar secretion levels provides evidence for interaction and should be explored further to understand if that is a function of induced stress response by the bacteria, or by the environment.

To our knowledge, this study is one of the first to classify the relationship between *A. brasilense* Sp7 and these valuable barley cultivars at early stages of growth. 'Barberousse' and 'Plaisant' were the most responsive to *A. brasilense* Sp7 treatment, though 'Plaisant' was perhaps the most intriguing , based on its early vigorous growth regardless of environment and PGPR treatment. 'Orria' is known for having lower biomass and slower proliferation at early growth stages, so is challenging for analyzing the early interaction with *A. brasilense* Sp7 inoculation, irrespective of growing environment. Ideally, the variety should be monitored at later growing times/at yield because of its importance of low biomass to create a more robust grain (I. Romagosa, personal communication, October 18, 2017). 'Albacete' is especially interesting in terms of its physiological interaction with *A. brasilense* Sp7 under conditions of abiotic stress because it is the only cultivar positively affected overall by inoculation *in vitro.*

There is relevance in combining the two growing scenarios tested since they render similar results for both inoculated and non-inoculated plant growth. The *in vitro* technique was useful at the earliest stages of growth since it provided an ongoing, clear image of the intrinsic root behavior of each cultivar during this time. In terms of sampling, advantages to this method

are that conditions can be meticulously controlled, and root analysis is easy to carry out. For one, the clear plastic bag makes it possible to track root growth on a daily basis without destructive sampling. Then at harvest, the roots can be carefully managed and root tips accurately quantified, as there is no need to wash soil from them, which often leads to breakage. However, depending on the objectives of the study, this method may not be ideal since it represents growth in the absence of an exogenous support system, and because its design probably induces abiotic stress with time as oxygen levels decrease. This method is not practical for studies of crops in higher stages of development.

4.6 Conclusions

- Sp7 inoculation increased the length, surface area and number of root tips in both systems and in the four treated cultivars in a similar way
- 'Barberousse' and 'Plaisant' were the most responsive to Sp7 treatment
- 'Albacete' was best protected by Sp7 under abiotic stress imposed by the *in vitro* system
- The utility of the *in vitro* system is only functional if project goals involve root analysis at early phenological stages

4.7 References

Adkins SW (1992) Cereal callus cultures: control of headspace gases can optimize the conditions for callus proliferation. *Australian Journal of Botany* 40:737–749.

Botta AL, Santacecilia A, Ercole C, Cacchio P, del Gallo M (2013) *In vitro* and *in vivo* inoculation of four endophytic bacteria on *Lycopersicon esculentum*. *Nature Biotechnology* 30 (6):666-674.

Bottcher I, Zeglauer K, Goring H (1988) Inducting and reversion of vitrification of plants cultured *in vitro*. *Journal of Plant Physiology* 66:94–98.

Burdman S, Jurkevitch E, Schwartzburd B, Hampel M, Okon Y (1998) Aggregation in *Azospirillum brasilense*: effects of chemical and physical factors and involvement of extracellular components. *Microbiology* 144 (7):1989-1999.

Cai J, Zeng Z, Connor JN, Huang CY, Melino V, Kumar P, Miklavcic SJ (2015) Rootgraph: a graphic optimization tool for automated image analysis of plant roots. *Journal of Experimental Botany* 66 (21):6551-6562.

Cao D, Lutz A, Hill CB, Callahan DL, Roessner U (2017) A quantitative profiling method of phytohormones and other metabolites applied to barley roots subjected to salinity stress. *Frontiers in Plant Science* 7:2070.

Cassán F, Perrig D, Sgroy V, Masciarelli O, Penna C, Luna V (2009) *Azospirillum brasilense* Az39 and *Bradyrhizobium japonicum* E109, inoculated singly or in combination, promote seed germination and early seedling growth in corn (*Zea mays* L.) and soybean (*Glycine max* L.). *European Journal of Soil Biology* 45:28–35.

Chanway CP, Nelson LM, Holl FB (1988) Cultivar-specific growth promotion of spring wheat (*Triticum aestivum* L.) by coexistent *Bacillus* species. *Canadian Journal of Microbiology* 34:925–929.

Comas LH, Eissenstat DM (2009) Patterns in root trait variation among 25 co-existing North American forest species. *New Phytologist* 182:919-928.

Correa OS, Romero AM, Montecchia MS, Soria MA (2007) Tomato genotype and Azospirillum inoculation modulate the changes in bacterial communities associated with roots and leaves. *Journal of Applied Microbiology* 102:781-786.

Creus CM, Graziano M, Casanovas EM, Pereyra MA, Simontacchi M, Puntarulo S, Barassi CA, Lamattina L (2005) Nitric Oxide is involved in the *Azospirillum brasilense*-induced lateral root formation in tomato. *Planta* 221:297-303.

Dobbelaere S, Croonenborghs A, Thys A, Vande Broek A, Vanderleyden J (1999) Phytostimulatory effect of *Azospirillum brasilense* wild type and mutant strains altered in IAA production on wheat. *Plant Soil* 212:153–162.

Döbereiner J, Marriel IE, Nery M (1976) Ecological distribution of *Spirillum lipoferum* Beijerinck. *Canadian Journal of Microbiology* 22 (10):1464-1473.

Franck T, Kavers C, Gaspar T, Dommes J, Deby C, Greimess R, Didier S, Deby-Dupont G (2004) Hyperhydricity of *Prunus avium* shoots cultured on gelreite: a controlled stress response. *Plant Physiology and Biochemistry* 42:519– 527.

Freitas F, Alves VD, Reis MAM (2011) Advances in bacterial exopolysaccharides: from production to biotechnological applications. *Trends in Biotechnology* 29 (8):388- 398.

Harari A, Kigel J, Okon Y (1988) Involvement of IAA in the interaction between *Azospirillum brasilense* and *Panicum miliaceum* roots. *Plant and Soil* 110:275–282.

Hartmann A, Baldani J (2006) The genus *Azospirillum*: In: Dworkin M., Falkow S., Rosenberg E., Schleifer K.-H., Stackebrandt E. (eds): *The Prokaryotes*. New York, Springer.

Hazarika BN (2006) Morpho-physiological disorders in *in vitro* culture of plants. Review. *Scientia Horticulturae* 108:105-120.

Kamnev A, Tugarova AV, Tarantilis PA, Gardiner PHE, Polissiou MG (2011) Comparing poly-3-hydroxybutyrate accumulation in *Azospirillum brasilense* strains Sp7 and Sp245: The effects of copper (II). *Applied Soil Ecology* 61:213-216.

Kevers C, Gaspar T (1986) Vitrification of carnation *in vitro*: changes in water content, extra cellular space, air volume and ion levels. *Chemistry of Vegetable Physiology and Agriculture* 24:647–653.

Lancashire PD, Bleiholder H, Langelüddecke P, Stauss R (1991) A uniform decimal code for growth stages of crops and weeds. *Annals of Applied Biology* 119: 561-601.

López-Castañeda C, Richards RA(1991) Variation in temperate cereals in rain-fed environments III. Water use and water-use efficiency. *Field Crops Research* 39:85-98.

Maene LJ, Debergh PC (1985) Liquid medium additions to establish tissue cultures to improve elongation and rooting *in vivo*. *Plant Cell, Tissue and Organ Culture* 5:23-33.

Mangmang J, Deaker R, Rogers G (2015) Response of lettuce seedlings fertilized with fish effluent to *Azospirillum brasilense* inoculation. *Biological Agriculture and Horticulture Journal* 31:61-71.

Michiels KW, Croes CL, Vanderlayden J (1991) Two different modes of attachment of *Azospirillum brasilense* Sp425 to wheat roots. *Journal of General Microbiology* 137:2241-2246.

Muñoz P, Voltas J, Araus JL, Igartua E, Romagosa I (1998) Changes over time in the adaptation of barley releases in north-eastern Spain. *Plant Breeding* 17:531-535.

Muthukumarasamy R, Revathi G, Loganathan P (2002) Effect of inorganic N on the population, *in vitro* colonization and morphology of *Acetobacter diazotrophicus* (syn *Gluconacetobacter diazotrophicus*). *Plant and Soil* 243:91–102.

Muthukumarasamy R, Revathi G, Lakshminarasimhan C (1999) Diazotrophic associations in sugar cane cultivation in South India. *Journal of Tropical Agriculture* 76:171-8.

Naseem H, Bano A (2014) Role of plant growth-promoting rhizobacteria and their exopolysaccharide in drought tolerance of maize. *Journal of Plant Interactions* 9:689–701.

Nowak J (1998) Benefits of in vitro "biotization" of plant tissue cultures with microbial inoculants. *In Vitro Cellular & Developmental Biology – Plant* 34:122–130.

Okon Y, Kapulnik Y (1986) Development and function of *Azospirillum*-inoculated roots. *Plant and Soil* 90:3–16.

de Oliveira ALM, de Canuto EL, Urquiaga S, Reis VM, Baldani JI (2006) Yield of micropropagated sugarcane varieties in different soil types following inoculation with diazotrophic bacteria. *Plant Soil* 284:23-32.

Omar MNA, Osman MEH, Kasim WA, El-Daim IAA (2000) Improvement of salt tolerance mechanisms of barley cultivated under salt stress using *Azospirillum brasilense.* In: Ashraf M, Ozturk M, Habib-ur-Rehman A (eds) *Salinity and water stress improving crop efficiency*. Springer, Dordrecht, pp 133–147.

Perry PL, Ueno K, Shetty K (1999) Reversion to hyperhydration by addition of antibiotics to remove *Pseudomonas* in unhyperhydrated oregano tissue culture. *Process Biochemistry* 34:717–723.

Phan CT, Letouze R (1983) A comparative study of chlorophyll, phenolic and protein contents, and hydroxycinnamate. CoA ligase activity. *Plant Science Letters* 36:323–327.

Pierik RLM (2012) *In vitro* culture of higher plants. *Springer Science and Business Media*.

Rashid KN (2014) *The Response of wheat genotypes to inoculation with Azospirillum brasilense*. University of Sydney, Camperdown NSW, Australia.

dos Reis Junior BF, Massena Reis V, Urquiaga S, Dobereiner J (2000) Influence of nitrogen fertilisation on the population of diazotrophic bacteria *Herbaspirillum* spp. and *Acetobacter diazotrophicus* in sugar cane (*Saccharum* spp.). *Plant and Soil* 219:153–159.

Siddique KHM, Belford RK, Perry MW, Tennant D (1989) Growth, development and light interception of old and modern wheat cultivars in a Mediterranean-type environment. *Australian Journal of Agricultural Research* 40:473-487.

Spaepen S, Vanderleyden J (2011) Auxin and Plant-Microbe Interactions. *Cold Spring Harbor Perspectives in Biology* 3:a001438.

Tarrand JJ, Krieg NR, Dobereiner J (1978) A taxonomic study of the *Spirillum lipoferum* group, with descriptions of a new genus, *Azospirillum* gen. nov. and two species, Azospirillum lipoferum (Beijerinck) comb. nov. and *Azospirillum brasilense* sp. nov. *Canadian Journal of Microbiology* 24:967–980.

Teulat B, Merah O, This D (2001) Carbon Isotope Discrimination and Productivity in Field-grown Barley Genotypes. *Journal of Agronomy Crop Science* 187:33-39.

Vacheron J, Desbrosses G, Bouffaud ML, Touraine B, Moenne-Loccoz Y, Muller D, Legendre L, Wisniewski-Dye B, Prigent-Combaret C (2013) Plant growth-promoting rhizobacteria and root system functioning. *Frontiers in Plant Science* 4 (356):1-19.

Vacheron J, Renoud S, Muller D, Babalola OO, Prigent-Combaret C (2015) Chapter 19: Alleviation of Abiotic and Biotic Stresses in Plants by *Azospirillum.* In: Cassán FD, Okon Y, Creus CM (eds) *Handbook for Azospirillum*. Springer International Publishing, Switzerland, pp 333-365.

Voltas J, Romagosa I, Lafarga A, Armesto AP, Sombrero A, Araus JL (1999) Genotype by environment interaction for grain yield and carbon isotope discrimination of barley in Mediterranean Spain. *Australian Journal of Agricultural Research* 50:1263–1271.

Yau SK (2016) *Vernalization Requirement of Lebanese Barley Landraces*. Retrieved from http://wheat.pw.usda.gov/ggpages/BarleyNewsletter/42/yau.html. Access date April 2017.

Zahir ZA, Muhammad A, Frankenberger Jr WT (2003) Plant growth-promoting rhizobacteria: applications and perspectives in agriculture. *Advances in Agronomy* 81:97–168.

Zawoznik MS, Vázquez SC, Díaz Herrera SM, Groppa MD (2014) Search for endophytic diazotrophs in barley seeds. *Brazilian Journal of Microbiology* 45 (2):621-625.

Zhu GY, Dobbelaere S, Vanderleyden J (2002) Use of green florescent protein to visualize rice root colonization by *Azospirillum irakense* and *A. brasilense. Functional Plant Biology* 29 (11):1279-1285.

CHAPTER 5

Host-specific proteomic and growth analysis of maize and tomato seedlings inoculated with *Azospirillum brasilense* Sp7

(Published in Plant Physiology and Biochemistry, 2018, 129:381-393. Annex 3)

Chapter 5. Host-specific proteomic and growth analysis of maize and tomato seedlings inoculated with *Azospirillum brasilense* Sp7

5.0 Abstract

Azospirillum brasilense Sp7 (Sp7) is a diazotrophic, free-living plant growth-promoting rhizobacterium (PGPR) that is increasingly used for its ability to reduce stress and improve nutrient uptake by plants. To test the hypothesis that Sp7 interacts differently with the primary metabolism in C_3 and C_4 plants, differential proteomics were employed to study weekly protein expression in Sp7-treated maize *(Zea mays cv.* B73) and tomato (*Solanum lycopersicum* cv. Boludo) seedlings. Plant and root growth parameters were also monitored. Protein changes were most striking at the four-leaf stage (T1) for both species. Proteins related to metabolism and redox homeostasis were most abundant in tomato at T1, but later, plants experienced inhibited CB cycle and chloroplast development, indicating that perhaps photosynthetic proteins were damaged by reactive oxygen species (ROS). In maize, Sp7 first increased ROS-scavenging enzymes and decreased those related to metabolism, which ultimately reduced photoinhibition at later sampling times. Overall, the early interaction with maize is more complex and beneficial because the photosynthetic apparatus is protected by the C_4 mechanism, thereby improving the interaction of the PGPR with maize. Better seedling emergence and vigor were observed in inoculated maize compared to tomato too. This study provides an integrated perspective on the Sp7 strain-specific interactions with young C_3 and C_4 plants to modulate primary metabolism and photosynthesis.

5.1 Introduction

Azospirillum brasilense is one of the most well characterized free-living diazotrophic plant growth promoting rhizobacteria (PGPR) (Tarrand et al., 1978) that has been studied as an inoculant for both extensive and intensive cropping systems, and in multiple environments. The inoculation of *A. brasilense* to seeds and plants augments proliferation of lateral and adventitious roots, and increases the dry weight of root systems and plant aerial parts to significantly improve development, flowering and harvest output (Dobbelaere et al., 2001).

The principle mode of action of *A. brasilense* is production and liberation of regulatory vegetative growth substances directly affecting plant metabolism (Glick, 2012). Furthermore, biological nitrogen fixation (BNF) by this bacterium in plant tissues results in increased plant biomass and grain production (Cassán et al., 2009). Both organisms change their metabolic routines to accommodate each other's needs (Mus et al., 2016). Bacterial nitrogen metabolism must be altered so that nitrogen is excreted rather than incorporated into the microbial biomass, while the plant host directly interferes with bacterial amino acid biosynthesis, forcing the release of nitrogen as ammonia (NH_3) (Lodwig et al., 2003). These processes are especially impressive when considering that C_3 and C_4 photosynthetic pathways differ significantly in their levels of dependence on N-metabolism (Wang et al., 2014).

From molecular studies of plant-PGPR interactions, it is known that *Azospirillum* spp. affects primary and secondary plant metabolism both above and below ground (Beimalt and Sonnewald, 2006). To do so, the PGPR mainly alters the root enzymes, changing patterns of root exudation and stimulating levels of carbon compounds in root exudates (Lavania et al., 2006), as in the field-inoculation of maize with single or combined applications of *Azospirillum* and other PGPRs such as *Rhizophagus* that has led to modifications of secondary root metabolites (Walker et al., 2012). This modification effect has been surmised to represent an attempt by the bacteria to manipulate plant metabolism to gain access to nutrients (Parra-cota et al., 2014).

In the past, many studies claimed that *A. brasilense* has a higher affinity for C_3 plants, and C_4 plants are supposedly better colonized by other species such as *A. lipoferum* (Mengel and Viro, 1978; Reynders and Vlassak, 1982). Contemporary reviews have, however, cautioned that older studies are representative of historical assumptions likely related to the original isolation of *A. brasilense* from cereals and subsequent experimentation performed mostly on them (Pereg et al., 2016).

There are various *A. brasilense* strains, differing in their habitat and capacities as PGPR. Some of them are endophytic, such as *A. brasilense* Sp245, which is now considered as the type strain for this species (Baldani et al., 1986); but others like Sp7 are epiphytic, which was previously considered to be the type strain for the species (Tarrand et al., 1978). Sp7 responds strongly to the soil environment, sensing stress and contaminants more acutely (Kamnev et al.,

2012). Therefore, Sp7 has more potential to protect plants from soil pathogens since it blocks rhizospheric pathogen-plant interaction zones (Pereg 2015).

Special focus was given to the early vegetative phase of development because previous studies working with field-grown crops and *Azospirillum* demonstrated bacteria viability and density to be unchanged for 30 days post-sowing, then to sharply decline and be negligible 57 days post-sowing (El Zemrany *et al.,* 2006). There are, however, limited studies reporting the timing of proteomic changes taking place within the first 30-35 days. One of the most comprehensive studies on the maize proteome relays the proteomic profile of a nine-day old plant (at the 2-leaf stage) (Majeran *et al.*, 2010). The study provides a well-defined molecular template for the structural and metabolic transitions that occur during C_4 leaf differentiation. Considering changes in the maize rootzone has also been an important field of study because the maize root system is composed of various embryonic and postembryonic root types. Regardless, all of these roots form lateral roots, which have influence over the proteome composition of the primary root (Hochholdinger et al., 2004). Proteomic studies regarding tomato are more scant. For one, studies focusing on tomato proteome changes during early growth are virtually non-existant. The few that analyze the effects of PGPR on the proteome have found that PGPR promoted plant growth whilst improving redox status by means of increased glutathione ascorbate (GSH) (Ibort et al., 2018). Finally, in comparing maize and tomato, perhaps one of the most relevant and intriguing findings is that PGPR leads to attenuation of defense responses in maize to allow for colonization, while they activate defense responses in tomato (Shivaprasad et al., 2012; Thiebalt et al., 2014).

In this study, we attempt to establish expression trends of protein functional groups in C_3 (tomato), and C_4 (maize) plants inoculated with *A. brasilense* strain Sp7 (ATCC 29145), and test the hypothesis that Sp7 interacts differently with the primary metabolism of the two types of plants. For this, differential proteomics has been employed to quantify changes during early stages of Sp7-treated plant development. This data is compared with plant growth and physiological parameters.

5.2 Aims

- Determine how Sp7 interacts with the primary metabolism in C_3 and C_4 plants via proteomic analysis
- Compare proteomic results with gas exchange parameters to effectively interpret metabolic changes caused by Sp7 in C_3 and C_4 plants

5.3 Material and Methods

5.3.1 Experimental design

Two completely randomized single factor experiments were started with maize (*Zea mays* L., Mill. cv. B73) and tomato (*Lycopersicon esculentum* L., cv. Boludo) seeds. There were two treatment groups (20 biological replicates) per species. Treatments were: 1) the control (C), seeds soaked in sterile phosphate-buffered saline (PBS), and 2) seeds soaked in the same buffer, incorporating Sp7 (Sp7).

Sampling began at the four-leaf stage, principal growth stage 14 for both maize and tomato according to the BBCH scale, (Lancashire et al., 1991). Samples were taken weekly until stage 19, corresponding to late tillering. These sampling times corresponded to 16 (T1), 23 (T2), 30 (T3) and 35 (T4) days post-inoculation (dpi) for maize and 14 (T1), 21 (T2), 28 (T3) and 35 (T4) dpi for tomato. Physiologically, T1 coincided with the four-leaf stage, T2 with early tillering or the seven-leaf stage, and T3 and T4 with late tillering or the 9-12 leaf stages.

5.3.2 *Azospirillum brasilense* Sp7 inoculum preparation and inoculation

The *Azospirillum brasilense* Sp7 inoculum was prepared as described in Chapter 3 (Section 3.3.3.) (Bashan et al., 1993). Inoculation time and quantity were established according to an imbibition curve, estimating the time taken for each seed variety to imbibe 70% of its total potential. Seeds were surface sterilized with 4% NaOCl for 10 min (with constant agitation) and washed six times with SDW in a laminar flow hood. They were dried and inoculated with the rhizobacteria by imbibition.

5.3.3 Plant growth

Seeds were sown in 1L pots containing autoclaved commercial substrate (Traysubstrat®, Klasmann-Deilmann, Gmbh, Geeste, Germany) characterized by having an extra fine structure and pH 6. Plants were then grown under greenhouse conditions 18-25%RH, 25-30ºC, with supplementary lighting (12h photoperiod) and protected from insect attack by an anti-aphid mesh and automatic drip irrigation (1h, twice per day).

5.3.4 Growth analysis and bacterial recovery

For aerial parameters, the height of 10 random plants was measured per treatment and sample time. For root analysis, three plants were randomly chosen per treatment and sample time. The root mass was carefully washed with distilled water and stored in 70% ethanol at 4ºC until analysis. They were then scanned using an Epson Perfection V700 scanner. The images were analyzed with the WinRHIZO® program (Regent Instruments Inc., Quebec, ON, Canada, 2009).

Sp7 colonization assays were conducted at harvest of each sampling time, with three random samples taken from each treatment. The procedure was carried out according to Botta et al. (2013) with modifications. One hundred grams of plant roots were homogenized in 1mL sterile physiological solution (NaCl 0.9%). The homogenate was then serially diluted and plated in Petri dishes containing sterile nitrogen-free broth medium (NFb) supplemented with 15mL/L of 1:400 aqueous solution of Congo-red (CR) (Bashan et al., 1993). Bacterial colonies were counted after 48h incubation at 32°C. Controls were replicated in the same manner.

5.3.5 Leaf gas exchange parameters

Leaf gas exchange was monitored with an infrared gas analyzer (LI-6400XT LICOR Inc., Nebraska, USA) at the same hour (14h), at each sampling time. Measurements were taken of leaf CO_2 assimilation rate (A), transpiration rate (E) and intercellular CO_2 concentration (C_i) and instantaneous water-use efficiency (WUE_i [A/E]).

5.3.6 Total protein extraction

One gram of leaf tissue was collected per plant for each sampling time (3 plants per treatment), immersed in liquid nitrogen and stored at -80ºC. Each sample was measured to 0.1g and ground with 2mL of 10% trichloroacetic acid (TCA) in acetone + 20mM dithriothreitol (DTT) and a protease inhibitor (complete ULTRA Tablets, Mini, EDTA-free, EASYpack, Sigma) was added and mixed by vortex (Xu et al., 2008). After centrifugation at 14,000rpm and 4ºC for 30min, the supernatant was discarded, and the pellet washed three times with 2mL acetone + 20mM DTT, then air dried on ice (10-30min). The total protein was eluted in 100-250µL lysis buffer (PER 4, Sigma) and the total protein content was measured by the Bradford method (Bio-Rad Protein Assay Dye Reagent Concentrate) using bovine serum albumin (BSA) as a standard. Absorbance was measured at OD_{600}, using an Amersham Biosciences (Ultraspec 3100 Pro) spectrophotometer.

5.3.7 Protein analysis

Total protein extracts were measured to 100µg and separated by 2D-PAGE analytical gels. Three biological replicates were collected for each treatment. For preparative gels, 500µg of protein were used. Samples were mixed with rehydration buffer [7M urea, 2M thiourea, 1% C7BzO detergent, 40mM Trizma Base, 50mM DTT, 1% IPG buffer pH 3-10, and 0.002% bromophenol blue] in a total volume of 200µL. Isoelectric focusing (IEF) of passively rehydrated 18cm IPG strips (pH 5-8) was performed in a Protean IEF Cell system (Bio-Rad) following the manufacturer's instructions. IEF used a sequential gradient procedure of 50 V/20 C/14h. The current limit was 50µA per IPG strip. Focused strips were stored at -80ºC until the second dimension was performed. After IEF separation, the gel strips were incubated for 15min

in the equilibration buffer [375mM Trizma base, 6M urea, 20% glycerol, 2% SDS] containing 2% DTT, followed by 15min in the same buffer containing 2.5% iodoacetamide instead of DTT. Two equilibrated 18cm gel strips were loaded in each 12.5% polyacrylamide gel (22cm x 20cm x 1mm) for the second-dimension separation in an Ettan DALTsix Electrophoresis Unit (GE Healthcare). Electrophoresis was carried out in SDS-PAGE gels of 12.5%. Gels were stained with Flamingo™ Gel fluorochrome (Bio-Rad) according to the manufacturer's instructions. Images were acquired with the Versadoc MP4000 system (Bio-Rad) (Cueto-Ginzo et al., 2016).

5.3.8 Protein digestion and MS analysis

Selected spots were manually excised from gels, digested with trypsin using 96-well perforated plates and a MultiScreen™ HTS Vacuum Manifold (Millipore). Each gel piece containing the protein was minced, washed twice with deionized water and dehydrated with 50% ethanol in 50mM NH_4HCO_3 for 10min, and then with 100% ethanol for 10min. Gel pieces were then reduced with 10mM DTT in 50mM NH_4HCO_3 for 1h at 56ºC and alkylated with 55mM iodoacetamide in 50mM NH_4HCO_3 for 30min at room temperature in the dark. The gel pieces were washed twice in 50mM NH_4HCO_3 for 15min and dehydrated with 5% acetonitrile (ACN) in 25mM NH_4HCO_3 for 15min, twice with 50% ACN in 25mM NH_4HCO_3 for 15min, and finally with 100% ACN for 10min. After total ACN evaporation, 15µL of 20ng.µL^{-1} trypsin in 25mM NH_4HCO_3 was added and left at 4 ºC for 45 min to allow for full rehydration of the gel pieces. The gel pieces were then covered with 25mM NH_4HCO_3 and incubated at 37ºC overnight for proteolysis. Eluted peptides were then transferred to a new Eppendorf tube, and 1µl of the digested protein was used for a first peptide mass fingerprint (PMF) analysis. If necessary, the minced gel was washed three more times with 0.25% trifluoroacetic acid (TFA) in 50% v/v ACN, twice with 100% ACN, evaporated in a SpeedVac and then re-suspended in 5µL of 70% ACN- 0.1% TFA to collect remaining peptides. 1µL peptide solution was spotted per well on a MALDI target and allowed to evaporate at room temperature before being covered with 1µL of a saturated solution of a-cyano-4-hydroxycinnamic acid prepared in 50% v/v ACN containing 1% TFA. Mass calibrations were carried out using a standard peptide mixture. Mass spectra were acquired using Autoflex™ Speed MALDI-TOF/TOF mass spectrometer (Bruker Daltonics) (Cueto-Ginzo et al., 2016).

Protein identification was performed using MALDI-TOF mass fingerprint (PMF) and MALDI-TOF/TOF. PMF and MS/MS spectra were compared against SwissProt, NCBI and TrEMBL databases, using the search engine MASCOT algorithm (Version 2.4, Matrix Science, London, UK).

5.3.9 Statistical analysis

Growth data were statistically processed using a one-way ANOVA for each sampling time. Bradford protein quantification was assessed in the same way. The analysis was prepared with JMP® 12.1 (SAS Institute Inc.), and graphics were created with Apache OpenOffice 4.1.3 in OS X Yosemite 10.10.5. An F-ratio of 0.05 for a One-way ANOVA was used to evaluate the difference between averages.

Spot detection and gel analysis were first conducted with the PDQUEST program (Bio-Rad) and the second time, manually. Normalization was performed with the LOESS regression model. Only the spots present on all of the gel replicates were used for statistical analysis. Ratios between two expressed conditions were calculated as the mean of three independent values for each spot from the 2D gel electrophoresis analysis ± standard error. Standard error for each spot was calculated according to the following guidelines: 1) there must be a variation coefficient ≤ 50% among replicates, 2) spots must be present in all measured conditions, 3) expression ratios must be ≤0.5 or ≥ 2.0, and 4) spots must be validated *in visu*. Spots lacking quantitative signal, high quantitative variation between replicates, or with mixed proteins, were not considered for the analysis.

For each species and each sampling time, each protein population (spot) was quantified based on the average of the three biological replicates and then log2 transformed to normalize the data. Finally, to streamline data interpretation and increase analysis power, a stringent fold-change threshold of 2/-2 was used to control the false discovery rate, but in the case that no proteins reached this threshold (which was the case at T2 and T3), the boundary was slackened to 1.5/-1.5-fold change.

Proteins were categorized into the various functional groups: 1) photosynthesis, respiration, and chloroplast organization; 2) redox homeostasis and stress response (defense); 3) protein synthesis, conformation and transport; 4) metabolism and energy; 5) pathogenic cell lysis; 6) resistance; and 7) with unknown or not yet established function (Tables 7 and 8).

Table 7. Main characteristics and function of identified maize proteins corresponding to spots in Fig. 19(a).

SSP [a]	Protein name	Accession No. [b] (database)	Molecular Weight (Da)/pI [c]	Coverage %	No Peptides Matched/Total peptides	Score [d]	Function [e]
210	Chaperonin	ACG33530**	25559/8.67	64	12/27	160	4
402	Phosphoribulokinase Sedoheptulose-1,7-bisphosphatase	B4FQ59*** B6T2L2***	45121/5.84 42303/6.08	76 66	28/74 28/74	260 219	3,4
504	Phosphoglycerate kinase	NP_001147628**	50009/6.07	61	33/49	283	2
2103	Chlorophyll a-b binding protein 8	NP_001148598.2**	28966/8.94	13	3/3	210	1,2
2705	ATP synthase subunit beta, mitochondrial	P19023*	59181/6.01	44	24/76	156	1
3104	Cytochrome b6-f complex iron-sulfur subunit	B4FTU7***	21026/6.41	10	3/4	154	1
3205	-						7
3303	Fructose-biphosphate aldolase	ACG36798.1**	41924/7.63	64	26/73	248	4
4105	Germin-like protein	Q6TM44***	22101/6.02	13	2/2	166	2,4
4201	Lactoylglutathione lyase	ACG39003**	35311/6.62	47	21/37	201	2
4402	Malate dehydrogenase, cytoplasmic	NP_001105603**	35909/5.77	68	24/45	263	1
4601	Hypothetical protein	NP_001142788**	51917/6.12	51	24/41	271	7
4602	Methionine adenosyltransferase	AFW82691**	46392/6.03	63	26/50	292	4
5001	Ribulose-1,5-bisphosphate carboxylase/oxygenase small subunit	CAA70416**	19364/8.98	69	13/54	153	1
5103	Ribosome recycling factor	NP_001150478**	29328/9.22	29	8/16	419	7
5104	Dip protein ABA- and ripening-inducible-like protein	ABW06773.1**	15905 X	25	2/2	160	2
5203	TPA: glutathione transferase	DAA51780**	25584/6.21	45	17/38	181	2
5602	Bifunctional 3-phosphoadenosine 5-phosphosulfate synthetase 2	NP_001147427**	52493/8.30	43	22/31	242	1
5608	Plastid ADP-glucose pyrophosphorylase large subunit	NP_001106017**	55600/8.57	71	40/56	464	2,4
5704	ATP synthase CF1 alpha subunit	NP_043022**	55729/5.87	49	31/41	392	1
6001	Cytochrome b6-f complex iron-sulfur subunit	ACG28186**	24321/8.52	41	10/20	152	1,2
6102	TPA: hypothetical protein ZEAMMB73_927356	DAA59517**	32073/9.50	48	12/34	159	7
6307	NAD-dependent epimerase/dehydratase	B4FH62***	31917/9.11	66	20/24	340	4
6503	Fructose-bisphosphate aldolase, cytoplasmic isozyme 1	B6SSU6***	38464/6.26	54	18/21	292	1
6713	ATP synthase CF1 alpha subunit	NP_043022**	55729/5.87	63	37/46	495	1,4
7103	Chain A, Structure Of Glutathione S-Transferase Iii In Apo Form	1AW9_A**	23416/5.97	68	11/27	166	2
7202	NAD-dependent epimerase/dehydratase	B6T962***	27809/6.77	60	18/21	306	2
7607	Putative uncharacterized protein	B4FHK4***	42290/6.53	43	23/34	263	7
3801 3807	Transketolase	Q7SIC9 *	73347/5.47	65	46/72	449	1,4
8001	Ribulose bisphosphate carboxylase small chain, chloroplastic precursor	NP_001105294**	19310/9.10	62	18/61	166	1
8002	Photosystem I reaction center subunit IV A	ACG26704.1**	14885/9.79	7	1/1	56	1
8101	Putative peptidyl-prolyl cis-trans isomerase family protein	NP_001136688**	26599/X	X	12/X	135	2,4
8401	Glyceraldehyde-3-phosphate dehydrogenase 1 Glyceraldehyde-3-phosphate dehydrogenase A Glyceraldehyde-3-phosphate dehydrogenase 2	P08735* P09315* Q09054*	36614/6.46 43182/7.00 36633/6.41	48 48 46	19/55 18/55 16/55	178 166 135	2,4
8602	Alanine aminotransferase 2	NP_001151209*	53716/6.73	39	24/37	255	4
6706 6714	Beta-glucosidase2	AFW56713**	64308/6.75	47	35/43	423	5
3802 3805 4801 4802	NADP-dependent malic enzyme, chloroplastic precursor	NP_001105313**	70293/6.09	53	43/78	353	1,4
6409 7403 7404	Glyceraldehyde-3-phosphate dehydrogenase A, chloroplastic precursor	NP_001105414**	43182/7.00	61	25/46	264	4

a. Spot numbers refer to Fig. 3a identified either by fingerprint mass spectrometry MS (MALDI-TOF) or by MS/MS (MALDI TOF-TOF).
b. Accession number and molecular mass according to SwissProt (us.expasy.org/sprot)*, NCBI** and TrEMBL*** databases.
c. MW and pI were calculated from aminoacid sequence.
d Scores of proteins identified by peptide mass fingerprinting were determined according to Mowse values obtained either from MASCOT.
e. (1) Photosynthesis, respiration, and chloroplast organization; (2) Redox homeostasis and stress response (defense); (3) Protein synthesis, conformation and transport; (4) Metabolism and energy; (5) Pathogenic cell lysis; (6) Resistance (7) Unknown.

Table 8. Main characteristics and function of identified tomato proteins corresponding to spots in Fig. 19(b).

SSP [a]	Protein name	Accession No. [b] (database)	Molecular [c] Weight (Da)/pI	Coverage %	No Peptides Matched/Total peptides	Score [d]	Function [e]
1202	Chlorophyll a-b binding protein 3C	P07370 *	28225/5.15	3	1/7	31	1
2001	Cytochrome b6-f complex iron-sulfur subunit	Q69GY7 *	24593/8.20	6	1/5	33	1
2004	Ribulose bisphosphate carbox. small chain 2A	P07179 *	20493/6.59	48	11/46	134	1
5307 6206	Fructose-bisphosphate aldolase 2	XP_004233550 **	42872/6.07	53	18/47	203	1,4
2901 2902	Heat shock cognate protein 70 protein 1-like	XP_004250958 **	71498/5.10	52	31/44	301	3
3002	Glycine-rich RNA-binding protein-like isoform 3	XP_004230945 **	16386/5.27	71	15/29	215	6
3702	ATP synthase subunit alpha	Q2MIB5 *	55434/5.14	42	25/42	296	4
3709	Inositol-3-phosphate synthase	XP_004239994 **	56697/5.45	46	25/75	159	2
3802 3906 4908	ATP-dependent Clp protease ATP-binding subunit clpA homolog CD4B	XP_004252280 **	102418/5.99	43	40/56	379	4
4002 4003	Superoxide dismutase [Cu-Zn]	P14831 *	22328/5.77	12	2/2	132	2
740 7504	Ribulose bisphosphate carbox./oxygenase activase 1	O49074 *	50897/8.61	50	26/56	245	1
4606	Glutamate-1-semialdehyde 2,1-aminomutase	NP_001234690 **	51722/6.54	48	26/43	235	3
5001	ATP synthase epsilon chain	Q2MI94 *	14571/5.43	63	10/36	144	2,4
5201	BG125080.1 EST470726 tomato shoot/meristem	BG125080 ***	25967/9.18	6	3	297	3
5302	Ferredoxin--NADP reductase	XP_004232495 **	40774/8.37	61	27/39	270	1,2
5405	Phosphoglycerate kinase	XP_004243968**	50592/7.66	11	4/4	211	4
5901 5902	Transketolase	XP_004248560 **	80268/5.97	46	33/52	347	4
6101	Chlorophyll a-b binding protein 8	XP_004248217 **	29261/8.65	15	2/2	237	1
6208	Thioredoxin-like protein CDSP32	XP_004238392 **	33779/7.57	18	6/6	241	2
6304	mRNA binding protein precursor	NP_001234656 **	44084/7.10	38	21/45	228	6
6403	Malate dehydrogenase	XP_004247734 **	35703/5.91	72	24/53	259	1
6404	Monodehydroascorbate reductase-like	XP_004246547 **	47106/5.77	72	29/39	386	2,3
6406	ATP synthase gamma chain	XP_004232711**	41752/8.15	13	3/6	224	4
6505	S-adenosylmethionine synthase 3	NP_001234004 **	43082/5.76	60	26/44	276	4
6509 7508	GDP-mannose 3',5'-epimerase	NP_001234734 **	42828/5.88	45	21/32	248	4
7913	Glycine dehydrogenase [decarboxylating]	XP_004245101**	114020/6.69	5	5/5	199	1
7402 7405 8404	Chloroplast stem-loop binding protein of 41 kDa b	XP_004241412 **	42596/7.67	60	23/29	321	1
8404	Glyceraldehyde-3-phosphate dehydrogenase A	XP_004236849 **	42940/8.46	58	23/60	234	1
7906	5-ethyltetrahydropteroyltriglutamate--homocysteine methyltransferase-like	XP_004249374 **	85014/6.01	39	26/35	319	4
8101	BP903052.1 Solanum lycopersicum cDNA, clone	BP903052 ***	17598/6.99	56	10/40	134	7
8107	Triose phosphate isomerase (cytosolic isoform)	AAR11379 **	27251/5.73	11	2	155	4
8114	Protein thylakoid formation1	XP_004243305**	33558/8.69	7	3/3	50	3
8401	Glyceraldehyde-3-phosphate dehydrogenase	NP_001266254 **	32097/5.93	56	15/22	192	1,4
8506	Isocitrate dehydrogenase [NADP]-like	XP_004228607 **	47001/6.35	56	24/26	327	4
8509	S-adenosylmethionine synthase 2-like	XP_004249481**	43089/6.12	8	3/3	102	4
8602	Dihydrolipoamide dehydrogenase precursor	NP_001234770 **	53120/6.90	51	22/30	264	2,4

a. Spot numbers refer to Fig. 3a identified either by fingerprint mass spectrometry MS (MALDI-TOF) or by MS/MS (MALDI TOF-TOF).
b. Accession number and molecular mass according to SwissProt (us.expasy.org/sprot)*, NCBI** and TrEMBL*** databases.
c. MW and pI were calculated from aminoacid sequence.
d Scores of proteins identified by peptide mass fingerprinting were determined according to Mowse values obtained either from MASCOT.
e. (1) Photosynthesis, respiration, and chloroplast organization; (2) Redox homeostasis and stress response (defense); (3) Protein synthesis, conformation and transport; (4) Metabolism and energy; (5) Pathogenic cell lysis; (6) Resistance (7) Unknown.

5.4 Results

5.4.1 Colonization of *Zea mays* cv. B73 and *Solanum lycopersicum* cv. Boludo

Sp7 was detected on the root systems of maize and tomato plants seven days after inoculation. The number of Sp7 colonies from the surface sterilized roots of the plants was 10^5 cfu/g of moist root, confirming that the bacteria had indeed colonized the plants. In contrast, no *A. brasilense* colonies were observed in non-inoculated plants.

5.4.2 Plant growth parameters

Significant differences ($p<0.01$) between the heights of maize (B73) seedlings treated with Sp7 and corresponding control (C-) seedlings were observed when the plants were further developed (T3). In tomato, there was a highly significant ($p<0.001$) height difference between C- and Sp7 treated seedlings for T2, T3 and T4 (Figures 17a & 17b).

In terms of root length, there was highly significant variation between C- and Sp7-treated plants at T1 in maize (Figure 17c & 17d) and significant differences at T2 and T3. In tomato (Figure 17c & 17d) there was no significant difference between treatments at T1, though there were at T2 and T3.

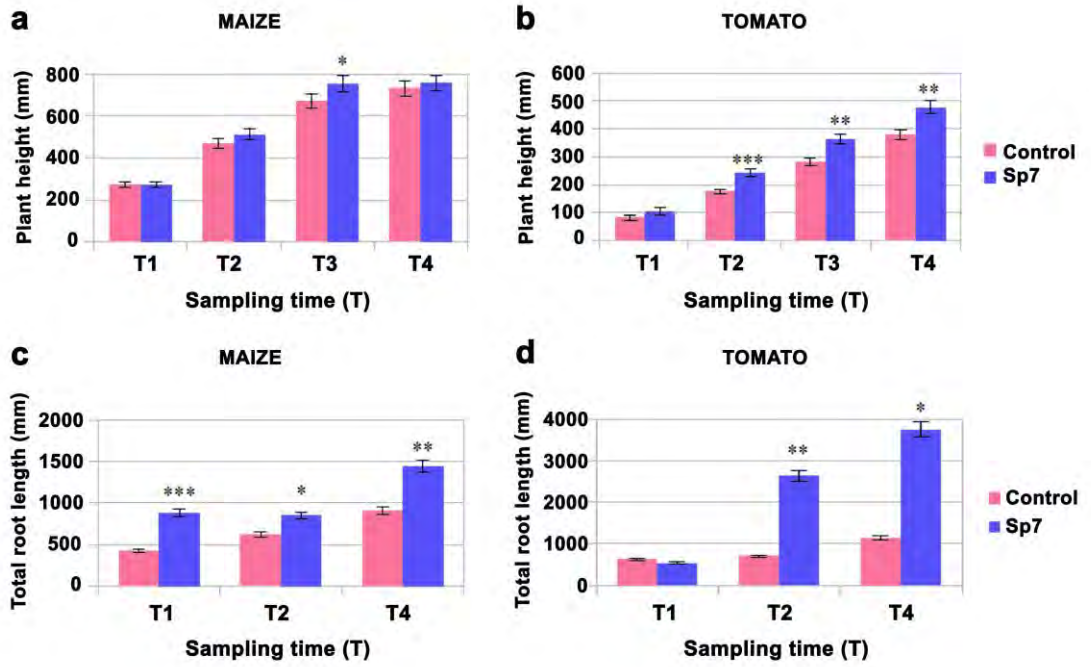

Figure 17. Plant height and root length. (a & b) Plant height (mm) of (a) maize and (b) tomato treated with *Azospirillum brasilense (*Sp7) *versus* control at different sampling times (T). (c & d) Root length (mm) of (c) maize and (d) tomato treated with Sp7 *versus* control. Asterisks indicate statistically significant differences between treatments for each sampling time: * ($p<0.05$), ** ($p<0.01$), *** ($p<0.001$).

5.4.3 Gas exchange is modulated by *A. brasilense* Sp7 treatments

In maize, changes in plant behavior induced by Sp7 were more immediate than those of tomato regarding augmenting photosynthesis. At T2 in maize, the photosynthetic rate (A) was significantly increased by Sp7 (Figure 18a). In tomato, A was similar between C- and Sp7 plants, until T3 and T4. At T3, the rate of Sp7 plants fell to be 66% lower than C- plants ($p<0.001$).

Differences in transpiration levels (E) (Figure 18b) were not apparent at T1 in either species. Sp7 maize plants transpired at a higher rate than C- plants throughout, reaching highly

significant values ($p<0.001$) at T3. In tomato, C- plants transpired 26% ($p<0.01$) more than Sp7 ones at T4.

Intercellular CO_2 concentrations (C_i) inversely reflect photosynthetic rates at T2 and T3 (Figure 18c). In maize, Sp7 plants had significantly higher ($p<0.01$) C_i T2. Then at T3 an T4, the opposite is true; as C- plants have significantly higher C_i In tomato, C_i concentrations were similar in Sp7 and C- plants at T1 and T4, but during the T2 and T3, Sp7 tomato plant C_i levels were 20-27% lower than C- plants ($p<0.05$). Instantaneous water use efficiency (WUE_i) values significantly differed between Sp7 and C- maize plants at T1 and T2, while differences between values in tomato were not significant (Figure 18d).

Maize E and stomatal conductance (g_s) were directly related, though g_s values were insignificant ($p>0.05$). Tomato g_s were significant, and values fluctuated from being 62% higher in Sp7 plants (over C-) at T2, to 74% lower than C- at T4 (Figure 18e).

5.4.4 Overall proteome changes identified via differential proteomics

Separation by 2-D gel electrophoresis of leaf protein extracts and comparative analysis with PDQuest software detected 43 differential spots that were significant in maize. In tomato, there were 41 significant spots. These spots did not always change significantly throughout the three sampling times, so only their significant changes are reported for each sampling time (Figures 19, 20 & 21).

Mechanisms involved in C_3 and C_4 plant response to Sp7 inoculation differ concerning timing and degree of protein changes. Sp7 decreases abundance of proteins related to photosynthesis and metabolism at T1 in the maize lifecycle, but increases those related to redox homeostasis, stress response, and pathogenesis. In tomato, proteins involved in photosynthetic processes and metabolism increased at T1, but not throughout. Most redox and stress-related proteins tended to have a delayed decrease in abundance, at T2, then gradually increased/recuperated their values at T3.

Only one protein within the 1.5-fold-change criterion could be isolated from maize at T2, and none from tomato; while three proteins of the same criterion could be isolated from tomato at T3, and none from maize.

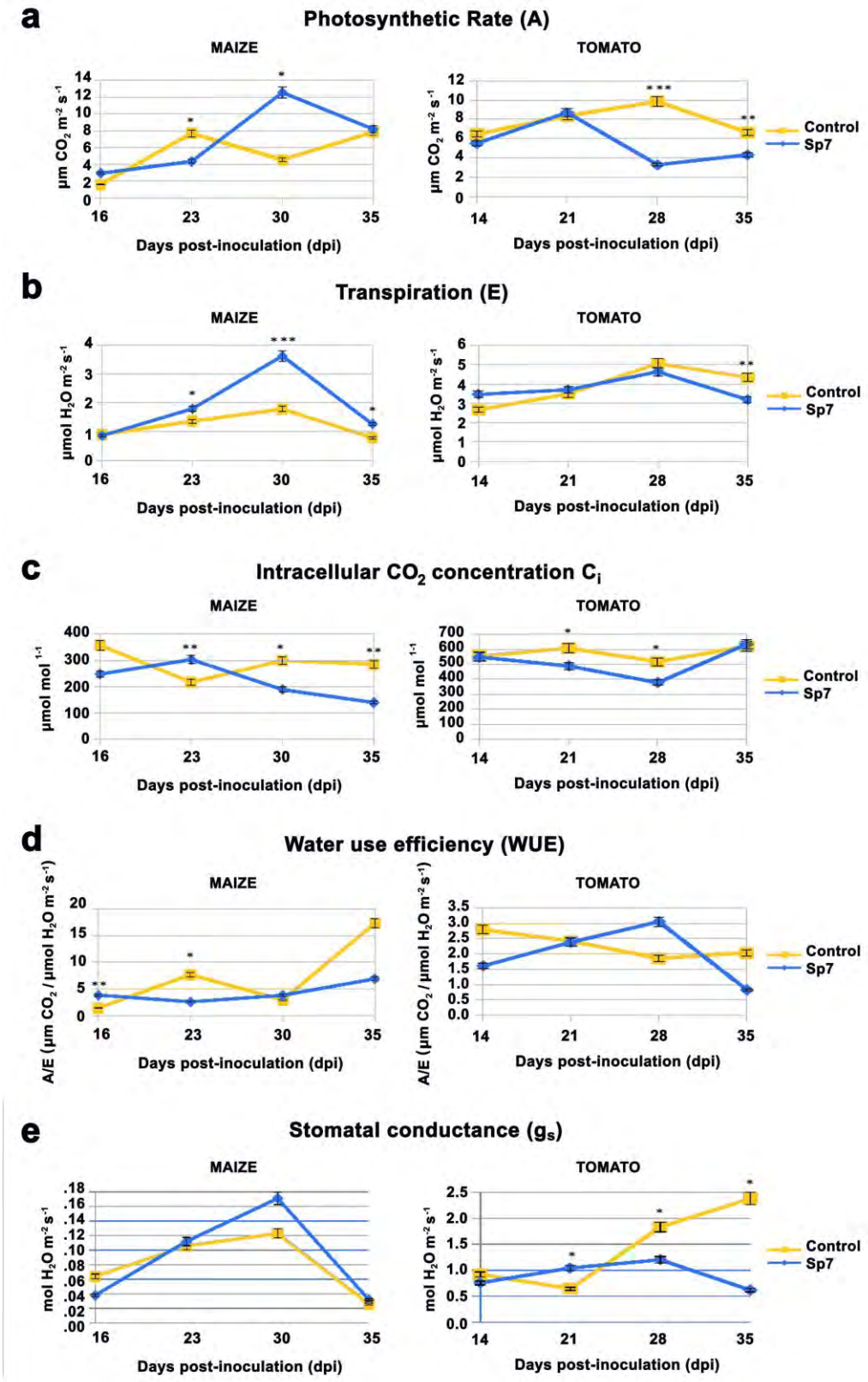

Figure 18. Gas exchange parameters in maize (left) and tomato (right) plants at different sampling times (T); *Azospirillum brasilense* (Sp7)-treated plants *versus* control. (a) Photosynthetic rate (A); (b) Transpiration (E); (c) Intercellular CO_2 concentration (C_i); (d) Water use efficiency (WUE_i); (e) Stomatal conductance (g_s). Asterisks indicate statistically significant differences between treatments for each sampling time : * ($p<0.05$), ** ($p<0.01$), *** ($p<0.001$).

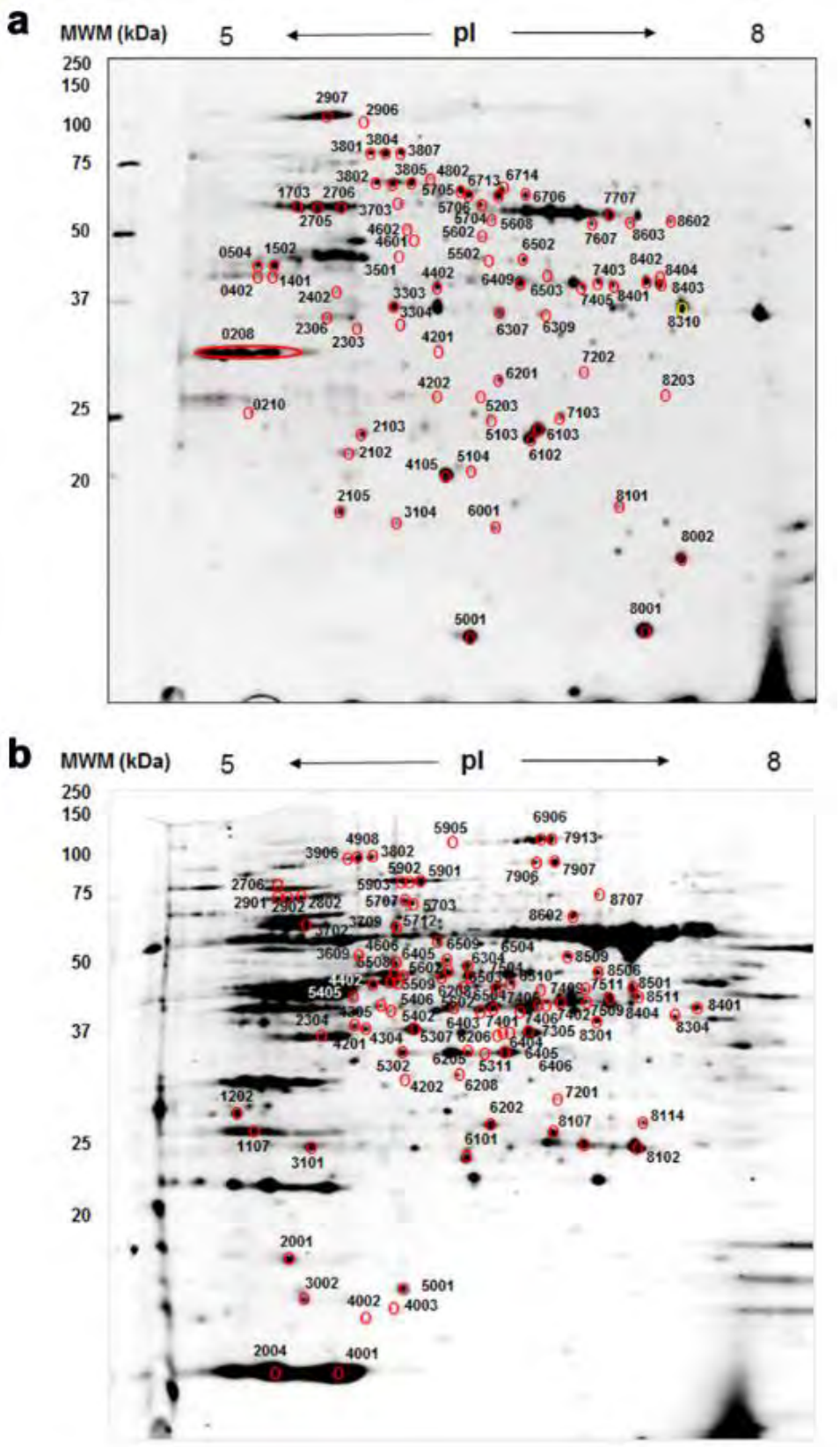

Figure 19. 2-D page gels of extracted proteins in maize and tomato plants. Representative 2-D PAGE gel image of (a) maize and (b) tomato with *Azospirillum brasilense* (Sp7) inoculation. Molecular markers are indicated as kDa. The representative spots and their numbers which show variation between treatments are indicated by the red circles.

A.

SSP	Sp7/C T1	T2	T3	Function
5104	**2.31			2
6706	**2.04			5
6714	*1.83			5
3205	*1.77			7
7103	*1.69		-0.53	2
7403		*1.58		4
3805			1.4	1,4
4801			1.31	1,4
5704	1.24			1
3807		1.22	0.82	1,4
5203	1.2			2
7202	1.19		-0.69	2
8401		1.12	1.07	1,4
6713			1.02	1,4
7607		1.04		7
6307	0.96			4
4802		0.84		1,4
5608		0.79		2,4
2705		0.79		2
3801			0.79	1,4
2103			0.77	1,2
8602		0.64		4
4602	0.57		-0.64	4
402	-0.35	-0.43		3,4
8001	-0.62			1
504	-0.68			2
7404	-0.71			4
5602	-0.73			1
201		-0.78		3
6409	-0.81			4
5001	-0.83	-0.43		1
4105		-0.91		2,4
4601	-1			7
4402		-1.05	-0.62	1
3802	-1.05		0.94	1,4
8101	-1.18	-0.76	0.88	2,4
5103		-1.18	-0.78	7
6102	-1.21			7
3104	-1.32	-0.49		1
8002	-1.43			1
6503	*-1.51			1
6001	*-1.94		0.98	1,2
3303	**-2.25			4

log2 FC: >2, >1.5, 1, 0, -1, <-1.5, <-2

B.

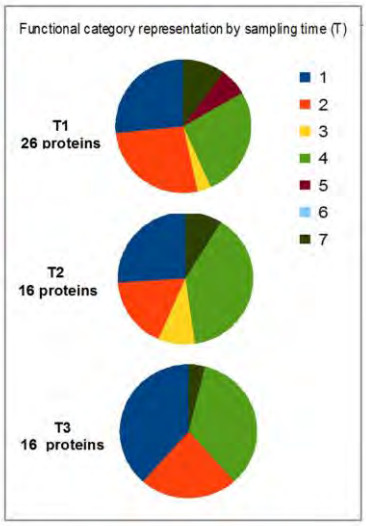

Figure 20. Maize heatmap (a) of differentially expressed proteins over three sampling times (T) and (b) relative expression of each functional category for each T. The heatmap color scale indicates differential regulation as the (log2) Fold Change of the *Azospirillum brasilense* (Sp7)-treated plant protein amount relative to control plants at each T. Analyzed spots were those in which the differences were more consistent (variation coefficient ≤50% among replicates, spots present in all measured conditions, measured ratios ≤0.5 or ≥2.0 and spots validated *in visu*. Proteins are annotated by spot numbers identified either by fingerprint mass spectrometry MS (MALDITOF) or by MS/MS (MALDI TOF-TOF) (Tables 1 and 2), and arranged according to relative expression levels; up-regulation is indicated in red, down-regulation in green. A value of 0, in grey, indicates no significant change in protein expression level. A single asterisk (*) indicates a>1.5 or < -1.5 FC, two asterisks (**) are >2 or < -2 FC. Differential expression is of proteins involved in biochemical pathways related to (1) Photosynthesis, respiration, and chloroplast organization; (2) Redox homeostasis and stress response; (3) Protein synthesis, conformation and transport; (4) Metabolism and energy; (5) Pathogenic cell lysis; (6) Resistance; (7) Unknown.

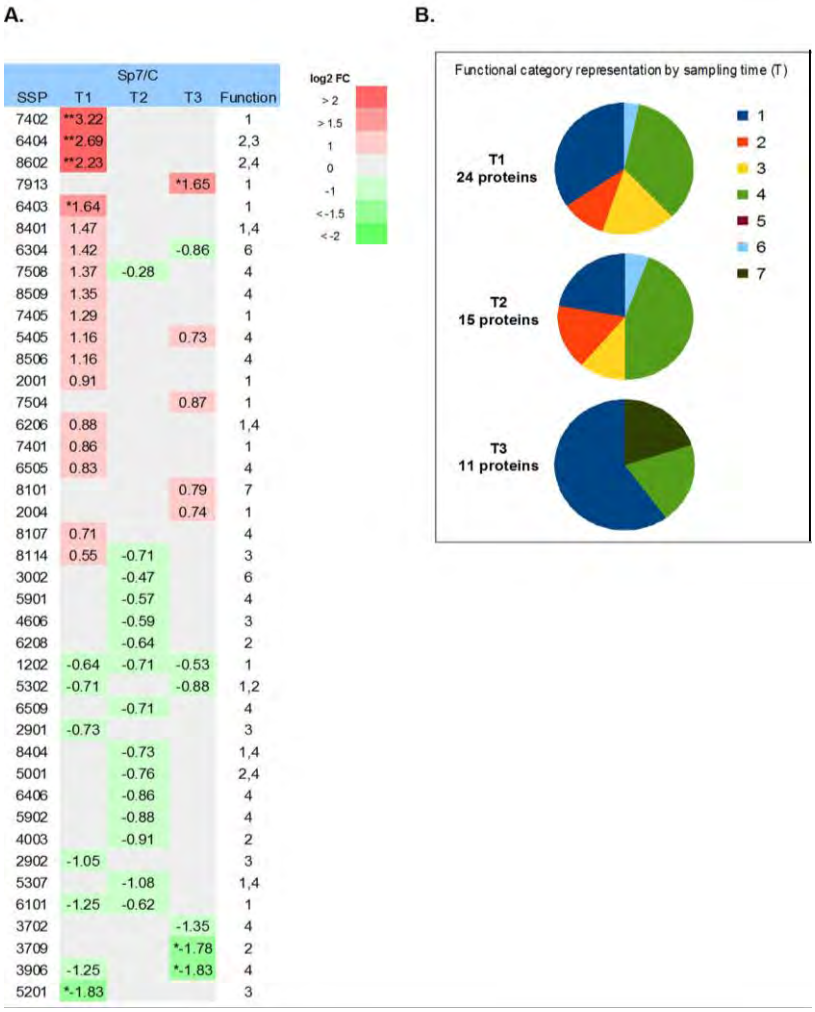

Figure 21. Tomato heatmap (a) of differentially expressed proteins over three sampling times (T) and (b) relative expression of each functional category for each T. The heatmap color scale indicates differential regulation as the (log2) Fold Change of the *Azospirillum brasilense* (Sp7)-treated plant protein amount relative to control plants at each T. Analyzed spots were those in which the differences were more consistent (variation coefficient ≤50% among replicates, spots present in all measured conditions, measured ratios ≤0.5 or ≥2.0 and spots validated *in visu*. Proteins are annotated by spot numbers identified either by fingerprint mass spectrometry MS (MALDITOF) or by MS/MS (MALDI TOF-TOF) (Tables 1 and 2), and arranged according to relative expression levels; up-regulation is indicated in red, down-regulation in green. A value of 0, in grey, indicates no significant change in protein expression level. A single asterisk (*) indicates a>1.5 or < -1.5 FC, two asterisks (**) are >2 or < -2 FC. Differential expression is of proteins involved in biochemical pathways related to (1) Photosynthesis, respiration, and chloroplast organization; (2) Redox homeostasis and stress response; (3) Protein synthesis, conformation and transport; (4) Metabolism and energy; (5) Pathogenic cell lysis; (6) Resistance; (7) Unknown.

5.4.5 Biological processes of shared proteins identified in response to *A. brasilense* Sp7 inoculation

There were ten proteins altered by *A. brasilense* Sp7 common to the two species (Table 9), but none of these proteins coincided in fitting the 1.5 or 2-fold-change criterion. At T1, the six common proteins were: cytochrome b6-f complex iron-sulfur subunit (EC 1.10.9.1) (cyt b6), fructose bisphosphate aldolase (EC 4.1.2.13) (FBA), glyceraldehyde-3-phosphate dehydrogenase (EC 1.2.1.9) (GAPDH), ribulose 1,5 bisphosphate carboxylase/oxygenase (EC 4.1.1.39) (Rubisco), phosphoglycerate kinase (EC 2.7.2.3) and S-Adenosyl-L-methionine (EC 2.1.1.41) (SAM). These proteins are mainly involved in photosynthesis, metabolism, or both. All except one protein (SAM) decreased in abundance in maize and increased in tomato. SAM increased in both species.

Table 9. Common proteins in maize (cv. B73) and tomato (cv. Boludo) plants that were altered on account of *Azospirillum brasilense* (Sp7) inoculation at each sampling time (T).

Sampling time	Protein	Corresponding spot(s)		Protein abundance: Sp7/C		Function
		Maize	Tomato	Maize	Tomato	
1	Cytochrome b6-f complex iron-sulfur subunit	3104, 6001	2001	↓↓	↑	1, 2
	Fructose bisphosphate aldolase	3303, 6503	6206	↓↓	↑	1,4
	Glyceraldehyde-3-phosphate dehydrogenase	7404, 6409	8401	↓↓	↑	1, 4
	Ribulose 1,5 bisphosphate carboxylase/oxygenase	5001, 8001	7401	↓↓	↑	1
	Phosphoglycerate kinase	504	5405	↓	↑	2,4
	Methionine (SAM)	4602	8509, 6505	↑	↑↑	4
2	ATP synthase	2705	5001, 6406	↑	↓↓	2, 4
	Glyceraldehyde-3-phosphate dehydrogenase	8401, 7403	8404	↑↑	↓	1, 4
	Transketolase	3807	5901, 5902	↑	↓↓	1, 4
3	ATP synthase	6713	3702	↑	↓	1, 4
	Chlorophyll A-B binding protein	2103	1202	↑	↓	1, 2

At T2 there were three proteins that changed in abundance in both species: ATP synthase (EC 3.6.3.14), GAPDH and transketolase (EC 2.2.1.1). All of these proteins are involved in plant metabolism and increased in abundance in maize, but decreased in tomato. Then at T3, the two common proteins were ATP synthase (photosynthesis and metabolism) and the chlorophyll A-B binding protein (EC 1.10.3.9) (photosynthesis and stress response). Similar to the common proteins at T2, these proteins both increased in abundance in maize, but decreased in tomato.

5.4.6 Early response to *A. brasilense* Sp7

At T1 in maize, the majority (62%) of the proteins decreased in abundance, and most were related to photosynthesis and metabolism, as well as protein synthesis and transport. In contrast, proteins related to redox homeostasis, stress response, and pathogenesis had an even rate of increased and decreased abundance. Protein alterations within the 2-fold change criterion were the dip protein (2.3-fold) and beta-glucosidase 2 (EC 3.2.1.21) (2-fold), related with redox homeostasis and DNA damage response, respectively. The most decreased protein was FBA (-2.25-fold), related with metabolism.

In tomato, 29% of the proteins decreased in abundance, and only one (unknown, but likely related to protein synthesis and transport) changed significantly (-1.83-fold). Alternatively, 71% of the proteins increased in abundance, and most were related with photosynthesis and protein synthesis. The most strikingly increased proteins were chloroplast stem-loop binding protein of 41 kDa b (3.2-fold) (CSP41), monohydroascorbate reductase-like (1.6.5.4) (2.7-fold), dihydrolipoamide dehydrogenase precursor (EC 1.8.1.4) (2.2-fold) and malate dehydrogenase (EC 1.1.1.38) (1.65-fold). These proteins are associated with photosynthesis, stress response and protein synthesis

5.4.7 Alteration to protein abundance in subsequent weeks/sampling times

The altered abundance of proteins in maize at T2 and T3 did not reach more than 2-fold, but there was only one instance of a protein exceeding a 1.5-fold change at T2: GAPDH, chloroplastic precursor (1.58-fold). This protein is involved in metabolism and energy, and falls within the trend for increased abundance of other proteins of the same functional category at both T2 and T3 in maize.

In tomato, Sp7 caused all proteins to decrease in abundance at T2, but none more that -1.5-fold. At T3, the most strikingly increased protein was glycine dehydrogenase (EC 1.4.1.10) (1.65-fold), related to photosynthesis, and the most decreased were NADPH-dependent thioredoxin reductase 3-like isoform 2/ Inositol-3-phosphate synthase (EC 1.8.1.9) (-1.78-fold), and ATP-dependent Clp protease ATP-binding subunit clpA homolog CD4B (EC 3.4.21.92) (-1.83-fold); related to redox homeostasis and protein synthesis, respectively.

5.5 Discussion

Progress has been made in identifying *A. brasilense* Sp7-regulated growth, nutrient content and yield in plants, but studies focusing on the proteomics of *A. brasilense* Sp7 in model plants are less common. The need for proteomic studies of PGPRs has indeed been addressed, as there is an exhaustive study (Cheng et al., 2010) comparing the impact of various PGPR on (symbiotic) plant proteomes; though *A. brasilense*, maize, and tomato are not included. In this study, we investigated how *A. brasilense* Sp7 interacts with the proteome of C_3 (tomato) and C_4 (maize) plants by inoculating seeds and comparing results to gas exchange parameters. Results have allowed us to characterize the early interaction of Sp7 with the developing seedlings. Within this framework, our analysis gives particular emphasis to T1 (four-leaf stage), where a total of 24 proteins were identified in tomato and 26 in maize, six of which were co-regulated in both species. Above all, it was at this sampling time that the highest number of proteins with striking differences were observed.

Physiological and gas exchange results indicated that inoculated maize seedlings had significantly enhanced root growth and WUE_i at the four-leaf stage. The ability of plants to withstand stresses has been attributed to their superior WUE_i, CO_2 fixation, long taproots and development of an extensive lateral root system in response to water shortage in the soil (Kadereit et al., 2003). Furthermore, better seedling emergence and earlier vegetative growth (i.e., seedling vigor) are considered to be essential traits for best WUE_i in cereals in Mediterranean conditions (Richards et al., 2002), so at least in this regard, we see that Sp7 inoculation has had a more profound and immediate effect on maize compared to tomato.

Of the proteins with expression changes in inoculated maize and tomato seedlings at the four-leaf stage, 90% had less than 2-fold expression changes. Comparing abundance of the most strikingly effected proteins at T1, our results show that proteins related to metabolism and redox homeostasis constituted the majority of the identified proteins for each species individually, as well as for the overlapping proteins. Specifically, in inoculated maize, the most striking accumulation of proteins was related to redox homeostasis and pathogenic cell lysis, and reduction was in those related to metabolism and energy. In inoculated tomato, there was a wider array (function-wise) of strikingly accumulated proteins, related to photosynthesis and respiration, redox homeostasis, protein synthesis, metabolism and energy.

In maize, the increased proteins were dip protein and beta-glucosidase2. The dip protein may be cross-influenced by both the plant and Sp7 since it holds a role in the production of abscisic acid (ABA) by plants under stress (Finn et al., 2017), and is synthesized by *A. brasilense* (Cohen et al., 2015). Beta-glucosidase2 is active in secondary plant metabolism, as well as catabolism of flavonoid glycosides during recovery from wounding stress and DNA damage (Roepke and Bozzo, 2015). However, since *A. brasilense* itself produces beta glucosidases, it is possible that the expression of exogenous beta-glucosidase leads to plant

phenotypes with increased phytohormone levels and increased resistance to biotic attack, as has been found in previous studies (Jin et al., 2011). Hence, we may be witnessing a "priming" effect, in which the PGPR is inducing ISR and the hormone pathways involved. The other increased protein was glutathione (within the 1.5-fold change criterion). Glutathione is vital in the transmission of ROS signaling as an interfacing molecule between ROS, NO, and protein Cys groups (Noctor et al., 2017), while it is also tightly interwoven with its role as a modulator of stress response hormones salicylic acid (SA), jasmonic acid (JA), and ethylene (ET) signaling pathways (Mhamdi et al., 2010; Han et al., 2013a,b; Datta et al., 2015), as well as plant development hormones auxin and ABA (Yu et al., 2013). Glutathione transferase redox imbalance triggers oxidation of crucial components of these hormonal signaling pathways, so its increase indicates that Sp7 inoculation induced reactions that counterbalance and substitute glyceraldehyde-3-phosphate dehydrogenase A (GAPDH) and ribulose 1,5 bisphosphate carboxylase/oxygenase (Rubisco) molecules participating in the CB cycle. Confirming this, fructose bisphosphatase aldolase (FBA) decreased in accumulation. This protein implies the active role of glycerate, and is involved in the carbon shuffle reactions replenishing Rubisco by oxygenation, an event signaling down-regulation of the entire CB cycle (Schimkat et al., 1990).

In tomato, increased proteins at T1 were chloroplast stem-loop binding protein of 41kDab (CSP41), monodehydroascorbate reductase-like (MDAR), dihydrolipoamide dehydrogenase precursor (DLD) and malate dehydrogenase (MDH). CSP41proteins are highly abundant RNA-binding proteins in the chloroplast stroma (Zybailov et al., 2008). Their function is critical in mature leaves when transcripts produced by phosphoenolpyruvate (PEP) become limiting and need to be stabilized and protected (Majeran et al., 2005). The presence of CSP41 increases transcripts for photosynthetic proteins and of some ribosomal RNAs, which in turn, maintains or increases the translational activity of chloroplasts (Leister, 2014). MDAR is an enzymatic component of the glutathione-ascorbate cycle also serving to protect cells against damage incurred by ROS (Leterrier et al., 2005). In other studies with tomato, MDAR was increased by stress conditions such as high salinity (Mittova et al., 2003), so our inoculated tomato plants had up-regulated redox homeostasis, like maize. Finally, DLD and MDH are both implicated in the tricarboxylic acid (TCA) cycle (Wang et al., 2017). Over-expression of DLD, also known as the L-protein component of the glycine decarboxylase protein (GDC-L), has been shown to lower CO_2 compensation points while causing higher net-CO_2 uptake rates and better growth (Timm et al., 2016). Meanwhile, the MDH increment suggests that Sp7 inoculation caused C_3 glutamate to rapidly turn-over as an intermediate in the photorespiratory N cycle and thereby down-regulate N metabolism in tomato (Nunes-Nesi et al., 2010).

Due to the great number of proteins involved in redox homeostasis at T1, combined with the importance of understanding the effects of redox homeostasis on subsequent plant processes and growth, we also compared all significant physiological parameters with altered

proteins that fell into the 1.5 fold-change criteria for subsequent growth stages. In maize at the seven-leaf stage (T2), GAPDH, a protein suggested to be an enzyme-forming part of the system protecting the cell against ROS (Jorrín-Novo et al., 2009), had increased abundance in inoculated plants. This increase coincided with significantly increased transpiration (E) and intracellular CO_2 concentration (C_i), but significantly decreased photosynthetic rate (A) and WUE_i. Then, a week later, at the end of tillering, there was a significant increase in A and E. Accumulation of intracellular ROS depends on a balance between the generation and detoxification of ROS via various ROS-scavenging enzymes. Several studies suggest that the combination of decreased levels of intracellular ROS and a reduced rate of photoinhibition can be achieved by engineering the production of ROS-scavenging enzymes in higher plants (Gururani et al., 2015). The Sp7 effect to maize appears to be similar; inoculation first instigated a stress-effect that increased ROS-scavenging enzymes, which ultimately reduced photoinhibition.

In the case of inoculated tomato, stomatal conductance (g_s) significantly increased at the seven-leaf (T2) stage and C_i decreased.Photosynthesis (A) plays a well-documented role in CO_2 regulation of stomatal apertures (g_s) by lowering the intercellular CO_2 concentration (C_i) in leaves (Mott, 1988), but in this scenario, A (and E) remained unchanged. Recent studies focusing on genetics have been trying to pinpoint the cause of C_i-dependent and C_i-independent induced stomatal opening; and one model points towards protein kinase abundance as a driver of fluctuations between C_i content and stomatal aperature (Engineer et al., 2016). Our gas exchange results coincided with 100% of the proteins slightly decreasing in abundance at T2, and phosphoglycerate kinase (PGK) (a metabolic kinase that moonlights as a protein kinase) was in this group. PGK catalyzes the ATP-dependent phosphorylation of 3-phosphoglycerate (3-PG) to 1,3-diphosphoglycerate and second step of the CB cycle, but it is so sensitive to the redox state that the oxidized enzyme has been shown to lose its activity (Tsukamoto et al., 2013). Therefore, the disconnect between A and g_s in the case of inoculation could be a result of oxidated and reduced PGK, or damaged photosynthetic mechanisms; both of which may have been caused by excessive ROS at T1.

At the nine-leaf stage (T3), inoculated tomato plants had significantly decreased A, C_i and g_s. Once again, there is discordance in the regulation between the three gas exchange parameters since down-regulated A and C_i should theoretically lead to up-regulated g_s. Furthermore, it has been reported that increased photosynthetic activity as a result of PGPR inoculation leads to higher N incorporation and therefore increased formation of chlorophyll (Baset Mia et al., 2010). Proteome data indicated that at this time, glycine dehydrogenase (GLDC) increased in abundance. GLDC is a photorespiratory intermediate whose increased abundance indicates inhibition of the CB cycle and up-regulation of photorespiratory metabolism (Timm et al., 2016). Furthermore, NADPH-dependent thioredoxin reductase

(NTRC) and ATP-dependent Clp protease both decreased in abundance. NTRC works against ROS, serving as part of the plant's defense system (Alscher et al., 2002), while ATP-dependent Clp protease is essential for chloroplast development and plant viability (Clarke, 2012). Taking tomato physiological and proteomic results together, joint analysis reveals that T3 Sp7-treated plants are less prone to fighting ROS, but do have inhibited CB cycle and chloroplast development. Therefore, we may presume that the main mechanism of photosynthesis diminution is either related to the direct effect of Sp7 on the physiological status of tomato plants at this specific growth stage; or by residual effects resulting from damage to the plant at earlier sampling times. Similar results have been reported for other PGPR and the effects that they have on runner bean and soybean at different growth stages (Marius et al., 2013; Zhang et al., 1997).

Despite the increase of photorespiratory proteins and decreased gas exchange parameters, plant height and root length continued to increase, especially at T3. This may be related to the effects of ROS. It has been found that ROS over-expression stimulates root elongation, calling for redox control of the cell cycle (Passardi et al., 2006). Stress induced presence of ROS and reactive nitrogen species (RNS) in specific tissues have also been found to affect root morphology by reducing primary root growth and promoting branching (Reichheld et al., 1999).

5.6 Conclusions

Sp7 interacts differently with the primary metabolism of the two plants. Results were most striking at the four-leaf stage for both species. Proteins related to metabolism and redox homeostasis were most abundant in tomato, though this was followed by an inhibited CB cycle and chloroplast development, indicating that photosynthetic proteins were damaged by ROS. In contrast, Sp7 inoculation to maize first instigated a stress-effect that increased ROS-scavenging enzymes, reducing photoinhibition. Sp7 inoculation induced reactions in maize that counterbalanced and substituted molecules participating in the CB cycle. Our findings differ from those of Shivaprasad et al. (2012) in that PGPR immediately leads to attenuation of defense responses in maize to allow for colonization because in our study, Sp7 tardily alters the defense response (which may then assist colonization). In contrast, Sp7-treated tomato plants indeed had activated defense and metabolic responses at the four-leaf stage. Finally, better seedling emergence and vigor was observed in inoculated maize compared to tomato. Overall, the early interaction of Sp7 with maize is more complex and beneficial than that with tomato because of the C_4 photosynthetic mechanism, thereby offsetting the stress involved in association and improving the interaction of the PGPR with maize.

5.7 References

Alscher RG, Erturk N, Heath LS (2002) Role of superoxide dismutases (SODs) in controlling oxidative stress in plants. *Journal of Experimental Biology* 53 (372):1331–1341.

Baldani VLD, Alvarez MAB, Baldani JI, Dobereiner J (1986). Establishment of inoculated *Azospirillum* spp in the rhizosphere and in root of field grown wheat and sorghum. *Plant Soil* 90:35–46.

Baset Mia MA, Shamsuddin ZH, Wahab Z, Marziah M (2010) Effect of plant growth promoting rhizobacterial (PGPR) inoculation on growth and nitrogen incorporation of tissue-cultured Musa plantlets under nitrogen-free hydroponics condition. *Australian Journal of Crop Science* 4 (2):85–90.

Bashan Y, Holguin G, Lifshitz R (1993) Isolation and characterization of plant growth-promoting rhizobacteria. In: Glick BR and Thompsom E (ed) *Methods in Plant Molecular Biology and Biotechnology*. CRC Press, Boca Raton, FL, USA, pp. 331–345.

Beimalt S, Sonnwald U (2014) Plant-microbe interactions to probe regulation of plant carbon metabolism. *Journal of Plant Physiology* 163:307–318.

Botta LA, Santacecilia A, Ercole C, Cacchio P, del Gallo M (2013) In vitro and in vivo inoculation of four endophytic bacteria on Lycopersicon esculentum. *Natural Biotechnology* 30 (6):666–674.

Cassán F, Perrig D, Sgroy V, Masciarelli O, Penna C, Luna V (2009) *Azospirillum brasilense* Az39 and Bradyrhizobium japonicum E109, inoculated singly or in combination, promote seed germination and early seedling growth in corn (*Zea mays* L.) and soybean (*Glycine max* L.). *European Journal of Soil Biology* 45:28–35.

Cheng Z, McConkey J, Glick BR (2010) Proteomic studies of plant-bacteria interactions. *Soil Biology and Biochemistry* 42:1673–1684.

Clarke AK (2012) The chloroplast ATP-dependent Clp protease in vascular plants- new dimensions and future challenges. *Physiologia Plantarum* 145 (1):235–244.

Cohen AC, Bottini R, Pontin M, Berli FJ, Moreno D, Boccanlandro H, Travaglia CN, Piccoli PN (2015) *Azospirillum brasilense* ameliorates the response of *Arabidopsis thaliana* to drought mainly via enhancement of ABA levels. *Physiologia Plantarum* 153 (1): 79–90.

Covshoff S, Hibberd JM (2012) Integrating C4 photosynthesis into C3 crops to increase yield potential. *Plant Biotechnology* 23:209–214.

Cueto-Ginzo AI, Serrano L, Sin E, Rodríguez R, Morales JG, Lade SB, Medina V, Achon MA (2016) Exogenous salicylic acid treatment delays initial infection and counteracts alterations induced by *Maize dwarf mosaic virus* in the maize proteome. *Physiological and Molecular Plant Pathology* 96:46–59.

Datta R, Kumar D, Sultana A, Hazra S, Bhattacharyya D, Chattopadhyay S (2015) Glutathione regulates 1-aminocyclopropane-1-carboxylate synthase transcription via WRKY33 and 1-aminocyclopropane-1-carboxylate oxidase by modulating messenger RNA stability to induce ethylene synthesis during stress. *Plant Physiology* 169:2963–2981.

Dobbelaere S, Croonenborghs A, Thys A, Ptacek D, Vanderleyden J, Dutto P, Labandera-Gonzalez C, Caballero-Mellado J, Aguirre JF, Kapulnik Y, Brener S, Burdman S, Kadouri D, Sarig S, Okon Y (2001) Responses of agronomically important crop to inoculation with *Azospirillum*. *Australian Journal of Plant Physiology* 28:871–879.

El Zemrany H, Corte, J, Lutz MP, Chabert A, Baudoin E, Haurat J, Maughan N, Felix D, Defago G, Bally R, Moenne-Loccoz Y (2006) Field survival of the phytostimulator Azospirillum lipoferum CRT1 and functional impact on maize crop, bio-degradation of crop residues, and soil faunal indicators in a context of decreasing nitrogen fertilisation. *Soil Biology and Biochemistry* 38:1712–1726.

Engineer C, Hashimoto-Sugimoto M, Negi J, Israelsson-Nordstrom M, Azoulay-Shemer T, Rappel W-J, Iba K., Schroeder J (2016) CO2 sensing and CO2 regulation of stomatal conductance: advances and open questions. *Trends in Plant Science* 21 (1):16–30.

Finn RD, Attwood TK, Babbitt PC, Bateman A, Bork P, Bridge AJ, Chang H-Y, Dosztányi Z, El-Gebali, S, Fraser M, Gough J, Haft D, Holliday GL, Huang H, Huang X, Letunic I, Lopez R, Lu S., Marchler-Bauer A, Mi H, Mistry J, Natal, DA, Necci M, Nuka G, Orengo CA, Park Y, Pesseat S, Piovesan D, Potter SC, Rawlings ND, Redaschi N, Richardson L, Rivoire C, Sangrador-Vegas A, Sigrist C, Sillitoe I, Smithers B, Squizzato S, Sutton G, Thanki N, Thomas PD, Tosatto SCE, Wu CH, Xenarios I, Yeh L-S, Young S-Y, Mitchell AL (2017). InterPro in 2017 — beyond protein family and domain annotations. *Nucleic Acids Research* Jan 2017.

Glick BR (2012) Plant growth-promoting bacteria: mechanisms and applications. *Scientifica* 2012, Article ID:963401.

Gururani MA, Venkatesh J, Tran L-SP (2015) Regulation of photosynthesis during abiotic stress-induced photoinhibition. *Molecular Plant* 8:1304–1302.

Han Y, Chaouch S, Mhamdi A, Queval G, Zechmann B, Noctor G (2013a). Functional analysis of Arabidopsis mutants points to novel roles for glutathione in coupling H2O2 to activation of salicylic acid accumulation and signaling. *Antioxidants & Redox Signaling* 18:2106–2121.

Han Y, Mhamdi A, Chaouch S, Noctor G (2013b) Regulation of basal and oxidative stress-triggered jasmonic acid-related gene expression by glutathione. *Plant Cell Environment* 36:1135–1146.

Hochholdinger F, Guo L, Schnable PS (2004) Lateral roots affect the proteome of the primary root of maize (*Zea mays* L.). *Plant Molecular Biology* 56 (3):397–412.

Ibort P, Imai H, Uemura M, Aroca R (2018) Proteomic analysis reveals that tomato interaction with plant growth promoting rhizobacteria is highly determined by ethylene perception. *Journal of Plant Physiology* 220:43–59.

Jin S, Kanagaraj A, Verma D, Lange T, Daniell H (2011) Release of hormones from conjugates: chloroplast expression of β-glucosidase results in elevated phytohormone levels associated with significant increase in biomass and protection from aphids or whiteflies conferred by sucrose esters. *Plant Physiology* 155:222–235.

Jorrín-Novo JV, Maldonado AM, Echevarría-Zomeño S, Valledor L, Castillejo MA, Curto M, Valero J, Sghaier B, Donoso G, Redondo I (2009) Plant proteomics update (2007-2008): second-generation proteomic techniques, an appropriate experimental design, and data analysis to fulfill MIAPE standards, increase plant proteome coverage and expand biological knowledge. *Journal of Proteomics* 72:285–314.

Kadereit G, Borsch T, Weising K, Freitag H (2003) Phylogeny of *amaranthaceae* and *chenopodiaceae* and the evolution of C-4 photosynthesis. *International Journal of Plant Science* 164:959–986.

Kamnev AA, Tugarova AV, Tarantilis PA, Gardiner PHE, Polissiou MG (2012) Comparing poly-3-hydroxybutyrate accumulation in *Azospirillum brasilense* strains Sp7 and Sp245: the effects of copper (II). *Applied Soil Ecology* 61:213–216.

Lancashire PD, Bleiholder H, Langelüddecke P, Stauss R (1991) An uniform decimal code for growth stages of crops and weeds. *Annals of Applied Biology* 119:561–601.

Lavania M, Chauhan PS, Chauhan SV, Singh HB, Nautiyal CS (2006) Induction of plant defense enzymes and phenolics by treatment with plant growth-promoting rhizobacteria *Serratia marcescens* NBRI1213. *Current Microbiology* 52:363–368.

Leister D (2014) Complex(iti)es of the ubiquitous RNA-binding CSP41 proteins. *Frontiers in Plant Science* 5 (255):1–4.

Leterrier M, Corpas FJ, Barroso JB, Sandalio LM, del Río LA (2005) Peroxisomal monodehydroascorbate reductase. Genomic clone characterization and functional analysis under environmental stress conditions. *Plant Physiology* 138 (4):2111–2123.

Lodwig EM, Hosie AH, Bourdès A, Findlay K, Allaway D, Karunakaran R, Downie J, Poole PS (2003) Amino-acid cycling drives nitrogen fixation in the legume-Rhizobium symbiosis. *Nature* 422:722–726.

Majeran W, Friso G, Ponnala L, Connolly B, Huang M, Reidel E, Zhang C, Asakura Y, Bhuiyan NH, Sun Q, Turgeon R, van Wijk KJ (2010) Structural and metabolic transitions of C4 leaf development and differentiation defined by microscopy and quantitative proteomics in maize. *The Plant Cell* 22:3509–3542.

Majeran W, Cai Y, Sun Q, van Wijk KJ (2005) Functional differentiation of bundle sheath and mesophyll maize chloroplasts determined by comparative proteomics. *The Plant Cell* 17 (11):3111–3140.

Marius S, Munteanu N, Stoleru V, Mihasan M (2013) Effects of inoculation with plant growth promoting rhizobacteria on photosynthesis, antioxidant status and yield of runner bean. *Romanian Biotechnological Letters* 18 (2):8132–8143.

Mengel K, Viro M (1978) The significance of plant energy status for the uptake and incorporation of NH4 nitrogen by young rice plants. *Soil Science and Plant Nutrition* 24 (3):407–416.

Mhamdi A, Hager J, Chaouch S, Queval G, Han Y, Taconnat Y, Saindrenan P, Issakidis-Bourguet E, Gouia H., Renou JP, Noctor G (2010) Arabidopsis GLUTATHIONE REDUCTASE 1 is essential for the metabolism of intracellular H_2O_2 and to enable appropriate gene expression through both salicylic acid and jasmonic acid signaling pathways. *Plant Physiology* 153:1144–1160.

Mittova V, Tal M, Volokita M, Guy M (2003) Up-regulation of the leaf mitochondrial and peroxisomal antioxidative systems in response to salt-induced oxidative stress in the wild salt-tolerant tomato species *Lycopersicon pennellii*. *Plant Cell Environment* 6:845–856.

Mott KA (1988) Do stomata respond to CO2 concentrations other than intercellular? *Plant Physiology* 86 (1):200–203.

Mus F, Crook MB, Garcia K, Garcia Costas A, Geddes BA, Kouri ED, Paramasivan P, Ryu M-H, Oldroyd GED, Poole PS, Udvardi MK, Voig CA, Ané J-M, Peters JW (2016) Symbiotic nitrogen fixation and the challenges to its extension to nonlegumes. *Applied Environmental Microbiology* 82:3698–3710.

Nunes-Nesi A, Fernie AR, Stitt M (2010) Metabolic and signaling aspects underpinning the regulation of plant carbon-nitrogen interactions. *Molecular Plant* 3 (6):973–966.

Noctor G, Reichheld JP, Foyer CH (2017) ROS-related redox regulation and signaling in plants. *Seminars in Cell and Developmental Biology* 80:3–12.

Okon Y, Albrecht SL, Burris RH (1977) Methods for growing Spirillum lipoferum and for counting it in pure culture and in association with plants. *Applied Environmental Microbiology* 33:85–88.

Parra-cota FI, Peña-Cabriales JJ, de los Santos-Villalobos S, Martínez-Gallardo NA, Délano-Frier JP (2014) *Burkholderia ambifaria* and *B. Caribensis* promote growth and increase yield in grain amaranth (*Amaranthus cruentus* and a. *Hypochondriacus*) by improving plant nitrogen uptake. *PLOS ONE* 9 (2): e88094.

Passardi F, Tognolli M, De Meyer M, Penel C, Dunand C (2006) Two cell wall associated peroxidases from Arabidopsis influence root elongation. *Planta* 223 (5):965–974.

Pereg L (2015) Chapter 10-*Azospirillum* cell aggregation, attachment, and plant interaction. In: Cassán FD, Okon Y, Creus CM (eds), *Handbook for Azospirillum*. Springer International Publishing, Switzerland, pp. 186–187.

Pereg L, de-Bashan LE, Bashan Y (2016) Assessment of affinity and specificity of *Azospirillum* for plants. *Plant Soil* 399:389–414.

Reichheld JP, Lardon TVF, Van Montagu M, Inzé D (1999) Specific checkpoints regulate plant cell cycle progression in response to oxidative stress. *The Plant Journal* 17 (6): 647–656.

Reynders L, Vlassak K (1982) Use of *Azospirillum brasilense* as biofertilizer in intensive wheat cropping. *Plant Soil* 66; 217.

Richards RA, Rebetzke GJ, Condon AG, van Herwaarden (2002) Breeding opportunities for increasing the efficiency of water use and crop yield in temperature cereals. *Crop Science* 42:111–121.

Roepke J, Bozzo GG (2015) *Arabidopsis thaliana* β-glucosidase BGLU15 attacks flavonol 3-O-β-glucoside-7-O-α-rhamnosides. *Phytochemistry* 109:14–24.

Schimkat D, Heineke D, Heldt HW (1990) Regulation of sedoheptulose-1,7-bisphosphatase by sedoheptulose-7-phosphate and glycerate, and of fructose-1,6-bisphosphatase by glycerate in spinach chloroplasts. *Planta* 181:97–103.

Shivaprasad PV, Chen H-M, Patel K, Bond DM, Santos BA, Baulcombe DC (2012) A microRNA superfamily regulates nucleotide binding site-leucine-rich repeats and other mRNAs. *Plant Cell* 24:859–874.

Tarrand JJ, Krieg NR, Dobereiner J (1978) A taxonomic study of *Spirillum lipoferum* group, with description of a new genus, *Azospirillum* gen nov. and two species. *Azospirillum lipoferum* (Beijerinck) comb. nov. and *Azospirillum brasilense* sp nov. *Canadian Journal of Microbiology* 24:967–980.

Thiebaut F, Rojas CA, Grativol C, Motta MR, Vieira T, Regulski M, Martienssen RA, Farinelli L, Hermerly AS, Ferreira CG (2014) Genome-wide identification of microRNA and siRNA responsive to endophytic beneficial diazotrophic bacteria in maize. *BMC Genomics* 15:766.

Timm S, Florian A, Fernie AR, Bauwe H (2016) The regulatory interplay between photorespiration and photosynthesis. *Journal of Experimental Botany* 67 (10):2923–2929.

Tsukamoto Y, Fukushima Y, Hara S, Hisabori T (2013) Redox control of the activity of phospholycerate kinase in Synechocystis sp. PCC6803. *Plant Cell Physiology* 54 (4):484–491.

Walker V, Couillerot O, Von Felten A, Bellvert F, Jansa J, Maurhofer M, Bally R, Moenne-Loccoz Y, Comte G (2012) Variation of secondary metabolite levels in maize seedling roots induced by inoculation with *Azospirillum*, *Pseudomona*s, and *Glomus* consortium under field conditions. *Plant Soil* 356:151–163.

Wang X, Xu C, Cai X, Wang Q, Dai S (2017) Heat-responsive photosynthetic signaling pathways in plants: insights from proteomics. *International Journal of Molecular Sciences* 18:2191.

Wang L, Czedik-Eysenberg A, Mertz RA, Si Y, Tohge T, Nunes-Nesi A, Arrivault S, Dedow LK, Bryant DW, Zhou W, Xu J, Weissmann S, Studer A, Li P, Zhang C, LaRue T, Shao Y, Ding Z, Sun Q, Patel RV, Turgeon R, Zhu X, Provart NJ, Mockler TC, Fernie AR, Stitt M, Liu P, Brutnell TP (2014) Comparative analysis of C4 and C3 photosynthesis in developing leaves of maize and rice. *Nature Biotechnology* 32 (11):1158–1170.

Xu Q, Ni H, Chen Q, Sun F, Zhou T, Lan Y, Zhou Y (2013) Comparative proteomic analysis reveals the cross-talk between the responses induced by H2O2 and by long-term Rice Black-streaked dwarf virus infection in rice. *PLOS ONE* 8 (11):e81640.

Yu X, Pasternak T, Eiblmeier M, Ditengou F, Kochersperger P, Sun J, Wang H, Rennenberg H, Teale W, Paponov I, Zhou W, Li C, Li X, Palme K (2013) Plastid-localized glutathione reductase2-regulated glutathione redox status is essential for Arabidopsis root apical meristem maintenance. *Plant Cell* 25:4451–4468.

Zhang F, Dashti N, Hynes RK, Smith DL (1997) Plant growth-promoting rhizobacteria and soybean [*Glycine max* (L) Merr] growth and physiology at suboptimal root zone temperatures. *Annals of Botany* 79 (3):243–249.

Zybailov B, Rutschow H, Friso G, Rudella A, Emanuelsson O, Sun Q, van Wijk KJ (2008) Sorting signals, N-terminal modifications and abundance of the chloroplast proteome. *PLOS ONE* 3, e1994.

CHAPTER 6

Differential proteomics analysis reveals that *Azospirillum brasilense* Sp7 promotes virus resistance in maize and tomato seedlings

(Submitted to European Journal of Plant Pathology, 2019. Annex 4)

Chapter 6. Differential proteomic analysis reveals that *Azospirillum brasilense* Sp7 promotes resistance to virus in maize and tomato seedlings

6.0 Abstract

Plant growth-promoting rhizobacteria such as *Azospirillum brasilense* Sp7 can protect plants against viruses but the molecular basis of this phenomenon is unclear. We therefore used differential proteomics to study two pathosystems in the presence and absence of Sp7 during early vegetative growth: tomato (*Solanum lycopersicum* L. cv. Boludo)/Potato virus X (PVX, KJ631111)/Sp7, and maize (*Zea mays* cv. B73)/Maize dwarf mosaic virus (MDMV, AM110558)/Sp7). In the maize/MDMV system, PDQuest revealed significant variations in the levels of 19 proteins compared to uninfected controls, including the upregulation of NADP-dependent malic enzyme as a form of host-specific viral anticipation, causing a simultaneous increase in the abundance of proteins related to photosynthesis and plastid functions. However, 42 proteins varied significantly in the maize/MDMV/Sp7 system, including the upregulation of radical-scavenging enzymes and proteins related to methionine metabolism, the glutathione-ascorbate cycle and photosynthesis, increasing the photosynthetic rate. In the tomato/PVX system, we observed significant variations in the levels of 58 proteins reflecting the disruption of the Calvin-Benson cycle, responses to oxidative stress and the inhibition of photosystem II (PSII) activity. We identified 26 proteins that varied in the tomato/PVX/Sp7 system, leading to increased virus resistance. PSII and plastid proteins transiently declined but partially recovered over time as the Calvin-Benson cycle was induced to compensate. Sp7 therefore triggers induced systemic resistance in both pathosystems without affecting the virus titer, although it does delay the appearance of MDMV. The role of ribulose-1.5-bisphosphate carboxylase/oxygenase small subunit as a host target for viruses is discussed in both pathosystems.

6.1 Introduction

The ability of *Azospirillum brasilense* Sp7 (hereafter, Sp7) and other plant growth-promoting rhizobacteria (PGPR) to control bacterial and fungal diseases is known to involve induced systemic resistance (ISR) in the host (Bashan and De Bashan, 2002; Tortora et al. 2011). However, PGPR can also protect plants against viruses, and the basis of this phenomenon has not been addressed in detail. Interactions between PGPR and viruses can improve plant growth and promote emergence (Al-Ani et al., 2013). In particular, *Azospirillum* species can protect tomato plants against yield losses caused by Cucumber mosaic virus (CMV) and its associated satellite RNA (Dashti et al., 2007), although they do not appear to reduce yield losses induced by Barley dwarf mosaic virus (BDMV) in wheat and barley (Al-Ani et al., 2011).

The interaction between PGPR and viruses is studied using model viruses such as Maize dwarf mosaic virus (MDMV) and Potato virus X (PVX). MDMV (genus *Potyvirus*, family *Potyviridae*) infects monocotyledonous plants, causing chlorotic mosaic or streaks on green leaf tissue, as well as shortened upper internodes (Matthews et al., 1982). Young plants are most susceptible to MDMV, and the most severe infections cause the termination of ear development. MDMV has caused up to 70% maize yield losses globally since 1960 (Kannan et al., 2018). PVX (genus *Potexvirus*, family *Alphaflexiviridae*) infects solanaceous dicotyledonous plants (Scholthof et al., 2011) and is the type species of its genus (Adams et al. 2005). Occasionally, PVX can cause >15% yield losses in tomato (Strand 2006). PVX interacts synergistically with other viruses to increase the overall virus titer and hence the severity of visible symptoms such as chlorosis, mosaicism and reduced leaf size (Van Regenmortel et al., 2004; Aguilar et al., 2015).

We have previously used the maize/MDMV and tomato/PVX pathosystems to investigate the proteomic effect of salicylic acid (SA) and systemic acquired resistance (SAR). We found that primary metabolism and reactive oxygen species (ROS) are tightly intertwined with the maize/MDMV pathosystem, but biocontrol using SA modulates the plant response to compensate for the negative effects of the virus, restoring physiological homeostasis to certain parts of the plant defense system (del Cueto-Ginzo et al., 2016a). In the tomato/PVX pathosystem, the inhibition of photosynthesis is lifted following the application of SA and the disease symptoms disappear. Most importantly, SA signaling controls the plant's stress response to the virus (Cueto-Ginzo et al. 2016b; Falcioni et al., 2014). In both pathosystems, SA slowed the accumulation of the virus and thus delayed the infection.

We hypothesized that Sp7 also has the ability to modulate plant responses to viruses and could provide a viable, environmentally-friendly alternative for disease control in both monocotyledonous and dicotyledonous plants. We therefore investigated the ability of Sp7 to

reduce the severity of infection in the maize/MDMV and tomato/PVX pathosystems using a differential proteomics approach to identify protein-level changes in the presence or absence of Sp7. We correlated the proteomic changes with the virus titer, photosynthetic parameters and physiological characteristics of the plants during early development.

6.2 Aims

- Employ differential proteomics to better understand maize/MDMV and tomato/PVX viral pathosystems
- Understand how Sp7 interferes at the molecular level of each pathosystem during early vegetative growth stages
- Compare proteomic data with other growth parameters to reach conclusions regarding metabolic changes

6.3 Material and Methods

6.3.1 Experimental design

Two completely randomized single-factor experiments were prepared using maize (*Zea mays* cv. B73) and tomato (*Solanum lycopersicum* L. cv. Boludo) seeds, with four treatment groups (20 biological replicates) per species. The first treatment group was the control (**C**), in which plants were grown from seeds soaked in sterile phosphate-buffered saline (PBS) (10 mM K_2PO_4/KH_2PO_4, 0.14 M NaCl, pH 7.2). In the second treatment group (**Sp7**), plants were grown from seeds soaked in a suspension of Sp7 in PBS prepared as described in the following section. In the third treatment group (**V**), plants were grown from seeds soaked in sterile PBS and were inoculated with either MDMV or PVX, as appropriate. In the fourth treatment group (**Sp7+V**), plants were grown from seeds soaked in a suspension of Sp7 and were subsequently inoculated with the virus, as above. The seeds were sown in 1-L pots containing autoclaved commercial substrate with a fine structure and a pH of 6.0 (Traysubstrat, Klasmann-Deilmann, Geeste, Germany). Plants were then grown under greenhouse conditions (18–25% relative humidity, 25–30 °C, 12-h photoperiod including supplementary lighting, automatic drip irrigation for 1 h twice daily, and an anti-aphid mesh to prevent infestation). Samples were taken at principal growth stage 14 for both maize and tomato according to the BBCH scale (Lancashire et al., 1991) and at weekly intervals thereafter, yielding four samples in total (corresponding to 2, 9, 16 and 21 days post-inoculation (dpi) with the virus). Physiologically in maize, 2 dpi coincided with the four-leaf stage, 9 dpi with early tillering, and 16 dpi and 21 dpi with late tillering. In tomato, 2 dpi coincided with the four-leaf stage, 9 dpi with the seven-leaf stage, 16 dpi with the nine-leaf stage and 21 dpi with the 12-leaf stage.

6.3.2 Preparation and application of bacterial suspension

The *Azospirillum brasilense* Sp7 inoculum was prepared as described in Chapter 3 (Section 3.3.3) and inoculation was performed as in Chapter 5 (Section 5.3.2).

6.3.3 Virus inoculation

In this study, we used viral strains: Potato virus X (PVX, KJ631111) and Maize dwarf mosaic virus (MDMV, AM110558)). Maize and tomato seedlings were inoculated with MDMV and PVX, respectively, when they were at the 3-leaf phenological growth stage, approximately two weeks after planting. MDMV was obtained from infected plants maintained in the greenhouse. Leaves that showed MDMV symptoms from plants tested positive by ELISA test were utilized for the inoculation. The PVX inoculant was made from freeze-dried tomato leaves that had been infected with virus and confirmed with enzyme-linked immunosorbent assay (ELISA).

For inoculation (of both species), a sterile mortar and pestle was placed over ice. Then, 50mL of the inoculation buffer [1M KH_2PO_4 pH 4.9 autoclaved and added to autoclaved 1M Na_2HPO_4 pH 9.6 in a ratio of 40:60; final pH of 7-7.2] was added to the mortar, along with 0.1g carborundum® and the vegetable material (2g freeze-dried and 1g fresh material). The mixture was ground by hand until it was a homogenous dark green liquid. This mixture (1mL) was manually rubbed into the bundle of the top two leaves with the thumb and forefinger, and all residues were washed away with distilled water.

6.3.4 Aerial and root growth analysis

The height of 10 biological replicates was measured per treatment at 9, 16 and 21 dpi for both species. For root analysis, three biological replicates were randomly selected per treatment at 9 and 21 dpi (because the analysis was destructive) and were analyzed using WinRHIZO as described in Chapter 5 (Section 5.3.4).

6.3.5 Bacterial recovery and viral disease assessment

Sp7 colonization assays were carried out 2 and 9dpi on three random samples from each treatment according to Botta et al. (2013) with modifications, as described in Chapter 5 (5.3.4).

Viral disease progress was also determined for each pathosystem at each sampling time (2, 9, 16 and 21 dpi) for both MDMV and PVX. To do so, a direct double-antibody sandwich (DAS)-ELISA was carried out as described by Clark and Bar-Joseph (1984) using polyclonal antisera specific for MDMV and PVX (Loewe Biochemical, Sauerlach, Germany), in Nalgene polystyrene plates (Thermo Fisher Scientific, Waltham, MA, USA). Samples were considered

positive when their average A_{405} value was three times higher than the average of three healthy controls. Positive (infected) plants were compared with 10 repetitions per treatment and sample time.

6.3.6 Leaf gas exchange parameters

Leaf gas exchange was monitored using an infrared gas analyzer (LICOR Biosciences, Lincoln, NE, USA) at the same hour (14.00h) for each sampling time. We measured the photosynthetic rate (A), transpiration rate (E), intercellular CO_2 concentration (C_i) and instantaneous water-use efficiency (WUE_i [A/E]).

6.3.7 Total protein extraction

Extraction was performed as described in Chapter 5 (5.3.6).

6.3.8 Protein analysis

Protein analysis was performed as described in Chapter 5 (5.3.7).

6.3.9 Protein digestion and mass spectrometry

Protein digestion and mass spectrometry analysis was performed as described in Chapter 5 (5.3.8).

6.3.10 Statistical analysis

Statistical analysis was performed as described in Chapter 5 (5.3.9). Proteins were grouped as previously described, with the addition of (8) Viral proteins.

6.4 Results

6.4.1 Sp7 colonization of maize and tomato

In maize and tomato plants grown from seeds imbibed with bacterial suspension, Sp7 was detected on the root systems at both 2 and 9 dpi. The number of Sp7 colonies recovered from the roots of the inoculated plants was 10^5 cfu g^{-1} of moist root tissue. No Sp7 colonies were recovered from the plants grown from seeds imbibed in sterile PBS.

6.4.2 Aerial and root growth

MDMV-infected maize plants were significantly shorter than controls at 9 ($p<0.05$) and 16 ($p<0.01$) dpi, whereas Sp7+MDMV plants were 25% shorter at 16 and 21dpi ($p<0.05$ and $p<0.01$, respectively) (Figure 22A). However, the opposite trend was observed for the tomato plants, where plants in all treatment groups (Sp7, PVX and Sp7+PVX) were significantly taller

(p<0.01) than controls at all sampling times (dpi) (Figure 22B). Notably, Sp7+PVX plants were 62% taller than controls.

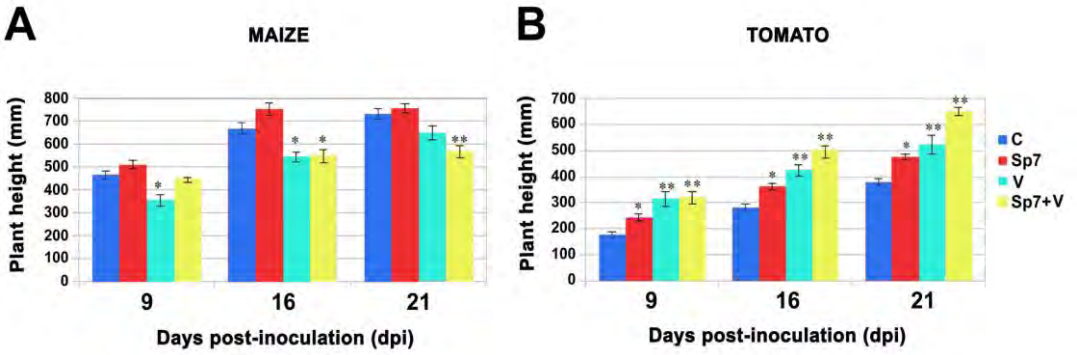

Figure 22. Plant height (mm) of (A) maize (cv. B73) and (B) tomato (cv. Boludo) subjected to different treatments: control (-), virus (V) (MDMV or PVX), *Azospirillum brasilense* (Sp7) and co-treatment (Sp7+MDMV or Sp7+PVX) at 9, 16 and 21 days post-inoculation (dpi). Graph error bars indicate standard error (SE) where n=10. Asterisks indicate statistically significant differences between treatments and controls for each sampling time: * (p<0.05), ** (p<0.01).

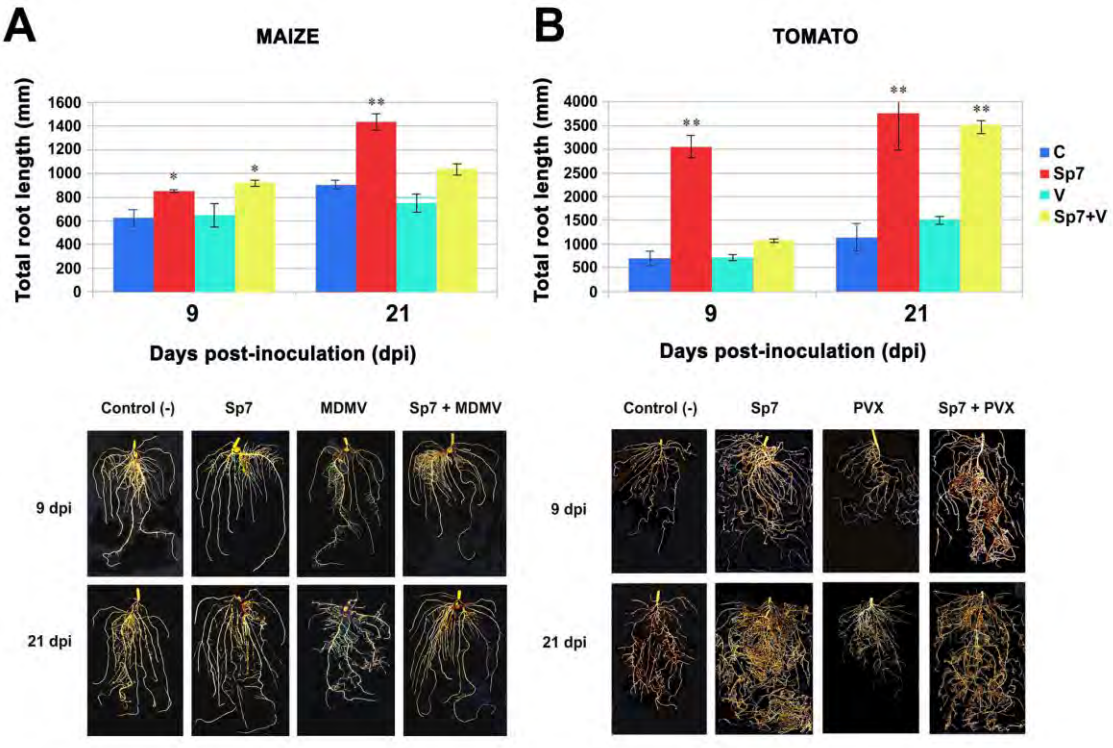

Figure 23. Root length (mm) and morphology of (A) maize (cv. B73) and (B) tomato (cv. Boludo). Graphs (above) indicate root length calculated from the scanned WinRHIZO® root representative images (below), and detail progressive root growth for plants at 9 and 21 days post-inoculation (dpi). Pictured are the four treatment groups: control (-), virus (MDMV or PVX), *Azospirillum brasilense* Sp7 (Sp7) and co-treatment (Sp7+MDMV or Sp7+PVX). Graph error bars indicate standard error (SE) where n=10. Asterisks indicate statistically significant differences between treatments and controls for each sampling time: * (p<0.05), ** (p<0.01).

In maize, there was significantly more root growth in the Sp7-treated plants at 9 and 21 dpi ($p<0.05$ and $p<0.01$, respectively). In the Sp7+MDMV group, the roots were 50% longer than controls at 9 dpi ($p<0.05$) (Figure 23A). PVX-infected tomato plants did not differ from controls in terms of root length, but Sp7-treated plants exhibited significantly longer roots ($p<0.05$) at both sampling times. Sp7+PVX plant roots were significantly longer ($p<0.05$) at 21dpi, i.e. 43% longer than in the controls (Figure 23B).

6.4.3 Photosynthesis and transpiration

The control plants typically showed the lowest levels of photosynthesis (*A*) and transpiration (*E*) in maize but the highest in tomato. At 9 and 16 dpi in maize, *A* was significantly higher for all treatment groups compared to controls, although at 21 dpi only the Sp7+MDMV treatment group remained significantly higher ($p<0.05$) than controls. In the MDMV plants, *E* was significantly higher than in controls at 9 dpi ($p<0.01$). *E* was higher in all treatments compared to controls at 16 dpi ($p<0.01$), but only the MDMV and Sp7+MDMV treatments showed significantly higher *E* values at 21 dpi ($p<0.01$) (Figures 24A and 24C).

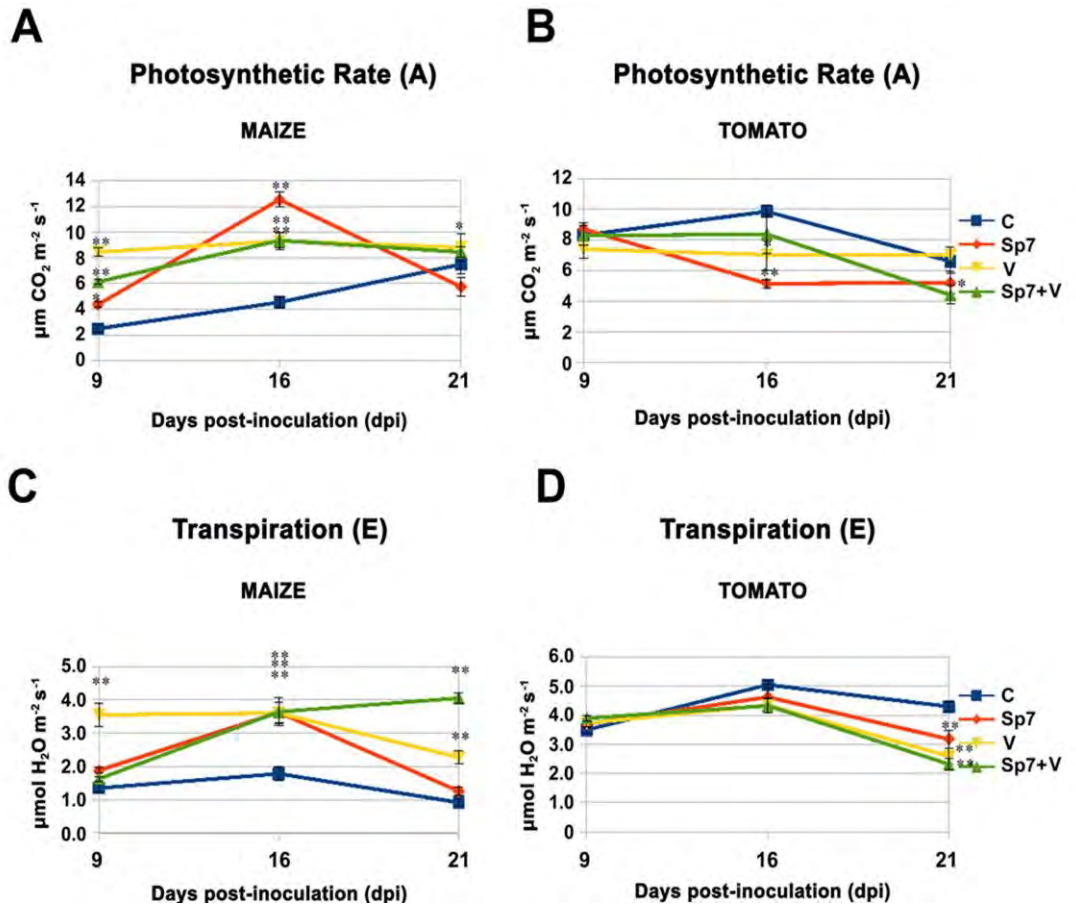

Figure 24. Gas exchange parameters Photosynthetic rate (A) and Transpiration (E) in (A) maize and (B) tomato plants at different days post-inoculation (dpi): control (C), *Azospirillum brasilense* (Sp7), virus inoculated (MDMV or PVX) and co-treated plants (Sp7+MDMV or Sp7+PVX). Graph error bars indicate standard error (SE) where n=10. Asterisks indicate statistically significant differences between treatments and controls for each sampling time: * ($p<0.05$), ** ($p<0.01$).

In tomato, there were no differences among treatment groups for *A* at 9 dpi. At 16 dpi, PVX and Sp7 plants showed significantly lower values of *A* than controls ($p<0.05$ and 0.01, respectively), but only the Sp7 plants retained a lower *E* value at 21 dpi ($p<0.05$). In tomato, significant differences in *E* were only observed at 21 dpi, when *E* was significantly ($p<0.01$) lower for all three treatment groups (Sp7, PVX and Sp7+PVX) compared to the controls (Figures 24B and 24D).

6.4.4 Viral titer

In maize, we observed a significant increase in viral titer at 16 dpi in the inoculated groups (75% in the MDMV plants and 766% in the Sp7+MDMV plants). These values dropped by 25% in both groups at 21 dpi. In both cases, for the titer was higher in the MDMV treatment group than the Sp7+MDMV treatment group (Figure 25A). The same analysis in tomato revealed earlier (9 dpi) peaks in viral titer representing increases of 800% and 600% in the PVX and Sp7+PVX treatment groups, respectively. At 16 dpi, the load decreased significantly by 55% in the PVX group and 25% in the Sp7+PVX group (Figure 25C).

6.4.5 Virus-induced proteome changes

The comparative analysis of leaf protein extracts by 2DGE and MALDI-TOF-MS/MS resulted in the detection of 19 spots with significant variation between MDMV-infected maize and controls (Table 10, Figures 25B and 26A) and 58 with variation between PVX-infected tomato and controls, 13 of which represented the same protein at 9 and 16 dpi (Table 11, Figures 25D and 26B). In MDMV-infected maize, no proteins showed a ≥1.5-fold change in abundance compared to control at 9 dpi and only one met the criterion at 16 dpi: NADP-dependent malic enzyme (NADP-ME) chloroplast precursor (EC 1.1.1.40; +1.50-fold and +1.93-fold for the two spots representing this protein). In PVX-infected tomato, several proteins showed a ≥1.5-fold change in abundance compared to control at 9 dpi and all of them were downregulated: glyceraldehyde-3-phosphate dehydrogenase A (GAPDH-A; EC 1.2.1.9; –1.5-fold); thioredoxin-like protein *CDSP32* (CDSP32; EC 1.8.1.9; –1.5-fold); transketolase (TKT; EC 2.2.1.1; –1.6-fold and –2-fold), fructose-bisphosphate aldolase (FBA; EC 4.1.2.13; –1.74-fold), and 5-methyltetrahydropteroyltriglutamate-homocysteine methyltransferase-like (MHM; EC 2.1.1.14; –2.4-fold). At 16 dpi, most proteins meeting the ≥1.5-fold change criterion were upregulated: glycine dehydrogenase (GLDC; EC 1.4.1.10; +1.85-fold and +3.22-fold), ribulose bisphosphate carboxylase small chain 2A (RBCS-2A; EC 4.1.1.39; +1.80-fold), and phosphoglycerate kinase (PGK; EC 2.7.2.3; +2.13-fold). The only protein to decrease at 16 dpi was NADPH-dependent thioredoxin reductase 3-like isoform 2 inositol-3-phosphate synthase (NTRC; EC 1.8.1.9; –2.5-fold). None of the proteins meeting the ≥1.5-fold change criterion were modulated in both species.

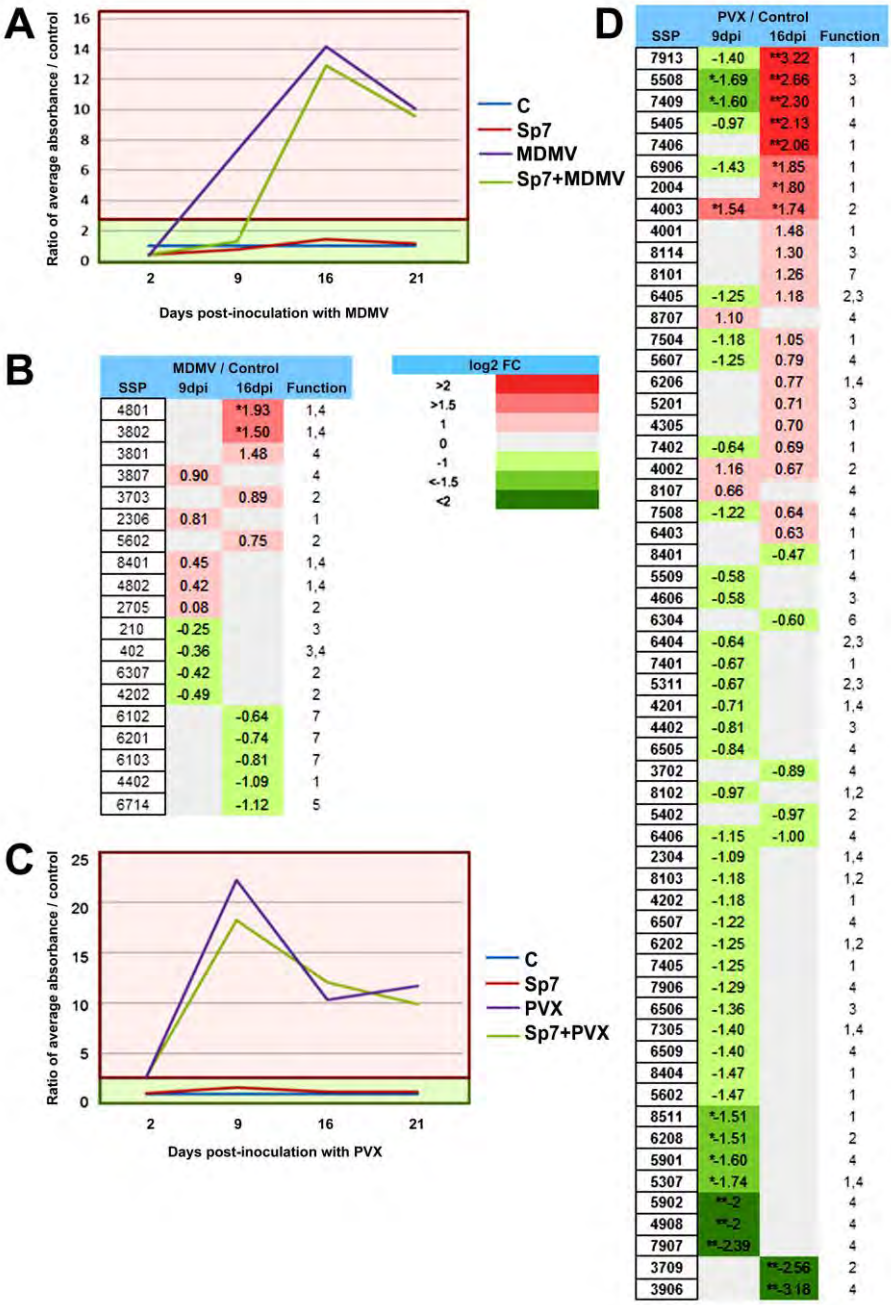

Figure 25. Maize dwarf mosaic virus (MDMV) and Potato virus X (PVX) viral progress and protein expression. (A) MDMV and (C) PVX DAS-ELISA (A_{405}) at 2, 9, 16 and 21 days post-inoculation (dpi) and (B) MDMV and (D) PVX heatmaps of differentially expressed proteins vs. controls at 9 and 16dpi for the four treatment groups Control (-), Virus (MDMV or PVX), *Azospirillum brasilense* (Sp7) and co-treatment (Sp7+MDMV or Sp7+PVX). Heatmap color scale indicates differential regulation as the (log2) Fold Change (FC) of the virus-inoculated plant protein amount relative to control plants at 9 and 16dpi. Analyzed spots were those in which the differences were more consistent (variation coefficient ≤50%) among replicates, spots present in all measured conditions, measured ratios ≤0.5 or ≥2.0 and spots validated *in visu*. Proteins correspond to those in Tables 10 and 11, and are arranged according to relative expression levels; up-regulation is indicated in red, down-regulation in green. A value of 0, in grey, indicates no significant change in protein expression level. (*) indicates a density change of >1.5 or<-1.5 FC, and (**) >2 or<-2 FC. Differential expression is of proteins involved in biochemical pathways related to (1) Photosynthesis, respiration, and chloroplast organization; (2) Redox homeostasis and stress response; (3) Protein synthesis, conformation and transport; (4) Metabolism and energy; (5) Pathogenic cell lysis; (6) Resistance; (7) Unknown; (8)Viral.

6.4.6 Sp7+V co-treatment proteome changes

Corresponding analysis of the plants grown from seeds imbibed with Sp7 revealed 42 spots that differed between Sp7+MDMV-treated maize and controls, and 26 spots that differed between Sp7+PVX-treated tomato and controls. In maize, both Sp7 and MDMV caused changes in the abundance of proteins. The Sp7 effect (Figure 27A) was only significant at 16 dpi for the proteins β-glucosidase 2 (EC 3.2.1.21; +1.79 and +1.82-fold) and MAT (+1.73-fold). The MDMV effect (Figure 27B) was significant at 9 dpi for ribulose-1.5-bisphosphate carboxylase/oxygenase small subunit (RBCS; EC 4.1.1.39; +1.61-fold) and hypothetical protein ZEAMMB73_873979 (+1.50-fold), and at 16 dpi for methionine adenosyltransferase (MAT; EC 1.97.1.4; +1.95-fold), GAPDH (+1.92-fold), NAD-dependent epimerase/dehydratase (EC 5.1.99.6; +1.90-fold) and ascorbate peroxidase (APX; EC 1.11.1.11; +1.54-fold). In tomato, the Sp7 effect (Figure 28A) exclusively caused the downregulation of proteins: GLDC (–2.18-fold) at 9 dpi and PVX movement and silencing protein TGBp1 (–1.64-fold). The PVX effect (Figure 28B) reduced the abundance of chloroplast stem-loop binding protein of 41 kDa b (CSP41b; –1.56-fold) and GLDC (–3.47-fold) at 9 dpi, and increased the of GAPDH-A/CSP41 (+1.82-fold) and thylakoid formation 1 (THF1; +1.63-fold) at 16 dpi.

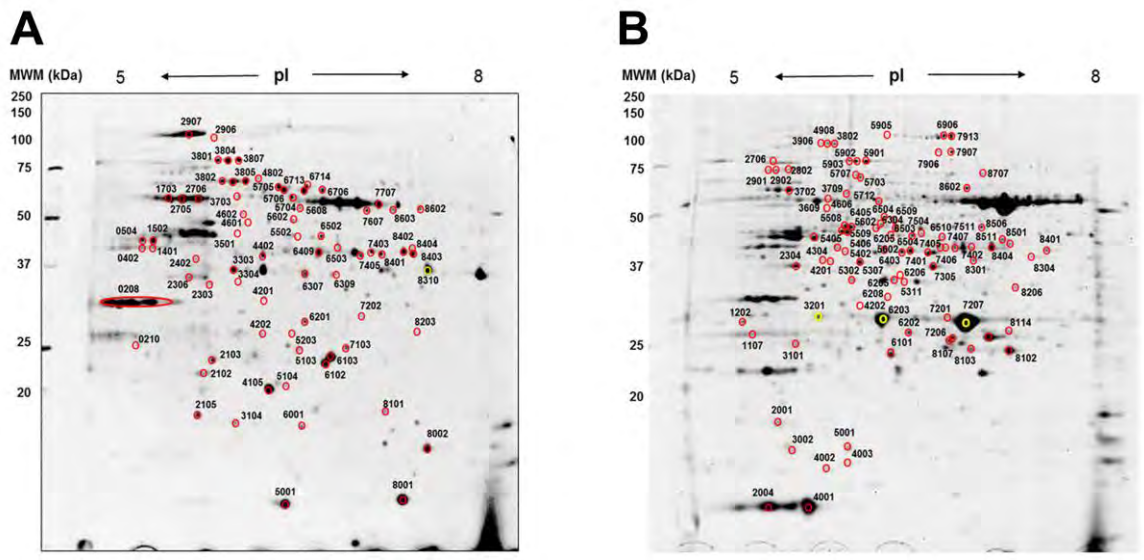

Figure 26. Representative 2-D page gels of extracted proteins from maize and tomato plants 21 days post inoculation (dpi). 2-D PAGE gel image of (A) maize and (B) tomato with Maize dwarf mosaic virus (MDMV) or Potato virus X (PVX) inoculation, respectively. Molecular markers are indicated in kDa. The representative spots and their numbers which show variation between treatments are indicated by the red circles, yellow circles indicate viral proteins.

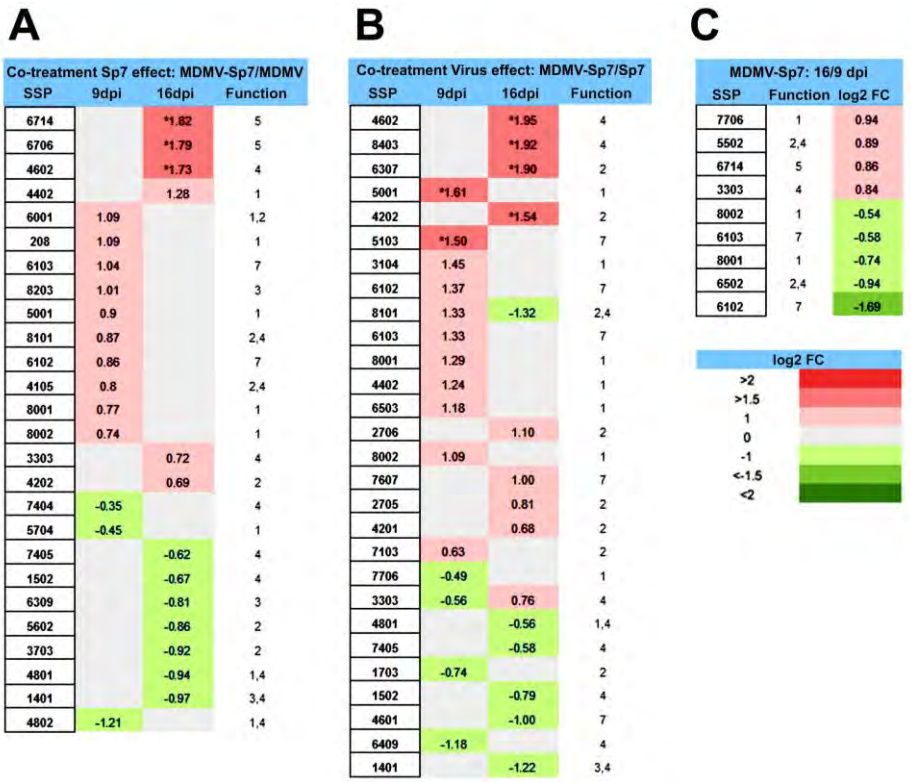

Figure 27. Maize heatmaps of differentially expressed proteins at 9 and 16 days post inoculation (dpi). Different effects of co-treatment *Azospirillum brasilense* Sp7 (Sp7)+Maize dwarf mosaic virus (MDMV) are highlighted in maps A&B: (A) the Sp7 effect (MDMV+Sp7/MDMV), (B) the MDMV effect (MDMV+Sp7/Sp7). Map (C) documents Sp7+MDMV proteins with significant change between 9 and 16dpi. Heatmap color scale indicates differential regulation as the (log2) fold change (FC) of the virus-inoculated plant protein amount relative to control plants at 9 and 16dpi. See Figure 25 legend for more information.

6.5 Discussion

We have previously demonstrated the unique ways in which Sp7 interacts with maize and tomato plants (Lade et al., 2018). The early interaction of Sp7 with maize is more complex and beneficial than the corresponding interaction with tomato because maize is a C_4 plant, allowing it to overcome the stress involved in the association with Sp7. In contrast, Sp7-treated tomato plants activate defense-related and metabolic responses at the four-leaf stage, but inhibit the Calvin-Benson cycle and chloroplast development because photosynthetic proteins are probably damaged by ROS when the plants are small. Here, we aimed to broaden our understanding of the Sp7–maize and Sp7–tomato interactions by including a model virus in each case. We first investigated the impact of MDMV and PVX alone on the host plant at the proteomic level, and then compared the effects of co-treatment. We anticipated that the effects of co-treatment would differ from the effect of the virus alone because (1) we have already reported the unique response of each host to Sp7 (Lade et al., 2018), (2) viruses also interact uniquely with their hosts (Maule 2001); and (3) synergy can occur in tritrophic interactions, and have been documented previously in the case of PVX (Van Regenmortel et al., 2004). In all experiments, we considered a response to be significant only if the fold change in protein abundance was ≥1.5.

Table 10. Main characteristics and function of identified maize proteins corresponding to spots in Figure 26A.

SSP [a]	Protein name	Accession No. [b] (database)	Molecular [c] Weight (Da)/pI	Coverage %	No Peptides Matched/Total peptides	Score [d]	Function [e]
208	Oxygen-evolving enhancer protein 1	ACG31595**	34783/5.59	68	34/50	303	1
210	Chaperonin	ACG33530**	25559/8.67	64	12/27	160	4
402 1401	Phosphoribulokinase Sedoheptulose-1,7-bisphosphatase	B4FQ59*** B6T2L2***	45121/5.84 42303/6.08	76 66	28/74 28/74	260 219	3,4
1502	Phosphogycerate kinase	NP_001147628**	50009/6.07	64	33/49	381	4
1703 2706	ATP synthase subunit beta, chloroplastic	P00827*	54064/5.31	59	31/73	211	2
2306	Chain A crystal structure of Ferredoxin	3VO1_A**	35835/5.43	70	32/45	320	1
2705	ATP synthase subunit beta, mitochondrial	P19023*	59181/6.01	44	24/76	156	2
3104	Cytochrome b6-f complex iron-sulfur subunit	B4FTU7***	21026/6.41	10	3/4	154	1
3303	Fructose-biphosphate aldolase	ACG36798.1**	41924/7.63	64	26/73	248	4
3703	Enolase 2	NP_001105371**	48418/5.70	61	29/53	295	2
3801 3807	Transketolase	Q7SIC9 *	73347/5.47	65	46/72	449	1,4
3802 4801 4802	NADP-dependent malic enzyme, chloroplastic precursor	NP_001105313**	70293/6.09	53	43/78	353	1,4
4105	Germin-like protein	Q6TM44***	22101/6.02	13	2/2	166	2,4
4201	Lactoylglutathione lyase	ACG39003**	35311/6.62	47	21/37	201	2
4202	Ascorbate peroxidase	NP_001152746**	27468/5.64	71	17/31		2
4402	Malate dehydrogenase, cytoplasmic	NP_001105603**	35909/5.77	68	24/45	263	1
4601	Hypothetical protein	NP_001142788**	51917/6.12	51	24/41	271	7
4602	Methionine adenosyltransferase	AFW82691**	46392/6.03	63	26/50	292	4
5001	Ribulose-1,5-bisphosphate carboxylase/oxygenase small subunit	CAA70416**	19364/8.98	69	13/54	153	1
5103	Ribosome recycling factor	NP_001150478**	29328/9.22	29	8/16	419	7
5602	Bifunctional 3-phosphoadenosine 5-phosphosulfate synthetase 2	NP_001147427**	52493/8.30	43	22/31	242	1
5704	ATP synthase CF1 alpha subunit	NP_043022**	55729/5.87	49	31/41	392	1
6001	Cytochrome b6-f complex iron-sulfur subunit	ACG28186**	24321/8.52	41	10/20	152	1,2
6102	TPA: hypothetical protein ZEAMMB73_927356	DAA59517**	32073/9.50	48	12/34	159	7
6103	Hypothetical protein ZEAMMB73_321092	DAA42743**	27411/8.97	49	13/30	185	7
6201	Hypothetical protein Putative uncharacterized protein	NP_001142128**	33566/5.96	41		114	7
6307	NAD-dependent epimerase/dehydratase	B4FH62***	31917/9.11	66	20/24	340	2
6309	50S ribosomal protein L1	NP_001150277**	37235/8.69	56	25/59	229	3
	guanine nucleotide-binding protein beta subunit-like protein	NP_001136800**	36670/6.13	67	18/59	196	3
6409 7404 7405	Glyceraldehyde-3-phosphate dehydrogenase A, chloroplastic precursor	NP_001105414**	43182/7.00	61	25/46	264	4
6503	Fructose-bisphosphate aldolase, cytoplasmic isozyme 1	B6SSU6***	38464/6.26	54	18/21	292	1
6706 6714	Beta-glucosidase2	AFW56713**	64308/6.75	47	35/43	423	5
7103	Chain A, Structure Of Glutathione S-Transferase Iii In Apo Form	1AW9_A**	23416/5.97	68	11/27	166	2
7607	Putative uncharacterized protein	B4FHK4***	42290/6.53	43	23/34	263	7
7706	Ribulose-1.5-bisphosphate carboxylase/oxygenase large subunit	NP_043033**	53295/6.33	59	42/84	341	1
8001	Ribulose bisphosphate carboxylase small chain, chloroplastic precursor	NP_001105294**	19310/9.10	62	18/61	166	1
8002	Photosystem I reaction center subunit IV A	ACG26704.1**	14885/9.79	7	1/1	56	1
8101	Putative peptidyl-prolyl cis-trans isomerase family protein	NP_001136688**	26599/X	X	12/X	135	2,4
8203	GTP-binding nuclear protein Ran-A1	NP_001131881**	25387/6.66	60	15/23	243	3
8310	Coat protein (MDMV) [f]	CAD91557**	34517/6.30	50	18/45	155	8
8401	Glyceraldehyde-3-phosphate dehydrogenase 1	P08735*	36614/6.46	48	19/55	178	1,4
	Glyceraldehyde-3-phosphate dehydrogenase A	P09315*	43182/7.00	48	18/55	166	
	Glyceraldehyde-3-phosphate dehydrogenase 2	Q09054*	36633/6.41	46	16/55	135	
8403	Glyceraldehyde-3-phosphate dehydrogenase 1, cytosolic	NP_001105413**	36600/6.46	53	21/44	232	4

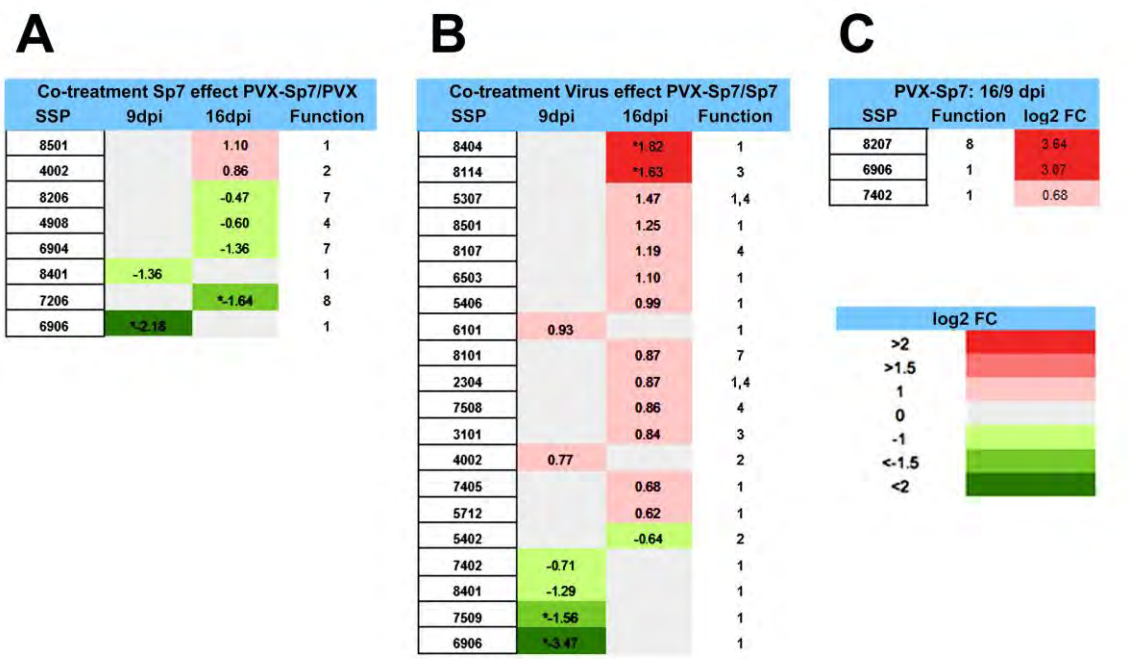

Figure 28. Tomato heatmaps of differentially expressed proteins at 9 and 16 days post inoculation (dpi). Different effects of co-treatment *Azospirillum brasilense* (Sp7)+ Potato virus X (PVX) are highlighted in maps A&B: (A) the Sp7 effect (PVX+Sp7/PVX), (B) the PVX effect (PVX+Sp7/Sp7). Map (C) documents Sp7+PVX proteins with significant change between 9 and 16dpi. Heatmap color scale indicates differential regulation as the (log2) fold change (FC) of the virus-inoculated plant protein amount relative to control plants at 9 and 16dpi. See Figure 25 legend for more information.

6.5.1 The proteomic effect of the virus alone on maize and tomato host plants

In MDMV-inoculated maize, there was a significant increase in the abundance of the plastidial precursor of NADP-ME, which is involved in the pathway that eliminates photorespiratory CO_2 loss in C_4 plants (Rao and Dixon 2016; UniProt Consortium, 2017). An increase in this enzyme in response to viruses has been reported before, leading to the belief that it is host-specific (Doubnerová et al., 2009). Most importantly, the upregulation of NADP-ME may be one of the earliest and most sensitive responses to impending virus infection in uninfected cells (Havelda and Maule 2000) and probably correlates with plant stress tolerance and antioxidant metabolism, which is localized mainly in the chloroplast (Romanowska et al., 2017). Whereas earlier studies reported the cytosolic production of NADP-ME (Doubnerová et al., 2009), here we provide evidence that the plastidial precursor of NADP-ME is involved in the MDMV/maize pathosystem.

← a. Spot numbers refer to Figure 26A, identified either by fingerprint mass spectrometry MS (MALDI-TOF) or by MS/MS (MALDI TOF-TOF). The representative spots and their numbers which show variation between treatments are indicated by the red circles, yellow circles indicate viral proteins.
b. Accession number and molecular mass according to SwissProt (us.expasy.org/sprot)*, NCBI ** and TrEMBL *** databases.
c. MW and pI were calculated from aminoacid sequence
d. Scores of proteins identified by peptide mass fingerprinting were determined according to Mowse values obtained either from MASCOT.
e. (1) Photosynthesis, respiration, and chloroplast organization; (2) Redox homeostasis and stress response (defense); (3) Protein synthesis, conformation and transport; (4) Metabolism and energy; (5) Pathogenic cell lysis; (6) Resistance; (7) Unknown; (8) Viral proteins.
f. Viral protein that is not represented in the heatmaps due to insignificant variation, but was detected.

Table 11. Main characteristics and function of identified tomato proteins corresponding to spots in Figure 26B.

SSP [a]	Protein name	Accession No. [b] (database)	Molecular [c] Weight (Da)/pI	Coverage %	No Peptides Matched/Total peptides	Score [d]	Function [e]
2004 4001	Ribulose bisphosphate carbox. small chain 2A	P07179 *	20493/6.59	48	11/46	134	1
2304 4201 5307 6206 7305	Fructose-bisphosphate aldolase 2	XP_004233550 **	42872/6.07	53	18/47	203	1,4
3101	Chaperonin 21 precursor	NP_001234423**	26603/6.85	58	13/36	177	3
3201 6203 7207 8103	Coat protein OS=Potato virus X [f]	P31798 *	25275/6.73	22	3/3	31	8
3702	ATP synthase subunit alpha	Q2MIB5 *	55434/5.14	42	25/42	296	4
3709	Inositol-3-phosphate synthase	XP_004239994 **	56697/5.45	46	25/75	159	2
3906 4908	ATP-dependent Clp protease ATP-binding subunit clpA homolog CD4B	XP_004252280 **	102418/5.99	43	40/56	379	4
4002 4003	Superoxide dismutase [Cu-Zn]	P14831 *	22328/5.77	12	2/2	132	2
4202	Magnesium-protoporphyrin O-methyltransferase-like	XP_004235845 **	35879/6.54	43	16/35	181	1
4305 5406 5602 6503 7401 7504	Ribulose bisphosphate carbox./oxygenase activase 1	O49074 *	50897/8.61	50	26/56	245	1
4402 5508	Elongation factor TuA	XP_004241515 **	56286/6.69	14	5/5	180	3
4606 6506	Glutamate-1-semialdehyde 2,1-aminomutase	NP_001234690 **	51722/6.54	48	26/43	235	3
5201	BG125080.1 EST470726 tomato shoot/meristem	BG125080 ***	25967/9.18	6	3	297	3
5311	Succinic semialdehyde reductase isofom2	NP_001233836 ** BAG16486	38941/8.50	4	2/2	92	2,3
5402	Quinone oxidoreductase-like protein At1g23740	XP_004238663 **	40976/7.74	12	4/4	143	2
5405 5509	Phosphoglycerate kinase	XP_004243968**	50592/7.66	11	4/4	211	4
5607	Diaminopimelate decarboxylase 1	XP_004230896**	53379/6.71	4	2/2	195	4
5712	Ribulose bisphosphate carboxylase/oxygenase large subunit	YP_514860**	53434/6.55	38	18/55	162	1
5901 5902	Transketolase	XP_004248560 **	80268/5.97	46	33/52	347	4
6202 8102 8103	Carbonic anhydrase	NP_001234048 **	34845/6.67	63	21/36	245	1,2
6101	Chlorophyll a-b binding protein 8	XP_004248217**	29261/8.65	15	2/2	237	1
6208	Thioredoxin-like protein CDSP32	XP_004238392 **	33779/7.57	18	6/6	241	2
6304	mRNA binding protein precursor	NP_001234656 **	44084/7.10	38	21/45	228	6
6403	Malate dehydrogenase	XP_004247734 **	35703/5.91	72	24/53	259	1
6404 6405	Monodehydroascorbate reductase-like	XP_004246547 **	47106/5.77	72	29/39	386	2,3
6406	ATP synthase gamma chain	XP_004232711**	41752/8.15	13	3/6	224	4
6503	Glyceraldehyde-3-phosphate dehydrogenase B	XP_0042238446**	51421/6.86	60	28/80	226	1
6505	S-adenosylmethionine synthase 3	NP_001234004 **	43082/5.76	60	26/44	276	4
6507	ATP sulfurylase 1	XP_004234020 **	52376/6.94	48	27/41	296	4
6509 7508	GDP-mannose 3',5'-epimerase	NP_001234734 **	42828/5.88	45	21/32	248	4
6904	Unknown protein						7
6906 7913	Glycine dehydrogenase [decarboxylating]	XP_004245101**	114020/6.69	5	5/5	199	1
7206	Movement and silencing protein TGBp1 OS=Potato virus X (strain X3)	P17780*	24695/6.31	42	5/5	350	8
7402 7405 7406 7409 7509 8404	Chloroplast stem-loop binding protein of 41 kDa b	XP_004241412 **	42596/7.67	60	23/29	321	1
7409 8404 8501 8511	Glyceraldehyde-3-phosphate dehydrogenase A	XP_004236849 **	42940/8.46	58	23/60	234	1
7906 7907	5-ethyltetrahydropteroyltriglutamate--homocysteine methyltransferase-like	XP_004249374 **	85014/6.01	39	26/35	319	4
8101	BP903052.1 Solanum lycopersicum cDNA, clone	BP903052 ***	17598/6.99	56	10/40	134	7
8107	Triose phosphate isomerase (cytosolic isoform)	AAR11379 **	27251/5.73	11	2	155	4
8114	Protein thylakoid formation1	XP_004243305**	33558/8.69	7	3/3	50	3
8206	Unknown protein						7
8401	Glyceraldehyde-3-phosphate dehydrogenase	NP_001266254 **	32097/5.93	56	15/22	192	1
8707	LEXYL2	BAC98299 **	69724/8.04	7	4/4	184	4

Photosynthesis (*A*) and transpiration (*E*) both increased significantly in MDMV-infected maize plants, although this pathosystem generally causes both parameters to decrease (Tu and Ford, 1968; Lindsey and Gudauskas, 1975). However, the growth of MDMV-infected plants becomes unsynchronized with healthy controls (Tosic and Misovic, 1967), and the negative correlation between light and infectivity suggests that enhanced photosynthesis and chloroplast function may play a positive role in defense responses during maize–virus interactions (Zhao et al., 2016). The sampling time at which *A* and *E* increased (16 dpi) is relatively early in the pathogenesis cycle, so together with protein data from this sampling time there is evidence that upregulated chloroplast function is an early defense response in maize, especially given that the reaction tapers off at 21 dpi. Coincidentally, the timing of this reaction corresponds with the increase in *A* and *E* caused by the treatment of maize plants with Sp7 as we previously reported (Lade et al., 2018). Sp7 similarly increases the abundance of ROS-scavenging enzymes to counter the initial stress and limit the degree of photo-inhibition, but MDMV infection uniquely activates NADP-ME to accomplish this.

In PVX-infected tomato, there was a prompt decrease at 9 dpi (seven-leaf stage) in proteins related to oxidative stress (CDSP32), the Calvin-Benson cycle (GAPDH-A, TKT and FBA), and amino acid metabolism (MHM). The depletion of these proteins provides evidence that the Calvin-Benson cycle was disturbed by PVX infection, inducing oxidative stress in the plants, as found in rice infected with the Rice black-streaked dwarf virus (Xu et al., 2013). At 16 dpi (nine-leaf stage), there was an increase in the abundance of proteins related to photosynthesis (RBCS), carbohydrate biosynthesis (PGK), and amino acid metabolism (GLDC), but a decrease in the abundance of NTRC, which is required for chlorophyll biosynthesis and chloroplast redox regulation (Lepistö et al., 2013). We also observed a lower photosynthetic rate and reduced chlorophyll levels at this time, which are typical plant stress responses to virus infection (Zechmann et al., 2003; Hooks et al., 2008). PVX can also disrupt plant growth (Hussein and Kamberoglu 2017) and modify the ultrastructure of the chloroplast membrane and grana stacks due to the plastidial localization of the PVX coat protein and virions (Qiao et al., 2009). Although PVX infection has not been directly correlated to the modulation of NTRC before, NTRC deficiency may perturb the chloroplast redox balance and increase oxidative stress (Ojeda et al., 2017). Loss of NTRC activity accelerated the spread of *Pseudomanas syringae* pv. *tomato* DC3000 disease-associated cell death and the accumulation

a. Spot numbers refer to Figure 26A, identified either by fingerprint mass spectrometry MS (MALDI-TOF) or by MS/MS (MALDI TOF-TOF). The representative spots and their numbers which show variation between treatments are indicated by the red circles, yellow circles indicate viral proteins.
b. Accession number and molecular mass according to SwissProt (us.expasy.org/sprot)*, NCBI ** and TrEMBL *** databases.
c. MW and pI were calculated from aminoacid sequence
d. Scores of proteins identified by peptide mass fingerprinting were determined according to Mowse values obtained either from MASCOT.
e. (1) Photosynthesis, respiration, and chloroplast organization; (2) Redox homeostasis and stress response (defense); (3) Protein synthesis, conformation and transport; (4) Metabolism and energy; (5) Pathogenic cell lysis; (6) Resistance; (7) Unknown; (8) Viral proteins.
f. Viral protein that is not represented in the heatmaps due to insignificant variation, but was detected.

of ROS (Ishiga et al., 2012). Our study is the first to confirm the same phenomenon in the tomato/PVX pathosystem.

The lower rate of photosynthesis we observed does not typically correspond with the increased abundance of RBCS-2A because this protein improves the photosynthetic capacity of leaves (Izumi et al., 2012). However, RBCS is often a target of viruses (Lin et al., 2011). RBCS plays an essential role in virus movement, host susceptibility and interaction (Zhao et al., 2013). Previous studies at the proteomic level have even suggested that certain viruses can recruit chloroplast photosynthesis-related proteins (CPRPs) such as RBCS to viral replication complexes (VRCs) during all infection stages (Brizard et al., 2006). Given the simultaneous increase in abundance of GLDC (indicating that the Calvin-Benson cycle is inhibited) and PGK, the plant appears to be trying to correct an imbalance in photosynthetic metabolism (Rosa-Tellez et al., 2017; Timm et al., 2016), probably caused by the hijacking of RBCS by the virus.

6.5.2 Physiology of co-treated plants

Our previous work revealed that Sp7 induces an early stress response in maize, resulting in the accumulation of ROS-scavenging enzymes, reducing photo-inhibition and increasing photosynthesis to counterbalance the loss of Calvin-Benson cycle products (Lade et al., 2018). Here we found that the Sp7+MDMV co-treatment also increases the level of ROS-scavenging enzymes, and boosts photosynthesis to an even greater degree than Sp7 alone, indicating a synergic interaction. In Sp7-treated tomato plants, ROS can also stimulate growth of the aerial tissues and embryonic root (Passardi et al., 2006; Lade et al., 2018) and this may also occur in PVX-infected plants. Although numerous studies have shown that PVX-infected plants grow to only 65% of the height of healthy controls (Balogun et al., 2002; Hussein and Kamberoglu, 2017), they considered longer periods of time than our study, with heights reported after 3 weeks (Hussein and Kamberoglu, 2017) or 7 weeks (Balogun et al., 2002). This indicates that PVX inoculated alone does not immediately impede plant aerial growth, but the stunting effects become apparent at around the time other visible symptoms emerge (3–4 weeks).

The co-treatment to tomato plants with PVX and Sp7 led to taller plants with longer roots. A similar phenomenon was reported when tomato plants were co-treated with PVX and ISR2000, an elicitor of SAR comprising yeast cell walls, *Lactobacillus acidophilus*, plant extracts and benzoic acid (Hussein and Kamberoglu, 2017). In plants treated with the elicitor alone, the increase in height was attributed to a combination of SAR (Yildiz and Aysan, 2005), a higher nitrogen content and a higher photosynthetic rate (Roshanpour et al. 2014). In the co-treatment, ISR2000 elicited the same mechanisms, not only inhibiting the virus but to also increasing the plant height by a further 10%, confirming a synergistic interaction. Our results

not only agreed with this finding, but revealed that the beneficial effect of the combined treatment is also exerted below ground.

6.5.3 The isolated effects of MDMV and Sp7 in co-treated maize plants

The comparison of proteomic data for the various treatments revealed distinct effects in the co-treated maize caused by Sp7 or MDMV. We restricted our analysis to proteins that showed a fold change of ≥1.5 in either the positive or negative direction and considered such changes significant. In the maize plants treated with MDMV and/or Sp7, all significant changes were positive, i.e. the relevant proteins became more abundant. MDMV had an effect on co-treated plants at 9 dpi by increasing the abundance of RBCS which correlated with a higher photosynthetic rate. Notably, the MDMV titer in the co-treated plants remained low at this sampling time, its increase being delayed by 7 days compared to the plants treated with MDMV alone. In virus-infected plants, RBCS fulfils two functions: (1) it becomes more active in the leaves, thus reducing oxygenation rates and boosting overall photosynthetic capacity (Tanaka et al., 2007; Morita et al., 2014), and (2) it can be recruited into VRCs. Our results provided evidence that RBCS participated in both roles at 9 dpi to benefit the host plant. The greater abundance of RBCS can reduce local susceptibility to infection, but facilitates long-distance virus movement (Zhao et al., 2012). The delayed increase in viral titer together with the higher rate of photosynthesis benefitted the plant by allowing it to grow more vigorously earlier on.

At 16 dpi, there was a significant increase in the abundance of Calvin-Benson cycle enzymes (such as MAT and GAPDH) as well as proteins linked to redox homeostasis (such as NAD-dependent epimerase/dehydratase and APX). In addition to their normal metabolic functions, all of these proteins have been linked to viral activity in previous studies. For example, the increased abundance of a Rice dwarf virus protein promoted the activity of S-adenosyl-L-methionine (SAM), a downstream product of MAT. SAM is one of the building blocks of ethylene. Many viruses cause infected plants to synthesize more ethylene, which benefits the viruses and facilitates infection. Plants that accumulate too much SAM are less able to defend themselves against viruses, whereas plants with low levels of SAM are better able to fight off viral infection (Zhao et al., 2017). The increased abundance of MAT indicates the upregulation of methionine metabolism, and thereby the synthesis of more ethylene, which may promote susceptibility or resistance depending on the overall levels. In our co-treated plants, the quantity of ethylene produced confers resistance.

A higher level of GAPDH typically implies either that CO_2 assimilation is accelerated by MDMV (Xu et al., 2013), or that ROS have accumulated in the plant (Jorrín-Novo et al., 2009). In agreement with the latter option, two redox homeostasis proteins (NAD-dependent epimerase/dehydratase and APX) that link antioxidant metabolites in the glutathione-ascorbate

cycle also became more abundant. Specifically, the glutathione-ascorbate cycle is responsible for detoxifying hydrogen peroxide (H_2O_2) and scavenging ROS (Ishikawa and Shigeoka, 2008). However, plants with higher levels of ascorbate can adapt to RNA virus infections more quickly, thus showing weaker symptoms and accumulating lower levels of ROS (Wang et al., 2011). Early, high-dose ascorbate treatments can alleviate symptoms of infection, and eventually inhibit virus replication with such efficacy that ascorbate is believed to participate in unique plant-defense machinery, in addition to H_2O_2 signaling (Wang et al., 2011). Our results fully support this finding.

The Sp7 effect was significant at 16 dpi for β-glucosidase 2 and MAT in co-treated maize plants. In our previous study considering the effect of Sp7 on maize metabolism, we concluded that because Sp7 itself produces β-glucosidases, the expression of exogenous β-glucosidases may induce phytohormone synthesis and thus increase resistance to biotic stress (Jin et al., 2011). This is synonymous with a priming effect, in which the PGPR activate ISR and the corresponding hormone pathways (Lade et al., 2018). The increased abundance of MAT is consistent with this effect, which is often linked to the upregulation of ethylene biosynthesis and ISR in the case of inoculation with PGPR (Kwon et al., 2010). The increase in MAT in the co-treated maize plants can be attributed to both the Sp7 and MDMV effects. The timing of MAT accumulation coincides with the significant increase in viral load in co-treated plants at 16 dpi. Given that the plants solely inoculated with MDMV exhibited similar viral titers at the same time, but did not accumulate high levels of MAT, we can deduce that the greater abundance of this protein in co-treated plants is indeed a product of the Sp7+MDMV interaction.

At 9 and 16 dpi, co-treated plants showed a significantly higher rate of photosynthesis (*A*). This was also the case for plants treated solely with MDMV, although the underlying mechanisms causing these changes are probably different in co-treated plants, based on the greater abundance of proteins involved in redox regulation, priming and defense-related processes. The chloroplasts are major sites for the generation of ROS, via the photosynthetic electron transport chain (Asada, 2006; Muhlenbock et al., 2008). We concluded that more efficient photosynthesis and chloroplast functions play a key role in defense during the early MDMV/maize pathogenesis cycle due to the greater abundance of NADP-ME. Sp7 must interfere with the NADP-ME signaling that typifies MDMV–maize interactions because although we observed similar reactions favoring the accumulation redox, antioxidant and hormone-related proteins in co-treated plants, different sets of proteins are involved (GAPDH, NAD-dependent epimerase/dehydratase and APX).

6.5.4 The isolated effects of PVX and Sp7 in co-treated tomato plants

In tomato, the PVX effect initially reduced the levels of CSP41, implying a decrease in the translational activity of chloroplasts (Leister, 2014), whereas the lower levels of GLDC reflect the upregulation of the Calvin-Benson cycle and the downregulation of photorespiration (Timm et al., 2016). These contrasting events indicate that lower levels of GLDC may compensate for the loss of CSP41b. The subsequent restoration of CSP41b levels at 16 dpi suggests that the PVX effect in co-treated tomato plants initially reduces photosynthesis-related protein accumulation but not permanently. The photosynthetic rate (*A*) in the co-treated plants was unchanged at this time, but fell significantly later on. In previous studies of the tomato/PVX pathosystem, similar declining levels of chlorophyll were attributed to SAR (Falcioni et al., 2014), indicating that there are many overlaps in the mechanisms of SAR and ISR (typically induced by Sp7).

GAPDH, which became more abundant at 16 dpi, may be a critical host factor that increases plant virus movement and replication (Kaido et al., 2014), and often leads to increased virulence of positive strand RNA viruses such as PVX. GAPDH also plays a variety of regulatory roles, inhibiting the replication of Tomato bushy stunt virus by modulating strand asymmetry (Huang and Nagy, 2011) and of Bamboo mosaic virus and its satellite RNA (Prasanth et al., 2011). This protein was not significantly affected by the isolated PVX infection in tomato but became more abundant in the co-treatment, indicating its abundance is dependent on the synergistic Sp7+PVX interaction.

THF1, which was also more abundant at 16 dpi, is involved in coronatine signaling (a jasmonate mimic) and provides defense against bacterial speck disease in tomato (Wangdi et al., 2010a). THF1 is located in the chloroplast and is thought to be involved in the maintenance of ROS homeostasis (Wangdi et al., 2010b). Current evidence suggests that THF1 may have multiple functions in the biogenesis of PSII and sugar signaling (Keren et al., 2005; Huang et al., 2006), namely that it is required for dynamic changes in PSII–LHCII complexes by physically interacting with Lhcb proteins (Huang et al., 2013). At 16 dpi, our results provided evidence that PVX inhibits PSII activity by reducing the abundance of NTRC and the photosynthetic rate, so the greater abundance of THF1 in Sp7+PVX plants indicates that co-treatment counteracts this effect.

Finally, the Sp7 effect reduced the abundance of the PVX movement and silencing protein (TGPp1) in co-treated plants, coinciding with falling viral titers at 16 dpi. Plants inoculated solely with PVX exhibited a nearly identical negative trend in viral titer, although TGPp1 levels were unchanged. Earlier studies showing that plants with similar viral titers can show great differences in the severity of symptoms indicate that the modulation of host gene

expression, especially the expression of genes involved in critical signaling pathways, is more likely responsible for symptom development (García-Marcos et al. 2009). In our case, Sp7 reduces the expression of the TGPp1 protein and subsequent modulation of related signaling pathways, ultimately leading to less susceptible and more vigorous plants.

6.6 Conclusions

Our study has revealed several novel characteristics of each plant/virus pathosystem. In the maize/MDMV system, we observed the significant and host-specific increase in plastidial NADP-ME, which anticipates viral infection and enhances photosynthesis and chloroplast functions to compensate. In the tomato/PVX system, immediate effects of the virus include the disruption of the Calvin-Benson cycle, an increase in oxidative stress, the inhibition of PSII activity and a lower photosynthetic rate. Even so, plant growth is not immediately affected, and only becomes apparent at the time plants develop other symptoms of infection. Finally, we identified RBCS as a target of PVX.

In general, co-treatment with a virus and Sp7 caused the differential regulation of more proteins than treatment with the virus alone, and there were indications of priming via ISR in both pathosystems. The viral titer was similar in the co-treatment and individual treatment, but co-treatment achieved better performance in both tomato (increase in plant height and root length) and maize (higher photosynthetic rate). Interestingly, we found that Sp7 does not reduce the viral load in either the tomato/PVX or maize/MDMV systems, but nevertheless achieves positive growth benefits in both plant species. In the case of maize/MDMV, Sp7 delays the increase in viral load by 7 days. We also observed a significant upregulation of ROS-scavenging enzymes, methionine metabolism and the glutathione-ascorbate cycle. In the tomato/PVX system, Sp7 modulated the abundance of several proteins that are integral to the balance between susceptibility and resistance, namely GAPDH, THF1 and TGPp1. Finally, the activity of PSII and proteins related to chloroplast activity initially decreased in the Sp7+PVX co-treatment but recovered over time due to the upregulation of the Calvin-Benson cycle. Our results provide insight into the interactions between Sp7, viruses and hosts plants and identify several mechanisms by which PGPR can protect plants from the detrimental effects of viral infections.

6.7 References

Aguilar E, Almendral D, Allende L, Pacheco R, Chung BM, Canto T, Tenllado F. (2015) The P25 protein of *Potato Virus X* (PVX) is the main pathogenicity determinant responsible for systemic necrosis in PVX-associated synergisms. *Journal of Virology* 89(4):2090-2103.

Al-Ani RA, Adhab MA, Matny ON (2013) Management of *potato virus Y* (PVY) in potato by some biocontrol agents under field conditions. *Advances in Environmental Biology* 7(3):441-444.

Al-Ani RA, Adhab MA, El-Muadhidi MA, Al-Fahad MA (2011) Induced systemic resistance and promotion of wheat and barley plants growth by biotic and non-biotic agents against barley yellow dwarf virus. *African Journal of Biotechnology* 10(56):12079-12084

Asada K (2006) Production and scavenging of reactive oxygen species in chloroplasts and their functions. *Plant Physiology* 141:391–396.

Balogun O S, Xu L, Teraoka T, Hosokawa D (2002) Effects of single and double infections with *potato virus X* and *Tobacco mosaic virus* on disease development, plant growth, and virus accumulation in tomato. *Fitopatologia Brasileira* 27:241–248

Bashan Y, Holguin G, de-Bashan L (2004) *Azospirillum*–plant relationships: physiological, molecular, agricultural, and environmental advances (1997–2003). *Canadian Journal of Microbiology* 50:521–577.

Bashan Y, de-Bashan LE (2002) Protection of tomato seedlings against infection by *Pseudomonas syringae* pv tomato using the plant growth promoting bacterium *Azospirillum brasilense*. *Applied Environmental Microbiology* 68:2637–2643.

Bashan Y, Holguin G, Lifshitz R (1993) Isolation and characterization of plant growth promoting rhizobacteria. In: B.R. Glick (Ed.), *Methods in Plant Molecular Biology and Biotechnology* (pp. 331–345) Boca Raton, FL, USA: CRC Press.

Botta LA, Santacecilia A, Ercole C, Cacchio P, del Gallo M (2013) *In vitro* and *in vivo* inoculation of four endophytic bacteria on *Lycopersicon esculentum*. *Nature Biotechnology* 30(6):666–674.

Brizard JP, Carapito C, Delalande F, Van Dorsselaer A, Brugidou C (2006) Proteome analysis of plant-virus interactome: comprehensive data for virus multiplication inside their hosts. *Molecular and Cellular Proteomics* 5:2279–2297.

CABI. (2018). *Invasive Species Compendium*. Wallingford, UK: CAB International. www.cabi.org/isc.

Clark MF, Bar-Joseph M (1984) Enzyme immunosorbent assay in plant virology. In: K Maramorosch & H Koprowski (eds.), *Methods in Virology*. Vol. 7 (pp. 51-58). New York: Academic Press.

Cueto-Ginzo AI, Serrano L, Sin E., Rodríguez R, Morales JG, Lade SB, Medina V, Achón, M.A. (2016a) Exogenous salicylic acid treatment delays initial infection and counteracts alterations induced by *Maize dwarf mosaic virus* in the maize proteome. *Physiological and Molecular Plant Pathology* 96:46–59.

Cueto-Ginzo AI, Serrano L, Bostock RM, Ferrio JP, Rodríguez R, Arcal L, Achón MA, Falcioni T, Luzuriaga WP, Medina V (2016b) Salicylic acid mitigates physiological and proteomic changes induced by the SPCP1 strain of *Potato virus X* in tomato plants. *Physiological and Molecular Plant Pathology*, 93:1-11.

Dashti NH, Montasser MS, Ali NY, Bhardwaj RG, Smith DL (2007) Nitrogen biofixing bacteria compensate for the yield loss caused by viral satellite RNA associated with cucumber mosaic virus in tomato. *The Plant Pathology Journal* 23(2):90-96.

Doubnerová V, Müller K, Čeřovská N, Synková H, Spoustová P, Ryšlavá H (2009) Effect of *Potato Virus Y* on the NADP-Malic enzyme from *Nicotiana tabacum* L.: mRNA, expressed protein and activity. *International Journal of Molecular Sciences* 10:3583-3598.

Falcioni T, Ferrio JP, Cueto AI, Giné J, Achón MA, Medina V (2014) Effect of salicylic acid treatment on tomato plant physiology and resistance to *Potato virus X* infection. *European Journal of Plant Pathology* 138:331-345.

García-Marcos A, Pacheco R, Martiáñez J, González-Jara P, Díaz-Ruíz JR, Tenllado F (2009). Transcriptional changes and oxidative stress associated with the synergistic interaction between *Potato virus X* and *Potato virus Y* and their relationship with symptom expression. *Molecular Plant-Microbe Interactions* 22:1431–1444.

Havelda Z, Maule AJ (2000) Complex spatial responses to cucumber mosaic virus infection in susceptible *Cucurbita pepo* cotyledons. *The Plant Cell* 12:1975-1985.

Haya, S, Ali B, Ahmad A (2007) Salicylic acid: biosynthesis, metabolism and physiological role in plants. In: S. Hayat & A. Ahmad (eds), *Salicylic Acid: a Plant Hormone* (pp.1E14). Dordrecht, The Netherlands: Springer.

Hooks CRR, Wright MG, Kabasaw DS, Manandhar R, Almeida RPP (2008) Effect of *banana bunchy top virus* infection on morphology and growth characteristics of banana. *Annals of Applied Biology* 1531):1–9.

Huang J, Taylor JP, Chen JG, Uhrig JF, Schnell DJ, Nakagawa T, Korth KL, Jones AM (2006) The plastid protein THYLAKOID FORMATION1 and the plasma membrane G-protein GPA1 interact in a novel sugar-signaling mechanism in *Arabidopsis*. *The Plant Cell* 18:1226–1238.

Huang TS, Nagy PD (2011) Direct inhibition of tombusvirus plus-strand RNA synthesis by a dominant negative mutant of a host metabolic enzyme, glyceraldehyde-3-phosphate dehydrogenase, in yeast and plants. *Journal of Virology* 85:9090–9102.

Huang W, Chen Q, Zhu Y, Hu F, Zhang L, Ma Z, He Z, Huang J (2013) Arabidopsis thylakoid formation 1 is a critical regulator for dynamics of PSII–LHCII complexes in leaf senescence and excess light. *Molecular Plant* 6 (5):1673-1691.

Hussein M, Kamberoglu MA (2017) The response to *Potato virus X* infection of tomato plants treated with ISR2000. *European Journal of Plant Pathology* 149 (4):807-815.

Ishiga Y, Ishiga T, Wangdi T, Mysore KS, Uppalapati SR (2012) NTRC and chloroplast-generated reactive oxygen species regulate *Pseudomonas syringae* pv. *tomato* disease development in tomato and *Arabidopsis. Molecular Plant-Microbe Interactions* 25 (3):294-306.

Ishikawa T, Shigeoka S (2008) Recent advances in ascorbate biosynthesis and the physiological significance of ascorbate peroxidase in photosynthesizing organisms. *Bioscience, Biotechnology and Biochemistry* 72:1143–1154

Jorrín-Novo JV, Maldonado AM, Echevarría-Zomeño S, Valledor L, Castillejo MA, Curto M, Valero J, Sghaier B, Donoso G, Redondo I (2009) Plant proteomics update (2007-2008): second-generation proteomic techniques, an appropriate experimental design, and data analysis to fulfill MIAPE standards, increase plant proteome coverage and expand biological knowledge. *Journal of Proteomics* 72:285–314.

Kaido M, Abe K, Mine A, Hyodo K, Taniguchi T, Taniguchi H, Mise K, Okuno T (2014) Gapdh-A recruits a plant virus movement protein to cortical virus replication complexes to facilitate viral cell-to-cell movement. *PLOS Pathology* 10:e1004505.

Kannan M, Ismail I, Bunawan H (2018) *Maize dwarf mosaic virus*: from genome to disease management. *Viruses*,10 (9):492.

Keren N, Ohkawa H, Welsh EA, Liberton M, Pakrasi HB (2005) Psb29, a conserved 22-kD protein, functions in the biogenesis of photosystem II complexes in *Synechocystis* and *Arabidopsis*. *The Plant Cell* 17:2768–2781

Kwon YS, Ryu C-M, Lee S, Park HB, Han KS, Lee JH, Lee K, Chung WS, Jeong MJ, Kim HK, Bae DW (2010). Proteome analysis of *Arabidopsis* seedlings exposed to bacterial volatiles. *Planta* 1370:1355–1370.

Leister D (2014) Complex(iti)es of the ubiquitous RNA-binding CSP41 proteins. *Frontiers in Plant Science* 5 (255):1–4.

Lepistö A, Pakula E, Toivola J, Krieger-Liszkay A, Vignols F, Rintamäki E (2013) Deletion of chloroplast NADPH-dependent thioredoxin reductase results in inability to regulate starch synthesis and causes stunted growth under short-day photoperiods. *Journal of Experimental Botany* 64:3843–3854.

Lin L, Luo Z, Yan F, Lu Y, Zheng H, Chen J (2011) Interaction between potyvirus P3 and ribulose-1,5 bisphosphatecarboxylase/ oxygenase (RubisCO) of host plants. *Virus Genes* 43: 90–92.

Lindsey DW, Gudauskas RT (1975) Effects of *maize dwarf mosaic virus* on water relations of corn. *Phytopathology* 65(4):434-440

Lade SB, Román C, Cueto-Ginzo AI, Serrano L, Sin E, Achón MA, Medina V (2018) Host-specific proteomic and growth analysis of maize and tomato seedlings inoculated with *Azospirillum brasilense* Sp7. *Plant Physiology and Biochemistry* 129:381-393.

Lancashire PD, Bleiholder H, Langelüddecke P, Stauss R (1991) An uniform decimal code for growth stages of crops and weeds. *Annals of Applied Biology* 119:561–601.

Maule AJ (2001) Virus and Host Plant Interactions. *Encyclopedia of Life Sciences* 1-7.

Matthews R (1982) The classification and nomenclature of viruses: Summary of results of meetings of the International Committee on Taxonomy of Viruses in Strasbourg. *Intervirology* 16:53–60.

Morita K, Hatanaka T, Misoo S, Fukayama H (2014) Unusual small subunit that is not expressed in photosynthetic cells alters the catalytic properties of Rubisco in rice. *Plant Physiology* 164:69–79.

Muhlenbock P, Szechynska-Hebda M, Plaszczyca M, Baudo M, Mateo A, Mullineaux PM, Parker JE, Karpinksa B, Karpinski S (2008) Chloroplast signaling and *LESION SIMULATING DISEASE1* regulate crosstalk between light acclimation and immunity in *Arabidopsis*. *The Plant Cell* 20:2339–2356.

Ojeda V, Pérez-Ruiz JM, González M, Nájera VA, Sahrawy M, Serrato AJ, Geigenberger P, Cejudo FJ (2017) NADPH thioredoxin reductase C and thioredoxins act concertedly in seedling development. *Plant Physiology* 174:1436-1448.

Okon Y, Albrecht SL, Burris RH (1977) Methods for growing *Spirillum lipoferum* and for counting it in pure culture and in association with plants. *Applied Environmental Microbiology* 33:85–88.

Passardi F, Tognolli M, De Meyer M, Penel C, Dunand C (2006) Two cell wall associated peroxidases from *Arabidopsis* influence root elongation. *Planta* 223 (5):965–974.

Prasanth KR, Huang YW, Liou MR, Wang RY, Hu CC, Tsai CH, Meng M, Lin NS, Hsu YH (2011) Glyceraldehyde 3-phosphate dehydrogenase negatively regulates the replication of Bamboo mosaic virus and its associated satellite RNA. *Journal of Virology* 85:8829–8840.

Qiao Y, Li HF, Wong SM, Fan ZF (2009) Plastocyanin transit peptide interacts with potato virus X coat protein, while silencing of plastocyanin reduces coat protein accumulation in chloroplasts and symptom severity in host plants. *Molecular Plant-Microbe Interactions* 22:1523–1534.

Radwan DEM, Lu G, Fayez KA, Mahmoud SY (2008) Protective action of salicylic acid against bean yellow mosaic virus infection in Vicia faba leaves. *Journal of Plant Physiology* 165:845-857.

Rao X, Dixon RA (2016) The differences between NAD-ME and NADP-ME subtypes of C4 photosynthesis: more than decarboxylating enzymes. *Frontiers in Plant Science* 7:1525.

Romanowska E, Buczynska A, Wasilewska W, Krupnik T, Drozak A, Rogowski P, Parys E, Zienkiewicz M (2017) Differenences in photosynthetic responses of NADP-ME type C4 species to high light. *Planta* 245:641-657.

Rosa-Téllez S, Anoman AD, Flores-Tornero M, Toujani W, Alseek S, Fernie AR, Nebauer SG, Muñoz-Bertomeu J, Segura J, Ros R (2017) Phosphoglycerate kinases are co-regulated to adjust metabolism and to optimize growth. *Plant Physiology* 176 (2):1182-1198.

Roshanpour N, Darzi MT, Hadi MHS (2014) Effects of plant growth promoter bacteria on biomass and yield of basil (*Ocimum basilicum* L.) *International Journal of Advanced Biological and Biomedical Research* 2 (6):2077–2085.

Scholthof K-BG, Adkins S, Czosnek H, Palukaitis P, Jacquot E, Hohn T, Hohn B, Saunders K, Candresse T, Ahlquist P, Hemenway C, Foster GD (2011) Top 10 plant viruses in molecular plant pathology. *Molecular Plant Pathology* 12:938–954.

Strand L (2006) Disease. In: L. Strand (ed), *Integrated Pest Management for Potatoes in the western United States* 2nd edn. (p. 95). University of California Division of Agriculture and Natural Resources.

Tanaka S, Sawaya MR, Kerfeld CA, Yeates TO (2007) Structure of the Rubisco chaperone RbcX from Synechocystis sp. PCC6803. *Acta Crystallography* D63:1109–1112.

The UniProt Consortium (2017) UniProt: the universal protein knowledge base. *Nucleic Acids Research*, 45:D158-D169.

Timm S, Florian A, Fernie AR, Bauwe H (2016) The regulatory interplay between photorespiration and photosynthesis. *Journal of Experimental Botany* 67 (10):2923–2929.

Tortora ML, Díaz-Ricci JC, Pedraza RO (2011). *Azospirillum brasilense* siderophores with antifungal activity against *Colletotrichum acutatum*. *Archives of Microbiology* 193:275–286.

Tosic M, Misovic M (1967). A study of the maize mosaic virus occurrence and its effect on the growth and yield of some corn varieties and hybrids. *Zastita Bilja* 93-95:173-180.

Tu JC, Ford RE (1968) Effect of maize dwarf mosaic virus infection on respiration and photosynthesis of corn. *Phytopathology* 58(3):282-284.

Van Regenmortel MHV, Mahy BWJ (2004). *Emerging issues in virus taxonomy. Emerging Infectious Diseases* 10 (1): 8- 13.

Wang SD, Zhu F, Yuan S, Yang H, Xu F, Shang J, Xu MY, Jia SD, Zhang ZW, Wang JH, Xi DH, Lin, HH (2011) The roles of ascorbic acid and glutathione in symptom alleviation to SA-deficient plants infected with RNA viruses. *Planta* 234:171–181.

Wangdi T, Uppalapati SR, Nagaraj S, Ryu C-M, Bender CL, Mysore KS (2010a) A role for chloroplast-localized *thylakoid formation 1 (ThF1)* in bacterial speck disease development. *Plant Signaling & Behavior* 5(4):425-427.

Wangdi T, Uppalapati SR, Nagaraj S, Ryu C-M, Bender CL, Mysore KS (2010b) A virus-induced gene silencing screen identifies a role for Thylakoid Formation1 in *Pseudomonas syringae* pv. tomato symptom development in tomato and *Arabidopsis*. *Plant Physiology* 152 (28):1–92.

Xu Q, Ni H, Chen Q, Sun F, Zhou T, Lan Y, Zhou Y (2013) Comparative proteomic analysis reveals the cross-talk between the responses induced by H2O2 and by longterm *Rice Black-streaked dwarf virus* infection in rice. *PLOS ONE*, 8(11):e81640.

Yildiz RC, Aysan Y (2005) Determination on effect of plant activators on tomato seedling infested with pathogen (*Clavibacter michiganensis subsp. michiganensis*) of bacterial wilt disease. Turkey 2nd seed congress 9-11 November, Adana, 359 pp.

Zechmann B, Muller M, Zellnig G (2003) Cytological modifications in *zucchini yellow mosaic virus* (ZYMV)-infected Styrian pumpkin plants. *Archives of Virology* 148:1119–1133.

Zhao J, Liu Q, Zhang H, Jia Q, Hong Y, Liu Y (2013) The rubisco small subunit is involved in *Tobamovirus* movement and *Tm-2*^{2}-mediated extreme resistance. *Plant Physiology* 161:374-383.

Zhao J, Zhang X, Hong Y, Liu Y (2016) Chloroplast in Plant-Virus Interaction. *Frontiers in Microbiology* 7:1565.

Zhao S, Hong W, Wu J, Wang Y, Ji S, Zhu S, Wei C, Zhang ., Li J (2017) A viral protein promotes host SAMS1 activity and ethylene production for the benefit of virus infection. *Elife* 1-22.

CHAPTER 7

Biochemical and molecular regulation of *Azospirillum brasilense* Sp7 x *Fusarium graminearum* interactions in early growth stages of high carotenoid maize

(Submitted to Molecular Plant-Microbe Interactions, 2019. Annex 5)

Chapter 7. Biochemical and molecular regulation of *Azospirillum brasilense* Sp7 x *Fusarium graminearum* interactions in early growth stages of high carotenoid maize

7.0 Abstract

High-carotenoid (HC) maize has clear benefits for human health. It is rich in pro-vitamin A and other nutritionally important carotenoids, and represents a cost-effective intervention particularly in developing countries. In addition to safety and efficacy studies, HC must be assessed for fitness prior to deployment. *Gibberella zeae* (anamorph *Fusarium graminearum*) (Fus) has devastating effects on maize when infection takes place early in the plant's life cycle. Priming seeds with plant growth-promoting rhizobacteria (PGPR) can promote seedling survival and reduce detrimental effects of this pathogen. The aims of this study were to compare HC with its near isogenic white maize inbred line M37W (WT), and test how the PGPR *Azospirillum brasilense* Sp7 (Sp7) interacts with HC to offset symptoms caused by Fus. Testing was performed in a temperature- and light-controlled growth chamber. We compared specific gene transcription data with the hormonal and defense response. HC seedlings were co-inoculated with Sp7 and Fus and four weeks after planting, the seedlings were tested for antioxidant capacity (FRAP) and total phenolic content (TPC), hormone profile of the plant immune system, expression of antioxidant turnover genes and hormonal transcription factors (TFs). Co-inoculation decreased disease severity in HC, promoted seedling survival, and increased concentrations of jasmonic and salicylic acids (JA and SA) as well as *Zea mays* gibberellin acid-regulated by MYB (ZmGAMYB) TF. Antioxidant and abscisic acid (ABA) turnover genes were strongly induced in co-inoculated HC plants, providing evidence that the antioxidant-hormone signaling network is mediated by up-regulated secondary metabolism.

7.1 Introduction

Fusarium graminareum (Fus) is a hemibiotrophic fungus that causes ear rot in maize plants with devastating consequences worldwide. The fungus leads to the production of mycotoxins (fumonisins) that pose a severe health concern to humans and animals alike. The three major factors influencing fungal development and mycotoxin production in maize kernels are environmental conditions, agricultural practices, and the susceptibility range of genotypes (Edwards 2004). More resistant maize (*Zea mays)* inbred lines have been shown to express defense-related genes in direct response to *Fusarium* spp. attack, indicating that resistance is likely due to constitutive defense mechanisms preventing fungal infection (Campos-Bermudez et al., 2013). Therefore, control of *F. graminareum* is typically based on integrated crop management (ICM), which combines the utilization of resistant or tolerant cultivars and agronomic (mostly chemical) applications (Panwar et al., 2014; Dinolfo et al., 2017).

The ultimate goal of ICM is to promote plant survival against abiotic and biotic stressors. There is, however, also the concept of crop biofortification, which is similar in that plants are strengthened by a compendium of factors, but unique in that its specific aim is producing nutritious and safe foods in a sufficient and sustainable manner. This can be achieved through three main approaches: transgenic, conventional, and agronomic, involving the use of biotechnology, crop breeding and fertilization strategies, respectively (Garg et al., 2018). Since biosynthetic pathways and plant metabolites are often changed in the process of biofortification, the side-effects or compound effects of multiple forms of biofortification may influence the final outcome of ICM. For example, transgenic biofortification often entails the simultaneous incorporation of genes involved in the enhancement of micronutrient concentration, their bioavailability, and reduction in the concentration of antinutrients. These changes can limit the bioavailability of nutrients in plants, redistribute micronutrients between tissues, or enhance the micronutrient concentration in the edible portions of commercial crops, thereby increasing the efficiency of biochemical pathways in edible tissues (Shewmaker et al., 1999; Agrawal et al., 2005; Yang et al., 2002).

Agronomic biofortification requires physical application of nutrients to improve the nutritional and health status of crops. One of the most biologically-sound applications in this regard are plant growth promoting rhizobacteria (PGPR), which enhance nutrient mobility from soil to edible plant parts, heighten their phytoavailability and improve plant nutritional status (Rengel et al., 1999; Smith and Read 2007). PGPR also have many mechanisms for mitigating phytopathogens, such as the production of siderophores, lytic enzymes, phytohormones and volatile organic compounds (Bhattacharyya and Jha 2012). *Azospirillum brasilense* Sp7 (Sp7) is one such PGPR found in the plant rhizosphere, which associates particularly well with maize (Bashan and de-Bashan 2010). Sp7 also produces growth-regulating substances, fixes atmospheric nitrogen, produces carotenoids and suppresses other microbes by producing

bacteriocins and phenylacetic acid (PAA) (Hartmann and Hurek 1988; Somers et al., 2005; Bashan and de-Bashan 2010).

Azospirillum spp. have been studied both *in vitro* and *in vivo* for their action against *Fusarium* spp. *In vitro* results showed that the PGPR reduces growth of *Fusarium* spp., likely due to the secretion of volatile inhibitory substances (Abdulkareem et al., 2014). *In vivo*, *A. brasilense* was found to displace pathogenic fungi in the leaves of teosinte, helping reduce the severity of the disease and promote plant growth (López-Reyes et al., 2017). Previous studies suggest that the observed effects of *A. brasilense* to suppress disease are due to a combination of *A. brasilense*-mediated production of catechol-like siderophores and salicylic acid (SA), which may induce resistance in the plants (Fernández and Pedraza 2013). Most commonly, beneficial microbes activate a combination of ethylene (ET) and jasmonic acid (JA) hormone signaling pathways, triggering APETALA2/Ethylene-responsive factor (AP2/ERF) and ZIM27 TFs, which in turn activate lipoxygenase (LOX3) or chitinase (CHIT) genes, and induced systemic resistance (ISR) (Pieterse et al., 2014).

The plant defense response is also up-regulated by hemibiotrophic pathogens like *Fusarium* spp., which trigger the SA hormone signaling pathway during pathogenesis and prime the plant to resist future attack via systemic acquired resistance (SAR). For this, the plant accumulates SA and activates WRKY transcription factors (TFs), leading to the expression and accumulation of pathogenesis related (PR) genes and proteins (Lanubile et al., 2017). ISR and SAR function independently from each other, but are connected by the non-expressor for pathogenesis-related genes 1 (NPR1), which is thought to act as a common regulator.

Maize is one of the most important staple crops in developing countries, and has been biofortified to accumulate a number of various vitamins, such as beta-carotene, folate, vitamins C and E as cost-effective interventions to improve human health (Garg et al., 2018). High carotenoid (HC) corn, which produces provitamin A (carotenoids) in its endosperm by expressing bacterial transgenes *Pantoea annatis crtI (PacrtI)* and *Zea mays phytoene synthase 1* (*ZmPSY1)* (Zhu et al., 2008), is particularly interesting to our study because carotenoids are potent antioxidants with positive implications for human and plant health alike. For one, carotenoids and tocopherols in plant/*Fusarium* interactions appear to quench free radicals produced by plant cells as an early response to fungal pathogen attack (Gutierrez-Gonzalez et al., 2013). Carotenoids also provide precursors for the synthesis of abscisic acid (ABA), a phytohormone that increases upon *F. graminearum* inoculation (in wheat) (Gunnaiah et al., 2012), and which is implicated in the integration of different stress-response signaling networks, including ISR (Asselbergh et al., 2008). There is also the theory that stress stimulates biosynthesis of carotenoids in photosynthetic tissue to dissipate excess absorbed energy through the xanthophyll cycle (García-Plazaola et al., 2012; Fanciullino et al., 2014).

In this study, we inoculated HC maize seedlings with *A. brasilense* Sp7 and examined the biochemical and molecular changes induced by fungal infection. The main purpose of our research was to test the hypothesis that agronomically biofortifying transgenic crops would improve plant defense regulation to offset symptoms induced by *F. graminareum*.

7.2 Aims

- Determine physiological differences between the rhizobacteria-inoculated and fungus-infected genotypes
- Identify hormonal pathways involved in the defense responses
- Test the degree to which interactions affect secondary metabolism (via gene transcription data, and by measuring phenolic content)
- Link specific gene and TF transcription profiles with the observed defense response

7.3 Material and Methods

7.3.1 Treatments

We used two maize (*Zea mays*) near-isogenic genotypes: a South-African white elite maize M37W lacking carotenoids in its endosperm (WT) and a high-carotenoid transgenic line (HC) previously created in our lab via combinatorial nuclear transformation of M37W. M37W seeds were obtained from The Council for Scientific and Industrial Research (CSIR, Pretoria, South Africa). HC expresses the transgenes *Zea mays phytoene synthase 1* (*Zmpsy1)* and *Pantoea annatis crtI (PacrtI)* and accumulates significant amounts of ß-carotene, lycopene, zeaxanthin and lutein in the endosperm, thereby giving it an orange phenotype (Zhu et al., 2008).

Seeds were either inoculated with Sp7 or PBS (controls) and sown in 5x5cm pots containing autoclaved commercial substrate (Traysubstrat®, Klasmann-Deilmann, Gmbh, Geeste, Germany) characterized by having an extra fine structure and pH of 6. For one week, or until the seedlings had reached the two-leaf stage, the pots were maintained in a growth chamber (1282 x 687 x 1487mm) at 23-25°C with a photoperiod of 16h light/8h dark cycle under 10,000lux fluorescent bulbs. Relative humidity was regulated at 90-95% and emerged plants were watered twice a week. To avoid cross-contamination, Sp7-inoculated and control pots were separated into different trays.

After a week, homogenous seedlings were selected for inoculating with Fus and transplanted in 0.3L pots. Fus millet inoculum was mixed into the soil at a rate of 0.6g/kg before transplanting the seeds. All pots were supplemented with 0.1g of 20-20-20 slow release fertilizer and returned to the same growth conditions (described above). Three weeks after

transplanting, when the mature conidia had begun to form in the infected cells (Oren et al., 2003), the plants were analyzed or harvested.

7.3.2 Sp7 and Fus inocula and inoculation

The *Azospirillum brasilense* Sp7 strain (ATCC 29145) (Sp7) was kindly provided by the "Colección Española de Cultivos Tipo" (CECT) of the Polytechnic University of Valencia (Spain). For the Sp7 suspension, a peptone yeast broth (PYB) liquid medium amended with $CaCl_2$ (0.04%) was prepared, as described by Döbereiner et al. (1976), and incubated at 32°C under constant agitation at 100rpm for 20h. The bacterial suspension was allowed to reach its late log-growth phase [absorbance of 1.0 at OD_{600} nm (determined via an Amersham Biosciences Ultraspec 3100 Pro spectrophotometer)], obtaining an ideal bacterial density of $1x10^8$cfu•mL^{-1}. The *Azospirillum brasilense* Sp7 inoculum was prepared as described in Chapter 3 (Section 3.3.3)

The maize seeds were disinfected with 70% ethanol for 2min, soaked in 1% sodium hypochlorite for 10min under constant agitation (100rpm), and washed six times with sterile distilled water. Seeds were dried on sterile autoclaved paper and inoculated with the rhizobacteria at $1x10^8$cfu•mL^{-1} (Bashan 1986); 1mL of the bacterial suspension was aliquoted for each WT and HC inoculated seed group and centrifuged at 5000rpm for 10min. The supernatant was removed and the pellet was re-suspended in 1mL of 1X PBS. The inoculum was vortexed, and 0.4mL of inoculum was added to each group of 10 seeds. The seeds and inoculum were sealed in 15mL Falcon tubes and agitated horizontally on a shaker for 4.5h. Inoculation time and quantity were established according to an imbibition curve, estimating the time taken for each seed variety to imbibe 70% of its total potential. Controls were handled the same was as inoculated seeds, but treated only with PBS.

The Fus inoculum was prepared with millet seed (*Panicum miliaceum L.*), as described by Idris et al., 2007; 150g millet seed and 200mL distilled water were mixed together in a 1L bottle, and autoclaved at 121ºC for 15min. Upon cooling, each bottle was inoculated with five 4mm discs cut from a fresh potato dextrose agar (PDA) culture of *Fusarium graminearum.* The inoculum was incubated at 27±1°C for one week and applied to the soil at a rate of 0.6g/L to pre-germinated (one-week old) seedlings.

7.3.3 Experimental Design

Inoculation was conducted in groups of 40 seeds per genotype (G) and treatment (T). One week after planting, germinated seeds were selected down to 20 for each G and T of the most homogenous seedlings and transferred to individual 0.3L pots. Each pot contained one seedling and was considered both as the randomization and as the observational unit. The

sampling was conducted three weeks after transplanting and five biological replicates of each G/T were chosen in a completely randomized design for each analysis.

7.3.4 Sampling and analysis of plants

Photosynthetic rates and related traits were determined for individual leaves at the final sampling time using a LCi portable photosynthesis system (ADC BioScientific, Great Amwell, UK) which measures net CO_2 assimilation (net photosynthetic rate). Measurements were taken using the last fully-expanded leaf between mid-morning and noon in the growth chamber. The leaf chlorophyll concentration was estimated *in situ* using a SPAD-520 portable chlorophyll meter (Minolta, Tokyo, Japan) on the same leaves used to measure gas exchange.

7.3.5 Physiological measurements

To determine moisture content, plants were first cut at ground level and roots cleaned with SDW. Stems with leaves and roots were weighed before and after drying for 72h at 65°C.

7.3.6 Verification of Sp7 and *Fusarium* presence

Sp7 colonization assays were conducted at sampling, with three random samples taken from each treatment. The procedure was carried out according to Botta et al. (2013) with modifications. One hundred grams of plant roots were homogenized in 1mL sterile physiological solution (NaCl 0.9%). The homogenate was then serially diluted and plated in Petri dishes containing sterile nitrogen-free broth medium (NFb) supplemented with 15mL/L of 1:400 aqueous solution of Congo-red (CR) (Bashan et al., 1993). Bacterial colonies were counted after 48h incubation at 32°C.

To verify that the colonies were indeed the Sp7 strain, we performed PCR with aliquots taken from stationary-phase cultures grown from the plate isolates, according to Shime-Hattori et al. (2011). The isolates were grown at 32ºC for 17h in Luria-Bertani (LB) broth supplemented with 2.5mmoll^{-1} $CaCl_2$ and 2.5mmol^{l-1} $MgCl_2$. The cultures were held at 95ºC for 5min, and the supernatants of cell lysates obtained were used as PCR templates. The presence of Sp7 16S rDNA was confirmed by PCR using 10µL of the crude bacterial lysate templates in a total volume of 25µL PCR reaction mix consisting of GoTaq DNA Polymerase with the reagents recommended by the manufacturer (Promega, Fitchburg, WI, USA). The PCR was run under the following conditions: 3min initial denaturation at 94ºC followed by 35 cycles of 30s denaturation at 94ºC, 30s annealing at 60ºC, and 1min extension at 72ºC with 5min final extension at 72ºC**.**

Fusarium graminareum presence in root tissues was tested for all treatments. In summary, 1cm-long pieces of roots were excised, rinsed with SDW and set to grow on selective *Fusarium* agar (SFA) for one week (Burgess et al., 1994), or until pink colonies had formed.

Pure cultures were then selected and grown in 500µL malt extract broth in Eppendorf tubes (2%*w/v* malt extract, 1% *w/v* peptone, 2% *w/v* glucose) for 2d at 25ºC in darkness. The mycelial extract was recovered by centrifugation (14,000rpm, 10min), and the DNA was extracted and amplified as described by Díaz-Gómez et al. (2016). Amplification reactions for DNA sequencing were conducted in volumes of 100µL containing 10ng template DNA, 4µL of each primer (10µM), 10µL of 10x PCR buffer, 2µL dNTPs (10mM), and 0.75µL Taq DNA polymerase ($5U\mu L^{-1}$). We ran the PCR under the following conditions: 3min initial denaturation at 95ºC followed by 35 cycles of 30s denaturation at 95ºC, 20s annealing at 62ºC, and 45s extension at 72ºC with 5min final extension at 72ºC (Demeke et al., 2005).

For both Sp7 and Fus detection assays, the PCR products were sequenced (StabVida, Caparica, Portugal). Sequences were analyzed and aligned using the Blast® search tool (National Center for Biotechnology Information, Bethesda, MD, USA) and Ugene (Okonechnikov et al., 2012). See Table 12 for 'Sp7' and 'Fus detection' primer sequences.

7.3.7 Hormone extraction and analysis

Cytokinins (trans-zeatin, tZ), indole-3-acetic acid (IAA), abscisic acid (ABA), salicylic acid (SA), jasmonic acid (JA) and the ethylene precursor 1-aminocyclopropane-1-carboxylic acid (ACC) were analyzed according to Gutierrez-Carbonell et al. (2015). Leaf samples were filtered through 13mm diameter Millex filters with 0.22µm pore size nylon membrane (Millipore, Bedford, MA, USA). Filtrated extract (10µl) was injected in a UHPLC-MS system consisting of an Accela Series UHPLC (ThermoFisher Scientific, Waltham, MA, USA) coupled to an Exactive mass spectrometer (ThermoFisher Scientific, Waltham, MA, USA) using a heated electrospray ionization (HESI) interface. Mass spectra were obtained using the Xcalibur software version 2.2 (ThermoFisher Scientific, Waltham, MA, USA). For hormone quantification, calibration curves were built for each analyte (1, 10, 50, and $100\mu gL^{-1}$) and corrected using $10\mu gL^{-1}$ deuterated internal standards. Recovery percentages ranged between 92 and 95%.

7.3.8 Total phenolic content and antioxidant capacity

Extraction and determination of total phenolic content (TPC) in leaf samples was done using the Folin-Ciocalteu Method (Singleton et al., 1999).as described by Giné-bordonaba and Terry (2016).

From the same methanolic extract used for TPC determinations, antioxidant capacity was determined by the standardized ferric reducing antioxidant power (FRAP) technique as described elsewhere. The FRAP was obtained by measuring the absorbance change at 593nm caused by the reduction of the Fe^{3+}-TPTZ complex to the ferrous form at pH 3.6. The FRAP reagent was freshly prepared by mixing 25mL of acetate buffer (300 mmol/L,

pH 3.6), 2.5mL of $FeCl_3 \cdot 6H_2O$ solution (20mmol/L). Briefly, 90µL extract was added with 90µL distilled water and 900µL FRAP reagent. The homogenate was incubated at 37°C for 60min, and absorbance was measured. Blanks were included replacing leaf extract volumes for acetone/water. Results were expressed as mmol Fe^{2+}/100g FW, using a $FeSO_4 \cdot 7H_2O$ calibration curve.

7.3.9 Total RNA isolation and cDNA synthesis

Total RNA was isolated using the RNeasy Plant Mini Kit (Qiagen, Valencia, CA, USA) and DNA was removed with DNase I (Rnase-free DNase Set, Qiagen). Total RNA was quantified using a Nanodrop 1000 spectrophotometer (Thermo Fisher Scientific, Vernon Hills, IL, USA), and 2µg total RNA was used as the template for first strand cDNA synthesis with Ominiscript reverse transcriptase (Qiagen) in a 20µl total reaction volume, following the manufacturer's recommendations.

7.3.10 Quantitative real-time RT-PCR

Quantitative real-time RT-PCR was used to analyze expression of genes and TFs (primers shown in Table 12) in a BioRad CFX96 system with 25-µl reaction mixtures containing 10ng cDNA, 1x iQ SYBR Green Supermix (BioRad, Hercules, CA, USA) and 0.2µM forward and reverse primers (Naqvi et al., 2011; Farré et al., 2013). Relative expression levels were calculated on the basis of serial dilutions of cDNA (125–0.2ng) which were used to generate standard curves for each gene. PCR was carried out in triplicate using 96-well optical reaction plates. The reaction conditions comprised an initial heating step at 95°C for 5min followed by 44 cycles of 95°C for 10s, 60°C for 35s and 72°C for 15s. Specificity was confirmed by product melt curve analysis over the temperature range 50–90°C with fluorescence acquired after every 0.5°C increase, and the fluorescence threshold values and gene expression data were calculated using BioRad CFX96™ software. Values represent the mean of 5 replicates ± SD. Amplification efficiencies were compared by plotting ΔCt values of different primer combinations in serial dilutions against the log of starting template concentrations using CFX96 software.

Table 12. DNA sequence of the primers used for PCR and RT qPCR.(maize)

Gene	Forward primer	Reverse primer
Sp7 detection* (Az16S-D)	5'-CCGCGGTAATACGAAGGGGGC-3'	5'-GCCTTCCTCCGGCTTGTCACCGGC-3'
Fusarium detection‡	5'-CTCCGGATATGTTGCGTCAA-3'	5'-GGTAGGTATCCGACATGGCAA-3'
ZmICS[1]	5'-GGCGAGATCCAATCACAGAT-3'	5'-CAGCATAATCATGCAAATAC-3'
ZmNCED4	5'-TCAAGCTCCAGGAGATGGTG-3'	5'-TCCAGAGGTGGAAGCAGAAG-3'
ZmCHI1[1]	5'-CGCGAGGAGAAAGAAAGCAA-3'	5'-CAACTACGCGACCAGAAAGG-3'
ZmZEP	5'-GAATGCCTGGCAAGAGAGTG-3'	5'-CCCTAGACCAACACCCAAGT-3'
ZmSOD4[2]	5'-TGGAGCACCAGAAGATGA-3'	5'-CTCGTGTCCACCCTTTCC-3'
ZmAPX[2]	5'-TGAGCGACCAGGACATTG-3'	5'-GAGGGCTTTGTCACTTGGT-3'
ZmLOX[3]	5'-CGCCATCATCGTCAAGAACA-3'	5'-ACTGCGGGTAGATCCATGAG-3'
ZmGAMYB[5]	5'-TGGGAACAGCCTTTATCTGCC-3'	5'-ATCCCCGCTTGGTCAACCT-3'
ZmNPR1[4]	5'-CCCGGTAGGAAGAAGAAGGG-3'	5'-AAGTCGGCGTAAATCACACG-3'
ZmPAL[1]	5'-GCTATCCGCTGTACCGTTTC-3'	5'-CAGCGGTTCACCATTCCATT-3'
ZmACO[1]	5'-CGACCTGCTCTTCAATCTGC-3'	5'-AGATGTGTTCGCACCTGGTA-3'
ZmCPK11[2]	5'-ACCTCTCCGAGCACCCCAAC-3'	5'-CCTCCACGACCCCGACAATG-3'
ZmEIN3	5'-GCAGCGAACAATCTGGACTT-3'	5'-ACGTGTCACTACTGCTCAT-3'
ZmERF1	5'-GATGAACGTGCTTTGACCGT-3'	5'-ACTTGCGAGTTACAGGGACA-3'
ZmWRKY	5'-AGCTCCACCTCCATCAACTC-3'	5'-ACTTGGGATCCTTGGTGAGC-3'
ZmAP2/EREPB	5'-ACGCACCCGTACTACTTCTT-3'	5'-TCCACTACCGACGAACAGTC-3'
ZmZIM27	5'-CGAGCAGCAAAGGTGTGTTA-3'	5'-TCCGCGATCAGAAGTTCACA-3'
ZmActin[ψ]	5'-CGATTGAGCATGGCATTGT-3'	5'-CCCACTAGCGTACAACGAA-3'

Primers as reported in:

*Shime-Hattori et al. (2011); ‡ Nicholson et al (1998); 1. Ding et al (2011); 2. Ding et al (2013); 3. Zehra et al (2017)

7.4 Results

7.4.1 Plant phenotypes and morphological characteristics

When comparing whole plant phenotypes, control and Sp7-inoculated plants were similar in that they both exhibited upright, full leaf structures that were continuous-green in color. In contrast, Fus plants were thinner, shorter and had leaf necrosis and extensive wilting. Co-treated (Sp7+Fus) plants were larger and more vigorous than any other treatment group, especially the HC genotype (Figure 29). Differences in chlorophyll content (SPAD) were highly significant for the interaction between genotype and treatment ($p=0.007$) (Figure 30). Fus HC had a 31% increase in chlorophyll content over WT ($p=0.025$), while in the case of co-treatment, Sp7+Fus HC had 34% less chlorophyll contents than WT ($p=0.005$).

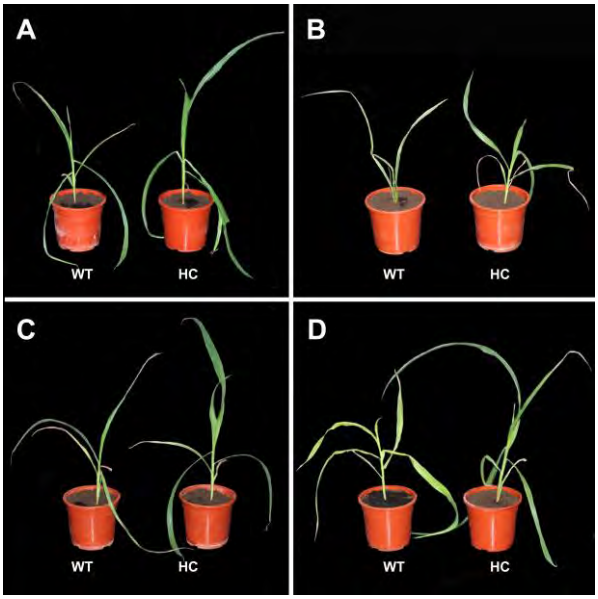

Figure 29. Representative plant phenotypes: (A) control, (B) *Fusarium*, (C) *Azospirillum brasilense* (Sp7) and (D) co-inoculated (Sp7+*Fusarium)* plants of wild type (WT) and high carotenoid (HC) maize.

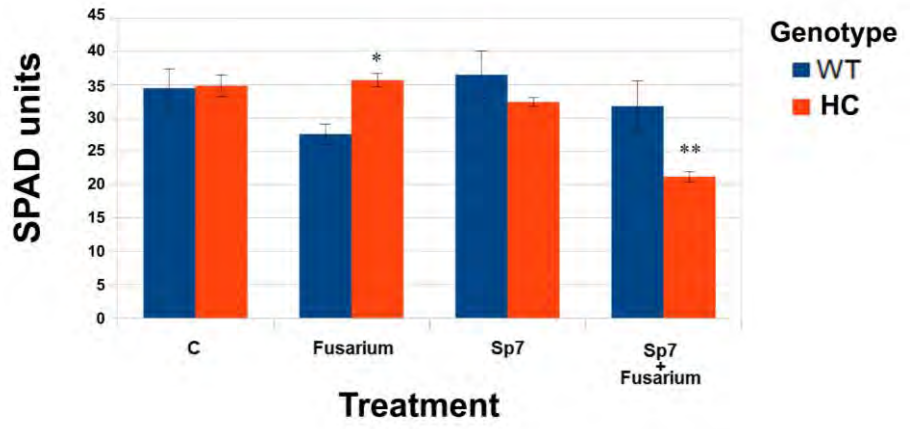

Figure 30. Leaf chlorophyll content (SPAD) for control (C), Fusarium (Fus), *Azospirillum brasilense* (Sp7) and co-inoculated (Sp7+*Fusarium*) plants of wild type (WT) and high carotenoid (HC) maize. Asterisks indicate statistically significant differences between treatments: *($p<0.05$), ** ($p<0.01$), *** ($p<0.001$). Values represent the average ± standard error for n=9.

Differences in leaf length were statistically significant among treatments ($p=0.002$) (Figure 31A). Specifically, Sp7 resulted in the leaves of both genotypes being 35% longer on average compared to controls ($p<0.001$). In a similar way, differences in total root moisture content (%) were highly significant ($p=0.006$) for treatment in a two-way ANOVA. On average, Sp7-inoculated plant roots contained nearly double the moisture of control, regardless of genotype ($p<0.05$) (Figure 31B).

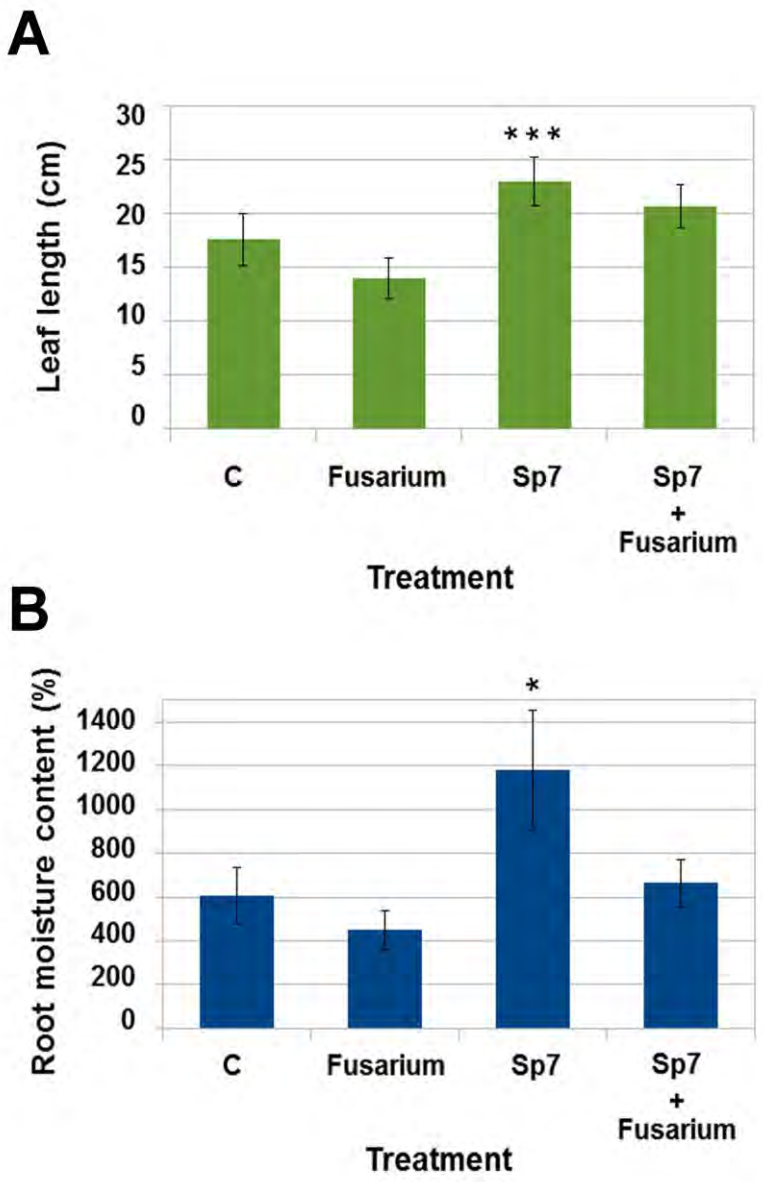

Figure 31. (A) Leaf length and (B) root moisture content for each treatment: control (C), *Fusarium* (Fus), *Azospirillum brasilense* (Sp7) and co-inoculation (Sp7+*Fusarium*). Asterisks indicate statistically significant differences between treatments: * ($p<0.05$), ** ($p<0.01$), *** ($p<0.001$). Values represent the average ± standard error for n=9.

Changes in leaf surface temperature were significant for the interaction between the genotype and treatment ($p=0.001$). Control HC plants were 6% warmer than WT ($p<0.001$), while Fus HC plants were 3% cooler than WT ($p=0.01$). Differences were non-significant between genotypes for Sp7 and Sp7+Fus treatments, indicating a standard up-regulation of plant temperature in response to Sp7 inoculation, regardless of fungal infection or genotype (Figure 32A).

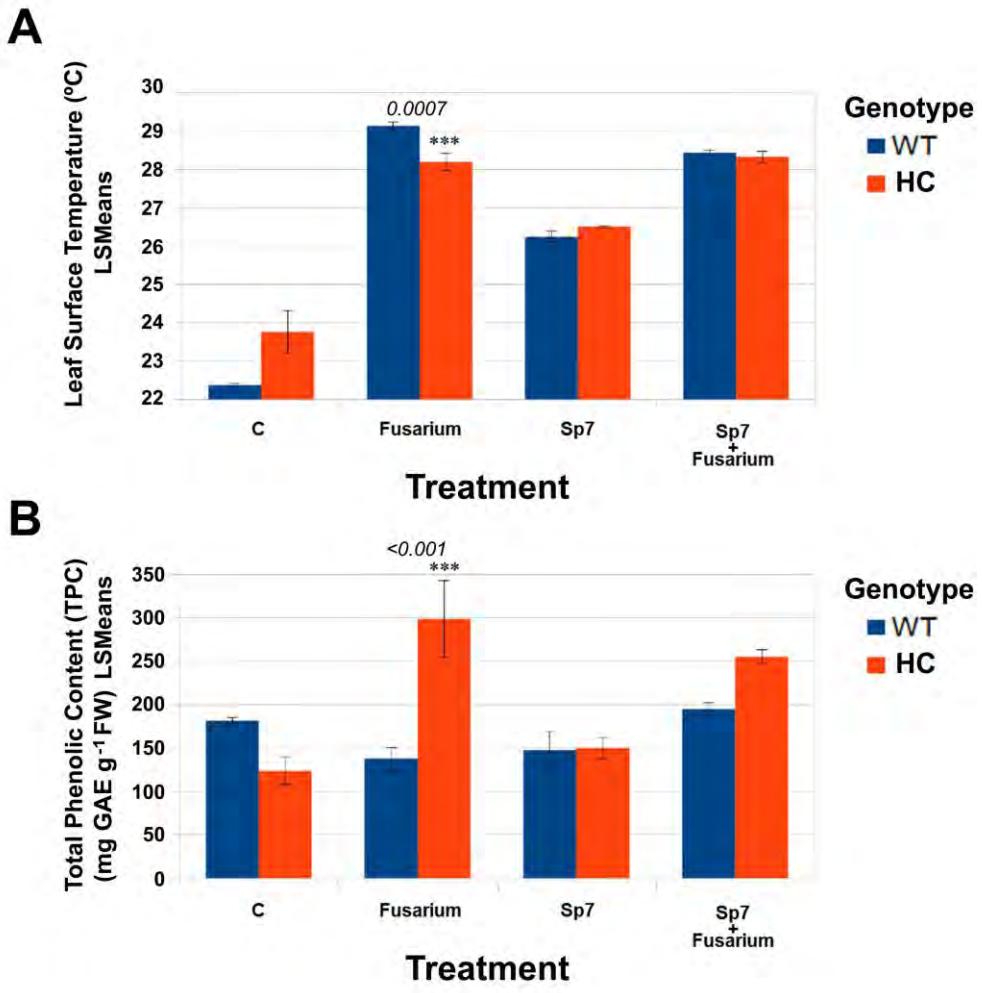

Figure 32. (A) Leaf temperature and (B) total phenolic content (TPC) for each treatment: control (C), *Fusarium* (Fus), *Azospirillum brasilense* (Sp7) and co-inoculation (Sp7+*Fusarium).* Least significant means between genotypes for each treatment are indicated with the p-value in each graph. Values represent the average ± standard error for n=9.

Total phenolic content (TPC) in leaves (Figure 32B) was highly correlated with antioxidant capacity (ferric reducing antioxidant power; FRAP) (Figure 33). A significant interaction was found between genotype and treatment highlighting the differential effect of the treatment among WT or HC genotypes. Inoculation with Sp7 or the combination of both Sp7+Fus did not alter or enhance, respectively, the TPC of leaves in both genotypes.

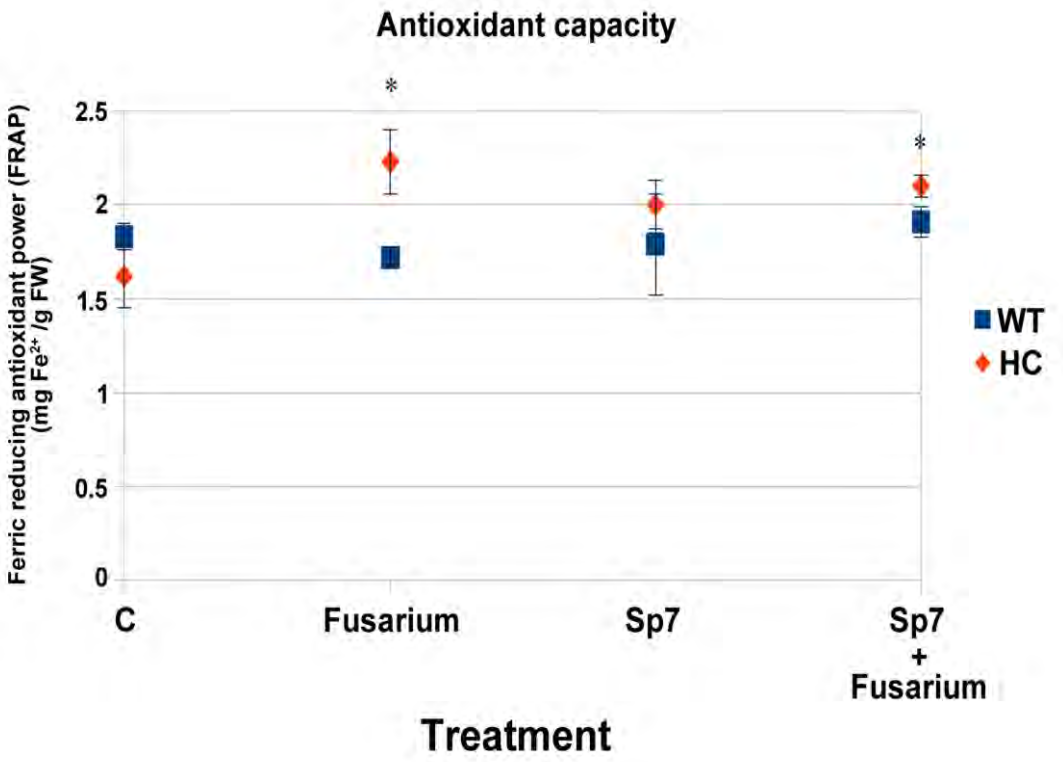

Figure 33. Antioxidant capacity measured by the Ferric reducing antioxidant power (FRAP; Fe2+/g FW) for each treatment: control (C), *Fusarium* (Fus), *Azospirillum brasilense* (Sp7) and co-inoculation (Sp7+*Fusarium*). Asterisks indicate statistically significant differences between treatments: * ($p<0.05$), ** ($p<0.01$), *** ($p<0.001$). Values represent the average ± standard error for n=9.

7.4.2 Hormone profiling and treatment group correlations

In leaves, six hormones (ACC, tZ, IAA, ABA, JA and SA) were measured and had significant interactions between genotype and treatment. In HC plants treated with Fus or Sp7+Fus, ACC decreased by 60-fold (compared to WT). In contrast, the accumulation of other hormones increased significantly in Sp7+Fus-treated HC plants if compared to WT; IAA increased 3-fold, JA increased 9-fold and SA 7-fold. HC plants only inoculated with Sp7 exhibited a 2-fold increase in ACC accumulation, and a 3-fold decrease in ABA compared to WT (Figure 34).

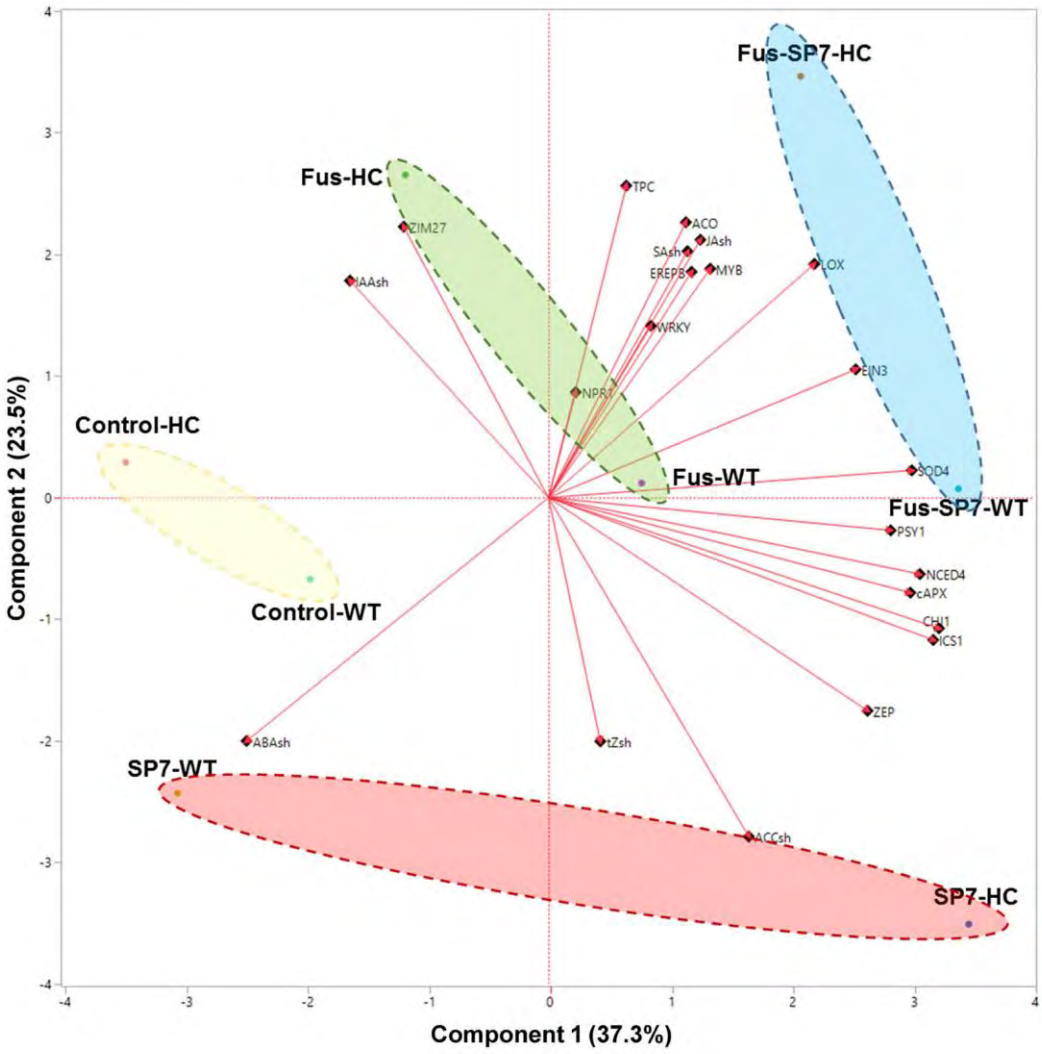

Figure 34. Principal component analysis (PCA) biplot characterizing leaf hormone accumulation, gene transcription and total phenolic content (TPC) trends in samples from the different treatments. Hormones are salicylic acid (SA), jasmonic acid (JA), 1-Aminocyclopropane-1-carboxylic acid deaminase (ACC), trans-Zeatin (tZ), indole-3-acetic acid (IAA) and abscisic acid (ABA). Genes are ZmICS, isochorismate; ZmSOD4, superoxide dismutase 4; ZmCHI1, chalcone isomerase; ZmAPX, ascorbate peroxidase; ZmLOX3, lipoxygenase; ZmZEP, zeaxanthin epoxidase; ZmMYB, transcription factor; ZmNCED4, 9-cis-epoxycarotenoid dioxygenase. Each dot represents the average of 3 (hormones) or 5 (gene transcription) independent measurements.

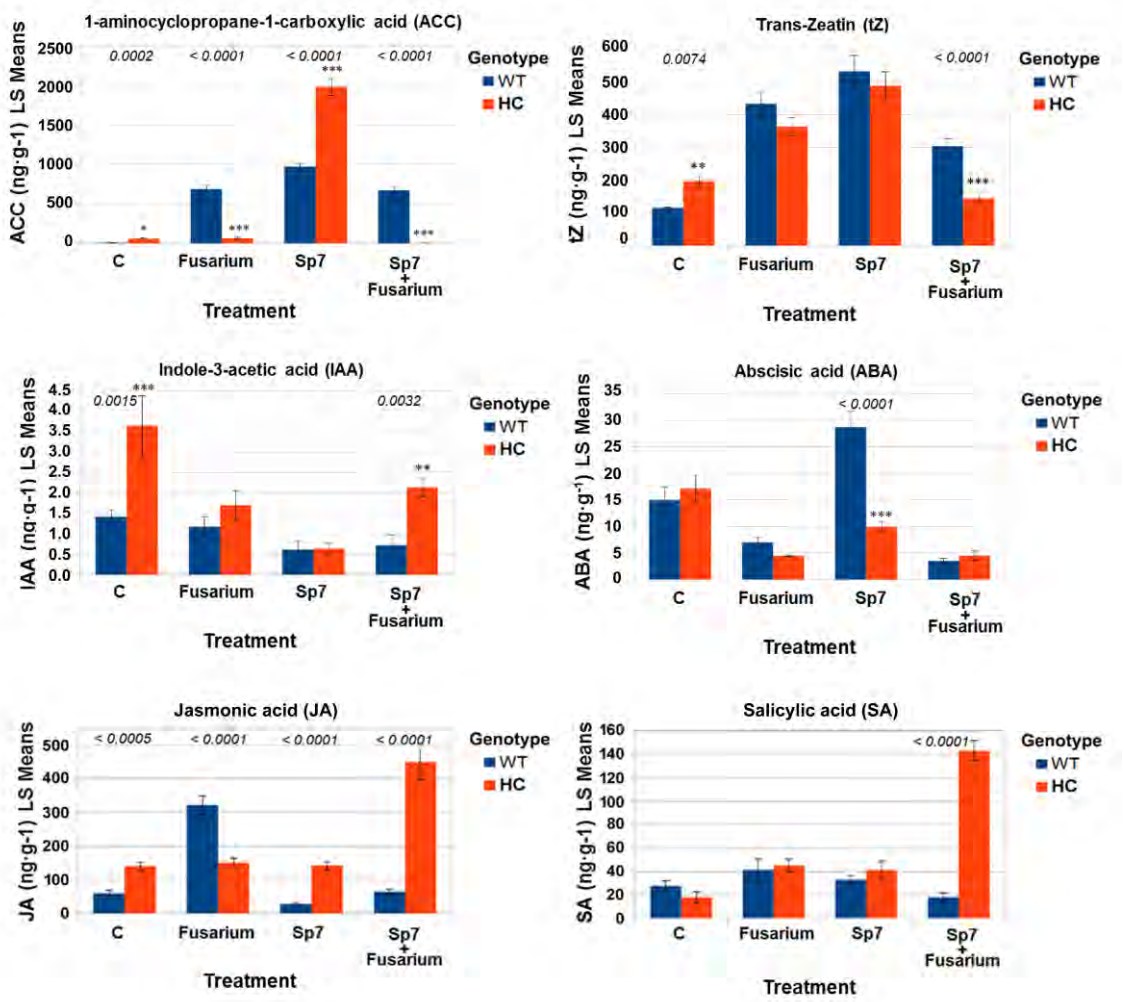

Figure 35. Hormone accumulation of 1-Aminocyclopropane-1-carboxylic acid deaminase (ACC), trans-Zeatin (tZ), indole-3-acetic acid (IAA), abscisic acid (ABA), jasmonic (JA) and salicylic acid (SA) in leaves for each treatment: control (C), *Fusarium* (Fus), *Azospirillum brasilense* (Sp7) and co-inoculation (Sp7+*Fusarium*). Least significant means between genotypes for each treatment are indicated with the p-value in each graph. Values represent the average ± standard error for n=9.

7.4.3 Expression of genes involved in redox homeostasis, flavonoid and carotenoid biosynthesis

For both genotypes, transcriptional changes of genes associated with secondary metabolism were most apparent in plants with Sp7+Fus treatment (Figure 36). In particular, there was an 14-fold transcriptional increase in superoxide dismutase 4 gene (*ZmSOD4*) in HC plants (compared to HC controls), and a 1.5-fold increase in Sp7+Fus WT plants compared to WT controls. Other significant transcriptional increases in Sp7+Fus-treated plants included chalcone isomerase (*ZmCHI1*) (6.6-fold for WT and 15-fold for HC, compared to their respective controls) and isochorismate (*ZmICS*) (2-fold for WT and 2.5-fold for HC), both involved in flavonoid biosynthesis; ascorbate peroxidase (*ZmAPX*) (1-fold for WT and 2.9-fold for HC), linked to redox reactions; and lipoxygenase (*ZmLOX3*) (14-fold for WT and 7.5-fold.

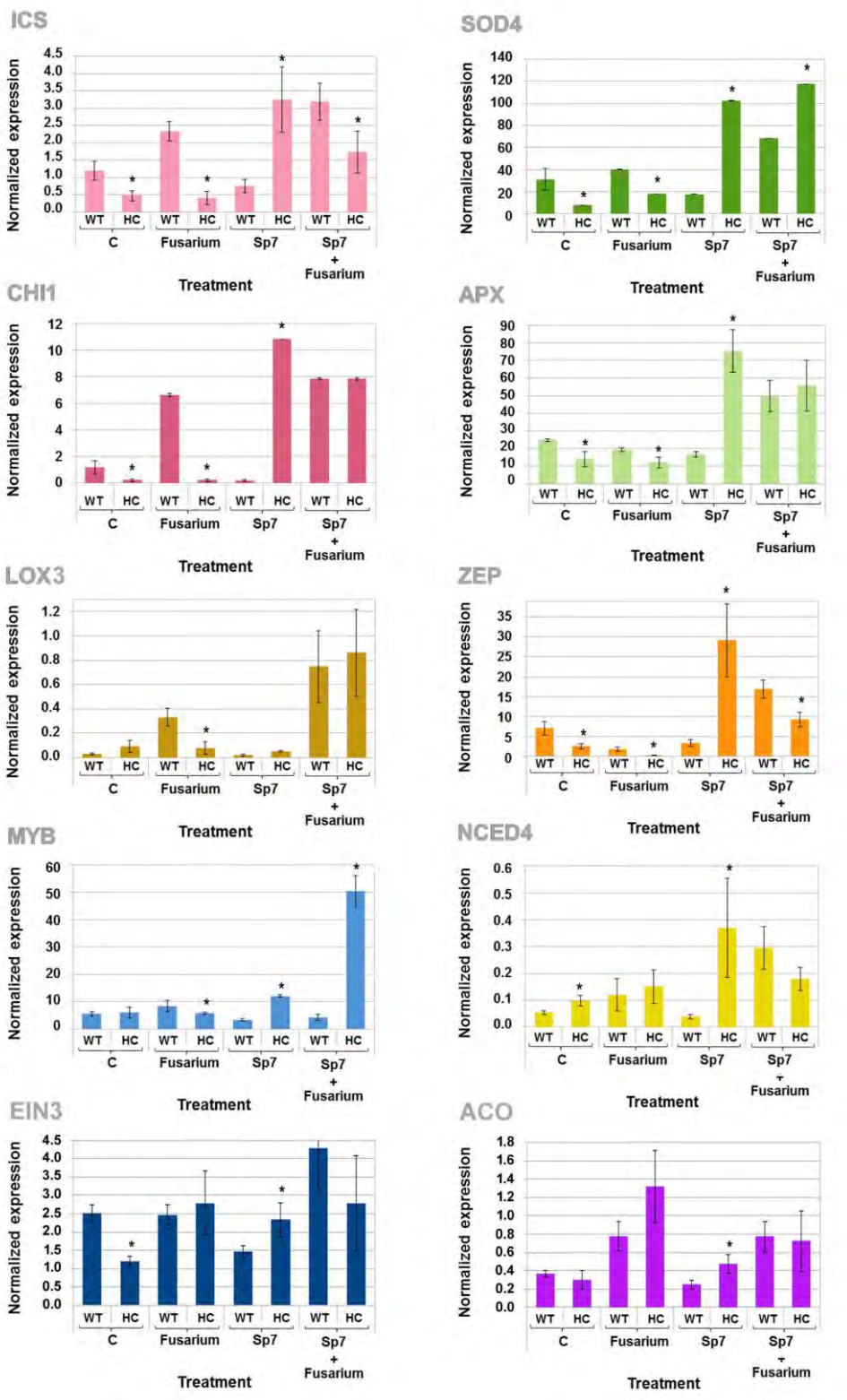

Figure 36. Quantitative real-time RT-PCR analysis of endogenous hormone pathway genes and in HC and WT plants grown with various treatments: control (C), *Fusarium* (Fus), *Azospirillum brasilense* (Sp7) and co-inoculation (Sp7+*Fusarium*). Data show relative mRNA levels in leaves, normalized against maize actin mRNA and presented as the mean of 5 biological replicates. (A) ZmICS, isochorismate; (B) ZmSOD4, superoxide dismutase 4; (C) ZmCHI1, chalcone isomerase; (D) ZmAPX, ascorbate peroxidase; (E) ZmLOX3, lipoxygenase; (F) ZmZEP, zeaxanthin epoxidase; (G) ZmMYB, myeloblastosis; (H) ZmNCED4, 9-cis-epoxycarotenoid dioxygenase, (I) ZmEIN3, Ethylene insensitive 3; (J) ZmACO. 1-aminocyclopropane-1-carboxylate oxygenase. Asterisks indicate a statistically significant difference between wild type and transgenic plants as determined by Student's t-test ($P < 0.05$; $n = 6$).

for HC), zeaxanthin epoxidase (*ZmZEP*) (1.4-fold for WT and 9-fold for HC) and 9-cis-epoxycarotenoid dioxygenase (*ZmNCED4*) (5-fold for WT and 0.8-fold for HC), all of which are intertwined with oxylipin and carotenoid biosynthesis, as well as ABA turnover.

Fusarium graminearum infection in WT plants caused increased transcription of flavonoid biosynthesis genes *ZmICS* (1.15-fold) and *ZmCHI1* (5.5-fold), as well as *ZmLOX3* (10-fold). Meanwhile in HC plants, Sp7 inoculation induced a similar reaction with the over-expression of *ZmICS* (5.5-fold), *ZmCHI1* (35-fold), *ZmSOD4* (11.5-fold) and *ZmAPX* (2-fold).

Of all transcription factors tested, the only one that exhibited significant variation between treatments and/or genotypes was the *Zea mays* gibberellin acid regulated by MYB (ZmGAMYB). In HC plants co-treated with Sp7+Fus, expression levels were 12-fold higher than respective (HC) controls (Figure 36).

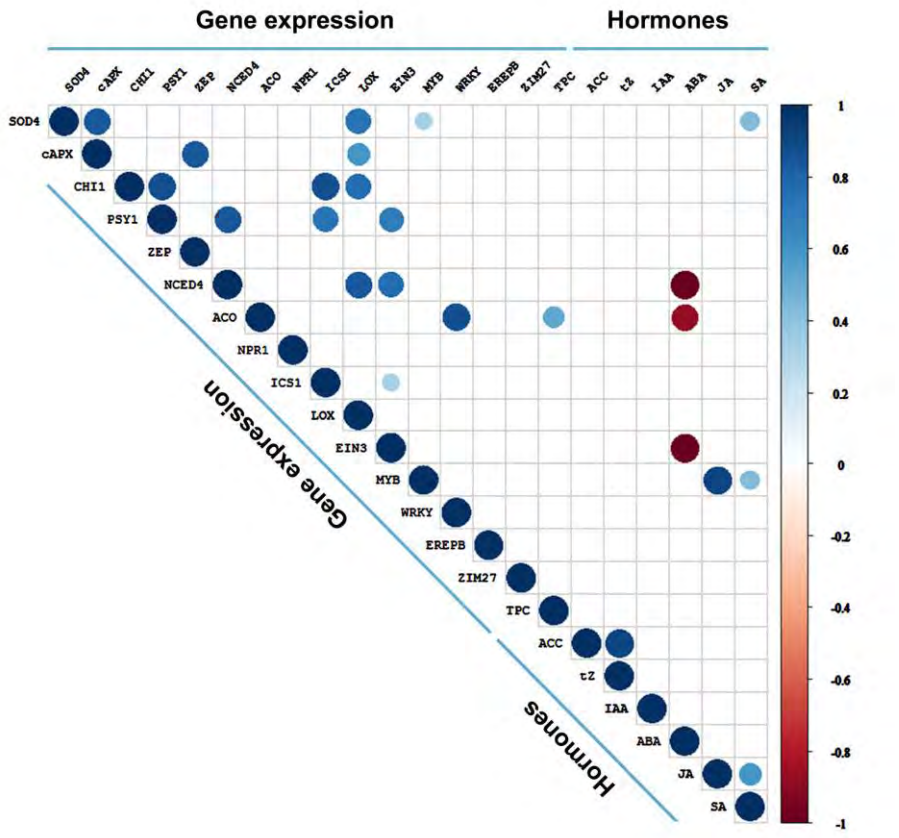

Figure 37. Correlation matrix relating gene expression and hormone data in plant leaves. Hormones are salicylic acid (SA), jasmonic acid (JA), 1-Aminocyclopropane-1-carboxylic acid deaminase (ACC), trans-Zeatin (tZ), indole-3-acetic acid (IAA) and abscisic acid (ABA). Genes are ZmICS, isochorismate; ZmSOD4, superoxide dismutase 4; ZmCHI1, chalcone isomerase; ZmAPX, ascorbate peroxidase; ZmLOX3, lipoxygenase; ZmZEP, zeaxanthin epoxidase; ZmMYB, myeloblastosis; ZmNCED4, 9-cis-epoxycarotenoid dioxygenase; ZmNCED4, 9-cis-epoxycarotenoid dioxygenase, ZmEIN3, Ethylene insensitive 3;ZmACO. 1-aminocyclopropane-1-carboxylate oxygenase.

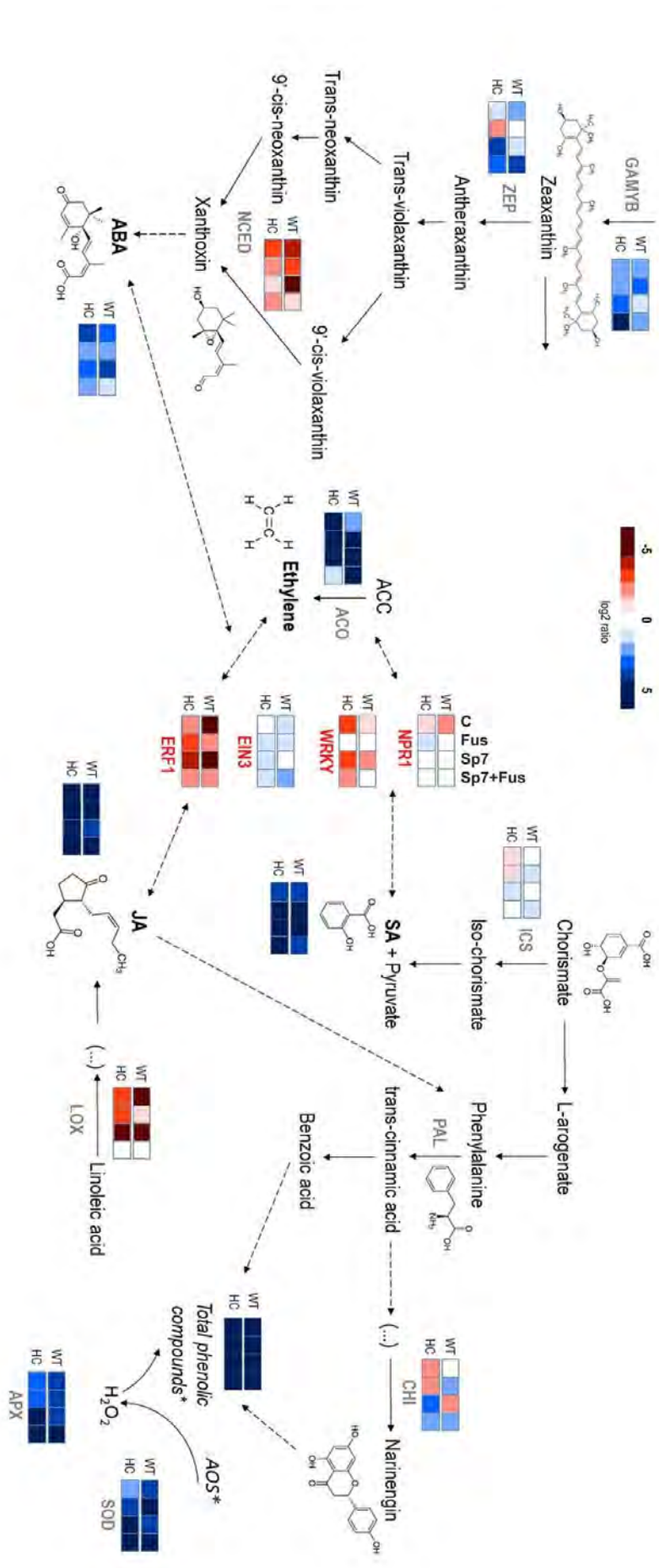

Figure 38. Gene and hormone regulatory network controlling carotenoid biosynthesis and the stress-related responses. The schema represents the regulatory network of carotenoid, flavonoid and redox-related genes in wild type (WT) and high carotenoid (HC) maize seedlings grown with various treatments: control (C), Fusarium (Fus), Azospirillum brasilense (Sp7) and co-inoculation (Sp7+Fusarium). The model is based on data obtained by qPCR for genes and by HPLC for hormone accumulation. Gene expression levels were normalized to the expression levels of ZmActin, and all values were log2 transformed to normalize the data. Blue indicates higher expression/accumulation while red indicates lower expression/accumulation relative to zero. Hormones are salicylic acid (SA), jasmonic acid (JA), 1-Aminocyclopropane-1-carboxylic acid deaminase (ACC), trans-Zeatin (tZ), indole-3-acetic acid (IAA) and abscisic acid (ABA). Genes are ZmICS, isochorismate; ZmSOD4, superoxide dismutase 4; ZmCHI1, chalcone isomerase; ZmAPX, ascorbate peroxidase; ZmLOX3, lipoxygenase; ZmZEP, zeaxanthin epoxidase; ZmMYB, transcription factor; ZmNCED4, 9-cis-epoxycarotenoid dioxygenase.

To further explore the relationship between all variables as well as the differential effect of the treatments on the different genotypes, a principal component analysis was carried out by combining hormonal, total phenolic content and gene expression data (23 variables; Fig. 34). Our results show that most of the variability between treatments was captured by the PC1 (37.3% of the total variability) while differences among genotypes for the same treatment where mainly related to PC2 (23.5% of the total variability). An exemption was found for Sp7 inoculated plants where the distinction between HC or WT genotypes was almost exclusively explained by the first principal component.

For all treatments and genotypes, gene expression was correlated with hormone accumulation, highlighting significant relationships within the regulatory network (Figure 37). In the matrix, several correlations were especially revealing. For one, ZmGAMYB was positively correlated with JA and SA, and *ZmSOD4* was correlated with SA. In contrast, ABA accumulation was antagonistic to *ZmEIN3*, *ZmACO* and *ZmNCED4*. Schematic representation of these findings (Figure 38) distinguishes the gene and hormone regulatory network controlling carotenoid biosynthesis and the stress-related responses for each genotype. Overall, there was consistency in results between genotypes, except for in the case of co-treatment, where ZmGAMYB correlated less with ABA and ACO hormone accumulation. For both genotypes, the up-regulation of ZmGAMYB and *ZmZEP* in the carotenoid pathway did not carry through to downstream gene expression, such as that of *ZmNCED4.* Although all hormones exhibited increased accumulation, the only active TF was ZmGAMYB.

7.5 Discussion

Crop systems are under extreme pressure to withstand environmental stress to meet growing demand. Sustainable management of crop welfare therefore requires the development of strategies that consider human and plant health alike. In order to effectively design and implement such programs, an integrated understanding of plant defense-related regulatory networks is crucial. In this study, we subjected HC maize seedlings to the combination of biotechnological and agronomic biofortification, with the aim of strengthening plants against *Fusarium graminareum* (Fus). Using high carotenoid (HC) transgenic seedlings provided a unique opportunity to investigate the compound effect of two forms of biofortification on defense-related biological processes. We found that inoculation with Sp7 offset symptoms incurred by Fus and that the genotypic diversity of the maize was a determining factor for variable transcriptional patterns and hormone concentrations in plants.

Analysis of chloroplastic activity, leaf growth and temperature elucidated aspects of above-ground plant physiology that were indicative of plant stress levels and susceptibility to fungal infection. WT plants had significantly less chlorophyll contents than HC and were visibly more susceptible to Fus infection than HC plants. Chloroplasts are highly sensitive to

stress factors (Romanowska et al., 2017; Zhao et al., 2016) and previous studies have shown that deoxynivalenol (DON), the *Fusarium* spp. trichothecene mycotoxin that inhibits eukaryotic protein synthesis, is responsible for cellular damage to chloroplasts (McLaughlin et al., 1977; Wojciechowski et al., 1995). WT plants also had weaker phenotypes and higher leaf temperatures, which is typical of plants exposed to pathogens and indicative of plant moisture stress, reduced water uptake efficiency and compromised evaporative cooling ability (Mengistu et al., 1987; Omer et al., 2007). The combined effect of Sp7+Fus affected the two genotypes in a different way than Fus alone, causing HC plant chlorophyll levels to drop significantly below those of WT. These results did not correspond with the fortified HC phenotype and stable leaf temperature that we observed, confirming a special interaction between the bacteria and fungus in HC plants which adversely affected photosynthesis-related cells, but did not physically stress the plant otherwise.

Fus-infection was a common denominator for increased TPC and FRAP in transgenic plants, evidencing up-regulated secondary metabolism (SM) stemming from the shikimate/phenylpropanoids pathway or through activation of other pathways generally leading to higher antioxidant content. In this way, it is possible that HC-specific flavonoids had pleiotropic effects on enzyme modification (Li et al., 2009). For example, we correlated TPC with *ZmACO,* the gene responsible for expression of ACC-oxidase (ACO), which converts ACC to ethylene in the presence of oxygen, and which over-expressed in Fus HC seedlings. Previous work has made similar connections regarding enhanced antioxidant capacity in plants via ethylene signaling (Xu et al., 2017). Ethylene signaling has even been found to regulate the relative abundance of two specific *F. graminareum*-related metabolites, smilaside A and smiglaside C, thereby affecting resistance against *F. graminareum* in maize seedling roots (Zhou et al., 2019). Antioxidant capacity is the result of synergistic or antagonistic effects from interactions between different polyphenol compositions among each other and with other components of the organism (Zhou et al., 2019). So, we provide evidence for the enhancement of plant antioxidant capacity by the interaction between Fus and HC, endogenous polyphenolic constituents and their reactions with ethylene precursors.

In this study, the up-regulation of antioxidant-related gene expression was not always correlated with increased TPC and FRAP. For instance, Sp7-inoculation in HC plants caused increased expression of *ZmSOD* and *ZmAPX*, despite no difference in TPC. Our results overall then revealed significant correlation between *ZmSOD* and SA, which was most evident in HC plants subjected to co-treatment. While previous studies have shown that antioxidants are strongly implicated in SA signaling (Foyer and Noctor 2005), we build upon this in providing evidence that the antioxidant-hormone signaling network is mediated by symbiotic partnerships such as that of Sp7 and HC. It is known that redox homeostasis is governed by the presence of large pools of antioxidants that absorb and buffer reductants and oxidants (Foyer and Noctor

2005). Symbiotic associations between organisms involve ROS-antioxidant interactions, leading to an enhancement of antioxidant status such that the symbiotic partnership is more resistant to environmental stress than either partner alone (Kranner et al., 2005). Sp7 inoculation demonstrates this type of relationship with the HC genotype, thereby increasing the plants' resistance against Fus. Why this enhancement is especially evident in HC but not in WT is still unclear and warrants further investigation, yet our results point out the putative role of several transcription factors.

In Sp7-inoculated HC seedlings that were infected with Fus, we also observed significantly increased accumulation of SA and JA hormones, and over-expression of the ZmGAMYB TF. The correlation matrix confirmed that ZmGAMYB was positively related with JA and SA, as well as *ZmSOD4.* In a similar study, chemical inducers SA, JA and the biocontrol agent *Trichoderma harzianum* induced the defense system against *F. oxysporum* f. sp. *lycopersici* infection by increasing expression of various antioxidant enzymes (Zehra et al., 2017). Our results reveal similar changes to the defense system with Sp7 as the biocontrol agent and *F. graminareum* as the pathogen, but go further by involving the ZmGAMYB TF as a potential regulatory hub of the antioxidant-related defense response in HC plants. There is the possibility that this interaction is connected to the redox state of the transgenic plants, which may be altered on account of the engineered carotenoid pathway. Even though earlier field trials found that HC demonstrated normal morphology and development, consistently with transgene expression strictly in the endosperm (Zhu et al., 2008; Zanga et al., 2016), other studies have found that alteration of the carotenoid biosynthetic pathway has pleiotropic effects on other main secondary metabolites with antioxidant activity *in planta* (Decourcelle et al., 2015; Zanga et al. 2018). Comparatively, MYB has proven to perceive the cellular redox state (Arratia-Quijada et al., 2012), and may coordinate secondary metabolism and oxidative stress response (Hong et al., 2013). The implication of SA and JA as a coordinated part of the same response also suggests that *ZmGAMYB* proteins are transcriptional common-ground for the two defense pathways elicited by each phytohormone. Previous work with other pathosystems has related SA and JA (Lanubile et al., 2017), but never have the two phytohormones been documented as sharing ZmGAMYB as with NPR1 (Dong 2004; Pieterse et al., 2012).

It is not unusual that ZmGAMYB over-expresses in response to up-regulated JA or SA hormone concentrations, though the response has generally been observed in the presence of each individual hormone, separately. ZmGAMYB is a member of the R2R3-class TFs, regulating gibberellin-responsive genes during germination (Gubler et al., 1995), as well as endosperm specific genes during seed development (Diaz et al., 2002). The family of R2R3-MYB-like TFs has repeatedly been implicated in JA-dependent defense responses (Ambawat et al., 2013), and in a variety of biological functions like phenylpropanoid metabolism (Hichri et al., 2011), biotic and abiotic stress (Lippold et al. 2009; Segarra et al. 2009), and hormone

responses (Urao et al. 1993). SA signal transduction pathways have also been connected with MYB (Raffaele et al. 2006); specifically, AtMYB96-mediated ABA signals enhanced pathogen resistance response by inducing SA biosynthesis, implicating MYB96 as a molecular link in ABA-SA crosstalk (Seo and Park 2010).

The SA and JA signaling pathways are thought to comprise the backbone of plant immunity (Pieterse et al., 2009; Pieterse et al., 2012; Shigenaga and Argueso, 2016), and to lead to the transcriptional activation of defense genes. Typically, SA has been tied to the WRKY TF family, and JA to ZIM27 (Lanubile et al., 2017). Previous studies have also shown that TF activation is skewed towards the MYB family in the case of certain pathosystems. For example, *Tobacco mosaic virus* (TMV) and an SA-induced tobacco gene were shown to encode a MYB TF to participate in SAR (Yang and Klessig 1996). In another case, at least two *Arabidopsis* MYB genes were induced by bacterial infection and hypersensitive cell death (Kranz et al. 1998); and finally there is one instance of a MYB gene being induced by fungal infection (Lee et al., 2001). Whereas earlier studies document MYB activation via the stress response to either bacterial or fungal infection, here we document the activation of ZmGAMYB in HC by bacterial and fungal co-infection.

Principle component analysis (PCA) indirectly correlated hormone accumulation of ABA with SA and JA. This sort of ABA-SA reciprocal antagonism in leaves has been well-documented in previous work (Cao et al., 2011). It has also been reported that engineered carotenoid modification can disturb ABA levels since ABA is a final product of the carotenoid pathway (Lindgren et al., 2003). Thus said, our results clearly showed that ABA was not different among WT or HC untreated genotypes. In terms of ABA signaling, our results emphasized a positive correlation between *ZmPSY1*, *ZmNCED4* and ZmEIN3. *ZmPSY1* and *ZmNCED4* are carotenoid to ABA biosynthesis, transport, turnover and catabolism genes, while ZmEIN3 is a TF responsible for regulating JA and ET signaling and cross-talk between all three pathways (JA, ET and SA) (Klessig et al., 2018). There was also positive correlation between *ZmNCED4* and *ZmLOX3,* which has been tied to the concomitant suppression of JA and SA-regulated pathways in roots (Gao et al., 2008). These relationships highlight the connection that carotenoid pathway genes have with hormone signaling genes, and while the exact mechanisms underlying their coordination still remains to be elucidated, our results imply the importance of up-regulated secondary metabolism in this response.

We also found that ABA accumulation was negatively correlated with up-regulated ZmEIN3, *ZmACO* and *ZmNCED4* gene expression. *ZmACO* and ZmEIN3 participate in ethylene conversion and signaling/crosstalk, respectively, and are typically regulated by ABA (Klessig et al., 2018), while *ZmNCED4* is a rate-limiting enzyme for ABA biosynthesis (Mou et al., 2016). The inverse relationships between ABA accumulation and downstream gene expression reiterates that another source is likely regulating ethylene-mediated processes, such

as an alteration of the redox state The mechanisms controlling ABA hormone accumulation are less known than those governing ABA turnover gene expression, though it has been suggested that there are unknown regulatory mechanisms integrating the activities of different ABA-metabolism pathways to match ABA level to stress severity (Kalladan et al., 2017). More recent work has found that ABA regulates the internal metabolic functions to alleviate the harms of environmental stresses by integrating with antioxidant responses and triggering the pre-transcriptional induction of NADPH oxidases (NOXs) to modulate NADPH oxidase for ROS generation (Asad et al., 2019). Over-expression of the ABA-synthesis enzyme NCED may lead to a small (or null) increase in ABA, but larger increases in the ABA catabolite phaseic acid (Qin and Zeevaart, 2002). In our study, this might be the case as demonstrated by correlation analysis, but also specifically in co-treated and Sp7 HC plants, since plants demonstrated up-regulation of ABA-related gene *ZmNCED4*, but no change in ABA hormone accumulation.

7.6 Conclusions

This study examined the relationship between *Azospirillum brasilense* Sp7 and *Fusarium graminareum* in high carotenoid transgenic maize plants, finding that their interaction adversely affects photosynthesis-related mechanisms, but enhances plant antioxidant capacity, as well as the expression of genes involved in the carotenoid pathway, hormone signaling and ethylene production generally leading to improved resistance to Fus and better agronomic performance. The combined effect of Sp7 and Fus on HC genotypes revealed a complex cross-talk between hormones with genes involved in the antioxidant and carotenoid pathway thereby , providing evidence that the antioxidant-hormone signaling network may be triggered by an up-regulation of the plant secondary metabolism.

We also show a likely implication of the ZmGAMYB transcription factor in the cellular redox state, and as a putative candidate transcription factor for coordinating the up-regulation of the plant secondary metabolism, the oxidative stress response and the hormonal cross-talk in HC plants. Besides, salicylic and jasmonic acid seem to act as a coordinated part of the same response, suggesting that ZmGAMYB proteins are transcriptional common-ground for the two defense pathways elicited by each phytohormone. To the best of our knowledge, this is the first study documenting the activation of ZmGAMYB by bacterial and fungal co-infection.

7.7 References

Abdulkareem M, Aboud HM, Saood HM, Shibly MK (2014) Antagonistic activity of some plant growth rhizobacteria to *Fusarium graminearum*. *International Journal of Phytopathology* 03 (01):49-54.

Agrawal PK, Kohli A, Twyman RM, Christou P (2005) Transformation of plants with multiple cassettes generates simple transgene integration patterns and high expression levels. *Molecular Breeding* 16:247–60.

Ambawat S, Sharma P, Yadav NR, Yadav RC (2013) MYB transcription factor genes as regulators for plant responses: an overview. *Physiology and Molecular Biology of Plants* 19 (3):307-321.

Arratia-Quijada J, Sánchez O, Scazzocchio C, Aguirre J (2012) FlbD, a Myb transcription factor of *Aspergillus nidulans*, is uniquely involved in both asexual and sexual differentiation. *Eukaryotic Cell* 11 (9):1132.

Asad MAU, Zakari SA, Zhao Q, Zhou L, Ye Y, Cheng F (2019) Abiotic stresses intervene with ABA signaling to induce destructive metabolic pathways leading to death: premature lead senescence in plants. *International Journal of Molecular Science* 20 (256):1-23.

Asselbergh B, De Vleesschauwer D, Höfte M (2008) Global switches and fine-tuning – ABA modulates plant pathogen defense. *Molecular Plant Microbe Interactions* 21:709–719.

Bashan Y, de-Bashan LE (2010) Chapter two – how the plant growth-promoting bacterium *Azospirillum* promotes plant growth – a critical assessment. *Advances in Agronomy* 108:77–136.

Bashan Y, Holguin G, Lifshitz R (1993) Isolation and characterization of plant growth-promoting rhizobacteria. In: Glick BR (ed) *Methods in Plant Molecular Biology and Biotechnology*. CRC Press, Boca Raton, FL, pp 331–345.

Bashan Y (1986) Significance of timing and level of inoculation with rhizosphere bacteria on wheat plants. *Soil Biology and Biochemistry* 18:297-301

Bhattacharyya PN, Jha DK (2012) Plant growth-promoting rhizobacteria (PGPR): emergence in agriculture. *World Journal of Microbiology and Biotechnology* 28 1327–1350.

Botta LA, Santacecilia A, Ercole C, Cacchio P, del Gallo M (2013) In vitro and in vivo inoculation of four endophytic bacteria on *Lycopersicon esculentum*. *Nature Biotechnology* 30 (6):666–674.

Burgess LW, Summerell BA, Bullock S, Gott KP, Backhouse D (1994) *Laboratory manual for Fusarium research*. Lab manual, 3rd ed. University of Sydney and Botanic Garden, Sydney, Australia.

Campos-Bermudez VA, Fauguel CM, Tronconi MA, Casati P, Presello DA, Andreo CS (2013) Transcriptional and metabolic changes associated to the infection by *Fusarium verticillioides* in maize inbreds with contrasting ear rot resistance. *PLOS ONE* 8 (4):e61580.

Cao FY, Yoshioka K, Desveaux D (2011) The roles of ABA in plant pathogen interactions. *Journal of Plant Research* 124:489–499.

Decourcelle M, Perez-Fons L, Baulande S, Steiger S, Couvelard L, Hem S, Zhu C, Capell T, Christou P, Fraser P, Sandmann G (2015) Combined transcript, proteome and metabolite analysis of transgenic maize seeds engineered for enhanced carotenoid synthesis reveals pleiotrophic effects in core metabolism. *Journal of Experimental Botany* 66:3141–3150.

Demeke T, Clear RM, Patrick SK, Gaba D (2005) Species-specific PCR-based assays for the detection of *Fusarium* species and a comparison with the whole seed agar plate method and trichothecene analysis. *International Journal of Food Microbiology* 103:271–284.

Diaz I, Vicente-Carbajosa J, Abraham Z, Martinez M, Isabel-La Moneda I, Carbonero P (2002) The GAMYB protein from barley interacts with the DOF transcription factor BPBF and activates endosperm-specific genes during seed development. *The Plant Journal* 29:453-464.

Díaz-Gómez J, Marín S, Nogareda C, Sanchis V, Ramos AJ (2016) The effect of enhanced carotenoid content of transgenic maize grain on fungal colonization and mycotoxin content. *Mycotoxin Research* 32 (4):221-228.

Ding L, Xu H, Kong Z, Zhang L, Xue S, Jia H, Ma Z (2011) Resistance to hemi-biotrophic *F. graminaerum* is associated with coordinated and ordered expression of diverse defense signalling pathways. *PLOS ONE* 6 (4):e19008.

Dinolfo MI, Castañares E, Stengelin SA (2017) *Fusarium*–Plant Interaction: State of the Art – a Review. *Plant Protection Science* 53:61-70.

Döbereiner J, Marriel IE, Nery M (1976) Ecological distribution of *Spirillum lipoferum* Beijerinck. *Canadain Journal of Microbiology* 22 (10):1464-1473.

Dong X (2004) NPR1, all things considered. *Curren Opinion in Plant Biology* 7:547–52.

Edwards SG (2004) Influence of agricultural practices on *Fusarium* infection of cereals and subsequent contamination of grain by trichothecene mycotoxins. *Toxicology Letters* 153:29-35.

Fanciullino AL, Bidel LPR, Urban L (2014) Carotenoid responses to environmental stimuli: integrating redox and carbon controls into a fruit model. *Plant Cell Environment* 37:273-289.

Farré G, Maiam Rivera S, Alves R, Vilaprinyo E, Sorribas A, Canela R, Naqvi S, Sandmann G, Capell T, Zhu C, Christou P (2013) Targeted transcriptomics and metabolic profiling reveals temporal bottlenecks in the maize carotenoid pathway that can be addressed by multigene engineering. *The Plant Journal* 75:441–455.

Foyer CH, Noctor G (2005) Redox homeostasis and antioxidant signaling: a metabolic interface between stress perception and physiological responses. *The Plant Cell* 17:1866-1875.

Gao X, Starr J, Göbel C, Engelberth J, Feussner I, Tumlinson J, Kolomiets M (2008) Maize 9-Lipoxygenase ZmLOX3 Controls Development, Root-Specific Expression of Defense Genes, and Resistance to Root-Knot Nematodes. *Molecular Plant-Microbe Interactions* 21(1):98-109.

Garg M, Sharma N, Sharma S, Kapoor P, Kumar A, Chunduri V, Arora P (2018) Biofortified crops generated by breeding, agronomy and transgenic approaches are improving lives of millions of people around the world. *Frontiers in Nutrition* 5:12.

Giné-Bordonaba J, Terry LA (2016) Effect of deficit irrigation and methyl jasmonate application on the composition of strawberry (*Fragaria x ananassa*) fruit and leaves. *Scientia Horticulturae* 199 (16): 63-70.

Gubler F, Kalla R, Roberts JK, Jacobsen JV (1995) Gibberellin-regulated expression of a myb gene in barley aleurone cells: evidence for Myb transactivation of a high-pI alpha-amylase gene promoter. *Plant Cell* 7:1879-1891.

Gunnaiah R, Kushalappa AC, Duggavathi R, Fox S, Somers DJ (2012) Integrated metabolo-proteomic approach to decipher the mechanisms by which wheat QTL (Fhb1) contributes to resistance against *Fusarium graminearum*. *PLOS ONE* 7: 7.

Gutierrez-Carbonell E, Lattanzio G. Albacete A, Rio JJ, Kehr J, Abadía A, Grusak MA, Abadía J, López-Millán AF (2015) Effects of Fe deficiency on the protein profile of *Brassica napus* phloem sap. *Proteomics* 15 (22):3835-3853.

Gutierrez-Gonzalez JJ, Wise ML, Garvin DF (2013) A developmental profile of tocol accumulation in oat seeds. *Journal of Cereal Science* 57:79–83.

Hartmann A, Hurek T (1988) Effect of carotenoid overproduction on oxygen tolerance of nitrogen fixation in *Azospirillum brasilense* Sp7. *Journal of General Microbiology* 134:449–2455.

Hichri I, Barrieu F, Bogs J, Kappel C, Delrot S, Lauvergeat V (2011) Recent advances in the transcriptional regulation of the flavonoid biosynthetic pathway. *Journal of Experimental Botany* 62 (8):2465–2483.

Hong S-Y, Roze LV, Linz JE (2013) Oxidative stress-related transcription factors in the regulation of secondary metabolism. *Toxins* 5:683-702.

Idris HA, Labuschagne N, Korsten L (2007) Screening rhizobacteria for biological control of *Fusarium* root and crown rot of sorghum in Ethiopia. *Biological Control* 40 (1):97-106.

Jin X, Bai C, Bassie L, Nogareda C, Romagosa I, Twyman RM, Christou P, Zhu C (2018) ZmPBF and ZmGAMYB transcription factors independently transactivate the promoter of the maize (*Zea mays*) β-carotene hydroxylase 2 gene. *New Phytologist.* doi: 10.1111/nph.15614.

Kalladan R, Lasky JR, Chang TZ, Sharma S, Juenger TE, Verslues PE (2017) Natural variation identifies genes affecting drought-induced abscisic acid accumulation in *Arabidopsis thaliana. Proceedings of the National Academy of Sciences of the United States of America* 114 (43):11536-11541.

Klessig DF, Choi HW, Dempsey D'MA (2018) Systemic acquired resistance and salicylic acid: past, present and future. *Molecular Plant-Microbe Interactions* 31(9).

Kranner I, Cram WJ, Zorn M, Wornik S, Yoshimura I, Stabentheiner E, Pfeifhofer W (2005) Antioxidants and photoprotection in a lichen as compared with its isolated symbiotic partners. *Proceedings of the National Academy of Sciences of the United States of America* 102:3141–3146.

Kranz HD, Denekamp M, Greco R, Jin HL, Leyva A, Meissner R, Petroni K, Urzainqui A, Bevan M, Martin C, Smeekens, S, Tonelli C, Paz-Ares J, Weisshaar B (1998) Towards functional characterisation of the members of the R2R3-MYB gene family from *Arabidopsis thaliana*. *The Plant Journal* 16:263–76.

Kyndt T, Nahar K, Haeck A, Verbeek R, Demeestere K, Gheysen G (2017) Interplay between carotenoids, abscisic acid and jasmonate guides the compatible rice-*Meloidogyne graminicola* interaction. *Frontiers in Plant Science* 8 (951):1-11.

Lanubile A, Maschietto V, Borrelli VM, Stagnati L, Logrieco AF, Marocco A (2017) Molecular basis of resistance to *Fusarium* ear rot in maize. *Frontiers in Plant Science* 8:1774.

Lee MW, Qi M, Yang Y (2001) A novel jasmonic acid-inducible rice MYB gene associates with fungal infection and host cell death. *Molecular Plant Microbe Interactions* 14:527–535.

Li X, Wu X, Huang L (2009) Correlation between Antioxidant Activities and Phenolic Contents of Radix Angelicae Sinensis (Danggui). *Molecules* 14:5349-5361.

Lippold F, Sanchez DH, Musialak M, Schlereth A, Scheible WR, Hincha DK, Udvardi MK (2009) AtMyb41 regulates transcriptional and metabolic responses to osmotic stress in *Arabidopsis*. *Plant Physiology* 149:1761–1772.

López-Reyes L, Carcaño-Montiel MG, Tapia-López L, Medina-de la Rosa G, Tapia-Hernández RA (2017) Antifungal and growth-promoting activity of *Azospirillum brasilense* in *Zea mays* L. ssp. Mexicana. *Archives of Phytopathology and Plant Protection* 50 (13-14):727-743.

Matsushima R (2014) Thin Sections of Technovit 7100 Resin of Rice Endosperm and Staining. *Bio-protocol* 4 (18):e1239.

McLaughlin CS, Vaughan MH, Campbell IM, Wei CM, Stafford ME, Hansen BS (1977) Inhibition of protein synthesis by trichothecenes. In: Rodricks JV, Hesseltine CW, Mehlman MA (eds.) *Mycotoxins in human and animal health* (Proceedings of a conference on mycotoxins in human and animal health). Pathotox Publishers, IL, USA, pp 263–273.

Mengistu A, Tachibana H, Epstein AH, Bidne KG, Hatfield JD (1987) Use of leaf temperature to measure the effect of brown stem rot and soil moisture stress and its relations to yields of soybeans. *Plant Disease* 71:632–634.

Mou W, Li D, Bu J, Jiang Y, Khan ZU, Luo Z, Mao L, Ying T (2016) Comprehensive Analysis of ABA Effects on Ethylene Biosynthesis and Signaling during Tomato Fruit Ripening. *PLOS ONE* 11(4):e0154072.

Naqvi S, Zhu C, Farre G, Sandmann G, Capell T, Christou P (2011) Synergistic metabolism in hybrid corn reveals bottlenecks in the carotenoid pathway and leads to the accumulation of extraordinary levels of the nutritionally important carotenoid zeaxanthin. *Plant Biotechnology* J 9:384–393.

Nicholson P, Simpson DR, Weston G, Rezanoor HN, Lees AK, Parry DW, Joyce D (1998) Detection and quantification of *Fusarium culmorum* and *Fusarium graminearum* in cereals using PCR assays. *Physiology and Molecular Plant Pathology* 53:17–37.

Okonechnikov K, Golosova O, Fursov M, the UGENE team (2012) Unipro UGENE: a unified bioinformatics toolkit. *Bioinformatics* 28:1166-1167.

Omer M, Locke JC, Frantz JM (2007) Using Leaf Temperature as a Nondestructive Procedure to Detect Root Rot Stress in Geranium. *Hort Technology* 17 (4):532-536.

Oren L, Ezrati S, Cohen D, Sharon A (2003). Early events in the *Fusarium verticilloides*-Maize interaction characterized by using a green florescent protein-expressing transgenic isolate. *Applied Environmental Microbiology* 69 (3):1695-1701.

Panwar V, Aggarwal A, Singh G, Verma A, Sharma I, Saharan MS (2014) Efficacy of foliar spray of Trichoderma isolates against *Fusarium graminearum* causing head blight (head scab) of wheat. *Journal of Wheat Research* 6 (1):1-5.

Pieterse CMJ, Leon-Reyes A, Van der Ent S, Van Wees SCM (2009) Networking by small-molecule hormones in plant immunity. *Nature Chemical Biology* 5:308-316.

Pieterse CMJ, Zamioudis C, Berendsen RL, Weller DM, Van Wees SCM, Bakker PAHM (2014) Induced systemic resistance by beneficial microbes. *Annual Review of Phytopathology* 52:16.1-16.29.

Pieterse CMJ, Van der Does D, Zamioudis C, Leon-Reyes A, Van Wees SCM (2012) Hormonal modulation of plant immunity. *Annual Review of Cell and Developmental Biology* 28:489–521.

Qin X, Zeevaart JAD (2002) Overexpression of a 9-cis-epoxycarotenoid dioxygenase gene in Nicotiana plumbaginifolia increases abscisic acid and phaseic acid levels and enhances drought tolerance. *Plant Physiology* 128:544–551.

Raffaele S, Rivas S, Roby D (2006) An essential role for salicylic acid in AtMYB30-mediated control of the hypersensitive cell death program in *Arabidopsis*. *FEBS Letters* 580:3498–3504.

Richardson KC, Jarrett L, Finke EH (1960) Embedding in epoxy resins for ultrathin sectioning in electron microscopy. *Stain Technology* 35:313.

Rengel Z, Batten GD, Crowley DE (1999) Agronomic approaches for improving the micronutrient density in edible portions of field crops. *Field Crops Research* 60:27–40.

Romanowska E, Buczynska A, Wasilewska W, Krupnik T, Drozak A, Rogowski P, Parys E, Zienkiewicz M (2017) Differences in photosynthetic responses of NADP-ME type C4 species to high light. *Planta* 245:641-657.

Ross, AF (1961) Systemic acquired resistance induced by localized virus infections in plants. *Virology* 14:340–58.

Segarra G, Van der Ent, S, Trillas I, Pieterse CMJ (2009) MYB72, a node of convergence in induced systemic resistance triggered by a fungal and a bacterial beneficial microbe. *Plant Biology* 11:90–96.

Seo PJ, Park CM (2010) MYB96-mediated abscisic acid signals induce pathogen resistance response by promoting salicylic acid biosynthesis in *Arabidopsis*. *New Phytologist* 186:471–483.

Shewmaker CK, Sheehu JA, Daley M, Colburn S, Ke DY (1999) Seed-specific overexpression of phytoene synthase: increase in carotenoids and metabolic effects. *Plant Journal* 20:41–412.

Shigenaga A M, Argueso CT (2016) No hormone to rule them all: Interactions of plant hormones during the responses of plants to pathogens. *Seminars in Cell and Developmental Biology* 56:174-189

Shime-Hattori A, Kobayashi S, Ikeda S, Asano R, Shime H, Shinano T (2011) A rapid and simple PCR method for identifying isolates of the genus *Azospirillum* within populations of rhizosphere bacteria. *Journal of Applied Microbiology* 111:915-924.

Singleton VL, Orthofer R, Lamuela-Raventos RM (1999) Analysis of total phenols and other oxidation substrates and antioxidants by means of Folin-Ciocalteu reagent. *Methods in Enzymology* 299:152–178.

Smith SE, Read DJ (2007) *Mycorrhizal Symbiosis,* 3rd ed. Elsevier, London, UK.

Somers E, Ptacek D, Gysegom P, Srinivasan M, Vanderleyden J (2005) *Azospirillum brasilense* produces the auxin-like phenylacetic acid by using the key enzyme for indole-3-acetic acid biosynthesis. *Applied Environmental Microbiology* 71:1803–1810.

Urao T, Yamaguchi-Shinozaki K, Urao S, Shinozaki K (1993) An *Arabidopsis* myb homolog is induced by dehydration stress and its gene product binds to the conserved MYB recognition sequence. *Plant Cell* 5:1529–1539.

Wojciechowski S, Chelkowski J, Kostecki M (1995) Influence of deoxynivalenol on electrolyte leakage in cereal seedling leaves. *Acta Physiologiae Plantarum* 17:357–360.

Xu L, Yue Q, Bian F, Sun H, Zhai H, Yao, Y (2017) Melatonin Enhances Phenolics Accumulation Partially via Ethylene Signaling and Resulted in High Antioxidant Capacity in Grape Berries. *Frontiers in Plant Science* 8:1426.

Yang SH, Moran DL, Jia HW, Bicar EH, Lee M, Scott MP (2002) Expression of a synthetic porcine alpha-lactalbumin gene in the kernels of transgenic maize. *Transgenic Research* 11:11–20.

Yang Y, Klessig DF (1996). Isolation and characterization of a tobacco mosaic virus-inducible myb oncogene homolog from tobacco. *PNAS* 93:14972–14977.

Zanga D, Sanahuja G, Eizaguirre M, Albajes R, Christou P, Capell T, Fraser P, Gerrisch C, López C (2018) Carotenoids moderate the effectiveness of a Bt gene against the European corn borer, *Ostrinia nubilalis. PLOS ONE* 13(7):e0199317.

Zanga D, Capell T, Slafer GA, Christou P, Savin R (2016) A carotenogenic mini-pathway introduced into white corn does not affect development or agronomic performance. *Scientific Reports* 6:38288.

Zehra A, Meena M, Dubey MK, Aamir M, Upadhyay RS (2017) Synergistic effects of plant defense elicitors and *Trichoderma harzianum* on enhanced induction of antioxidant defense system in tomato against *Fusarium* wilt disease. *Botanical Studies* 58:44.

Zhao J, Zhang X, Hong Y, Liu Y (2016) Chloroplast in Plant-Virus Interaction. *Frontiers in Microbiology* 7:1565.

Zhou S, Zhang YK, Kremling KA, Ding Y, Bennett JS, Bae JS, Kim DK, Ackerman HH, Kolomiets MV, Schmelz EA, Schroeder FC, Buckler ES, Jander G (2019) Ethylene signaling regulates natural variation in the abundance of antifungal acetylated diferuloylsucroses and *Fusarium graminearum* resistance in maize seedling roots. *New Phytologist* 221 (4):2096-2111.

Zhu C, Naqvi S, Breitenback J, Sandmann G, Christou P, Capell T (2008) Combinatorial genetic transformation generates a library of metabolic phenotypes for the carotenoid pathway in maize. *Proceedings of the National Academy of Sciences of the United States of America* 105 (47):18232-18237.

CHAPTER 8

Azospirillum brasilense Sp7 modulates homeostasis of Fe-biofortified rice seedlings

(Manuscript in preparation, 2019)

Chapter 8. *Azospirillum brasilense* Sp7 modulates homeostasis of Fe-biofortified rice seedlings

8.0 Abstract

Iron (Fe) homeostasis in rice is a complex process governed by an array of promiscuous metal ligands and transporters. Effectively controlling some of these elements has led to Fe-biofortification of the rice endosperm to benefit human health, but there are still many questions regarding the mechanisms that regulate the Fe-deficiency response to improve plant health. Plant growth-promoting rhizobacteria (PGPR) are a biological root additive that produce siderophores and help plants assimilate stress. We investigated Fe homeostasis in Fe-biofortified rice seedlings inoculated with the PGPR *Azospirillum brasilense* (Sp7) at planting. Dry biomass accumulation, metals, siderophore, nitrogen and chlorophyll contents were measured in leaf tissues at early vegetative stages. We evaluated the expression of key endogenous Fe-homeostasis genes and compared results to the physiological state of the seedlings. Sp7 increased the expression of *OsNAS2*, *OsTOM1*, *OsDMAS1, OsYSL15* and *OsIRO2* as well as Fe and Zn accumulation in seedlings (leaves), without changing plant mugineic acid (MA) levels. Notably, *OsIRO2* was up-regulated by Sp7 regardless of Fe supply. Sp7 also exerted influence over root-bound MA homeostasis. Finally, the inverse regulation between *OsNAS1* and *OsNAS2* indicated that these two genes may work in tandem to regulate Fe equilibrium in seedlings. This study shows how gene expression is affected by Sp7 in Fe-deficient rice, drawing attention to how the simultaneous use of two biofortification strategies work together to positively effect plants under stress.

8.1 Introduction

Iron (Fe) stress can be caused either by deficiency or by excess (Connolly and Guerinot, 2002). When the soil is aerated and in alkaline pH, Fe is oxidized as insoluble iron oxides, but in anaerobic conditions such as flooded soils, pH decreases and there is a reduction of insoluble ferric iron (Fe^{3+}) to soluble ferrous iron (Fe^{2+}) (Morrissey and Guerinot, 2009). Fe deficiency can cause alterations in root morphology (Morrissey and Guerinot, 2009) and chlorosis of young leaves (Kobayashi and Nishizawa, 2014), while high Fe^{2+} levels can be directly and indirectly toxic to plants (Mongon et al., 2014). Direct toxicity occurs when there is too much absorption and excessive accumulation of elemental Fe in tissues, causing brown-dark spots in the leaves (leaf-bronzing) (Morrissey and Guerinot, 2009). Indirect damage is caused by the prevention of the uptake, transport and utilization of other nutrients (e.g.: P, K, Ca and Zn) due to the iron plaque that forms when Fe^{3+} is deposited in the apoplast of rice roots (Zhang et al., 2014). Both situations affect plant growth, development and productivity, leading to significant yield losses in cultivated rice in the regions of Africa, Asia and South America (Shahid et al., 2014).

Rice (*Oryza sativa* L.) roots prevent Fe imbalances and acquire adequate amounts of soluble Fe from the rhizosphere by relying on the combination of two Fe acquisition strategies (I and II). Strategy I is a reduction-based pathway using ferric-chelate reductases, while Strategy II involves the release of chelating Fe-phytosiderophore (Fe-PS) complexes by plant roots that solubilize Fe^{3+} and transport it to the plant (Cline et al., 1984; Römheld and Marschner, 1986). Fe-PSs are in the mugineic acid (MA) family (Ma and Nomoto, 1994) and their biosynthesis follows the methionine cycle (Ma et al., 1995). They consist of 2'-deoxymugineic acid (DMA), biosynthesized from S-adenosyl-L-methionine (SAM) through a nicotianamine (NA) intermediate (Mori et al., 1987; Shojima et al., 1989), and three enzymes: NA synthase (NAS) (Higuchi et al., 1999), NA aminotransferase (NAAT) (Takahashi et al., 1999), and DMA synthase (Bashir et al., 2006). In the rhizosphere, DMA chelates and solubilizes Fe, then transports it to the plant via the Transporter Of Mugineic acids 1 (*TOM1*) (Nozoye et al., 2007, 2011). The resultant Fe^{3+}-MA complexes are absorbed by root cells via the Yellow Stripe-Like (YSL) protein OsYSL15, located in the plasma membrane (Inoue et al., 2009; Curie et al., 2001). Once Fe is loaded into the xylem, chelators such as citrate, NA, and DMA are involved in transport within the plant (Jeong and Guerinot, 2009), along with the expression of *OsNAS1*, *OsNAS2*, *OsNAAT1* and *OsDMAS1* genes (Inoue et al. 2003; Bashir et al. 2006).

Due to the insolubility of elemental Fe in an aerobic atmosphere, microorganisms have also evolved the capacity to generate siderophores that form soluble complexes with Fe^{3+}, as well as specific receptor proteins that recognize these complexes and facilitate Fe transport into the cells (Neilands, 1982). The specificity of the transport systems enable micro-organisms to compete with other organisms for available Fe (Weinberg 1984). In the case of pathogenic

bacteria, competition involves interacting with the hosts' Fe-binding proteins (Neilands & Leong, 1986). Studies with beneficial plant growth-promoting rhizobacteria (PGPR), on the other hand, have shown how the plants' high-specificity, high-affinity Fe uptake systems exert a strong influence on the microbial environment and increase Fe-solubilisation in the rhizosphere to improve plant growth (Schroth & Hancock, 1982; Pii et al., 2015). PGPR also up-regulate N_2-fixation in Fe-deficient conditions (Fernández-Scavino and Pedraza 2013). Bacterial Fe-homeostasis is essential so that bacteria can acquire sufficient Fe to function, but resist toxicity caused by Fe-mediated production of reactive oxygen species (ROS) (Braun 1997; Cornelis and Matthijs 2002), restricting the expression of bacterial Fe-acquisition systems to environments where Fe stores are depleted (Dave and Dube 2000; Ellerman and Arthur, 2017).

Azospirillum brasilense Sp7 (Sp7) is a free-living, diazotrophic PGPR (Tarrand et al., 1978) used as a root inoculant for plants in cropping systems. The primary benefits of Sp7 stem from its production of regulatory vegetative growth substances directly affecting plant metabolism (Glick, 2012; Lade et al., 2018) and its ability to carry out biological nitrogen fixation (BNF) (Cassán et al., 2009). Sp7 is also valued for its ability to produce siderophores, especially since not all strains of *A. brasilense* are able to do so (Bachhawat and Ghosh 1987b; Tortora et al., 2011). While Sp7 is an epiphytic bacterial strain, rendering it comparatively less productive of siderophores than other endophytic strains of *Azospirillum* spp. (Tortora et al., 2011), it is also highly responsive to the soil environment, perceiving stress and contaminants acutely (Kamnev et al., 2012). For this reason, Sp7 is often chosen as an inoculant to help plants attenuate the effects of abiotic and biotic stresses (Bashan et al., 2004). Consequently, most of the existing literature regarding siderophore production by Sp7 relates to its role as a biocontrol agent used to limit the growth of soil-borne phytopathogens (Tortora et al., 2011), or bioremediate toxic metals from the soil (Kamnev et al., 2005). *Azospirillum brasilense* has a high necessity for Fe because it is needed as a co-factor in bacterial enzymes involved in redox reactions and N_2 fixation, such as nitrogenase (Andrews 1998; Pedraza 2015). *Azospirillum brasilense* initiates biosynthesis of its siderophore, spirilobactin (a catechol), in Fe-deficient soils and induces the synthesis of several high-molecular-weight proteins that act as high-affinity Fe carriers to scavenge Fe from both the rhizosphere and/or from plant tissue (Bachhawat and Gosh 1987a, b, 1989).

Even when there is a high amount of Fe in the soil, which can be toxic to the plant, little is accumulated in rice grains. Therefore, in parts of the world where rice is the staple crop, Fe deficiency has major consequences on human health, causing anemia and even death (Arcanjo et al., 2013; Aung et al., 2013). Biofortification is a way to help solve this problem because it is a sustainable method that can promote the movement of Fe to grains, and decrease Fe absorption inhibitors (Schuler and Bauer 2012). The use of siderophore-producing microbes has proven to be a better approach over other conventional methods of agronomic

biofortification such as chemical fertilizer application (Khan et al., 2019), but the specific relationship between *Azospirillum* and rice to enhance Fe content in plants and grains requires more study. To address this need, we have conducted a study evaluating Fe homeostasis characteristics in Sp7-inoculated plants grown in Fe-sufficient and Fe-deficient soil conditions. To better understand and characterize Sp7 changes to Fe homeostasis, we compared transgenically Fe-biofortified rice plants (RB92) with wild type (WT) plants. Fe-homeostasis of RB92 has been well-characterized in previous work (Banakar et al., 2017). Our study focused on the early vegetative growth stages of rice because it is when seedlings are highly susceptible to Fe deficiency and secrete very low amounts of DMA (Mori et al., 1991), and because Sp7 has been shown to increase the vigor of young seedlings (Lade et al., 2018). Furthermore, *Azospirillum* spp. is most viable and unchanged as an inoculant for 30 days post-sowing, then sharply declines and can become negligible 57 days post-sowing (El Zemrany et al., 2006).

We hypothesized that Sp7 synergistically interacts with plant siderophores to promote Fe acquisition and translocation into leaf tissues under conditions of Fe-deficiency. We therefore explored the effects of Sp7 on the Fe homeostasis of rice seedlings by examining molecular and biochemical changes to plants grown in soils containing Fe or not. We identified plant transcription factors (TFs) involved in the Fe-deficiency response, and gauged how root inoculation with Sp7 affects gene expression, siderophore and metal accumulation. Special interest was given to the expression of Fe-related homeostasis genes and TFs in aerial plant parts because Fe allocation and transport into leaf tissues is mediated by siderophore-Fe complexes (Hell and Stephan, 2002).

8.2 Aims

- Explore the effects of Sp7 on the Fe homeostasis of RB92 seedlings grown in Fe-deficient soil conditions
- Identify TFs and hormones instrumental in the Fe-deficiency response in WT and RB92 plants
- Gauge how root inoculation with Sp7 affects expression of Fe-related genes and metal accumulation

8.3 Materials and Methods

8.3.1 Plant material, Sp7 inoculation and Fe uptake studies

We used two near-isogenic rice genotypes: *Oryza sativa* L. cv EYI 105, referred to herein as wild-type (WT), and a biofortified transgenic line (RB92) that had been engineered previously to co-express *OsNAS1* and *HvNAATb* (Banakar 2016). RB92 has increased abundance of NA and DMA (124- and 8-fold, respectively), as well as increased accumulation

of Fe (7.5-fold) and Zn (3.8-fold) in the endosperm (Banakar 2016). In recent work by Banakar et al. (2017), plants expressing the same genes as RB92 were found to have a homeostatic mechanism for limiting Fe and Zn over-loading in the endosperm, causing the sequestration of excess minerals to the roots, culm, middle leaf and flag leaf. For this, the plant regulates metal uptake in the roots, sequesters metals in vacuoles and employs endogenous metal transporters; the secondary effects that such mechanisms have on the plant is still largely unknown.

The *Azospirillum brasilense* Sp7 strain (ATCC 29145) (Sp7) was kindly provided by the "Colección Española de Cultivos Tipo" (CECT) of the Polytechnic University of Valencia (Spain). For the Sp7 suspension, a peptone yeast broth (PYB) liquid medium supplemented with $CaCl_2$ (0.04%) was prepared, as described by Döbereiner et al. (1976), and incubated at 32°C under constant agitation at 100rpm for 20h. The bacterial suspension was allowed to reach its late log-growth phase [absorbance of 1.0 at OD_{600} nm (determined via an Amersham Biosciences Ultraspec 3100 Pro spectrophotometer)], obtaining an ideal bacterial density of $1x10^8 cfu \cdot mL^{-1}$.

Rice seeds were disinfected with 70% ethanol for 2min, soaked in 1% sodium hypochlorite for 10min under constant agitation (100rpm), and washed six times with sterile distilled water. Seeds were dried on sterile autoclaved paper and inoculated with the rhizobacteria at $1x10^8$cfu per mL (Bashan 1986); 1mL of the bacterial suspension was aliquoted for each WT and RB92 inoculated seed group and centrifuged at 5000rpm for 10min. The supernatant was poured out and the pellet was re-suspended in 1mL of 1X PBS. The inoculum was vortexed, and 0.2mL of inoculum was added to each group of 50 seeds. The seeds and inoculum were sealed in 15mL falcon tubes and put into horizontal agitation for 2h 50min. Inoculation time and quantity were established according to an imbibition curve, estimating the time taken for each seed variety to imbibe 70% of its total potential. Non-inoculated seeds of each cultivar served as controls and were handled the same was as inoculated seeds, but treated only with PBS.

Once seeds from both lines were treated with either PBS or Sp7, they were planted *in vitro* in MS medium lacking Fe (Murashige and Skoog 1962). Seeds germinated and grew in a growth chamber (1282 x 687 x 1487mm) at 23-25°C with a photoperiod of 16h light/8h dark cycle under 10,000lux fluorescent bulbs for 5d. Seedlings were then transferred to independent floating trays containing autoclaved commercial substrate (Traysubstrat®, Klasmann-Deilmann, Gmbh, Geeste, Germany). The roots of five random seedlings from each line were screened for Sp7 presence at transfer. All seedlings were watered for 3w with nutrient solution (Kobayashi et al., 2005) containing 100μM $FeCl_3$.

Twenty seedlings of equivalent height each from RB92-Sp7 and -PBS (and WT controls) were then transferred to independent trays in isolation with nutrient solution containing 100μM $FeCl_3$ (normal feeding), or the same omitting $FeCl_3$ (Fe-starvation). Fresh

nutrient solution was provided every other day and the pH of the solution was adjusted to 5.3 with 0.1M KOH (Banakar et al., 2017). Every week, the nutrient solution was completely replaced. Seedlings were maintained as above for an additional 3 weeks. Samples were collected from five seedlings per group and pooled as roots or leaves for each analysis. Five random seedlings from each line and treatment regime were screened (again) for Sp7 presence in the roots at sampling.

8.3.2 Experimental design

The experiment was designed with four treatment groups for the two genotypes: PBS (Fe-starvation), Fe (normal feeding regime), Sp7 (Fe-starved but inoculated) and Fe+Sp7 (normal feeding and inoculated). Sp7 or PBS inoculation was conducted in groups of 40 seeds per genotype (G) and treatment (T). Five days after planting *in vitro*, germinated seeds were selected down to 20 (for each G and T) of the most homogenous seedlings and transferred to the independent floating trays. Each tray well contained one seedling and was considered both as the randomization as well as the observational unit. Sampling was conducted six weeks after transplanting and five biological replicates of each G/T were chosen in a completely randomized design for each analysis.

8.3.3 Screening for Sp7 presence

Sp7 colonization assays were conducted at transfer and at sampling, with five random samples taken from each treatment. The procedure was carried out according to Botta et al. (2013) with modifications and as described in Chapter 5 (Section 5.3.4) (Bashan et al., 1993).

To verify that the colonies were indeed the Sp7 strain, we performed PCR with aliquots taken from stationary-phase cultures grown from the plate isolates, according to Shime-Hattori et al. (2011). The isolates were grown at 32ºC for 17h in Luria-Bertani (LB) broth supplemented with 2.5mmoll^{-1} $CaCl_2$ and 2.5mmol^{l-1} $MgCl_2$. The cultures were held at 95ºC for 5min, and the supernatants of cell lysates obtained were used as PCR templates. The presence of Sp7 16S rDNA was confirmed by PCR using 10µL of the crude bacterial lysate templates in a total volume of 25µL PCR reaction mix consisting of GoTaq DNA Polymerase with the reagents recommended by the manufacturer (Promega, Fitchburg, WI, USA). The PCR was run under the following conditions: 3min initial denaturation at 94ºC followed by 35 cycles of 30s denaturation at 94ºC, 30s annealing at 60ºC, and 1min extension at 72ºC with 5min final extension at 72ºC.

The PCR products were sequenced by StabVida; Caparica, Portugal. Sequences were analyzed and aligned using the Blast® search tool (National Center for Biotechnology Information, Bethesda, MD, USA) and Ugene (Okonechnikov et al., 2012). See Table 13 for 'Sp7' primer sequences.

8.3.4 Analysis of metal and phytosiderophore levels

The metal content of the roots and leaves was determined in diluted samples by inductively coupled plasma mass spectrometry (ICP-MS) using an Agilent 7700X instrument (Agilent Technologies, Santa Clara, CA, USA) as previously described (Banakar et al., 2017).

The most effective way of understanding how the genotype/Fe/Sp7 interaction affects the mobilization of metals in the plant is measuring *in planta* PS concentrations of DMA and NA. NA and DMA levels in roots and leaves were determined by HPLC-electrospray ionization (ESI)-time of flight (TOF)-MS (Xuan et al., 2006) with the modifications described by Banakar et al. (2017).

8.3.5 Total RNA isolation and cDNA synthesis

Total leaf RNA was isolated using the RNeasy Plant Mini Kit (Qiagen, Valencia, CA, USA) and DNA was removed with DNase I (RNase-free DNase Set, Qiagen). Total RNA was quantified using a Nanodrop 1000 spectrophotometer (Thermo Fisher Scientific, Vernon Hills, IL, USA), and 2µg total RNA was used as the template for first strand cDNA synthesis with Ominiscript reverse transcriptase (Qiagen) in a 20µl total reaction volume, following the manufacturer's recommendations.

Table 13. DNA sequence of the primers used for PCR and RT qPCR. (rice)

Gene	Forward primer	Reverse primer
Sp7 detection* (Az16S-D)	5'-CCGCGGTAATACGAAGGGGGC-3'	5'-GCCTTCCTCCGGCTTGTCACCGGC-3'
OsNAS1[5]	5'-GTTCAGCTCCCTCGTGCTCGCTGCGCA-3'	5'-CACGTCGGCGGTGTGGAACGCCATG-3'
OsNAS2‡	5'-GTCCTCATCTCCACCAGCA-3'	5'-GAGGGGTTGAGGTGGAAGAT-3'
OsNAS3‡	5'-GCACCAGAAGATGGAGGACA-3'	5'-TGGTGAGGTAGCAAGCGATG-3'
OsDMAS1‡	5'-TCCAAGGGCAAGACCGTAG-3'	5'-ATCCTCTGCCTCTCCTCCTC-3'
OsNAAT1‡	5'-GATGGCGACTTGGTTGGGT-3'	5'-GCTCCCTGAATGAAAGTTGCT-3'
HvNAATb[5]	5'-AGGATCCATGGCCACCGTACGCCAGAGCGACG-3'	5'-AAAGCTTCTAGCAATCATCGCTCGAATTTCTC-3'
OsYSL15[1]	5'-GAGCTTCGCCATCGACAT-3'	5'-TTGTTCATCTTGTTCCAAGCA-3'
OsIRO2[1]	5'-GAAGGTCTTCACTTCATCAGTTCA-3'	5'-TGATCGTTCCTTCACTTCTCTG-3'
OsIRO3[1]	5'-GCGAGCTGGGTAATATGCTAGA-3'	5'-ATCCGGGTGGTGTCAGTTAG-3'
OsTOM1[2]	5'-CACCAGTTGCAGATCGTATAGGGAGGAA-3'	5'-TCGGAAATCATTGGATTTGCTA-3'
OsIDEF1[3]	5'-ATGGACGACATGGTGCTCC-3'	5'-CTAGGGATTTGTTGTCTGCT-3'
OsIDEF2[4]	5'-CTCGAGTCTAGAATGGCTCAAACTTGCTTGCC-3'	5'-TTAATCTGCATGCTCCCATTCTTC-3'

Primers as reported in: *Shime-Hattori et al. (2011); ‡ Banakar et al (2017); 1. Zheng et al (2010); 2. Jin et al (2014); 3. Kobayashi et al (2012); 4. Ogo et al. (2008); 5. Gómez-Anduro (2011).

8.3.6 Quantification of endogenous gene expression

Quantitative real-time PCR was carried out to measure steady state mRNA levels in leaves of the endogenous genes listed in Table 13. We chose to examine the transcription of genes related to Strategy II Fe acquisition because this strategy involves the secretion of MA siderophores, opposed to Strategy I, which relies upon the excretion of proton and phenolic compounds to increase solubility of ferric ions/Fe (Kobayashi et al., 2012; Selby-Pham et al., 2017). *OsActin1* was used as a reference gene due to its stable expression and reliability as a reference gene (Cheng et al., 2007; Lee et al., 2011).

We used a BioRad CFX96 system with 25-µl reaction mixtures containing 10ng cDNA, 1x iQ SYBR Green Supermix (BioRad, Hercules, CA, USA) and 0.2µM forward and reverse primers (Naqvi et al., 2011; Farré et al., 2013). Relative expression levels were calculated on the basis of serial dilutions of cDNA (125–0.2ng) which were used to generate standard curves for each gene. PCR was carried out in triplicate using 96-well optical reaction plates. The reaction conditions comprised an initial heating step at 95°C for 5min followed by 44 cycles of 95°C for 10s, 60°C for 35s and 72°C for 15s. Specificity was confirmed by product melt curve analysis over the temperature range 50–90°C with fluorescence acquired after every 0.5°C increase, and the fluorescence threshold values and gene expression data were calculated using BioRad CFX96™ software. Values represent the mean of 5 replicates ± SD. Amplification efficiencies were compared by plotting ΔCt values of different primer combinations in serial dilutions against the log of starting template concentrations using CFX96 software.

8.3.7 Statistical analysis

Siderophore, metals, chlorophyll and nitrogen data were processed using a two-way analysis of variance (ANOVA) to quantify the overall effect of the anticipated genotype (G) x treatment (T) interaction and the related effects. Least significant difference was used for mean separation, and an individual error rate of 95% was considered in all tests. JMP software version Pro 11.0.0 was used for all analyses (SAS Institute, Cary, NC, USA), and graphics were created with Apache OpenOffice 4.1.3 in OS X Yosemite 10.10.5.

For qRT-PCR data, differences between RB92 and WT seedlings and the differences among treatments were tested by comparison of means using Student's t-test ($P<0.05$). All genes listed in Table 13 were analyzed but only ones with significant values are reported.

8.4 Results

8.4.1 Chlorophyll contents, metals, nitrogen and dry biomass accumulation

Chlorophyll contents (in SPAD units) were higher (1.6-fold on average) in RB92 leaves than WT leaves for all treatments. This difference was significant in the case of PBS ($p<0.001$), Fe ($p<0.006$), and Sp7+Fe ($p<0.001$) (Figures 39A and 39B).

Significant accumulation of metals was only observed in RB92 leaves of Sp7-inoculated seedlings. Despite Fe-starvation, Fe and Zn levels were 327% and 257% ($p<0.001$) higher compared to WT (Figure 40).

Compared to WT, RB92 leaf nitrogen content (%N) was significantly lower ($p<0.001$) for Fe and Sp7+Fe treatment groups (Figure 41A). When denied Fe supply, there was no significant difference in %N between genotypes. In roots, RB92 always has significantly lower ($p<0.001$) N than WT, regardless of Sp7 inoculation or Fe-supply (Figure 41B).

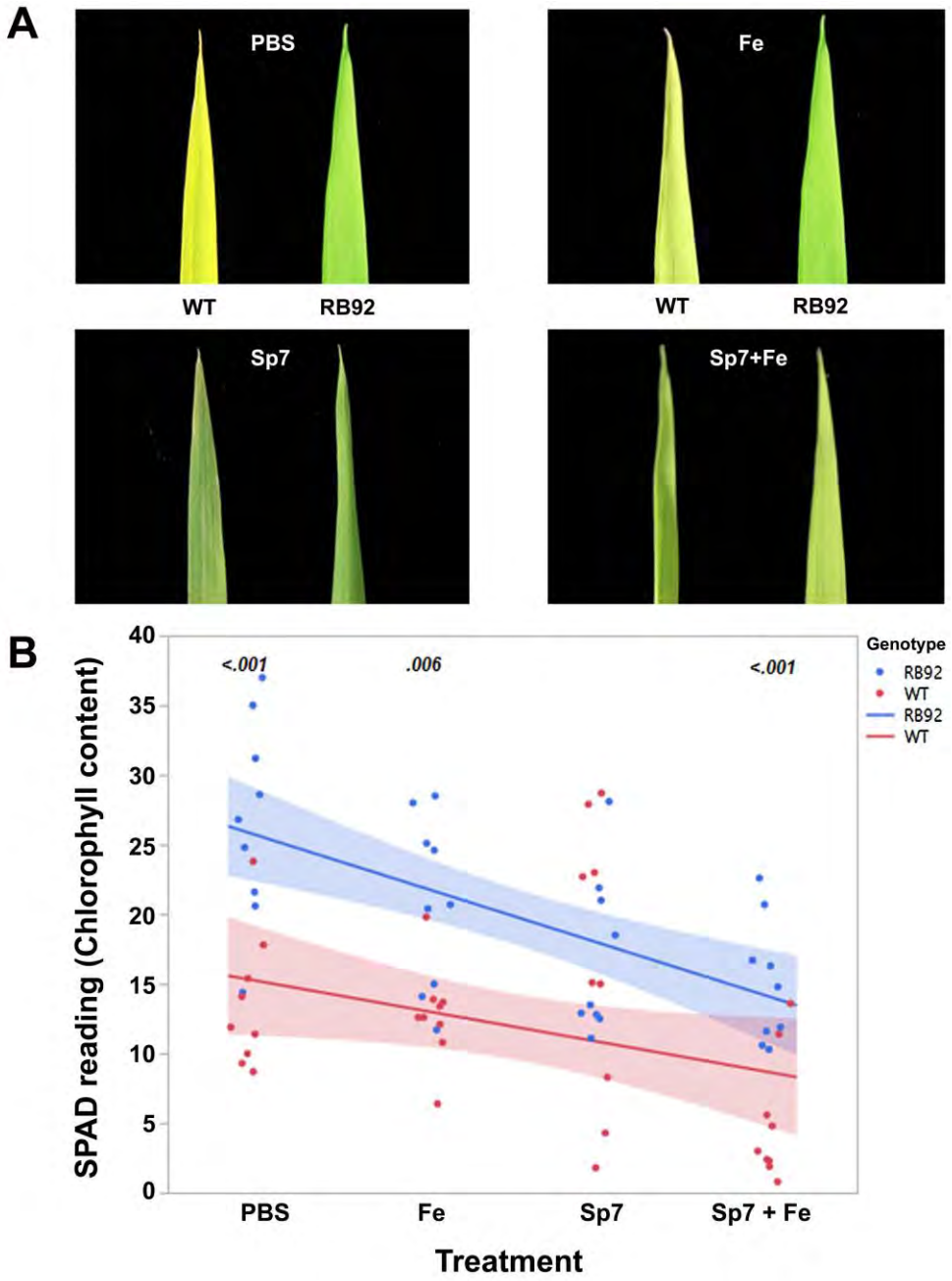

Figure 39. (A) Representative plant phenotypes of wild-type (WT) and Fe-biofortified (RB92) rice seedlings grown with various soil treatments: control (PBS), 100µM $FeCl_3$ (Fe), *Azospirillum brasilense* (Sp7) and Sp7+Fe. (B) Relative SPAD reading of WT and RB92 plants in each treatment group. Least significant means between genotypes for each treatment are indicated with the p-value above data plots.

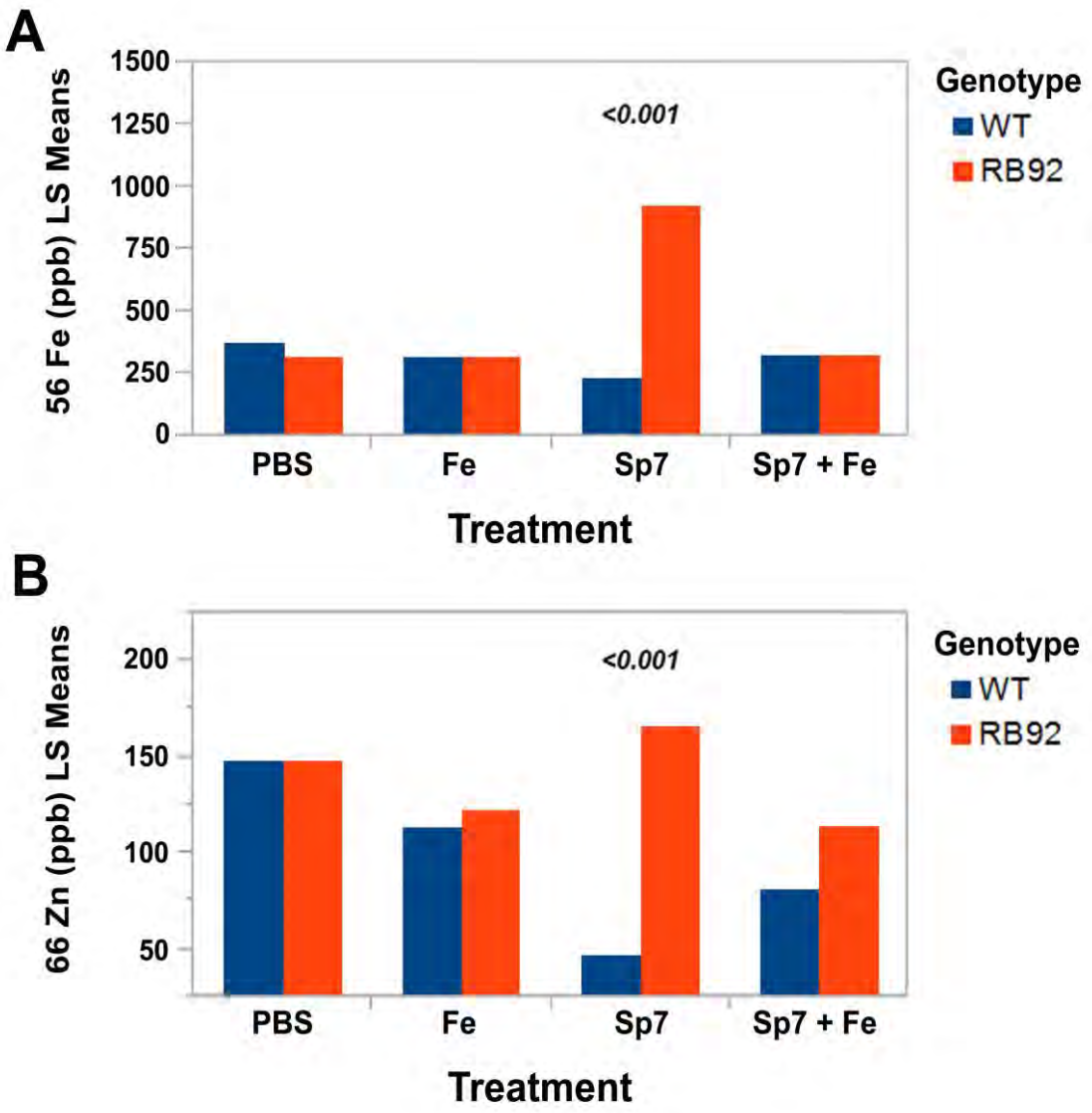

Figure 40. Iron (Fe) and Zinc (Zn) accumulation in roots (A) and leaves (B) of wild-type (WT) and Fe-biofortified (RB92) rice seedlings grown with various soil treatments: control (PBS), 100µM $FeCl_3$ (Fe), *Azospirillum brasilense* (Sp7) and Sp7+Fe. Least significant means between genotypes for each treatment are indicated with the p-value above data plots.

Dry biomass accumulation was always higher in RB92 seedlings in both roots and leaves. The weight of RB92 roots was 40-60% heavier than WT for PBS, Fe and Sp7 treatment groups; while roots treated with Sp7+Fe were 291% heavier than WT. In leaves, RB92 seedlings subjected to Fe-starvation (PBS and Sp7 treatment groups) were 40% heavier than WT, while those supplied with Fe (Fe and Sp7+Fe) were 179% and 291% heavier than WT, respectively (Figure 42).

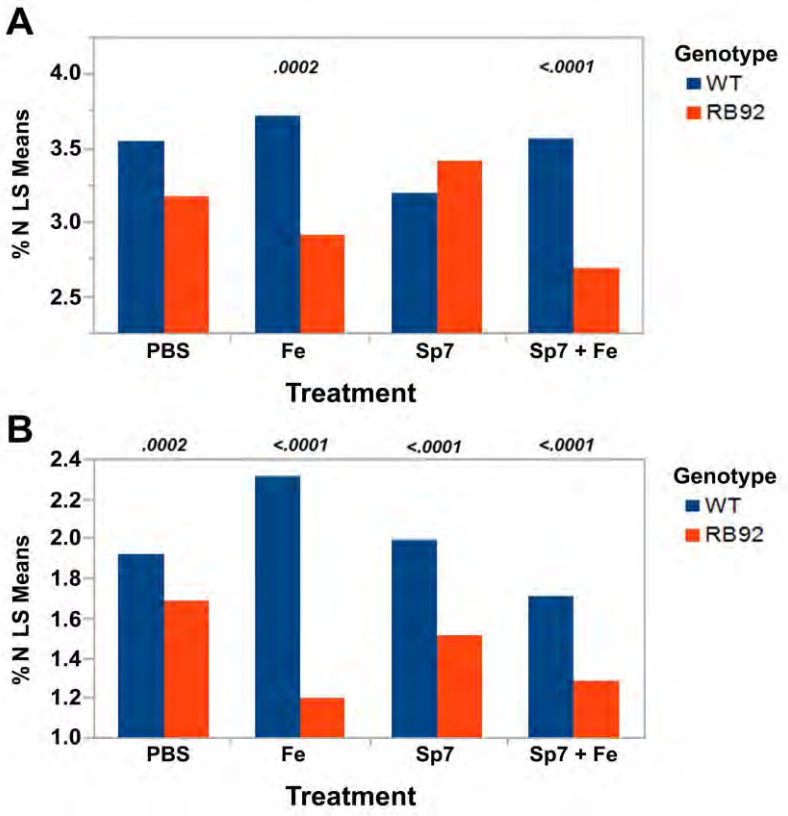

Figure 41. Nitrogen accumulation (%) in roots (A) and leaves (B) of wild-type (WT) and Fe-biofortified (RB92) rice seedlings grown with various soil treatments: control (PBS), 100µM $FeCl_3$ (Fe), *Azospirillum brasilense* (Sp7) and Sp7+Fe. Least significant means between genotypes for each treatment are indicated with the p-value above data plots.

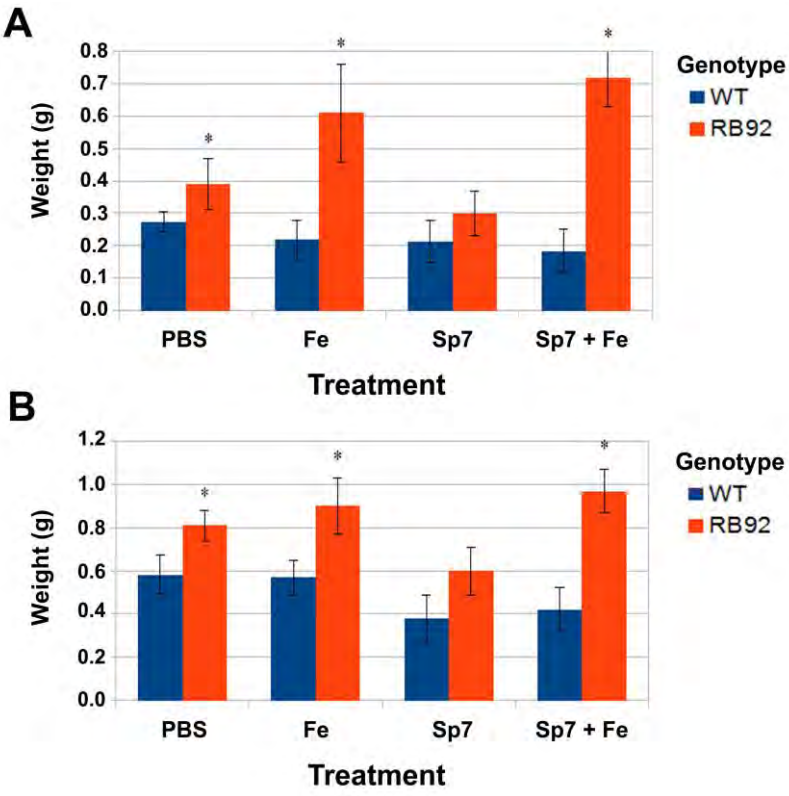

Figure 42. Dry biomass accumulation in roots (A) and leaves (B) grown with various treatments: control (PBS), 100µM $FeCl_3$ (Fe), *Azospirillum brasilense* (Sp7) and Sp7+Fe. Bars represent standard error (n=5), and asterisks (*) represent a significant difference ($p<0.05$) between RB92 and WT plants.

8.4.2 Siderophore levels in roots and leaves

DMA levels in RB92 roots were significantly higher than in WT roots for PBS (6-fold) and Fe (4.5-fold) treatment groups. RB92 roots treated with Sp7 and Sp7+Fe did not exhibit significant differences in DMA levels compared to controls. In leaves, RB92 seedlings fed with Fe and Sp7+Fe had significantly higher NA (24-fold and 20-fold, respectively) and DMA levels (1.3-fold and 2.6-fold, respectively) than WT seedlings (Figure 43). Sp7-inoculated seedlings subjected to Fe-starvation did not have a significant change in siderophore accumulation in neither leaves nor roots.

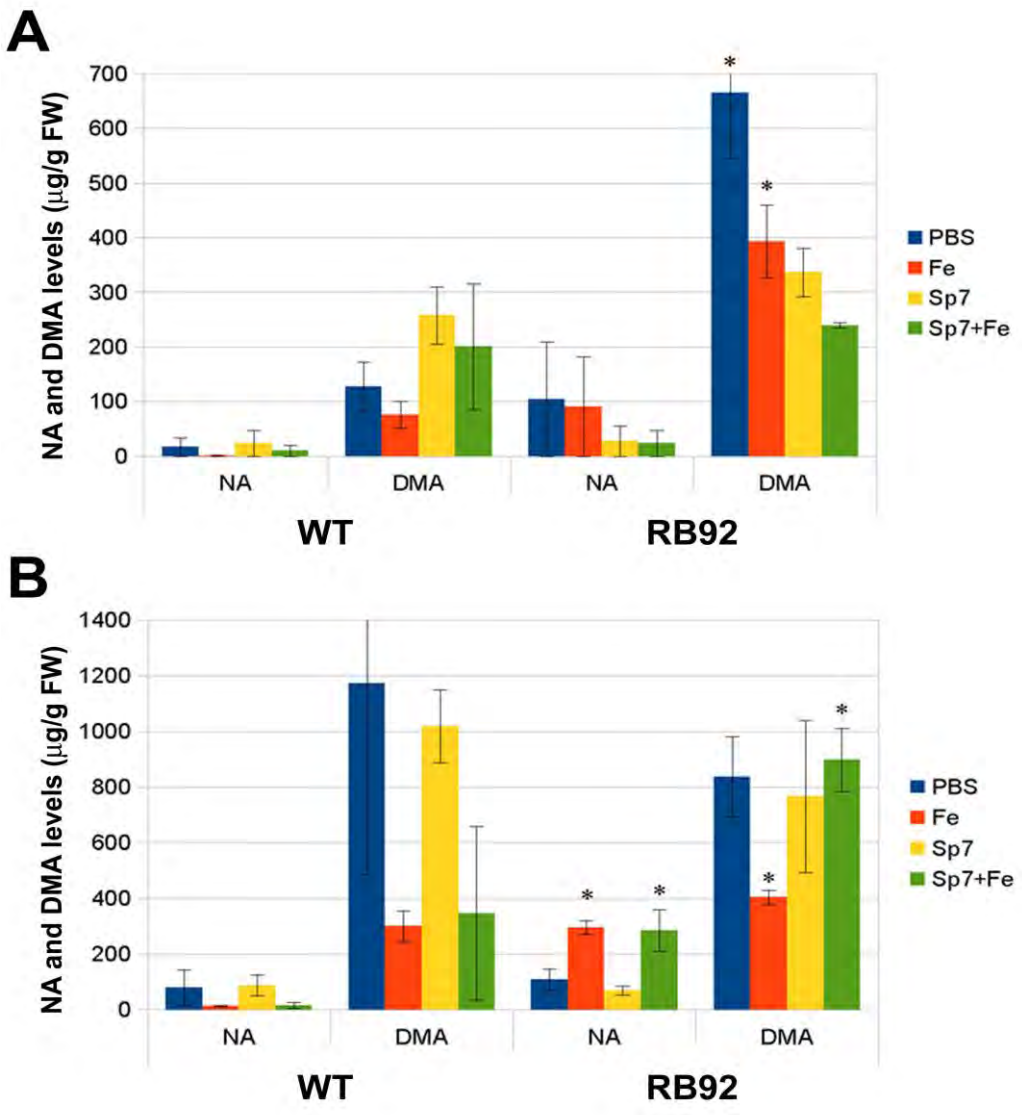

Figure 43. Nicotianamine (NA) and deoxy-2'-mugeinic acid (DMA) accumulation in roots (A) and leaves (B) of wild-type (WT) and Fe-biofortified (RB92) rice seedlings grown with various soil treatments: control (PBS), 100µM $FeCl_3$ (Fe), *Azospirillum brasilense* (Sp7) and Sp7+Fe. NA and DMA concentrations are expressed as µg/g FW. Asterisks (*) represent a significant difference ($p<0.05$) between RB92 and WT plants.

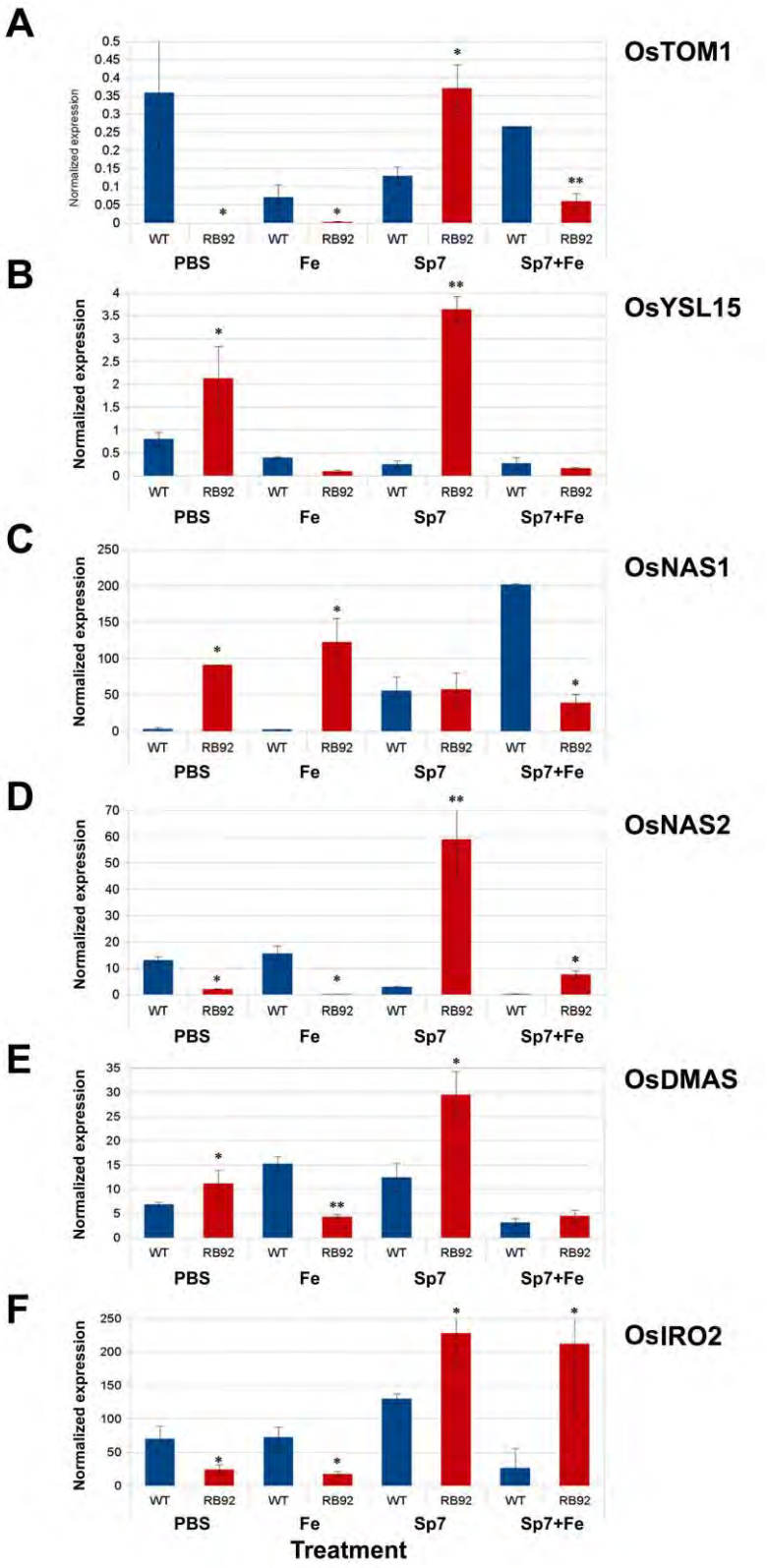

Figure 44. Quantitative real-time (qRT)-PCR analysis of endogenous Fe-homeostasis genes in wild-type (WT) and Fe-biofortified (RB92) rice seedlings grown with various soil treatments: control (PBS), 100µM $FeCl_3$ (Fe), *Azospirillum brasilense* (Sp7) and Sp7+Fe. (A) OsTOM1, Transporter Of Mugineic acids 1; (B) OsYSL15, Yellow Stripe-Like 15; (C) OsNAS1, Nicotianamine 1; (D) OsNAS2, Nicotianamine 2; (E) OsDMAS1, 2'-deoxymugineic acid synthase; (F) OsIRO2. Bars represent standard error (n=5), and * represents a significant difference ($p<0.05$) between RB92 and WT plants.

8.4.3 Gene expression

OsTOM1 was significantly lower in RB92 seedlings lacking Sp7, compared to WT ($p<0.05$) (35-fold lower for PBS and 5-fold lower for Fe). In Sp7-inoculated (Fe-starved) seedling leaves, *OsTOM1* expressed 3-fold higher in RB92 compared to WT ($p<0.05$), but 4-fold lower in Fe+Sp7 RB92 (Figure 44A).

OsYSL15 over-expressed in all RB92 seedling leaves subjected to Fe-starvation (2.75-fold for PBS and 14-fold for Sp7). Additionally, there was a significant increase between means for the two treatment groups, PBS being lower than Sp7 (Figure 44B).

OsNAS1 over-expressed in RB92 seedling leaves ($p<0.05$) when Sp7 was not present. That is, *OsNAS1* expressed 95-fold higher in PBS RB92 compared to PBS WT, and 125-fold higher in Fe RB92 compared to Fe WT (Figure 44C). *OsNAS2,* on the other hand, over-expressed in RB92 seedling leaves ($p<0.05$) only when Sp7 was present, regardless of feeding regime; it expressed 20-fold higher in Sp7 RB92 compared to Sp7 WT, and 8-fold higher in Sp7+Fe RB92 (Figure 44D).

OsDMAS1 over-expressed in all RB92 seedlings subjected to Fe-starvation (1.8-fold increase in PBS and 2.32-fold increase in Sp7), compared to their respective WT. *OsDMAS1* under-expressed in Fe RB92 (3-fold decrease) compared to WT (Figure 44E).

Finally, *OsIRO2* over-expressed in RB92 whenever Sp7 was present, regardless of Fe supply (1.25-fold increase for Sp7 and 8-fold increase for Sp7+Fe); and under-expressed in RB92 in the absence of Sp7 (a 2.5-fold decrease for PBS and 3.75-fold decrease for Fe) (Figure 44F).

8.5 Discussion

Iron biofortification of rice plants is critical for improving human health in parts of the world where rice is the staple crop (Slamet-Loedin et al., 2015). Great lengths have been taken to improve the nutritional value and Fe contents of rice grains, while comparatively less attention has been given to understanding how these nutritionally superior plants assimilate abiotic or biotic stress. Knowing how Fe biofortified plants behave under stress will facilitate the design of more specialized and sustainable crop management programs.

Within this context, the study of plant growth-promoting rhizobacteria (PGPR) is appealing because PGPR can counterbalance plant stress *and* biofortify edible plant parts (Garg et al., 2018). Considering the roles of PGPR, we designed our study to test the efficacy of the PGPR *Azospirillum brasilense* Sp7 on plant Fe homeostasis. To do so, we inoculated wild type (WT) and transgenically Fe-biofortified (RB92) rice seedlings, then grew plants in Fe-sufficient and Fe-deficient soil conditions. We found that in Fe-deficient soil conditions, RB92 roots accumulated significant amounts of DMA and increased gene activity related to NA/DMA uptake, transport and synthesis. Transcriptional regulators and efflux transporters decreased in

activity. Since these regulators and transporters usually up-regulate in response to Fe deficiency, their decrease indicated that RB92 seedlings are less susceptible to Fe deficiency than WT plants. Previous studies have also shown that plants with lower susceptibility to Fe deficiency over-expressed NAS genes and had higher levels of accumulated Fe (Wang et al., 2013; Nozoye et al., 2014b). Comparatively, RB92 plants did not need to accumulate higher levels of Fe or Zn to be less susceptible to Fe deficiency.

The roots of RB92 seedlings accumulated more DMA than WT regardless of Fe deficiency, and Sp7 inoculation attenuated this effect. Fe-deficient conditions typically induce the over-expression of MA biosynthesis genes and increased accumulation of DMA in roots (Selby-Pham et al., 2017). Increased NA production feeds DMA biosynthesis, rather than NA accumulation, and increased DMA is likely utilized for the altered chelation of Fe in the roots of Fe-deficient rice (Selby-Pham et al., 2017). Our finding that Sp7 inoculation correlated with lowered DMA accumulation in RB92 regardless of Fe supply provides evidence that Sp7 exerts influence over root-bound MA homeostasis. It is known that Sp7 produces siderophores and has positive effects on plant redox homeostasis and growth. Soon after inoculation, Sp7 solubilizes Fe in the rhizosphere, making it more available to plants because bacterial siderophores also act as signal molecules or regulators of the microbe-plant interaction (Scavino and Pedraza 2013). We have shown that the signaling between plant and microbes is two-way, and susceptible to change depending upon the plant's siderophore status.

In the absence of Sp7, *OsNAS1* expression was significantly higher in RB92 seedlings (coinciding directly with root DMA accumulation). Transcriptional changes included compensatory-like expression patterns between *OsNAS1* and *OsNAS2*, with differences being more pronounced in RB92 seedlings. These results were in contrast to a comprehensive study by Inoue et al., (2003) which analyzed the three *OsNAS* gene homologues in rice and found *OsNAS1* and *OsNAS2* to be very similar. They found that both genes were differentially regulated by Fe and typically expressed in cells involved in its long-distance transport, in Fe sufficient roots, and in leaves and roots of Fe-deficient seedlings. *OsNAS1* always expressed slightly stronger than *OsNAS2* in leaves, but they were mostly homologous otherwise. In our study, *OsNAS2* expression increased in RB92 Sp7 leaves, though there was not a significant increase in NA or DMA accumulation, countering previous reports finding that the disturbance of Fe homeostasis in plants over-expressing *OsNAS2* might be related to the overproduction of DMA and NA, which increases the chelating capacity of Fe and disrupts an unknown Fe-sensing mechanism (Nozoye et al., 2014a). Our results offer evidence that over-expression of *OsNAS2* is indeed related to altered Fe homeostasis, though there is no evidence that it is the gene responsible for ubiquitous MA accumulation. When *OsNAS2* over-expressed, *OsNAS1* expression consistently decreased, so this may be a way in which the seedling maintains MA equilibrium via compensatory regulation towards Fe homeostasis.

In our experiment, *OsIRO2*, *OsTOM1* and *OsNAS2* had similar expression patterns in RB92 seedlings. These three genes all possess sequences homologous to the Fe-deficiency responsive *cis-acting elements* IDE1 and IDE2 in their promoter regions at a higher rate than genes whose expression is not affected by Fe deficiency (Kobayashi et al., 2003). Rice genes involved in Fe acquisition are coordinately regulated by conserved mechanisms in response to Fe deficiency, and IDE-mediated regulation plays a significant role (Kobayashi et al., 2005). *OsNAS2* and *OsTOM1* contain IDE1 (GATGC) *and* IDE2 (CA(A/C)G(T/C)(T/C/A)(T/C/A) elements in their 1.5 kb promoter regions, with an induction ratio greater than 2.0 in Fe-deficient roots (Kobayashi et al., 2005; Nozoye et al., 2015). *OsIRO2* only has IDE1 elements, while *OsNAS1* and *OsDMAS1* only contain IDE2 elements (Kobayashi et al., 2005). IDE elements are typically identified by IDEF1 and IDEF2, TFs from the ABI3/VP1 and NAC TF families, respectively, that bind to them and regulate the response to Fe deficiency (Durrett et al., 2007; Duy et al., 2007; Kobayashi et al., 2009). Expression levels of these TFs and the genes they regulate are typically analogous; for example, IDEF1 over-expression causes up-regulation of *OsIRO2* (though IDEF1 expression itself is not regulated by Fe) (Lemanceau 2009). When we tested the expression of IDEF1 in our study, however, expression was below detection levels despite *OsIRO2* up-regulation. *OsIRO2* is a Fe deficiency-inducible bHLH TF regulating the Fe-deficiency response in graminaceous plants (Goto et al., 1999; Ogo et al., 2006). Over-expression of *OsIRO2* has been suggested to increase the availability of Fe in plants, cooperating with root-specific or leaf-specific TFs to promote gene expression in a tissue-specific manner under Fe-deficient conditions (Ogo et al., 2007). Although *OsIRO2* interacts with the IDEF1 TF under certain conditions, this is not the case for RB92; implying that there is an alternative mechanism responsible for the regulation of *OsIRO2* and other *IDE*-containing genes.

In RB92 seedlings, *OsIRO2* expression increased with Sp7 inoculation, regardless of exogenous Fe supply. The mode of action of *OsIRO2* has been likened to that of some gene promoters where stress-responsive and site-specific regulatory regions occur separately, indicating that different TFs bind to these regions (Elliott and Shirsat, 1998; Ogo et al., 2007). In addition to possessing IDE, *OsIRO2* has a G-box core binding sequence (CACGTGG), which is often present among Fe deficiency-inducible gene promoters in rice (Ogo et al., 2006, 2008). The G-box element is involved in response to abscisic acid, methyl-jasmonate, anaerobiosis, PR genes and ethylene induction (Yoshihara et al., 1996; Siberil et al., 2001; Kaur et al., 2017). Notably, there is crossover in what may constitute G-box activation with protein products that are typically up-regulated by Sp7-induced ISR, such as plant hormones, including ethylene (Vacheron et al., 2015; Elias et al., 2018). Conversely, the promoters of the ISR-primed genes are significantly enriched for a *cis-acting* G-box-like (AACGTG) motif, such as MYC2, which functions as a key transcriptional regulator of JA-dependent defenses (Memelink 2009; Fukami

et al., 2018). The lack of interaction between *OsIRO2* and IDEF1 in RB92 seedlings and the ubiquitous up-regulation of *OsIRO2* in the presence of Sp7 inoculation, thereby provide evidence that the *OsIRO2* G-box motif is bound by protein products of the ISR response induced by Sp7 (Kosová et al. 2011; Lade et al., 2018), leading to its up-regulation in the absence of IDEF1 expression. If true, this hypothesis would define the molecular basis for why plants benefit from PGPR siderophore production by activating ISR (Iavicoli et al., 2003; Bakker et al., 2007; Zamioudis et al., 2015). Sp7 is known to have genotype-specific interaction (Correa et al., 2007), providing explanation for our finding that *OsIRO2* was up-regulated in RB92 seedlings, but not in WT under the same conditions. In fact, transcriptome profiling of the bacterial strain- rice genotype interactions revealed that around 83% of the differentially expressed genes are combination-specific. Since most of the differentially expressed genes are involved in primary metabolism, transport, regulation of transcription and protein fate, individual genotypic variations could be the most important driving force of rice gene expression upon *Azospirillum* spp. inoculation (Drogue et al., 2014).

The expression levels of *OsIRO2* increased while *OsNAS1* decreased in RB92 seedlings regardless of treatment group. All other genes related to the Fe-deficiency response up-regulated like *OsIRO2*. Typically, *OsIRO2* positively regulates genes related with the Strategy II Fe-deficiency response because it is widely conserved among graminaceous plants (Ogo et al., 2006, 2007, 2011). The current proposed model for the role of *OsIRO2* in the Fe gene regulation network is that it dictates regulation of all down-stream genes, while genes containing the binding sequence (G-box) in their promoter regions are completely dependent upon its expression (Ogo et al., 2007). *OsNAS1* is one of these genes (Higuchi et al., 2001), and since it has both IDE2 elements and a G-box, it has been linked to the expression of some Fe deficiency inducible TFs, which might also be involved in the indirect regulation of *OsIRO2* downstream genes (Ogo et al., 2007). *OsNAS1* fails to express completely in Fe-sufficient leaves, and its expression is directly related to the degree of leaf chlorosis in Fe deficient plants (Higuchi et al., 2001). The leaves of Sp7 RB92 seedlings did not suffer Fe deficiency symptoms, based on mineral accumulation and SPAD results. Therefore, we highlight a dissonance between the expression of *OsNAS1* and other homeostasis genes, based on the actual Fe status of the plant leaves. *OsNAS1* expression has repeatedly been shown to be intertwined with Fe status of plant leaves: as in the simultaneous over-expression of *OsNAS1* and increased NA which were implied in increasing metals accumulation in plant shoots (Takahashi et al., 2003; Douchkov et al., 2005; Kim et al., 2005), or how NAS was up-regulated by synthetic siderophores treatment to increase Fe uptake (Dellagi et al., 2005; Aznar et al., 2014).

The significant accumulation of metals in Sp7 RB92 leaf tissues occurred despite Fe-deficient soil conditions, and coincided with the specific over-expression of *OsTOM1*. *OsNAS2* also over-expressed in these seedlings, indicating a synergism between the two genes. These

two genes exhibited similar (albeit down-regulated) expression patterns in Fe-deficient WT seedlings inoculated with Sp7 as well. Previous studies have reported that Fe deficiency typically increases expression of *OsNAS2* with *OsTOM1* (Kobayashi et al., 2012), as we observed in RB92 seedlings. The decreased expression of these genes in Fe-deficient Sp7 WT seedlings is therefore paradoxical, but may be due to the interaction between Sp7 and the genotype. Previous work has documented the coordination of *OsNAS2* with *OsTOM1* in their similar diurnal expression patterns (Curie and Briat 2003), while both possess IDE elements 1 and 2, which exhibit synergism with each other (Kobayashi et al., 2003). The Transporter of MAs (TOM) gene family plays important roles in the maintenance of metal homeostasis through the secretion of DMA into the soil, and in the translocation of metals to sink areas in plants. It has even been suggested that the TOM family is involved in NA-mediated metal translocation (Nozoye et al. 2015). Altered expression of *OsTOM1* in transgenic rice has been highly correlated withPS secretion from the roots, and over-expression resulted in increased tolerance to Fe deficiency (Nozoye et al. 2015). Under Fe-deficient conditions, *TOM1* expression was observed in the whole root cell and in leaves, with expression patterns similar to those of genes involved in DMA biosynthesis (Dinneny et al., 2008; Higuchi et al., 1999; Ishimaru et al., 2010). Therefore, *TOM1* is involved in DMA secretion from the root, efflux of DMA to the phloem and xylem for internal Fe transport, as well as translocation inside the plant (Dinneny et al., 2008; Ishimaru et al., 2006; Kobayashi et al., 2012). The interaction between *OsNAS2, OsTOM1* and *OsIRO2* in Sp7 RB92 seedlings led to synergistically up-regulated translocation of Fe to plant leaves.

Previous studies have shown that in Fe deficient soil, plant N contents and PS accumulation are directly related to effectively mobilize absorbed Fe (Ali et al., 2015). In the same way, increasing soil N supply enhances Fe mobilization in Fe-deficient plants by inducing the release of root PS (Aciksoz et al., 2011). In our study, WT seedlings employed this dynamic, but in RB92 seedlings, N was indirectly related with PS accumulation in both roots and leaves. Specifically, RB92 leaf N contents dropped significantly lower than their WT counterparts in function of Fe-supply, regardless of Sp7 inoculation. Fe is a key cofactor in the *A. brasilense* nitrogenase enzyme that helps the plant assimilate atmospheric nitrogen (Pedraza 2015), which is why Fe and N activity is usually directly related in *A. brasilense*-inoculated plants. However, in RB92 seedlings supplied with sufficient soil Fe, Sp7 activity did not affect N accumulation. Instead, seedlings had significantly increased levels of DMA, which is well-known for its role in reinforcing nitrate assimilation, in addition to chelating Fe (Araki et al., 2015). *Azospirillum* spp. has been shown to counteract the plant response to nitrate induction without compromising plant N nutrition (Pii et al., 2019). Therefore, the over-expression of DMA may be the plants' compensation for any negative influence that Sp7 has on innate nitrate induction in the plant.

8.6 Conclusions

This study intended to explain how plant genes and siderophore production adjusts to Fe-deficiency, using the PGPR *Azospirillum brasilense* Sp7 and a transgenically biofortified rice to elicit plant mechanisms attenuating Fe deficiency-induced stress. What we found was that Sp7 interacted with the already biofortified RB92 plant line to increase metal accumulation in seedling leaf tissue. We also unravelled as yet unknown elements explaining how plant genes adjust to the Fe-deficiency response based on genotype. The Fe deficiency responses elucidated how Sp7 inoculation and the ISR response may interact with Fe homeostasis gene expression. Sp7 exerted influence over root-bound MA homeostasis, which also may be responsible for modulating Fe-homeostasis gene expression. Our findings emphasize that further study of *cis/trans* interactions will contribute greatly to the understanding of the network regulating plant responses to Fe deficiency. Overall, this work shows how gene expression is affected by Sp7 in Fe-deficient rice, drawing attention to how the simultaneous use of two biofortification strategies work together to positively effect plants under stress.

8.7 References

Aciksoz SB, Ozturk L, Gokmen OO, Römheld V, Cakmak I (2011) Effect of nitrogen on root release of phytosiderophores and root uptake of Fe(III)-phytosiderophore in Fe-deficient wheat plants. *Physiologia Plantarum* 142:287-296.

Ali NS, Hassan WF, Janno FO (2015) Soil iron and nitrogen availability and their uptake by maize plants as related to mineral and bio nitrogen fertilizers application. *Agriculture and Biology Journal of North America* 6 (5):118-122.

Andrews SC (1998) Iron storage in bacteria. *Advances in Microbial Physiology* 40:281-351.

Araki R, Namba K, Murata Y, Murata J (2015) Phytosiderophores revisited: 2'-deoxymugineic acid-mediated iron uptake triggers nitrogen assimilation in rice (*Oryza sativa*) seedlings. *Plant Signaling & Behavior* 10:6, e1031940.

Arcanjo FPN, Santos PR, Arcanjo CPC (2013) Daiky and weekly iron supplementation are effective in increasing hemoglobin and reducing anemia in infants*, Journal of Tropical Pediatry* 59:175.179.

Aung MS, Masuda H, Kobayashi T, Nakanishi H, Yamakawa T, Nishizawa NK (2013) Iron biofortification of myanmar rice. *Frontiers in Plant Science* 4:158.

Aznar A, Chen NW, Rigault M, Riache N, Joseph D, Desmaele D, Mouille G, Boutet S, Soubigou-Taconnat L, Renou JP, Thomine S, Expert D, Dellagi A (2014) Scavenging iron: a novel mechanism of plant immunity activation by microbial siderophores. *Plant Physiology* 164 (4):2167–83.

Bachhawat AK, Ghosh S (1987a) Isolation and characterisation of the outer membrane proteins of *Azospirillum brasilense*. *Journal of General Microbiology* 133:1751-1758.

Bachhawat AK, Ghosh S (1987b) Iron transport in *Azospirillum brasilense*: role of the siderophore, spirilobactin. *Journal of General Microbiology* 133:1759-1765.

Bachhawat AK, Ghosh S (1989) Temperature inhibition of Siderophore production in *Azospirillum brasilense. Journal of Bacteriology* 171 (7):4092-4094.

Bakker PA, Pieterse CM, van Loon LC (2007) Induced systemic resistance by fluorescent *Pseudomonas* spp. *Phytopathology* 97 (2):239–43.

Banakar R (2016) *'Mechanisms controlling the selective iron and zinc biofortification of rice*', PhD thesis, University of Lleida, Lleida Spain.

Banakar R, Fernández AA, Abadía J, Capell T, Christou P (2017) The expression of heterologous Fe (III) phytosiderophore transporter HvYS1 in rice increases Fe uptake, translocation and seed loading and excludes heavy metals by selective Fe transport. *Plant Biotechnology Journal* 15(4):423-432.

Bashan Y (1986) Significance of timing and level of inoculation with rhizosphere bacteria on wheat plants. *Soil Biology and Biochemistry* 18:297-301.

Bashan Y, Holguin G, De-Bashan LE (2004) *Azospirillum*-plant relationships: physiological, molecular, agricultural, and environmental advances (1997-2003). *Canadian Journal of Microbiology* 50:521-577.

Bashan Y, Holguin G, Lifshitz R (1993) Isolation and characterization of plant growth-promoting rhizobacteria. In: B.R. Glick (ed.) *Methods in Plant Molecular Biology and Biotechnology* (Boca Raton, FL: CRC Press), pp 331–345.

Bashir K, Inoue H, Nagasaka S, Takahashi M, Nakanishi H, Mori S, Nishizawa NK (2006) Cloning and characterization of deoxymugineic acid synthase genes from graminaceous plants. *Journal of Biological Chemistry* 281:32395-402.

Becker M, Asch F (2005) Iron Toxicity in Rice—Conditions and Management Concepts. *Journal of Plant Nutrition and Soil Science* 168:558-573.

Botta LA, Santacecilia A, Ercole C, Cacchio P, del Gallo M (2013) In vitro and in vivo inoculation of four endophytic bacteria on *Lycopersicon esculentum*. *Natural Biotechnology* 30 (6):666–674.

Cassán F, Perrig D, Sgroy V, Masciarelli O, Penna C, Luna V (2009) *Azospirillum brasilense* Az39 and *Bradyrhizobium japonicum* E109, inoculated singly or in combination, promote seed germination and early seedling growth in corn (*Zea mays* L.) and soybean (*Glycine max* L). *European Journal of Soil Biology* 45:28–35.

Cheng L, Wang F, Shou H, Huang F, Zheng L, He F, Li J, Zhao F, Ueno D, Ma J, Wu P (2007) Mutation in nicotianamine aminotransferase stimulated the Fe (II) acquisition system and led to iron accumulation in rice. *Plant Physiology* 145:1647–1657.

Cline GR, Reid CPP, Szaniszlo PJ (1984) Effects of a hydroxamate siderophore on iron absorption by sunflower and sorghum. *Plant Physiology* 76:36-39.

Connolly EL, Guerinot M (2002) Iron stress in plants. *Genome Biology* 3(8):1024.1-1024.4.

Cornelis P, Matthijs. S (2002) Diversity of siderophore-mediated iron uptake systems in fluorescent pseudomonads: Not only pyoverdines. *Environmental Microbiology* 4:787.

Correa OS, Romero AM, Montecchia MS, Soria MA (2007) Tomato genotype and *Azospirillum* inoculation modulate the changes in bacterial communities associated with roots and leaves. *Journal of Applied Microbiology* 102:781–786.

Curie C, Briat JF (2003) Iron transport and signaling in plants. *Annual Review of Plant Biology* 54:183-206.

Curie C, Panaviene Z, Loulergue C, Dellaporta SL, Briat J-F, Walker EL (2001) Maize yellow stripe1 encodes a membrane protein directly involved in Fe(III) uptake. *Nature* 409:346-9.

Dave BP, Dube HC (2000) Regulation of siderophore production by iron Fe (III) in certain fungi and fluorescent *Pseudomonas*. *Indian Journal of Experimental Biology* 38:297–299.

Dellagi A, Rigault M, Segond D, Roux C, Kraepiel Y, Cellier F, Briat JF, Gaymard F, Expert D. (2005) Siderophore mediated up-regulation of *Arabidopsis* ferritin expression in response to *Erwinia chrysanthemi* infection. *The Plant Journal*. 43 (2):262–72.

Dinneny JR, Long TA, Wang JY, Jung JW, Mace D, Pointer S, Barron C, Brady SM, Schiefelbein J, Benfey PN (2008) Cell identity mediates the response of *Arabidopsis* roots to abiotic stress. *Science* 320:942–5.

Döbereiner J, Marriel IE, Nery M (1976). Ecological distribution of *Spirillum lipoferum* Beijerinck. *Canadian Journal of Microbiology* 22 (10):1464-1473.

Douchkov D, Gryczka C, Stephan UW, Hell R, Baumlein H (2005) Ectopic expression of nicotianamine synthase genes results in improved iron accumulation and increased nickel tolerance in transgenic tobacco. *Plant Cell and Environment* 28:365–374.

Drogue B, Sanguin H, Chamam A, Mozar M, Llauro C, Panaud O, Prigent-Combaret C, Picault N, Wisniewski-Dyé F (2014) Plant root transcriptome profiling reveals a strain-dependent response during *Azospirillum*-rice cooperation. *Frontiers in Plant Science* 5(607):1-14.

Durrett TP, Gassmann W, Rogers EE (2007) The FRD3-mediated efflux of citrate into the root vasculature is necessary for efficient iron translocation. *Plant Physiology* 144:197–205.

Duy D, Wanner G, Meda AR, von Wirén N, Soll J, Philippar K (2007) PIC1, an ancient permease in *Arabidopsis* chloroplasts, mediates iron transport. *Plant Cell* 19: 986–1006.

El Zemrany H, Cortet J, Lutz, MP, Chabert A, Baudoin E, Haurat J, Maughan N, Felix D, Defago G, Bally R, Moenne-Loccoz Y (2006) Field survival of the phytostimulator *Azospirillum lipoferum* CRT1 and functional impact on maize crop, biodegradation of crop residues, and soil faunal indicators in a context of decreasing nitrogen fertilisation. *Soil Biology and Biochemistry* 38:1712–1726.

Elias JM, Guerrero-Molina MF, Martínez-Zamora MG, Díaz-Ricci JC, Pedraza RO (2018) Role of ethylene and related gene expression in the interaction between strawberry plants and the plant growth-promoting bacterium *Azospirillum brasilense*. *Plant Biology* 20:490–496.

Ellerman M, Arthur JC (2017) Siderophore-mediated iron acquisition and modulation of host-bacterial interactions. *Free Radical Biology and Medicine* 105:68-78.

Elliott KA, Shirsat AH (1998) Promoter regions of the extA extensin gene from *Brassica napus* control activation in response to wounding and tensile stress. *Plant Molecular Biology* 37:675–687.

Farré G, Rivera SM, Alves R, Vilaprinyo E, Sorribas A, Canela R, Naqvi S, Sandmann G, Capell T, Zhu, C, Christou P (2013) Targeted transcriptomics and metabolic profiling reveals temporal bottlenecks in the maize carotenoid pathway that can be addressed by multigene engineering. *The Plant Journal* 75:441–455.

Fernández-Scavino A, Pedraza RO (2013) The role of siderophores in plant-growth promoting bacteria. In: *Bacteria in Agrobiology: Crop Productivity*. Maheshwari DK, Saraf M, Aeron A (eds) Springer, Heidelberg, pp 265-285.

Fukami J, Cerezini P, Hungria M (2018) *Azospirillum*: benefits that go far beyond biological nitrogen fixation. *AMB Express* 8 (73):1-12.

Garg M, Sharma N, Sharma S, Kapoor P, Kumar A, Chunduri V, Arora P (2018) Biofortified crops generated by breeding, agronomy and transgenic approaches are improving lives of millions of people around the world. *Frontiers in Nutrition* 5:12.

Glick BR (2012) Plant growth-promoting bacteria: mechanisms and applications. *Scientifica* 2012: 963401.

Gómez-Anduro G, Ceniceros-Ojeda EA, Casados-Vázquez LE, Bencivenni C, Sierra-Beltrán A, Murillo-Amador B, Tiessen A (2011) Genome-wide analysis of the beta-glucosidase gene family in maize (*Zea* mays L. var B73). *Plant Molecular Biology* 77:159-183.

Goto F, Yoshihara T, Shigemoto N, Toki S, Takaiwa F (1999) Iron fortification of rice seed by the soybean ferritin gene. *Natural Biotechnology* 17:282–86.

Hell R, Stephan UW (2002) Iron uptake, trafficking and homeostasis in plants. *Planta* 216:541-551.

Higuchi K, Suzuki K, Nakanishi H, Yamaguchi H, Nishizawa NK, Mori S (1999) Cloning of nicotianamine synthase genes, novel genes involved in the biosynthesis of phytosiderophores. *Plant Physiology* 119:471-80.

Higuchi K, Watanabe S, Takahashi M, Kawasaki S, Nakanishi H, Nishizawa N K, Mori S (2001) Nicotianamine synthase gene expression differs in barley and rice under Fe-deficient conditions. *The Plant Journal* 25:159–167.

Iavicoli A, Boutet E, Buchala A, Metraux JP (2003) Induced systemic resistance in *Arabidopsis thaliana* in response to root inoculation with *Pseudomonas fluorescens* CHA0. *Molecular Plant-Microbe Interactions* 16 (10):851–858.

Inoue H, Higuchi K, Takahashi M, Nakanishi H, Mori S, Nishizawa NK (2003) Three rice nicotianamine synthase genes, *OsNAS1, OsNAS2,* and *OsNAS3* are expressed in cells involved in long-distance transport of iron and differentially regulated by iron. *The Plant Journal* 36:366-381.

Inoue H, Kobayashi T, Nozoye T, Takahashi M, Kakei Y, Suzuki K, Nakazono M, Nakanishi H, Mori S, Nishizawa NK (2009) Rice OsYSL15 is an iron-regulated iron(III)-deoxymugineic acid transporter expressed in the roots and is essential for iron uptake in early growth of the seedlings. *Journal of Biological Chemistry* 284:3470-9.

Ishimaru Y, Suzuki M, Tsukamoto T, Suzuki K, Nakazono M, Kobayashi T, Wada Y, Watanabe S, Matsuhashi S, Takahashi M, Nakanishi H, Mori S, Nishizawa NK. (2006) Rice plants take up iron as an $Fe3^{+}$-phytosiderophore and as $Fe2^{+}$. *The Plant Journal* 45 (3):335–346.

Ishimaru Y, Masuda H, Bashir K, Inoue H, Tsukamoto T, Takahashi M, Nakanishi H, Aoki N, Hirose T, Ohsugi R, Nishizawa NK (2010) Rice metal-nicotianamine transporter, OsYSL2, is required for the long-distance transport of iron and manganese. *Plant Journal* 62:379–390.

Jeong J, Guerinot ML (2009) Homing in on iron homeostasis in plants. *Trends in Plant Science* 14:280–85.

Jin CW, Ye YQ, Zheng SJ (2014) An underground tale: contribution of microbial activity to plant iron acquisition via ecological processes. *Annals of Botany* 113:7-18.

Kamnev AA, Tugarova AV, Antonyuk LP, Tarantilis PA, Polissiou MG, Gardiner PHE (2005) Effects of heavy metals on plant-associated rhizobacteria: Comparison of endophytic and non-endophytic strains of *Azospirillum brasilense*. *Journal of Trace Elements in Medicine and Biology* 19:91-95.

Kamnev AA, Tugarova AV, Tarantilis PA, Gardiner PHE, Polissiou MG (2012) Comparing poly-3-hydroxybutyrate accumulation in *Azospirillum brasilense* strains Sp7 and Sp245: the effects of copper(II). *Applied Soil Ecology* 61:213–216.

Kaur A, Pati PK, Pati AM, Nagpal AK (2017) *In-silico* analysis of cis-acting regulatory elements of pathogenesis-related proteins of *Arabidopsis thaliana* and *Oryza sativa. PLOS ONE.* 12 (9):e0184523.

Khan A, Singh J, Upadhayay VK, Singh AV, Shah S (2019) Chapter 13: Microbial biofortification: a green technology through plant growth-promoting microorganisms. In: Shah S et al. (eds.) *Sustainable Green Technologies for Environmental Management*. Springer Nature, Singapore, pp.261.

Kim S, Takahashi M, Higuchi K, Tsunoda K, Nakanishi H, Yoshimura E, Mori S, Nishizawa NK (2005) Increased nicotianamine biosynthesis confers enhanced tolerance of high levels of metals, in particular nickel, to plants. *Plant Cell Physiology* 46:1809.

Kobayashi T, Yoshihara T, Jiang T, Goto F, Nakanishi H, Mori S, Nishizawa NK (2003) Combined deficiency of iron and other divalent cations mitigates the symptoms of iron deficiency in tobacco plants, *Physiologia Plantarum* 119:400–408.

Kobayashi T, Suzuki M, Inoue H, Itai RN, Takahashi M, Nakanishi H, Mori S, Nishizawa NK (2005) Expression of iron-acquisition-related genes in iron-deficient rice is coordinately induced by partially conserved iron-deficiency-responsive elements. *Journal of Experimental Botany* 56:1305–1316.

Kobayashi T, Itai RN, Ogo Y, Kakei Y, Nakanishi H, Takahashi M, Nishizawa NK (2009) The rice transcription factor IDEF1 is essential for the early response to iron deficiency, and induces vegetative expression of late embryo-genesis abundant genes. *The Plant Journal* 60:948–961.

Kobayashi T, Itai RN, Aung MS, Senoura T, Nakanishi H, Nishizawa NK (2012) The rice transcription factor IDEF1 directly binds to iron and other divalent metals for sensing cellular iron status. *The Plant Journal* 69:81–91.

Kobayashi T, Nishizawa NK (2012) Iron uptake, translocation and regulation in higher plants. *Annual Review of Plant Biology* 63:131-152.

Kobayashi T, Nishizawa NK (2014) Iron sensors and signals in response to iron deficiency. *Plant Science* 224:36-43.

Kosová K, Vítámvás P, Prášil IT, Renaut J (2011) Plant proteome changes under abiotic stress - Contribution of proteomics studies to understanding plant stress response. *Journal of Proteomics* 74 (8):1301–22.

Lade SB, Román C, Cueto-Ginzo AI, Serrano L, Sin E, Achón MA, Medina V (2018) Host-specific proteomic and growth analysis of maize and tomato seedlings inoculated with *Azospirillum brasilense* Sp7. *Plant Physiology and Biochemistry* 129:381-393.

Lee S, Person DP, Hansen TH, Husted S, Schjoerring JK, Kim S-Y, Jeon US, Kim YK, Kakei Y, Masuda H, Nishizawa NK, An G (2011) Bio-available zinc in rice seeds is increased by activation tagging of nicotianamine synthase. *Plant Biotechnology Journal* 9:865–873.

Lemanceau P, Expert D, Gaymard G, Bakker PAHM, Briat J-F (2009) Role of iron in plant-microbe interactions. In: Van Loon LC (ed) *Advances in Botanical Research, Vol. 51.* Academic Press, Burlington, pp 491-549.

Ma JF, Nomoto K (1994) Incorporation of label from C-13-labeled, H-2-labeled and N-15-labeled methionine molecules during the biosynthesis of 2'-deoxymugineic acid in roots of wheat. *Plant Physiology* 105:607–610.

Ma JF, Shinada T, Matsuda C, Nomoto K (1995) Biosynthesis of phytosiderophores, mugineic acids, associated with methionine cycling. *Journal of Biological Chemistry* 270:16549-16554.

Memelink J (2009) Regulation of gene expression by jasmonate hormones. *Phytochemistry* 70:1560–70.

Mongon J, Konnerup D, Colmer TD, Rerkasem B (2014) Responses of rice to Fe2+ in aerated and stagnant conditions: growth, root porosity and radial oxygen loss barrier. *Functional Plant Biology* 41 (9), 922-929.

Mori S, Nishizawa N (1987) Methionine as a dominant precursor of phytosiderophores in graminaceae plants. *Plant Cell Physiology* 28:1081-1092.

Mori S, Nishizawa N, Hayashi H, Chino M, Yoshimura E, Ishihara J (1991) Why are young rice plants highly susceptible to iron deficiency? *Plant and Soil* 130:143-156.

Morrissey J, Guerinot ML (2009) Iron uptake and transport in plants: the good, the bad, and the ionome. *Chemical Reviews* 109(10):4553-4567

Murashige T, Skoog F (1962) A revised medium for rapid growth and bioassays with tobacco tissue cultures. *Physiologia Plantarum* 15:473–497.

Naqvi S, Zhu C, Farre G, Sandmann G, Capell T, Christou P (2011) Synergistic metabolism in hybrid corn reveals bottlenecks in the carotenoid pathway and leads to the accumulation of extraordinary levels of the nutritionally important carotenoid zeaxanthin. *Plant Biotechnology Journal* 9:384–393.

Neilands JB (1982) Microbial envelope proteins related to iron. *Annual Review of Microbiology* 36:285-310.

Neilands JB, Leong SA (1986) Siderophores in relation to plant growth and disease. *Annual Review of Plant Physiology* 31:187-208.

Nozoye T, Inoue H, Takahashi M, Ishimaru Y, Nakanishi H, Mori S, Nishizawa NK (2007) The expression of iron homeostasis-related genes during rice germination. *Plant Molecular Biology* 64:35- 47.

Nozoye T, Nagasaka S, Kobayashi T, Takahashi M, Sato Y, Uozumi N, Nakanishi H, Nishizawa NK (2011) Phytosiderophore efflux transporters are crucial for iron acquisition in graminaceous plants. *Journal of Biological Chemistry* 286:5446-5454.

Nozoye T, Tsunoda K, Nagasaka S, Bashir K, Takahashi M, Kobayashi T, Nakanishi H, Nishizawa NK (2014a) Rice nicotianamine synthase localizes to particular vesicles for proper function. *Plant Signaling and Behavior* 9:e28660.

Nozoye T, Nagasaka S, Bashir K, Takahashi M, Kobayashi T, Nakanishi H, Nishizawa NK (2014b) Nicotianamine synthase 2 localizes to the vesicles of iron-deficient rice roots, and its mutation in the YXXφ or LL motif causes the disruption of vesicle formation or movement in rice. *The Plant Journal* 77:246-260.

Nozoye T, Nagasaka S, Kobayashi T, Sato Y, Uozumi N, Nakanishi H, Nishizawa NK (2015) The phytosiderophore efflux transporter TOM2 is involved in metal transport in rice. *Journal of Biological Chemistry* 290 (46):27688-27699.

Ogo Y, Itai RN, Kobayashi T, Aung MS, Nakanishi H, Nishizawa NK (2011) OsIRO2 is responsible for iron utilization in rice and improves growth and yield in calcareous soil. *Plant Molecular Biology* 75:593–605.

Ogo Y, Itai RN, Nakanishi H, Inoue H, Kobayashi T, Suzuki M, Takahashi M, Mori S, Nishizawa NK (2006) Isolation and characterization of IRO2, a novel iron-regulated bHLH transcription factor in graminaceous plants. *Journal of Experimental Botany* 57:867-78.

Ogo Y, Itai RN, Nakanishi H, Inoue H, Kobayashi T, Takahashi M, Mori S, Nishizawa NK (2007) The rice bHLH protein OsIRO2 is an essential regulator of the genes involved in Fe uptake under Fe-deficient conditions. *The Plant Journal* 51:366-377.

Ogo Y, Kobayashi T, Itai RN, Nakanishi H, Kakei Y, Takahashi M, Toki S, Mori S, Nishizawa N (2008) A novel NAC transcription factor, IDEF2, that recognizes the iron deficiency-responsive element 2 regulates the genes involved in iron homeostasis in plants. *The Journal of Biological Chemistry* 283 (19):13407-13417.

Okonechnikov K, Golosova O, Fursov M, the UGENE team (2012) Unipro UGENE: a unified bioinformatics toolkit. *Bioinformatics* 28:1166-1167.

Pedraza RO (2015) Chapter 14: Siderophores production by *Azospirillum*: biological importance, assessing methods and biocontrol activity. In: Cassán FD, Okon Y, Creus CM (eds) *Handbook for Azospirillum: Technical Issues and Protocols.* Springer International Publishing, Switzerland. p 253.

Pii Y, Penn A, Terzano R, Crecchio C, Mimmo T, Cesco S (2015) Plant-microorganism-soil interactions influence the Fe availability in the rhizosphere of cucumber plants. *Plant Physiology and Biochemistry* 87:45-52.

Pii Y, Aldrighetti A, Valentinuzzi F, Mimmo T, Cesco S (2019) *Azospirillum brasilense* inoculation counteracts the induction of nitrate uptake in maize plants. *Journal of Experimental Botany* 70(4):1313–1324.

Römheld V, Marschner H (1986) Evidence for a specific uptake system for iron phytosiderophore in roots of grasses. *Plant Physiology* 80:175–180.

Sahrawat KL (2004) Iron Toxicity in Wetland Rice and the Role of Other Nutrients. *Journal of Plant Nutrition* 27:1471-1504.

Scavino AF, Pedraza RO (2013) Chapter 11: The role of siderophores in plant growth-promoting bacteria. In: Maheshwari DK (ed) *Bacteria in Agrobiology: Crop Productivity*. Springer-Verlag, Berlin Heidelberg, pp 265-285.

Schroth MN, Hancock JG (1982) Disease suppressive soil and root colonizing bacteria. *Science* 216:1376-1381.

Schuler M, Bauer P (2012) Strategies for iron biofortification of crop plants. In: Kapiris K (ed) *Food Quality, InTech*. Available from:
http://www.intechopen.com/books/food-quality/strategies- for-iron-biofortification-of-crop-plants.

Selby-Pham J, Lutz A, Moreno-Moyano LT, Boughton BA, Roessner U, Johnson AAT (2017) Diurnal changes in transcript and metabolite levels during the iron deficiency response of rice. *Springer Open Access* 10:14.

Shahid M, Nayak AK, Shukla AK, Tripathi R, Kumar A, Raja R, Panda BB, Meher J, Bhattacharyya P, Dash D (2014) Mitigation of iron toxicity and Iron, Zinc, and Manganese nutrition of Wetland Rice Cultivars (Oryza sativa L.) grown in iron-toxic soil. *CLEAN – Soil, Air, Water* 42:1604-1609.

Shime-Hattori A, Kobayashi S, Ikeda S, Asano R, Shime H, Shinano T (2011) A rapid and simple PCR method for identifying isolates of the genus *Azospirillum* within populations of rhizosphere bacteria. *Journal of Applied Microbiology* 111:915-924.

Shojima S, Nishizawa NK, Mori S (1989) Establishment of a cell-free system for the biosynthesis of nicotianamine. *Plant Cell Physiology* 30:673-677.

Siberil Y, Doireau P, Gantet P. (2001) Plant bZIP G-box binding factors Modular structure and activation mechanisms. *European Journal of Biochemistry* 268 (22):5655-66.

Slamet-Loedin IH, Johnson-Beebout SE, Impa S, Tsakirpaloglou N (2015) Enriching rice with Zn and Fe while minimizing Cd risk. *Frontiers in Plant Science* 6:1–9.

Takahashi M, TeradaY, Nakai I, Nakanishi H, Yoshimura E, Mori S, Nishizawa N (2003) Role of nicotianamine in the intracellular delivery of metals and plant reproductive development. *Plant Cell* 15:1263–1280.

Takahashi M, Yamaguchi H, Nakanishi H, Shioiri T, Nishizawa NK, Mori S (1999) Cloning two genes for nicotianamine aminotransferase, a critical enzyme in iron acquisition (Strategy II) in graminaceous plants. *Plant Physiology* 121:947-56.

Tarrand JJ, Krieg NR, Dobereiner J (1978) A taxonomic study of *Spirillum lipoferum* group, with description of a new genus, *Azospirillum* gen nov. and two species. *Azospirillum lipoferum* (Beijerinck) comb. nov. and *Azospirillum brasilense* sp nov. *Canadian Journal of Microbiology* 24:967–980.

Tortora ML, Díaz-Ricci JC, Pedraza RO (2011) *Azospirillum brasilense* siderophores with antifungal activity against *Colletotrichum acutatum*. *Archives of Microbiology* 193 (4):275-286.

Vacheron J, Renoud S, Muller D, Babalola OO, Prigent-Combaret C (2015) Chapter 19: Alleviation of abiotic and biotic stresses in plants by *Azospirillum*. In: Cassán FD, Okon Y, Creus CM (eds) *Handbook for Azospirillum: Technical Issues and Protocols.* Springer International Publishing, Switzerland, pp 333–365.

Wang M, Gruissem W, Bhullar NK (2013) Nicotianamine synthase overexpression positively modulates iron homeostasis-related genes in high iron rice. *Frontiers in Plant Science* 29 (4):156.

Weinberg ED (1984) Iron withholding: a defense against infection and neoplasia. *Physiological Reviews* 64:65-107.

Xuan Y, Scheuermann EB, Meda AR, Hayen H, von Wirén N, Weber G. (2006) Separation and identification of phytosiderophores and their metal complexes in plants by zwitterionic hydrophilic interaction liquid chromatography coupled to electrospray ionization mass spectrometry. *Journal of Chromatography A* 1136 (1):73–81.

Yoshihara T, Washida H, Takaiwa F. (1996) A 45-bp proximal region containing AACA and GCN4 motif is sufficient to confer endosperm-specific expression of the rice storage protein glutelin gene *GluA-3*. *FEBS Letters* 383:213-218.

Zamioudis C, Korteland J, Van Pelt JA, van Hamersveld M, Dombrowski N, Bai Y, Hanson J, Van Verk MC, Ling HQ, Schulze-Lefert P, Pieterse CM (2015) Rhizobacterial volatiles and photosynthesis-related signals coordinate MYB72 pression in *Arabidopsis* roots during onset of induced systemic resistance and iron deficiency responses. *The Plant Journal* 84(2):309–22.

Zhang M, Pinson SRM, Tarpley L, Huang XY, Lahner B, Yakubova E, Baxter I, Guerinot ML, Salt DE (2014) Mapping and validation of quantitative trait loci associated with concentrations of 16 elements in unmilled rice grain. *Theoretical and Applied Genetics* 127:137-165.

Zheng L, Ying Y, Wang L, Wang F, Whelan J, Shou H (2010) Identification of a novel iron regulated basic helix-loop-helix protein involved in Fe homeostasis in *Oryza sativa. BMC Plant Biology* 10 (166):1-9.

CHAPTER 9

General Discussion

9.1 General Discussion

Crop biofortification by plant growth-promoting rhizobacteria (PGPR) can lead to an increase in the nutrient content of edible plant parts (Garg et al., 2018). Effective use of PGPR provide a promising way to sustainably produce nutritious and safe food for human consumption, addressing one of the world's greatest challenges: food insecurity. At the same time, PGPR play an important role enhancing plant growth and productivity, and act as an environmentally-friendly biocontrol agent (Khan et al., 2019). These functions address the other issue affecting food insecurity: crop loss due to pre-harvest diseases (Miller et al., 2017). The ability of PGPR to modulate the metabolism and immune system of their plant hosts is one of their most coveted attributes in terms of crop health. However, quantifying the ways in which PGPR affect molecular mechanisms of their hosts poses a significant challenge because these reactions are both host- and species-specific (Correa et al., 2007; Drogue et al., 2014). Having a clear understanding of these interactions is crucial because they are determinate in the plants' survival against biotic and abiotic stresses.

An additional complexity is posed by the increasingly common use of other modes of biofortification that alter the host genetic makeup, thereby broadening genotypic diversity within plant species and among cultivars (Farré 2012). Biotechnological methods can lead to the integration of entire metabolic pathways, synergistically augmenting the activity of a PGPR *in planta*, or rendering its influence null altogether (Vacheron et al., 2015). An advantage to designing biofortification programs that simultaneously employ various strategies (agronomic, transgenic and/or breeding) is that modern biotechnological advancements can be integrated with biological crop management for a sustainable outcome. However, before this can happen, the interplay between plants, stress, and biofortification must be closely examined and well-defined so that the interactions can be optimized to promote both plant and human health.

Azospirillum brasilense Sp7 (Sp7) is a PGPR that agronomically biofortifies plants by solubilizing soil nutrients and moving them to plant tissues and organs (Patidar and Mali 2004). Sp7 also improves plant health by association because it stimulates growth, increases fixed soil nitrogen available to the plant, and induces systemic resistance (ISR), which up-regulates the plant defense response and primes it against future stress (van Loon et al., 1998; Dobbelaere et al., 2001; Cassán et al., 2009). Nearly every interaction that Sp7 has with its environment (the soil, plant, nutrients, organic sugars, pH, oxygen supply, etc.) has the potential to impact bacterial root colonization, along with subsequent reactions elicited in the associated host plant (Cassán et al., 2015). Even the individual components of different inoculation buffers (Chapter 3) can modulate these interactions and differentially influence plant metabolic processes.

Azospirillum spp. interacts differently with plant metabolism depending on the species (Mus et al., 2016). This is thought to be because the association between PGPR and host plant(s) is ancient (Lambers et al., 2009) and has probably been shaped by coevolutionary

processes. Both primary and secondary metabolic functions in the plant are pivotal in the PGPR-plant-stress interaction. Previous work has suggested that rhizobacteria can have strain-dependent effects on the secondary metabolism of plants without influencing the physiological functions that are related to primary metabolism and involved directly in plant development and growth (Walker et al., 2011). However, in comparing the reactions of Sp7 in two different species and in four distinct cultivars (Chapters 4 & 5), we have shown otherwise, especially at incipient stages of vegetative development.

Ongoing research of individual plant stressors provides evidence for overlapping receptors, signaling pathways and responses between different stresses of the same nature and between biotic and abiotic stresses. The characterization of hub genes and common components in multiple stress resistance offers considerable potential for the development of multiple stress-resistant crop cultivars, appropriate for sustainable agricultural practices (Miller et al., 2017). Furthermore, when PGPR elicit different plant pathways simultaneously, this often confers additive responses that are more effective than single-elicited pathways (Vacheron et al., 2015). Regardless, a primary mode of action of Sp7 is the production and liberation of regulatory vegetative growth substances (phytohormones) directly affecting plant metabolism (Glick, 2012). Phytohormones play critical regulatory roles within complex signaling systems that respond to internal and external cues to modulate interactions between plant genomes and their environment (Castillo et al., 2015). These interactions include developmental growth, as well as plant responses to biotic or abiotic stresses (Feussner and Wasterback 2002). The activity of hormones is determined by their interaction with each other, as well as their availability, which is a consequence of hormone metabolism, distribution, signal efficiency, perception and transduction. In turn, hormone crosstalk and signaling affects plant gene expression and protein activity control related to metabolism and stress (Castillo et al., 2015).

The "theory of multiple mechanisms" encapsulates the collective ontogeny of these biochemical and molecular processes elicited by *Azospirillum* spp. Specifically, it is defined as: the bacterium acting in a cumulative or sequential pattern to activate ISR, resulting from hormonal, metabolic and transcriptional mechanisms occurring simultaneously or consecutively (Bashan and de-Bashan, 2010). The mechanisms include the production or metabolism of plant phytohormones; solubilization of metals and siderophore synthesis; and altering plant metabolism and production of secondary metabolites. Our work showcases the variability of the multiple mechanisms induced by Sp7, emphasizing how the mechanisms are altered by different genetic features of the host plant (Chapters 4 - 8), abiotic (Chapters 3, 4 & 8) and biotic (Chapters 6 & 7) stresses. Proteins related to ISR are abundant in Sp7-inoculated plants (Chapters 5 & 6), and transgenic plants interact with Sp7 and stress to synergistically up-regulate certain transcription factors (TFs) (Chapters 7 & 8). Considering that TFs are an important cornerstone of gene regulatory networks controlling the expression of multiple genes

and hormones involved in stress responses, and that genomes can alter TF-DNA binding dynamics through epigenetic regulation (Zhang et al., 2009), there is inevitable molecular overlap between ISR-incited protein up-regulation (proven TF-binding agents) and TF over-expression (Singh et al., 2002).

The molecular mechanisms mediating transient TF-DNA binding are rapid and dynamic transcriptional and post-translational interactions that translate to long-term temporal regulation of genomes (Alon 2007). It is for this reason that characterizing all possible regulatory interactions within a genome is an arduous task, and even more so when key plant enzymes in metabolic pathways have been modified towards biofortification. However, the characterization of hub genes and delineation of plant gene network topologies is a promising approach to generate novel plant phenotypes, since rewiring of gene regulatory networks through mutations in TF coding and regulatory regions has been found a principle driver of crop domestication (Century et al., 2008; Swift and Coruzzi 2017). The conclusions obtained in this thesis provide important insights into how Sp7 intervenes in multiple mechanisms of the various plant types tested, supporting the hypothesis that inoculating already biofortified plants with Sp7 has favorable effects on plant metabolism and stress response.

9.2. References

Alon U (2007) Network motifs: theory and experimental approaches. *Nature Reviews Genetics* 8(6):450–461.

Bashan Y, de-Bashan LE (2010) Chapter 2: How the plant growth-promoting bacterium *Azospirillum* promotes plant growth- a critical assessment. In: Sparks DL (ed) *Advances in Agronomy*, Volume 108. Academic Press, pp 77-136.

Cassán F, Perrig D, Sgroy V, Masciarelli O, Penna C, Luna V (2009) *Azospirillum brasilense* Az39 and Bradyrhizobium japonicum E109, inoculated singly or in combination, promote seed germination and early seedling growth in corn (*Zea mays* L.) and soybean (*Glycine max* L.). *European Journal of Soil Biology* 45:28–35.

Castillo P, Molina R, Andrade A, Vigliocco A, Alemano S, Cassán FD (2015) Chapter 7: Phytohormones and other plant growth regulators produced by PGPR: the genus *Azospirillum.* In: Cassán FD, Okon Y, Creus CM (eds.) *Handbook for Azospirillum*: *Technical issues and protocols.* Springer International Publishing, Switzerland, p. 115.

Century K, Reuber TL, Ratcliffe OJ (2008) Regulating the regulators: The future prospects for transcription-factor-based agricultural biotechnology products. *Plant Physiology* 147(1):20–29.

Correa OS, Romero AM, Montecchia MS, Soria MA (2007) Tomato genotype and *Azospirillum* inoculation modulate the changes in bacterial communities associated with roots and leaves. *Journal of Applied Microbiology* 102:781–786.

Dobbelaere S, Croonenborghs A, Thys A, Ptacek D, Vanderleyden J, Dutto P, Labandera-Gonzalez C, Caballero-Mellado J, Aguirre JF, Kapulnik Y, Brener S, Burdman S, Kadouri D, Sarig S, Okon Y (2001) Responses of agronomically important crop to inoculation with *Azospirillum*. *Australian Journal of Plant Physiology* 28:871–879.

Drogue B, Sanguin H, Chamam A, Mozar M, Llauro C, Panaud O, Prigent-Combaret C, Picault N, Wisniewski-Dyé. Plant root transcriptome profiling reveals a strain-dependent response during *Azospirillum*-rice cooperation. *Frontiers in Plant Science* 5(607):1-14.

Farré G (2012) Towards vitamin biofortification in staple cereal crops in a socio-political and food security context. Dissertation, University of Lleida.

Feussner I, Wasternack C (2002) The lipoxygenase pathway. *Annual Reviews in Plant Biology* 53:275-297.

Garg M, Sharma N, Sharma S, Kapoor P, Kumar A, Chunduri V, Arora P (2018) Biofortified crops generated by breeding, agronomy and transgenic approaches are improving lives of millions of people around the world. *Frontiers in Nutrition* 5:12.

Glick BR (2012) Plant growth-promoting bacteria: mechanisms and applications. *Scientifica*: 963401.

Khan A, Singh J, Upadhayay VK, Singh AV, Shah S (2019) Chapter 13: Microbial biofortification: a green technology through plant growth-promoting microorganisms. In: Shah S et al. (eds.) *Sustainable Green Technologies for Environmental Management*. Springer Nature, Singapore, pp.261.

Lambers H, Mougel C, Jaillard B, Hinsinger P (2009) Plant–microbe–soil interactions in the rhizosphere: an evolutionary perspective. *Plant and Soil* 321:83–115.

Miller RNG, Alves GSC, Van Sluys M-A (2017) Plant immunity: unravelling the complexity of plant responses to biotic stresses. *Annals of Botany* 119:681-687.

Mus F, Crook MB, Garcia K, Garcia Costas A, Geddes BA, Kouri ED, Paramasivan P, Ryu M-H, Oldroyd GED, Poole PS, Udvardi MK, Voigt CA, Ané J-M, Peters JW (2016) Symbiotic nitrogen fixation and the challenges to its extension to nonlegumes. *Applied Environmental Microbiology* 82: 3698–3710.

Patidar M, Mali AL (2004) Effect of farmyard manure, fertility levels and bio-fertilizers on growth, yield and quality of *Sorghum* (*Sorghum bicolor*). *Indian Journal of Agronomy* 2(49):117–20.

Singh KB, Foley RC, Oñate-Sánchez L (2002) Transcription factors in plant defense and stress responses. *Current Opinions in Plant Biology* 5: 430–436.

Swift J, Coruzzi G (2017) A matter of time – how transient transcription factor interactions create dynamic gene regulatory networks. *Biochim Biophys Acta* 1860(1): 75-83.

Vacheron J, Renoud S, Muller D, Babalola OO, Prigent-Combaret (2015) Chapter 19: Alleviation of abiotic and biotic stresses in plants by *Azospirillum.* In: Cassán FD, Okon Y, Creus CM (eds.) *Handbook for Azospirillum*: *Technical issues and protocols.* Springer International Publishing, Switzerland, p. 333.

van Loon LC, Bakker PAHM, Pieterse CJM (1998) Systemic resistance induced by rhizosphere bacteria. *Annual Review in Phytopathology* 36:453-483.

Walker V, Bertrand C, Bellvert F, Moënne-Loccoz Y, Bally R, Comte G (2011) Host plant secondary metabolite profiling shows a complex, strain-dependent response of maize to plant growth-promoting rhizobacteria of the genus *Azospirillum*. *New Phytologist* 189:494:506.

Zhang X, Bernatavichute YV, Cokus S, Pellegrini M, Jacobsen SE (2009) Genome-wide analysis of mono-, di- and trimethylation of histone H3 lysine 4 in *Arabidopsis thaliana*. *Genome Biology* 10(6): R62.

CHAPTER 10

General Conclusions

General Conclusions

1. Seed inoculation with *Azospirillum brasilense* Sp7 modulates barley growth at early vegetative stages of seedling development, irrespective of growing conditions (*in vitro* vs *in vivo*), but varies according to cultivar

2. *Azospirillum brasilense* Sp7 positively influences maize-seedling growth regardless of inoculation buffer choice. However, seedlings inoculated with phosphate buffered saline (PBS) +Sp7 exhibit higher C adsorption, compared to those inoculated with magnesium sulfate ($MgSO_4$) +Sp7, indicating that there are subtle differences in interactions between the buffer components and Sp7

3. The primary metabolism of tomato and maize seedlings is affected differently by *Azospirillum brasilense* Sp7. In tomato, Sp7 increases the abundance of proteins related to metabolism and redox homeostasis but inhibits the Calvin Benson (CB) cycle and chloroplast development, leading to damaged photosynthetic proteins by reactive oxygen species (ROS). In maize, Sp7 tardily alters the defense response, which assists in colonization of the plant growth-promoting rhizobacteria (PGPR); this also leads to increased ROS-scavenging enzymes and reduced photoinhibition

4. *Azospirillum brasilense* Sp7 causes better maize seedling emergence, and has a more complex and beneficial interaction with maize (compared to tomato) because of the C_4 mechanism

5. *Azospirillum brasilense* Sp7 does not affect viral titer of Maize dwarf mosaic virus (MDMV) nor Potato virus X (PVX), but does incite induced systemic resistance (ISR), restored chloroplast activity and up-regulated CB cycle. This delays detection of MDMV at early stages of maize development and increases the tolerance of tomato plants to PVX

6. *Azospirillum brasilense* Sp7 mitigates symptoms of *Fusarium graminareum* in high carotenoid (HC) biofortified maize, observable at both the macro- and molecular level

7. Up-regulated SA and JA in *Azospirillum brasilense* Sp7-inoculated HC maize seedlings is a coordinated part of the same cellular response as ZmGAMYB

proteins. Therefore, ZmGAMYB is proposed as a candidate transcription factor responsible for activating the SAR and ISR defense pathways elicited by each phytohormone

8. *Azospirillum brasilense* Sp7 exerts influence over root-bound mugeinic acid (MA) homeostasis in rice seedlings, for both wild-type (WT) and iron accumulating (RB92) genotypes

9. Under Fe-starvation, *Azospirillum brasilense* Sp7 induces significant accumulation of Fe and Zn in Fe-biofortified rice seedling leaf tissues, as well as up-regulation of Fe-homeostasis genes. The *OsIRO2* TF and *OsTOM1* gene are implicated as having a unique role in coordinating this interaction

10. A *trans*-acting factor might play a significant role in the exogenous alteration of the Fe-homeostasis pathway in rice seedlings, based on the Fe-homeostasis genes elicited in inoculated seedlings and the previously identified mode(s) of action of Sp7. Specifically, we identify the *OsIRO2* G-box motif as the *cis*-acting factor for interacting with protein products that are up-regulated by *Azospirillum brasilense* Sp7 inoculation and the subsequent ISR response

FUTURE PROSPECTS & RECOMMENDATIONS

Future prospects and recommendations

The results presented in this thesis provide important insights into the molecular processes underlying *Azospirillum brasilense* Sp7 inoculation to economically important crops. The simultaneous use of various biofortification strategies has been proven effective for the up-regulation of plant defense against both biotic and abiotic stressors, with TF activation and coordinated hormone signaling playing a central role in these responses.

There were many environmental factors that were not analyzed in this study, but are important to consider, such as soil pH and composition, and the biodiversity of microorganisms, especially other PGPR. Furthermore, all studies that were not subjected to timed samplings would have benefitted tremendously from information detailing the evolution of hormone accumulation and signaling (gene transcription) related to physiological plant stage.

My preliminary work called for many more studies to fully understand the stress responses elicited by the two buffers + Sp7. Future proposed work in this regard includes: measure transcription of Mg-responsive genes in roots, quantify Mg^{+2} interaction with N-metabolism and phytohormone signaling pathways, measure amino acid flux, ATPase activity and K^{+} concentrations in the plant related to PBS+Sp7.

For the Sp7-HC maize study, the most important pending future experiment is to conduct assays that confirm the action of the ZmGAMYB TF in the hormone pathways, via mutants or hormone treatments. RNA needs to be collected from root tissue and all gene transcription data should be collected just as it was for leaves, to compare with hormone data; this was a limitation in my experiments because I test seedlings, but plants were often too small to render enough root material to test. Proteomic and/or metabolomic analyses would clarify outstanding questions regarding changes to secondary metabolism, and phenolic compounds observed. Finally, there is still much to study in regards to ET metabolism, ACC accumulation and ABA/H_2O_2 signaling pathways.

Continued work with Sp7-RB92 rice requires proteomic and hormone analysis, focusing on the G-box element and how it is involved in response to ABA, JA, anaerobiosis, PR genes and ET induction. Study of *cis/trans* interactions between the G-box motif and Sp7 elicited proteins is required to confirm the relationship between the promoters of ISR-primed genes and OsIRO2. Finally, further experiments could analyze bacterial siderophore (catechol) activity related to Fe homeostasis in the plant since catechols improve siderophore use efficiency.

OUTPUTS

Outputs

1. Publications

Lade SB, Villarroyo AL, Fernández ÁA, Abadia J, Garcia PB, Albacete A, Muñoz P, Christou P, Medina V (2019) *Azospirillum brasilense* Sp7 modulates homeostasis in Fe-biofortified rice seedlings. *Manuscript in preparation*.

Lade SB, Giné-Bordonaba J, Albacete A, Serrano L, Segarra J, Christou P, Medina V (2019) Biochemical and molecular regulation of *Azospirillum brasilense* Sp7 x *Fusarium graminearum* interactions influence hormones in early growth stages of high carotenoid maize. Submitted to *Molecular Plant-Microbe Interactions.* Under revision. (see **Annex 5**)

Lade SB, Román C, Cueto-Ginzo AI, Serrano L, Sin E, Achón MA, Medina V (2019) Differential proteomic analysis reveals that *Azospirillum brasilense* Sp7 promotes virus resistance in maize and tomato seedlings. Submitted to *European Journal of Plant Pathology*. Under revision. (see **Annex 4**)

Lade SB, Nicholson-Sabaté, Medina V (2019) Response of maize (*Zea Mays* L. Mill cv. B73) seedlings to *Azospirillum brasilense* Sp7 in common inoculation buffers PBS and $MgSO_4$. Submitted to *Cereal Research Communications*. Under revision. (see **Annex 1**)

Lade SB, Román C, Cueto-Ginzo AI, Serrano L, Sin E, Achón MA, Medina V (2018) Host-specific proteomic and growth analysis of maize and tomato seedlings inoculated with *Azospirillum brasilense* Sp7. *Plant Physiology and Biochemistry* 129: 381-393. **(See Annex 3)**

Lade SB, Román C, Cueto-Ginzo AI, Maneiro L, Muñoz P, Medina V (2018) Root development in agronomically distinct six-rowed barley (*Hordeum vulgare* L.) cultivars inoculated with *Azospirillum brasilense* Sp7. *Plant Breeding Journal* 137: 338-345. **(See Annex 2)**

Lade SB, Giné-Bordonaba J, Albacete A, Serrano L, Segarra J, Christou P, Medina V (2018). *Azospirillum brasilense* Sp7 x *Gibberella zeae* interactions in early growth stages of high carotenoid corn (Abstr.). *Phytopathology* 108:S1.1. https://doi.org/10.1094/PHYTO-108-10-S1.132.

Bortesi L, Zhu C, Zischewski J, Perez L, Bassie L, Nadi R, Forni G, **Lade SB**, Soto E, Jin X, Medina V, Villorbina G, Muñoz P, Farré G, Fischer R, Twyman RM, Capell T, Christou P, Schillberg S (2016) Patterns of CRISPR/Cas9 activity in plants, animals and microbes. *Plant Biotechnology Journal* 14 (12): 2203-2216.

Lade SB, Medina V (2016) CRISPR-Cas9 como herramienta en el control de enfermedades de las plantas. Boletín Informativo de la Sociedad Española de Fitopatología 93: 48-58. **(See Annex 6)**

Cueto-Ginzo AI, Serrano L, Sin E, Rodríguez R, Morales JG, **Lade SB**, Medina V, Achón MA (2016) Exogenous salicylic acid treatment delays initial infection and counteracts alterations induced by Maize dwarf mosaic virus in the maize proteome. *Physiological and Molecular Plant Pathology* 95: 47-59.

Cueto-Ginzo AI, Aparicio F, Achón MA, Pallás V, Arcal L, **Lade SB**, Medina V (2015) Characterization of a new Spanish Potato Virus X (PVX) inducing symptoms in tomato. *Journal of Plant Pathology 97* (2): 369-372.

2. Participation in congresses

2.1 Oral presentations

Lade, S.B., Giné-Bordonaba, J., Albacete, A., Serrano, L., Segarra, J., Christou, P., Medina, V. (2018, October). *Resistance and synergy in the early Azospirillum brasilense (Sp7) x Fusarium graminareum interaction: Wild type (WT) vs. High carotenoid (HC) corn*. Presentation at the XIX Congreso de la Sociedad Española de Fitopatología, Toledo, Spain.

2.2 Posters

Lade, S.B., Giné-Bordonaba, J., Albacete, A., Serrano, L., Segarra, J., Christou, P., Medina, V. (2018, August). *Azospirillum brasilense (Sp7) x Gibberella zeae interactions in early growth stages of high carotenoid corn activate the MYB transcription factor to up-regulate hormone response*. Poster at the International Congress of Plant Pathology (ICPP), Boston, USA.

Lade, S.B., Román, C., Cueto-Ginzo, A.I., Serrano, L., Sin, E., Achón, M.A., Medina, V. (2017, June). *Azospirillum brasilense (Sp7) increases the viral load while counteracting oxidative stress and alleviating negative physiological effects induced by viruses in tomato and maize.* Poster at the XIV Congreso Nacional de Virología, Cadiz, Spain.

Lade, S.B., Román, C., Cueto-Ginzo, A.I., Rodriguez, R., Serrano, L., Meler, P., Sin, E., Achón, M.A., Medina, V. (2017, June). *Host-specific proteomic and growth analysis of C3 and C4 plants inoculated with Azospirillum brasilense (Sp7).* Poster at the XXII Reunion de la Sociedad Española de Fisiología Vegetal- XV Spanish Portuguese Congress of Plant Pathology, Barcelona, Spain

3. Presentations

Lade, S.B. (2018, March). *The effects of Azospirillum brasilense (Sp7) on iron homeostasis and bronzing in rice plants.* Presentation for the PVCF Departmental Seminar, University of Lleida, Lleida, Spain.

Lade, S.B. (2017, May). *Crispr-Cas9 genome editing and broad virus resistance*. Presentation for third year Virology students, University of Lleida, Lleida, Spain.

ANNEXES

ANNEX 1

Lade SB, Nicholson-Sabaté, Medina V (2019) Response of maize (*Zea mays* L. Mill cv. B73) seedlings to *Azospirillum brasilense* Sp7 in common inoculation buffers PBS and $MgSO_4$ (*Submitted to Cereal Research Communications)*

PBS and $MgSO_4$ buffers differentially affect the response of maize (*Zea Mays* L. Mill cv. B73) seedlings to *Azospirillum brasilense* Sp7

Sarah Boyd LADE*, Nathan NICHOLSON-SABATÉ, Vicente MEDINA

Department of Plant Production and Forestry Science, University of Lleida-Agrotecnio Center, Av. Alcalde Rovira Roure, 191, 25198 Lleida, Spain

The effect of *Azospirillum brasilense* Sp7 (Sp7) on maize (*Zea mays*, Mill cv. B73) seedlings was examined using phosphate buffered saline (PBS) or magnesium sulfate ($MgSO_4$) as the inoculation buffer. Maize seeds were inoculated, then seedling height, leaf chlorophyll levels, and root parameters were analyzed with WinRHIZO® at an early vegetative stage of plant development. Scanning and transmission electron microscope (SEM & TEM) analysis was conducted to evaluate bacterial binding to plant roots. $MgSO_4$+Sp7 caused a significant increase in the abundance of thick lateral roots, but rendered plants stunted compared to other treatment groups. Relative chlorophyll contents significantly increased in seedlings inoculated with PBS+Sp7. SEM & TEM elucidated that buffer choice does not interfere with bacterial binding to roots. Both inoculation buffers yield distinct benefits for plant growth, but also evidently promote stress that is mitigated by Sp7. These results form the basis of a narrative considering that Sp7 differentially affects an associated plant depending upon buffer choice.

Key words : PGPR, cereal crops, nutrients, root morphology

Abbreviations: Phosphate buffered saline (PBS); *Azospirillum brasilense* Sp7 (Sp7); Plant-growth promoting rhizobacteria (PGPR); Jasmonic acid (JA); Ethylene (ET); nitrogen-free broth (Nfb); Okon, Albrecht and Burris (OAB); tryptone yeast extract and glucose (TYG); Lauria-Bertani (LB); Congo-red (CR)

* Corresponding author: SB Lade, email: sarahb.lade@pvcf.udl.cat

Introduction

Fertilizer is one of the most important components for increasing crop growth rates. Nonetheless, chemical fertilizers pose the risk of eutrophication due to excessive nutrient enrichment of water systems from farm runoff (Carpenter et al., 1998). Plant-growth promoting rhizobacteria (PGPRs) have been found to offer the same benefits to crops as chemical fertilizers, which is why they have been examined extensively as a viable replacement option (Barassi et al., 2007).

Azospirillum brasilense is a well-studied PGPR that helps the host plant fix nitrogen (Bashan and Holguin 1996), increases plant growth by inciting root hair proliferation, facilitates water and nutrient uptake (Barassi et al., 2007), influences phytohormone production (Perrig et al., 2007), and reduces biotic and abiotic stresses (Bashan and Holguin 1997; Lugtenberg and Kamilova 2009). In this regard, *A. brasilense* provokes the defense mechanism *induced systemic resistance* (ISR) in plants upon association (Alström 1991). ISR relies on jasmonic acid (JA) and ethylene (ET) phytohormone signal transduction pathways to 'prime', or sensitize distal plant parts for enhanced pathogen defense (Van Peer et al., 1991). At the onset, priming is rather elusive because it does not involve direct activation of resistance, so is nearly invisible at the protein or transcriptome level. As a result, ISR is normally studied in combination with stress factors, which is when changes in JA and ET up-regulation are made perceivable (Verhagen et al., 200; Wang et al., 2005). A primed plant exhibits several other physiological changes that help delay disease progression, such as enhanced callose deposition (Ton et al., 2005) and more rapid stomatal closure (Kumar et al., 2012).

The conditions in which *A. brasilense* grows can also greatly influence some of its plant-growth promoting properties (Bashan and Bashan 2011). A number of studies have been carried out to weigh the impact of various culture media on the growth of *Azospirillum* spp., both in small-scale operations and commercially. Typically, a nitrogen free broth (Nfb) is the standard growth media. It has ammonium chloride (NH_4Cl) serving as the nitrogen (N) source and organic acids, such as malate, succinate, gluconate or glycerol as carbon (C) sources (Bashan and Bashan 2011). Carbon sources have been optimized since supplying them is fundamental for promoting efficient C metabolism in *Azospirillum* spp. (Hartmann and Zimmer 1994). Considering this, the most effective culture media identified and utilized to date are OAB (Okon, Albrecht and Burris 1977), and tryptone yeast extract & glucose (TYG) (Bashan et al., 2011).

Once cultured, the next step in manual delivery of the PGPR to the plant or seed is the inoculation buffer. There is no universal carrier for PGPRs, and choosing the proper formula has been identified as a strain-specific process (Rivera et al., 2014). Even still, there is little literature that makes distinction between the buffers, or classifies them by strain. A number of solid, liquid, oil and gel-based formulas have been developed; liquid inoculants being the most economical for small-scale use (Mugilan et al., 2011). In the case of *Azospirillum* spp., liquid inoculant buffer options include PBS (Cohen et al., 2009), magnesium sulfate ($MgSO_4$) (Mangmang et al., 2015), 0.9% sodium chloride (NaCl) (Bashan and Levanony 1985), 66mM phosphate buffer (Creus et al., 1997) and Lauria-Bertani (LB)-broth (Khalid et al. 2017). Most studies with *A. brasilense* Sp7 (Sp7) in particular use PBS, though $MgSO_4$ has appeared in more contemporary works.

Azospirillum brasilense has been repeatedly studied for mitigating salinity stress in the rhizosphere because it accumulates amino acids such as proline and glutamate (Bashan and Holguin 1997), which act as osmoprotectants (Casanovas et al., 2002,

2003). Glutamate is central to N-metabolism in plants, and most assimilated N passes through this step before it is re-distributed to major N metabolites (Forde et al., 2007). Furthermore, the exopolysaccharides produced by A. *brasilense* restrict sodium (Na^{+1}) influx into roots (Ashraf et al., 2004). In this way, studies addressing the efficacy of *A. brasilense* in the control of salinity conveniently use phosphate or LB buffers, probably because both magnesium (Mg^{+2}) and Na^{+1} ions can disrupt the binding of rhizobacteria to roots (Gafny et al., 1985). It is not, however, known to what extent the Na^{+1} concentration in PBS disrupts bacterial binding compared to that of Mg^{+2} in $MgSO_4$. Study has shown that increasing $MgSO_4$ supply increased the concentration of total Mg and decreased the concentration of Ca in both roots and shoots irrespective of anion form supplied with Mg, such as sulfur (S). There is no significant difference in S concentration in the roots in *Arabidopsis* grown in the medium containing SO_4^{2-} concentration ranging from 250 to 10250µM. This is maybe an alternative explanation on why S has relatively little influence on the morphology of the root (Niu et al., 2014).

The aims of our study are to investigate the effects of PBS and $MgSO_4$ buffers on the phenotype of Sp7-inoculated maize seedlings and determine if and how Sp7 binding and activity is modulated by two common buffers. Based on previous research, we hypothesize that inoculation buffer components in will distinctly alter the way in which Sp7 interacts with seedlings, affecting plant growth overall.

Material and Methods

Experimental design and general information

The experiment consisted of 4 seed treatments 1) PBS, 2) PBS+Sp7, 3) $MgSO_4$, 4) $MgSO_4$+Sp7) with ten biological replicas each, and arranged in a completely randomized design. Maize seeds were sown in 0.3L pots filled with autoclaved commercial substrate (Traysubstrat®, Klasmann-Deilmann, Gmbh, Geeste, Germany) characterized by having an extra fine structure and pH of 6, which was sufficient for this study since ranges for N-fixation by *Azospirillum* spp. are between 5.5 and 9 (Day and Döbereiner 1976). Both inoculated and non-inoculated (control) maize seeds were maintained in a greenhouse on the Escola Tecnica Superior d' Enginyeria Agraria (ETSEA) Campus at the University of Lleida, in Catalonia, Spain. They were maintained at 70-80% humidity, 25-30ºC, and protected from insect attack by an anti-aphid mesh. Automatic drip irrigation without nutrient amendment was administered in the morning and evening every day for an hour.

Imbibition curve preparation

A water imbibition curve was defined for maize. Initially, groups of ten maize (*Zea mays* L. Mill cv. B73) seeds (with five replicates) were disinfected with 70% ethanol (EtOH) for 2min. Seeds were then disinfected with 4% sodium hypochlorite (NaClO) for 15min (under constant agitation) and subsequently rinsed six times with sterile distilled water (SDW). Finally, seeds were dried on sterile paper.

The seeds, prepared as above, were weighed and moved to 50mL Falcon tubes containing SDW and maintained at 30ºC for 30min. The seeds were removed from the SDW and briefly allowed to dry on sterile distilled paper. Group seed weight was recorded. This process was repeated until the seeds stopped water uptake. A linear regression model was calculated from the curve and it was estimated that to imbibe 70% of its potential, the seeds should be left for 156min to absorb 0.05mL.

Azospirillum brasilense Sp7 inoculum preparation and inoculation

The *Azospirillum brasilense* Sp7 strain was kindly provided by the *Colección Española de Cultivos Tipo* (acc. CECT 590) at the Polytechnic University of Valencia (Spain). The material arrived freeze-dried and was cultivated in Petri® dishes containing sterile nitrogen free broth medium (Nfb) supplemented with 15mL/L of 1:400 aqueous solution of Congo-red (CR) (Bashan et al., 1993) for 48h.

To prepare the Sp7 suspension, OAB liquid media [per liter for Solution A: (g/L)DL-malic acid, 5; NaOH, 3; $MgSO_4 \cdot 7H_2O$, 0.2; $CaCl_2$, 0.02; NaCl, 0.1; NH_4Cl, 1; yeast extract, 0.1; $FeCl_3$, 0.01; (mg/1) $NaMoO_4 \cdot 2H_2O$, 2; $MnSO_4$, 2.1; H_3BO_3, 2.8; $Cu(NO_3)_2 \cdot 3H_2O$, 0.04; $ZnSO_4 \cdot 7H_2O$, 0.24 – per 100mL for Solution B: (g/L) K_2HPO_4, 6; KH_2PO_4, 4 - Solution A+B post-autoclaving, pH 6.8] was prepared as described by Okon et al. (1977), inoculated with a single Sp7 colony selected from the CR medium and incubated at 32°C in constant agitation (8.96g) for 48 hours. The bacterial suspension was allowed to reach its late-log growth phase with an absorbance of 0.399nm at OD_{600} (using an Amersham Biosciences Ultraspec 3100 Pro spectrophotometer); a concentration yielding approximately $1.16x10^8 cfu \cdot mL^{-1}$ based on a previously established bacterial curve.

All seeds were disinfected with 4% NaClO for 15min (under constant agitation) and washed six times with SDW in the laminar flow hood. They were laid out to dry on sterile autoclaved paper until all water had evaporated. Seeds were then inoculated with the rhizobacteria via soaking at approximately $1.16x10^8 cfu \cdot mL^{-1}$ per seed. To do so, 10mL of the bacterial suspension was aliquoted for each inoculated seed group of ten and pelleted by centrifuging at 448g for 10min. When PBS was used as inoculation buffer, the supernatant was poured off and the bacterial pellet was washed twice with 1xPBS adjusted to a pH of 7.4 (per L for 10xPBS: 80g NaCl, 2g KH_2PO_4, 29g Na_2HPO_4 12 H_2O, 2g KCl, 2g NaN_3). Then 0.056 mL 1X PBS was added to the tube together with ten sterile maize seeds and vortexed. In the case of $MgSO_4$, the bacterial pellet was washed twice with autoclaved 30mM $MgSO_4$, and then resuspended in the same volume of buffer solution as for PBS (Mangmang et al., 2015). For control groups, ten sterile seeds were placed in tubes with buffer only. All treatments and controls were left in horizontal agitation at 8.96g to imbibe as previously described.

Plant measurements

Maize leaf arch height and chlorophyll contents (SPAD 502Plus, Konica Minolta) were recorded four weeks after planting. Arch height was measured from the soil surface to the arch of the uppermost leaf that was at least 50% emerged from the whorl.

Root structure analysis

Plant roots from all treatments were washed, extended on glass and photographed. Photographs were scanned and analyzed with WinRHIZO® (version 2009; Regent Instruments Inc., Quebec, ON, Canada).

Transmission electron microscopy (TEM)

To visualize the *Azospirillum* polar flagella, a drop of bacterial suspension in OAB was applied onto a Formvar©-covered electron microscope 200mesh copper grid for 1min.

The liquid was absorbed by filter paper, then a drop of the staining solution (1% uranyl acetate in water) was applied to the grid and allowed to absorb for 30s. After drying, the specimen was ready to be introduced into the electron beam of an EM 910 Transmission Electron Microscope (Zeiss, Oberkochen, Germany). A minimum of two grids per treatment were analysed (Borisov et al., 2009).

Scanning electron microscopy (SEM)

To visualize the biofilm formed by bacterial root colonization with scanning electron microscopy (SEM), root pieces were excised for both treatment groups and controls, and fixed in 3% (v/v) glutaraldehyde solution buffered with 0.1M phosphate buffer (pH 7.4) for 3h at room temperature. They were then postfixed in 1% (v/v) osmium tetraoxide in the same buffer. Specimens were washed three times in sterile distilled water and treated with aqueous solution of uranyl acetate 2% (w/v) for 40min. After fixation, samples were dehydrated through a graded ethanol series (30–100%) followed with acetone (100%), critical-point dried, mounted on aluminum stubs, coated with gold and examined with a Jeold JSM-6300 scanning electron microscope (Guerrero-Molina et al., 2012).

Statistical analysis

Statistical analyses were conducted for all the obtained data for each treatment group by using a one-way ANOVA test and Tukey's HSD test. Analyses were processed with JMP® 12.1 (SAS Institute Inc.), while software and graphics were created with Microsoft Excel 2016. The F-ratio of 0.05 for a One-way ANOVA was used to evaluate the difference between averages.

Results

Chlorophyll contents (SPAD) was significantly higher in treatments with PBS+Sp7 ($p<0.05$) than other treatment groups (Figure 1). Scanned images of the washed roots reflected qualitative differences between root systems (Figure 2).

FIGURE 1
FIGURE 2

WinRHIZO® analysis evidenced the efficacy of Sp7, detailing value increases in all root parameters over treatments without Sp7 (Tables 1 and 2). Then, subjecting the WinRHIZO® data to a one-way ANOVA statistical analysis revealed the abundance of certain root diameters to be significant between treatment groups. $MgSO_4$+Sp7 inoculated seedlings had significantly more abundance of roots measuring 2.0-2.5mm and 4.5-5.0mm than other treatment groups (Table 2).

TABLE 1
TABLE 2

Plant arch height (Figure 3) was significantly shorter for $MgSO_4$+Sp7 seedlings compared to other groups. This finding was disproportional to increased root hair proliferation in $MgSO_4$+Sp7 seedlings (Table 1).

FIGURE 3

FIGURE 4

TEM examination of root microorganisms confirmed that the size of Sp7 bacterial cells is variable in general. There were some spiral shaped cells (typical to the *Azospirillum* genus) (Figure 4A), but the most abundant Sp7 phenotype was smaller (1.2x2-3µm) exhibiting a polar flagella (Figure 4B). All inoculated plants revealed different degrees of bacterial colonization and biofilm formation on the root surfaces, but from these figures, there was not a clear pattern or influence based on buffer (Figure 4C). The higher magnification in Figure 4D shows the Sp7 adherence to the root.

Discussion

Azospirillum brasilense Sp7 inoculation has repeatedly been shown to enhance plant growth (Bashan et al., 2006; Fukami et al., 2016). Our work expands upon these findings by demonstrating the specific ways in which Sp7 modulates plant growth depending upon buffer choice. When Sp7 is inoculated with PBS or $MgSO_4$ buffers, plant root diameter, height and leaf chlorophyll contents are differentially affected. Furthermore, we have found that these differences are not attributed to variations in bacterial binding to roots.

Plants inoculated with $MgSO_4$+Sp7 had a higher frequency of thick root hairs, but plant height was stunted relative to other treatment groups. This combination of events is unusual since Sp7 priming typically enhances plant growth overall, both above and below ground (Correa et al., 2007). A similar study reporting stunting in the presence of PGPR attributed it to other sources of unforeseen stress. Pathogenesis-related (PR) proteins were also detected, implying the activation of systemic acquired resistance (SAR) (Maurhofer et al., 1994). Proteomic analysis would enhance our findings, and help to understand this affect.

The $MgSO_4$ buffer augments the abundance of thicker root hairs compared to PBS in inoculated plants. There are several possible explanations for this: a) Sp7 potentiates the interaction of the buffer elements with early Mg-responsive genes in root hairs (Guo et al. 2016); b) Mg^{+2} in the buffer improves N_2 fixation by Sp7, thereby increasing plant root growth (Peng et al., 2018); c) high Mg-supply decreases starch and sucrose accumulation in leaves, but increases root concentrations, enhancing carbohydrate import into associated rhizobia (Peng et al., 2018). In the case of Sp7, enhanced carbohydrate supply would potentiate its hormone production, which stimulates plant root hair development.

Finally, PBS+Sp7 inoculation causes significant increases in chlorophyll production. Increased chlorophyll contents reflects C gain in the C-assimilation process through photosynthesis; and higher C absorption is often a byproduct of stress (Hernández-González et al. 2010). Work carried out with a similar PGPR, *Bacillus thuringiensis*, revealed that the bacteria was instrumental in reducing salt-stress in the plant by targeting the up-regulation of chloroplast proteins (Subramanian et al., 2016). Accordingly, the NaCl present in the PBS buffer may exert stress on the plant, but Sp7 works to positively counterbalance this reaction by increasing chloroplast activity.

Our findings suggest that both common buffers tested interact with the plant to stimulate small stress reactions that are mitigated by Sp7, and that Sp7 root binding is not affected by either of the buffers tested. In conclusion, PBS is the most suitable buffer to use because plants inoculated with PBS+Sp7 exhibit higher C adsorption in leaf tissues, while $MgSO_4$+Sp7 presents a distress element that leads to stunted plant height.

References

Alström, S. 1991. Induction of disease resistance in common bean susceptible to halo blight bacterial pathogen after seed bacterization with rhizosphere pseudomonads. J. Gen. Appl. Microbiol. **37**:495–501.

Ashraf, M., Hasnain, S., Berge, O., Mahmood, T. 2004. Inoculating wheat seedlings with exopolysaccharide-producing bacteria restricts sodium uptake and stimulates plant growth under salt stress. Biol. Fertil. Soil. **40**:157–162.

Barassi, C.A., Sueldo, R.J., Creus, C.M., Carrozzi, L.E., Casanovas, E.M., Pereyra, M.A. 2007. *Azospirillum* spp., a dynamic soil bacterium favourable to vegetable crop production. Dyn. Soil Dyn. Plant **1**:68–82.

Barassi, C., Fasciglione, G., Casanovas, E. 2015. *Azospirillum* spp. and Related PGPRs Inocula Use in Intensive Agriculture. In: Cassán, F.D., Okon, Y., Creus, C.M. (eds), Handbook for *Azospirillum*. Springer International Publishing, Switzerland, pp. 447-466.

Bashan, Y., Levanony, H. 1985. An improved selection technique and medium for the isolation and enumeration of *Azospirillum brasilense.* Can. J. Microbiol. **31**:947-952.

Bashan, Y., Holguin, G., Lifshitz, R. 1993. Isolation and characterization of plant growth-promoting rhizobacteria. In: Glick, B.R., Thompson, J.E. (eds), Methods in Plant Molecular Biology and Biotechnology. CRC Press, Boca Raton, FL, USA.

Bashan, Y., Holguin, G. 1996. Nitrogen-fixation by *Azospirillum brasilense* cd is promoted when co-cultured with a mangrove rhizosphere bacterium (*Staphilococus sp.*). Soil Biol. Biochem. **28**(12):1651-1660.

Bashan, Y., Holguin, G. 1997. *Azospirillum*-plant relationships: environmental and physiological advances (1990–1996). Can. J. Microbiol. **43**:103–121.

Bashan, Y., Bustillos, J.J., Leyva, L.A., Hernandez, J.P., Bacilio, M. 2006. Increase in auxiliary photoprotective photosynthetic pigments in wheat seedlings induced by *Azospirillum brasilense*. Biol. Fertil. Soils **42**(4):279-285.

Bashan, Y., Trejo, A., de-Bashan, L.E. 2011. Development of two culture media for mass cultivation of *Azospirillum* sp. and for production of inoculants to enhance plant growth. Biol. Fertil. Soils **47**:963–969.

Borisov, I.V., Schelud'ko, A.V., Petrova, L.P., Katsy, E.I. 2009. Changes in *Azospirillum brasilense* motility and the effect of wheat seedling exudates. Microbiol. Res. **164**:578—587.

Carpenter, S.R., Caraco, N.F., Correll, D.L., Howarth, R.W., Sharpley, A.N., Smith, V.H. 1998. Nonpoint Pollution of Surface Waters with Phosphorous and Nitrogen. Ecol. Appl. **8**(3):559-568.

Casanovas, E.M., Barassi, C.A., Sueldo, R.J. 2002. *Azospirillum* inoculation mitigates water stress effects in maize seedlings. Cereal Res. Commun. **30**:343–350.

Casanovas, E.M., Barassi, C.A., Andrade, F.H., Sueldo, R.J. 2003. *Azospirillum*- inoculated maize plant responses to irrigation restraints imposed during flowering. Cereal Res. Commun. **31**:395–402.

Cohen, A.C., Travaglia, C.N., Bottini, R., Piccoli, P.N. 2009. Participation of abscisic acid and gibberellins produced by endophytic *Azospirillum* in the alleviation of drought effects in maize. Botany **87**:455-462.

Correa, O.S., Romero, A.M., Montecchia, M.S., Soria, M.A. 2007. Tomato genotype and *Azospirillum* inoculation modulate the changes in bacterial communities associated with roots and leaves. J. Appl. Microbiol. **102**:781–786.

Creus, C.M., Sueldo, R.J., Barassi, C.A. 1997. Shoot growth and water status in *Azospirillum*-inoculated wheat seedling grown under osmotic and salt stresses. Plant Physiol. Biochem. **35**(12):939-944.

Day, D.M., Döbereiner, J. 1976. Physiological aspects of N_2-fixation by a *Spirillum* from *Digitaria* roots. Soil Biol. Biochem. **8**:45-50.

Forde, B.G., Lea, P.J. 2007. Glutamate in plants: metabolism, regulation, and signaling. J. Exp. Bot. **58**:2339–2358.

Fukami, J., Nogueira, M.A., Araujo, R.S., Hungria, M. 2016. Accessing inoculation methods of maize and wheat with *Azospirillum brasilense*. AMB Express **6**(3).

Gafny, R., Okon, Y., Kapulnik, Y. 1985. Adsorption of *Azospirillum brasilense* to corn roots. Soil Biol. Biochem. **18**(1):69-75.

Guerrero-Molina, M.F., Winik, B.C., Pedraza, R.O. 2012. More than rhizosphere colonization of strawberry plants by *Azospirillum brasilense*. Appl. Soil Ecol. **61**:205-212.

Guo, W.L., Nazim, H., Liang, Z., Yang, D. 2016. Magnesium deficiency in plants: an urgent problem. Crop J. **4**:83-91.

Hartmann, A., Zimmer, W. 1994. Physiology of *Azospirillum*. In: Okon, Y. (ed), *Azospirillum*/plant associations. CRC Press, Boca Raton, pp. 15-39.

Hernández-González, O., Yoisura, S.V., Larqué-Saavedra, A. 2010. Photosynthesis, transpiration, stomatal conductance, chlorophyll fluorescence and chlorophyll content in *Brosimum alicastrum*. Bothalia Journal **44**(6):165-176.

Khalid, M., Bilal, M., Hassani, D., Iqbal, H.M.N., Wang, H., Huang, D. 2017. Mitigation of salt stress in white clover (*Trifolium repens*) by *Azospirillum brasilense* and its inoculation effect. Bot. Stud. 58 (1):5.

Kumar, A.S., Lakshmanan, V., Caplan, J.L., Powell, D., Czymmek, K.J., Levia, D.F., Bais, H.P. 2012. Rhizobacteria *Bacillus subtilis* restricts foliar pathogen entry through stomata. Plant J. **72**:694–706.

Li, P., Cao, W., Fang, H., Xu, S., Yin, S., Zhang, Y., Lin, D., Wang, J., Chen, Y., Xu, C., Yang, Z. 2017. Transcriptomic Profiling of the Maize (*Zea mays* L.) Leaf Response to Abiotic Stresses at the Seedling Stage. Front. Plant Sci. **8**:290.

Lugtenberg, B., Kamilova, F. 2009. Plant-Growth-Promoting Rhizobacteria. Ann. Rev. Microbiol. **63**:541-556.

Mangmang, J.S., Deaker, R., Rogers, I. 2015. Early seedling growth response of lettuce, tomato and cucumber to *Azospirillum brasilense* inoculated by soaking and drenching. J. Hortic. Sci. **42**(1):37-46.

Maurhofer, M., Hase, C., Meuwly, P., Métraux, J.P., Défago, G. 1994. Induction of systemic resistance of tobacco to tobacco necrosis virus by the root-colonizing *Pseudomonas fluorescens* strain CHA0: Influence of the *gacA* gene and of pyoverdine production. Phytopathology **84**:139–146.

Mugilan, I., Gayathri, P., Elumalai, E.K., Elango, R. 2011. Studies on improve survivability and shelf life of carrier using liquid inoculation of *Pseudomonas striata*. Int. J. Pharm. Bio. **2**(4):1271-1275.

Niu, Y.F., Jin, G.L., Zhang, Y.S. 2014. Root development under control of magnesium availability. Plant Signal. Behav. **9**:e29720.

Okon, Y., Albrecht, S.L., Burris, R.H. 1977. Methods for growing *Spirillum lipoferum* and for counting it in pure culture and in association with plants. Appl. Environ. Microbiol. **33**:85-88.

Perrig, D., Boiero, M.L., Masciarelli, O.A., Penna, C., Ruiz, O.A., Cassán, F.D., Luna, M.V. 2007. Plant-growth-promoting compounds produced by two agronomically important strains of *Azospirillum brasilense*, and implications for inoculant formulation. Appl. Microbiol. Biotechnol. **75**:1143–1150.

Rivera, D., Obando, M., Barbosa, H., Rojas Tapias, D., Bonilla, R. 2014. Evaluation of polymers for the

399 liquid rhizobial formulation and their influence in the Rhizobium-Cowpea interaction. Univ. Sci. **19**
400 (3):265-275.
401
402 Subramanian, S., Souleimanov, A., Smith, D.L. 2016. Proteomic studies on the effects of lipo-
403 chitooligosaccharide and thuricin 17 under unstressed and salt stressed conditions in *Arabidopsis*
404 *thaliana*. Front. Plant Sci. **7**:1314.
405
406 Ton, J., Jakab, G., Toquin, V., Flors, V., Iavicoli, A., Maeder, M.N., Métraux, J.P., Mauch-Mani, B.
407 2005. Dissecting the β-aminobutyric acid–induced priming phenomenon in *Arabidopsis*. Plant Cell
408 **17**:987–99.
409
410 Van Peer, R., Niemann, G.J., Schippers, B. 1991. Induced resistance and phytoalexin accumulation in
411 biological control of Fusarium wilt of carnation by *Pseudomonas* sp. strain WCS417r. Phytopathology
412 **81**:728–34.
413
414 Verhagen, B.W.M., Glazebrook, J., Zhu, T., Chang, H.-S., Van Loon, L.C., Pieterse, C.M.J. 2004. The
415 transcriptome of rhizobacteria-induced systemic resistance in *Arabidopsis*. Mol. Plant Microbe Interact.
416 **17**:895–908.
417
418 Wang, Y.Q., Ohara, Y., Nakayashiki, H., Tosa, Y., Mayama, S. 2005. Microarray analysis of the gene
419 expression profile induced by the endophytic plant growth–promoting rhizobacteria, *Pseudomonas*
420 *fluorescens* FPT9601-T5 in *Arabidopsis*. Mol. Plant Microbe Interact. **18**:385–96.
421
422 Venable, J.H., Coggeshall, R. 1965. A simplified lead citrate stain for use in electron microscopy. J. Cell
423 Biol. **25**:407–408.

Table 1. WinRHIZO® root values for four inoculation treatments in maize seedlings.

	PBS	$MgSO_4$	PBS+Sp7	$MgSO_4$+Sp7
Total length (cm)	245.50	265.06	336.23	346.81
Average diameter (cm)	0.76	0.49	0.80	0.86
Total surface area (cm^2)	61.10	68.79	85.06	92.36
Total projected area (cm^2)	19.41	21.88	28.73	29.39
Total volume (cm^3)	1.23	1.42	1.71	1.96

Table 2. Total root area (cm^2) in function of diameter class (mm) for four inoculation treatments in maize seedlings.

Root diameter class (mm)	**Inoculation treatment and total root area (cm^2) in function of root diameter class**			
	PBS	**$MgSO_4$**	**PBS+Sp7**	**$MgSO_4$+Sp7**
0.1-0.5	133	144	198	196
0.5-1.0	71	73.8	77	91.8
1.5-2.0	8.76	9.25	10.40	14.40
2.0-2.5	3.0	4.3	3.62	6.0*
2.5-3.0	5.34	2.0	1.44	2.95
3.0-3.5	0.6	0.86	2.75	1.80
3.5-4.0	0.32	0.61	0.55	1.12
4.0-4.5	0.17	0.02	0.32	0.68
4.5-5.0	0.11	0.69	0.32	1.07*

Data was subjected to a one-way ANOVA test and values with an asterisk (*) denote significant differences between treatments ($p<0.05$).

212

Figure Legends

Figure 1. Relative chlorophyll contents of maize seedlings subjected to four inoculation treatments. Statistical differences ($p<0.05$) are denoted by different letters and error bars represent a 5% standard error (SE).

Figure 2. Representative images of maize seedling root systems with four inoculation treatments: PBS, $MgSO_4$, PBS+Sp7 and $MgSO_4$+Sp7. Images are the most representative example from sample groups of five (per treatment). C.) bar = 10cm.

Figure 3. Average highest leaf arch height (cm). Statistical differences ($p<0.05$) are denoted by different letters and error bars represent a 5% SE.

Figure 4. Electron microscopy (EM) images of *Azospirillum brasilense* (Sp7). A-B. Transmission electron microscopy (TEM) images of Sp7. C-D. Scanning electron micrographs (SEM) of Sp7-treated maize roots (bars: A & B = 2.5µm, C = 2µm, D = 6µm).

451 **Figure 1.**
452

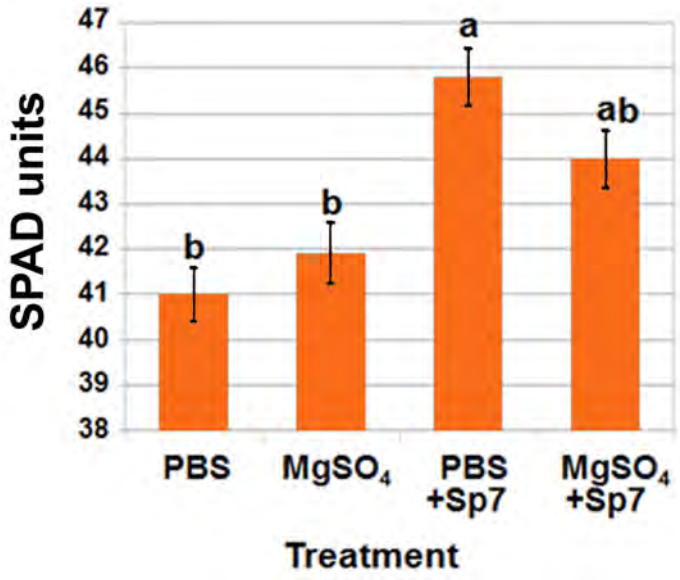

454 **Figure 2.**

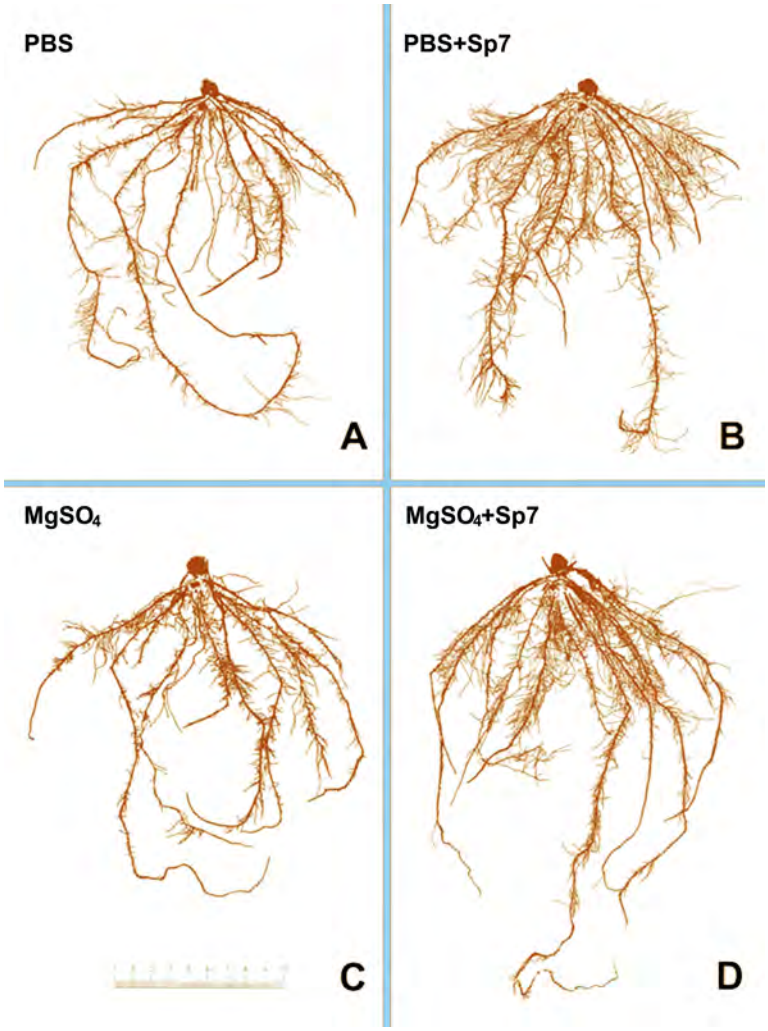

214

456 **Figure 3.**

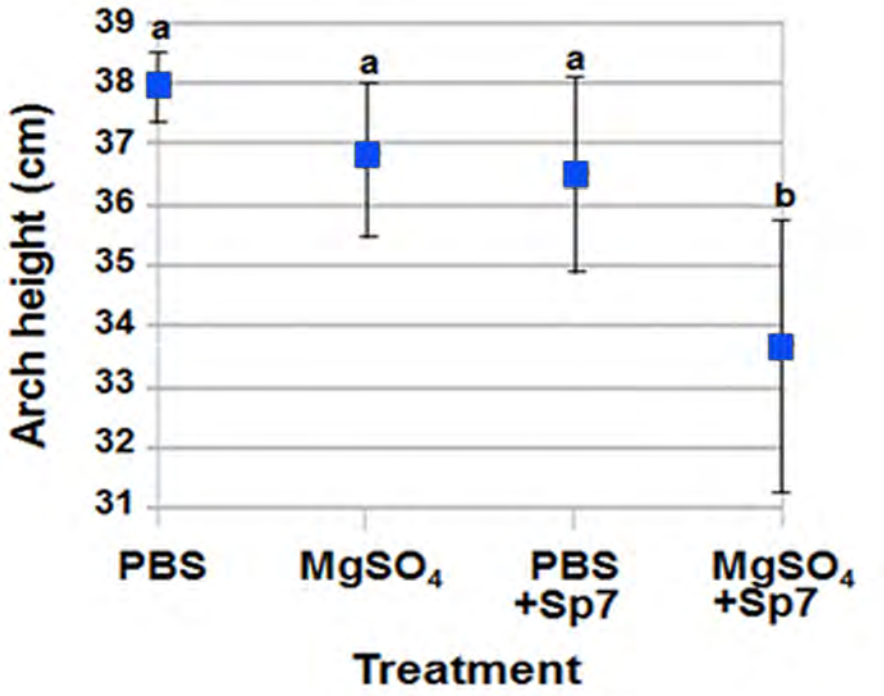

458 **Figure 4.**
459

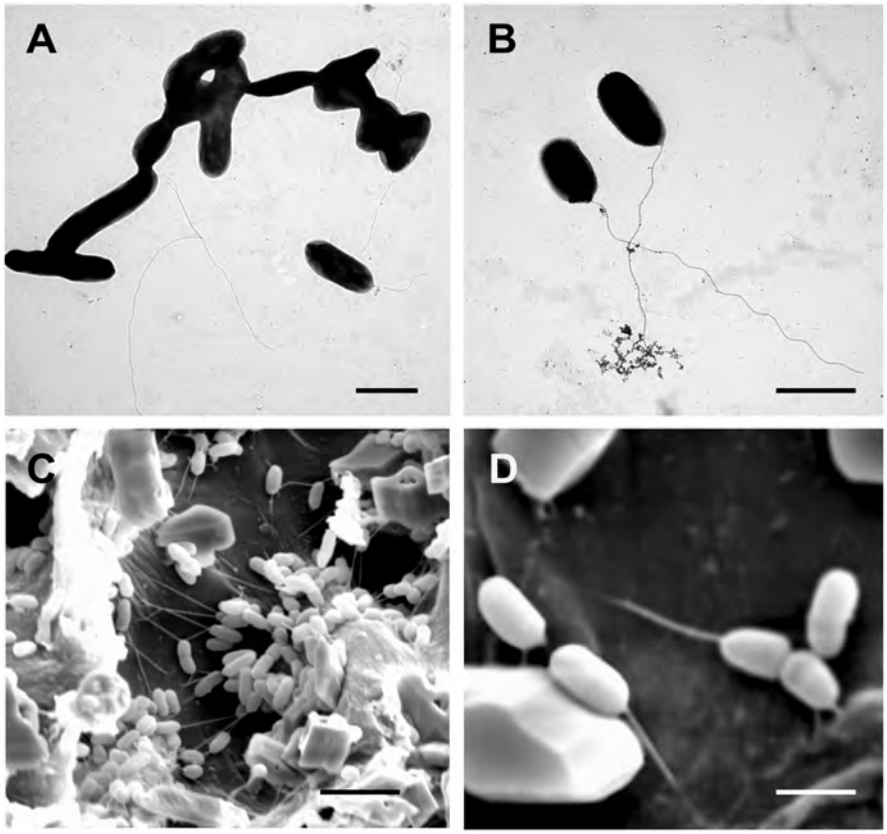

215

ANNEX 2

Lade SB, Román C, Cueto-Ginzo AI, Maneiro L, Muñoz P, Medina V (2018) Root development in agronomically distinct six-rowed barley (*Hordeum vulgare* L.) cultivars inoculated with *Azospirillum brasilense* Sp7. *Plant Breeding Journal* 137: 338-345.

Received: 24 June 2017 | Accepted: 3 March 2018

DOI: 10.1111/pbr.12593

ORIGINAL ARTICLE

WILEY Plant Breeding

Root development in agronomically distinct six-rowed barley (*Hordeum vulgare*) cultivars inoculated with *Azospirillum brasilense* Sp7

Sarah B. Lade[1] | Carla Román[1] | Ana I. Cueto-Ginzo[1] | Laura Maneiro[2] | Pilar Muñoz[1,3] | Vicente Medina[1,3]

[1]Escola Tècnica Superior d'Enginyeria Agrària (ETSEA), Departament de Producció Vegetal i Ciència Forestal, Universitat de Lleida, Lleida, Spain

[2]Biomolecular Lab., Department of Introduction to Agricultural Sciences, National University of Mar del Plata, Balcarce, Argentina

[3]AGROTECNIO Center, Escola Tècnica Superior d'Enginyeria Agrària (ETSEA), Universitat de Lleida, Lleida, Spain

Correspondence
Sarah B. Lade, Escola Tècnica Superior d´ Enginyeria Agrària (ETSEA), Departament de Producció Vegetal i Ciència Forestal, Universitat de Lleida, Lleida Spain.
Email: sarahb.lade@pvcf.udl.cat

Funding information
MINCYT, Grant/Award Number: AGL2010-15691

Communicated by: E. Igartua

Abstract

The growth-promoting rhizobacteria *Azospirillum brasilense* Sp7 positively affects many crops, but its influence on barley remains to be fully investigated. The aim of this study was to track early root growth of four barley cultivars that are widely used in Spanish breeding programmes under different growing scenarios. Different growth conditions are hypothesized to affect the response of young plants to *A. brasilense* Sp7, so seeds were inoculated with *A. brasilense* Sp7 and directly sown in the growth chamber, or planted in vitro. Plant height was measured and root structure analysed with the WinRHIZO program. *Azospirillum brasilense* Sp7 inoculation increased the length, surface area and number of root tips in both systems and in most cultivars in a similar way. Cultivars 'Barberousse' and 'Plaisant' were the most responsive to *A. brasilense* Sp7 treatment, while 'Albacete' was especially interesting in terms of its physiological interaction with *A. brasilense* Sp7 under abiotic stress imposed by the in vitro system. The utility of the in vitro system is criticized.

KEYWORDS
Azospirillum brasilense Sp7, root analysis, six-rowed barley

1 | INTRODUCTION

Barley (*Hordeum vulgare* L.) is especially important in the Mediterranean area, where the yield of certain crops is evaluated by their adaptability or tolerance to abiotic stress, mainly drought (López-Castañeda & Richards, 1994; Teulat, Merah, & This, 2001). Among the agronomic practices that favour the adaptation of barley to unfavourable environments, the use of plant growth-promoting rhizobacteria (PGPR), such as *Azospirillum brasilense* (Tarrand et al., 1979), is increasingly popular. Its ability to increase auxin production in host plants leads to greater root surface area (Spaepen & Vanderleyden, 2011), which in turn alleviates adaptive stress to drought by increasing the absorption of water and minerals (Vacheron et al., 2013). *Azospirillum brasilense* inoculation has been shown to induce early vigorous growth, which is important in providing assimilates for grain filling when drought or any other kind of stress occurs postanthesis (Siddique, Belford, Perry, & Tennant, 1989).

The most influential theory regarding the precise mode of action of *A. brasilense* in plants against abiotic stress suggests crosstalk between two stress signalling pathways by means of priming and initiating induced systemic response (ISR) in the plant (Omar et al., 2000; Vacheron, Renoud, Muller, Babalola, & Prigent-Combaret, 2015). Regardless of this overarching mechanism, *A. brasilense*-induced processes observed in plants are tightly intertwined with and influenced by the host plant's genetic makeup (Correa, Romero, Montecchia, & Soria, 2007). In this way, understanding the genotype-by-environment (G × E) interaction, or barley cultivar × *A. brasilense* treatment interaction (C × T), can help elucidate genotype–inoculum specificities, which can be harnessed to ensure the ontogenesis of a relationship that imparts a positive plant

response. Investigation into this relationship can complement breeders' goals by optimizing economically important traits, substantiating that they are not diminished by the inoculum (Rashid, 2014).

The possible relationship between *A. brasilense* and barley has been confirmed in previous studies (Zawoznik, Vázquez, Díaz Herrera, & Groppa, 2014), and it has been observed that different genotypes indeed influence the activity of rhizobacteria differently, leading to distinct root architecture and/or exudation profiles (Comas & Eissenstat, 2009). As such, four-six-rowed, winter-type barley cultivars characterized for their contrasting agronomic performance in the Mediterranean area have been chosen as subjects herein, viz., 'Albacete,' 'Barberousse,' 'Plaisant' and 'Orria.' These cultivars are traditionally classified and distinguished primarily by their vulnerability to drought (Voltas et al., 1999). Likewise, the genotype of the bacterial strain also influences the plant–bacterial interaction. In this work, the *Azospirillum* Sp7 strain has been selected because it responds more acutely to exogenously induced abiotic stress factors. Sp7 is an epiphyte, only colonizing plant root surfaces and thus remaining more closely connected to the outer environment (Kamnev, Tugarova, Tarantilis, Gardiner, & Polissiou, 2011).

In general, field performance of the bacteria in the rhizosphere is affected by soil-related factors as well, such as nitrogen content (Muthukumarasamy, Revathi, & Lakshminarasimhan, 1999; Muthukumarasamy, Revathi, & Loganathan, 2002), soil type (de Oliveira, de Canuto, Urquiaga, Reis, & Baldani, 2006), soil sterility or any support system (or lack thereof) (dos Reis Junior, Massena Reis, Urquiaga, & Döbereiner, 2000). So to investigate this relationship, we have two selected distinct growing scenarios: (1) direct sowing in sterile soil under growth chamber conditions, and (2) a media-less in vitro premise, fit for sterile laboratory conditions. This work explores the two distinct environments held under constant experimental conditions to analyse the effects of *A. brasilense* Sp7 on barley root systems. To best summarize the overall effect of the C × T interaction, a two-way ANOVA is conducted to understand each studied parameter. Findings can help uncover mechanisms underlying the barley/*A. brasilense* Sp7 interaction in different scenarios for each of these cultivars.

2 | MATERIALS AND METHODS

2.1 | Barley cultivars

The seeds of the four selected barley cultivars ('Albacete,' 'Barberousse,' 'Plaisant' and 'Orria') were obtained from the Aula Dei Experimental Station of the CSIC of Zaragoza, Spain. 'Albacete' is an inbred line that was first cultivated in the middle of the 20th century, within a local heterogeneous population of landowners in the Spanish province of Albacete. It is drought-tolerant and with a stable grain yield, which is the reason why it has been cultivated across vast expanses in dry zones for decades. 'Barberousse' was released in France in 1980. It was obtained from the cross [259 711/(Hatif de Grignon/Ares)/Ager] and is sensitive to drought. However, it is known for its high productivity and adaptability (Farré et al., 2011). 'Plaisant' is another French cultivar that was obtained in 1982. It has a strong vernalization requirement, causing late heading and slow maturing, so it often performs poorly in Mediterranean environments. It is grown for malt and originates from a rather narrow genetic base (Yau, 2016). Finally, 'Orria' is a productive Spanish cultivar of CIMMYT origin, well-adapted to fertile, rain-fed environments. It was released in 1993 and is commonly used as a parental line for crossing with other cultivars (Muñoz, Voltas, Araus, Igartua, & Romagosa, 1998). 'Barberousse,' 'Orria' and 'Plaisant' have been found to suffer acutely from the effect of terminal heat and drought stresses on grain growth, whereas 'Albacete' is rather insensitive to these climatic factors, but performs poorly in environments favouring a high grain weight due to its susceptibility to lodging (Voltas et al., 1999).

2.2 | *Azospirillum brasilense* inoculum and inoculation method

The *Azospirillum brasilense* Sp7 strain (ATCC 29145) was kindly provided by the "Colección Española de Cultivos Tipo" (CECT) of the Polytechnic University of Valencia (Spain). For the *A. brasilense* Sp7 suspension, a peptone yeast broth liquid medium amended with $CaCl_2$ 0.04% was prepared, as described by Döbereiner, Marriel, and Nery (1976), and incubated at 32°C under constant agitation at 100 rpm for 20 hr. At this point, the bacterial suspension had reached its late log-growth phase, with an absorbance of 1.0 at $OD_{600\ nm}$ (determined via an Amersham Biosciences Ultraspec 3100 Pro spectrophotometer). This yielded an ideal bacterial density of 1×10^8 cfu/ml.

The seeds of the four above-mentioned cultivars were disinfected with 70% ethanol for 2 min, soaked in 1% sodium hypochlorite for 10 min under constant agitation (100 rpm) and washed six times with sterile distilled water. Seeds were dried on sterile autoclaved paper until all water had evaporated. They were then inoculated with the rhizobacteria via the seed-coat contamination method at 1×10^8 cfu/ml. To do so, 1 ml of the bacterial suspension was aliquoted for each of the four seed groups and centrifuged at 2319.85 RCF (g) 5000 rpm for 10 min. The supernatant was poured out, and the pellet was resuspended in 1 ml of 1× PBS: 80 g NaCl, 2 g KH_2PO_4, 29 g $Na_2HPO_4{\cdot}12H_2O$ and 2 g KCl and adjusted to a pH of 7.4 (per litre for 10× PBS). Then, the inoculum was vortexed, and between 0.21 and 0.24 ml of the inoculum was added to each tube of 30 seeds, depending on the cultivar (see Table 1). The tubes were put into horizontal agitation for 30 min to 1 hr 15 min, depending on the previously defined imbibition time for each cultivar

TABLE 1 Time and volume of inoculum solution (ml) required to achieve 70% seed imbibition in 30 seeds for four barley cultivars: 'Albacete,' 'Barberousse,' 'Plaisant' and 'Orria'

Cultivar	70% Imbibition absorbance (ml)	Time (hr:min)
Albacete	0.21	00:30
Barberousse	0.24	01:15
Plaisant	0.18	01:05
Orria	0.22	01:00

(Table 1). Non-inoculated (control) seeds of each cultivar served as the controls and were "inoculated" with PBS only. Note that only a total of 18 inoculated seeds were needed per cultivar (nine for direct sowing and nine in vitro), but inoculation was conducted in groups of 30 according to the imbibition curve so as to select and plant the most homogenous seeds postinoculation.

2.3 | Direct sowing (under growth chamber conditions)

For direct sowing (Figure S1), the treatments were defined as *A. brasilense*-inoculated seeds or non-inoculated seeds that were treated solely with PBS buffer and served as the controls. Each pot contained one seed and was considered both as the randomization unit and the observational unit. Then, each treatment was replicated nine times per cultivar in a completely randomized design. The seeds were planted in 0.3-L pots filled with autoclaved commercial substrate (Traysubstrat®, Klasmann-Deilmann, Gmbh, Geeste, Germany) characterized by having an extra fine structure and pH of 6. Both inoculated and non-inoculated (control) barley seeds were sown and maintained in a growth chamber (1,282 × 687 × 1,487 mm) at 23–25°C with a photoperiod of 16-hr light/8-hr dark cycle under 10,000 lux fluorescent bulbs. Relative humidity was regulated at 90%–95%, and emerged plants were watered twice a week by flooding. Forty-five days after sowing, when the seedlings started to tiller and had reached a phenological growth stage of 21 according to the BBCH scale (Lancashire, Bleiholder, Langelüddecke, & Stauss, 1991), root development analysis was performed. Roots were gently washed with distilled water, extended on glass and scanned with an Epson Perfection V700 modified flatbed scanner at an optical resolution of 4,800 dots per inch.

2.4 | In vitro procedure

For the in vitro assay, the experimental units for inoculated and non-inoculated (controls) were adjusted to the in vitro model. Three barley seeds were arranged linearly on a piece of sterile cardboard humidified with sterile distilled water and placed in a sterile transparent plastic bag (55-oz. 19 × 30 cm, Nasco Whirl-Pak® sampling bag; Sigma-Aldrich). Each bag of three seeds served as a randomization unit and was replicated three times per treatment and per cultivar in a completely randomized design. Closed bags were maintained at 23–25°C (Figure S2) in the dark for five days, then moved into the growth chamber (conditions described above) for 10 more days. After 15 days, which was enough time for all seeds to germinate and reach stages 09–10 according to the BBCH scale, images of the plastic bags with germinated seeds were obtained with a scanner, as performed at the end of the previous assay.

2.5 | Plant growth analysis

For both direct sowing and in vitro assays, root development analysis was performed to evaluate length (cm), surface area (cm^2) and number of root tips using WinRHIZO software (version 2009; Regent Instruments Inc., Quebec, ON, Canada). Root imaging tools, such as WinRHIZO, use a skeletonization method to generate root representation and to count root tips by counting endpoints of the root skeleton. Via user-defined average root thickness of primary roots, it is then possible to obtain an estimate of the number of primary roots and the number of lateral roots contained in that image (Cai et al., 2015). Directly sown samples were also analysed for plant height at 45 days after planting. Effects of the treatment, growth characteristics, cultivars and their interactions were determined using the linear model in the case of direct sowing and the linear mixed model for in vitro, whereby bag was held as the random factor. Both direct sowing and in vitro growing scenarios called for a two-way analysis of variance (ANOVA) to quantify the overall effect of the anticipated G × E interaction (in this case defined as cultivar × treatment interaction, or C × T) and the related effects. Least significant difference was used for mean separation, and an individual error rate of 95% was considered in all tests. JMP® software version Pro 11.0.0 was used for all analyses (SAS Institute, Cary, NC, USA).

To clarify how each cultivar specifically reacts to Sp7 inoculation compared to the control, and irrespective of the other cultivars, one-way ANOVAs were run for each cultivar. The cultivar was modelled as the independent effect and root growth parameters as dependent. In the case of in vitro growth, the bag was modelled as an additional random effect, just as in the two-way ANOVA.

3 | RESULTS

The cultivar rank order for overall plant performance according to the parameters studied was 'Plaisant,' 'Barberousse,' 'Orria' and 'Albacete.' That is to say barley cv. 'Plaisant' had the most positive growth for both treatments in nearly all parameters measured under both growing scenarios (Table 2).

Two-way ANOVA did not reveal any significant C × T interactions, although it was clear that *A. brasilense* Sp7 had an overall positive effect on plant growth. Specifically, 'Barberousse,' 'Plaisant' and

TABLE 2 Relative overall growth of each barley cultivar ('Albacete,' 'Barberousse,' 'Orria' and 'Plaisant') ±*SE*, regardless of treatment: direct sowing vs. *in vitro*

Method	Cultivar	Length (cm)	Area (cm^2)	Tips (#)
Direct sowing	Plaisant	508 ± 53	496 ± 52	50 ± 8
	Orria	377 ± 26	362 ± 22	26 ± 3
	Barberousse	333 ± 22	325 ± 20	28 ± 6
	Albacete	238 ± 24	244 ± 24	15 ± 1
In vitro	Plaisant	45 ± 4	162 ± 16	36 ± 7
	Orria	46 ± 2	122 ± 9	22 ± 3
	Barberousse	47 ± 4	109 ± 8	22 ± 4
	Albacete	43 ± 3	86 ± 7	19 ± 2

'Albacete' were significantly and positively affected by *A. brasilense* in the direct sowing assay, whereas 'Albacete' was the only cultivar significantly affected by *A. brasilense* treatment in vitro. Effect tests revealed the random factor "bag" to indeed be significant for all in vitro growth parameters.

For direct sowing under growth chamber conditions, the cultivar (C) effect was highly significant for all root parameters analysed: length (cm), surface area (cm^2) and number of tips (Table 3). The effect of *A. brasilense* Sp7 treatment (T) on all root parameters was also significant, especially for the number of tips.

For all radicular parameters in which the T effect was significant under direct sowing, inoculated plants with *Azospirillum* Sp7 had larger values than their non-inoculated counterparts of the same cultivar. Overall, root length increased proportionally for each inoculated cultivar over its non-inoculated counterpart, although one-way ANOVA revealed that 'Barberousse' was the only cultivar to exhibit significantly longer inoculated roots ($p = .034$). Similarly, 'Barberousse' was also the only cultivar to exhibit significantly more root surface area in inoculated plants compared with non-inoculated ones ($p = .028$). The number of root tips was significantly higher for inoculated 'Albacete' ($p = .037$) and 'Plaisant' cultivars ($p = .057$) over their non-inoculated controls.

Inoculated and non-inoculated plants of the same cultivar showed a mixed trend for plant height. Inoculated 'Barberousse' and 'Plaisant' plants were slightly taller than their control counterparts, whereas those of 'Albacete' and 'Orria' were shorter (Figure 1d).

For the in vitro-grown plants, the C effect was significant for root area and number of tips, but not for root length. Neither the T effect nor the C × T interaction was not significant for any of the parameters studied.

In vitro one-way analysis revealed that 'Albacete' was the only cultivar to exhibit significantly longer roots ($p = .029$) (Figure 2a) and a significantly larger root surface area ($p = .025$) (Figure 2b) when inoculated. Interestingly, there were quantifiable differences in the root surface area of non-inoculated cultivars, suggesting rooting capacity to be intrinsic for each cultivar in this growing scenario. Figure 2c depicts the mean number of root tips; a trend towards more root tips was observed in *A. brasilense* Sp7-inoculated seedlings of 'Albacete,' 'Plaisant' and 'Barberousse,' compared with their untreated counterparts.

4 | DISCUSSION

On the whole, this study concurs with literature in that *A. brasilense* Sp7-inoculated root systems display a significant increase in the number and length of root tips, and root surface area (Creus et al., 2005; Dobbelaere, Croonenborghs, Thys, Vande Broek, & Vanderleyden, 1999), adding that such effects take hold irrespective of growing conditions. Although isolated effects (C and T) are significant, there is not any significant interaction between the barley cultivars and *A. brasilense* treatments (C × T) under either growing environment tested.

Seedlings that were directly sown under growth chamber conditions have significantly different growth among inoculated cultivars, indicating an intrinsic variation in cultivar performance. Particularly, 'Barberousse' is the only cultivar to exhibit increased root length and significantly greater root surface area in inoculated plants over non-inoculated ones when directly sown. Historically, 'Barberousse' is the "least drought-tolerant" and most stress-prone cultivar of those studied, lying grounds for the precedent that it has a different degree of responsiveness to *A. brasilense* Sp7 inoculation. Previous studies suggest two different reasons for these varying degrees of reactivity. For one, Cao, Lutz, Hill, Callahan, and Roessner (2017) found that unique barley varieties have different gibberellic acid 4 (GA_4)-dependent growth mechanisms and ICA (auxin phytohormone) differentials when under (salinity) stress, reiterating the intrinsic variation of various cultivars' hormonal responses to stressful situations. It still remains in question as to how exactly *A. brasilense* induces ISR and

TABLE 3 Effect tests of two-way analysis of variance (ANOVA). Mean squares for the terms of the two-way analyses of variance for variables measured at the two experimental set-ups

		Length	Surface area	Number of tips	Plant height
Direct sowing					
Cultivar	3	19,854,247***	199,668***	3,849***	266.64***
Treatment	1	6,337,490*	48,996*	2,201**	1.97
C × T	3	96,897	1,297	487	9.79
Residual	64	1,132,884	10,280	277	36.07
In vitro					
Cultivar	3	43.2	1,672.4**	1,006*	
Treatment	1	483.01	562.7	675	
C × T	3	83.06	13.1	169	
Bag (C × T)	16	189.35*	205.5*	251	
Residual	48	76.72	75.2	150	

*, **, *** significant *F* value for $p < .05$, <.01 and <.001, respectively.

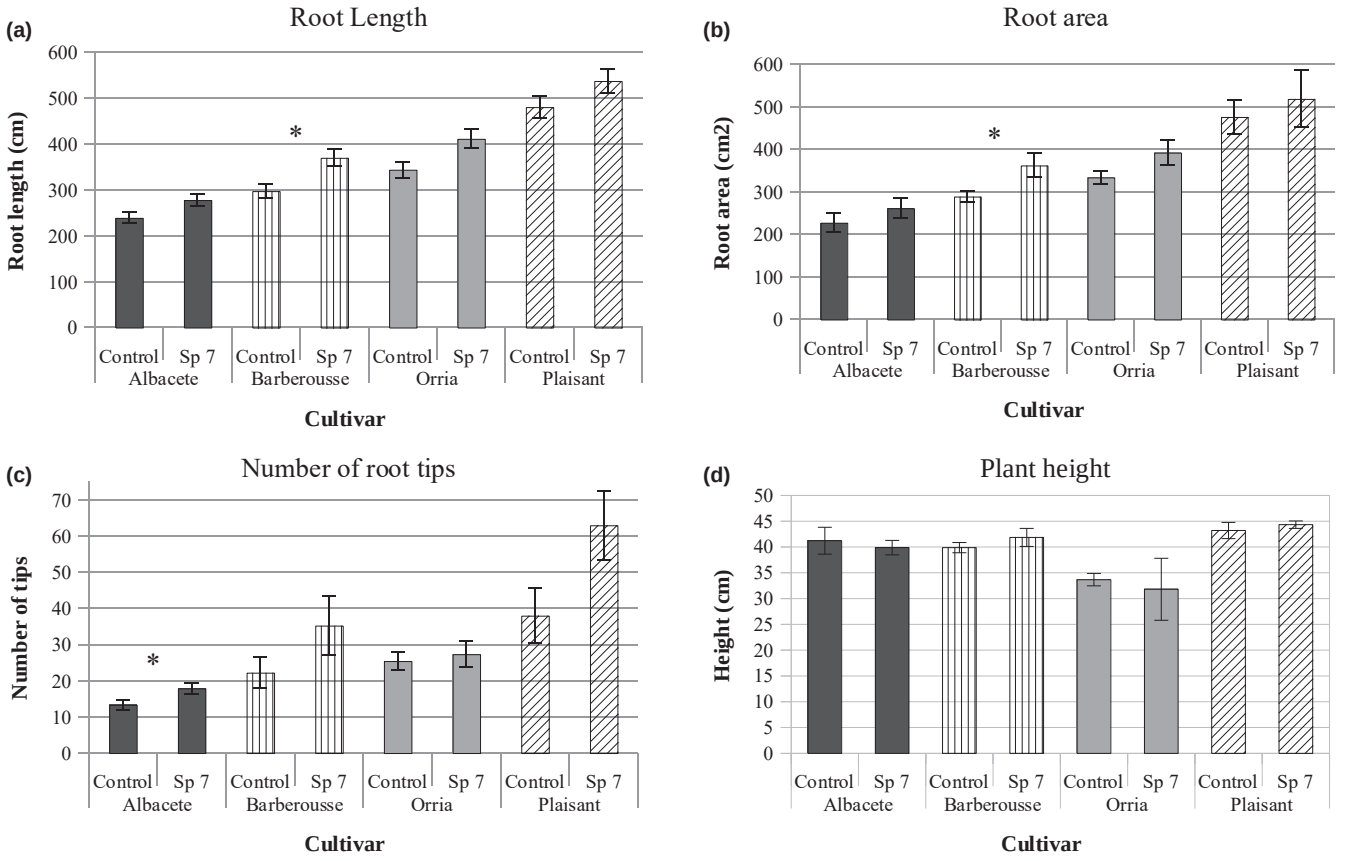

FIGURE 1 Direct sowing: *Azospirillum brasilense* Sp7 vs. Control. Four barley cultivars ('Albacete,' 'Barberousse,' 'Orria' and 'Plaisant') treated with *Azospirillum brasilense* Sp7, or untreated (control), were evaluated for (a) root length (cm), (b) root area (cm^2), (c) number of root tips and (d) height (cm), 45 days after sowing in pots. Error bars indicate the mean ± standard error (*SE*) (Student's *t* test, $p < .05$) between treatments for each cultivar, individually. Significant differences between treatments are indicated with an asterisk (*)

the hormonal crosstalk, connecting stress signalling pathways that play into the unique biology of each cultivar.

Various studies relating PGPRs to increased drought tolerance attribute increased root surface area to the production of bacterial exopolysaccharides, which in turn provide additional proteins and soluble sugars to enhance plant growth, maintain soil moisture and content and increase drought tolerance of plants (Freitas, Alves, & Reis, 2011; Naseem & Bano, 2014). As the cultivars in our study have different degrees of drought tolerance, it is hypothesized that they would in turn require different amounts of bacterial exopolysaccharides to produce a uniform response. The concentration of inoculated bacteria was uniform for all cultivars, which is probably why we see a variety of responses between cultivars.

'Albacete' exhibits a significant up-regulation of number of tips in directly sown inoculated plants, although it has the lowest number of root tips. Comparatively, 'Albacete' is historically the more drought-tolerant cultivar, and while it has the least number of intrinsic root tips, they are the most sensitive to proliferation after inoculation. 'Albacete' also exhibited significantly longer roots for inoculated in vitro-grown plants.

Longer roots of *A. brasilense*-treated plants grown in vitro have also been observed in other species, such as lettuce (Mangmang, Deaker, & Rogers, 2015) and tomato (Botta, Santacecilia, Ercole, Cacchio, & del Gallo, 2013). In cereals (e.g., sorghum and wheat), on the other hand, inoculation of high concentration of *Azospirillum* was documented to inhibit root elongation (Harari, Kigel, & Okon, 1988; Okon & Kapulnik, 1986), and the effects on root elongation at various bacterial concentrations are recognized to be regulated by phytohormones (Cassán et al., 2009; Hartmann & Baldani, 2006). More specifically, Harari et al. (1988) reported that the inconsistency of the effects of *Azospirillum* on root elongation could be the result of the antagonistic actions of IAA and other growth regulators produced by bacteria in any particular condition. Several studies have shown that the beneficial effects of PGPRs are dependent on matching specific strains of PGPR with crop species, specific cultivars, soils, inoculation methods and growing conditions (Chanway, Nelson, & Holl, 1988; Nowak, 1998; Zahir, Muhammad, & Frankenberger, 2003). As such, we can conclude that the interaction between "Albacete," the concentration of Sp7 and the in vitro growing conditions used herein do not induce antagonistic growth regulators.

The in vitro method utilized is specific in that it does not involve nutrient-rich solid or semi-solid media. This situation was elected to circumvent a common side effect of in vitro growth in agar, which has been referenced to have a limited supply of oxygen (O_2), causing

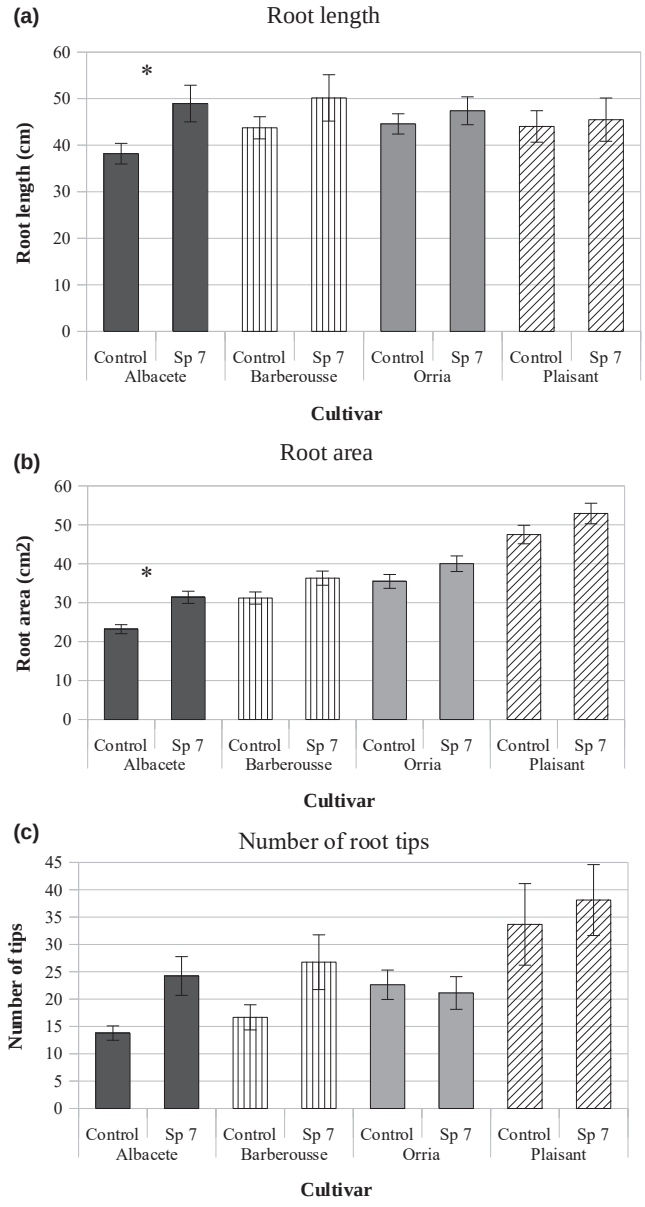

FIGURE 2 *In vitro* growth: *Azospirillum brasilense* Sp7 vs. Control. Four barley cultivars ('Albacete,' 'Barberousse,' 'Orria' and 'Plaisant') treated with *Azospirillum brasilense* Sp7 or untreated (control) were evaluated for (a) root length (cm), (b) root area (cm^2) and (c) number of root tips, 15 days after sowing in Nasco Whirl-Pak® sampling bags. Error bars indicate the mean ± standard error (Student's *t* test, $p < .05$) between treatments for each cultivar, individually. Significant differences between treatments are indicated with an asterisk (*)

poorly formed root hairs and tips (Maene & Debergh, 1985; Pierik, 2012). Such growth conditions would have contributed an additional factor affecting root tip number and overall surface area, which is why the bags were employed. In practice, using an agar-free in vitro environment was not ideal either, as the bag effect was significant too.

Even still, the treatment effect revealed in vitro inoculation of *A. brasilense* Sp7 to significantly augment root surface area and cause a trend for a greater number of tips over controls. Treatment therefore relieves the stress caused by the bags to some extent.

The Whirl-Pak® bags were sealed without any oxygen intake or escape, thus creating the possibility for an environment with decreased O_2 concentrations. Situations of low O_2 concentrations in vitro are often the catalyst for a number of other disorders, such as excessive ethylene gas accumulation (Hazarika, 2006) and in more serious cases hyperhydricity by which the plants suffer decreased protein and chlorophyll contents (Franck et al., 2004; Phan & Letouze, 1983), low phenolics (Perry, Ueno, & Shetty, 1999), increased water content (Bottcher, Zeglauer, & Goring, 1988) and altered ion composition (Kevers & Gaspar, 1986). Ethylene is a plant growth regulator produced by plants under stress, and when it accumulates excessively around roots, this can lead to less hairy root formation (Adkins, 1992).

Finally, if inoculant imbibition were considered a potential factor influencing growth, it is worth mentioning that the cultivar 'Albacete' imbibed the inoculant twice as fast as any other cultivar (Table 1). The attachment of *A. brasilense* to roots is divided into two steps: 1) a weak, reversible and unspecified binding governed by bacterial surface proteins, capsular polysaccharides and flagella; 2) an irreversible attachment phase that happens up to 16 hr after inoculation and is mediated by bacterial surface polysaccharides (Zhu, Dobbelaere, & Vanderleyden, 2002). Extracellular polysaccharide production has also been related to the process of flocculation of *Azospirillum* cells (Burdman, Jurkevitch, Schwartzburd, Hampel, & Okon, 1998). In vitro growth conditions lack a crucial component in anchoring kinetics (soil), so in the case of 'Albacete,' our results suggest that faster absorption leads to firmer anchoring, regardless of the growing environment. Anchoring may also be more efficient because of the specific chemistry of 'Albacete' seed secretions and the dynamics of extracellular polysaccharides required for *A. brasilense* Sp7 adhesion (Michiels, Croes, & Vanderlayden, 1991). This precedence is further substantiated by a related study, in which the change in sugar metabolism was found to vary among different barley varieties, and when looking at the main monosaccharides in plant roots, such as fructose and glucose, it was apparent that different cultivars had different metabolic sugar adaptations when subjected to stress (Cao et al., 2017). Henceforth, *A. brasilense* Sp7 colonization of barley cultivars based on sugar secretion levels provides evidence for interaction and should be explored further to understand whether that is a function of induced stress response by the bacteria or by the environment.

To our knowledge, this study is one of the first to classify the relationship between *A. brasilense* Sp7 and these valuable barley cultivars at early stages of growth. 'Barberousse' and 'Plaisant' were the most responsive to *A. brasilense* Sp7 treatment, although 'Plaisant' was perhaps the most intriguing, based on its early vigorous growth regardless of environment and PGPR treatment. 'Orria' is known for having lower biomass and slower proliferation at early growth stages to create a more robust grain at heading; therefore, its low response in its early interaction with *A. brasilense* Sp7 inoculation, irrespective of growing environment, is to be expected (I. Romagosa, personal communication, October 18, 2017). To better understand the relationship that 'Orria' has with inoculation with regard to the other cultivars, it should be studied at yield, when its growth is optimal. 'Albacete' is especially interesting in terms of its physiological interaction with *A. brasilense*

Sp7 under conditions of abiotic stress because it is the only cultivar positively affected overall by inoculation in vitro.

There is relevance in combining the two growing scenarios tested as they render similar results for both inoculated and non-inoculated plant growth. The in vitro technique was useful at the earliest stages of growth as it provided an ongoing, clear image of the intrinsic root behaviour of each cultivar during this time. In terms of sampling, advantages to this method are that conditions can be meticulously controlled, and root analysis is easy to carry out. For one, the clear plastic bag makes it possible to track root growth on a daily basis without destructive sampling. Then at harvest, the roots can be carefully managed and root tips accurately quantified, as there is no need to wash soil from them, which often leads to breakage. However, depending on the objectives of the study, this method may not be ideal as it represents growth in the absence of an exogenous support system, and as its design probably induces abiotic stress with time as oxygen levels decrease. This method is not practical for studies of crops in higher stages of development.

ACKNOWLEDGEMENTS

This work was supported by the MINCYT (project ref. AGL2010-15691). The authors would like to thank Drs. Jordi Voltas and Ignacio Romagosa for the manuscript revision.

CONFLICT OF INTEREST

The authors have no conflict of interest to declare.

AUTHOR CONTRIBUTIONS

SL, PM and VM analysed the data and wrote the manuscript. CR, AIC and LM were involved in plant cultivation and sample collection. CR, AIC and VM designed the experiments.

ORCID

Sarah B. Lade http://orcid.org/0000-0002-9549-903X

REFERENCES

Adkins, S. W. (1992). Cereal callus cultures: Control of headspace gases can optimize the conditions for callus proliferation. *Australian Journal of Botany*, *40*, 737–749. https://doi.org/10.1071/BT9920737

Botta, A. L., Santacecilia, A., Ercole, C., Cacchio, P., & del Gallo, M. (2013). *In vitro* and *in vivo* inoculation of four endophytic bacteria on *Lycopersicon esculentum*. *Nature Biotechnology*, *30*(6), 666–674.

Bottcher, I., Zeglauer, K., & Goring, H. (1988). Inducting and reversion of vitrification of plants cultured *in vitro*. *Journal of Plant Physiology*, *66*, 94–98.

Burdman, S., Jurkevitch, E., Schwartzburd, B., Hampel, M., & Okon, Y. (1998). Aggregation in *Azospirillum brasilense*: Effects of chemical and physical factors and involvement of extracellular components. *Microbiology*, *144* (7), 1989–1999. https://doi.org/10.1099/00221287-144-7-1989

Cai, J., Zeng, Z., Connor, J. N., Huang, C. Y., Melino, V., Kumar, P., & Miklavcic, S. J. (2015). Rootgraph: A graphic optimization tool for automated image analysis of plant roots. *Journal of Experimental Botany*, *66*(21), 6551–6562. https://doi.org/10.1093/jxb/erv359

Cao, D., Lutz, A., Hill, C. B., Callahan, D. L., & Roessner, U. (2017). A quantitative profiling method of phytohormones and other metabolites applied to barley roots subjected to salinity stress. *Frontiers in Plant Science*, *7*, 2070.

Cassán, F., Perrig, D., Sgroy, V., Masciarelli, O., Penna, C., & Luna, V. (2009). *Azospirillum brasilense* Az39 and *Bradyrhizobium japonicum* E109, inoculated singly or in combination, promote seed germination and early seedling growth in corn (*Zea mays* L.) and soybean (*Glycine max* L.). *European Journal of Soil Biology*, *45*, 28–35. https://doi.org/10.1016/j.ejsobi.2008.08.005

Chanway, C. P., Nelson, L. M., & Holl, F. B. (1988). Cultivar-specific growth promotion of spring wheat (*Triticum aestivum* L.) by coexistent *Bacillus* species. *Canadian Journal of Microbiology*, *34*, 925–929. https://doi.org/10.1139/m88-164

Comas, L. H., & Eissenstat, D. M. (2009). Patterns in root trait variation among 25 co-existing North American forest species. *New Phytologist*, *182*, 919–928. https://doi.org/10.1111/j.1469-8137.2009.02799.x

Correa, O. S., Romero, A. M., Montecchia, M. S., & Soria, M. A. (2007). Tomato genotype and Azospirillum inoculation modulate the changes in bacterial communities associated with roots and leaves. *Journal of Applied Microbiology*, *102*, 781–786. https://doi.org/10.1111/j.1365-2672.2006.03122.x

Creus, C. M., Graziano, M., Casanovas, E. M., Pereyra, M. A., Simontacchi, M., Puntarulo, S., … Lamattina, L. (2005). Nitric oxide is involved in the *Azospirillum brasilense*-induced lateral root formation in tomato. *Planta*, *221*, 297–303. https://doi.org/10.1007/s00425-005-1523-7

Dobbelaere, S., Croonenborghs, A., Thys, A., Vande Broek, A., & Vanderleyden, J. (1999). Phytostimulatory effect of *Azospirillum brasilense* wild type and mutant strains altered in IAA production on wheat. *Plant and Soil*, *212*, 153–162. https://doi.org/10.1023/A:1004658000815

Döbereiner, J., Marriel, I. E., & Nery, M. (1976). Ecological distribution of *Spirillum lipoferum* Beijerinck. *Canadian Journal of Microbiology*, *22*(10), 1464–1473. https://doi.org/10.1139/m76-217

Farré, A., I. Lacasa Benito, L. Cistué, J. H. de Jong, I. Romagosa, and J. Jansen, 2011: Linkage map construction involving a reciprocal translocation. *Theoretical Applied Genetics 122*, 1029–1037.

Franck, T., Kavers, C., Gaspar, T., Dommes, J., Deby, C., Greimess, R., … Deby-Dupont, G. (2004). Hyperhydricity of *Prunus avium* shoots cultured on gelrite: A controlled stress response. *Plant Physiology and Biochemistry*, *42*, 519–527. https://doi.org/10.1016/j.plaphy.2004.05.003

Freitas, F., Alves, V. D., & Reis, M. A. M. (2011). Advances in bacterial exopolysaccharides: From production to biotechnological applications. *Trends in Biotechnology*, *29*(8), 388–398. https://doi.org/10.1016/j.tibtech.2011.03.008

Harari, A., Kigel, J., & Okon, Y. (1988). Involvement of IAA in the interaction between *Azospirillum brasilense* and *Panicum miliaceum* roots. *Plant and Soil*, *110*, 275–282. https://doi.org/10.1007/BF02226808

Hartmann, A., & Baldani, J. (2006). The genus *Azospirillum*. In M. Dworkin, S. Falkow, E. Rosenberg, K.-H. Schleifer & E. Stackebrandt (Eds.), *The prokaryotes* (pp. 114–140). New York, NY: Springer.

Hazarika, B. N. (2006). Morpho-physiological disorders in *in vitro* culture of plants. Review. *Scientia Horticulturae*, *108*, 105–120. https://doi.org/10.1016/j.scienta.2006.01.038

Kamnev, A., Tugarova, A. V., Tarantilis, P. A., Gardiner, P. H. E., & Polissiou, M. G. (2011). Comparing poly-3-hydroxybutyrate accumulation in *Azospirillum brasilense* strains Sp7 and Sp245: The effects of copper(II). *Applied Soil Ecology*, *61*, 213–216.

Kevers, C., & Gaspar, T. (1986). Vitrification of carnation *in vitro*: Changes in water content, extra cellular space, air volume and ion levels. *Chemistry of Vegetable Physiology and Agriculture*, *24*, 647–653.

Lancashire, P. D., Bleiholder, H., Langelüddecke, P., & Stauss, R. (1991). A uniform decimal code for growth stages of crops and weeds. *Annals of Applied Biology*, *119*, 561–601. https://doi.org/10.1111/j.1744-7348.1991.tb04895.x

López-Castañeda, C., & Richards, R. A. (1994). Variation in temperate cereals in rain-fed environments III. Water use and water-use efficiency. *Field Crops Research*, *39*, 85–98.

Maene, L. J., & Debergh, P. C. (1985). Liquid medium additions to establish tissue cultures to improve elongation and rooting *in vivo*. *Plant Cell, Tissue and Organ Culture*, *5*, 23–33. https://doi.org/10.1007/BF00033566

Mangmang, J., Deaker, R., & Rogers, G. (2015). Response of lettuce seedlings fertilized with fish effluent to *Azospirillum brasilense* inoculation. *Biological Agriculture and Horticulture Journal*, *31*, 61–71. https://doi.org/10.1080/01448765.2014.972982

Michiels, K. W., Croes, C. L., & Vanderlayden, J. (1991). Two different modes of attachment of *Azospirillum brasilense* Sp425 to wheat roots. *Journal of General Microbiology*, *137*, 2241–2246. https://doi.org/10.1099/00221287-137-9-2241

Muñoz, P., Voltas, J., Araus, J. L., Igartua, E., & Romagosa, I. (1998). Changes over time in the adaptation of barley releases in north-eastern Spain. *Plant Breeding*, *17*, 531–535.

Muthukumarasamy, R., Revathi, G., & Lakshminarasimhan, C. (1999). Diazotrophic associations in sugar cane cultivation in South India. *Journal of Tropical Agriculture*, *76*, 171–178.

Muthukumarasamy, R., Revathi, G., & Loganathan, P. (2002). Effect of inorganic N on the population, *in vitro* colonization and morphology of *Acetobacter diazotrophicus* (syn *Gluconacetobacter diazotrophicus*). *Plant and Soil*, *243*, 91–102. https://doi.org/10.1023/A:1019963928947

Naseem, H., & Bano, A. (2014). Role of plant growth-promoting rhizobacteria and their exopolysaccharide in drought tolerance of maize. *Journal of Plant Interactions*, *9*, 689–701. https://doi.org/10.1080/17429145.2014.902125

Nowak, J. (1998). Benefits of in vitro "biotization" of plant tissue cultures with microbial inoculants. *In Vitro Cellular & Developmental Biology – Plant*, *34*, 122–130. https://doi.org/10.1007/BF02822776

Okon, Y., & Kapulnik, Y. (1986). Development and function of *Azospirillum*-inoculated roots. *Plant and Soil*, *90*, 3–16. https://doi.org/10.1007/BF02277383

de Oliveira, A. L. M., de Canuto, E. L., Urquiaga, S., Reis, V. M., & Baldani, J. I. (2006). Yield of micropropagated sugarcane varieties in different soil types following inoculation with diazotrophic bacteria. *Plant and Soil*, *284*, 23–32. https://doi.org/10.1007/s11104-006-0025-0

Omar, M. N. A., Osman, M. E. H., Kasim, W. A., & El-Daim, I. A. A. (2000) Improvement of salt tolerance mechanisms of barley cultivated under salt stress using *Azospirillum brasilense*. *Salinity and water stress* (6th ed.). Dordrecht, the Netherlands: Springer.

Perry, P. L., Ueno, K., & Shetty, K. (1999). Reversion to hyperhydration by addition of antibiotics to remove *Pseudomonas* in unhyperhydrated oregano tissue culture. *Process Biochemistry*, *34*, 717–723. https://doi.org/10.1016/S0032-9592(98)00146-0

Phan, C. T., & Letouze, R. (1983). A comparative study of chlorophyll, phenolic and protein contents, and hydroxycinnamate. CoA ligase activity. *Plant Science Letters*, *36*, 323–327. https://doi.org/10.1016/0304-4211(83)90071-8

Pierik, R. L. M. (2012). *In vitro* culture of higher plants. Dordrecht, the Netherlands: Springer Science and Business Media.

Rashid, K. N. (2014). *The response of wheat genotypes to inoculation with Azospirillum brasilense*. Camperdown, NSW: University of Sydney.

dos Reis Junior, B. F., Massena Reis, V., Urquiaga, S., & Döbereiner, J. (2000). Influence of nitrogen fertilisation on the population of diazotrophic bacteria *Herbaspirillum* spp. and *Acetobacter diazotrophicus* in sugar cane (*Saccharum* spp.). *Plant and Soil*, *219*, 153–159. https://doi.org/10.1023/A:1004732500983

Siddique, K. H. M., Belford, R. K., Perry, M. W., & Tennant, D. (1989). Growth, development and light interception of old and modern wheat cultivars in a Mediterranean-type environment. *Australian Journal of Agricultural Research*, *40*, 473–487.

Spaepen, S., & Vanderleyden, J. (2011). Auxin and plant-microbe interactions. *Cold Spring Harbor Perspectives in Biology*, *3*, a001438.

Tarrand, J. J., N. R. Krieg, and J. Döbereiner, 1978: A taxonomic study of the *Spirillum lipoferum* group, with descriptions of a new genus, *Azospirillum gen*. nov. and two species, *Azospirillum lipoferum* (Beijerinck) comb. nov. and *Azospirillum brasilense* sp. nov. *Canadian Journal of Microbiology 24*, 967–980.

Teulat, B., Merah, O., & This, D. (2001). Carbon isotope discrimination and productivity in field-grown barley genotypes. *Journal of Agronomy Crop Science*, *187*, 33–39. https://doi.org/10.1046/j.1439-037X.2001.00496.x

Vacheron, J., Desbrosses, G., Bouffaud, M. L., Touraine, B., Moenne-Loccoz, Y., Muller, D., … Prigent-Combaret, C. (2013). Plant growth-promoting rhizobacteria and root system functioning. *Frontiers in Plant Science*, *4*(356), 1–19.

Vacheron, J., Renoud, S., Muller, D., Babalola, O. O., & Prigent-Combaret, C. (2015). Chapter 19: Alleviation of abiotic and biotic stresses in plants by *Azospirillum*. In F. D. Cassán, Y. Okon & C. M. Creus (Eds.), *Handbook for Azospirillum* (pp. 333–365). Basel, Switzerland: Springer International Publishing.

Voltas, J., Romagosa, I., Lafarga, A., Armesto, A. P., Sombrero, A., & Araus, J. L. (1999). Genotype by environment interaction for grain yield and carbon isotope discrimination of barley in Mediterranean Spain. *Australian Journal of Agricultural Research*, *50*, 1263–1271. https://doi.org/10.1071/AR98137

Yau, S. K. (2016). *Vernalization Requirement of Lebanese Barley Landraces*. Retrieved from http://wheat.pw.usda.gov/ggpages/BarleyNewsletter/42/yau.html.

Zahir, Z. A., Muhammad, A., & Frankenberger, W. T. Jr (2003). Plant growth promoting rhizobacteria: Applications and perspectives in agriculture. *Advances in Agronomy*, *81*, 97–168. https://doi.org/10.1016/S0065-2113(03)81003-9

Zawoznik, M. S., Vázquez, S. C., Díaz Herrera, S. M., & Groppa, M. D. (2014). Search for endophytic diazotrophs in barley seeds. *Brazilian Journal of Microbiology*, *45*(2), 621–625. https://doi.org/10.1590/S1517-83822014000200033

Zhu, G. Y., Dobbelaere, S., & Vanderleyden, J. (2002). Use of green florescent protein to visualize rice root colonization by *Azospirillum irakense* and *A. brasilense*. *Functional Plant Biology*, *29*(11), 1279–1285. https://doi.org/10.1071/FP02120

SUPPORTING INFORMATION

Additional supporting information may be found online in the Supporting Information section at the end of the article.

How to cite this article: Lade SB, Román C, Cueto-Ginzo AI, Maneiro L, Muñoz P, Medina V. Root development in agronomically distinct six-rowed barley (*Hordeum vulgare*) cultivars inoculated with *Azospirillum brasilense* Sp7. *Plant Breed*. 2018;137:338–345. https://doi.org/10.1111/pbr.12593

ANNEX 3

Lade SB, Román C, Cueto-Ginzo AI, Serrano L, Sin E, Achón MA, Medina V (2018) Host-specific proteomic and growth analysis of maize and tomato seedlings inoculated with *Azospirillum brasilense* Sp7. *Plant Physiology and Biochemistry* 129: 381-393.

Plant Physiology and Biochemistry 129 (2018) 381–393

Contents lists available at ScienceDirect

Plant Physiology and Biochemistry

journal homepage: www.elsevier.com/locate/plaphy

Research article

Host-specific proteomic and growth analysis of maize and tomato seedlings inoculated with *Azospirillum brasilense* Sp7

Sarah Boyd Lade*, Carla Román, Ana Isabel Cueto-Ginzo, Luis Serrano, Ester Sin, Maria Angels Achón, Vicente Medina

Department of Plant Production and Forestry Science, University of Lleida – Agrotecnio Center, Lleida, Spain

ARTICLE INFO

Keywords:
Plant-growth-promoting rhizobacteria (PGPR)
Sp7
Proteomics
ROS
Photosynthesis

ABSTRACT

Azospirillum brasilense Sp7 (Sp7) is a diazotrophic, free-living plant growth-promoting rhizobacterium (PGPR) that is increasingly used for its ability to reduce stress and improve nutrient uptake by plants. To test the hypothesis that Sp7 interacts differently with the primary metabolism in C_3 and C_4 plants, differential proteomics were employed to study weekly protein expression in Sp7-treated maize *(Zea mays cv.* B73) and tomato (*Solanum lycopersicum* cv. Boludo) seedlings. Plant and root growth parameters were also monitored. Protein changes were most striking at the four-leaf stage (T1) for both species. Proteins related to metabolism and redox homeostasis were most abundant in tomato at T1, but later, plants experienced inhibited Calvin-Benson (CB) cycle and chloroplast development, indicating that photosynthetic proteins were damaged by reactive oxygen species (ROS). In maize, Sp7 first increased ROS-scavenging enzymes and decreased those related to metabolism, which ultimately reduced photoinhibition at later sampling times. Overall, the early interaction with maize is more complex and beneficial because the photosynthetic aparatus is protected by the C_4 mechanism, thereby improving the interaction of the PGPR with maize. Better seedling emergence and vigor were observed in inoculated maize compared to tomato. This study provides an integrated perspective on the Sp7 strain-specific interactions with young C_3 and C_4 plants to modulate primary metabolism and photosynthesis.

1. Introduction

Azospirillum brasilense is one of the most well characterized free-living diazotrophic plant growth-promoting rhizobacteria (PGPR) (Tarrand et al., 1978) that has been studied as an inoculant for both extensive and intensive cropping systems, and in multiple environments. The inoculation of *A. brasilense* to seeds and plants augments proliferation of lateral and adventitious roots, and increases the dry weight of root systems and plant aerial parts to significantly improve development, flowering and harvest output (Dobbelaere et al., 2001).

The principle mode of action of *A. brasilense* is production and liberation of regulatory vegetative growth substances directly affecting plant metabolism (Glick, 2012). Furthermore, biological nitrogen fixation (BNF) by this bacterium results in increased plant biomass and grain production (Cassán et al., 2009). Both organisms change their metabolic routines to accommodate each other's needs (Mus et al., 2016). Bacterial nitrogen metabolism must be altered so that nitrogen is excreted rather than incorporated into the microbial biomass, while the plant host directly interferes with bacterial amino acid biosynthesis, forcing the release of nitrogen as ammonia (Lodwig et al., 2003).

From molecular studies of plant-PGPR interactions, it is known that *Azospirillum* spp. affects primary and secondary plant metabolism both above and below ground (Beimalt and Sonnewald, 2014). To do so, the PGPR mainly alters the root enzymes, changing patterns of root exudation and stimulating levels of carbon compounds in root exudates (Lavania et al., 2006), as in the field-inoculation of maize with single or combined applications of *Azospirillum* and other PGPRs such as *Rhizophagus* that has led to modifications of secondary root metabolites (Walker et al., 2012). This modification effect has been surmised to represent an attempt by the bacteria to manipulate plant metabolism to gain access to nutrients (Parra-cota et al., 2014).

Given the fundamental differences between C_4 and C_3 photosynthetic pathways and the unique dependence of each on N-metabolism (Wang et al., 2014), alongside the propensity for *Azospirillum* to interact uniquely with the metabolism of its host, thereby creates an interesting puzzle that has proven challenging to understand. In the past, studies claimed that *A. brasilense* has a higher affinity for C_3 plants, and C_4 plants are supposedly better colonized by other species such as *A. lipoferum* (Mengel and Viro, 1978; Reynders and Vlassak, 1982). Contemporary reviews have, however, cautioned that older

* Corresponding author.
E-mail address: sarahb.lade@pvcf.udl.cat (S.B. Lade).

https://doi.org/10.1016/j.plaphy.2018.06.024
Received 21 May 2018; Received in revised form 16 June 2018; Accepted 16 June 2018
Available online 19 June 2018

studies are representative of historical assumptions likely related to the original isolation of *A. brasilense* from cereals and subsequent experimentation performed mostly on them (Pereg et al., 2016). In this study, we have chosen tomato and maize to represent C_3 and C_4 crops, respectively. Both of these species are model in that they are economically important and have sequenced genomes. Furthermore, they are the most widely studied species falling in to their respective monocot and dicot categories (Covshoff and Hibberd, 2012).

There are various *A. brasilense* strains, differing in their habitat and capacities as PGPR. Some are endophytic, such as *A. brasilense* Sp245, which is now considered as the type strain for this species (Baldani et al., 1986); but others like Sp7 are epiphytic, which was previously considered to be the type strain for the species (Tarrand et al., 1978). Sp7 responds strongly to the soil environment, sensing stress and contaminants more acutely (Kamnev et al., 2012). Therefore, Sp7 has more potential to protect plants from soil pathogens since it blocks rhizospheric pathogen-plant interaction zones (Pereg, 2015).

In most studies of field-grown crops, special focus was given to the early vegetative phase of development because and *Azospirillum* demonstrated bacteria viability and density to be unchanged for 30 days post-sowing, then to sharply decline and be negligible 57 days post-sowing (El Zemrany et al., 2006). There are, however, limited studies reporting the timing of proteomic changes taking place within the first 30–35 days. One of the most comprehensive studies on the maize proteome outlines the proteomic profile of a nine-day old plant (at the 2-leaf stage) (Majeran et al., 2010). The study provides a well-defined molecular template for the structural and metabolic transitions that occur during C_4 leaf differentiation. Considering changes in the maize root zone has also been an important field of study because the maize root system is composed of various embryonic and postembryonic root types. Regardless, all of these roots form lateral roots, which have influence over the proteome composition of the primary root (Hochholdinger et al., 2004). Proteomic studies regarding tomato are more scant. For one, studies focusing on tomato proteome changes during early growth are virtually non-existant. The few that analyze the effects of PGPR on the proteome have found that PGPR promoted plant growth whilst improving redox status by means of increased *glutathione ascorbate* (GSH) (Ibort et al., 2018). Finally, in comparing maize and tomato, perhaps one of the most relevant and intriguing findings is that PGPR leads to attenuation of defense responses in maize to allow for colonization, while they activate defense responses in tomato (Shivaprasad et al., 2012; Thiebaut et al., 2014).

In this study, we attempt to establish expression trends of protein functional groups in model C_3 and C_4 plants (tomato and maize, respectively) inoculated with *A. brasilense* strain Sp7 (ATCC 29145), and test the hypothesis that Sp7 interacts differently with the primary metabolism of the two types of plants. For this, differential proteomics has been employed to quantify changes during early stages of Sp7-treated plant development. This data is compared with plant growth and physiological parameters.

2. Materials and methods

2.1. Experimental design

Two completely randomized single factor experiments were started with maize (*Zea mays* L., Mill. cv. B73) and tomato (*Lycopersicon esculentum* L., cv. Boludo) seeds. There were two treatment groups (20 biological replicates) per species. Treatments were: 1) the control (C), seeds soaked in sterile phosphate-buffered saline (PBS) [10 mM K_2PO_4-KH_2PO_4, 0.14 M NaCl, pH 7.2], and 2) seeds soaked in the same buffer, incorporating Sp7.

Sampling began at principal growth stage 14 for both maize and tomato according to the BBCH scale (Lancashire et al., 1991), and continued weekly until stage 19 for both species. In maize, sampling times 1–4 corresponded to 16 (T1), 23 (T2), 30 (T3) and 35 (T4) days post-inoculation (dpi). Physiologically, T1 coincided with the four-leaf stage, T2 with early tillering, and T3 and T4 with late tillering.

In tomato, sampling times 1–4 corresponded to 14 (T1), 21 (T2), 28 (T3) and 35 (T4) dpi. Physiologically, T1 also coincided with the four-leaf stage, T2 with the seven-leaf stage, and T3 with the 9-leaf stage and T4 with the 12-leaf stage.

2.2. Azospirillum brasilense Sp7 inoculum preparation and inoculation

A freeze-dried vial of *Azospirillum brasilense* Sp7 strain was kindly provided by the *Colección Española de Cultivos Tipo* (acc. CECT 590), Polytechnic University of Valencia (Spain). It was cultivated in Petri dishes containing sterile nitrogen-free broth medium (NFb) supplemented with 15 mL/L of 1:400 aqueous solution of Congo-red (CR) (Bashan et al., 1993) for 48 h. *Azospirillum brasilense* Sp7 inoculum was prepared as described by Okon et al. (1977) in OAB liquid media inoculated with a single colony selected from the CR medium and incubated at 32 °C with constant agitation (100 rpm) for 48 h. The bacterial suspension was allowed to reach late log growth phase [absorbance of 0.399 nm at OD_{600} (using an Amersham Biosciences Ultraspec 3100 Pro spectrophotometer)], at a concentration yielding 1.16×10^8 cfu mL^{-1}.

Inoculation time and quantity were established according to an imbibition curve, estimating the time taken for each seed variety to imbibe 70% of its total potential. Seeds were surface sterilized with 4% NaOCl for 10 min (with constant agitation) and washed six times with sterile distilled water (SDW) in a laminar flow hood. They were dried and inoculated with the rhizobacteria by imbibition.

2.3. Plant growth

Seeds were sown in 1 L pots containing autoclaved commercial substrate (Traysubstrat®, Klasmann-Deilmann, Gmbh, Geeste, Germany) characterized by having an extra fine structure and pH 6. Plants were then grown under greenhouse conditions 18–25% HR, 25–30 °C, with supplementary lighting (12 h photoperiod) and protected from insect attack by an anti-aphid mesh and automatic drip irrigation (1 h, twice per day).

2.4. Growth analysis and bacterial recovery

For aerial parameters, the height of 10 random plants was measured per treatment and sample time. For root analysis, three plants were randomly chosen per treatment and sample time. The root mass was carefully washed with distilled water and stored in 70% ethanol at 4 °C until analysis. They were then scanned using an Epson Perfection V700 scanner. The images were analyzed with the WinRHIZO program (Regent Instruments Inc., Quebec, ON, Canada, 2009).

Sp7 colonization assays were conducted at harvest of each sampling time, with three random samples taken from each treatment. The procedure was carried out according to Botta et al. (2013) with modifications. One hundred grams of plant roots were homogenized in 1 mL sterile physiological solution (NaCl 0.9%). The homogenate was then serially diluted and plated on CR medium. Bacterial colonies were counted after 2–3 days incubation, depending on the growth rate of each plate, at 32 °C. Controls were replicated in the same manner.

2.5. Leaf gas exchange parameters

Leaf gas exchange was monitored with an infrared gas analyzer (LI-6400XT LICOR Inc., Nebraska, USA) at the same hour (14 h), at each sampling time. Measurements were taken of leaf CO_2 assimilation rate (A), transpiration rate (E) and intercellular CO_2 concentration (C_i) and instantaneous water-use efficiency (WUE_i [A/E]).

2.6. Total protein extraction

One gram of leaf tissue was collected per plant for each sampling time (3 plants per treatment), immersed in liquid nitrogen and stored at −80 °C. Each sample was measured to 0.1 g and ground with 2 mL of 10% trichloroacetic acid (TCA) in acetone + 20 mM dithriothreitol (DTT) and a protease inhibitor (complete ULTRA Tablets, Mini, EDTA-free, EASYpack, Sigma) was added and mixed by vortex (Xu et al., 2013). After centrifugation at 14,000 rpm and 4 °C for 30 min, the supernatant was discarded, and the pellet washed three times with 2 mL acetone +20 mM DTT, then air dried on ice (10–30 min). The total protein was eluted in 100–250 μL lysis buffer (PER 4, Sigma) and the total protein content was measured by the Bradford method (Bio-Rad Protein Assay Dye Reagent Concentrate) using bovine serum albumin (BSA) as a standard. Absorbance was measured at OD_{600}, using an Amersham Biosciences (Ultraspec 3100 Pro) spectrophotometer.

2.7. Protein analysis

Total protein extracts were measured to 100 μg and separated by 2D-PAGE analytical gels. Three biological replicates were collected for each treatment. For preparative gels, 500 μg of protein were used. Samples were mixed with rehydration buffer [7 M urea, 2 M thiourea, 1% C7BzO detergent, 40 mM Trizma Base, 50 mM DTT, 1% IPG buffer pH 3–10, and 0.002% bromophenol blue] in a total volume of 200 μL. Isoelectric focusing (IEF) of passively rehydrated 18 cm IPG strips (pH 5–8) was performed in a Protean IEF Cell system (Bio-Rad) following the manufacturer's instructions. IEF used a sequential gradient procedure of 50 V/20 C/14 h. The current limit was 50 μA per IPG strip. Focused strips were stored at −80 °C until the second dimension was performed. After IEF separation, the gel strips were incubated for 15 min in the equilibration buffer [375 mM Trizma base, 6 M urea, 20% glycerol, 2% SDS] containing 2% DTT, followed by 15 min in the same buffer containing 2.5% iodoacetamide instead of DTT. Two equilibrated 18 cm gel strips were loaded in each 12.5% polyacrylamide gel (22 cm × 20 cm x 1 mm) for the second-dimension separation in an Ettan DALTsix Electrophoresis Unit (GE Healthcare). Electrophoresis was carried out in SDS-PAGE gels of 12.5%. Gels were stained with Flamingo™ Gel fluorochrome (Bio-Rad) according to the manufacturer's instructions. Images were acquired with the Versadoc MP4000 system (Bio-Rad) (Cueto-Ginzo et al., 2016).

2.8. Protein digestion and MS analysis

Spots were manually excised from gels, digested with trypsin in 96-well perforated plates using a MultiScreen™ HTS Vacuum Manifold (Millipore). Each gel piece containing the protein was minced, washed twice with deionized water and dehydrated with 50% ethanol in 50 mM NH_4HCO_3 for 10 min, and then with 100% ethanol for 10 min. Gel pieces were then reduced with 10 mM DTT in 50 mM NH_4HCO_3 for 1 h at 56 °C and alkylated with 55 mM iodoacetamide in 50 mM NH_4HCO_3 for 30 min at room temperature in the dark. The gel pieces were washed twice in 50 mM NH_4HCO_3 for 15 min and dehydrated with 5% acetonitrile (ACN) in 25 mM NH_4HCO_3 for 15 min, twice with 50% ACN in 25 mM NH_4HCO_3 for 15 min, and finally with 100% ACN for 10 min. After total ACN evaporation, 15 μL of 20 ng μL^{-1} trypsin in 25 mM NH_4HCO_3 was added and left at 4 °C for 45 min to allow for full rehydration of the gel pieces. The gel pieces were then covered with 25 mM NH_4HCO_3 and incubated at 37 °C overnight for proteolysis. Eluted peptides were then transferred to a new Eppendorf tube, and 1 μL of the digested protein was used for a first peptide mass fingerprint (PMF) analysis. If necessary, the minced gel was washed three more times with 0.25% trifluoroacetic acid (TFA) in 50% v/v ACN, twice with 100% ACN, evaporated in a SpeedVac and then re-suspended in 5 μL of 70% ACN- 0.1% TFA to collect remaining peptides. 1 μL peptide solution was spotted per well on a MALDI target and allowed to evaporate at room temperature before being covered with 1 μL of a saturated solution of α-cyano-4-hydroxycinnamic acid prepared in 50% v/v ACN containing 1% TFA. Mass calibrations were carried out using a standard peptide mixture. Mass spectra were acquired using Autoflex™ Speed MALDI-TOF/TOF mass spectrometer (Bruker Daltonics) (Cueto-Ginzo et al., 2016).

Protein identification was performed using MALDI-TOF mass fingerprint (PMF) and MALDI-TOF/TOF. PMF and MS/MS spectra were compared against SwissProt, NCBI and TrEMBL databases, using the search engine MASCOT algorithm (Version 2.4, Matrix Science, London, UK).

2.9. Statistical analysis

Growth data were statistically processed using a one-way ANOVA for each sampling time. Bradford protein quantification was assessed in the same way. The analysis was prepared with JMP® 12.1 (SAS Institute Inc.), and graphics were created with Apache OpenOffice 4.1.3 in OS X Yosemite 10.10.5. An F-ratio of 0.05 for a One-way ANOVA was used to evaluate the difference between averages.

Spot detection and gel analysis were first conducted with the PDQUEST program (Bio-Rad) and the second time, manually. Normalization was performed with the LOESS regression model. Only the spots present on all of the gel replicates were used for statistical analysis. Ratios between two expressed conditions were calculated as the mean of three independent values for each spot from the 2D gel electrophoresis analysis ± standard error. Standard error for each spot was calculated according to the following guidelines: 1) there must be a variation coefficient ≤50% among replicates, 2) spots must be present in all measured conditions, 3) expression ratios must be ≤ 0.5 or ≥2.0, and 4) spots must be validated in visu. Spots lacking quantitative signal, high quantitative variation between replicates, or with mixed proteins, were not considered for the analysis.

For each species and each sampling time, each protein population (spot) was quantified based on the average of the three biological replicates and then log2 transformed to normalize the data. Finally, to streamline data interpretation and increase analysis power, a stringent fold-change threshold of 2/-2 was used to control the false discovery rate, but in the case that no proteins reached this threshold (which was the case at T2 and T3), the boundary was slackened to 1.5/-1.5-fold change.

Proteins were categorized into the various functional groups: 1) photosynthesis, respiration, and chloroplast organization; 2) redox homeostasis and stress response (defense); 3) protein synthesis, conformation and transport; 4) metabolism and energy; 5) pathogenic cell lysis; 6) resistance; and 7) with unknown or not yet established function (Tables 1 and 2).

3. Results

3.1. Colonization of Zea mays cv. B73 and Solanum lycopersicum cv. Boludo

Sp7 was detected on the root systems of maize and tomato plants seven days after inoculation. The number of Sp7 colonies from the surface sterilized roots of the plants was 10^5 CFU g of moist root, confirming that the bacteria had indeed colonized the plants. In contrast, no *A. brasilense* colonies were observed in non-inoculated plants.

3.2. Plant growth parameters

Significant differences ($p < 0.01$) between the heights of maize (B73) seedlings treated with Sp7 and corresponding control (C-) seedlings were observed when the plants were further developed (T3). In tomato, there was a highly significant ($p < 0.001$) height difference between C- and Sp7 treated seedlings for T2, T3 and T4 (Fig. 1a and b).

Table 1
Main characteristics and function of identified maize proteins corresponding to spots in Fig. 3.

SSP [a]	Protein name	Accession No. [b] (database)	Molecular Weight (Da)/pI [c]	Coverage %	No Peptides Matched/Total peptides	Score [d]	Function [e]
210	Chaperonin	ACG33530**	25559/8.67	64	12/27	160	4
402	Phosphoribulokinase Sedoheptulose-1,7-bisphosphatase	B4FQ59*** B6T2L2***	45121/5.84 42303/6.08	76 66	28/74 28/74	260 219	3,4
504	Phosphoglycerate kinase	NP_001147628**	50009/6.07	61	33/49	283	2
2103	Chlorophyll *a-b* binding protein 8	NP_001148598.2**	28966/8.94	13	3/3	210	1,2
2705	ATP synthase subunit beta, mitochondrial	P19023*	59181/6.01	44	24/76	156	2
3104	Cytochrome b6-f complex iron-sulfur subunit	B4FTU7***	21026/6.41	10	3/4	154	1
3205	–						7
3303	Fructose-biphosphate aldolase	ACG36798.1**	41924/7.63	64	26/73	248	4
4105	Germin-like protein	Q6TM44***	22101/6.02	13	2/2	166	2,4
4201	Lactoylglutathione lyase	ACG39003**	35311/6.62	47	21/37	201	2
4402	Malate dehydrogenase, cytoplasmic	NP_001105603**	35909/5.77	68	24/45	263	1
4601	Hypothetical protein	NP_001142788**	51917/6.12	51	24/41	271	7
4602	Methionine adenosyltransferase	AFW82691**	46392/6.03	63	26/50	292	4
5001	Ribulose-1,5-bisphosphate carboxylase/oxygenase small subunit	CAA70416**	19364/8.98	69	13/54	153	1
5103	Ribosome recycling factor	NP_001150478**	29328/9.22	29	8/16	419	7
5104	Dip protein ABA- and ripening-inducible-like protein	ABW06773.1**	15905 X	25	2/2	160	2
5203	TPA: glutathione transferase	DAA51780**	25584/6.21	45	17/38	181	2
5602	Bifunctional 3-phosphoadenosine 5-phosphosulfate synthetase 2	NP_001147427**	52493/8.30	43	22/31	242	1
5608	Plastid ADP-glucose pyrophosphorylase large subunit	NP_001106017**	55600/8.57	71	40/56	464	2,4
5704	ATP synthase CF1 alpha subunit	NP_043022**	55729/5.87	49	31/41	392	1
6001	Cytochrome b6-f complex iron-sulfur subunit	ACG28186**	24321/8.52	41	10/20	152	1,2
6102	TPA: hypothetical protein ZEAMMB73_927356	DAA59517**	32073/9.50	48	12/34	159	7
6307	NAD-dependent epimerase/dehydratase	B4FH62***	31917/9.11	66	20/24	340	4
6503	Fructose-bisphosphate aldolase, cytoplasmic isozyme 1	B6SSU6***	38464/6.26	54	18/21	292	1
6713	ATP synthase CF1 alpha subunit	NP_043022**	55729/5.87	63	37/46	495	1,4
7103	Chain A, Structure Of Glutathione S-Transferase Iii In Apo Form	1AW9_A**	23416/5.97	68	11/27	166	2
7202	NAD-dependent epimerase/dehydratase	B6T962***	27809/6.77	60	18/21	306	2
7607	Putative uncharacterized protein	B4FHK4***	42290/6.53	43	23/34	263	7
3801 3807	Transketolase	Q7SIC9*	73347/5.47	65	46/72	449	1,4
8001	Ribulose bisphosphate carboxylase small chain, chloroplastic precursor	NP_001105294**	19310/9.10	62	18/61	166	1
8002	Photosystem I reaction center subunit IV A	ACG26704.1**	14885/9.79	7	1/1	56	1
8101	Putative peptidyl-prolyl *cis*-trans isomerase family protein	NP_001136688**	26599/X	X	12/X	135	2,4
8401	Glyceraldehyde-3-phosphate dehydrogenase 1	P08735*	36614/6.46	48	19/55	178	1,4
	Glyceraldehyde-3-phosphate dehydrogenase A	P09315*	43182/7.00	48	18/55	166	
	Glyceraldehyde-3-phosphate dehydrogenase 2	Q09054*	36633/6.41	46	16/55	135	
8602	Alanine aminotransferase 2	NP_001151209*	53716/6.73	39	24/37	255	4
6706 6714	Beta-glucosidase2	AFW56713**	64308/6.75	47	35/43	423	5
3802 3805 4801 4802	NADP-dependent malic enzyme, chloroplastic precursor	NP_001105313**	70293/6.09	53	43/78	353	1,4
6409 7403 7404	Glyceraldehyde-3-phosphate dehydrogenase A, chloroplastic precursor	NP_001105414**	43182/7.00	61	25/46	264	4

[a] Spot numbers refer to Fig. 3a identified either by fingerprint mass spectrometry MS (MALDI-TOF) or by MS/MS (MALDI TOF-TOF).
[b] Accession number and molecular mass according to SwissProt (us.expasy.org/sprot)*, NCBI** and TrEMBL*** databases.
[c] MW and pI were calculated from aminoacid sequence.
[d] Scores of proteins identified by peptide mass fingerprinting were determined according to Mowse values obtained either from MASCOT.
[e] (1) Photosynthesis, respiration, and chloroplast organization; (2) Redox homeostasis and stress response (defense); (3 Protein synthesis, conformation and transport; (4) Metabolism and energy; (5) Pathogenic cell lysis; (6) Resistance (7) Unknown.

In terms of root length, there was highly significant variation between C- and Sp7-treated plants at T1 in maize (Fig. 1a and b) and significant differences at T2 and T3. In tomato (Fig. 1c and d) there was no significant difference between treatments at T1, though there were at T2 and T3.

3.3. Gas exchange is modulated by A. brasilense treatments

In maize, changes in plant behavior induced by Sp7 were more immediate than those of tomato regarding augmenting photosynthesis. At T2 in maize, the photosynthetic rate (A) was significantly increased by Sp7 (Fig. 2a). In tomato, A was similar between C- and Sp7 plants, until T3 and T4. At T3, the rate of Sp7 plants was 66% lower than C-plants ($p < 0.001$).

Differences in transpiration levels (E) (Fig. 2b) were not apparent at T1 in either species. Sp7-treated maize plants transpired at a higher rate than C- plants throughout, reaching highly significant values ($p < 0.001$) at T3. In tomato, C- plants transpired 26% ($p < 0.01$) more than the Sp7-treated plants at T4.

Intercellular CO_2 concentrations (C_i) inversely reflect photosynthetic rates at T2 and T3 (Fig. 2c). In maize, Sp7-treated plants had significantly higher ($p < 0.01$) C_i at T2. Then at T3 an T4, the opposite is true; as C- plants had significantly higher C_i In tomato, C_i concentrations were similar in Sp7 and C- plants at T1 and T4, but during the T2 and T3, Sp7 tomato plant C_i levels were 20–27% lower than C-plants ($p < 0.05$). Instantaneous water use efficiency (WUE_i) values

Table 2
Main characteristics and function of identified tomato proteins corresponding to spots in Fig. 3.

SSP [a]	Protein name	Accession No. [b] (database)	Molecular Weight (Da)/pI [c]	Coverage %	No Peptides Matched/Total peptides	Score [d]	Function [e]
1202	Chlorophyll *a-b* binding protein 3C	P07370*	28225/5.15	3	1/7	31	1
2001	Cytochrome b6-f complex iron-sulfur subunit	Q69GY7*	24593/8.20	6	1/5	33	1
2004	Ribulose bisphosphate carbox. small chain 2A	P07179*	20493/6.59	48	11/46	134	1
5307 6206	Fructose-bisphosphate aldolase 2	XP_004233550**	42872/6.07	53	18/47	203	1,4
2902	Heat shock cognate protein 70 protein 2	P27322*	71062/5.08	41	26/52	195	3
2901 2902	Heat shock cognate protein 70 protein 1-like	XP_004250958**	71498/5.10	52	31/44	301	3
3002	Glycine-rich RNA-binding protein-like isoform 3	XP_004230945**	16386/5.27	71	15/29	215	6
3702	ATP synthase subunit alpha	Q2MIB5*	55434/5.14	42	25/42	296	4
3709	Inositol-3-phosphate synthase	XP_004239994**	56697/5.45	46	25/75	159	2
3906	ATP-dependent Clp protease ATP-binding subunit clpA homolog CD4B	XP_004252280**	102418/5.99	43	40/56	379	4
4003	Superoxide dismutase [Cu-Zn]	P14831*	22328/5.77	12	2/2	132	2
7401 7504	Ribulose bisphosphate carbox./oxygenase activase 1	O49074*	50897/8.61	50	26/56	245	1
4606	Glutamate-1-semialdehyde 2,1-aminomutase	NP_001234690**	51722/6.54	48	26/43	235	3
5001	ATP synthase epsilon chain	Q2MI94*	14571/5.43	63	10/36	144	2,4
5201	BG125080.1 EST470726 tomato shoot/meristem	BG125080***	25967/9.18	6	3	297	3
5302	Ferredoxin–NADP reductase	XP_004232495**	40774/8.37	61	27/39	270	1,2
5405	Phosphoglycerate kinase	XP_004243968**	50592/7.66	11	4/4	211	4
5901 5902	Transketolase	XP_004248560**	80268/5.97	46	33/52	347	4
6101	Chlorophyll *a-b* binding protein 8	XP_004248217**	29261/8.65	15	2/2	237	1
6208	Thioredoxin-like protein CDSP32	XP_004238392**	33779/7.57	18	6/6	241	2
6304	mRNA binding protein precursor	NP_001234656**	44084/7.10	38	21/45	228	6
6403	Malate dehydrogenase	XP_004247734**	35703/5.91	72	24/53	259	1
6404	Monodehydroascorbate reductase-like	XP_004246547**	47106/5.77	72	29/39	386	2,3
6406	ATP synthase gamma chain	XP_004232711**	41752/8.15	13	3/6	224	4
6505	S-adenosylmethionine synthase 3	NP_001234004**	43082/5.76	60	26/44	276	4
6509 7508	GDP-mannose 3′,5′-epimerase	NP_001234734**	42828/5.88	45	21/32	248	4
7913	Glycine dehydrogenase [decarboxylating]	XP_004245101**	114020/6.69	5	5/5	199	1
7402 7405 8404	Chloroplast stem-loop binding protein of 41 kDa b	XP_004241412**	42596/7.67	60	23/29	321	1
8404	Glyceraldehyde-3-phosphate dehydrogenase A	XP_004236849**	42940/8.46	58	23/60	234	4
7906	5-ethyltetrahydropteroyltriglutamate–homocysteine methyltransferase-like	XP_004249374**	85014/6.01	39	26/35	319	4
8101	BP903052.1 Solanum lycopersicum cDNA, clone	BP903052***	17598/6.99	56	10/40	134	7
8107	Triose phosphate isomerase (cytosolic isoform)	AAR11379**	27251/5.73	11	2	155	4
8114	Protein thylakoid formation1	XP_004243305**	33558/8.69	7	3/3	50	3
8401	Glyceraldehyde-3-phosphate dehydrogenase	NP_001266254**	32097/5.93	56	15/22	192	1,4
8506	Isocitrate dehydrogenase [NADP]-like	XP_004228607**	47001/6.35	56	24/26	327	4
8509	S-adenosylmethionine synthase 2-like	XP_004249481**	43089/6.12	8	3/3	102	4
8602	Dihydrolipoamide dehydrogenase precursor	NP_001234770**	53120/6.90	51	22/30	264	2,4

[a] Spot numbers refer to Fig. 3b identified either by fingerprint mass spectrometry MS (MALDI-TOF) or by MS/MS (MALDI TOF-TOF).
[b] Accession number and molecular mass according to SwissProt (us.expasy.org/sprot)*, NCBI** and TrEMBL*** databases.
[c] MW and pI were calculated from aminoacid sequence.
[d] Scores of proteins identified by peptide mass fingerprinting were determined according to Mowse values obtained either from MASCOT.
[e] (1) Photosynthesis, respiration, and chloroplast organization; (2) Redox homeostasis and stress response (defense); (3) Protein synthesis, conformation and transport; (4) Metabolism and energy; (5) Resistance; (6) Unknown.

significantly differed between Sp7 and C- maize plants at T1 and T2, while differences between values in tomato were not significant (Fig. 2d).

Maize E and stomatal conductance (g_s) were directly related, though g_s values were insignificant ($p > 0.05$). Tomato g_s were significant, and values fluctuated from being 62% higher in Sp7 plants (over C-) at T2, to 74% lower than C- at T4 (Fig. 2e).

3.4. Overall proteome changes identified via differential proteomics

Separation by 2-D gel electrophoresis of leaf protein extracts and comparative analysis with PDQuest software detected 43 differential spots that were significant in maize. In tomato, there were 41 significant spots. These spots did not always change significantly throughout the three sampling times, so only their significant changes are reported for each sampling time (Figs. 3–5).

Mechanisms involved in C_3 and C_4 plant response to Sp7 inoculation differ concerning timing and degree of protein changes. Sp7 decreases abundance of proteins related to photosynthesis and metabolism at T1 in the maize lifecycle, but increases those related to redox homeostasis, stress response, and pathogenesis. In tomato, proteins involved in photosynthetic processes and metabolism increased at T1, but not throughout. Most redox and stress-related proteins tended to have a delayed decrease in abundance, at T2, then gradually increased/recuperated their values at T3.

Only one protein within the 1.5-fold-change criterion could be isolated from maize at T2, and none from tomato; while three proteins of the same criterion could be isolated from tomato at T3, and none from maize.

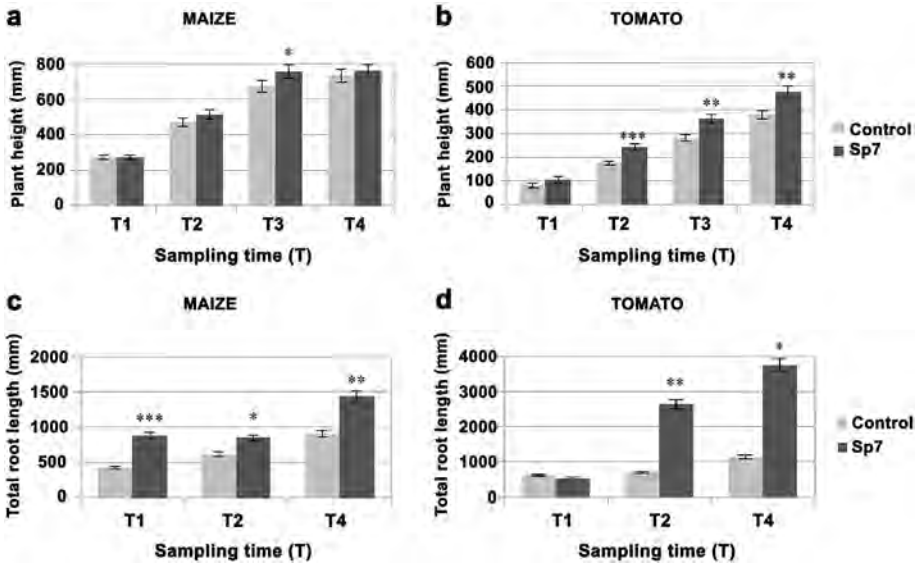

Fig. 1. Plant height and root length. (a & b) Plant height (mm) of (a) maize and (b) tomato treated with Sp7 vs controls at different sampling times (T). **(c & d)** Root length (mm) of (c) maize and (d) tomato treated with Sp7 vs controls. Asterisks indicate statistically significant differences between treatments for each sampling time: * ($p < 0.05$), ** ($p < 0.01$), *** ($p < 0.001$).

3.5. Biological processes of shared proteins identified in response to A. brasilense Sp7 inoculation

There were ten proteins altered by *A. brasilense* Sp7 common to the two species (Table 3), but none of these proteins coincided in fitting the 1.5 or 2-fold-change criterion. At T1, the six common proteins were: *cytochrome b6-f complex iron-sulfur subunit* (EC 1.10.9.1), *fructose bisphosphate aldolase* (EC 4.1.2.13), *glyceraldehyde-3-phosphate dehydrogenase* (EC 1.2.1.9), *ribulose 1,5 bisphosphate carboxylase/oxygenase* (EC 4.1.1.39) (*Rubisco), phosphoglycerate kinase* (EC 2.7.2.3) and *S-Adenosyl-L-methionine* (EC 2.1.1.41) (*SAM*). These proteins are mainly involved in photosynthesis, metabolism, or both. All except one protein (*SAM*) decreased in abundance in maize and increased in tomato. *SAM* increased in both species.

At T2 there were three proteins that changed in abundance in both species: *ATP synthase* (EC 3.6.3.14), *glyceraldehyde-3-phosphate dehydrogenase* and *transketolase* (EC 2.2.1.1). All of these proteins are involved in plant metabolism and increased in abundance in maize, but decreased in tomato. Then at T3, the two common proteins were *ATP synthase* (photosynthesis and metabolism) and the *chlorophyll A-B binding protein* (EC 1.10.3.9) (photosynthesis and stress response). Similar to the common proteins at T2, these proteins both increased in abundance in maize, but decreased in tomato.

3.6. Early response to A. brasilense Sp7

At T1 in maize, the majority (62%) of the proteins decreased in abundance, and most were related to photosynthesis and metabolism, as well as protein synthesis and transport. In contrast, proteins related to redox homeostasis, stress response, and pathogenesis had an even rate of increased and decreased abundance. Protein alterations within the 2-fold change criterion were the *dip protein* (2.3-fold) and *beta-glucosidase 2* (EC 3.2.1.21) (2-fold), related with redox homeostasis and DNA damage response, respectively. The most decreased protein was *fructose bisphosphotase-aldolase* (−2.25-fold), related with metabolism.

In tomato, 29% of the proteins decreased in abundance, and only one (unknown, but likely related to protein synthesis and transport) changed significantly (−1.83-fold). Alternatively, 71% of the proteins increased in abundance, and most were related with photosynthesis and protein synthesis. The most strikingly increased proteins were *chloroplast stem-loop binding protein of* 41 kDa b (3.2-fold), *monohydroascorbate reductase-like* (1.6.5.4) (2.7-fold), *dihydrolipoamide dehydrogenase precursor* (EC 1.8.1.4) (2.2-fold) and *malate dehydrogenase* (EC 1.1.1.38) (1.65-fold). These proteins are associated with photosynthesis, stress response and protein synthesis.

3.7. Alteration to protein abundance in subsequent weeks/sampling times

The altered abundance of proteins in maize at T2 and T3 did not reach more than 2-fold. There was one case of a 1.5-fold change at T2: *glyceraldehyde-3-phosphate dehydrogenase A, chloroplastic precursor* (1.58-fold). This protein is involved in metabolism, and falls within the trend for increased abundance of other proteins of the same functional category at both T2 and T3 in maize.

In tomato, Sp7 caused all proteins to decrease in abundance at T2, but none more than −1.5-fold. At T3, the most strikingly increased protein was *glycine dehydrogenase* (EC 1.4.1.10) (1.65-fold), related to photosynthesis, and the most decreased were *NADPH-dependent thioredoxin reductase 3-like isoform 2/Inositol-3-phosphate synthase* (EC 1.8.1.9) (−1.78-fold), and *ATP-dependent Clp protease ATP-binding subunit clpA homolog CD4B* (EC 3.4.21.92) (−1.83-fold); related to redox homeostasis and protein synthesis, respectively.

4. Discussion

Progress has been made in identifying *A. brasilense* Sp7-regulated growth, nutrient content and yield in plants, but studies focusing on the proteomics of *A. brasilense* Sp7 in model plants are less common. The need for proteomic studies of PGPRs has indeed been addressed, as there is an exhaustive study (Cheng et al., 2010) comparing the impact of various PGPR on (symbiotic) plant proteomes; though *A. brasilense*, maize, and tomato are not included. In this study, we investigated how *A. brasilense* Sp7 interacts with the proteome of C_3 (tomato) and C_4 (maize) plants by inoculating seeds and comparing results to gas exchange parameters. Results have allowed us to characterize the early interaction of Sp7 with the developing seedlings. Within this framework, our analysis gives particular emphasis to T1 (four-leaf stage), where a total of 24 proteins were identified in tomato and 26 in maize, six of which were co-regulated in both species. Above all, it was at this sampling time that the highest number of proteins with striking differences were observed.

Physiological and gas exchange results indicated that inoculated maize seedlings had significantly enhanced root growth and WUE_i at the four-leaf stage. The ability of plants to withstand stresses has been attributed to their superior WUE_i, CO_2 fixation, long taproots and development of an extensive lateral root system in response to water shortage in the soil (Kadereit et al., 2003). Furthermore, better seedling emergence and earlier vegetative growth (i.e., seedling vigor) are

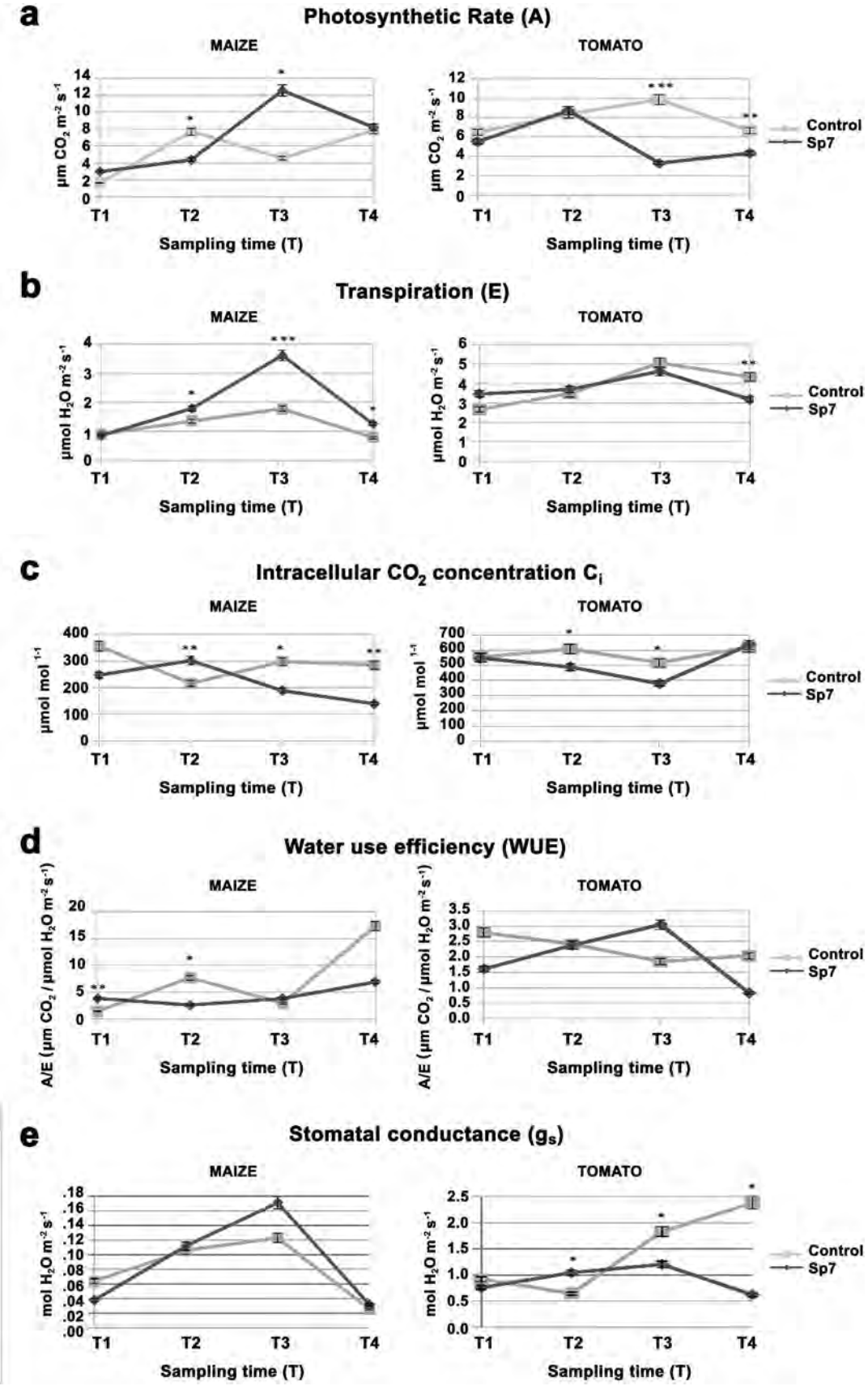

Fig. 2. Gas exchange parameters in maize (left) and tomato (right) plants at different sampling times (T); Sp7-treated plants vs controls. (a) Photosynthetic rate (A); **(b)** Transpiration (E); **(c)** Intercellular CO_2 concentration (C_i); **(d)** Water use efficiency (WUE_i); **(e)** Stomatal conductance (g_s). Asterisks indicate statistically significant differences between treatments for each sampling time: * ($p < 0.05$), ** ($p < 0.01$), *** ($p < 0.001$).

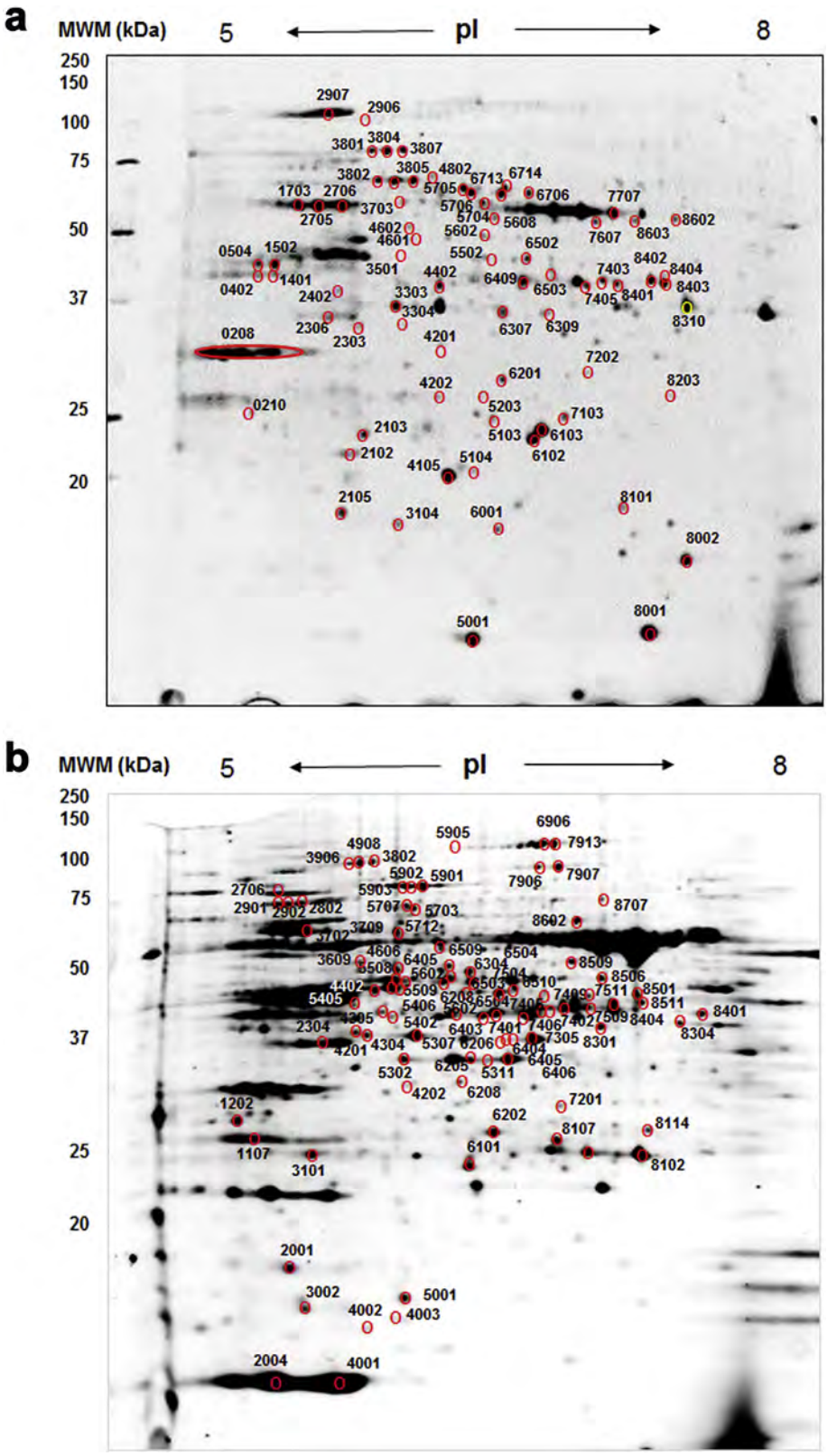

Fig. 3. 2-D page gels of extracted proteins from maize and tomato plants. Representative 2-D PAGE gel image of **(a)** maize and **(b)** tomato with Sp7 inoculation. Molecular markers are indicated in kDa. The representative spots and their numbers which show variation between treatments are indicated by the red circles. (For interpretation of the references to color in this figure legend, the reader is referred to the Web version of this article.)

considered to be essential traits for best WUE_i in cereals in Mediterranean conditions (Richards et al., 2002), so at least in this regard, we see that Sp7 inoculation has had a more profound and immediate effect on maize compared to tomato.

Of the proteins with expression changes in inoculated maize and tomato seedlings at the four-leaf stage, 90% had less that 2-fold

A.

	Sp7/C			
SSP	T1	T2	T3	Function
7402	**3.22			1
6404	**2.69			2,3
8602	**2.23			2,4
7913			*1.65	1
6403	*1.64			1
8401	1.47			1,4
6304	1.42		-0.86	6
7508	1.37	-0.28		4
8509	1.35			4
7405	1.29			1
5405	1.16		0.73	4
8506	1.16			4
2001	0.91			1
7504			0.87	1
6206	0.88			1,4
7401	0.86			1
6505	0.83			4
8101			0.79	7
2004			0.74	1
8107	0.71			4
8114	0.55	-0.71		3
3002		-0.47		6
5901		-0.57		4
4606		-0.59		3
6208		-0.64		2
1202	-0.64	-0.71	-0.53	1
5302	-0.71		-0.88	1,2
6509		-0.71		4
2901	-0.73			3
8404		-0.73		1,4
5001		-0.76		2,4
6406		-0.86		4
5902		-0.88		4
4003		-0.91		2
2902	-1.05			3
5307		-1.08		1,4
6101	-1.25	-0.62		1
3702			-1.35	4
3709			*-1.78	2
3906	-1.25		*-1.83	4
5201	*-1.83			3

log2 FC
>2
> 1.5
1
0
-1
< -1.5
< -2

B.

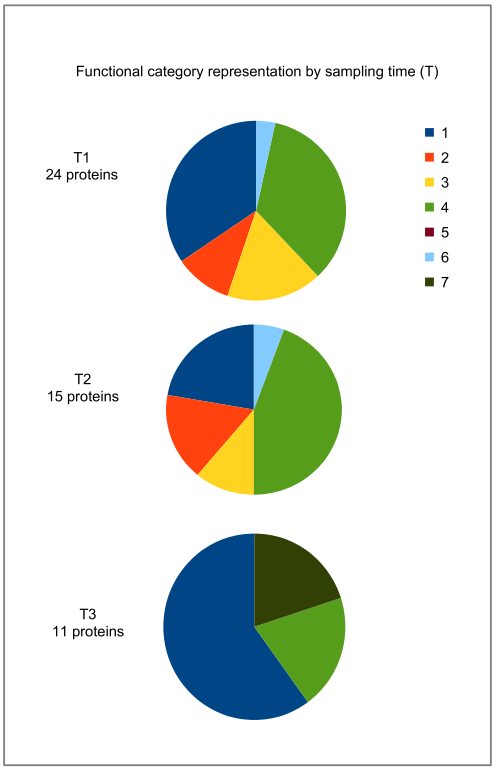

Fig. 4. Tomato heatmap (a) of differentially expressed proteins over 3 sampling times (T) and (b) relative expression of each functional category for each T. The heatmap color scale indicates differential regulation as the (log2) Fold Change of the Sp7-treated plant protein amount relative to Control plants at each T. Analyzed spots were those in which the differences were more consistent (variation coefficient ≤50% among replicates, spots present in all measured conditions, measured ratios ≤0.5 or ≥2.0 and spots validated in visu. Proteins are annotated by spot numbers identified either by fingerprint mass spectrometry MS (MALDI-TOF) or by MS/MS (MALDI TOF-TOF) (Tables 1 and 2), and arranged according to relative expression levels; up-regulation is indicated in red, down-regulation in green. A value of 0, in grey, indicates no significant change in protein expression level. A single asterisk (*) indicates a > 1.5 or < -1.5 FC, two asterisks (**) are > 2 or < -2 FC. Differential expression is of proteins involved in biochemical pathways related to **(1)** Photosynthesis, respiration, and chloroplast organization; **(2)** Redox homeostasis and stress response; **(3)** Protein synthesis, conformation and transport; **(4)** Metabolism and energy; **(5)** Pathogenic cell lysis; **(6)** Resistance; **(7)** Unknown. (For interpretation of the references to color in this figure legend, the reader is referred to the Web version of this article.)

expression changes. Comparing abundance of the most strikingly effected proteins at T1, our results show that proteins related to metabolism and redox homeostasis constituted the majority of the identified proteins for each species individually, as well as for the overlapping proteins. Specifically, in inoculated maize, the most striking accumulation of proteins was related to redox homeostasis and pathogenic cell lysis, and reduction was in those related to metabolism and energy. In inoculated tomato, there was a wider array (function-wise) of strikingly accumulated proteins, related to photosynthesis and respiration, redox homeostasis, protein synthesis, metabolism and energy.

In maize, the increased proteins were *dip* protein and *beta-glucosidase2*. The *dip* protein may be cross-influenced by both the plant and Sp7 since it holds a role in the production of abscisic acid (ABA) by plants under stress (Finn et al., 2017), and is synthesized by *A. brasilense* (Cohen et al., 2015). *Beta-glucosidase2* is active in secondary plant metabolism, as well as catabolism of flavonoid glycosides during recovery from wounding stress and DNA damage (Roepke and Bozzo, 2015). However, since *A. brasilense* itself produces *beta glucosidases*, it is

A.

SSP	Sp7/C T1	T2	T3	Function
5104	**2.31			2
6706	**2.04			5
6714	*1.83			5
3205	*1.77			7
7103	*1.69		-0.53	2
7403		*1.58		4
3805			1.4	1,4
4801			1.31	1,4
5704	1.24			1
3807		1.22	0.82	1,4
5203	1.2			2
7202	1.19		-0.69	2
8401		1.12	1.07	1,4
6713			1.02	1,4
7607		1.04		7
6307	0.96			4
4802		0.84		1,4
5608		0.79		2,4
2705		0.79		2
3801			0.79	1,4
2103			0.77	1,2
8602		0.64		4
4602	0.57		-0.64	4
402	-0.35	-0.43		3,4
8001	-0.62			1
504	-0.68			2
7404	-0.71			4
5602	-0.73			1
201		-0.78		3
6409	-0.81			4
5001	-0.83	-0.43		1
4105		-0.91		2,4
4601	-1			7
4402		-1.05	-0.62	1
3802	-1.05		0.94	1,4
8101	-1.18	-0.76	0.88	2,4
5103		-1.18	-0.78	7
6102	-1.21			7
3104	-1.32	-0.49		1
8002	-1.43			1
6503	*-1.51			1
6001	*-1.94		0.98	1,2
3303	**-2.25			4

log2 FC: >2, >1.5, 1, 0, -1, <-1.5, <-2

B.

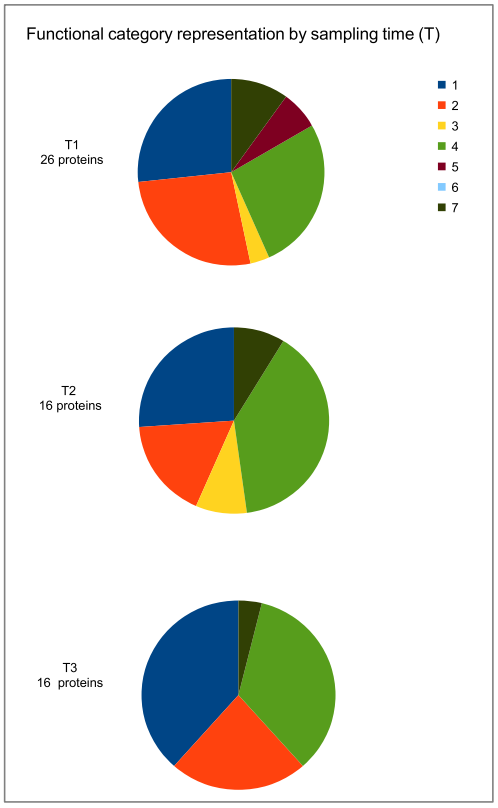

Fig. 5. Maize heatmap (a) of differentially expressed proteins over 3 sampling times (T) and (b) relative expression of each functional category for each T. The heatmap color scale indicates differential regulation as the (log2) Fold Change of the Sp7-treated plant protein amount relative to Control plants at each T. Analyzed spots were those in which the differences were more consistent (variation coefficient ≤50% among replicates, spots present in all measured conditions, measured ratios ≤0.5 or ≥2.0 and spots validated in visu. Proteins are annotated by spot numbers identified either by fingerprint mass spectrometry MS (MALDI-TOF) or by MS/MS (MALDI TOF-TOF) (Tables 1 and 2), and arranged according to relative expression levels; up-regulation is indicated in red, down-regulation in green. A value of 0, in grey, indicates no significant change in protein expression level. A single asterisk (*) indicates a > 1.5 or < -1.5 FC, two asterisks (**) are > 2 or < -2 FC. Differential expression is of proteins involved in biochemical pathways related to **(1)** Photosynthesis, respiration, and chloroplast organization; **(2)** Redox homeostasis and stress response; **(3)** Protein synthesis, conformation and transport; **(4)** Metabolism and energy; **(5)** Pathogenic cell lysis; **(6)** Resistance; **(7)** Unknown. (For interpretation of the references to color in this figure legend, the reader is referred to the Web version of this article.)

possible that the expression of exogenous *beta-glucosidases* leads to plant phenotypes with increased phytohormone levels and increased resistance to biotic attack, as has been found in previous studies (Jin et al., 2011). Hence, we may be witnessing a "priming" effect, in which the PGPR is inducing ISR and the hormone pathways involved. The other increased protein was *glutathione* (within the 1.5-fold change criterion). *Glutathione* is vital in the transmission of ROS signaling as an interfacing molecule between ROS, NO, and protein Cys groups (Noctor et al., 2017), while it is also tightly interwoven with its role as a modulator of stress response hormones salicylic acid (SA), jasmonic acid (JA), and ethylene (ET) signaling pathways (Mhamdi et al., 2010; Han et al., 2013a,b; Datta et al., 2015), as well as plant development hormones auxin and ABA (Yu et al., 2013). *Glutathione transferase* redox imbalance triggers oxidation of crucial components of these hormonal signaling pathways, so its increase indicates that Sp7 inoculation induced reactions that counterbalance and substitute GAPDH and Rubisco molecules participating in the CB cycle. Confirming this, *fructose bisphosphatase aldolase* decreased in accumulation. This protein implies the active role of glycerate, and is involved in the carbon shuffle reactions replenishing Rubisco by oxygenation, an event signaling down-regulation of the entire CB cycle (Schimkat et al., 1990).

In tomato, increased proteins at T1 were *chloroplast stem-loop binding protein of* 41 kDa b (CSP41), *monodehydroascorbate reductase-like* (MDAR), *dihydrolipoamide dehydrogenase precursor* (DLD) and *malate dehydrogenase* (MDH). CSP41proteins are highly abundant RNA-binding proteins in the chloroplast stroma (Zybailov et al., 2008). Their

Table 3
Common proteins in maize (cv. B73) and tomato (cv. Boludo) plants that were altered on account of *Azospirillum brasilense* (Sp7) inoculation at each Sampling time.

Sampling time	Protein	Corresponding spot(s)		Protein abundance: Sp7/C		Function
		Maize	Tomato	Maize	Tomato	
1	Cytochrome b6-f complex iron-sulfur subunit	3104, 6001	2001	↓↓	↑	1, 2
	Fructose bisphosphate aldolase	3303, 6503	6206	↓↓	↑	1,4
	Glyceraldehyde-3-phosphate dehydrogenase	7404, 6409	8401	↓↓	↑	1, 4
	Ribulose 1,5 bisphosphate carboxylase/oxygenase	5001, 8001	7401	↓↓	↑	1
	Phosphoglycerate kinase	504	5405	↓	↑	2,4
	Methionine (SAM)	4602	8509, 6505	↑	↑↑	4
2	ATP synthase	2705	5001, 6406	↑	↓↓	2, 4
	Glyceraldehyde-3-phosphate dehydrogenase	8401, 7403	8404	↑↑	↓	1, 4
	Transketolase	3807	5901, 5902	↑	↓↓	1, 4
3	ATP synthase	6713	3702	↑	↓	1, 4
	Chlorophyll A-B binding protein	2103	1202	↑	↓	1, 2

function is critical in mature leaves when transcripts produced by *phosphoenolpyruvate* (PEP) become limiting and need to be stabilized and protected (Majeran et al., 2005). The presence of CSP41 increases transcripts for photosynthetic proteins and of some ribosomal RNAs, which in turn, maintains or increases the translational activity of chloroplasts (Leister, 2014). MDAR is an enzymatic component of the glutathione-ascorbate cycle also serving to protect cells against damage incurred by ROS (Leterrier et al., 2005). In other studies with tomato, MDAR was increased by stress conditions such as high salinity (Mittova et al., 2003), so our inoculated tomato plants had up-regulated redox homeostasis, like maize. Finally, DLD and MDH are both implicated in the tricarboxylic acid (TCA) cycle (Wang et al., 2017). Overexpression of DLD, also known as the L-protein component of the *glycine decarboxylase* protein (GDC-L), has been shown to lower CO_2 compensation points while causing higher net-CO_2 uptake rates and better growth (Timm et al., 2016). Meanwhile, the MDH increment suggests that Sp7 inoculation caused C_3 glutamate to rapidly turn-over as an intermediate in the photorespiratory N cycle and thereby down-regulate N metabolism in tomato (Nunes-Nesi et al., 2010).

Due to the great number of proteins involved in redox homeostasis at T1, combined with the importance of understanding the effects of redox homeostasis on subsequent plant processes and growth, we also compared all significant physiological parameters with altered proteins that fell into the 1.5 fold-change criteria for subsequent growth stages. In maize at the seven-leaf stage (T2), *glyceraldehyde-3-phosphate dehydrogenase A* (GAPDH), a protein suggested to be an enzyme-forming part of the system protecting the cell against ROS (Jorrín-Novo et al., 2009), had increased abundance in inoculated plants. This increase coincided with significantly increased transpiration (E) and intracellular CO_2 concentration (C_i), but significantly decreased photosynthetic rate (A) and WUE_i. Then, a week later, at the end of tillering, there was a significant increase in A and E. Accumulation of intracellular ROS depends on a balance between the generation and detoxification of ROS via various ROS-scavenging enzymes. Several studies suggest that the combination of decreased levels of intracellular ROS and a reduced rate of photoinhibition can be achieved by engineering the production of ROS-scavenging enzymes in higher plants (Gururani et al., 2015). The Sp7 effect to maize appears to be similar; inoculation first instigated a stress-effect that increased ROS-scavenging enzymes, which ultimately reduced photoinhibition.

In the case of inoculated tomato, stomatal conductance (g_s) significantly increased at the seven-leaf (T2) stage and C_i decreased. Photosynthesis (A) plays a well-documented role in CO_2 regulation of stomatal apertures (g_s) by lowering the intercellular CO_2 concentration (C_i) in leaves (Mott, 1988), but in this scenario, A (and E) remained unchanged. Recent studies focusing on genetics have been trying to pinpoint the cause of C_i-dependent and C_i-independent induced stomatal opening; and one model points towards *protein kinase* abundance as a driver of fluctuations between C_i content and stomatal aperature (Engineer et al., 2016). Our gas exchange results coincided with 100% of the proteins slightly decreasing in abundance at T2, and *phosphoglycerate kinase* (PGK) (a metabolic kinase that moonlights as a protein kinase) was in this group. PGK catalyzes the ATP-dependent phosphorylation of *3-phosphoglycerate* (3-PG) to *1,3-diphosphoglycerate* and second step of the CB cycle, but it is so sensitive to the redox state that the oxidized enzyme has been shown to lose its activity (Tsukamoto et al., 2013). Therefore, the disconnect between A and g_s in the case of inoculation could be a result of oxidated and reduced PGK, or damaged photosynthetic mechanisms; both of which may have been caused by excessive ROS at T1.

At the nine-leaf stage (T3), inoculated tomato plants had significantly decreased A, C_i and g_s. Once again, there is discordance in the regulation between the three gas exchange parameters since down-regulated A and C_i should theoretically lead to up-regulated g_s. Furthermore, it has been reported that increased photosynthetic activity as a result of PGPR inoculation leads to higher N incorporation and therefore increased formation of chlorophyll (Baset Mia et al., 2010). Proteome data indicated that at this time, *glycine dehydrogenase* (GLDC) increased in abundance. GLDC is a photorespiratory intermediate whose increased abundance indicates inhibition of the CB cycle and up-regulation of photorespiratory metabolism (Timm et al., 2016). Furthermore, *NADPH-dependent thioredoxin reductase* (NTRC) and *ATP-dependent Clp protease* both decreased in abundance. NTRC works against ROS, serving as part of the plant's defense system (Alscher et al., 2002), while *ATP-dependent Clp protease* is essential for chloroplast development and plant viability (Clarke, 2012). Taking tomato physiological and proteomic results together, joint analysis reveals that T3 Sp7-treated plants are less prone to fighting ROS, but do have inhibited CB cycle and chloroplast development. Therefore, we may presume that the main mechanism of photosynthesis diminution is either related to the direct effect of Sp7 on the physiological status of tomato plants at this specific growth stage; or by residual effects resulting from damage to the plant at earlier sampling times. Similar results have been reported for other PGPR and the effects that they have on runner bean and soybean at different growth stages (Marius et al., 2013; Zhang et al., 1997).

Despite the increase of photorespiratory proteins and decreased gas exchange parameters, plant height and root length continued to increase, especially at T3. This may be related to the effects of ROS. It has been found that ROS overexpression stimulates root elongation, calling for redox control of the cell cycle (Passardi et al., 2006). Stress induced presence of ROS and reactive nitrogen species (RNS) in specific tissues have also been found to affect root morphology by reducing primary root growth and promoting branching (Reichheld et al., 1999).

5. Conclusions

Sp7 interacts differently with the primary metabolism of the two

plants. Results were most striking at the four-leaf stage for both species. Proteins related to metabolism and redox homeostasis were most abundant in tomato, though this was followed by an inhibited CB cycle and chloroplast development, indicating that photosynthetic proteins were damaged by ROS. In contrast, Sp7 inoculation to maize first instigated a stress-effect that increased ROS-scavenging enzymes, reducing photoinhibition. Sp7 inoculation induced reactions in maize that counterbalanced and substituted molecules participating in the CB cycle. Our findings differ from those of Shivaprasad et al. (2012) in that PGPR immediately leads to attenuation of defense responses in maize to allow for colonization because in our study, Sp7 tardily alters the defense response (which may then assist colonization). In contrast, Sp7-treated tomato plants indeed had activated defense and metabolic responses at the four-leaf stage. Finally, better seedling emergence and vigor was observed in inoculated maize compared to tomato. Overall, the early interaction of Sp7 with maize is more complex and beneficial than that with tomato because the photosynthetic apparatus is protected by the C_4 mechanism, thereby offsetting the stress involved in association and improving the interaction of the PGPR with maize.

Contributions

SL and VM analyzed the data and wrote the manuscript. AIC, CR, LS, ES, and MAA were involved in plant cultivation, sample collection, and proteomic analysis. AIC, CR, LS, and VM designed the experiments.

Funding

We thank the MINCyT of Spain for supporting this research with project ref. AGL2010-15691. SL was supported by the UdL-Jade Plus Grant for pre-doctoral researchers and AIC by the UdL-IMPULS program.

Declarations of interest

None.

Acknowledgements

The authors would like to especially thank Dr. Isabel Sanchez for helping with the Proteomic analysis, and Dr. Paul Christou for comments on the manuscript.

References

Alscher, R.G., Erturk, N., Heath, L.S., 2002. Role of superoxide dismutases (SODs) in controlling oxidative stress in plants. J. Exp. Biol. 53 (372), 1331–1341.
Baldani, V.L.D., Alvarez, M.A.B., Baldani, J.I., Dobereiner, J., 1986. Establishment of inoculated *Azospirillum* spp in the rhizosphere and in root of field grown wheat and sorghum. Plant Soil 90, 35–46.
Baset Mia, M.A., Shamsuddin, Z.H., Wahab, Z., Marziah, M., 2010. Effect of plant growth promoting rhizobacterial (PGPR) inoculation on growth and nitrogen incorporation of tissue-cultured Musa plantlets under nitrogen-free hydroponics condition. Aust. J. Crop. Sci. 4 (2), 85–90.
Bashan, Y., Holguin, G., Lifshitz, R., 1993. Isolation and characterization of plant growth-promoting rhizobacteria. In: Methods in Plant Molecular Biology and Biotechnology. CRC Press, Boca Raton, FL, USA, pp. 331–345.
Beimalt, S., Sonnwald, U., 2014. Plant-microbe interactions to probe regulation of plant carbon metabolism. J. Plant Physiol. 163, 307–318.
Botta, L.A., Santacecilia, A., Ercole, C., Cacchio, P., del Gallo, M., 2013. *In vitro* and *in vivo* inoculation of four endophytic bacteria on *Lycopersicon esculentum*. N. Biotech. 30 (6), 666–674.
Cassán, F., Perrig, D., Sgroy, V., Masciarelli, O., Penna, C., Luna, V., 2009. *Azospirillum brasilense* Az39 and *Bradyrhizobium japonicum* E109, inoculated singly or in combination, promote seed germination and early seedling growth in corn (*Zea mays* L.) and soybean (*Glycine max* L. Eur. J. Soil Biol. 45, 28–35.
Cheng, Z., McConkey, J., Glick, B.R., 2010. Proteomic studies of plant-bacteria interactions. Soil Biol. Biochem. 42, 1673–1684.
Clarke, A.K., 2012. The chloroplast ATP-dependent Clp protease in vascular plants- new dimensions and future challenges. Physiol. Plantarum 145 (1), 235–244.
Cohen, A.C., Bottini, R., Pontin, M., Berli, F.J., Moreno, D., Boccanlandro, H., Travaglia, C.N., Piccoli, P.N., 2015. *Azospirillum brasilense* ameliorates the response of *Arabidopsis thaliana* to drought mainly via enhancement of ABA levels. Physiol. Plantarum 153 (1), 79–90.
Covshoff, S., Hibberd, J.M., 2012. Integrating C4 photosynthesis into C3 crops to increase yield potential. Plant Biotechnol. 23, 209–214.
Cueto-Ginzo, A.I., Serrano, L., Sin, E., Rodríguez, R., Morales, J.G., Lade, S.B., Medina, V., Achon, M.A., 2016. Exogenous salicylic acid treatment delays initial infection and counteracts alterations induced by *Maize dwarf mosaic virus* in the maize proteome. Physiol. Mol. Plant Pathol. 96, 46–59.
Datta, R., Kumar, D., Sultana, A., Hazra, S., Bhattacharyya, D., Chattopadhyay, S., 2015. Glutathione regulates 1-aminocyclopropane-1-carboxylate synthase transcription via WRKY33 and 1-aminocyclopropane-1-carboxylate oxidase by modulating messenger RNA stability to induce ethylene synthesis during stress. Plant Physiol. 169, 2963–2981.
Dobbelaere, S., Croonenborghs, A., Thys, A., Ptacek, D., Vanderleyden, J., Dutto, P., Labandera-Gonzalez, C., Caballero-Mellado, J., Aguirre, J.F., Kapulnik, Y., Brener, S., Burdman, S., Kadouri, D., Sarig, S., Okon, Y., 2001. Responses of agronomically important crop to inoculation with *Azospirillum*. Aust. J. Plant Physiol. 28, 871–879.
El Zemrany, H., Cortet, J., Lutz, M.P., Chabert, A., Baudoin, E., Haurat, J., Maughan, N., Felix, D., Defago, G., Bally, R., Moenne-Loccoz, Y., 2006. Field survival of the phytostimulator *Azospirillum lipoferum* CRT1 and functional impact on maize crop, biodegradation of crop residues, and soil faunal indicators in a context of decreasing nitrogen fertilisation. Soil Biol. Biochem. 38, 1712–1726.
Engineer, C., Hashimoto-Sugimoto, M., Negi, J., Israelsson-Nordstrom, M., Azoulay-Shemer, T., Rappel, W.-J., Iba, K., Schroeder, J., 2016. CO_2 sensing and CO_2 regulation of stomatal conductance: advances and open questions. Trends Plant Sci. 21 (1), 16–30.
Finn, R.D., Attwood, T.K., Babbitt, P.C., Bateman, A., Bork, P., Bridge, A.J., Chang, H.-Y., Dosztányi, Z., El-Gebali, S., Fraser, M., Gough, J., Haft, D., Holliday, G.L., Huang, H., Huang, X., Letunic, I., Lopez, R., Lu, S., Marchler-Bauer, A., Mi, H., Mistry, J., Natale, D.A., Necci, M., Nuka, G., Orengo, C.A., Park, Y., Pesseat, S., Piovesan, D., Potter, S.C., Rawlings, N.D., Redaschi, N., Richardson, L., Rivoire, C., Sangrador-Vegas, A., Sigrist, C., Sillitoe, I., Smithers, B., Squizzato, S., Sutton, G., Thanki, N., Thomas, P.D., Tosatto, S.C.E., Wu, C.H., Xenarios, I., Yeh, L.-S., Young, S.-Y., Mitchell, A.L., 2017. InterPro in 2017 — beyond protein family and domain annotations. Nucleic Acids Res Jan 2017.
Glick, B.R., 2012. Plant growth-promoting bacteria: mechanisms and applications. Scientifica 2012, 963401.
Gururani, M.A., Venkatesh, J., Tran, L.-S.P., 2015. Regulation of photosynthesis during abiotic stress-induced photoinhibition. Mol. Plant 8 1304–1302.
Han, Y., Chaouch, S., Mhamdi, A., Queval, G., Zechmann, B., Noctor, G., 2013a. Functional analysis of Arabidopsis mutants points to novel roles for glutathione in coupling H_2O_2 to activation of salicylic acid accumulation and signaling. Antioxidants Redox Signal. 18, 2106–2121.
Han, Y., Mhamdi, A., Chaouch, S., Noctor, G., 2013b. Regulation of basal and oxidative stress-triggered jasmonic acid-related gene expression by glutathione. Plant Cell Environ. 36, 1135–1146.
Hochholdinger, F., Guo, L., Schnable, P.S., 2004. Lateral roots affect the proteome of the primary root of maize *(Zea mays L.)*. Plant Mol. Biol. 56 (3), 397–412.
Ibort, P., Imai, H., Uemura, M., Aroca, R., 2018. Proteomic analysis reveals that tomato interaction with plant growth promoting rhizobacteria is highly determined by ethylene perception. J. Plant Physiol. 220, 43–59.
Jin, S., Kanagaraj, A., Verma, D., Lange, T., Daniell, H., 2011. Release of hormones from conjugates: chloroplast expression of β-glucosidase results in elevated phytohormone levels associated with significant increase in biomass and protection from aphids or whiteflies conferred by sucrose esters. Plant Physiol. 155, 222–235.
Jorrín-Novo, J.V., Maldonado, A.M., Echevarría-Zomeño, S., Valledor, L., Castillejo, M.A., Curto, M., Valero, J., Sghaier, B., Donoso, G., Redondo, I., 2009. Plant proteomics update (2007-2008): second-generation proteomic techniques, an appropriate experimental design, and data analysis to fulfill MIAPE standards, increase plant proteome coverage and expand biological knowledge. J. Proteom. 72, 285–314.
Kadereit, G., Borsch, T., Weising, K., Freitag, H., 2003. Phylogeny of amaranthaceae and chenopodiaceae and the evolution of C-4 photosynthesis. Int. J. Plant Sci. 164, 959–986.
Kamnev, A.A., Tugarova, A.V., Tarantilis, P.A., Gardiner, P.H.E., Polissiou, M.G., 2012. Comparing poly-3-hydroxybutyrate accumulation in *Azospirillum brasilense* strains Sp7 and Sp245: the effects of copper(II). Appl. Soil Ecol. 61, 213–216.
Lancashire, P.D., Bleiholder, H., Langelüddecke, P., Stauss, R., 1991. An uniform decimal code for growth stages of crops and weeds. Ann. Appl. Biol. 119, 561–601.
Lavania, M., Chauhan, P.S., Chauhan, S.V., Singh, H.B., Nautiyal, C.S., 2006. Induction of plant defense enzymes and phenolics by treatment with plant growth-promoting rhizobacteria *Serratia marcescens* NBRI1213. Curr. Microbiol. 52, 363–368.
Leister, D., 2014. Complex(iti)es of the ubiquitous RNA-binding CSP41 proteins. Front. Plant Sci. 5 (255), 1–4.
Leterrier, M., Corpas, F.J., Barroso, J.B., Sandalio, L.M., del Río, L.A., 2005. Peroxisomal monodehydroascorbate reductase. Genomic clone characterization and functional analysis under environmental stress conditions. Plant Physiol. 138 (4), 2111–2123.
Lodwig, E.M., Hosie, A.H., Bourdès, A., Findlay, K., Allaway, D., Karunakaran, R., Downie, J., Poole, P.S., 2003. Amino-acid cycling drives nitrogen fixation in the legume-Rhizobium symbiosis. Nature 422, 722–726.
Majeran, W., Friso, G., Ponnala, L., Connolly, B., Huang, M., Reidel, E., Zhang, C., Asakura, Y., Bhuiyan, N.H., Sun, Q., Turgeon, R., van Wijk, K.J., 2010. Structural and metabolic transitions of C4 leaf development and differentiation defined by microscopy and quantitative proteomics in maize. Plant Cell 22, 3509–3542.
Majeran, W., Cai, Y., Sun, Q., van Wijk, K.J., 2005. Functional differentiation of bundle sheath and mesophyll maize chloroplasts determined by comparative proteomics. Plant Cell 17 (11), 3111–3140.

Marius, S., Munteanu, N., Stoleru, V., Mihasan, M., 2013. Effects of inoculation with plant growth promoting rhizobacteria on photosynthesis, antioxidant status and yield of runner bean. Rom. Biotechnol. Lett. 18 (2), 8132–8143.
Mengel, K., Viro, M., 1978. The significance of plant energy status for the uptake and incorporation of NH4 nitrogen by young rice plants. Soil Sci. Plant Nutr. 24 (3), 407–416.
Mhamdi, A., Hager, J., Chaouch, S., Queval, G., Han, Y., Taconnat, Y., Saindrenan, P., Issakidis-Bourguet, E., Gouia, H., Renou, J.P., Noctor, G., 2010. *Arabidopsis* GLUTATHIONE REDUCTASE 1 is essential for the metabolism of intracellular H2O2 and to enable appropriate gene expression through both salicylic acid and jasmonic acid signaling pathways. Plant Physiol. 153, 1144–1160.
Mittova, V., Tal, M., Volokita, M., Guy, M., 2003. Up-regulation of the leaf mitochondrial and peroxisomal antioxidative systems in response to salt-induced oxidative stress in the wild salt-tolerant tomato species *Lycopersicon pennellii*. Plant Cell Environ. 6, 845–856.
Mott, K.A., 1988. Do stomata respond to CO_2 concentrations other than intercellular. Plant Physiol. 86 (1), 200–203.
Mus, F., Crook, M.B., Garcia, K., Garcia Costas, A., Geddes, B.A., Kouri, E.D., Paramasivan, P., Ryu, M.-H., Oldroyd, G.E.D., Poole, P.S., Udvardi, M.K., Voigt, C.A., Ané, J.-M., Peters, J.W., 2016. Symbiotic nitrogen fixation and the challenges to its extension to nonlegumes. Appl. Environ. Microbiol. 82, 3698–3710.
Nunes-Nesi, A., Fernie, A.R., Stitt, M., 2010. Metabolic and signaling aspects underpinning the regulation of plant carbon-nitrogen interactions. Mol. Plant 3 (6) 973–966.
Noctor, G., Reichheld, J.P., Foyer, C.H., 2017. ROS-related redox regulation and signaling in plants. Semin. Cell Dev. Biol. 80, 3–12.
Okon, Y., Albrecht, S.L., Burris, R.H., 1977. Methods for growing *Spirillum lipoferum* and for counting it in pure culture and in association with plants. Appl. Environ. Microbiol. 33, 85–88.
Parra-cota, F.I., Peña-Cabriales, J.J., de los Santos-Villalobos, S., Martínez-Gallardo, N.A., Délano-Frier, J.P., 2014. *Burkholderia ambifaria* and *B. Caribensis* promote growth and increase yield in grain amaranth (*Amaranthus cruentus* and *a. Hypochondriacus*) by improving plant nitrogen uptake. PLoS One 9 (2), e88094.
Passardi, F., Tognolli, M., De Meyer, M., Penel, C., Dunand, C., 2006. Two cell wall associated peroxidases from Arabidopsis influence root elongation. Planta 223 (5), 965–974.
Pereg, L., 2015. Chapter 10-*Azospirillum* cell aggregation, attachment, and plant interaction. In: Cassan, F.D. (Ed.), Handbook for Azospirillum. Springer International Publishing, Switzerland, pp. 186–187.
Pereg, L., de-Bashan, L.E., Bashan, Y., 2016. Assessment of affinity and specificity of *Azospirillum* for plants. Plant Soil 399, 389–414.
Reichheld, J.P., Lardon, T.V.F., Van Montagu, M., Inzé, D., 1999. Specific checkpoints regulate plant cell cycle progression in response to oxidative stress. Plant J. 17 (6), 647–656.
Reynders, L., Vlassak, K., 1982. Use of *Azospirillum brasilense* as biofertilizer in intensive wheat cropping. Plant Soil 66, 217.
Richards, R.A., Rebetzke, G.J., Condon, A.G., van Herwaarden, 2002. Breeding opportunities for increasing the efficiency of water use and crop yield in temperature cereals. Crop Sci. 42, 111–121.
Roepke, J., Bozzo, G.G., 2015. Arabidopsis thaliana β-glucosidase BGLU15 attacks flavonol 3-O-β-glucoside-7-O-α-rhamnosides. Phytochemistry 109, 14–24.
Schimkat, D., Heineke, D., Heldt, H.W., 1990. Regulation of sedoheptulose-1,7-bisphosphatase by sedoheptulose-7-phosphate and glycerate, and of fructose-1,6-bisphosphatase by glycerate in spinach chloroplasts. Planta 181, 97–103.
Shivaprasad, P.V., Chen, H.-M., Patel, K., Bond, D.M., Santos, B.A., Baulcombe, D.C., 2012. A microRNA superfamily regulates nucleotide binding site-leucine-rich repeats and other mRNAs. Plant Cell 24, 859–874.
Tarrand, J.J., Krieg, N.R., Dobereiner, J., 1978. A taxonomic study of *Spirillum lipoferum* group, with description of a new genus, *Azospirillum* gen nov. and two species. *Azospirillum lipoferum* (Beijerinck) comb. nov. and *Azospirillum brasilense* sp nov. Can. J. Microbiol. 24, 967–980.
Thiebaut, F., Rojas, C.A., Grativol, C., Motta, M.R., Vieira, T., Regulski, M., Martienssen, R.A., Farinelli, L., Hermerly, A.S., Ferreira, C.G., 2014. Genome-wide identification of microRNA and siRNA responsive to endophytic beneficial diazotrophic bacteria in maize. BMC Genom. 15, 766.
Timm, S., Florian, A., Fernie, A.R., Bauwe, H., 2016. The regulatory interplay between photorespiration and photosynthesis. J. Exp. Bot. 67 (10), 2923–2929.
Tsukamoto, Y., Fukushima, Y., Hara, S., Hisabori, T., 2013. Redox control of the activity of phospholycerate kinase in *Synechocystis* sp. PCC6803. Plant Cell Physiol. 54 (4), 484–491.
Walker, V., Couillerot, O., Von Felten, A., Bellvert, F., Jansa, J., Maurhofer, M., Bally, R., Moenne-Loccoz, Y., Comte, G., 2012. Variation of secondary metabolite levels in maize seedling roots induced by inoculation with *Azospirillum, Pseudomonas, and Glomus* consortium under field conditions. Plant Soil 356, 151–163.
Wang, X., Xu, C., Cai, X., Wang, Q., Dai, S., 2017. Heat-responsive photosynthetic signaling pathways in plants: insights from proteomics. Int. J. Mol. Sci. 18, 2191.
Wang, L., Czedik-Eysenberg, A., Mertz, R.A., Si, Y., Tohge, T., Nunes-Nesi, A., Arrivault, S., Dedow, L.K., Bryant, D.W., Zhou, W., Xu, J., Weissmann, S., Studer, A., Li, P., Zhang, C., LaRue, T., Shao, Y., Ding, Z., Sun, Q., Patel, R.V., Turgeon, R., Zhu, X., Provart, N.J., Mockler, T.C., Fernie, A.R., Stitt, M., Liu, P., Brutnell, T.P., 2014. Comparative analysis of C4 and C3 photosynthesis in developing leaves of maize and rice. Nat. Biotechnol. 32 (11), 1158–1170.
Xu, Q., Ni, H., Chen, Q., Sun, F., Zhou, T., Lan, Y., Zhou, Y., 2013. Comparative proteomic analysis reveals the cross-talk between the responses induced by H_2O_2 and by long-term *Rice Black-streaked dwarf virus* infection in rice. PLoS One 8 (11), e81640.
Yu, X., Pasternak, T., Eiblmeier, M., Ditengou, F., Kochersperger, P., Sun, J., Wang, H., Rennenberg, H., Teale, W., Paponov, I., Zhou, W., Li, C., Li, X., Palme, K., 2013. Plastid-localized glutathione reductase2-regulated glutathione redox status is essential for Arabidopsis root apical meristem maintenance. Plant Cell 25, 4451–4468.
Zhang, F., Dashti, N., Hynes, R.K., Smith, D.L., 1997. Plant growth-promoting rhizobacteria and soybean [*Glycine max* (L) Merr] growth and physiology at suboptimal root zone temperatures. Ann. Bot. 79 (3), 243–249.
Zybailov, B., Rutschow, H., Friso, G., Rudella, A., Emanuelsson, O., Sun, Q., van Wijk, K.J., 2008. Sorting signals, N-terminal modifications and abundance of the chloroplast proteome. PLoS One 3, e1994.

ANNEX 4

Lade SB, Román C, Cueto-Ginzo AI, Serrano L, Sin E, Achón MA, Medina V (2019) Differential proteomic analysis reveals that *Azospirillum brasilense* Sp7 promotes virus resistance in maize and tomato seedlings. (*Submitted to European Journal of Plant Pathology)*

European Journal of Plant Pathology

Differential proteomic analysis reveals that Azospirillum brasilense Sp7 promotes virus resistance in maize and tomato --

Manuscript Draft--

Manuscript Number:	EJPP-D-19-00012
Full Title:	Differential proteomic analysis reveals that Azospirillum brasilense Sp7 promotes virus resistance in maize and tomato seedlings
Article Type:	Original Article
Keywords:	Plant growth-promoting rhizobacteria (PGPR); Sp7; proteomics; Maize dwarf mosaic virus (MDMV); Potato virus X (PVX)
Corresponding Author:	Sarah Boyd Lade Universitat de Lleida Lleida, SPAIN
Corresponding Author Secondary Information:	
Corresponding Author's Institution:	Universitat de Lleida
Corresponding Author's Secondary Institution:	
First Author:	Sarah Boyd Lade
First Author Secondary Information:	
Order of Authors:	Sarah Boyd Lade
	Carla Román
	Ana Isabel del Cueto-Ginzo
	Luis Serrano
	Ester Sin
	María Angeles Achón
	Vicente Medina
Order of Authors Secondary Information:	
Funding Information:	Universitat de Lleida (0-1-2018-013363-2) — Mrs. Sarah Boyd Lade
	MINCYT (AGL2010-15691) — Dr. Ana Isabel del Cueto-Ginzo
Abstract:	The interaction of a plant growth-promoting rhizobacteria (PGPR) Azospirillum brasilense Sp7 (Sp7) was studied in two pathosystems: tomato (Solanum lycopersicum L. cv. Boludo)/Potato virus X (PVX, KJ631111)/Sp7 and maize (Zea mays cv. B73)/Maize dwarf mosaic virus (MDMV, AM110558)/Sp7). Differential proteomics was employed during early vegetative growth stages to better understand these viral pathosystems and how Sp7 interferes at the molecular level of each. PDQuest proteome discrimination revealed a significant variation in 19 proteins in the maize/MDMV interaction. Namely, there was a significant increase in the NADP-dependent malic enzyme (NADP-ME), which was a form of host-specific viral anticipation, and caused simultaneous increase in photosynthesis- and chloroplast-related proteins. 42 proteins varied significantly in maize/MDMV/Sp7; ROS-scavenging enzymes increased, as well as the proteins related with methionine metabolism, the glutathione-ascorbate cycle and photosynthesis. Photosynthetic rate (A) increased ubiquitously. There were 58 proteins with variation in tomato/PVX that were connected to disruption of the Calvin-Benson (CB) cycle, up-regulation of oxidative stress and inhibition of

	photosystem II (PSII) activity. NADPH-dependent thioredoxin reductase 3-like isoform 2 Inositol-3-phosphate synthase (NTRC) perturbed chloroplast redox balance. 26 proteins varied in the tomato/PVX/Sp7 interaction and lowered tomato plant susceptibility to viral attack. PSII and proteins related to chloroplast activity initially decreased, but were partially restored with time due to up-regulated CB cycle. Sp7 incites ISR in both pathosystems, but does not affect viral titer in either; though it does delay the appearance of MDMV. The role of ribulose-1.5-bisphosphate carboxylase/oxygenase small subunit (RBCS) as a viral target is discussed in both pathosystems.
Suggested Reviewers:	Francisco Manuel Cazorla Professor, University of Malaga cazorla@uma.es Biological control of plant pathogens and microbiology
	Deanna Funnell-Harris, PhD Associate Professor (Adjunct) USDA-ARS Deanna.Funnell-Harris@ARS.USDA.GOV Modification of plant metabolism to improve defense; beneficial microorganisms
	Christer Magnusson Research Professor, Norsk Institutt for Biookonomi christer.magnusson@nibio.no Viruses, bacteria and nematodes in forestry, agriculture and horticulture
	Luis Rubio Academic Researcher, Instituto Valenciano de Investigaciones Agrarias rubio_luimig@gva.es Virology

Differential proteomic analysis reveals that Azospirillum brasilense (Sp7) promotes virus resistance in maize and tomato seedlings

Sarah Boyd Lade*, Carla Román, Ana Isabel del Cueto-Ginzo, Luis Serrano, Ester Sin, María Angeles Achón, Vicente Medina

Department of Plant Production and Forestry Science, University of Lleida – Agrotecnio Center, Av. Alcalde Rovira Roure, 191, 25198 Lleida, Spain

Key words: Plant growth-promoting rhizobacteria (PGPR), Sp7, proteomics, Maize dwarf mosaic virus (MDMV), Potato virus X (PVX)

Abstract

The interaction of a plant growth-promoting rhizobacteria (PGPR) *Azospirillum brasilense* Sp7 (Sp7) was studied in two pathosystems: tomato (*Solanum lycopersicum* L. cv. Boludo)/*Potato virus X* (PVX, KJ631111)/Sp7 and maize (*Zea mays* cv. B73)/*Maize dwarf mosaic virus* (MDMV, AM110558)/Sp7). Differential proteomics was employed during early vegetative growth stages to better understand these viral pathosystems and how Sp7 interferes at the molecular level of each.

PDQuest proteome discrimination revealed a significant variation in 19 proteins in the maize/MDMV interaction. Namely, there was a significant increase in the NADP-dependent malic enzyme (NADP-ME), which was a form of host-specific viral anticipation, and caused simultaneous increase in photosynthesis- and chloroplast-related proteins. 42 proteins varied significantly in maize/MDMV/Sp7; ROS-scavenging enzymes increased, as well as the proteins related with methionine metabolism, the glutathione-ascorbate cycle and photosynthesis. Photosynthetic rate (A) increased ubiquitously.

There were 58 proteins with variation in tomato/PVX that were connected to disruption of the Calvin-Benson (CB) cycle, up-regulation of oxidative stress and inhibition of photosystem II (PSII) activity. *NADPH-dependent thioredoxin reductase 3-like isoform 2 Inositol-3-phosphate synthase* (NTRC) perturbed chloroplast redox balance. 26 proteins varied in the tomato/PVX/Sp7 interaction and lowered tomato plant susceptibility to viral attack. PSII and proteins related to chloroplast activity initially decreased, but were partially restored with time due to up-regulated CB cycle.

Sp7 incites ISR in both pathosystems, but does not affect viral titer in either; though it does delay the appearance of MDMV. The role of *ribulose-1.5-bisphosphate carboxylase/oxygenase small subunit* (RBCS) as a viral target is discussed in both pathosystems.

* Corresponding author: sarahb.lade@pvcf.udl.cat

Introduction

The beneficial effect of *Azospirillium* and other plant growth promoting rhizobacteria (PGPR) in the control of bacterial and fungal diseases is well known for its activation of induced systemic resistance (ISR) in the plant (Bashan and De Bashan, 2002; Tortora et al. 2011), but its antiviral action has been comparatively less studied. The interaction of other PGPR with various viruses has been found to improve plant growth and stimulate plant emergence (Al-Ani et al., 2013). *Azospirillum* spp., in particular, compensates the yield loss induced by *Cucumber mosaic virus* (CMV) and its associated RNA satellite in tomato plants (Dashti et al., 2007), but no significant differences were found between treatments to reduce yield losses induced by *Barley dwarf mosaic virus* (BDMV) in wheat and barley (Al-Ani et al., 2011).

Maize dwarf mosaic virus (MDMV) is a *Potyvirus* in the *Potyviridae* family affecting monocotyledonous plants (Matthews et al., 1982). Infected plants exhibit chlorotic mosaic or streaks on green leaf tissue, as well as shortened upper internodes. Young plants are the most susceptible to MDMV damage. In worst cases, plants undergo the termination of ear development. MDMV infection has caused up to 70% corn yield loss globally since 1960 (Kannan et al., 2018).

Potato virus X (PVX) is a scientifically important virus that infects solanaceous dicotyledonous plants (Scholthof et al., 2011) and is the type species of *Potexvirus* genus in the *Alphaflexiviridae* family (Adams et al. 2005). Occasionally, yield loss in tomato plants infected by PVX may exceed 15% (Strand 2006). PVX infection is more relevant when other viruses are present since it interacts synergistically with them to increase viral titer, as well as visible symptoms of chlorosis, mosaic and reduced leaf size (Van Regenmortel et al., 2004; Aguilar et al., 2015).

Previous work in our lab has dealt with understanding proteomic intricacies of the maize/MDMV and tomato/PVX pathosystems under the influence of salicylic acid (SA) applications and systemic acquired resistance (SAR) activation. We found that in the case of maize/MDMV, primary metabolism and reactive oxygen species (ROS) are tightly intertwined with the pathosystem, but biocontrol like SA modulates the plant response to compensate for the negative effects incurred by the virus, restoring physiological homeostasis to certain plant defense-related components (del Cueto-Ginzo et al., 2016a). In tomato/PVX, reduced photosynthesis is restored and viral symptoms disappear with SA applications. Most importantly, SA signaling controls the plant's stress response to the virus (Cueto-Ginzo et al. 2016b; Falcioni et al., 2014). In both pathosystems, SA slowed the rate of viral accumulation.

We hypothesize that *Azospirillum brasilense* Sp7 (Sp7) can mitigate viral responses in the plant in both mono- and dicot-species. If so, it will pose a viable, environmentally-friendly alternative for controlling viral infections. Thus, our main objective has been to examine the efficacy of inoculating plants with Sp7 to palliate virosis in two widespread pathosystems; maize/MDMV and tomato/PVX. In order to better understand the biochemical mechanisms driving the studied interactions, we compared the proteomic profile of each pathosystem with virus titer in the plant, plant photosynthetic parameters and physiological changes at various sample times post-inoculation and during early stage of development.

Materials and methods

Experimental design

Two completely randomized single factor experiments were started with maize (*Zea mays* cv. B73) and tomato (*Solanum lycopersicum* L. cv. Boludo) seeds. There were four treatment groups (20 biological replicates) per species. Treatments were: 1) control (**C**), no treatment, plants from seeds just soaked in sterile phosphate-buffered saline (PBS) [10mM K_2PO_4-KH_2PO_4, 0.14M NaCl, pH 7.2]; 2) **Sp7,** *Azospirillum brasilense* Sp7 treatment/application (see below), plants from seeds soaked in the same buffer, but incorporating Sp7; 3) **V,** virus treatment/inoculation (see below), maize or tomato plants inoculated with either MDMV or PVX, respectively; 4) **Sp7+V**, co-treatment, plants from seeds treated with Sp7 and inoculated with virus.

Seeds were sown in 1 L pots containing autoclaved commercial substrate (Traysubstrat®, Klasmann-Deilmann, Gmbh, Geeste, Germany) characterized by having an extra fine structure and pH 6. Plants were then grown under greenhouse conditions 18–25% HR, 25–30 °C, with supplementary lighting (12 h photoperiod) and protected from insect attack by an anti-aphid mesh and automatic drip irrigation (1 h, twice per day).

There were four samplings for each species; the first was at principal growth stage 14 for both maize and tomato according to the BBCH scale (Lancashire et al., 1991), and the following were each subsequent week, for three weeks. Sampling times corresponded to 2, 9, 16 and 21 days post-inoculation (dpi) with the virus. Physiologically in maize, 2 dpi coincided with the four-leaf stage, 9 dpi with early tillering, 16 dpi and 21 dpi with late tillering. In tomato, 2 dpi also coincided with the four-leaf stage, 9 dpi with the seven-leaf stage, 16 dpi with the 9-leaf stage and 21 dpi with the 12-leaf stage.

Azospirillum brasilense Sp7 preparation and application

A freeze-dried vial of *Azospirillum brasilense* Sp7 (Sp7) strain was kindly provided by the Colección Española de Cultivos Tipo (acc. CECT 590), Polytechnic University of Valencia (Spain). It was cultivated in Petri dishes containing sterile nitrogen-free broth medium (NFb) supplemented with 15 mL/L of 1:400 aqueous solution of Congo-red (CR) (Bashan et al., 1993) for 48 h. Sp7 inoculum was prepared as described by Okon et al. (1977) in OAB liquid media inoculated with a single colony selected from the CR medium and incubated at 32 °C with constant agitation (100 rpm) for 48 h. The bacterial suspension was allowed to reach late log growth phase [absorbance of 0.399 nm at OD600 (using an Amersham Biosciences Ultraspec 3100 Pro spectrophotometer)], at a concentration yielding 1.16 x 10^8 cfu mL^{-1}.

Inoculation time and quantity were established according to a previously established imbibition curve, estimating the time taken for each seed variety to imbibe 70% of its total potential. Seeds were surface sterilized with 4% NaOCl for 10 min (with constant agitation) and washed six times with sterile distilled water (SDW) in a laminar flow hood. They were dried and inoculated with the rhizobacteria by imbibition.

Virus inoculation

In this study, we used viral strains: *Potato virus X* (PVX, KJ631111) and *Maize dwarf mosaic virus* (MDMV, AM110558)). Maize and tomato seedlings were inoculated with MDMV and PVX, respectively, when they were at the 3-leaf phenological growth stage, approximately two weeks after planting. MDMV was obtained from infected plants maintained in the greenhouse. Leaves that showed MDMW symptoms from plants tested positive by ELISA test were utilized for the

inoculation. The PVX inoculant was made from freeze-dried tomato leaves that had been infected with virus and confirmed with enzyme-linked immunosorbent assay (ELISA).

For inoculation (of both species), a sterile mortar and pestle was placed over ice. Then, 50 mL of the inoculation buffer [1M KH_2PO_4 pH 4.9 autoclaved and added to autoclaved 1 M Na_2HPO_4 pH 9.6 in a ratio of 40:60; final pH of 7-7.2] was added to the mortar, along with 0.1g carborundum® and the vegetable material (2 g freeze-dried and 1 g fresh material). The mixture was ground by hand until it was a homogenous dark green liquid. This mixture (1 mL) was manually rubbed into the bundle of the top two leaves with the thumb and forefinger, and all residues were washed away with distilled water.

Aerial and root growth analysis

The height of 10 biological replicates was measured per treatment at 9, 16 and 21 dpi for both species. For root analysis, three biological replicates were randomly chosen per treatment at 9 and 21 dpi (since the analysis was destructive). The root mass was washed with distilled water and stored in 70% ethanol at 4 °C until analysis. They were then scanned using an Epson Perfection V700 scanner to quantify root mass and length. The images were analyzed with the WinRHIZO program (Regent Instruments Inc., Quebec, ON, Canada, 2009).

Bacterial recovery and viral disease assessment

Sp7 colonization assays were conducted at 2 and 9 dpi, with three random samples taken from each treatment. The procedure was carried out according to Botta et al. (2013) with modifications. One hundred grams of plant roots were homogenized in 1 mL sterile physiological solution (NaCl 0.9%). The homogenate was then serially diluted and plated on CR medium. Bacterial colonies were counted after 2–3 days incubation, depending on the growth rate of each plate, at 32°C. Controls were replicated in the same manner.

Viral disease progress was also checked for each pathosystem at each sampling time (2, 9, 16 and 21 dpi) for both MDMV and PVX. To do so, a direct type double-antibody sandwich (DAS-) ELISA was conducted according to the protocol described by Clark and Bar-Joseph in 1984. Polyclonal commercial antisera were used against MDMV and PVX (Loewe Biochemical GmbH), and solid support was added by polystyrene plates (Nunc™). Samples were considered positive when their average absorbance values (A_{405}) were three times higher than the average of three healthy controls. Positive (infected) plants were compared with 10 repetitions per treatment and sample time.

Leaf gas exchange parameters

Leaf gas exchange was monitored with an infrared gas analyzer (LI- 6400XT LICOR Inc., Nebraska, USA) at the same hour (14 h), at each sampling time. Measurements were taken of photosynthetic rate (A), transpiration rate (E), intercellular CO_2 concentration (C_i) and instantaneous water-use efficiency (WUE_i [A/E]).

Total protein extraction

One gram of leaf tissue was collected per plant for each sampling time (three biological replicates per treatment), immersed in liquid nitrogen and stored at −80 °C. Each sample was measured to 0.1 g and ground with 2 mL of 10% trichloroacetic acid (TCA) in acetone + 20 mM dithriothreitol (DTT) and a protease inhibitor (complete ULTRA Tablets, Mini, EDTAfree, EASYpack, Sigma) was added and mixed by vortex (Xu et al., 2013). After centrifugation at 14,000 rpm and 4 °C for 30 min, the supernatant was discarded, and the pellet washed three times with 2 mL acetone +20 mM DTT, then air dried on ice (10–30 min). The total protein was eluted in 100–250 µL lysis buffer (PER 4, Sigma) and the total protein content was measured by the Bradford method (Bio-Rad Protein Assay Dye Reagent Concentrate) using bovine serum albumin (BSA) as a standard. Absorbance was measured at A_{600}, using an Amersham Biosciences (Ultraspec 3100 Pro) spectrophotometer.

Protein analysis

Total protein extracts were measured to 100 µg and separated by 2D-PAGE analytical gels. Three biological replicates were collected for each treatment. For preparative gels, 500 µg of protein were used. Samples were mixed with rehydration buffer [7M urea, 2M thiourea, 1% C7BzO detergent, 40mM Trizma Base, 50mM DTT, 1% IPG buffer pH 3–10, and 0.002% bromophenol blue] in a total volume of 200 µL. Isoelectric focusing (IEF) of passively rehydrated 18 cm IPG strips (pH 5–8) was performed in a Protean IEF Cell system (Bio-Rad) following the manufacturer's instructions. IEF used a sequential gradient procedure of 50 V/20 C/14 h. The current limit was 50 µA per IPG strip. Focused strips were stored at −80 °C until the second dimension was performed. After IEF separation, the gel strips were incubated for 15 min in the equilibration buffer [375mM Trizma base, 6M urea, 20% glycerol, 2% SDS] containing 2% DTT, followed by 15 min in the same buffer containing 2.5% iodoacetamide instead of DTT. Two equilibrated 18 cm gel strips were loaded in each 12.5% polyacrylamide gel (22 cmÅ~20 cm x 1 mm) for the second-dimension separation in an Ettan DALTsix Electrophoresis Unit (GE Healthcare). Electrophoresis was carried out in SDS-PAGE gels of 12.5%. Gels were stained with Flamingo™ Gel fluorochrome (Bio-Rad) according to the manufacturer's instructions. Images were acquired with the Versadoc MP4000 system (Bio-Rad) (Cueto-Ginzo et al., 2016a).

Protein digestion and MS analysis

Spots were manually excised from gels, digested with trypsin in 96- well perforated plates using a MultiScreen™ HTS Vacuum Manifold (Millipore). Each gel piece containing the protein was minced, washed twice with deionized water and dehydrated with 50% ethanol in 50mM NH_4HCO_3 for 10 min, and then with 100% ethanol for 10 min. Gel pieces were then reduced with 10mM DTT in 50mM NH_4HCO_3 for 1 h at 56 °C and alkylated with 55mM iodoacetamide in 50mM NH_4HCO_3 for 30 min at room temperature in the dark. The gel pieces were washed twice in 50mM NH_4HCO_3 for 15 min and dehydrated with 5% acetonitrile (ACN) in 25mM NH_4HCO_3 for 15 min, twice with 50% ACN in 25mM NH_4HCO_3 for 15 min, and finally with 100% ACN for 10 min. After total ACN evaporation, 15 µL of 20ngµL−1 trypsin in 25mM NH_4HCO_3 was added and left at 4 °C for 45 min to allow for full rehydration of the gel pieces. The gel pieces were then covered with 25mM NH_4HCO_3 and incubated at 37 °C overnight for proteolysis. Eluted peptides were then transferred to a new Eppendorf tube, and 1 µL of the digested protein was used for a first peptide mass fingerprint (PMF) analysis. If

necessary, the minced gel was washed three more times with 0.25% trifluoroacetic acid (TFA) in 50% v/v ACN, twice with 100% ACN, evaporated in a SpeedVac and then re-suspended in 5 µL of 70% ACN- 0.1% TFA to collect remaining peptides. 1 µL peptide solution was spotted per well on a MALDI target and allowed to evaporate at room temperature before being covered with 1 µL of a saturated solution of α-cyano-4 hydroxycinnamic acid prepared in 50% v/v ACN containing 1% TFA. Mass calibrations were carried out using a standard peptide mixture. Mass spectra were acquired using Autoflex™ Speed MALDI-TOF/TOF mass spectrometer (Bruker Daltonics) (Cueto-Ginzo et al., 2016b).

Protein identification was performed using MALDI-TOF mass fingerprint (PMF) and MALDI-TOF/TOF. PMF and MS/MS spectra were compared against SwissProt, NCBI and TrEMBL databases, using the search engine MASCOT algorithm (Version 2.4, Matrix Science, London, UK).

Statistical analysis

Growth data were statistically processed using a one-way ANOVA for each sampling time. Bradford protein quantification was assessed in the same way. The analysis was prepared with JMP® 12.1 (SAS Institute Inc.), and graphics were created with Apache OpenOffice 4.1.3 in OS X Yosemite 10.10.5. An F-ratio of 0.05 for a One-way ANOVA was used to evaluate the difference between averages.

Spot detection and gel analysis were first conducted with the PDQUEST program (Bio-Rad) and the second time, manually. Normalization was performed with the LOESS regression model. Only the spots present on all of the gel replicates were used for statistical analysis. Ratios between two expressed conditions were calculated as the mean of three independent values for each spot from the 2D gel electrophoresis analysis±standard error. Standard error for each spot was calculated according to the following guidelines: 1) there must be a variation coefficient ≤50% among replicates, 2) spots must be present in all measured conditions, 3) expression ratios must be≤0.5 or ≥2.0, and 4) spots must be validated *in visu*. Spots lacking quantitative signal, high quantitative variation between replicates, or with mixed proteins, were not considered for the analysis.

For each species and each sampling time, each protein population (spot) was quantified based on the average of the three biological replicates and then log2 transformed to normalize the data. Finally, to streamline data interpretation and increase analysis power, a stringent fold-change threshold of 1.5/-1.5 was used to control the false discovery rate.

Proteins were categorized into the various functional groups: 1) photosynthesis, respiration, and chloroplast organization; 2) redox homeostasis and stress response (defense); 3) protein synthesis, conformation and transport; 4) metabolism and energy; 5) pathogenic cell lysis; 6) resistance; 7) with unknown or not yet established function; and 8) viral proteins.

Results

Sp7 colonization of maize and tomato

Sp7 was detected on the root systems of maize and tomato plants at both 2 and 9 dpi. The number of Sp7 colonies recovered from the roots of the inoculated plants was 10^5 CFU/g of moist root. No Sp7 colonies were obtained from non-inoculated

plants.

Aerial and root growth

MDMV-infected plants were significantly shorter than controls at 9 ($p<0.05$) and 16 ($p<0.01$) dpi, while Sp7+MDMV plants were 25% shorter at 16 and 21 dpi ($p<0.05$ and $p<0.01$, respectively) **(Fig. 1A)**. In tomato, the trend was opposite, and all treatment groups were significantly taller ($p<0.01$) than controls at all sampling times (dpi) **(Fig. 1B)**. Notably, Sp7+PVX plants were 62% taller than controls.

In maize, root growth was significantly greater for Sp7-treated plants at 9 and 21 dpi ($p<0.05$ and $p<0.01$, respectively). Sp7+MDMV plant roots were 50% longer than controls at 9 dpi ($p<0.05$) **(Fig. 2A)**. PVX-infected tomato plants did not differ from controls in their root length, but Sp7-treated plants exhibited significantly longer roots ($p<0.05$) at both sampling times. Sp7+PVX plant roots were significantly longer ($p<0.05$) at 21 dpi, exhibiting a 43% increase in length over controls **(Fig. 2B)**.

Photosynthesis and transpiration

In general, control plants exhibited the lowest levels of photosynthesis (A) and transpiration (E) in maize, but the highest in tomato. At 9 and 16 dpi in maize, A was significantly higher for all treatment groups compared to controls. At 21 dpi, Sp7+MDMV was the only treatment group that remained significantly higher ($p<0.05$) than controls. For E, MDMV plants were significantly higher than controls at 9 dpi ($p<0.01$). All treatments were higher at 16 dpi ($p<0.01$), and only MDMV and Sp7+MDMV were significantly higher at 21 dpi ($p<0.01$) **(Figs. 3A and 3C)**.

In tomato, there were no differences among treatment groups for A at 9 dpi. At 16 dpi, PVX and Sp7 plants were significantly lower than controls ($p<0.05$ and 0.01, respectively); then at 21 dpi, only Sp7 plants were lower ($p<0.05$). In the case of E for tomato, there were only significant results at 21 dpi, when all treatments Sp7, PVX and Sp7+PVX were significantly lower than controls ($p<0.01$) **(Figs. 3B and 3D)**.

Viral titer

ELISA analysis to maize leaves revealed significant increase in viral titer of 75% and 766% at 16 dpi for MDMV and Sp7+MDMV plants, respectively. Values dropped slightly (-25%) at 21 dpi for both treatments. In both cases, there was a trend for titer values to always be relatively higher for MDMV treatments (than Sp7+MDMV) **(Fig. 4A)**.

The same analysis in tomato revealed earlier (significant) peaks in viral titer of 800% and 600% increase in PVX and Sp7+PVX treatments at 9 dpi, respectively. Then at 16 dpi, the load dropped for significantly for both treatments -55% and -25% for PVX and Sp7+PVX treatments, respectively **(Fig. 4C)**.

Virus-induced proteome changes

Separation by 2-D gel electrophoresis of leaf protein extracts and comparative analysis with PDQuest software detected 19

differential spots that showed significant variation in MDMV-infected maize **(Table 1, Figs. 5A and 4B)**. In PVX-infected tomato, there were 58; 13 of which represented the same protein at both 9 and 16 dpi **(Table** 2, **Figs. 5B and 4D)**.

In maize, the *NADP-dependent malic enzyme* (NADP-ME)*, chloroplastic precursor* (EC 1.1.1.40) (1.50- and 1.93-fold) was the only protein within the 1.5-fold-change criterion that increased abundance at 16 dpi. There were no significant changes at 9 dpi. In tomato, the proteins following the same criterion that changed in abundance at 9 dpi were: *glyceraldehyde-3-phosphate dehydrogenase A* (GAPDH-A) (EC 1.2.1.9) (-1.5-fold); *thioredoxin-like protein CDSP32* (CDSP32) (EC 1.8.1.9) (-1.5-fold); and *transketolase* (TKT) (EC 2.2.1.1) (-1.6-fold and -2-fold), *fructose-bisphosphate aldolase* (FBA) (EC 4.1.2.13) (-1.74-fold), and *5-methyltetrahydropteroyltriglutamate-homocysteine methyltransferase-like* (MHM) (EC 2.1.1.14) (-2.4-fold). At 16 dpi, *glycine dehydrogenase* (GLDC) (EC 1.4.1.10) (1.85 and 3.22-fold) and *ribulose bisphosphate carboxylase small chain 2A* (RBCS-2A) (EC 4.1.1.39) (1.80-fold); as well as *phosphoglycerate kinase* (PGK) (EC 2.7.2.3) (2.13-fold) increased in abundance. The only protein to decrease at 16 dpi was *NADPH-dependent thioredoxin reductase 3-like isoform 2 Inositol-3-phosphate synthase* (NTRC) (EC 1.8.1.9) (-2.5-fold). None of the significantly altered proteins falling within the 1.5-fold change criterion were common between the two species.

Sp7+Virus co-treatment proteome changes

There were 42 differential spots that showed variation in Sp7+MDMV-treated maize. In Sp7+PVX-treated tomato, there were 26. In maize, both the Sp7- and MDMV-effects on co-treatment led to significantly increased abundance in proteins. The MDMV effect **(Fig. 6B)** was significant for co-treatment at 9 dpi for *ribulose-1.5-bisphosphate carboxylase/oxygenase small subunit* (RBCS) (EC 4.1.1.39) (1.61-fold) and *hypothetical protein ZEAMMB73_873979* (1.50-fold). At 16 dpi, proteins *methionine adenosyltransferase* (MAT) (EC 1.97.1.4) (1.95-fold), GAPDH (1.92-fold), *NAD-dependent epimerase/dehydratase* (EC 5.1.99.6) (1.90-fold) and *ascorbate peroxidase* (APX) (EC 1.11.1.11) (1.54-fold) increased in abundance. The Sp7 effect **(Fig. 6A)** was only significant at 16 dpi for proteins *beta-glucosidase 2* (EC 3.2.1.21) (1.79 and1.82-fold) and MAT (1.73-fold).

In tomato, the PVX effect **(Fig. 7B)** caused decreased protein abundance at 9 dpi for *chloroplast stem-loop binding protein of 41 kDa b* (CSP41b) (-1.56-fold) and GLDC (-3.47-fold); and increased protein abundance at 16 dpi for GAPDH-A/ CSP41 (1.82-fold) and *thylakoid formation 1* (THF1) (1.63-fold). In contrast, the Sp7-effect **(Fig. 7A)** resulted in exclusively decreased protein abundance of GLDC (-2.18-fold) at 9 dpi and *movement and silencing protein TGBp1 OS=Potato virus X* (strain X3) (-1.64-fold) at 16 dpi.

Discussion

The results of this study expound upon those of our previous study, in which we demonstrated the unique ways that Sp7 interacts with maize or tomato plants (Lade et al., 2018). Comparatively, the early interaction of Sp7 with maize is more complex and beneficial than with tomato because the photosynthetic apparatus is protected by the C_4 mechanism, thereby offsetting the stress involved in Sp7 association and improving the interaction of the PGPR with maize. Sp7-treated tomato plants had activated defense and metabolic responses at the four-leaf stage, but inhibited CB cycle and chloroplast development because photosynthetic proteins are most likely damaged by ROS when plants are small. In the current study,

we aimed to broaden our understanding of how maize and tomato interact with Sp7 by adding a viral interaction. We first document how MDMV and PVX altered the plant proteomes when inoculated alone, then report on the effects of co-treatment (virus+Sp7). The observed plant-Sp7 dynamic(s) were not expected to be the same in maize and tomato in the current experiment with the added factor of virus since 1) the plants have already exhibited unique response in how they respond to Sp7 alone (Lade et al., 2018), 2) viruses interact distinctly with their hosts (Maule 2001) and 3) synergisms were a possibility, especially in the case of PVX (Van Regenmortel et al., 2004).

Transcriptional profiles of maize and tomato under viral infection

In MDMV-inoculated maize, the chloroplastic precursor to the *NADP-dependent malic enzyme* (NADP-ME) significantly increased in abundance. This protein is involved in the pathway that eliminates photorespiratory CO_2 loss in C_4 plants (Rao and Dixon 2016; The Uniprot Consortium, 2017), and has increased in abundance in specific plant-virus interactions in the past, leading to the belief that it is host-specific (Doubnerová et al., 2009). Most importantly, up-regulation of NADP-ME has been suggested to be one of the earliest signaling responses to impending infection in uninfected cells (Havelda and Maule 2000). It is highly sensitive to the temporal and spatial advance of viral infection (Havelda and Maule 2000), and likely corresponds to plant stress tolerance and antioxidant metabolism that is largely localized in the chloroplast (Romanowska et al., 2017). Whereas earlier studies showed cytosolic production of NADP-ME (Doubnerová et al., 2009), here we provide an example of the chloroplastic precursor of NADP-ME in an as yet undocumented potyvirus/plant pathosystem: MDMV/maize.

Photosynthesis (A) and transpiration (E) both increased significantly in MDMV-infected maize plants, though this pathosystem generally causes a decrease in A and E (Tu and Ford, 1968; Lindsey and Gudauskas, 1975). Given, however, the dissimultaneous stages of growth typical to MDMV-infected plants (Tosic and Misovic, 1967), there is the likelihood that infected plants are growing at a different rate than controls. Furthermore, the negative correlation between light and infectivity suggest that enhanced photosynthesis and chloroplast function play a positive role in defense response during plant-virus interactions in maize plants (Zhao et al., 2016). The sampling time at which A and E increased (16 dpi) is relatively early in the pathogenesis cycle, so together with protein data from this sampling time, there is evidence that up-regulated chloroplast function is an early defense response in the maize plant; especially because the reaction tapers off at 21 dpi. Coincidentally, the timing of this reaction co-occurs with the up-regulation of A and E resulting from Sp7 treatment to maize, documented in our previous work (Lade et al., 2018). Evolution of these reactions is similar in that Sp7 also instigates the increased abundance of ROS-scavenging enzymes to counter the initial stress effect and decrease photoinhibition, but unique in that MDMV infection activates NADP-ME to accomplish this.

In PVX-inoculated tomato, there was a prompt decrease at 9 dpi (seven-leaf stage) in proteins related with oxidative stress (CDSP32), the Calvin-Benson (CB) cycle (GAPDH-A, *transketolase* and FBA), and amino acid metabolism (MHM). The decreased abundance of these proteins provides evidence that the CB cycle was disturbed by PVX infection, putting the plants under oxidative stress, as found in rice infected with the fijivirus (*Reoviridae* family) *Rice black-streaked dwarf virus* (RBSDV) (Xu et al., 2013).

At 16 dpi (nine-leaf stage), there was an increase in the abundance of proteins related to photosynthesis (RBCS), carbohydrate biosynthesis (PGK), and amino acid metabolism (GLDC), but a decrease in the abundance of *NADPH-*

dependent thioredoxin reductase 3-like isoform 2 Inositol-3-phosphate synthase (NTRC); a protein required for chlorophyll biosynthesis and chloroplast redox regulation (Lepistö et al., 2013). We also observed lowered chlorophyll contents and photosynthetic rates at this time, which are typical products of stress physiology in plants infected with virus (Zechmann et al., 2003; Hooks et al., 2008). Studies specific to PVX have further reported unfavorable influence over plant physiological processes such as disturbed plant growth (Hussein and Kamberoglu 2017), as well as ultrastructural alteration of chloroplast membrane and grana stacks due to the chloroplastic localization of PVX coat protein (CP) and viral particles (Qiao et al., 2009). While PVX has not been directly correlated to the alteration of NTRC before, it has been acknowledged that NTRC deficiency may perturb chloroplast redox balance (Ojeda et al., 2017) and increase oxidative stress. A loss-of-function analysis of NTRC resulted in the accelerated spreading of *Pseudomanas syringae* pv. tomato DC3000 disease-associated cell death, along with enhanced reactive oxygen species (ROS) accumulation (Ishiga et al., 2012). So, our study is the first to confirm the same in the tomato/PVX pathosystem.

The trend for decreased photosynthesis that we observed in our study does not typically correspond with the increased abundance of RBCS-2A since this protein procures leaf photosynthetic capacity (Izumi et al., 2012). It can, however, be explained if considering the frequent role of RBCS as a viral target (Lin et al., 2011). RBCS plays an essential role in virus movement, host susceptibility and the interaction (Zhao et al., 2013). Previous proteomic analysis has even suggested that certain viruses are capable of recruiting CPRPs like RBCS to their viral replication complexes (VRCs) during all infection stages (Brizard et al., 2006). So with the simultaneous increase in abundance of GLDC (indicating that the CB mechanism is inhibited) and PGK, the plant is attempting to correct an imbalance in photosynthetic metabolism (Rosa-Tellez et al., 2017; Timm et al., 2016), likely incurred by the viral hijacking of RBCS.

Physiology of co-treated plants

Previous work revealed that Sp7 first instigated a stress-effect in maize, increasing ROS-scavenging enzymes, reducing photoinhibition and increasing photosynthesis to induce reactions that counterbalance and substituted molecules participating in the CB cycle (Lade et al., 2018). Herein, Sp7+MDMV also instigate an increase in ROS-scavenging enzymes, and increase photosynthesis (to an even greater degree than just Sp7 inoculation), indicating synergy.

For Sp7-treated tomato plants, ROS is also a potential stimulant underlying aerial and radicular growth (Passardi et al., 2006; Lade et al., 2018) that may affect PVX-infected plants as well. Though numerous studies on the effects of PVX-inoculation to tomato plants report that the average height of infected plants is around 65% that of healthy controls (Balogun et al., 2002; Hussein and Kamberoglu, 2017), these studies differ from ours in that they were done over longer periods of time, and heights were reported after three (Hussein and Kamberoglu, 2017) or seven weeks (Balogun et al., 2002). Therefore, we conclude that when inoculated alone, PVX does not immediately impede plant aerial growth, but rather it takes approximately the same amount of time as for plants to begin to develop visible symptoms of infection (three to four weeks).

Co-treatment to tomato plants led to taller plants with longer roots. A relevant study which measured the changes in tomato plants co-treated with PVX and systemic acquired resistance (SAR) elicitor ISR2000 comprised of yeast cell wall, *Lactobacillus acidophilus*, plant extracts and benzoic acid (Hussein and Kamberoglu, 2017) also recorded significantly taller plants. In plants that were only treated with the elicitor (ISR2000), increased height was ascribed to a combination of

SAR (Yildiz and Aysan, 2005), the enhancement of nitrogen content and increased photosynthetic rate (Roshanpour et al. 2014). For co-treatment, ISR2000 elicited the same mechanisms to not only hinder the negative effect of the virus but to also increase plant height by 10%. This proved that co-treated plants develop even better, and exhibit synergy. Our results not only corroborated this finding, but also confirmed that the same beneficial effect (due to the combined treatment) is present below ground.

The isolated effects of MDMV and Sp7 in co-treated maize plants

Comparing proteomic data of the various treatments revealed distinct effects in co-treated maize due to the Sp7 factor or the MDMV factor. For one, all significant proteins exhibited an increase in abundance. MDMV had an effect on co-treated plants at 9 dpi by increasing RBCS together with photosynthetic rate. Notably, the MDMV viral titer in co-treated plants remained low at this sampling time; and its increase was delayed by one week in comparison to MDMV-infected plants. As aforementioned, RBCS has dual function when virus is present in the plant as 1) up-regulating leaf catalytic activity, decreasing oxygenation rates and positively regulating the plant's photosynthetic capacity (Tanaka et al., 2007; Morita et al., 2014), or 2) as a viral target for VRCs. Based on our results, there is evidence that RBCS participated in both its active roles at this sampling time to benefit the host plant. Increased abundance of RBCS has been shown to reduce local susceptibility to infection, but increase its long-distance movement (Zhao et al., 2012). So, the delay in viral titer together with up-regulated photosynthesis benefitted the plant, allowing it to grow more vigorously earlier on.

At 16 dpi, there was a significant increase in abundance of proteins related to metabolism and the CB cycle, like MAT and GAPDH; as well as proteins linked to redox homeostasis, like *NAD-dependent epimerase/dehydratase* and APX. Despite their standard functions, all of these proteins have been connected with viral activity in previous studies. For example, the increased abundance of a rice dwarf virus (RDV) viral protein led to more activity of S-adenosyl-L-methionine (SAM), a downstream enzyme of MAT. SAM constitutes one of the building blocks needed to produce ethylene. Many viruses cause infected plants to make more ethylene, which, depending upon levels, benefits the viruses and aids them to infect. It has been proven that plants with too much SAM are less able to defend themselves against virus, while plants that lack SAM are better able to fight off viral infection (Zhao et al., 2017). So the increased abundance of a SAM precursor (MAT) indicates up-regulation of methionine metabolism, and thereby the creation of more ethylene, which depending on levels, may perpetuate plant susceptibility or resistance; in the case of our co-treated plants, it is resistance.

The increase in GAPDH typically implies either that CO_2 assimilation is sped up by the MDMV effect (Xu et al., 2013), or that there is increased reactive oxygen species (ROS) within the plant (Jorrín-Novo et al., 2009). To corroborate the later, two redox homeostasis proteins (*NAD-dependent epimerase/dehydratase* and APX) that link antioxidant metabolites in the glutathione-ascorbate cycle increased in abundance as well. Specifically, the glutathione-ascorbate cycle is responsible for detoxifying hydrogen peroxide (H_2O_2) and scavenging ROS molecules (Ishikawa and Shigeoka, 2008). Infected plants with higher ascorbate content (APX) have, however, been shown to adapt to RNA virus infections better, thus exhibiting weaker symptoms and less ROS accumulation (Wang et al., 2011). Early and high-dose ascorbate treatment regimes alleviated viral symptoms, and eventually inhibited virus replication with such efficacy that ascorbate is believed to participate in unique plant-defense machinery, in addition to the hydrogen peroxide signal (Wang et al., 2011). Our results provide the evidence to fully support this finding.

The Sp7 effect was significant at 16 dpi for *beta-glucosidase 2* and MAT in co-treated maize plants. From our previous work analyzing the effects of Sp7 on maize metabolism, we concluded that since *A. brasilense* itself produces beta glucosidases, it is possible that the expression of exogenous beta-glucosidases leads to plant phenotypes with increased phytohormone levels and increased resistance to biotic attack (Jin et al., 2011). This is synonymous with a "priming" effect, in which the PGPR activates ISR and the hormone pathways involved (Lade et al., 2018). The increased abundance of MAT reiterates this effect, as it has often been tied to up-regulation of ethylene biosynthesis and ISR in the case of inoculation with PGPR (Kwon et al., 2010). So, MAT increases in the case of co-treatment, and can be attributed to both the Sp7- and MDMV- effects. The timing of MAT accumulation coincides with the significant increase in viral load in co-treated plants at 16 dpi. Since plants solely inoculated with MDMV exhibited similar viral titers at the same time, but did not over-accumulate MAT, we can deduce that increased abundance of this protein in co-treated plants is indeed a product of the interaction Sp7+MDMV.

At 9 and 16 dpi, co-treated Sp7+MDMV plants had significantly higher photosynthesis (A) rates. Plants treated solely with MDMV also exhibited higher A, though the underlying mechanisms causing these changes are probably different in co-treated plants, based on the increased abundance of proteins involved in redox regulation, priming and defense-related processes. The chloroplasts are major sites of the production of reactive oxygen species (ROS), and the photosynthetic electron transport chain is responsible for ROS generation (Asada, 2006; Muhlenbock et al., 2008). We concluded that more efficient photosynthesis and chloroplast function play a positive role in defense response during plant-virus interactions for the early MDMV/maize pathogenesis cycle on account of increased abundance of NADP-ME. Sp7 must interfere with signaling of NADP-ME typical to the viral interaction because although we observe similar reactions favoring the increased abundance of redox, antioxidant and hormone-related proteins in co-treated plants, the specific expressing proteins are distinct (GAPDH, *NAD-dependent epimerase/dehydratase* and APX).

The isolated effects of PVX and Sp7 in co-treated tomato plants

In tomato, the PVX effect caused an initial decrease in CSP41, implying a decrease in the translational activity of chloroplasts (Leister, 2014). Meanwhile, the decrease in GLDC indicates up-regulation of the CB cycle and down-regulation of photorespiratory metabolism (Timm et al., 2016). These contrasting events indicate that decreased abundance of GLDC may be a compensatory mechanism for decreased CSP41b. The subsequent restoration of CSP41b abundance at 16 dpi implies that the PVX effect in co-treated plants initially decreases photosynthesis-related protein accumulation in tomato, but not permanently. Photosynthetic rate (A) in co-treated plants was unchanged at this time, but dropped significantly later. In past studies regarding the tomato/PVX pathosystem, similar results of decreased plant chlorophyll content were ascribed to SAR (Falcioni et al., 2014); indicating that there are many overlaps in the mechanisms involved in SAR and ISR (typically induced by Sp7).

GAPDH, which increased in abundance at 16 dpi, has been implied as a crucial host factor involved in increasing plant virus movement and replication (Kaido et al., 2014), and often precludes increased virulence of positive strand RNA viruses like PVX. What's more, GAPDH plays a variety of regulatory roles, such as the inhibition of *Tomato bushy stunt virus* replication by modulating strand asymmetry (Huang and Nagy, 2011) and negative regulation of the replication of *Bamboo mosaic virus* and its sat-RNA (Prasanth et al., 2011). It is notable that this protein is not significantly affected by

the isolated PVX infection in tomato, but expresses with co-treatment, so it's increased abundance is a product of Sp7+PVX.

THF1, which also increased in abundance at 16 dpi, is involved in coronatine- (COR) (a jasmonate mimic) signaling and has been shown to defend against bacterial speck disease in tomato (Wangdi et al., 2010a). THF1 is located in the chloroplast and is speculated to be involved in maintenance of ROS homeostasis (Wangdi et al., 2010b). Current evidence suggests that THF1 may have multiple functions in the biogenesis of PSII and sugar signaling (Keren et al., 2005; Huang et al., 2006), namely that it is required for dynamic changes of PSII–LHCII complexes via its physical interaction with Lhcb proteins (Huang et al., 2013). At 16 dpi our results provided evidence that PVX causes inhibition of PSII activity by decreasing the abundance of NTRC and the photosynthetic rate; so the increased abundance of THF1 in Sp7+PVX plants indicates that co-treatment counteracts this effect.

Finally, the Sp7 effect led to decreased abundance of the *movement and silencing protein TGPp1 OS=Potato virus X* (TGPp1) in co-treated plants, coinciding with a drop in viral titer (at 16 dpi). Plants only inoculated with PVX exhibited a nearly identical negative trend in viral titer, though TGPp1 was unchanged. Earlier studies showing that plants with similar levels of viral titer can still have dramatic differences in symptom severities conclude that alteration of host gene expression, especially the expression of genes involved in critical signal pathways, is more likely responsible for the symptom development (García-Marcos et al. 2009). In our case, Sp7 is responsible for decreased expression of the TGPp1 protein, and subsequent modulation of related signaling pathways, ultimately leading to less susceptible and more vigorous plants.

Conclusions

First, we can conclude several novelties related to each viral pathosystem studied. In the maize/MDMV interaction, we observed the significant and host-specific increase in chloroplastic NADP-ME. Its increase is believed to be a form of viral anticipation and enhanced photosynthesis and chloroplast function complement its increase. In the tomato/PVX pathosystem, immediate effects of PVX in tomato include disruption of the CB cycle, oxidative stress, inhibited PSII activity and decreased photosynthetic rate. Despite this, PVX does not immediately impede plant growth. Instead, growth inhibition takes approximately the same amount of time as for plants to develop visible symptoms of infection. Finally, we identify RBCS as a viral (PVX) target.

In general, Sp7+Virus co-treatment led to more proteins being differentially regulated than plants inoculated with virus alone and there are signs of priming via ISR in both pathosystems. Viral titer augments with co-treatment nearly to the same degree as with virus alone, though it promotes better plant performance in both tomato (height and root length) and maize (photosynthetic rate). It is a novel finding that Sp7 does not reduce viral load when co-inoculated in tomato and maize plants, but still changes factors inducing positive growth in both plant species. In the case of maize/MDMV, Sp7 delays viral load by one week. We also observed a significant up-regulation in ROS-scavenging enzymes, methionine metabolism and the glutathione-ascorbate cycle. Tomato/PVX/Sp7 led to changed abundance of several proteins that are integral factors in rendering tomato plants less susceptible to viral attack: GAPDH, THF1 and TGPp1. Finally, PSII and proteins related to chloroplast activity initially decreased with Sp7+PVX, but were restored with time due to up-regulated CB cycle.

In this study, we have reached conclusions regarding the isolated pathosystems (maize/MDMV and tomato/PVX).

Additionally, we offer findings and insights regarding the modifications of these pathosystems by Sp7, which favors ISR induction and the up-regulation of responses promoting lower susceptibility to virus.

Acknowledgements

We thank the MINCyT of Spain for supporting this research with project ref. AGL2010-15691. SL was supported by the UdL-Jade Plus Grant for pre-doctoral researchers and AIC by the UdL-IMPULS program. The authors would like to especially thank Dr. Isabel Sanchez for helping with the Proteomic analysis.

Compliance with ethical standards

The paper has not been submitted elsewhere for publication, in whole or in part.

Conflict of interest

The authors declare that they have no conflict of interest regarding the publication of this paper.

Human and animal studies

The research did not involve any Human Participants and/or Animals.

Informed consent

Informed consent was obtained from all individual participants included in the study.

References

Aguilar, E., Almendral, D., Allende, L., Pacheco, R., Chung, B.M., Canto, T., & Tenllado, F. (2015). The P25 Protein of *Potato Virus X* (PVX) Is the Main Pathogenicity Determinant Responsible for Systemic Necrosis in PVX-Associated Synergisms. *Journal of Virology*, 89(4), 2090-2103 .

Al-Ani, R.A., Adhab, M.A., & Matny, O.N. (2013). Management of *potato virus Y* (PVY) in potato by some biocontrol agents under field conditions. *Advances in Environmental Biology*, 7(3), 441-444.

Al-Ani, R.A., Adhab, M.A., El-Muadhidi, M.A., & Al-Fahad, M.A. (2011). Induced systemic resistance and promotion of wheat and barley plants growth by biotic and non-biotic agents against barley yellow dwarf virus. *African Journal of Biotechnology*, 10(56), 12079-12084

Asada, K.(2006). Production and scavenging of reactive oxygen species in chloroplasts and their functions. *Plant Physiology*, 141, 391–396.

Balogun, O. S., Xu, L., Teraoka, T., & Hosokawa, D. (2002). Effects of single and double infections with *potato virus X* and *Tobacco mosaic virus* on disease development, plant growth, and virus accumulation in tomato. *Fitopatologia Brasileira*, 27, 241–248

Bashan, Y., Holguin, G., & de-Bashan, L. (2004). *Azospirillum*–plant relationships: physiological, molecular, agricultural, and environmental advances (1997–2003). *Canadian Journal of Microbiology*, 50, 521–577.

Bashan, Y., & de-Bashan, L.E. (2002). Protection of tomato seedlings against infection by *Pseudomonas syringae* pv tomato using the plant growth promoting bacterium *Azospirillum brasilense*. *Applied Environmental Microbiology*, 68, 2637–2643.

Bashan, Y., Holguin, G., & Lifshitz, R. (1993). Isolation and characterization of plant growth promoting rhizobacteria. In B.R. Glick (Ed.), *Methods in Plant Molecular Biology and Biotechnology* (pp. 331–345) Boca Raton, FL, USA: CRC Press.

Botta, L.A., Santacecilia, A., Ercole, C., Cacchio, P., & del Gallo, M. (2013). *In vitro* and *in vivo* inoculation of four endophytic bacteria on *Lycopersicon esculentum*. *Nature Biotechnology*, 30(6), 666–674.

Brizard, J. P., Carapito, C., Delalande, F., Van Dorsselaer, A., & Brugidou, C. (2006). Proteome analysis of plant-virus interactome: comprehensive data for virus multiplication inside their hosts. *Molecular and Cellular Proteomics*, 5, 2279–2297.

CABI. (2018). Invasive Species Compendium. Wallingford, UK: CAB International. www.cabi.org/isc.

Clark, M.F., & Bar-Joseph, M. (1984). Enzyme immunosorbent assay in plant virology. In K Maramorosch & H Koprowski (Eds.), *Methods in Virology*. Vol. 7 (pp. 51-58). New York: Academic Press.

Cueto-Ginzo, A.I., Serrano, L., Sin, E., Rodríguez, R., Morales, J.G., Lade, S.B., Medina, V., & Achon, M.A. (2016a). Exogenous salicylic acid treatment delays initial infection and counteracts alterations induced by *Maize dwarf mosaic virus* in the maize proteome. *Physiological and Molecular Plant Pathology*, 96, 46–59.

Cueto-Ginzo A.I., Serrano, L., Bostock, R.M., Ferrio, J.P., Rodríguez, R., Arcal, L., Achón, M.A., Falcioni, T., Luzuriaga, W.P., & Medina, V. (2016b). Salicylic acid mitigates physiological and proteomic changes induced by the SPCP1 strain of *Potato virus X* in tomato plants. *Physiological and Molecular Plant Pathology*, 93, 1-11.

Dashti, N.H., Montasser, M.S., Ali, N.Y., Bhardwaj, R.G., & Smith, D.L. (2007). Nitrogen biofixing bacteria compensate for the yield loss caused by viral satellite RNA associated with cucumber mosaic virus in tomato. *The Plant Pathology Journal*, 23(2), 90-96.

Doubnerová, V., Müller, K., Čeřovská, N., Synková, H., Spoustová, P., & Ryšlavá, H. (2009). Effect of *Potato Virus Y* on the NADP-Malic Enzyme from *Nicotiana tabacum* L.: mRNA, Expressed Protein and Activity. *International Journal of Molecular Sciences*, 10, 3583-3598.

Falcioni, T., Ferrio, J.P., Cueto, A.I., Giné, J., Achón, M.A., & Medina, V. (2014). Effect of salicylic acid treatment on tomato plant physiology and resistance to *Potato virus X* infection. *European Journal of Plant Pathology*, 138, 331e345.

García-Marcos, A., Pacheco, R., Martiáñez, J., González-Jara, P., Díaz-Ruíz, J. R., & Tenllado, F. (2009). Transcriptional changes and oxidative stress associated with the synergistic interaction between *Potato virus X* and *Potato virus Y* and their relationship with symptom expression. *Molecular Plant-Microbe Interactions*, 22, 1431–1444.

Havelda, Z., & Maule, A.J. (2000). Complex spatial responses to cucumber mosaic virus infection in susceptible *Cucurbita pepo* cotyledons. *The Plant Cell*, 12, 1975-1985.

Hayat, S., Ali, B., & Ahmad, A. (2007). Salicylic acid: biosynthesis, metabolism and physiological role in plants. In S. Hayat & A. Ahmad (Eds.), *Salicylic Acid: a Plant Hormone* (pp.1E14). Dordrecht, The Netherlands: Springer.

Hooks, C. R. R.,Wright, M.G.,Kabasaw, D. S., Manandhar, R.,& Almeida, R. P. P. (2008). Effect of *banana bunchy top virus* infection on morphology and growth characteristics of banana. *Annals of Applied Biology*, 153(1), 1–9.

Huang, J., Taylor, J.P., Chen, J.G., Uhrig, J.F., Schnell, D.J., Nakagawa, T., Korth, K.L., & Jones, A.M. (2006). The plastid protein THYLAKOID FORMATION1 and the plasma membrane G-protein GPA1 interact in a novel sugar-signaling mechanism in *Arabidopsis*. *Plant Cell*, 18, 1226–1238.

Huang, T.S., & Nagy, P.D. (2011). Direct inhibition of tombusvirus plus-strand RNA synthesis by a dominant negative mutant of a host metabolic enzyme, glyceraldehyde-3-phosphate dehydrogenase, in yeast and plants. *Journal of Virology*,

588 85, 9090–9102.
589
590 Huang, W., Chen, Q., Zhu, Y., Hu, F., Zhang, L., Ma, Z., He, Z., & Huang, J. (2013). Arabidopsis Thylakoid Formation 1 Is
591 a Critical Regulator for Dynamics of PSII–LHCII Complexes in Leaf Senescence and Excess Light. *Molecular Plant*, 6(5),
592 1673-1691.
593
594 Hussein, M., & Kamberoglu, M.A. (2017). The response to *Potato virus X* infection of tomato plants treated with ISR2000.
595 *European Journal of Plant Pathology*, 149(4), 807-815.
596
597 Ishiga, Y., Ishiga, T., Wangdi, T., Mysore, K.S., & Uppalapati, S.R. (2012). NTRC and chloroplast-generated reactive
598 oxygen species regulate *Pseudomonas syringae* pv. *Tomato* disease development in tomato and *Arabadopsis. Molecular*
599 *Plant-Microbe Interactions*, 25(3), 294-306.
600
601 Ishikawa, T., & Shigeoka, S. (2008). Recent advances in ascorbate biosynthesis and the physiological significance of
602 ascorbate peroxidase in photosynthesizing organisms. *Bioscience, Biotechnology and Biochemistry*, 72, 1143–1154
603
604 Jorrín-Novo, J.V., Maldonado, A.M., Echevarría-Zomeño, S., Valledor, L., Castillejo, M.A., Curto, M., Valero, J., Sghaier,
605 B., Donoso, G., & Redondo, I. (2009). Plant proteomics update (2007-2008): second-generation proteomic techniques, an
606 appropriate experimental design, and data analysis to fulfill MIAPE standards, increase plant proteome coverage and
607 expand biological knowledge. *Journal of Proteomics*, 72, 285–314.
608
609 Kaido, M., Abe, K., Mine, A., Hyodo, K., Taniguchi, T., Taniguchi, H., Mise, K., & Okuno, T. (2014). Gapdh-A recruits a
610 plant virus movement protein to cortical virus replication complexes to facilitate viral cell-to-cell movement. *PloS*
611 *Pathology*, 10, e1004505.
612
613 Kannan, M., Ismail, I., & Bunawan, H. (2018). *Maize dwarf mosaic virus*: from genome to disease management. *Viruses*,
614 10(9), 492.
615
616 Keren, N., Ohkawa, H., Welsh, E.A., Liberton, M., & Pakrasi, H.B. (2005). Psb29, a conserved 22-kD protein, functions in
617 the biogenesis of photosystem II complexes in *Synechocystis* and *Arabidopsis*. *Plant Cell*, 17, 2768–2781
618
619 Kwon, Y. S., Ryu, C.-M., Lee, S., Park, H. B., Han, K. S., Lee, J. H., Lee, K., Chung, W.S., Jeong, M.J., Kim, H.K., & Bae,
620 D.W. (2010). Proteome analysis of *Arabidopsis* seedlings exposed to bacterial volatiles. *Planta* 1370, 1355–1370.
621
622 Leister, D. (2014). Complex(iti)es of the ubiquitous RNA-binding CSP41 proteins. *Frontiers in Plant Science*, 5(255), 1–4.
623
624 Lepistö, A., Pakula, E., Toivola, J., Krieger-Liszkay, A., Vignols, F., & Rintamäki, E. (2013). Deletion of chloroplast
625 NADPH-dependent thioredoxin reductase results in inability to regulate starch synthesis and causes stunted growth under
626 short-day photoperiods. *Journal of Experimental Botany*, 64, 3843–3854.
627
628 Lin, L., Luo, Z., Yan, F., Lu, Y., Zheng, H., & Chen, J. (2011). Interaction between potyvirus P3 and ribulose-1,5
629 bisphosphatecarboxylase/ oxygenase (RubisCO) of host plants. *Virus Genes*, 43, 90–92.
630
631 Lindsey, D.W., & Gudauskas, R.T. (1975). Effects of maize dwarf mosaic virus on water relations of corn. *Phytopathology*,
632 65(4), 434-440
633
634 Lade, S.B., Román, C., Cueto-Ginzo, A.I., Serrano, L., Sin, E., Achón, M.A., & Medina, V. (2018). Host-specific proteomic
635 and growth analysis of maize and tomato seedlings inoculated with *Azospirillum brasilense* Sp7. *Plant Physiology and*
636 *Biochemistry*, 129, 381-393.
637
638 Lancashire, P.D., Bleiholder, H., Langelüddecke, P., & Stauss, R. (1991). An uniform decimal code for growth stages of
639 crops and weeds. *Annals of Applied Biology*, 119, 561–601.
640
641 Maule, A.J. (2001). Virus and Host Plant Interactions. *Encyclopedia of Life Sciences*, 1-7.
642
643 Matthews, R. (1982). The classification and nomenclature of viruses: Summary of results of meetings of the International

644 Committee on Taxonomy of Viruses in Strasbourg. *Intervirology*, 16, 53–60.
645
646 Morita, K., Hatanaka, T., Misoo, S., & Fukayama, H. (2014). Unusual small subunit that is not expressed in photosynthetic
647 cells alters the catalytic properties of Rubisco in rice. *Plant Physiology*, 164, 69–79.
648
649 Muhlenbock, P., Szechynska-Hebda, M., Plaszczyca, M., Baudo, M., Mateo, A., Mullineaux, P.M., Parker, J.E., Karpinksa,
650 B., Karpinski, S. (2008). Chloroplast signaling and *LESION SIMULATING DISEASE1* regulate crosstalk between light
651 acclimation and immunity in *Arabidopsis*. *Plant Cell*, 20, 2339–2356.
652
653 Ojeda, V., Pérez-Ruiz, J.M., González, M., Nájera, V.A., Sahrawy, M., Serrato, A.J., Geigenberger, P., & Cejudo, F.J. (2017).
654 NADPH thioredoxin reductase C and thioredoxins act concertedly in seedling development. *Plant Physiology*, 174, 1436-
655 1448.
656
657 Okon, Y., Albrecht, S.L., & Burris, R.H. (1977). Methods for growing *Spirillum lipoferum* and for counting it in pure culture
658 and in association with plants. *Applied Environmental Microbiology*, 33, 85–88.
659
660 Passardi, F., Tognolli, M., De Meyer, M., Penel, C., & Dunand, C. (2006). Two cell wall associated peroxidases from
661 *Arabidopsis* influence root elongation. *Planta*, 223(5), 965–974.
662
663 Prasanth, K.R., Huang, Y.W., Liou, M.R., Wang, R.Y., Hu, C.C., Tsai, C.H., Meng, M., Lin, N.S., & Hsu, Y.H. (2011).
664 Glyceraldehyde 3-phosphate dehydrogenase negatively regulates the replication of Bamboo mosaic virus and its associated
665 satellite RNA. *Journal of Virology*, 85, 8829–8840.
666
667 Qiao, Y., Li, H.F., Wong, S. M., & Fan, Z.F. (2009). Plastocyanin transit peptide interacts with potato virus X coat protein,
668 while silencing of plastocyanin reduces coat protein accumulation in chloroplasts and symptom severity in host plants.
669 *Molecular Plant-Microbe Interactions*, 22, 1523–1534.
670
671 Radwan, D.E.M., Lu, G., Fayez, K.A., & Mahmoud, S.Y. (2008). Protective action of salicylic acid against bean yellow
672 mosaic virus infection in Vicia faba leaves. *Journal of Plant Physiology*, 165, 845-857.
673
674 Rao, X., & Dixon, R.A. (2016). The differences between NAD-ME and NADP-ME subtypes of C4 photosynthesis: more
675 than decarboxylating enzymes. *Frontiers in Plant Science*, 7, 1525.
676
677 Romanowska, E., Buczynska, A., Wasilewska, W., Krupnik, T., Drozak, A., Rogowski, P., Parys, E., & Zienkiewicz, M.
678 (2017). Differenences in photosynthetic responses of NADP-ME type C4 species to high light. *Planta*, 245, 641-657.
679
680 Rosa-Téllez, S., Anoman, A.D., Flores-Tornero, M., Toujani, W., Alseek, S., Fernie, A.R., Nebauer, S.G., Muñoz-Bertomeu,
681 J., Segura, J., & Ros, R. (2017). Phosphoglycerate kinases are co-regulated to adjust metabolism and to optimize growth.
682 *Plant Physiology*, 176(2), 1182-1198.
683
684 Roshanpour, N., Darzi, M. T., & Hadi, M. H. S. (2014). Effects of plant growth promoter bacteria on biomass and yield of
685 basil (*Ocimum basilicum* L.) *International Journal of Advanced Biological and Biomedical Research*, 2(6), 2077–2085.
686
687 Scholthof, K.-B. G., Adkins, S., Czosnek, H., Palukaitis, P., Jacquot, E., Hohn, T., Hohn, B., Saunders, K., Candresse, T.,
688 Ahlquist, P., Hemenway, C., & Foster, G.D. (2011). Top 10 plant viruses in molecular plant pathology. *Molecular Plant*
689 *Pathology*, 12, 938–954.
690
691 Strand, L. (2006). Disease. In L. Strand (Ed), *Integrated Pest Management for Potatoes in the western United States* 2nd edn.
692 (p. 95). University of California Division of Agriculture and Natural Resources.
693
694 Tanaka, S., Sawaya, M.R., Kerfeld, C.A., & Yeates, T.O. (2007). Structure of the Rubisco chaperone RbcX from
695 Synechocystis sp. PCC6803. *Acta Crystallography*, D63, 1109–1112.
696
697 The UniProt Consortium. (2017). UniProt: the universal protein knowledgebase. *Nucleic Acids Research*, 45, D158-D169.
698
699 Timm, S., Florian, A., Fernie, A.R., & Bauwe, H. (2016). The regulatory interplay between photorespiration and

photosynthesis. *Journal of Experimental Botany*, 67(10), 2923–2929.

Tortora, M.L., Díaz-Ricci. J.C., & Pedraza, R.O. (2011). *Azospirillum brasilense* siderophores with antifungal activity against *Colletotrichum acutatum*. *Archives of Microbiology*, 193, 275–286.

Tosic, M., & Misovic, M. (1967). A study of the maize mosaic virus occurrence and its effect on the growth and yield of some corn varieties and hybrids. *Zastita Bilja*, 93-95, 173-180.

Tu, J.C., & Ford, R.E. (1968). Effect of maize dwarf mosaic virus infection on respiration and photosynthesis of corn. *Phytopathology*, 58(3), 282-284.

Van Regenmortel, M.H.V., & Mahy, B.W.J. (2004). *Emerging issues in virus taxonomy. Emerging Infectious Diseases*, 10(1), 8- 13.

Wang, S.D., Zhu, F., Yuan, S., Yang, H., Xu, F., Shang, J., Xu, M.Y., Jia, S.D., Zhang, Z.W., Wang, J.H., Xi, D.H., & Lin, H.H. (2011). The roles of ascorbic acid and glutathione in symptom alleviation to SA-deficient plants infected with RNA viruses. *Planta*, 234, 171–181.

Wangdi, T., Uppalapati, S.R., Nagaraj, S., Ryu, C.-M., Bender, C.L., & Mysore, K.S. (2010a). A role for chloroplast-localized *thylakoid formation 1 (ThF1)* in bacterial speck disease development. *Plant Signaling & Behavior*, 5(4), 425-427.

Wangdi, T., Uppalapati, S.R., Nagaraj, S., Ryu, C.-M., Bender, C.L., & Mysore, K.S. (2010b). A virus-induced gene silencing screen identifies a role for Thylakoid Formation1 in *Pseudomonas syringae* pv. tomato symptom development in tomato and *Arabidopsis*. *Plant Physiology*, 152(28), 1–92.

Xu, Q., Ni, H., Chen, Q., Sun, F., Zhou, T., Lan, Y., & Zhou, Y. (2013). Comparative proteomic analysis reveals the cross-talk between the responses induced by H2O2 and by longterm *Rice Black-streaked dwarf virus* infection in rice. *PLoS One*, 8(11), e81640.

Yildiz, R.C., & Aysan, Y. (2005). Determination on effect of plant activators on tomato seedling infested with pathogen (*Clavibacter michiganensis subsp. michiganensis*) of bacterial wilt disease. Turkey 2nd seed congress 9-11 November, Adana, 359 pp.

Zechmann, B., Muller, M., & Zellnig, G. (2003) Cytological modifications in *zucchini yellow mosaic virus* (ZYMV)-infected Styrian pumpkin plants. *Archives of Virology*, 148, 1119–1133.

Zhao, J., Liu, Q., Zhang, H., Jia, Q., Hong, Y., & Liu, Y. (2013). The rubisco small subunit is involved in *Tobamovirus* movement and *Tm-2*^{2}-mediated extreme resistance. *Plant Physiology*, 161, 374-383.

Zhao, J., Zhang, X., Hong, Y., & Liu, Y. (2016). Chloroplast in Plant-Virus Interaction. *Frontiers in Microbiology*, 7, 1565.

Zhao, S., Hong, W., Wu, J., Wang, Y., Ji, S., Zhu, S., Wei, C., Zhang, J., & Li, J. (2017). A viral protein promotes host

Table 1. Main characteristics and function of identified maize proteins corresponding to spots in Figs. 4 & 6.

SSP [1]	Protein name	Accession No. [2] (database)	Molecular Weight (Da)/pI [3]	Coverage %	No Peptides Matched/Total peptides	Score [4]	Function [5]
208	Oxygen-evolving enhancer protein 1	ACG31595**	34783/5.59	68	34/50	303	1
210	Chaperonin	ACG33530**	25559/8.67	64	12/27	160	4
402 1401	Phosphoribulokinase Sedoheptulose-1,7-bisphosphatase	B4FQ59*** B6T2L2***	45121/5.84 42303/6.08	76 66	28/74 28/74	260 219	3,4
1502	Phosphogycerate kinase	NP_001147628**	50009/6.07	64	33/49	381	4
1703 2706	ATP synthase subunit beta, chloroplastic	P00827*	54064/5.31	59	31/73	211	2
2306	Chain A crystal structure of Ferredoxin	3VO1_A**	35835/5.43	70	32/45	320	1
2705	ATP synthase subunit beta, mitochondrial	P19023*	59181/6.01	44	24/76	156	2
3104	Cytochrome b6-f complex iron-sulfur subunit	B4FTU7***	21026/6.41	10	3/4	154	1
3303	Fructose-biphosphate aldolase	ACG36798.1**	41924/7.63	64	26/73	248	4
3703	Enolase 2	NP_001105371**	48418/5.70	61	29/53	295	2
3801 3807	Transketolase	Q7SIC9 *	73347/5.47	65	46/72	449	1,4
3802 4801 4802	NADP-dependent malic enzyme, chloroplastic precursor	NP_001105313**	70293/6.09	53	43/78	353	1,4
4105	Germin-like protein	Q6TM44***	22101/6.02	13	2/2	166	2,4
4201	Lactoylglutathione lyase	ACG39003**	35311/6.62	47	21/37	201	2
4202	Ascorbate peroxidase	NP_001152746**	27468/5.64	71	17/31		2
4402	Malate dehydrogenase, cytoplasmic	NP_001105603**	35909/5.77	68	24/45	263	1
4601	Hypothetical protein	NP_001142788**	51917/6.12	51	24/41	271	7
4602	Methionine adenosyltransferase	AFW82691**	46392/6.03	63	26/50	292	4
5001	Ribulose-1,5-bisphosphate carboxylase/oxygenase small subunit	CAA70416**	19364/8.98	69	13/54	153	1
5103	Ribosome recycling factor	NP_001150478**	29328/9.22	29	8/16	419	7
5602	Bifunctional 3-phosphoadenosine 5-phosphosulfate synthetase 2	NP_001147427**	52493/8.30	43	22/31	242	1
5704	ATP synthase CF1 alpha subunit	NP_043022**	55729/5.87	49	31/41	392	1
6001	Cytochrome b6-f complex iron-sulfur subunit	ACG28186**	24321/8.52	41	10/20	152	1,2
6102	TPA: hypothetical protein ZEAMMB73_927356	DAA59517**	32073/9.50	48	12/34	159	7
6103	Hypothetical protein ZEAMMB73_321092	DAA42743**	27411/8.97	49	13/30	185	7
6201	Hypothetical protein Putative uncharacterized protein	NP_001142128**	33566/5.96	41		114	7
6307	NAD-dependent epimerase/dehydratase	B4FH62***	31917/9.11	66	20/24	340	2
6309	50S ribosomal protein L1 guanine nucleotide-binding protein beta subunit-like protein	NP_001150277** NP_001136800**	37235/8.69 36670/6.13	56 67	25/59 18/59	229 196	3 3
6409 7404 7405	Glyceraldehyde-3-phosphate dehydrogenase A, chloroplastic precursor	NP_001105414**	43182/7.00	61	25/46	264	4
6503	Fructose-bisphosphate aldolase, cytoplasmic isozyme 1	B6SSU6***	38464/6.26	54	18/21	292	1
6706 6714	Beta-glucosidase2	AFW56713**	64308/6.75	47	35/43	423	5
7103	Chain A, Structure Of Glutathione S-Transferase Iii In Apo Form	1AW9_A**	23416/5.97	68	11/27	166	2
7607	Putative uncharacterized protein	B4FHK4***	42290/6.53	43	23/34	263	7
7706	Ribulose-1.5-bisphosphate carboxylase/oxygenase large subunit	NP_043033**	53295/6.33	59	42/84	341	1
8001	Ribulose bisphosphate carboxylase small chain, chloroplastic precursor	NP_001105294**	19310/9.10	62	18/61	166	1
8002	Photosystem I reaction center subunit IV A	ACG26704.1**	14885/9.79	7	1/1	56	1
8101	Putative peptidyl-prolyl cis-trans isomerase family protein	NP_001136688**	26599/X	X	12/X	135	2,4

8203	GTP-binding nuclear protein Ran-A1	NP_001131881**	25387/6.66	60	15/23	243	3
8310	Coat protein (MDMV)[6]	CAD91557**	34517/6.30	50	18/45	155	8
8401	Glyceraldehyde-3-phosphate dehydrogenase 1	P08735*	36614/6.46	48	19/55	178	1,4
	Glyceraldehyde-3-phosphate dehydrogenase A	P09315*	43182/7.00	48	18/55	166	
	Glyceraldehyde-3-phosphate dehydrogenase 2	Q09054*	36633/6.41	46	16/55	135	
8403	Glyceraldehyde-3-phosphate dehydrogenase 1, cytosolic	NP_001105413**	36600/6.46	53	21/44	232	4

[1] Spot numbers refer to Figs. 4 & 6, identified either by fingerprint mass spectrometry MS (MALDI-TOF) or by MS/MS (MALDI TOF-TOF). The representative spots and their numbers which show variation between treatments are indicated by the red circles, yellow circles indicate viral proteins.
[2] Accession number and molecular mass according to SwissProt (us.expasy.org/sprot)*, NCBI ** and TrEMBL *** databases.
[3] MW and pI were calculated from aminoacid sequence
[4] Scores of proteins identified by peptide mass fingerprinting were determined according to Mowse values obtained either from MASCOT.
[5] (1) Photosynthesis, respiration, and chloroplast organization; (2) Redox homeostasis and stress response (defense); (3) Protein synthesis, conformation and transport; (4) Metabolism and energy; (5) Pathogenic cell lysis; (6) Resistance; (7) Unknown; (8) Viral proteins.

Table 2. Main characteristics and function of identified tomato proteins corresponding to spots in Figs. 4 & 7.

SSP [1]	Protein name	Accession No. [2] (database)	Molecular Weight (Da)/pI [3]	Coverage %	No Peptides Matched/Total peptides	Score [4]	Function [5]
2004 4001	Ribulose bisphosphate carbox. small chain 2A	P07179 *	20493/6.59	48	11/46	134	1
2304 4201 5307 6206 7305	Fructose-bisphosphate aldolase 2	XP_004233550 **	42872/6.07	53	18/47	203	1,4
3101	Chaperonin 21 precursor	NP_001234423**	26603/6.85	58	13/36	177	3
3201 6203 7207 8103	Coat protein OS=Potato virus X[6]	P31798 *	25275/6.73	22	3/3	31	8
3702	ATP synthase subunit alpha	Q2MIB5 *	55434/5.14	42	25/42	296	4
3709	Inositol-3-phosphate synthase	XP_004239994 **	56697/5.45	46	25/75	159	2
3906 4908	ATP-dependent Clp protease ATP-binding subunit clpA homolog CD4B	XP_004252280 **	102418/5.99	43	40/56	379	4
4002 4003	Superoxide dismutase [Cu-Zn]	P14831 *	22328/5.77	12	2/2	132	2
4202	Magnesium-protoporphyrin O-methyltransferase-like	XP_004235845 **	35879/6.54	43	16/35	181	1
4305 5406 5602 6503 7401 7504	Ribulose bisphosphate carbox./oxygenase activase 1	O49074 *	50897/8.61	50	26/56	245	1
4402 5508	Elongation factor TuA	XP_004241515 **	56286/6.69	14	5/5	180	3
4606 6506	Glutamate-1-semialdehyde 2,1-aminomutase	NP_001234690 **	51722/6.54	48	26/43	235	3
5201	BG125080.1 EST470726 tomato shoot/meristem	BG125080 ***	25967/9.18	6	3	297	3
5311	Succinic semialdehyde reductase isofom2	NP_001233836 ** BAG16486	38941/8.50	4	2/2	92	2,3
5402	Quinone oxidoreductase-like protein At1g23740	XP_004238663 **	40976/7.74	12	4/4	143	2
5405 5509	Phosphoglycerate kinase	XP_004243968**	50592/7.66	11	4/4	211	4
5607	Diaminopimelate decarboxylase 1	XP_004230896**	53379/6.71	4	2/2	195	4
5712	Ribulose bisphosphate carboxylase/oxygenase large subunit	YP_514860**	53434/6.55	38	18/55	162	1
5901 5902	Transketolase	XP_004248560 **	80268/5.97	46	33/52	347	4
6202 8102 8103	Carbonic anhydrase	NP_001234048 **	34845/6.67	63	21/36	245	1,2
6101	Chlorophyll a-b binding protein 8	XP_004248217**	29261/8.65	15	2/2	237	1
6208	Thioredoxin-like protein CDSP32	XP_004238392 **	33779/7.57	18	6/6	241	2
6304	mRNA binding protein precursor	NP_001234656 **	44084/7.10	38	21/45	228	6
6403	Malate dehydrogenase	XP_004247734 **	35703/5.91	72	24/53	259	1
6404 6405	Monodehydroascorbate reductase-like	XP_004246547 **	47106/5.77	72	29/39	386	2,3
6406	ATP synthase gamma chain	XP_004232711**	41752/8.15	13	3/6	224	4
6503	Glyceraldehyde-3-phosphate dehydrogenase B	XP_0042238446**	51421/6.86	60	28/80	226	1
6505	S-adenosylmethionine synthase 3	NP_001234004 **	43082/5.76	60	26/44	276	4
6507	ATP sulfurylase 1	XP_004234020 **	52376/6.94	48	27/41	296	4
6509 7508	GDP-mannose 3',5'-epimerase	NP_001234734 **	42828/5.88	45	21/32	248	4
6904	Unknown protein						7
6906 7913	Glycine dehydrogenase [decarboxylating]	XP_004245101**	114020/6.69	5	5/5	199	1
7206	Movement and silencing protein TGBp1 OS=Potato virus X (strain X3)	P17780*	24695/6.31	42	5/5	350	8
7402 7405 7406 7409 7509 8404	Chloroplast stem-loop binding protein of 41 kDa b	XP_004241412 **	42596/7.67	60	23/29	321	1
7409 8404 8501	Glyceraldehyde-3-phosphate dehydrogenase A	XP_004236849 **	42940/8.46	58	23/60	234	1

8511							
7906 7907	5-ethyltetrahydropteroyltriglutamate--homocysteine methyltransferase-like	XP_004249374 **	85014/6.01	39	26/35	319	4
8101	BP903052.1 Solanum lycopersicum cDNA, clone	BP903052 ***	17598/6.99	56	10/40	134	7
8107	Triose phosphate isomerase (cytosolic isoform)	AAR11379 **	27251/5.73	11	2	155	4
8114	Protein thylakoid formation1	XP_004243305**	33558/8.69	7	3/3	50	3
8206	Unknown protein						7
8401	Glyceraldehyde-3-phosphate dehydrogenase	NP_001266254 **	32097/5.93	56	15/22	192	1
8707	LEXYL2	BAC98299 **	69724/8.04	7	4/4	184	4

[1] Spot numbers refer to Figs. 4 & 7, identified either by fingerprint mass spectrometry MS (MALDI-TOF) or by MS/MS (MALDI TOF-TOF). The representative spots and their numbers which show variation between treatments are indicated by the red circles, yellow circles indicate viral proteins.
[2] Accession number and molecular mass according to SwissProt (us.expasy.org/sprot)*, NCBI ** and TrEMBL *** databases.
[3] MW and pI were calculated from aminoacid sequence
[4] Scores of proteins identified by peptide mass fingerprinting were determined according to Mowse values obtained either from MASCOT.
[5](1) Photosynthesis, respiration, and chloroplast organization; (2) Redox homeostasis and stress response (defense); (3) Protein synthesis, conformation and transport; (4) Metabolism and energy; (5) Pathogenic cell lysis; (6) Resistance; (7) Unknown; (8) Viral proteins.

Figure 1. Plant height (mm) of (A) maize (cv. B73) and (B) tomato (cv. Boludo) subjected to different treatments: control (-), Virus (MDMV or PVX), A. brasilense Sp7

Click here to access/download;line figure;Figure 1.jpg

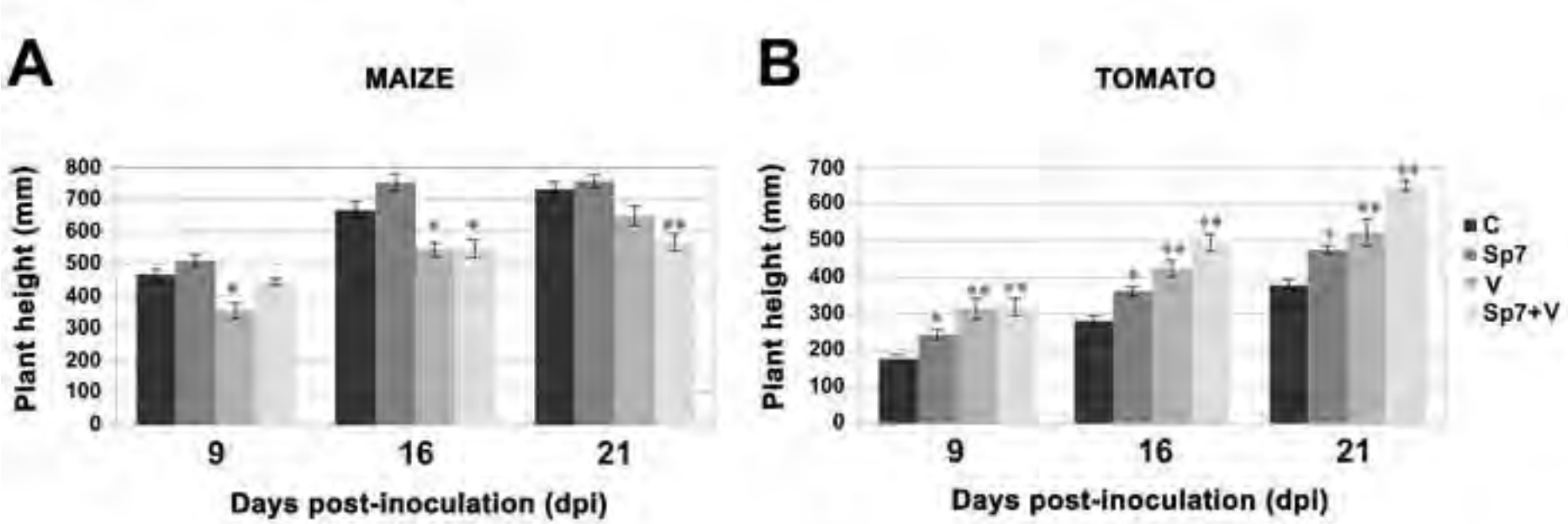

Figure 2. Root length (mm) and morphology of (A) maize (cv. B73) and (B) tomato (cv. Boludo). Graphs (above) indicate root length calculated from the scanned Winrhizo©

Click here to access/download;line figure;Figure 2.jpg

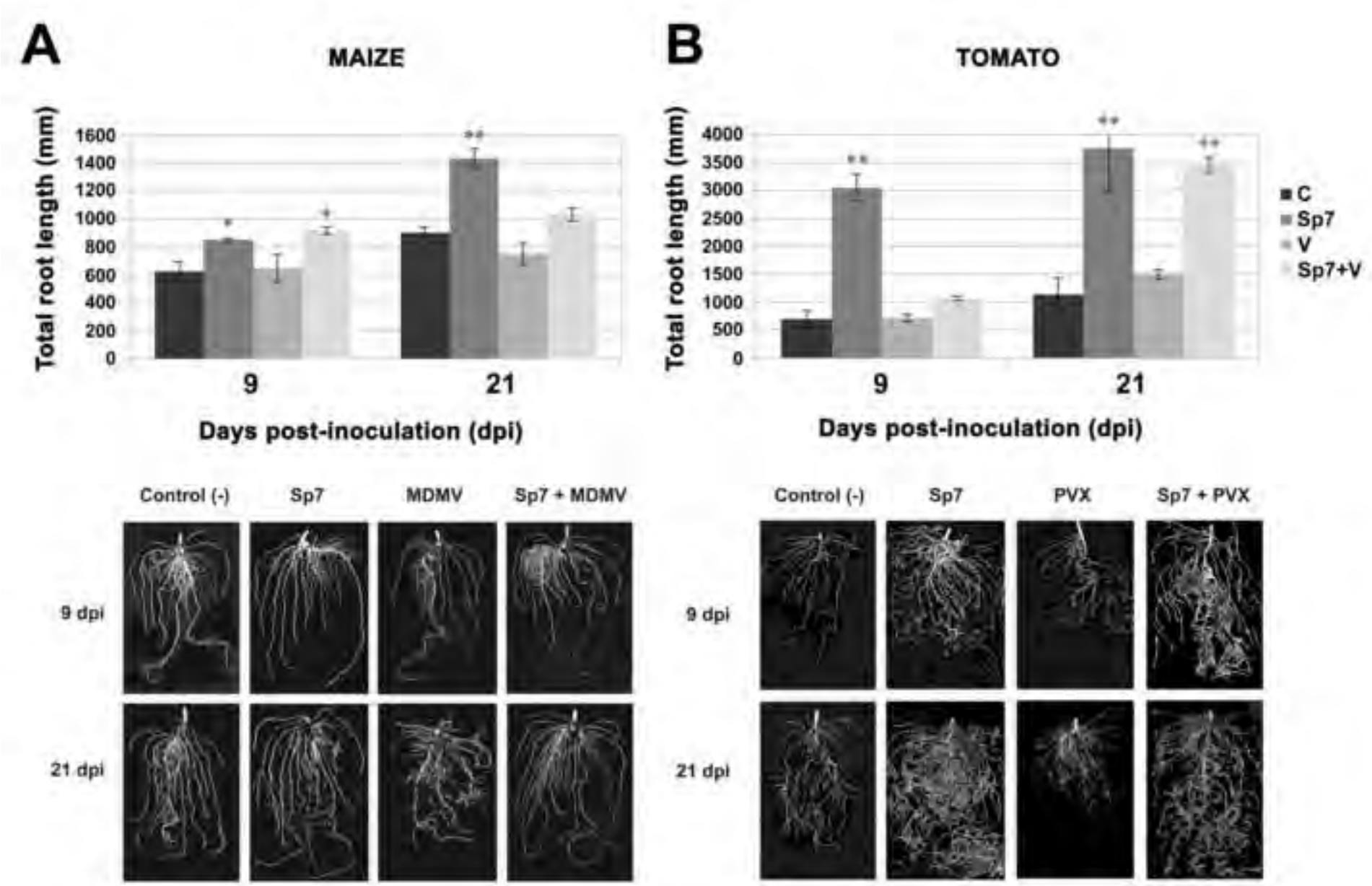

Figure 3. Gas exchange parameters Photosynthetic rate (A) and Transpiration (E) in (A) maize and (B) tomato plants at different days post-inoculation (dpi); control (C), A.

Click here to access/download;colour figure;Figure 3.jpg

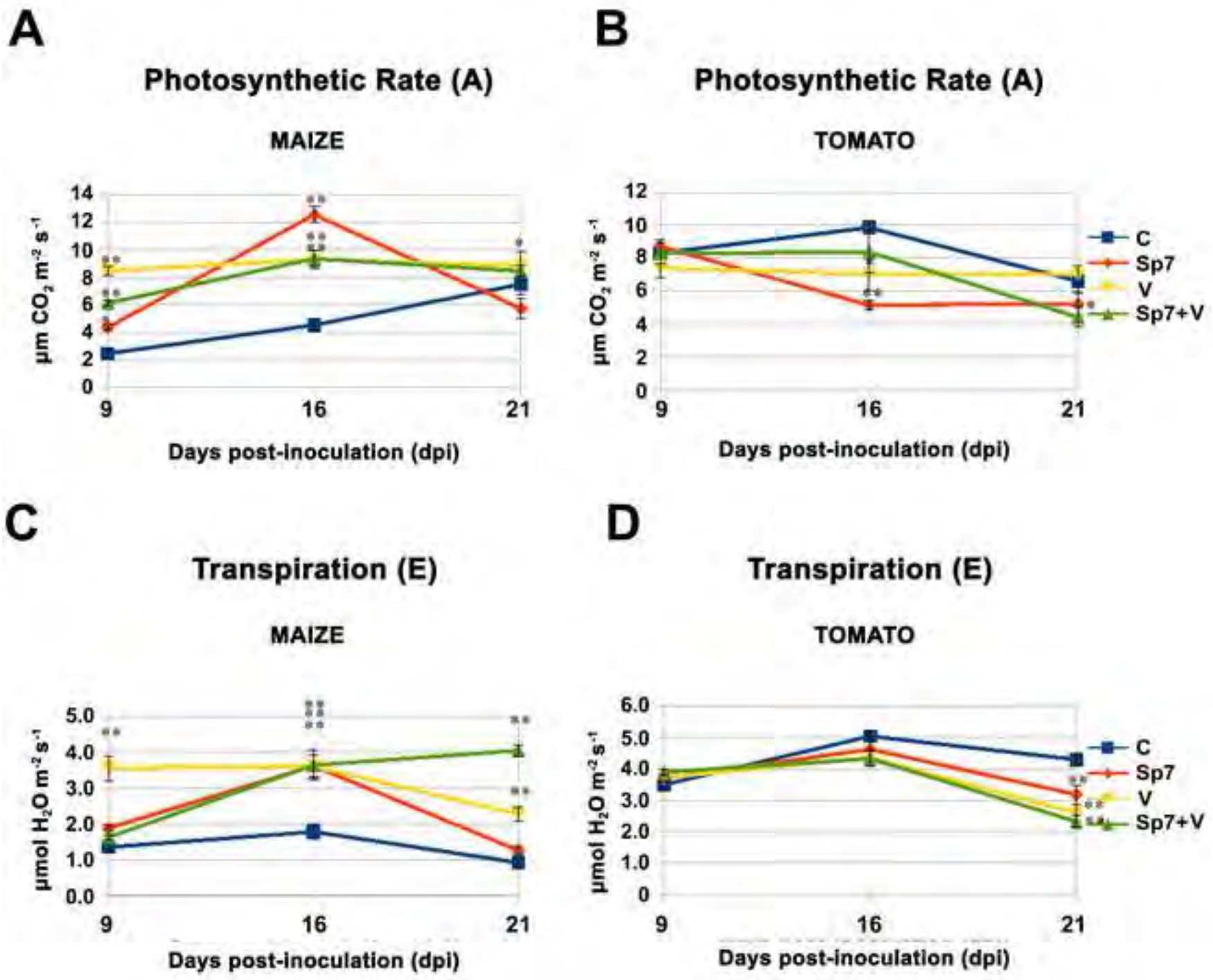

Figure 4. Maize dwarf mosaic virus (MDMV) and Potato virus X (PVX) viral progress and protein expression. (A) MDMV and (C)

Click here to access/download;colour figure;Figure 4.jpg

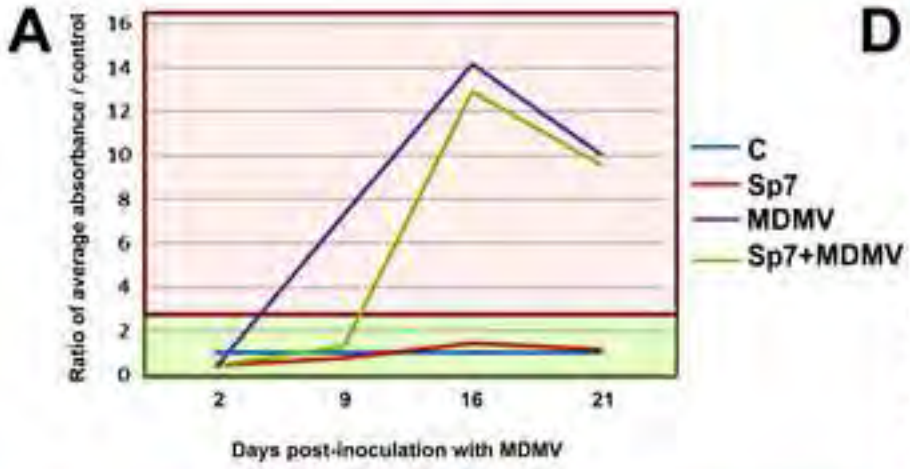

B

MDMV / Control			
SSP	9dpi	16dpi	Function
4801		*1.93	1,4
3802		*1.50	1,4
3801		1.48	4
3807	0.90		4
3703		0.89	2
2306	0.81		1
5602		0.75	2
8401	0.45		1,4
4802	0.42		1,4
2705	0.08		2
210	-0.25		3
402	-0.36		3,4
6307	-0.42		2
4202	-0.49		2
6102		-0.64	7
6201		-0.74	7
6103		-0.81	7
4402		-1.09	1
6714		-1.12	5

log2 FC
>2
>1.5
1
0
-1
<-1.5
<-2

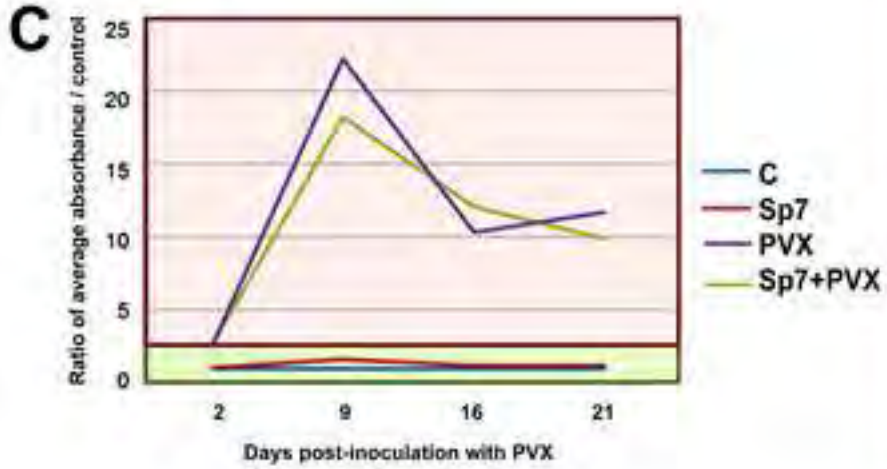

D

PVX / Control			
SSP	9dpi	16dpi	Function
7913	-1.40	[illegible]	1
5508	*-1.69	[illegible]	3
7409	*-1.60	[illegible]	1
5405	-0.97	[illegible]	4
7406		[illegible]	1
6906	-1.43	*1.85	1
2004		*1.80	1
4003	*1.54	*1.74	2
4001		1.46	1
8114		1.30	3
8101		1.26	7
6405	-1.25	1.18	2,3
8707	1.10		4
7504	-1.18	1.05	1
5607	-1.25	0.79	4
6206		0.77	1,4
5201		0.71	3
4305		0.70	1
7402	-0.64	0.69	1
4002	1.16	0.67	2
8107	0.66		4
7508	-1.22	0.64	4
6403		0.63	1
8401		-0.47	1
5509	-0.58		4
4606	-0.58		3
6304		-0.60	6
6404	-0.64		2,3
7401	-0.67		1
5311	-0.67		2,3
4201	-0.71		1,4
4402	-0.81		3
6505	-0.84		4
3702		-0.89	4
8102	-0.97		1,2
5402		-0.97	2
6406	-1.15	-1.00	4
2304	-1.09		1,4
8103	-1.18		1,2
4202	-1.18		1
6507	-1.22		4
6202	-1.25		1,2
7405	-1.25		1
7906	-1.29		4
6506	-1.36		3
7305	-1.40		1,4
6509	-1.40		4
8404	-1.47		1
5602	-1.47		1
8511	*-1.51		1
6208	*-1.51		2
5901	*-1.60		4
5307	*-1.74		1,4
5902	[illegible]		4
4908	[illegible]		4
7907	[illegible]		4
3709		[illegible]	2
3906		[illegible]	4

Figure 5. Representative 2-D page gels of extracted proteins from maize and tomato plants 21 dpi. 2-D PAGE gel image of (A) maize and (B) tomato with MDMV or PVX

Click here to access/download;colour figure;Figure 5.jpg

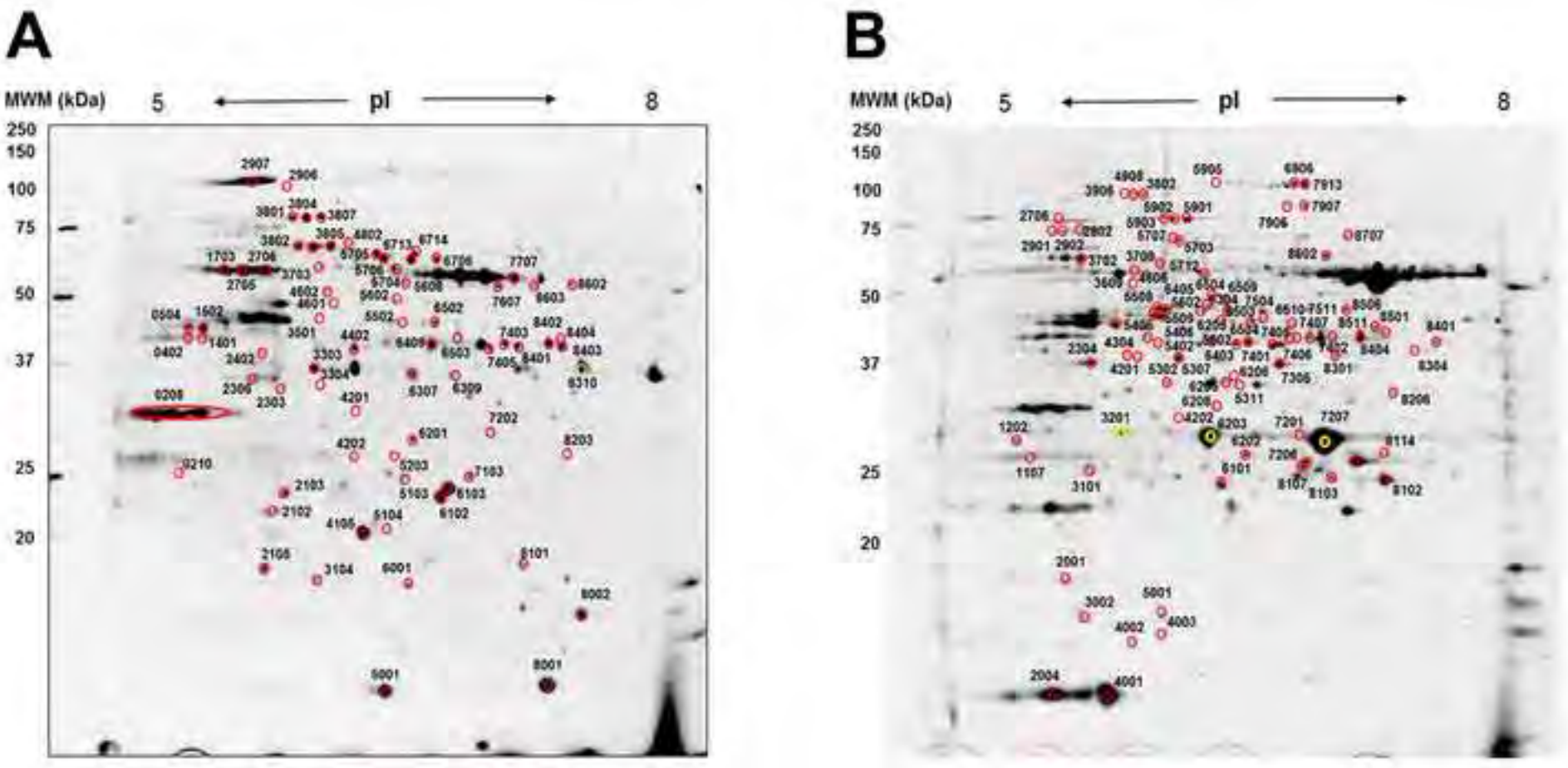

Figure 6. Maize heatmaps of differentially expressed proteins at 9 and 16 days post inoculation (dpi). Different effects of co-treatment (A. brasilense Sp7 (Sp7)+Maize

Click here to access/download;colour figure;Figure 6.jpg

274

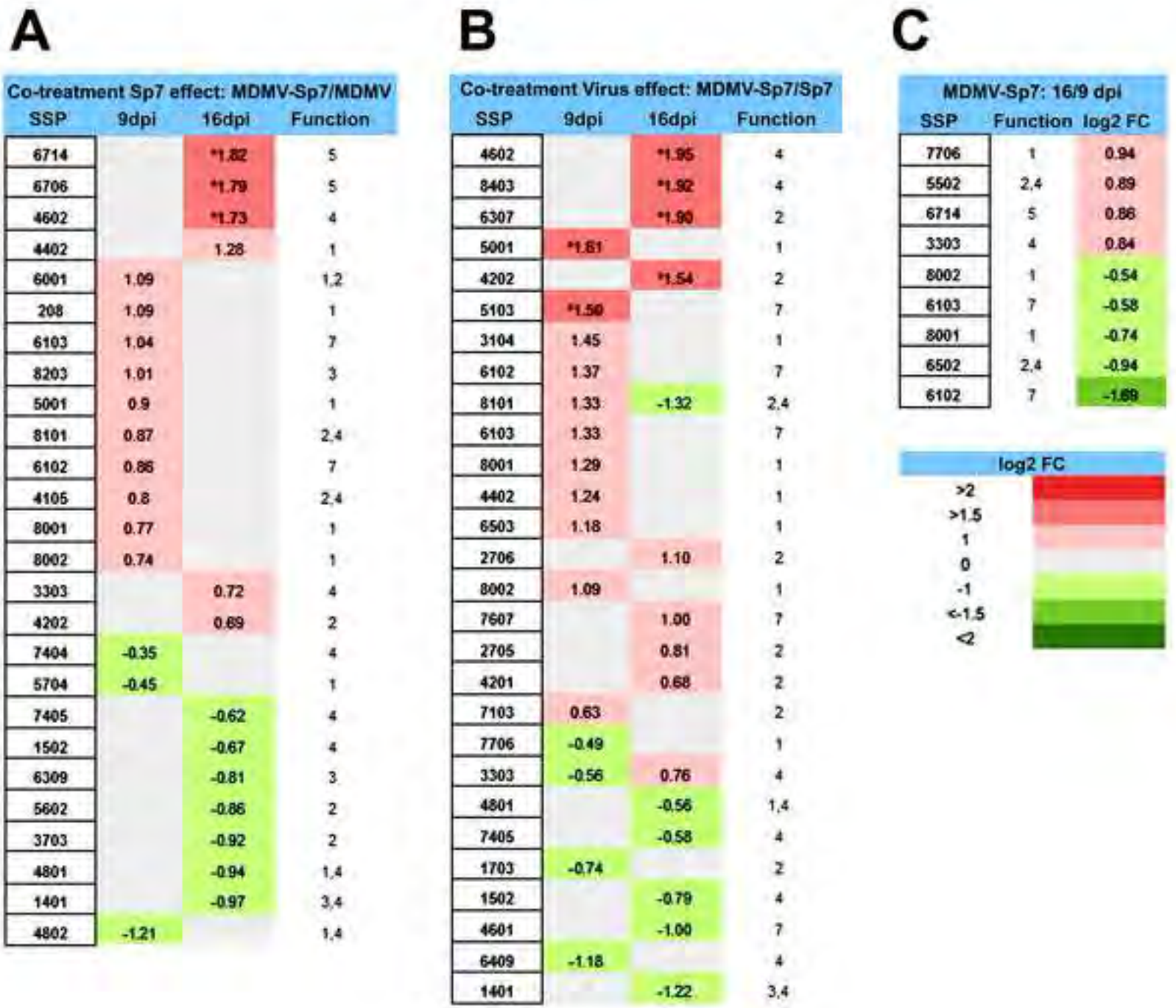

Figure 7. Tomato heatmaps of differentially expressed proteins at 9 and 16 days post inoculation (dpi). Different effects of co-treatment (A. brasilense Sp7 (Sp7)+ Potato

Click here to access/download;colour figure;Figure 7.jpg

ANNEX 5

Lade SB, Giné-Bordonaba J, Albacete A, Serrano L, Segarra J, Christou P, Medina V (2019) Biochemical and molecular regulation of *Azospirillum brasilense* Sp7 x *Fusarium graminearum* interactions influence hormones in early growth stages of high carotenoid maize (*Submitted to Molecular Plant-Microbe Interactions*)

Molecular Plant-Microbe Interactions® MPMI

Biochemical and molecular regulation of Azospirillum brasilense Sp7 x Fusarium graminearum interactions in early growth stages of high carotenoid maize

Journal:	*Molecular Plant-Microbe Interactions*
Manuscript ID	MPMI-04-19-0109-R
Manuscript Type:	Research
Date Submitted by the Author:	24-Apr-2019
Complete List of Authors:	Lade, Sarah; University of Lleida School of Agricultural and Forestry Engineering, PVCF Giné-Bordonaba, Jordi; IRTA Albacete, Alfonso; CEBAS Serrano, Luis Segarra, Joan; Universitat de Lleida Escola Tecnica Superior d'Enginyeria Agraria Christou, Paul; Agrotecnio Medina, Vicente; Univesitat de Lleida, Producció Vegetal i Ciència Forestal; Agrotecnio Center,
Area That Best Describes Your Manuscript:	Bacteria-plant symbiosis, genetics and gene regulation < Bacteria-plant symbiosis, molecular signaling < Bacteria-plant symbiosis

Biochemical and molecular regulation of *Azospirillum brasilense* Sp7 x *Fusarium graminearum* interactions in early growth stages of high carotenoid maize

Sarah B. Lade[1*], Jordi Giné-Bordonaba[2], Alfonso Albacete[3], Luis Serrano[1], Joan Segarra[1], Paul Christou[1,4], Vicente Medina[1]

1. Department of Plant Production and Forestry Science, University of Lleida-Agrotecnio Center, Av. Alcalde Rovira Roure, 191, 25198 Lleida, Spain
2. Institute for Food and Agricultural Research and Technology (IRTA), XaRTA-Postharvest, Edifici Fruitcentre, Parc Científic I Tecnològic Agroalimentari de Lleida, Parc de Gardeny, 25003 Lleida, Spain
3. Department of Plant Nutrition, CEBAS-CSIC, Campus Universitario de Espinardo, Espinardo, E-30100 Murcia, Spain
4. ICREA, Catalan Institute for Research and Advanced Studies, Passeig Lluís Companys 23, 08010 Barcelona, Spain

*Corresponding author: Sarah B. Lade, sarahb.lade@pvcf.udl.cat

Abstract

High-carotenoid (HC) maize has clear benefits for human health. It is rich in pro-vitamin A and other nutritionally important carotenoids, and represents a cost-effective intervention particularly in developing countries. In addition to safety and efficacy studies, HC must be assessed for fitness prior to deployment. *Gibberella zeae* (anamorph *Fusarium graminearum*) (Fus) has devastating effects on maize when infection takes place early in the plant's life cycle. Priming seeds with plant growth-promoting rhizobacteria (PGPR) can promote seedling survival and reduce detrimental effects of this pathogen. The aims of this study were to compare HC with its near isogenic white maize inbred line M37W (WT), and test how the PGPR *Azospirillum brasilense* Sp7 (Sp7) interacts with HC to offset symptoms caused by Fus. Testing was performed in a temperature- and light-controlled growth chamber. We compared specific gene transcription data with the hormonal and defense response. HC seedlings were co-inoculated with Sp7 and Fus and four weeks after planting, the seedlings were tested for antioxidant capacity (FRAP) and total phenolic content (TPC), hormone profile of the plant immune system, expression of antioxidant turnover genes and hormonal transcription factors (TFs). Co-inoculation decreased disease severity in HC, promoted seedling survival, and increased concentrations of jasmonic and salicylic acids (JA and SA) as well as *Zea mays* gibberellin acid-regulated by MYB (ZmGAMYB) TF. Antioxidant and abscisic acid (ABA) turnover genes were strongly induced in co-inoculated HC plants, providing evidence that the antioxidant-hormone signaling network is mediated by up-regulated secondary metabolism.

Keywords

Pathogen; defense; PGPR; biofortified crops; beta-carotene, phenols

Introduction

Fusarium graminareum (Fus) is a hemibiotrophic fungus that causes ear rot in maize plants with devastating consequences worldwide. The fungus leads to the production of mycotoxins (fumonisins) that pose a severe health concern to humans and animals alike. The three major factors influencing fungal development and mycotoxin production in maize kernels are environmental conditions, agricultural practices, and the susceptibility range of different genotypes (Edwards 2004). More resistant maize (*Zea mays)* inbred lines have been shown to express defense-related genes in direct response to *Fusarium* spp. attack, indicating that resistance is likely due to constitutive defense mechanisms preventing fungal infection (Campos-Bermudez et al., 2013). Therefore, control of *F. graminareum* is typically based on integrated crop management (ICM) strategies, which combines the utilization of resistant or tolerant cultivars and agronomic (mostly chemical) applications (Panwar et al., 2014; Dinolfo et al., 2017).

The ultimate goal of ICM is to promote plant survival against abiotic and biotic stressors. There is, however, also the concept of crop biofortification, which is similar in that plants are strengthened by a compendium of factors, but unique in that its specific aim is producing nutritious and safe foods in a sufficient and sustainable manner. This can be achieved through three main approaches: transgenic, conventional, and agronomic, involving the use of biotechnology, crop breeding and fertilization strategies, respectively (Garg et al., 2018). Since biosynthetic pathways and plant metabolites are often changed in the process of biofortification, the side-effects or compound effects of simultaneous use of various biofortification strategies may influence the final outcome of ICM. For example, transgenic biofortification often entails the concurrent incorporation of genes involved in the enhancement of micronutrient concentration, their bioavailability, and reduction in the concentration of antinutrients. These changes can limit the bioavailability of nutrients in plants, redistribute micronutrients between tissues, or enhance the micronutrient concentration in the edible portions of commercial crops, thereby increasing the efficiency of

biochemical pathways in edible tissues (Shewmaker et al., 1999; Agrawal et al., 2005; Yang et al., 2002).

Agronomic biofortification requires physical application of nutrients to improve the nutritional and health status of crops. One of the most biologically-sound applications in this regard are plant growth promoting rhizobacteria (PGPR), which enhance nutrient mobility from soil to edible plant parts, heighten their phytoavailability and improve plant nutritional status (Rengel et al., 1999; Smith and Read 2007). PGPR also have many mechanisms for mitigating phytopathogens, such as the production of siderophores, lytic enzymes, phytohormones and volatile organic compounds (Bhattacharyya and Jha 2012). *Azospirillum brasilense* Sp7 (Sp7) is one such PGPR found in the plant rhizosphere, which associates particularly well with maize (Bashan and de-Bashan 2010). Sp7 also produces growth-regulating substances, fixes atmospheric nitrogen, produces carotenoids and suppresses other microbes by producing bacteriocins and phenylacetic acid (PAA) (Hartmann and Hurek 1988; Somers et al., 2005; Bashan and de-Bashan 2010).

Azospirillum spp. have been studied both *in vitro* and *in vivo* for their action against *Fusarium* spp*. In vitro* results showed that the PGPR reduces growth of *Fusarium* spp., likely due to the secretion of volatile inhibitory substances (Abdulkareem et al., 2014). *In vivo*, *A. brasilense* was found to displace pathogenic fungi in the leaves of teosinte, helping reduce the severity of the disease and promote plant growth (López-Reyes et al., 2017). Previous studies suggest that the observed effects of *A. brasilense* to suppress disease are due to a combination of *A. brasilense*-mediated production of catechol-like siderophores and salicylic acid (SA), which may induce resistance in the plants (Fernández and Pedraza 2013). Most commonly, beneficial microbes activate a combination of ethylene (ET) and jasmonic acid (JA) hormone signaling pathways, triggering APETALA2/Ethylene-responsive factor (AP2/ERF) and ZIM27 TFs, which in turn activate lipoxygenase (LOX) or chitinase (CHIT) genes, and induced systemic resistance (ISR) (Pieterse et al., 2014).

The plant defense response is also up-regulated by hemibiotrophic pathogens like *Fusarium* spp., which trigger the SA hormone signaling pathway during pathogenesis and prime the plant to resist future attack via systemic acquired resistance (SAR). For this, the plant accumulates SA and activates WRKY transcription factors (TFs), leading to the expression and accumulation of pathogenesis related (PR) genes and proteins (Lanubile et

282

al., 2017). ISR and SAR function independently from each other, but are connected by the non-expressor for pathogenesis-related genes 1 (NPR1), which is thought to act as a common regulator.

Maize is one of the most important staple crops in developing countries, and has been biofortified to accumulate a number of various vitamins, such as beta-carotene, folate, vitamins C and E as cost-effective interventions to improve human health (Garg et al., 2018). High carotenoid (HC) corn, which produces provitamin A (carotenoids) in its endosperm by expressing bacterial transgenes *Pantoea annatis crtI (PacrtI)* and *Zea mays phytoene synthase 1* (*ZmPSY1)* (Zhu et al., 2008), is particularly interesting to our study because carotenoids are potent antioxidants with positive implications for human and plant health alike. For one, carotenoids and tocopherols in plant/*Fusarium* interactions appear to quench free radicals produced by plant cells as an early response to fungal pathogen attack (Gutierrez-Gonzalez et al., 2013). Carotenoids also provide precursors for the synthesis of abscisic acid (ABA), a phytohormone that increases upon *F. graminearum* inoculation (in wheat) (Gunnaiah et al., 2012), and which is implicated in the integration of different stress-response signaling networks, including ISR (Asselbergh et al., 2008). There is also the theory that stress stimulates biosynthesis of carotenoids in photosynthetic tissue to dissipate excess absorbed energy through the xanthophyll cycle (García-Plazaola et al., 2012; Fanciullino et al., 2014).

In this study, we inoculated HC maize seedlings with *A. brasilense* Sp7 and examined the biochemical and molecular changes induced by fungal infection. The main purpose of our research was to test the hypothesis that agronomically biofortifying transgenic crops would improve plant defense regulation to offset symptoms induced by *F. graminareum*. To do so, we determine physiological differences between the rhizobacteria-inoculated and fungus-infected genotypes, identify hormonal pathways involved in the defense responses, test the degree to which interactions affect secondary metabolism (via gene transcription data, and by measuring phenolic content) and link specific gene and TF transcription profiles with the observed defense response.

Results

Plant phenotypes and morphological characteristics

When comparing whole plant phenotypes, control and Sp7-inoculated plants were similar in that they both exhibited upright, full leaf structures that were continuous-green in color. In contrast, Fus plants were thinner, shorter and had leaf necrosis and extensive wilting. Co-treated (Sp7+Fus) plants were larger and more vigorous than any other treatment group, especially for the HC genotype (Figure 1).

Figure 1

Differences in leaf length were statistically significant among treatments ($p=0.002$) (Figure 2A). Specifically, Sp7 resulted in the leaves of both genotypes being 35% longer on average compared to controls ($p<0.001$). In a similar way, differences in total root moisture content (%) were highly significant ($p=0.006$) when comparing different treatments. On average, Sp7-inoculated plant roots had nearly twice the water content than control or plants inoculated with Fus or both Sp7+Fus, regardless of genotype ($p<0.05$) (Figure 2B).

Figure 2

Changes in leaf surface temperature were significant for the interaction between the genotype and treatment ($p=0.001$). Control HC plants were 6% warmer than WT ($p<0.001$), while Fus HC plants were 3% cooler than WT ($p=0.01$). Differences were non-significant between genotypes for Sp7 and Sp7+Fus treatments, indicating a standard up-regulation of plant temperature in response to Sp7 inoculation, regardless of fungal infection or genotype (Figure 3A). Differences in chlorophyll content (SPAD) were highly significant for the interaction between genotype and treatment ($p=0.007$) (Figure 3B). Fus HC had a 31% increase in chlorophyll content over WT ($p=0.025$), while in the case of co-treatment, Sp7+Fus HC had 34% less chlorophyll contents than WT ($p=0.005$).

Figure 3

Total phenolic content (TPC) in leaves (Figure 4A) was highly correlated with antioxidant capacity (ferric reducing antioxidant power; FRAP) (Figure 4B). A significant interaction was found between genotype and treatment highlighting the differential effect of the treatment among WT or HC genotypes. For instance, Fus inoculation resulted in -0.17-fold lower or 1.5-fold higher TPC, if compared to control plants, for WT or HC, respectively. In contrast, inoculation with Sp7 or the combination of both Sp7+Fus did not alter or enhance, respectively, the TPC of leaves in both genotypes.

Figure 4

Hormone profiling

In leaves, six hormones (ACC, tZ, IAA, ABA, JA and SA) were measured and had significant interactions between genotype and treatment. In HC plants treated with Fus or Sp7+Fus, ACC decreased by 60-fold (compared to WT). In contrast, the accumulation of other hormones increased significantly in Sp7+Fus-treated HC plants if compared to WT; IAA increased 3-fold, JA increased 9-fold and SA 7-fold. HC plants only inoculated with Sp7 exhibited a 2-fold increase in ACC accumulation, and a 3-fold decrease in ABA compared to WT (Figure 5).

Figure 5

Expression of genes involved in redox homeostasis, flavonoid and carotenoid biosynthesis

For both genotypes, transcriptional changes of genes associated with secondary metabolism were most apparent in plants inoculated with Sp7+Fus (Figure 6). In particular, there was a 14-fold transcriptional increase in superoxide dismutase 4 gene (*ZmSOD4*) in HC plants (compared to HC controls), and a 1.5-fold increase in Sp7+Fus WT plants compared to WT controls. Other significant transcriptional increases in Sp7+Fus-treated plants included chalcone isomerase (*ZmCHI1*) (6.6-fold for WT and 15-fold for HC, compared to their respective controls) and isochorismate (*ZmICS*) (2-fold for WT and 2.5-fold for HC), both involved in flavonoid biosynthesis. Ascorbate peroxidase (*ZmAPX*) (1-fold for WT and 2.9-fold for HC), linked to redox reactions; and lipoxygenase (*ZmLOX3*) (14-fold for WT and 7.5-fold for HC), zeaxanthin epoxidase (*ZmZEP*) (1.4-fold for WT and 9-fold for HC) and 9-cis-epoxycarotenoid dioxygenase (*ZmNCED4*) (5-fold for WT and 0.8-fold for HC), all of which are intertwined with oxylipin and carotenoid biosynthesis, as well as ABA turnover.

Fusarium graminearum infection in WT plants caused increased transcription of flavonoid biosynthesis genes *ZmICS* (1.15-fold) and *ZmCHI1* (5.5-fold), as well as *ZmLOX3* (10-fold). Meanwhile in HC plants, Sp7 inoculation induced a similar reaction with the over-expression of *ZmICS* (5.5-fold), *ZmCHI1* (35-fold), *ZmSOD4* (11.5-fold) and *ZmAPX* (2-fold).

Of all transcription factors tested, the only one that exhibited significant variation between treatments and/or genotypes was the *Zea mays* gibberellin acid regulated by MYB

(ZmGAMYB). In HC plants co-treated with Sp7+Fus, expression levels were 12-fold higher than in the respective controls (HC; Figure 6).

Figure 6

To further explore the relationship between all variables as well as the differential effect of the treatments on the different genotypes, a principal component analysis was carried out by combining hormonal, total phenolic content and gene expression data (23 variables; Figure 7). Our results show that most of the variability between treatments was captured by the PC1 (37.3% of the total variability) while differences among genotypes for the same treatment where mainly related to PC2 (23.5% of the total variability). An exemption was found for Sp7 inoculated plants where the distinction between HC or WT genotypes was almost exclusively explained by the first principal component. Interestingly, the variables TPC, SA, JA, ACO, and transcription factor expression of EREPB, MYB and WRKY clustered (positively) on component 2. In a similar way, SOD4, PSY1, NCED4, APX, CHI1 and ICS1 all had large positive loadings on component 1. ABA had strong negative loading for both components 1 and 2.

Figure 7

For all treatments and genotypes, gene expression was correlated with hormone accumulation, highlighting significant relationships within their regulatory network (Figure 8). In the correlation matrix, several relationships were especially revealing. For instance, ZmGAMYB was positively correlated with *ZmSOD4,* JA and SA; while *ZmSOD4* was only correlated with SA. In contrast, ABA accumulation was antagonistic to *ZmEIN3*, *ZmACO* and *ZmNCED4*. *ZmEIN3* positively correlated with *ZmPSY1* and *ZmNCED4* of carotenoid biosynthesis, while *ZmNCED4* was also (positively) correlated with *ZmLOX3*, which is involved in root-specific defense signaling pathways. *ZmACO* was positively correlated with TPC and the ZmWRKY TF. Schematic representation of these findings (Figure 9) distinguishes the gene and hormone regulatory network controlling carotenoid biosynthesis and the stress-related responses for each genotype. Overall, there was consistency in results between genotypes, except for in the case of co-treatment, where ZmGAMYB correlated less with ABA and ACO hormone accumulation. For both genotypes, the up-regulation of ZmGAMYB and *ZmZEP* in the carotenoid pathway did not carry through to downstream gene expression, such as that of *ZmNCED4.* Although all hormones exhibited increased

accumulation, the only active TF was ZmGAMYB.

Figure 8

Figure 9

Discussion

Rapid climate change and population growth put pressure on crop systems to withstand stress. Sustainable management of crop welfare therefore requires the development of strategies that consider human and plant health alike. In order to effectively design and implement such programs, an integrated understanding of plant defense-related regulatory networks is crucial. In this study, we subjected HC maize seedlings to the combination of biotechnological and agronomic biofortification, with the aim of strengthening plants against *Fusarium graminareum* (Fus). Using high carotenoid (HC) transgenic seedlings provided a unique opportunity to investigate the compound effect of two forms of biofortification on defense-related biological processes. We found that inoculation with Sp7 offset symptoms incurred by Fus and that the genotypic diversity of the maize was a determining factor for variable transcriptional patterns and hormone concentrations in plants.

Analysis of chloroplastic activity, leaf growth and temperature elucidated aspects of above-ground plant physiology that were indicative of plant stress levels and susceptibility to fungal infection. WT plants had significantly less chlorophyll contents than HC and were visibly more susceptible to Fus infection than HC plants. Chloroplasts are highly sensitive to stress factors (Romanowska et al., 2017; Zhao et al., 2016) and previous studies have shown that deoxynivalenol (DON), the *Fusarium* spp. trichothecene mycotoxin that inhibits eukaryotic protein synthesis, is responsible for cellular damage to chloroplasts (McLaughlin et al., 1977; Wojciechowski et al., 1995). WT plants also had weaker phenotypes and higher leaf temperatures, which is typical of plants exposed to pathogens and indicative of plant moisture stress, reduced water uptake efficiency and compromised evaporative cooling ability (Mengistu et al., 1987; Omer et al., 2007). The combined effect of Sp7+Fus affected the two genotypes in a different way than Fus alone, causing HC plant chlorophyll levels to drop significantly below those of WT. These results did not correspond with the fortified HC phenotype and stable leaf temperature that we observed, confirming a special interaction between the bacteria and fungus in HC plants which adversely affected photosynthesis-

related cells, but did not physically stress the plant otherwise.

Fus-infection was a common denominator for increased TPC and FRAP in transgenic plants, evidencing up-regulated secondary metabolism (SM) stemming either from the shikimate/phenylpropanoids pathway or through activation of other pathways generally leading to higher antioxidant content. For example, we correlated TPC with *ZmACO,* the gene responsible for expression of ACC-oxidase (ACO), which converts ACC to ethylene in the presence of oxygen, and which over-expressed in Fus HC seedlings. Previous work has made similar connections regarding enhanced antioxidant capacity in plants via ethylene signaling (Xu et al., 2017). Ethylene signaling has even been found to regulate the relative abundance of two specific *F. graminareum*-related metabolites, smilaside A and smiglaside C, thereby affecting resistance against *F. graminareum* in maize seedling roots (Zhou et al., 2019).

In this study, the up-regulation of antioxidant-related gene expression was not always correlated with increased TPC and FRAP, suggesting that enzymatic antioxidants but not specific antioxidant metabolites were triggered in response to the plant-pathogen or plant-. PGPR-interaction. For instance, Sp7-inoculation in HC plants caused increased expression of *ZmSOD* and *ZmAPX*, enzymes responsible to scavenge H_2O_2, despite no difference in TPC. Our results also revealed significant correlation between *ZmSOD* and SA, which was most evident in HC plants subjected to co-treatment or Sp7-inoculation. While previous studies have shown that antioxidants are strongly implicated in SA signaling (Foyer and Noctor 2005), we build upon this in providing evidence that the antioxidant-hormone signaling network is mediated by symbiotic partnerships such as that resulting from the interaction between Sp7 and HC. It is known that redox homeostasis is governed by the presence of large pools of antioxidants that absorb and buffer reductants and oxidants (Foyer and Noctor 2005). Symbiotic associations between organisms involve ROS-antioxidant interactions, leading to an enhancement of antioxidant status such that the symbiotic partnership is more resistant to environmental stress than either partner alone (Kranner et al., 2005). Sp7 inoculation demonstrates this type of relationship with the HC genotype, thereby increasing the plants' resistance against Fus. Why this enhancement is especially evident in HC but not in WT is still unclear and warrants further investigations, yet our results point out the putative role of several transcription factors.

In Sp7-inoculated HC seedlings that were infected with Fus, we also observed significantly increased accumulation of SA and JA hormones, and over-expression of the ZmGAMYB TF. The correlation matrix confirmed that ZmGAMYB was positively related with JA and SA, as well as *ZmSOD4.* In a similar study, chemical inducers SA, JA and the biocontrol agent *Trichoderma harzianum* induced the defense system against *F. oxysporum* f. sp. *lycopersici* infection by increasing expression of various antioxidant enzymes (Zehra et al., 2017). Our results reveal similar changes to the defense system with Sp7 as the biocontrol agent and *F. graminareum* as the pathogen, but go further by involving the ZmGAMYB TF as a potential regulatory hub of the antioxidant-related defense response in HC plants. There is the possibility that this interaction is connected to the redox state of the transgenic plants, which may be altered on account of the engineered carotenoid pathway. Even though earlier field trials found that HC demonstrated normal morphology and development, consistently with transgene expression strictly in the endosperm (Zhu et al., 2008; Zanga et al., 2016), other studies have found that alteration of the carotenoid biosynthetic pathway has pleiotropic effects on other main secondary metabolites with antioxidant activity *in planta* (Decourcelle et al., 2015; Zanga et al. 2018). Comparatively, MYB has proven to perceive the cellular redox state (Arratia-Quijada et al., 2012), and may coordinate secondary metabolism and oxidative stress response (Hong et al., 2013). The implication of SA and JA as a coordinated part of the same response also suggests that *ZmGAMYB* proteins are transcriptional common-ground for the two defense pathways elicited by each phytohormone. Previous work with other pathosystems has related SA and JA (Lanubile et al., 2017), but never have the two phytohormones been documented as both having a connection with ZmGAMYB, as with NPR1 or ABA (Dong 2004; Pieterse et al., 2012).

It is not unusual that ZmGAMYB over-expresses in response to up-regulated JA or SA hormone concentrations, though the response has generally been observed in the presence of each individual hormone, separately. ZmGAMYB is a member of the R2R3-class TFs, regulating gibberellin-responsive genes during germination (Gubler et al., 1995), as well as endosperm specific genes during seed development (Diaz et al., 2002). The family of R2R3-MYB-like TFs has repeatedly been implicated in JA-dependent defense responses (Ambawat et al., 2013), and in a variety of biological functions like phenylpropanoid

metabolism (Hichri et al., 2011), biotic and abiotic stress (Lippold et al. 2009; Segarra et al. 2009), and hormone responses (Urao et al. 1993). SA signal transduction pathways have also been connected with MYB (Raffaele et al. 2006); specifically, AtMYB96-mediated ABA signals enhanced pathogen resistance response by inducing SA biosynthesis, implicating MYB96 as a molecular link in ABA-SA crosstalk (Seo and Park 2010).

The SA and JA signaling pathways are thought to comprise the backbone of plant immunity (Pieterse et al., 2009; Pieterse et al., 2012; Shigenaga and Argueso, 2016), and to lead to the transcriptional activation of defense genes. Typically, SA has been tied to the WRKY TF family, and JA to ZIM27 (Lanubile et al., 2017). Previous studies have also shown that TF activation is skewed towards the MYB family in the case of certain pathosystems. For example, *Tobacco mosaic virus* (TMV) and an SA-induced tobacco gene were shown to encode a MYB TF to participate in SAR (Yang and Klessig 1996). In another case, at least two *Arabidopsis* MYB genes were induced by bacterial infection and hypersensitive cell death (Kranz et al. 1998); and finally there is one instance of a MYB gene being induced by fungal infection (Lee et al., 2001). Whereas earlier studies document MYB activation via the stress response to either bacterial or fungal infection, here we document the activation of ZmGAMYB in HC by bacterial and fungal co-infection.

Principle component analysis (PCA) indirectly correlated hormone accumulation of ABA with SA and JA. This sort of ABA-SA reciprocal antagonism in leaves has been well-documented in previous work (Cao et al., 2011). It has also been reported that engineered carotenoid modification can disturb ABA levels (Lindgren et al., 2003) since ABA is a final product of the carotenoid pathway. Thus said, our results clearly showed that ABA was not different among WT or HC untreated genotypes. In terms of ABA signaling, our results emphasized a positive correlation between *ZmPSY1*, *ZmNCED4* and ZmEIN3*. ZmPSY1* and *ZmNCED4* are carotenoid to ABA biosynthesis, transport, turnover and catabolism genes*,* while ZmEIN3 is a TF responsible for regulating JA and ET signaling and cross-talk between all three pathways (JA, ET and SA) (Klessig et al., 2018). There was also positive correlation between *ZmNCED4* and *ZmLOX3,* which has been tied to the concomitant suppression of JA and SA-regulated pathways in roots (Gao et al., 2008). These relationships highlight the connection that carotenoid pathway genes have with hormone signaling genes, and while the exact mechanisms underlying their coordination still remains to be elucidated, our results

290

imply the importance of up-regulated secondary metabolism in this response.

We also found that ABA accumulation was negatively correlated with up-regulated ZmEIN3, *ZmACO* and *ZmNCED4* gene expression. *ZmACO* and ZmEIN3 participate in ethylene conversion and signaling/crosstalk, respectively, and are typically regulated by ABA (Klessig et al., 2018), while *ZmNCED4* is a rate-limiting enzyme for ABA biosynthesis (Mou et al., 2016). The inverse relationships between ABA accumulation and downstream gene expression reiterates that another source is likely regulating ethylene-mediated processes, such as an alteration of the redox state. The mechanisms controlling ABA hormone accumulation are less known than those governing ABA turnover gene expression, though it has been suggested that there are unknown regulatory mechanisms integrating the activities of different ABA-metabolism pathways to match ABA level to stress severity (Kalladan et al., 2017). More recent work has found that ABA regulates the internal metabolic functions to alleviate the harms of environmental stresses by integrating with antioxidant responses and triggering the pre-transcriptional induction of NADPH oxidases (NOXs) to modulate NADPH oxidase for ROS generation (Asad et al., 2019). Over-expression of the ABA-synthesis enzyme NCED may lead to a small (or null) increase in ABA, but larger increases in the ABA catabolite phaseic acid (Qin and Zeevaart, 2002). In our study, this might be the case as demonstrated by correlation analysis, but also specifically in co-treated and Sp7 HC plants, since plants demonstrated up-regulation of ABA-related gene *ZmNCED4*, but no change in ABA hormone accumulation.

Conclusions

This study examined the relationship between *Azospirillum brasilense* Sp7 and *Fusarium graminareum* in high carotenoid transgenic maize plants, finding that their interaction adversely affects photosynthesis-related mechanisms, but enhances plant antioxidant capacity, as well as the expression of genes involved in the carotenoid pathway, hormone signaling and ethylene production generally leading to improved resistance to Fus and better agronomic performance. The combined effect of Sp7 and Fus on HC genotypes revealed a complex cross-talk between hormones with genes involved in the antioxidant and carotenoid pathway thereby providing evidence that the antioxidant-hormone signaling network may be triggered by an up-regulation of the plant secondary metabolism.

We also show a likely implication of the ZmGAMYB transcription factor in the cellular redox state, and as a putative candidate transcription factor for coordinating the up-regulation of the plant secondary metabolism, the oxidative stress response and the hormonal cross-talk in HC plants. Besides, salicylic and jasmonic acid seem to act as a coordinated part of the same response, suggesting that ZmGAMYB proteins are transcriptional common-ground for the two defense pathways elicited by each phytohormone. To the best of our knowledge, this is the first study documenting the activation of ZmGAMYB by bacterial and fungal co-infection.

Material and Methods

Treatments

We used two maize (*Zea mays*) near-isogenic genotypes: a South-African white elite maize M37W lacking carotenoids in its endosperm (WT) and a high-carotenoid transgenic line (HC) previously created in our lab via combinatorial nuclear transformation of M37W. M37W seeds were obtained from The Council for Scientific and Industrial Research (CSIR, Pretoria, South Africa). HC expresses the transgenes *Zea mays phytoene synthase 1* (*Zmpsy1)* and *Pantoea annatis crtI (PacrtI)* and accumulates significant amounts of ß-carotene, lycopene, zeaxanthin and lutein in the endosperm, thereby giving it an orange phenotype (Zhu et al., 2008).

Seeds were either inoculated with Sp7 or PBS (controls) and sown in 5x5cm pots containing autoclaved commercial substrate (Traysubstrat®, Klasmann-Deilmann, Gmbh, Geeste, Germany) characterized by having an extra fine structure and pH of 6. For one week, or until the seedlings had reached the two-leaf stage, the pots were maintained in a growth chamber (1282 x 687 x 1487mm) at 23-25°C with a photoperiod of 16h light/8h dark cycle under 10,000lux fluorescent bulbs. Relative humidity was regulated at 90-95% and emerged plants were watered twice a week. To avoid cross-contamination, Sp7-inoculated and control pots were separated into different trays.

After a week, homogenous seedlings were selected for inoculating with Fus and transplanted in 0.3L pots. Fus millet inoculum was mixed into the soil at a rate of 0.6g/kg before transplanting the seeds. All pots were supplemented with 0.1g of 20-20-20 slow release fertilizer and returned to the same growth conditions (described above). Three weeks

292

after transplanting, when the mature conidia had begun to form in the infected cells (Oren et al., 2003), the plants were analyzed or harvested.

Sp7 and Fus inocula and inoculation

The *Azospirillum brasilense* Sp7 strain (ATCC 29145) (Sp7) was kindly provided by the "Colección Española de Cultivos Tipo" (CECT) of the Polytechnic University of Valencia (Spain). For the Sp7 suspension, a peptone yeast broth (PYB) liquid medium amended with $CaCl_2$ (0.04%) was prepared, as described by Döbereiner et al. (1976), and incubated at 32°C under constant agitation at 100rpm for 20h. The bacterial suspension was allowed to reach its late log-growth phase [absorbance of 1.0 at OD_{600} nm (determined via an Amersham Biosciences Ultraspec 3100 Pro spectrophotometer)], obtaining an ideal bacterial density of $1x10^8 cfu \bullet mL^{-1}$.

The maize seeds were disinfected with 70% ethanol for 2min, soaked in 1% sodium hypochlorite for 10min under constant agitation (100rpm), and washed six times with sterile distilled water. Seeds were dried on sterile autoclaved paper and inoculated with the rhizobacteria at $1x10^8 cfu \bullet mL^{-1}$ (Bashan 1986); 1mL of the bacterial suspension was aliquoted for each WT and HC inoculated seed group and centrifuged at 5000rpm for 10min. The supernatant was removed and the pellet was re-suspended in 1mL of 1X PBS. The inoculum was vortexed, and 0.4mL of inoculum was added to each group of 10 seeds. The seeds and inoculum were sealed in 15mL Falcon tubes and agitated horizontally on a shaker for 4.5h. Inoculation time and quantity were established according to an imbibition curve, estimating the time taken for each seed variety to imbibe 70% of its total potential. Controls were handled the same was as inoculated seeds, but treated only with PBS.

The Fus inoculum was prepared with millet seed (*Panicum miliaceum L.*), as described by Idris et al., 2007; 150g millet seed and 200mL distilled water were mixed together in a 1L bottle, and autoclaved at 121ºC for 15min. Upon cooling, each bottle was inoculated with five 4mm discs cut from a fresh potato dextrose agar (PDA) culture of *Fusarium graminearum.* The inoculum was incubated at 27±1°C for one week and applied to the soil at a rate of 0.6g/L to pre-germinated (one-week old) seedlings.

Experimental Design

Inoculation was conducted in groups of 40 seeds per genotype (G) and treatment (T). One week after planting, germinated seeds were selected down to 20 for each G and T of the most homogenous seedlings and transferred to individual 0.3L pots. Each pot contained one seedling and was considered both as the randomization and as the observational unit. The sampling was conducted three weeks after transplanting and five biological replicates of each G/T were chosen in a completely randomized design for each analysis.

Sampling and analysis of plants

Photosynthetic rates and related traits were determined for individual leaves at the final sampling time using a LCi portable photosynthesis system (ADC BioScientific, Great Amwell, UK) which measures net CO_2 assimilation (net photosynthetic rate). Measurements were taken using the last fully-expanded leaf between mid-morning and noon in the growth chamber. The leaf chlorophyll concentration was estimated *in situ* using a SPAD-520 portable chlorophyll meter (Minolta, Tokyo, Japan) on the same leaves used to measure gas exchange.

A two-way analysis of variance (ANOVA) was conducted to quantify the overall effect of the interaction(s) between genotypes, treatments and the related effects for all measurements. Least significant difference was used for mean separation, and an individual error rate of 95% was considered in all tests. JMP□ software version Pro 11.0.0 was used for all analyses (SAS Institute, Cary, NC, USA).

Physiological measurements

To determine moisture content, plants were first cut at ground level and roots cleaned with SDW. Stems with leaves and roots were weighed before and after drying for 72h at 65°C.

Verification of Sp7 and Fusarium presence

Sp7 colonization assays were conducted at sampling, with three random samples taken from each treatment. The procedure was carried out according to Botta et al. (2013) with modifications. One hundred grams of plant roots were homogenized in 1mL sterile physiological solution (NaCl 0.9%). The homogenate was then serially diluted and plated in Petri dishes containing sterile nitrogen-free broth medium (NFb) supplemented with 15mL/L of

294

1:400 aqueous solution of Congo-red (CR) (Bashan et al., 1993). Bacterial colonies were counted after 48h incubation at 32°C.

To verify that the colonies were indeed the Sp7 strain, we performed PCR with aliquots taken from stationary-phase cultures grown from the plate isolates, according to Shime-Hattori et al. (2011). The isolates were grown at 32ºC for 17h in Luria-Bertani (LB) broth supplemented with 2.5mmol1^{-1} $CaCl_2$ and 2.5mmol$^{1-1}$ $MgCl_2$. The cultures were held at 95ºC for 5min, and the supernatants of cell lysates obtained were used as PCR templates. The presence of Sp7 16S rDNA was confirmed by PCR using 10µL of the crude bacterial lysate templates in a total volume of 25µL PCR reaction mix consisting of GoTaq DNA Polymerase with the reagents recommended by the manufacturer (Promega, Fitchburg, WI, USA). The PCR was run under the following conditions: 3min initial denaturation at 94ºC followed by 35 cycles of 30s denaturation at 94ºC, 30s annealing at 60ºC, and 1min extension at 72ºC with 5min final extension at 72ºC.

Fusarium graminareum presence in root tissues was tested for all treatments. In summary, 1cm-long pieces of roots were excised, rinsed with SDW and set to grow on selective *Fusarium* agar (SFA) for one week (Burgess et al., 1994), or until pink colonies had formed. Pure cultures were then selected and grown in 500µL malt extract broth in Eppendorf tubes (2%*w/v* malt extract, 1% *w/v* peptone, 2% *w/v* glucose) for 2d at 25ºC in darkness. The mycelial extract was recovered by centrifugation (14,000rpm, 10min), and the DNA was extracted and amplified as described by Díaz-Gómez et al. (2016). Amplification reactions for DNA sequencing were conducted in volumes of 100µL containing 10ng template DNA, 4µL of each primer (10µM), 10µL of 10x PCR buffer, 2µL dNTPs (10mM), and 0.75µL Taq DNA polymerase (5UμL^{-1}). We ran the PCR under the following conditions: 3min initial denaturation at 95ºC followed by 35 cycles of 30s denaturation at 95ºC, 20s annealing at 62ºC, and 45s extension at 72ºC with 5min final extension at 72ºC (Demeke et al., 2005).

For both Sp7 and Fus detection assays, the PCR products were sequenced (StabVida, Caparica, Portugal). Sequences were analyzed and aligned using the Blast® search tool (National Center for Biotechnology Information, Bethesda, MD, USA) and Ugene (Okonechnikov et al., 2012). See Table 1 for 'Sp7' and 'Fus detection' primer sequences.

Hormone extraction and analysis

Cytokinins (trans-zeatin, tZ), indole-3-acetic acid (IAA), abscisic acid (ABA), salicylic acid (SA), jasmonic acid (JA) and the ethylene precursor 1-aminocyclopropane-1-carboxylic acid (ACC) were analyzed according to Gutierrez-Carbonell et al. (2015). Leaf samples were filtered through 13mm diameter Millex filters with 0.22µm pore size nylon membrane (Millipore, Bedford, MA, USA). Filtrated extract (10µl) was injected in a UHPLC-MS system consisting of an Accela Series UHPLC (ThermoFisher Scientific, Waltham, MA, USA) coupled to an Exactive mass spectrometer (ThermoFisher Scientific, Waltham, MA, USA) using a heated electrospray ionization (HESI) interface. Mass spectra were obtained using the Xcalibur software version 2.2 (ThermoFisher Scientific, Waltham, MA, USA). For hormone quantification, calibration curves were built for each analyte (1, 10, 50, and 100µgL^{-1}) and corrected using 10µgL^{-1} deuterated internal standards. Recovery percentages ranged between 92 and 95%.

Total phenolic content and antioxidant capacity

Extraction and determination of total phenolic content (TPC) in leaf samples was done using the Folin-Ciocalteu Method (Singleton et al., 1999) as described by Giné-bordonaba and Terry (2016).

From the same methanolic extract used for TPC determinations, antioxidant capacity was determined by the standardized ferric reducing antioxidant power (FRAP) technique as described elsewhere. The FRAP was obtained by measuring the absorbance change at 593nm caused by the reduction of the Fe^{3+}-TPTZ complex to the ferrous form at pH 3.6. The FRAP reagent was freshly prepared by mixing 25mL of acetate buffer (300 mmol/L, pH 3.6), 2.5mL of $FeCl_3 \cdot 6H_2O$ solution (20mmol/L). Briefly, 90µL extract was added with 90µL distilled water and 900µL FRAP reagent. The homogenate was incubated at 37°C for 60min, and absorbance was measured. Blanks were included replacing leaf extract volumes for acetone/water. Results were expressed as mmol Fe^{2+}/100g FW, using a $FeSO_4 \cdot 7H_2O$ calibration curve.

Total RNA isolation and cDNA synthesis

Total RNA was isolated using the RNeasy Plant Mini Kit (Qiagen, Valencia, CA, USA) and DNA was removed with DNase I (Rnase-free DNase Set, Qiagen). Total RNA was

296

quantified using a Nanodrop 1000 spectrophotometer (Thermo Fisher Scientific, Vernon Hills, IL, USA), and 2µg total RNA was used as the template for first strand cDNA synthesis with Ominiscript reverse transcriptase (Qiagen) in a 20µl total reaction volume, following the manufacturer's recommendations.

Quantitative real-time RT-PCR

Quantitative real-time RT-PCR was used to analyze expression of genes and TFs (primers shown in Table 1) in a BioRad CFX96 system with 25-µl reaction mixtures containing 10ng cDNA, 1x iQ SYBR Green Supermix (BioRad, Hercules, CA, USA) and 0.2µM forward and reverse primers (Naqvi et al., 2011; Farré et al., 2013). Relative expression levels were calculated on the basis of serial dilutions of cDNA (125–0.2ng) which were used to generate standard curves for each gene. PCR was carried out in triplicate using 96-well optical reaction plates. The reaction conditions comprised an initial heating step at 95°C for 5min followed by 44 cycles of 95°C for 10s, 60°C for 35s and 72°C for 15s. Specificity was confirmed by product melt curve analysis over the temperature range 50–90°C with fluorescence acquired after every 0.5°C increase, and the fluorescence threshold values and gene expression data were calculated using BioRad CFX96™ software. Values represent the mean of 5 replicates ± SD. Amplification efficiencies were compared by plotting ΔCt values of different primer combinations in serial dilutions against the log of starting template concentrations using CFX96 software. Statistical analysis was conducted to compare qRT-PCR with hormone data. To do so, R packages for principal component analysis (PCA) biplot and correlation matrix analysis were used.

Acknowledgments

The authors would like to thank Ignacio Romagosa for his help with statistical interpretation and Richard M. Bostock for the manuscript revision.

Conflict of Interest

The authors declare that they have no conflict of interest.

Literature cited

Abdulkareem, M., Aboud, H.M., Saood, H.M., and Shibly, M.K. 2014. Antagonistic activity of some plant growth rhizobacteria to *Fusarium graminearum*. Int. J. Phytopathol. 03 (01):49-54.

Agrawal, P.K., Kohli, A., Twyman, R.M., and Christou, P. 2005. Transformation of plants with multiple cassettes generates simple transgene integration patterns and high expression levels. Mol. Breed. 16:247–60.

Ambawat, S., Sharma, P., Yadav, N.R., and Yadav, R.C. 2013. MYB transcription factor genes as regulators for plant responses: an overview. Physiol. Mol. Biol. Plants. 19 (3):307-321.

Arratia-Quijada, J., Sánchez, O., Scazzocchio, C., and Aguirre, J. 2012. FlbD, a Myb transcription factor of *Aspergillus nidulans*, is uniquely involved in both asexual and sexual differentiation. Eukaryot. Cell 11 (9):1132.

Asad, M.A.U., Zakari, S.A., Zhao, Q., Zhou, L., Ye, Y., Cheng, F. 2019. Abiotic stresses intervene with ABA signaling to induce destructive metabolic pathways leading to death: premature lead senescence in plants. Int. J. Mol. Sci. 20 (256):1-23.

Ashraf, M.A., Iqbal, M., Rasheed, R., Hussain, I., Riaz, M., and Arif, M.S. 2018. Chapter 8: Environmental stress and secondary metabolites in plants: an overview. In: Ahmad P, Ahanger MA, Singh VP, Tripathi DK, Alam P, Alyemeni MN (eds) *Plant Metabolites and Regulation Under Environmental Stress.* Academic Press (Elsevier), London, UK, pp 153-167.

Asselbergh, B., De Vleesschauwer, D., and Höfte, M. 2008. Global switches and fine-tuning – ABA modulates plant pathogen defense. Mol. Plant-Microbe Interact. 21:709–719.

Bashan, Y., and de-Bashan, L.E. 2010. Chapter two – how the plant growth-promoting bacterium *Azospirillum* promotes plant growth – a critical assessment. Adv. Agro. 108:77–

136.

Bashan, Y., Holguin, G., and Lifshitz, R. 1993. Isolation and characterization of plant growth-promoting rhizobacteria. In: Glick BR (ed) *Methods in Plant Molecular Biology and Biotechnology*. CRC Press, Boca Raton, FL, pp 331–345.

Bashan, Y. 1986. Significance of timing and level of inoculation with rhizosphere bacteria on wheat plants. Soil Biol. Biochem. 18:297-301

Bhattacharyya, P.N., and Jha, D.K. 2012. Plant growth-promoting rhizobacteria (PGPR): emergence in agriculture. World J. Microbiol. Biotechnol. 28 1327–1350.

Botta, L.A., Santacecilia, A., Ercole, C., Cacchio, P., and del Gallo, M. 2013. In vitro and in vivo inoculation of four endophytic bacteria on *Lycopersicon esculentum*. Nat. Biotechnol. 30 (6):666–674.

Burgess, L.W., Summerell, B.A., Bullock, S., Gott, K.P., and Backhouse, D. 1994. *Laboratory manual for Fusarium research*. Lab manual, 3rd ed. University of Sydney and Botanic Garden, Sydney, Australia.

Campos-Bermudez, V.A., Fauguel, C.M., Tronconi, M.A., Casati, P., Presello, D.A., and Andreo, C.S. 2013. Transcriptional and metabolic changes associated to the infection by *Fusarium verticillioides* in maize inbreds with contrasting ear rot resistance. PLoS One 8 (4):e61580.

Cao, F.Y., Yoshioka, K., and Desveaux, D. 2011. The roles of ABA in plant pathogen interactions. J. Plant Res. 124:489–499.

Decourcelle, M., Perez-Fons, L., Baulande, S., Steiger, S., Couvelard, L., Hem, S., Zhu, C., Capell, T., Christou, P., Fraser, P., and Sandmann, G. 2015. Combined transcript, proteome and metabolite analysis of transgenic maize seeds engineered for enhanced carotenoid

synthesis reveals pleiotrophic effects in core metabolism. J. Exp. Bot. 66:3141–3150.

Demeke, T., Clear, R.M., Patrick, S.K., and Gaba, D. 2005. Species-specific PCR-based assays for the detection of *Fusarium* species and a comparison with the whole seed agar plate method and trichothecene analysis. Int. J. Food Microbiol. 103:271–284.

Diaz, I., Vicente-Carbajosa, J., Abraham, Z., Martinez, M., Isabel-La Moneda, I., and Carbonero, P. 2002. The GAMYB protein from barley interacts with the DOF transcription factor BPBF and activates endosperm-specific genes during seed development. Plant J. 29:453-464.

Díaz-Gómez, J., Marín, S., Nogareda, C., Sanchis, V., and Ramos, A.J. 2016. The effect of enhanced carotenoid content of transgenic maize grain on fungal colonization and mycotoxin content. Mycotoxin Res. 32 (4):221-228.

Ding, L., Xu, H., Kong, Z., Zhang, L., Xue, S., Jia, H., and Ma, Z. 2011. Resistance to hemi-biotrophic *F. graminaerum* is associated with coordinated and ordered expression of diverse defense signalling pathways. PloS One 6 (4):e19008.

Dinolfo, M.I., Castañares, E., and Stengelin, S.A. 2017. *Fusarium*–Plant Interaction: State of the Art – a Review. Plant. Protect. Sci. 53:61-70.

Döbereiner, J., Marriel, I.E., and Nery, M. 1976. Ecological distribution of *Spirillum lipoferum* Beijerinck. Can. J. Microbiol. 22 (10):1464-1473.

Dong, X. 2004. NPR1, all things considered. Curr. Opin. Plant Biol. 7:547–52.

Edwards, S.G. 2004. Influence of agricultural practices on *Fusarium* infection of cereals and subsequent contamination of grain by trichothecene mycotoxins. Toxicol. Lett. 153:29-35.

Fanciullino, A.L., Bidel, L.P.R., and Urban, L. 2014. Carotenoid responses to environmental

300

stimuli: integrating redox and carbon controls into a fruit model. Plant Cell Environ. 37:273-289.

Farré, G., Maiam Rivera, S., Alves, R., Vilaprinyo, E., Sorribas, A., Canela, R., Naqvi, S., Sandmann, G., Capell, T., Zhu, C., and Christou, P. 2013. Targeted transcriptomics and metabolic profiling reveals temporal bottlenecks in the maize carotenoid pathway that can be addressed by multigene engineering. Plant J. 75:441–455.

Foyer, C.H., and Noctor, G. 2005. Redox homeostasis and antioxidant signaling: a metabolic interface between stress perception and physiological responses. Plant Cell 17:1866-1875.

Garg, M., Sharma, N., Sharma, S., Kapoor, P., Kumar, A., Chunduri, V., and Arora, P. 2018. Biofortified crops generated by breeding, agronomy and transgenic approaches are improving lives of millions of people around the world. Front. Nutr. 5:12.

Gao, X., Starr, J., Göbel, C., Engelberth, J., Feussner, I., Tumlinson, J., and Kolomiets, M. 2008. Maize 9-Lipoxygenase ZmLOX3 Controls Development, Root-Specific Expression of Defense Genes, and Resistance to Root-Knot Nematodes. Mol. Plant-Microbe Int. 21(1):98-109.

Giné-Bordonaba, J., and Terry, L.A. 2016. Effect of deficit irrigation and methyl jasmonate application on the composition of strawberry (*Fragaria x ananassa*) fruit and leaves. Sci. Hortic. 199 (16): 63-70.

Gubler, F., Kalla, R., Roberts, J.K., and Jacobsen, J.V. 1995. Gibberellin-regulated expression of a myb gene in barley aleurone cells: evidence for Myb transactivation of a high-pI alpha-amylase gene promoter. Plant Cell 7:1879-1891.

Gunnaiah, R., Kushalappa, A.C., Duggavathi, R., Fox, S., and Somers, D.J. 2012. Integrated metabolo-proteomic approach to decipher the mechanisms by which wheat QTL (Fhb1) contributes to resistance against *Fusarium graminearum*. PloS One 7: 7.

Gutierrez-Carbonell, E., Lattanzio, G., Albacete, A., Rio, J.J., Kehr, J., Abadía, A., Grusak, M.A., Abadía, J., and López-Millán, A.F. 2015. Effects of Fe deficiency on the protein profile of *Brassica napus* phloem sap. Proteomics 15 (22):3835-3853.

Gutierrez-Gonzalez, J.J., Wise, M.L., and Garvin, D.F. 2013. A developmental profile of tocol accumulation in oat seeds. J. Cereal Sci. 57:79–83.

Hartmann, A., and Hurek, T. 1988. Effect of carotenoid overproduction on oxygen tolerance of nitrogen fixation in *Azospirillum brasilense* Sp7. J. Gen. Microbiol. 134:449–2455.

Hichri, I., Barrieu, F., Bogs, J., Kappel, C., Delrot, S., and Lauvergeat, V. 2011. Recent advances in the transcriptional regulation of the flavonoid biosynthetic pathway. J. Exp. Bot. 62 (8):2465–2483.

Hong, S-Y., Roze, L.V., and Linz, J.E. 2013. Oxidative stress-related transcription factors in the regulation of secondary metabolism. Toxins 5:683-702.

Idris, H.A., Labuschagne, N., and Korsten, L. 2007. Screening rhizobacteria for biological control of *Fusarium* root and crown rot of sorghum in Ethiopia. Biol. Control 40 (1):97-106.

Jin, X., Bai, C., Bassie, L., Nogareda, C., Romagosa, I., Twyman, R.M., Christou, P., and Zhu, C. 2018. ZmPBF and ZmGAMYB transcription factors independently transactivate the promoter of the maize (*Zea mays*) β-carotene hydroxylase 2 gene. New Phytol. doi: 10.1111/nph.15614.

Kalladan, R., Lasky, J.R., Chang, T.Z., Sharma, S., Juenger, T.E., and Verslues, P.E. 2017. Natural variation identifies genes affecting drought-induced abscisic acid accumulation in *Arabidopsis thaliana.* Proc. Natl. Acad. Sci. USA 114 (43):11536-11541.

Klessig, D.F., Choi, H.W, Dempsey, and D.'M.A. 2018. Systemic acquired resistance and

salicylic acid: past, present and future. Mol. Plant-Microbe Int. 31(9).

Kranner, I., Cram, W.J., Zorn, M., Wornik, S., Yoshimura, I., Stabentheiner, E., and Pfeifhofer, W. 2005. Antioxidants and photoprotection in a lichen as compared with its isolated symbiotic partners. Proc. Natl. Acad. Sci. USA 102:3141–3146.

Kranz, H.D., Denekamp, M., Greco, R., Jin, H.L., Leyva, A., Meissner, R., Petroni, K., Urzainqui, A., Bevan, M., Martin, C., Smeekens, S., Tonelli, C., Paz-Ares, J., and Weisshaar, B. 1998. Towards functional characterisation of the members of the R2R3-MYB gene family from *Arabidopsis thaliana*. Plant J. 16:263–276.

Kyndt, T., Nahar, K., Haeck, A., Verbeek, R., Demeestere, K., and Gheysen, G. 2017. Interplay between carotenoids, abscisic acid and jasmonate guides the compatible rice-Meloidogyne graminicola interaction. Front. Plant Sci. 8 (951):1-11.

Lanubile, A., Maschietto, V., Borrelli, V.M., Stagnati, L., Logrieco, A.F., and Marocco, A. 2017. Molecular basis of resistance to *Fusarium* ear rot in maize. Front. Plant Sci. 8:1774.

Lee, M.W., Qi, M., and Yang, Y. 2001. A novel jasmonic acid-inducible rice MYB gene associates with fungal infection and host cell death. Mol. Plant-Microbe Interact. 14:527–535.

Lippold, F., Sanchez, D.H., Musialak, M., Schlereth, A., Scheible, W.R., Hincha, D.K., and Udvardi, M.K. 2009. AtMyb41 regulates transcriptional and metabolic responses to osmotic stress in *Arabidopsis*. Plant Physiol. 149:1761–1772.

López-Reyes, L., Carcaño-Montiel, M.G., Tapia-López, L., Medina-de la Rosa, G., and Tapia-Hernández, R.A. 2017, Antifungal and growth-promoting activity of *Azospirillum brasilense* in *Zea mays* L. ssp. Mexicana. Arc. Phytopath. Plant Prot. 50 (13-14):727-743.

Matsushima, R. 2014. Thin sections of Technovit 7100 resin of rice endosperm and staining.

Bio-protocol 4 (18):e1239.

McLaughlin, C.S., Vaughan, M.H., Campbell, I.M., Wei, C.M., Stafford, M.E., and Hansen, B.S. 1977. Inhibition of protein synthesis by trichothecenes. In: Rodricks JV, Hesseltine CW, Mehlman MA (eds.) *Mycotoxins in human and animal health* (Proceedings of a conference on mycotoxins in human and animal health). Pathotox Publishers, IL, USA, pp 263–273.

Mengistu, A., Tachibana, H., Epstein, A.H., Bidne, K.G., and Hatfield, J.D. 1987. Use of leaf temperature to measure the effect of brown stem rot and soil moisture stress and its relations to yields of soybeans. Plant Dis. 71:632–634.

Mou, W., Li, D., Bu, J., Jiang, Y., Khan, Z.U., Luo, Z., Mao, L., Ying, T. 2016. Comprehensive analysis of ABA effects on ethylene biosynthesis and signaling during tomato fruit ripening. PLoS ONE 11(4):e0154072.

Naqvi, S., Zhu, C., Farre, G., Sandmann, G., Capell, T., and Christou, P. 2011. Synergistic metabolism in hybrid corn reveals bottlenecks in the carotenoid pathway and leads to the accumulation of extraordinary levels of the nutritionally important carotenoid zeaxanthin. Plant Biotechnol. J. 9:384–393.

Nicholson, P., Simpson, D.R., Weston, G., Rezanoor, H.N., Lees, A.K., Parry, D.W., and Joyce, D. 1998. Detection and quantification of *Fusarium culmorum* and *Fusarium graminearum* in cereals using PCR assays. Physiol. Mol. Plant P. 53:17–37.

Okonechnikov, K., Golosova, O., Fursov, M, and team, U. 2012. Unipro UGENE: a unified bioinformatics toolkit. Bioinformatics 28:1166-1167.

Omer, M., Locke, J.C., and Frantz, J.M. 2007. Using Leaf Temperature as a Nondestructive Procedure to Detect Root Rot Stress in Geranium. Horttechnology 17 (4):532-536.

Oren, L., Ezrati, S., Cohen, D., and Sharon, A. 2003. Early events in the *Fusarium*

304

verticilloides-Maize interaction characterized by using a green florescent protein-expressing transgenic isolate. Appl. Environ. Microbiol. 69 (3):1695-1701.

Panwar, V., Aggarwal, A., Singh, G., Verma, A., Sharma, I., and Saharan, M.S. 2014. Efficacy of foliar spray of Trichoderma isolates against *Fusarium graminearum* causing head blight (head scab) of wheat. J. Wheat Res. 6 (1):1-5.

Pieterse, C.M.J., Zamioudis, C., Berendsen, R.L., Weller, D.M., Van Wees, S.C.M., and Bakker, P.A.H.M. 2014. Induced systemic resistance by beneficial microbes. Annu. Rev. Phytopath. 52:16.1-16.29.

Pieterse, C.M.J., Van der Does, D., Zamioudis, C., Leon-Reyes, A., and Van Wees, S.C.M. 2012. Hormonal modulation of plant immunity. Annu. Rev. Cell Dev. Biol. *28*:489–521.

Pieterse, C.M.J., Leon-Reyes, A., Van der Ent, S., and Van Wees, S. C. M. 2009. Networking by small-molecule hormones in plant immunity. Nat. Chem. Biol. 5:308-316.

Qin, X., and Zeevaart, J.A.D. 2002. Overexpression of a 9-cis-epoxycarotenoid dioxygenase gene in Nicotiana plumbaginifolia increases abscisic acid and phaseic acid levels and enhances drought tolerance. Plant Physiol. 128:544–551.

Raffaele, S., Rivas, S., and Roby, D. 2006. An essential role for salicylic acid in AtMYB30-mediated control of the hypersensitive cell death program in *Arabidopsis*. FEBS Lett. 580:3498–3504.

Richardson, K.C., Jarrett, L., and Finke, E.H. 1960. Embedding in epoxy resins for ultrathin sectioning in electron microscopy. Stain Technol. 35:313.

Rengel, Z., Batten, G.D., and Crowley, D.E. 1999. Agronomic approaches for improving the micronutrient density in edible portions of field crops. Field Crops Res. 60:27–40.

Romanowska, E., Buczynska, A., Wasilewska, W., Krupnik, T., Drozak, A., Rogowski, P., Parys, E., and Zienkiewicz, M. 2017. Differences in photosynthetic responses of NADP-ME type C4 species to high light. Planta 245:641-657.

Ross, A.F. 1961. Systemic acquired resistance induced by localized virus infections in plants. Virology 14:340–58.

Segarra, G., Van der Ent, S., Trillas, I., and Pieterse, C.M.J. 2009. MYB72, a node of convergence in induced systemic resistance triggered by a fungal and a bacterial beneficial microbe. Plant Biol. 11:90–96.

Seo, P.J., and Park, C.M. 2010. MYB96-mediated abscisic acid signals induce pathogen resistance response by promoting salicylic acid biosynthesis in *Arabidopsis*. New Phytol. 186:471–483.

Shewmaker, C.K., Sheehu, J.A., Daley, M., Colburn, S., and Ke, D.Y. 1999. Seed-specific overexpression of phytoene synthase: increase in carotenoids and metabolic effects. Plant J. 20:41–412.

Shigenaga, A. M., and Argueso, C. T. 2016. No hormone to rule them all: Interactions of plant hormones during the responses of plants to pathogens. Sem. Cell Dev. Biol. 56:174-189.

Shime-Hattori, A., Kobayashi, S., Ikeda, S., Asano, R., Shime, H., and Shinano, T. 2011. A rapid and simple PCR method for identifying isolates of the genus *Azospirillum* within populations of rhizosphere bacteria. J. Appl. Microbiol. 111:915-924.

Singleton, V.L., Orthofer, R., and Lamuela-Raventos, R.M. 1999. Analysis of total phenols and other oxidation substrates and antioxidants by means of Folin-Ciocalteu reagent. Methods in Enzymol. 299:152–178.

Smith, S.E., and Read, D.J. 2007. Mycorrhizal Symbiosis, 3rd ed. Elsevier, London, UK.

306

Somers, E., Ptacek, D., Gysegom, P., Srinivasan, M., and Vanderleyden, J. 2005. *Azospirillum brasilense* produces the auxin-like phenylacetic acid by using the key enzyme for indole-3-acetic acid biosynthesis. Appl. Environ. Microbiol. 71:1803–1810.

Urao, T., Yamaguchi-Shinozaki, K., Urao, S., and Shinozaki, K. 1993. An *Arabidopsis* myb homolog is induced by dehydration stress and its gene product binds to the conserved MYB recognition sequence. Plant Cell 5:1529–1539.

Wojciechowski, S., Chelkowski, J., and Kostecki, M. 1995. Influence of deoxynivalenol on electrolyte leakage in cereal seedling leaves. Acta Physiol. Plant. 17:357–360.

Xu, L., Yue, Q., Bian, F., Sun, H., Zhai, H. and Yao, Y. 2017. Melatonin Enhances Phenolics Accumulation Partially via Ethylene Signaling and Resulted in High Antioxidant Capacity in Grape Berries. Front. Plant Sci. 8:1426.

Yang, S.H., Moran, D.L., Jia, H.W., Bicar, E.H., Lee, M., and Scott, M.P. 2002. Expression of a synthetic porcine alpha-lactalbumin gene in the kernels of transgenic maize. Transgenic Res. 11:11–20.

Yang, Y., and Klessig, D.F, 1996. Isolation and characterization of a tobacco mosaic virus-inducible myb oncogene homolog from tobacco. Proc. Natl. Acad. Sci. USA 93:14972–14977.

Zanga, D., Sanahuja, G., Eizaguirre, M., Albajes, R., Christou, P., Capell, T., Fraser, P., Gerrisch, C., and López, C. 2018. Carotenoids moderate the effectiveness of a Bt gene against the European corn borer, *Ostrinia nubilalis.* PLoS One 13(7):e0199317.

Zanga, D., Capell, T., Slafer, G.A., Christou, P., and Savin, R. 2016. A carotenogenic mini-pathway introduced into white corn does not affect development or agronomic performance. Sci. Rep. 6:38288.

Zehra, A., Meena, M., Dubey, M.K., Aamir, M., and Upadhyay, R.S. 2017. Synergistic effects

of plant defense elicitors and *Trichoderma harzianum* on enhanced induction of antioxidant defense system in tomato against *Fusarium* wilt disease. Bot. Stud. 58:44.

Zhao, J., Zhang, X., Hong, Y., and Liu, Y. 2016. Chloroplast in Plant-Virus Interaction. Front. Microbiol. 7:1565.

Zhou, S., Zhang, Y.K., Kremling, K.A., Ding, Y., Bennett, J.S., Bae, J.S., Kim, D.K., Ackerman, H.H., Kolomiets, M.V., Schmelz, E.A., Schroeder, F.C., Buckler, E.S., and Jander, G. 2019. Ethylene signaling regulates natural variation in the abundance of antifungal acetylated diferuloylsucroses and *Fusarium graminearum* resistance in maize seedling roots. New Phytol. 221 (4):2096-2111.

Zhu, C., Naqvi S., Breitenback, J., Sandmann, G., Christou, P., and Capell, T. 2008. Combinatorial genetic transformation generates a library of metab c phenotypes for the carotenoid pathway in maize. Proc. Natl. Acad. Sci. USA 105 (47):18232-18237.

Table 1. DNA sequence of the primers used for PCR and RT qPCR

Gene	Forward primer	Reverse primer
Sp7 detection* (Az16S-D)	5'-CCGCGGTAATACGAAGGGGGC-3'	5'-GCCTTCCTCCGGCTTGTCACCGGC-3'
Fusarium detection‡	5'-CTCCGGATATGTTGCGTCAA-3'	5'-GGTAGGTATCCGACATGGCAA-3'
ZmICS[1]	5'-GGCGAGATCCAATCACAGAT-3'	5'-CAGCATAATCATGCAAATAC-3'
ZmNCED4	5'-TCAAGCTCCAGGAGATGGTG-3'	5'-TCCAGAGGTGGAAGCAGAAG-3'
ZmCHI1[1]	5'-CGCGAGGAGAAAGAAAGCAA-3'	5'-CAACTACGCGACCAGAAAGG-3'
ZmZEP	5'-GAATGCCTGGCAAGAGAGTG-3'	5'-CCCTAGACCAACACCCAAGT-3'
ZmSOD4[2]	5'-TGGAGCACCAGAAGATGA-3'	5'-CTCGTGTCCACCCTTTCC-3'
ZmAPX[2]	5'-TGAGCGACCAGGACATTG-3'	5'-GAGGGCTTTGTCACTTGGT-3'
ZmLOX3[3]	5'-CGCCATCATCGTCAAGAACA-3'	5'-ACTGCGGGTAGATCCATGAG-3'
ZmGAMYB[5]	5'-TGGGAACAGCCTTTATCTGCC-3'	5'-ATCCCCGCTTGGTCAACCT-3'
ZmNPR1[4]	5'-CCCGGTAGGAAGAAGAAGGG-3'	5'-AAGTCGGCGTAAATCACACG-3'
ZmPAL[1]	5'-GCTATCCGCTGTACCGTTTC-3'	5'-CAGCGGTTCACCATTCCATT-3'
ZmACO[1]	5'-CGACCTGCTCTTCAATCTGC-3'	5'-AGATGTGTTCGCACCTGGTA-3'
ZmCPK11[2]	5'-ACCTCTCCGAGCACCCCAAC-3'	5'-CCTCCACGACCCCGACAATG-3'
ZmEIN3	5'-GCAGCGAACAATCTGGACTT-3'	5'-ACGTGTCACTACTGCTCAT-3'
ZmERF1	5'-GATGAACGTGCTTTGACCGT-3'	5'-ACTTGCGAGTTACAGGGACA-3'
ZmWRKY	5'-AGCTCCACCTCCATCAACTC-3'	5'-ACTTGGGATCCTTGGTGAGC-3'
ZmAP2/EREPB	5'-ACGCACCCGTACTACTTCTT-3'	5'-TCCACTACCGACGAACAGTC-3'
ZmZIM27	5'-CGAGCAGCAAAGGTGTGTTA-3'	5'-TCCGCGATCAGAAGTTCACA-3'
ZmActin[Ψ]	5'-CGATTGAGCATGGCATTGT-3'	5'-CCCACTAGCGTACAACGAA-3'

Primers as reported in: *Shime-Hattori et al. (2011); ‡ Nicholson et al (1998); 1. Ding et al (2011); 2. Ding et al (2013); 3. Zehra et al (2017); 4. Rubio et al., 2017; 5. Jin et al (2018); Ψ Berman et al. (2017)

Figure Legends

Figure 1. Representative plant phenotypes: (A) control, (B) *Fusarium*, (C) *Azospirillum brasilense* (Sp7) and (D) co-inoculated (Sp7+*Fusarium)* plants of wild type (WT) and high carotenoid (HC) maize.

Figure 2. (A) Leaf length and (B) root moisture content for each treatment: control (C), *Fusarium* (Fus), *Azospirillum brasilense* (Sp7) and co-inoculation (Sp7+*Fusarium*). Asterisks indicate statistically significant differences between treatments: * ($p<0.05$), ** ($p<0.01$), *** ($p<0.001$). Values represent the average ± standard error for n=9.

Figure 3. (A) Leaf temperature and (B) Leaf chlorophyll content (SPAD) for control (C), *Fusarium* (Fus), *Azospirillum brasilense* (Sp7) and co-inoculated (Sp7+*Fusarium*) plants of wild type (WT) and high carotenoid (HC) maize. Asterisks indicate statistically significant differences between treatments: *($p<0.05$), ** ($p<0.01$), *** ($p<0.001$). Least significant means between genotypes for each treatment are indicated with the p-value in each graph. Values represent the average ± standard error for n=9.

Figure 4. (A) Total phenolic content (TPC) and (B) Ferric reducing antioxidant power (FRAP; Fe2+/g FW) for each treatment: control (C), *Fusarium* (Fus)*, Azospirillum brasilense* (Sp7) and co-inoculation (Sp7+*Fusarium).* Asterisks indicate statistically significant differences between treatments: * ($p<0.05$), ** ($p<0.01$), *** ($p<0.001$). Least significant means between genotypes for each treatment are indicated with the p-value in each graph. Values represent the average ± standard error for n=9.

Figure 5. Hormone accumulation of 1-Aminocyclopropane-1-carboxylic acid deaminase (ACC), trans-Zeatin (tZ), indole-3-acetic acid (IAA), abscisic acid (ABA), jasmonic (JA) and salicylic acid (SA) in leaves for each treatment: control (C), *Fusarium* (Fus), *Azospirillum brasilense* (Sp7) and co-inoculation (Sp7+*Fusarium*). Least significant means between genotypes for each treatment are indicated with the p-value in each graph. Values represent the average ± standard error for n=9.

310

Figure 6. Quantitative real-time RT-PCR analysis of endogenous hormone pathway genes and in HC and WT plants grown with various treatments: control (C), *Fusarium* (Fus), *Azospirillum brasilense* (Sp7) and co-inoculation (Sp7+*Fusarium*). Data show relative mRNA levels in leaves, normalized against maize actin mRNA and presented as the mean of 5 biological replicates. ZmICS, isochorismate; ZmSOD4, superoxide dismutase 4; ZmCHI1, chalcone isomerase; ZmAPX, ascorbate peroxidase; ZmLOX3, lipoxygenase; ZmZEP, zeaxanthin epoxidase; ZmMYB, myeloblastosis; ZmNCED4, 9-cis-epoxycarotenoid dioxygenase; ZmEIN3, ethylene insensitive 3; ZmACO, 1-aminocyclopropane-1-carboxylate oxygenase.

Figure 7. Principal component analysis (PCA) biplot characterizing leaf hormone accumulation, gene transcription and total phenolic content (TPC) trends in samples from the different treatments. Hormones are salicylic acid (SA), jasmonic acid (JA), 1-Aminocyclopropane-1-carboxylic acid deaminase (ACC), trans-Zeatin (tZ), indole-3-acetic acid (IAA) and abscisic acid (ABA). Genes are ZmICS, isochorismate; ZmSOD4, superoxide dismutase 4; ZmCHI1, chalcone isomerase; ZmAPX, ascorbate peroxidase; ZmLOX3, lipoxygenase; ZmZEP, zeaxanthin epoxidase; ZmMYB, myeloblastosis; ZmNCED4, 9-cis-epoxycarotenoid dioxygenase; ZmEIN3, ethylene insensitive 3; ZmACO, 1-aminocyclopropane-1-carboxylate oxygenase. Each dot represents the average of 3 (hormones) or 5 (gene transcription) independent measurements.

Figure 8. Correlation matrix relating gene expression and hormone data in plant leaves. Hormones are salicylic acid (SA), jasmonic acid (JA), 1-Aminocyclopropane-1-carboxylic acid deaminase (ACC), trans-Zeatin (tZ), indole-3-acetic acid (IAA) and abscisic acid (ABA). Genes are ZmICS, isochorismate; ZmSOD4, superoxide dismutase 4; ZmCHI1, chalcone isomerase; ZmAPX, ascorbate peroxidase; ZmLOX3, lipoxygenase; ZmZEP, zeaxanthin epoxidase; ZmMYB, myeloblastosis ZmNCED4, 9-cis-epoxycarotenoid dioxygenase; ZmEIN3, ethylene insensitive 3; ZmACO, 1-aminocyclopropane-1-carboxylate oxygenase.

Figure 9. Gene and hormone regulatory network controlling carotenoid biosynthesis and the

stress-related responses. The schema represents the regulatory network of carotenoid, flavonoid and redox-related genes in wild type (WT) and high carotenoid (HC) maize seedlings grown with various treatments: control (C), *Fusarium* (Fus), *Azospirillum brasilense* (Sp7) and co-inoculation (Sp7+*Fusarium*). The model is based on data obtained by qPCR for genes and by HPLC for hormone accumulation. Gene expression levels were normalized to the expression levels of ZmActin, and all values were log2 transformed to normalize the data. Blue indicates higher expression/accumulation while red indicates lower expression/accumulation relative to zero. Hormones are salicylic acid (SA), jasmonic acid (JA), 1-Aminocyclopropane-1-carboxylic acid deaminase (ACC), trans-Zeatin (tZ), indole-3-acetic acid (IAA) and abscisic acid (ABA). Genes are ZmICS, isochorismate; ZmSOD4, superoxide dismutase 4; ZmCHI1, chalcone isomerase; ZmAPX, ascorbate peroxidase; ZmLOX3, lipoxygenase; ZmZEP, zeaxanthin epoxidase; ZmMYB, myeloblastosis; ZmNCED4, 9-cis-epoxycarotenoid dioxygenase; ZmEIN3, ethylene insensitive 3; ZmACO, 1-aminocyclopropane-1-carboxylate oxygenase.

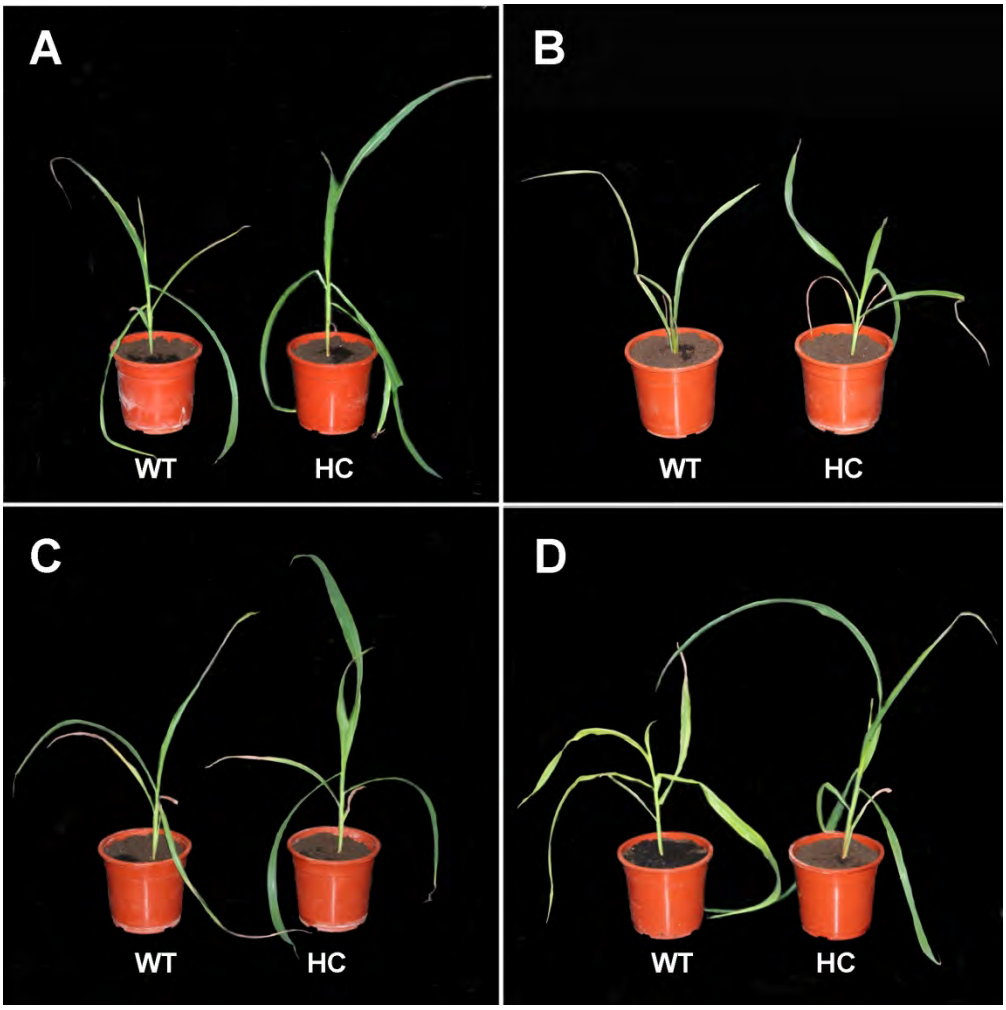

Figure 1. Representative plant phenotypes: (A) control, (B) Fusarium, (C) Azospirillum brasilense (Sp7) and (D) co-inoculated (Sp7+Fusarium) plants of wild type (WT) and high carotenoid (HC) maize.

180x180mm (300 x 300 DPI)

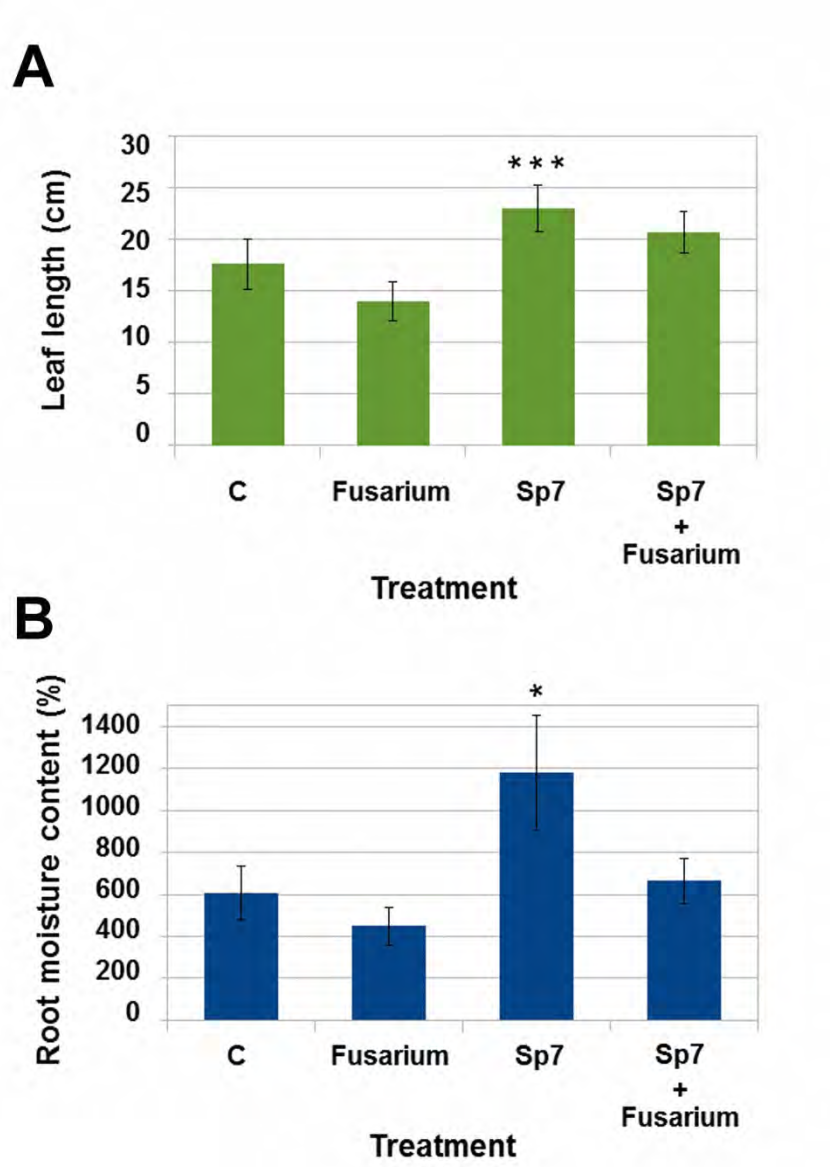

Figure 2. (A) Leaf length and (B) root moisture content for each treatment: control (C), Fusarium (Fus), Azospirillum brasilense (Sp7) and co-inoculation (Sp7+Fusarium). Asterisks indicate statistically significant differences between treatments: * ($p<0.05$), ** ($p<0.01$), *** ($p<0.001$). Values represent the average ± standard error for n=9.

326x468mm (300 x 300 DPI)

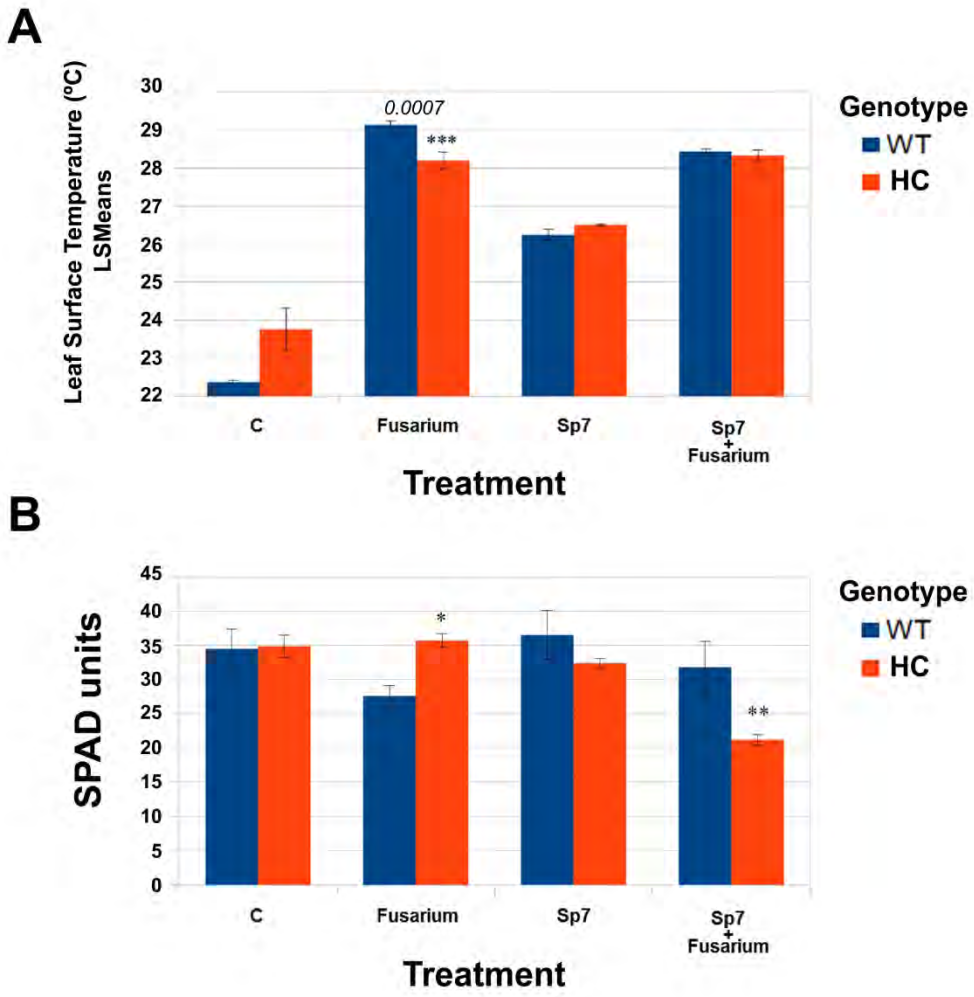

Figure 3. (A) Leaf temperature and (B) Leaf chlorophyll content (SPAD) for control (C), Fusarium (Fus), Azospirillum brasilense (Sp7) and co-inoculated (Sp7+Fusarium) plants of wild type (WT) and high carotenoid (HC) maize. Asterisks indicate statistically significant differences between treatments: *($p<0.05$), ** ($p<0.01$), *** ($p<0.001$). Least significant means between genotypes for each treatment are indicated with the p-value in each graph. Values represent the average ± standard error for n=9.

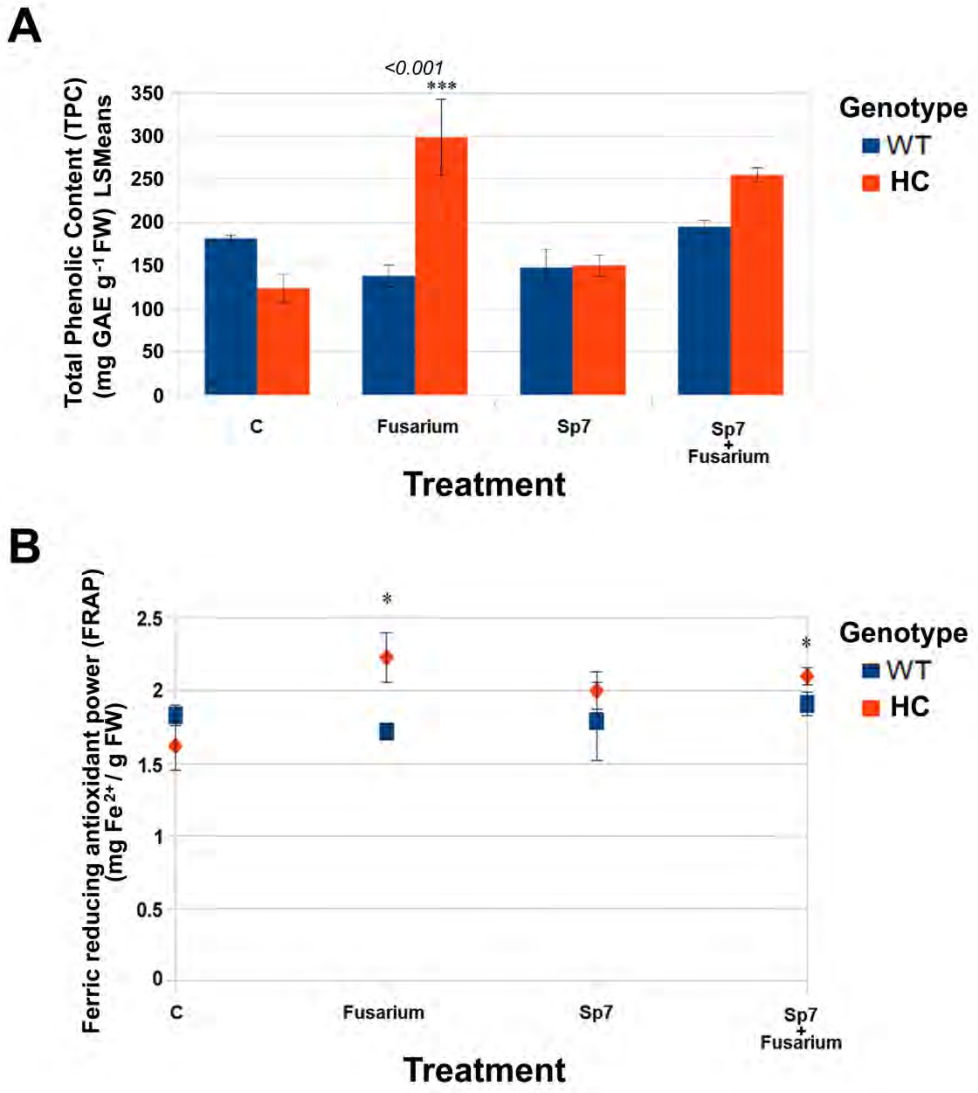

Figure 4. (A) Total phenolic content (TPC) and (B) Ferric reducing antioxidant power (FRAP; Fe2+/g FW) for each treatment: control (C), Fusarium (Fus), Azospirillum brasilense (Sp7) and co-inoculation (Sp7+Fusarium). Asterisks indicate statistically significant differences between treatments: * ($p<0.05$), ** ($p<0.01$), *** ($p<0.001$). Least significant means between genotypes for each treatment are indicated with the p-value in each graph. Values represent the average ± standard error for n=9.

316

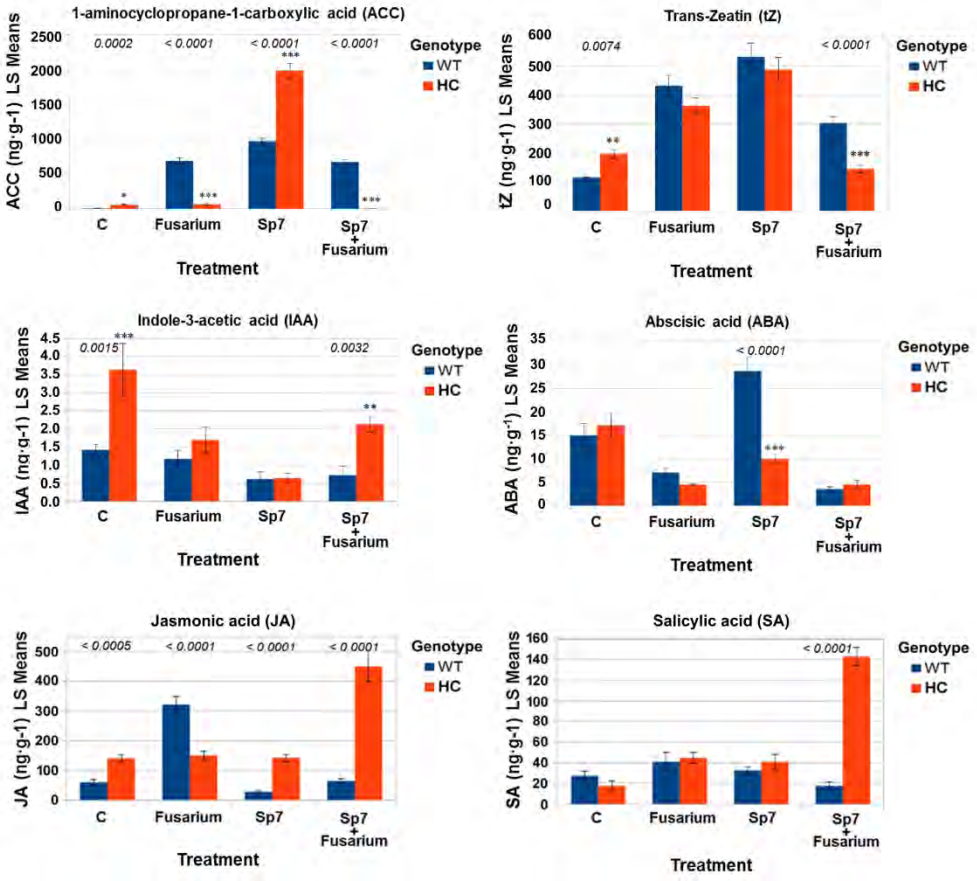

Figure 5. Hormone accumulation of 1-Aminocyclopropane-1-carboxylic acid deaminase (ACC), trans-Zeatin (tZ), indole-3-acetic acid (IAA), abscisic acid (ABA), jasmonic (JA) and salicylic acid (SA) in leaves for each treatment: control (C), Fusarium (Fus), Azospirillum brasilense (Sp7) and co-inoculation (Sp7+Fusarium). Least significant means between genotypes for each treatment are indicated with the p-value in each graph. Values represent the average ± standard error for n=9.

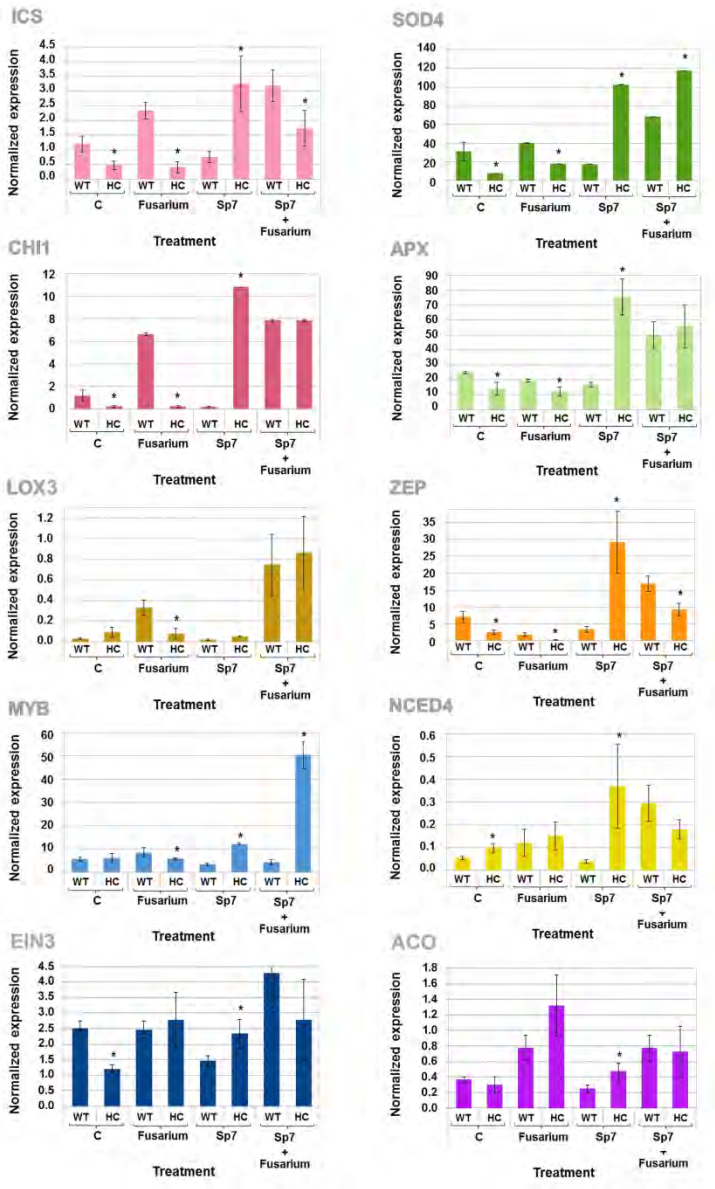

Figure 6. Quantitative real-time RT-PCR analysis of endogenous hormone pathway genes and in HC and WT plants grown with various treatments: control (C), Fusarium (Fus), Azospirillum brasilense (Sp7) and co-inoculation (Sp7+Fusarium). Data show relative mRNA levels in leaves, normalized against maize actin mRNA and presented as the mean of 5 biological replicates. ZmICS, isochorismate; ZmSOD4, superoxide dismutase 4; ZmCHI1, chalcone isomerase; ZmAPX, ascorbate peroxidase; ZmLOX3, lipoxygenase; ZmZEP, zeaxanthin epoxidase; ZmMYB, myeloblastosis; ZmNCED4, 9-cis-epoxycarotenoid dioxygenase; ZmEIN3, ethylene insensitive 3; ZmACO, 1-aminocyclopropane-1-carboxylate oxygenase.

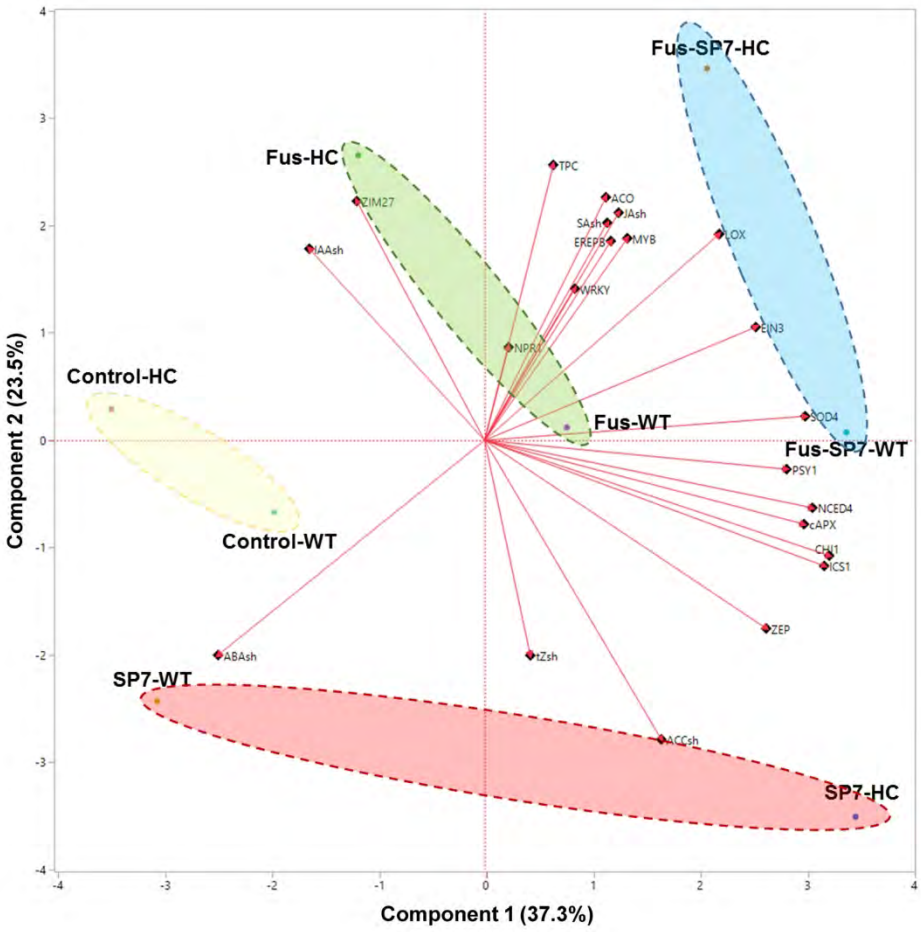

Figure 7. Principal component analysis (PCA) biplot characterizing leaf hormone accumulation, gene transcription and total phenolic content (TPC) trends in samples from the different treatments. Hormones are salicylic acid (SA), jasmonic acid (JA), 1-Aminocyclopropane-1-carboxylic acid deaminase (ACC), trans-Zeatin (tZ), indole-3-acetic acid (IAA) and abscisic acid (ABA). Genes are ZmICS, isochorismate; ZmSOD4, superoxide dismutase 4; ZmCHI1, chalcone isomerase; ZmAPX, ascorbate peroxidase; ZmLOX3, lipoxygenase; ZmZEP, zeaxanthin epoxidase; ZmMYB, myeloblastosis; ZmNCED4, 9-cis-epoxycarotenoid dioxygenase; ZmEIN3, ethylene insensitive 3; ZmACO, 1-aminocyclopropane-1-carboxylate oxygenase. Each dot represents the average of 3 (hormones) or 5 (gene transcription) independent measurements.

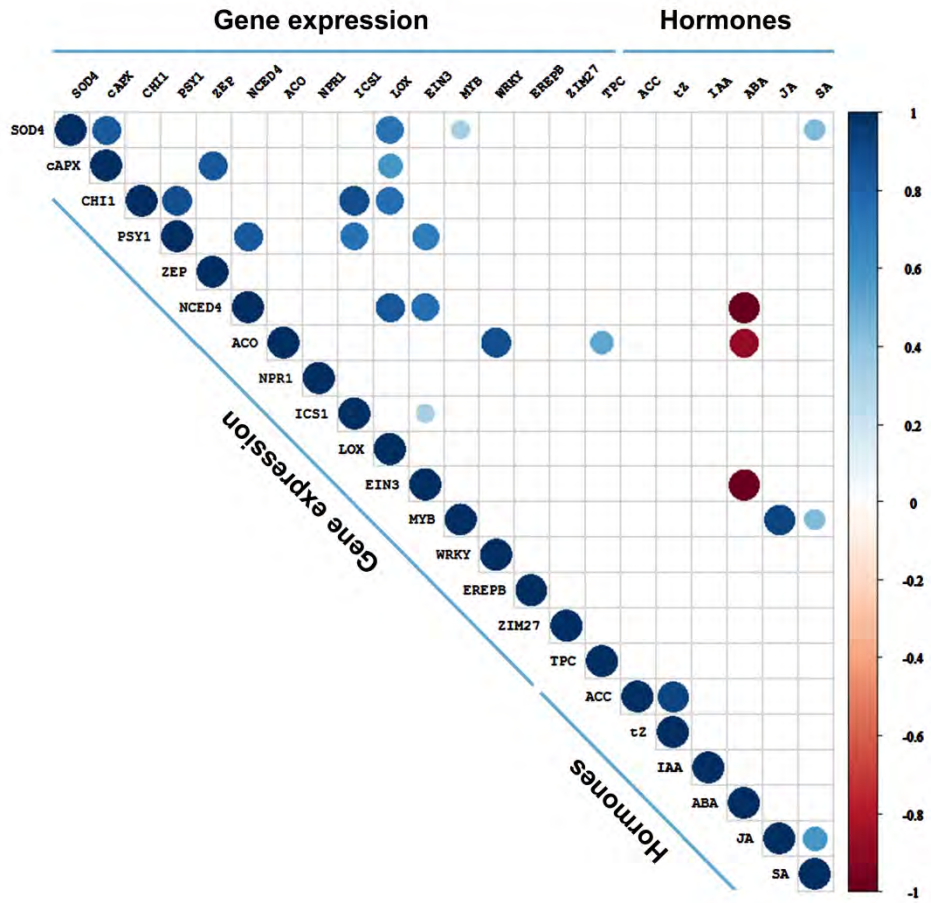

Figure 8. Correlation matrix relating gene expression and hormone data in plant leaves. Hormones are salicylic acid (SA), jasmonic acid (JA), 1-Aminocyclopropane-1-carboxylic acid deaminase (ACC), trans-Zeatin (tZ), indole-3-acetic acid (IAA) and abscisic acid (ABA). Genes are ZmICS, isochorismate; ZmSOD4, superoxide dismutase 4; ZmCHI1, chalcone isomerase; ZmAPX, ascorbate peroxidase; ZmLOX3, lipoxygenase; ZmZEP, zeaxanthin epoxidase; ZmMYB, myeloblastosis ZmNCED4, 9-cis-epoxycarotenoid dioxygenase; ZmEIN3, ethylene insensitive 3; ZmACO, 1-aminocyclopropane-1-carboxylate oxygenase.

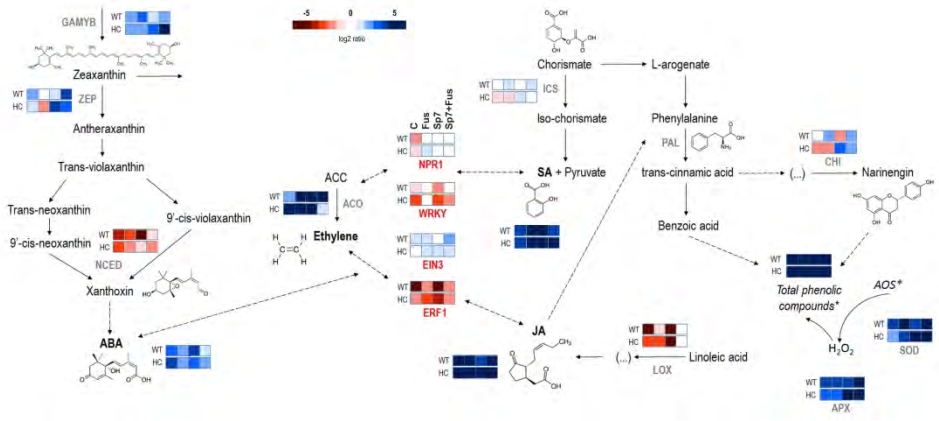

Figure 9. Gene and hormone regulatory network controlling carotenoid biosynthesis and the stress-related responses. The schema represents the regulatory network of carotenoid, flavonoid and redox-related genes in wild type (WT) and high carotenoid (HC) maize seedlings grown with various treatments: control (C), Fusarium (Fus), Azospirillum brasilense (Sp7) and co-inoculation (Sp7+Fusarium). The model is based on data obtained by qPCR for genes and by HPLC for hormone accumulation. Gene expression levels were normalized to the expression levels of ZmActin, and all values were log2 transformed to normalize the data. Blue indicates higher expression/accumulation while red indicates lower expression/accumulation relative to zero. Hormones are salicylic acid (SA), jasmonic acid (JA), 1-Aminocyclopropane-1-carboxylic acid deaminase (ACC), trans-Zeatin (tZ), indole-3-acetic acid (IAA) and abscisic acid (ABA). Genes are ZmICS, isochorismate; ZmSOD4, superoxide dismutase 4; ZmCHI1, chalcone isomerase; ZmAPX, ascorbate peroxidase; ZmLOX3, lipoxygenase; ZmZEP, zeaxanthin epoxidase; ZmMYB, myeloblastosis; ZmNCED4, 9-cis-epoxycarotenoid dioxygenase; ZmEIN3, ethylene insensitive 3; ZmACO, 1-aminocyclopropane-1-carboxylate oxygenase.

ANNEX 6

Lade SB, Medina V (2016) CRISPR-Cas9 como herramienta en el control de enfermedades de las plantas. *Boletín Informativo de la Sociedad Espanola de Fitopatologia* 93: 48-58.

CRISPR/Cas9 COMO HERRAMIENTA EN EL CONTROL DE ENFERMEDADES DE LAS PLANTAS

Sarah b. LADE, vicente MEDINA

Grupo "Interaccio Planta-Microorganisme-vector" (IMPLAMIC) y centro AGROTECNIO Universidad de Lleida. Avda. Alcalde Rovira Roure 191, 25198 Lleida

Parece que, gracias a una tecnología revolucionaria, ha llegado el momento para los fitopatólogos de descubrir con más facilidad el misterio que envuelve la genómica de la co-evolución planta/patógeno, así como los factores del huésped que controlan la resistencia de las plantas o vulnerabilidad a la infección. Desde que fuera identificado y reproducido el sistema inmunitario adaptativo de los procariotas, basado en repeticiones palindrómicas cortas agrupadas y regularmente interespaciadas ("clustered regularly interspaced short palindromic repeats"), también llamado sistema CRISPR, y, concretamente, el Tipo II asociado a una nucleasa ("CRISPR-associated nuclease 9"), o CRISPR/Cas9, son muchos los grupos de investigación que han empezado a utilizarlo y perfeccionarlo como una técnica de mutación génica. Este sistema se compone básicamente de una enzima de restricción, diseñada a partir de las CRISPR, que induce una mutación dirigida en el ADN gracias a un ARN sintético quimera que actúa como guía (sgRNA[1]) y a la secuencia específica de una nucleasa, Cas9, que le acompaña. La Cas9 es guiada de una forma muy precisa por el sgRNA hacia la secuencia diana del ADN adyacente a un protoespaciador (PAM, "protospacer adjacent motif NGG")[2]. Una vez localizado el locus, la Cas9 actúa sobre el ADN causando roturas en sus dos cadenas ("double strand breaks" o DSBs), que son reparadas por una de las dos rutas intracelulares existentes: unión no homóloga ("non homologous joining" o NHEJ), produciendo pequeñas inserciones/delecciones ("indels") y desplazamientos ("frameshifts"), o reparación homóloga directa ("homology-directed repair" o HDR) provocando mutaciones puntuales específicas o inserción de secuencias (Van der Oost et al., 2014; Jian, 2015) (**Figura 1**).

La tecnología CRISPR/Cas9, en el caso de su aplicación a plantas[3], se ha aplicado tanto en plantas modelo (*Arabidopsis thaliana, Nicotiana benthamiana*) como en plantas cultivadas (trigo, sorgo, arroz, soja) y con diferentes planteamientos (Belhaj et al., 2013, 2015; Jiang et al., 2013; Shan et al., 2013) (ver explicación esquemática del proceso en **Figura 2**). La mayoría de los proyectos que utilizan esta herramienta de edición del genoma van dirigidos a obtener y conocer los efectos de mutaciones inducidas. Así, mediante el sistema CRISPR/Cas9 se han planificado mutaciones que modifican uno o varios genes ("knock out"), pero también se producen otras fuera del objetivo ("off-target" o "target out")[4]; se buscan métodos para evitar ésta últimas (Schiml et al., 2014); o se silencian rutas y/o activan genes (Bortesi & Fischer, 2015), explorando así aspectos nuevos de la genómica funcional de las plantas con lo que su desarrollo está creciendo exponencialmente. En todos los trabajos, se destaca la importancia de CRISPR/Cas9 dentro del campo de la ingeniería genética, o en su marco actual más amplio, la llamada biología sintética, llegando a considerarla incluso como una tecnología revolucionaria (Doudna & Charpentier, 2014).

[1] sgRNA supone la fusion sintética de dos ARNs no codificantes: Crispr RNA (crRNA) y un ARN trans-activador (tracrRNA) (Jinek et al., 2012). El sgRNA está formado por 20-22 nucleótidos diseñados y sintetizados como oligonucleótidos. Lei et al., (2014) han desarrollado diseños de sgRNAs para más de 20 especies de plantas. También se han desarrollado muchos vectores y "kits" para la edición, mediante CRISPR-Cas9, de genomas de (Xing et al., 2014; Kumar and Jain, 2015).

[2] El motivo adyacente pro-espaciador (PAM; NGG/NAG) se sitúa en el extremo 3' inmediatamente después del punto diana.

[3] Ver revisión de Hsu, Lander & Zhang (2014) sobre otras aplicaciones del sistema CRISPR-Cas9.

[4] Ver revisión de Endo (2015) sobre el significado e importancia de tales mutaciones.

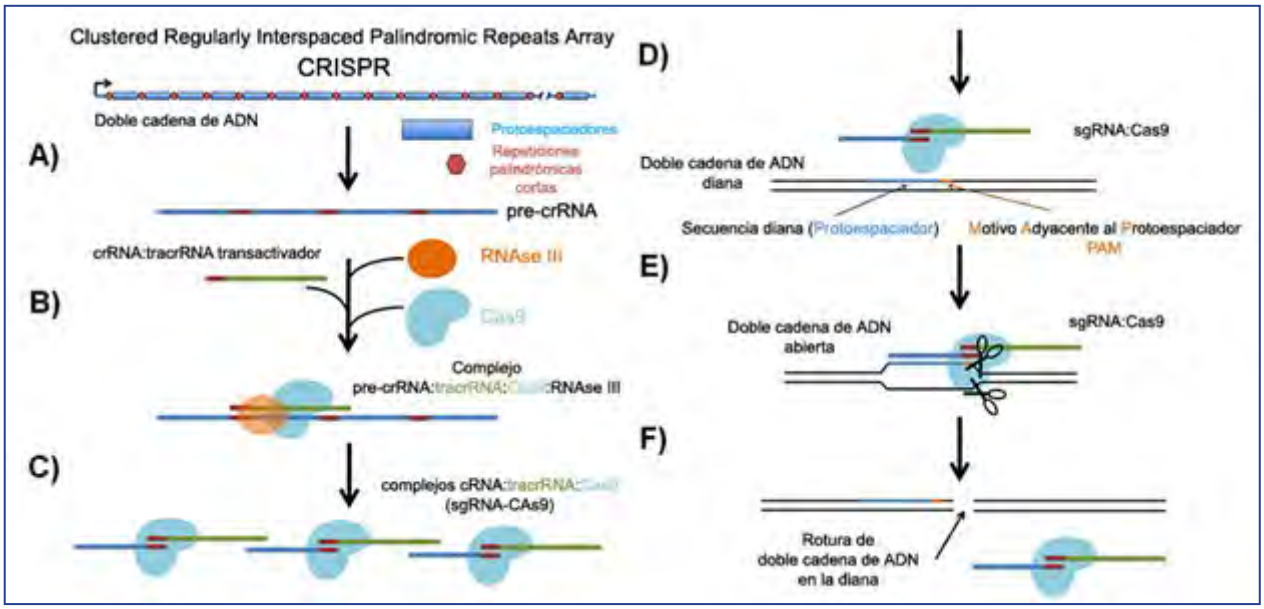

Figura 1. Esquema del sistema CRISPR/Cas9 endógeno. **(A)** La matriz CRISPR se transcribe para hacer el CRISPR RNA inicial (pre-crRNA). **(b)** El pre-crRNA es procesado produciéndose crRNAs individuales mediante un crRNA transactivador (tracrRNA) o crRNA homólogo a las repeticiones palindrómicas. El tracrRNA ayuda a atraer a las enzimas ARNasa III y Cas9, que en conjunto separan los crRNAs individuales. **(C)** La nucleasa crRNA y Cas9 forman complejos crRNA (ARN localizador de CRISPR) o sgRNA (ARN guía). **(D)** Cada complejo sgRNA-Cas9 busca la secuencia de ADN complementario al sgRNA. En el sistema de CRISPR tipo II una secuencia diana potencial sólo es válida si contiene un motivo especial adyacente al protoespaciador (PAM) directamente después del punto de unión del sgRNA. **(E)** Una vez unido el complejo, Cas9 se separa la diana de ADN de doble cadena y se une a ambas cadenas después de PAM. **(F)** El sgRNA: desenlaza los complejos Cas9 después de la ruptura de doble cadena (traducido y adaptado de Addgene, https://www.addgene.org/crispr/plant).

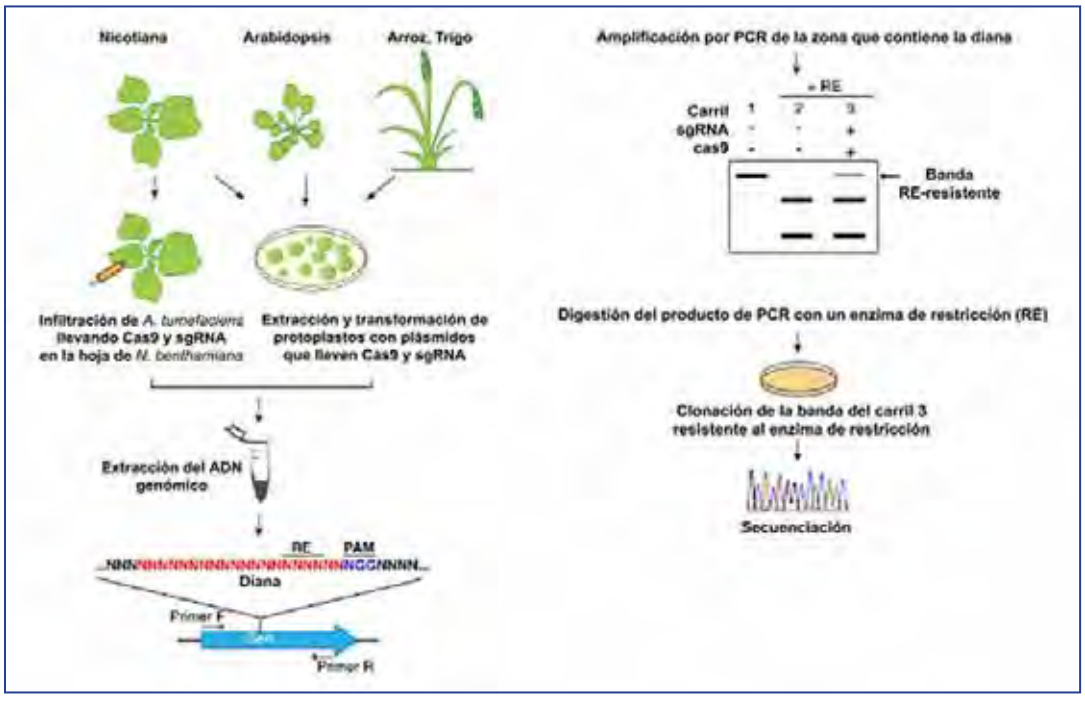

Figura 2. Diagrama explicativo del proceso de edición del genoma mediante CRISPR/Cas9 en plantas experimentales (*Nicotiana benthamiana, Arabidopsis thaliana*) y en plantas de cultivo (arroz, trigo). La nucleasa Cas9 y el sgRNA coinciden con el gen de interés y son co-expresados, usando como vector *Agrobacterium tumefaciens*, en hojas de *N. benthamiana* o en protoplastos transfectados de *Arabidopsis*, trigo o arroz. A continuación, el ADN genómico se extrae de los tejidos de las hojas o de los protoplastos y se amplifica por PCR con los cebadores que flanquean el sitio de destino o diana. La presencia de mutaciones inducidas por sgRNA Cas9 se pueden detectar fácilmente mediante un enzima de restricción (RE) apropiado. La banda RE-resistente (carril 3) se puede clonar. La naturaleza exacta de las mutaciones a continuación, se revela mediante la secuenciación de clones individuales (traducido y adaptado de Belhaj et al., 2013).

Este artículo no pretende ser una revisión completa sobre el uso del sistema CRISPR/Cas9, pues sólo comenta algunos trabajos recientes y relacionados con Patología Vegetal, concretamente aquellos implicados en el control de fitopatógenos o estrés biótico. No se resumen, pues, publicaciones más centradas en el estudio del genoma de los microorganismos que pueden incluir fitopatógenos como, por ejemplo, el realizado por Louwen et al. (2014) sobre el papel que tiene el sistema CRISPR-Cas en la virulencia de las bacterias patógenas, y que recoge entre otras informaciones, su aplicación en la caracterización de tres grupos de cepas de Erwinia amylovora según su distribución geográfica (Rezzonico et al., 2011). Ni tampoco los relacionados con el estrés abiótico, aunque éstos se superpongan algo en esta revisión, porque, hasta la fecha, no se han llevado a cabo estudios precisos que relacionen CRISPR/Cas9 y el control de la respuesta abiótica. No obstante, como la modulación de la tolerancia al estrés abiótico está gobernada por múltiples genes implicados en la señalización y regulación de rutas metabólicas, y el sistema CRISPR/Cas9 puede actuar sobre genes múltiples y funcionalmente redundantes, seguramente pronto se publicarán trabajos que los relacionen (Jain, 2015). También se dejan a un lado las importantes implicaciones que tiene el sistema CRISPR/Cas9 en terapia génica humana y/o animal[5], así como la terapia general en plantas, entendiendo que este artículo divulgativo es sólo una contribución más para destacar la relevancia del sistema CRISPR/Cas9 también en Patología Vegetal.

Así, pues, y como ejemplos, nos centramos sólo en cuatro trabajos o líneas e investigación. El primer trabajo a comentar es el de Fang y Tilere (2016), que añade información sobre la genómica funcional de *Phytophthora sojae* y el posible uso de tal información en el control de la enfermedad que induce. El segundo es el logro conseguido por Wang et al. (2014), al obtener una cepa de trigo resistente a oídio usando el sistema CRISPR/Cas9. Un tercer bloque de estudios supone el control de enfermedades inducidas por infecciones simples y múltiples de geminivirus, concretamente del complejo viral relacionado con el virus del rizado amarillo del tomate o virus de la cuchara, *Tomato yellow leaf curl virus* (TYLCV) y de la cepa severa del virus de las puntas rizadas de la remolacha, *Beet severe curly top virus* (BSCTV) (Ali et al., 2015; Ji et al., 2015; Zaidi et al., 2016). Por último, se resume, el reciente trabajo de Chandrasekaran et al. (2016) en el que se consigue utilizando esta tecnología, conferir una amplia resistencia a diferentes géneros de virus fitopatógenos de la familia *Potyviridae* en pepino “no transgénico”. A partir de ellos se comentarán ciertos avances en el uso del sistema CRISPR, y el prometedor futuro que plantea su uso en Patología Vegetal[6].

Genómica funcional de *Phytophthora sojae*

En este estudio, se usó el sistema CRISPR/Cas9 para editar de forma sencilla y eficiente el genoma del estramenopila *Phytophthora sojae*. Para ello, Fang y Tilere (2016) utilizaron como diana, el gen efector Avr4/6 para la secuencia consenso RXLR (Arg-X-Leu-Arg), observando que en ausencia del patrón homólogo, la reparación de las roturas de dobles cadenas (DSBs) inducidas por Cas9 en *P. sojae* están mediadas por extremos no homólogos (NHEJ), dando como resultado, principalmente, a pequeñas inserciones/delecciones. La mayoría de los mutantes que obtuvieron fueron homocigotos, presumiblemente debido a la modificación de genes provocada por la escisión mediada por Cas9 de alelos no mutantes. Cuando estaba presente el ADN de los donantes, observaron reparación dirigida homóloga (HDR), que dio como resultado la sustitución del gen diana por el ADN de los donantes.

Al probar la virulencia específica de varios mutantes obtenidos mediante NHEJ

[5] Con importantes resultados, por ejemplo, en el control del virus del SIDA (Liao et al., 2015) y en la cura del cáncer (Kim et al., 2015).

[6] Para revisión del concepto y metodología relacionada con los diferentes sistemas CRISPR, incluso productos relacionados, disponibles ya en el mercado visitar, por ejemplo, http://www.scbt.com/crispr-cas9_system.html, o, http://onlinedigeditions.com/publication/frame.php?i=223322&p=&pn=&ver=flex.

y HDR, los autores no sólo confirmaron la contribución de AVR4/6 en el reconocimiento de los loci del gen R, Rps4 y Rps6 de soja, sino que también descubrieron la relación de estos dos loci con la resistencia. Así, concluyeron que el sistema CRISPR/Cas9 es una poderosa herramienta para el estudio de la genómica funcional en *P. sojae*, lo que puede proporcionar nuevas vías para un mejor control de este patógeno.

Resistencia a oidio en trigo harinero

Mediante las tecnologías TALEN (transcription activator-like effector nuclease) y CRISPR/Cas9, Wang et al. (2014) realizaron mutaciones en un genoma poliploide, como es el del trigo harinero (*Triticum aestivum*), concretamente mutaciones en tres homoalelos que determinan locus de resistencia a oídio (*Blumeria graminis* f.sp. *tritici*) (Mildew-resistance Locus, MLO) (Elliot et al., 2002), lo que supone la primera cita de modificación múltiple y simultánea de homoalelos. En el trabajo, se demuestra que la mutación inducida por TALEN de los tres homólogos TaMLO en la misma planta confiere amplia resistencia al oídio. Por otra parte, se utiliza la tecnología CRISPR/Cas9 para generar plantas transgénicas portadoras de mutaciones en el alelo TaMLO-A1, con lo que se concluye que la ingeniería dirigida a la inserción de ADN en el genoma de trigo harinero, a través de la recombinación no homóloga mediada por TALEN es viable, y proporciona un marco metodológico para mejorar cultivos poliploides.

Resistencia a geminivirus

Son dos los trabajos publicados (Ali et al., 2015; Ji et al., 2015) sobre el uso del sistema CRISPR/Cas9 para el control de geminivirus, el primero sobre el complejo viral del begomovirus *Tomato yellow leaf curl virus*

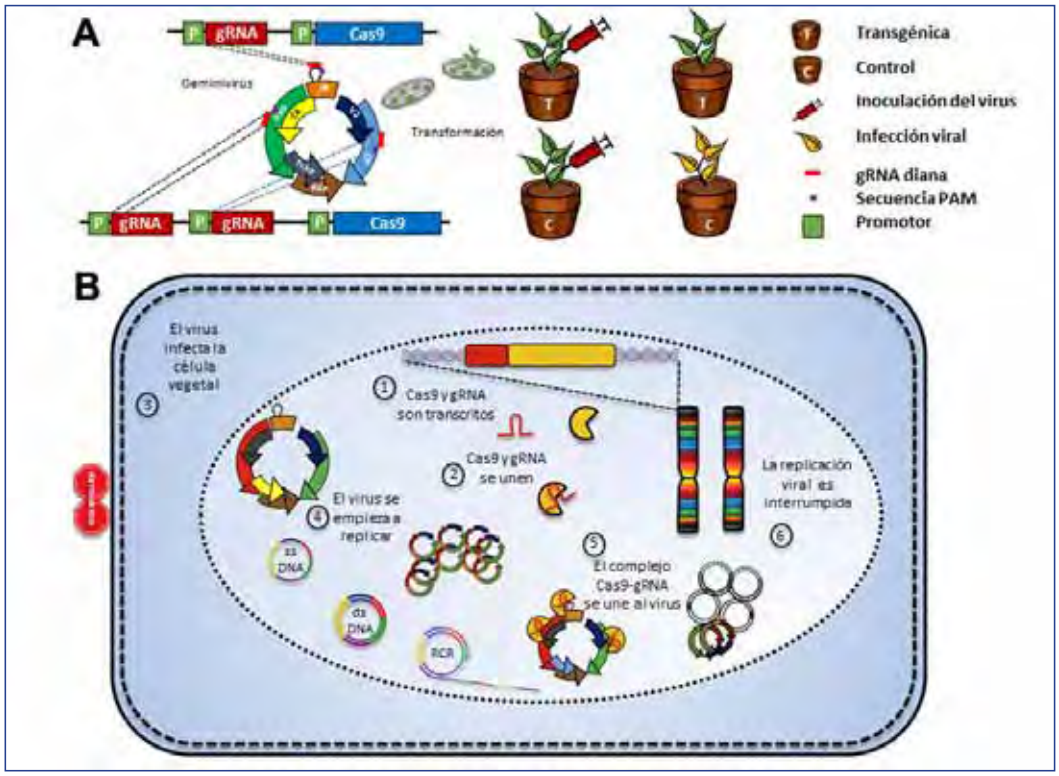

Figura 3. Sistema CRISPR/Cas9 utilizado para generar resistencia a virus fitopatógenos **(A)** Representación gráfica del genoma de un geminivirus y arquitectura molecular de los componentes del complejo CRISPR/Cas9 adaptado a las dianas del virus. Transformación estable del sistema CRISPR/Cas9 en plantas. Las plantas que expresan CRISPR/Cas9 son inoculadas con el virus (jeringa roja) y en condiciones controladas se observa si aparece resistencia. Las plantas transgénicas CRISPR/Cas9 (T) muestran resistencia al virus tras la agroinfección, mientras que las plantas no transgénicas inoculadas con el virus (C) desarrollan los síntomas típicos de la enfermedad, indicando susceptibilidad. **(b)** Interferencia de CRISPR/Cas9 con el virus en el núcleo celular. (1) Los componentes del complejo CRISPR/Cas9, gRNA y Cas9, se expresan a partir del genoma de la planta. (2) El complejo empieza a producir copias. (3) El virus infecta la célula. (4) El ADN de cadena sencilla (SSDNA) del geminivirus se replica y produce múltiples copias. (5) El complejo gRNA/Cas9 se une a los puntos diana de la doble cadena de DNA y (6) la rompe formando dobles roturas de la cadena (DSBs) que luego se reparan por unión no homóloga de los extremos (NHEJ). Las DSBs pueden conducir a la degradación del genoma viral (traducido de Zaidi et al., 2016).

(TYLCV), y el segundo sobre el curtovirus *Beet severe curly top virus* (BSCTV) (**Figura 3**).

Mediante la inserción de sgRNAs en *Tobacco rattle virus* (TRV) como plásmido vector y usando plantas de Nicotiana benthamiana que sobreexpresan la nucleasa Cas9 (Nb-Cas9OE), Ali et al. (2015) produjeron mutaciones y roturas en el fragmento de lectura abierta (ORF) y en la región intergénica (IR) de TYLCV. En primer lugar, diseñaron sgRNAs para modificar secuencias codificantes y no codificantes del genoma de TYLCV, que se insertaron en el genoma del vector TRV. Los sgRNAs se introdujeron así en las plantas Nb-Cas9OE, que diez días más tarde se agroinfiltraron con clones infecciosos de TYLCV. Se comprobó que se impedía la replicación viral y se reducía la expresión de síntomas de forma significativa. Por tanto, el sistema de CRISPR/Cas9 conduce a la degradación viral, gracias a las mutaciones introducidas en las secuencias diana. Además de estos claros resultados, los autores detectaron que todos los sgRNA-Cas9 tenían actividad de interferencia, pero aquellos dirigidos a la secuencia origen de replicación en la región intergénica (IR) del genoma de TYLCV eran los más eficaces. Por último, también observaron que, al

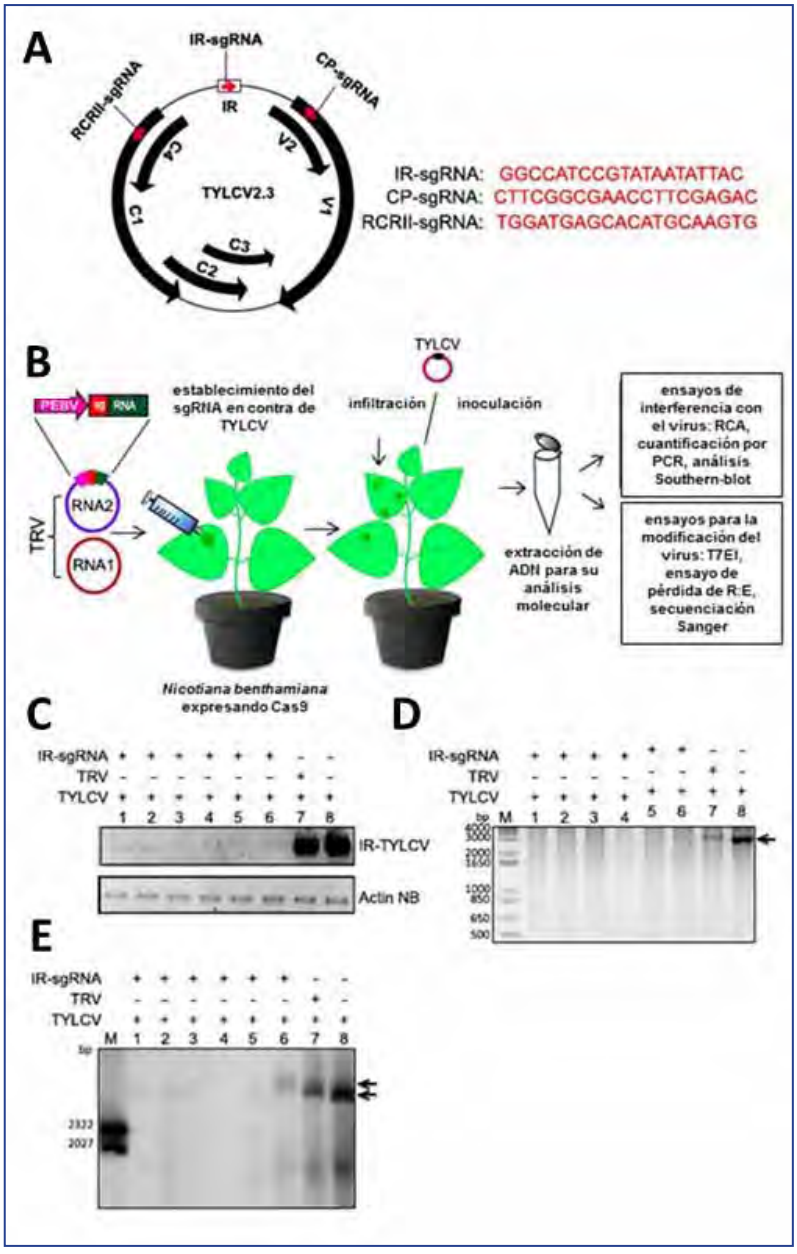

Figura 4. Interferencia mediada por CRISPR/Cas9 en la acumulación de *Tomato yellow leaf curl virus* (TYLCV). **(A)** Diagrama de la organización del genoma de TYLCV. La secuencia diana se muestra en rojo a la derecha arriba. **(b)** Esquema del diseño experimental. Se agroinfiltra, en plantas que expresan Cas9, *Agrobacterium* conteniendo *Tobacco rattle virus* (TRV) como vector y con sgRNA específico para el genoma de TYLCV. TYLCV es infiltrado también en las plantas con Cas9OE establecida la infección con TRV. Las muestras fueron recolectadas para realizar los análisis moleculares a los 10–21 días post-infiltración (dpi). **(C)** El análisis por PCR semi-cuantitativa del DNA de TYLCV indica que la infitración de TYLCV en las plantas Cas9OE acumula niveles más bajos que las plantas infiltradas con el vector TRV vacío. Se usa el genoma de *N. benthamiana* para normalizar. **(D)** Amplificación del genoma de TYLCV en los extractos vegetales. Las plantas con IR-sgRNA acumulan menos TYLCV-DNA que las que se inocularon con TYLCV y el vector TRV vacío. **(E)** Análisis mediante Southern blot de la acumulación de TYLCV-DNA en las plantas Cas9OE. EL TYLCV-DNA fue detectado mediante una sonda marcada con DIG ("DIG-labeled probe") contra una secuencia de 560-bp de la región IR. Las 6 plantas con IR-sgRNA que fueron infiltradas con TYLCV mostraron menor acúmulo de TYLCV-DNA que las que se inocularon con TYLCV y el vector TRV vacío. Las flechas en D y E indican la banda correspondiente a TYLCV-DNA (DIG: digoxigenina M: Marcador, NB: *N. benthamiana*, PEBV: promotor de Pea early browning virus, RE: enzima de restricción (autores: Ali et al., 2015).

programar un IR-sgRNA hacia la secuencia conservada (TAATATTAC) común a todos los geminivirus, se conseguía actuar sobre otros virus como *Merremia mosaic virus* (MeMV) (ver proceso experimental y resultados en **Figura 4**).

En el caso de BSCTV en *N. bethamiana* y, también, *Arabidopsis thaliana*, Ji et al. (2015) utilizaron una aproximación diferente para inhibir la replicación viral mediante el uso del sistema CRISPR/Cas9 en el momento de la conversión del ADN de cadena sencilla (ssDNA) a ADN de cadena doble (dsDNA) durante el proceso de replicación. Para determinar si el complejo sgRNA/Cas9 podía inhibir activamente la replicación viral, en lugar de inducir roturas mediante plásmidos (p-Cambia T DNA llevando 1,8 copias del genoma de BSCTV), se seleccionaron sgRNA diseñados para llevar a cabo ensayos discriminatorios. Los resultados revelaron que no sólo el sistema CRISPR-Cas dirigido contra geminivirus se podía establecer en plantas creando plantas transgénicas inmunes al virus, sino que se podían identificar sgRNAs anti-virales que reconocieran lugares en cualquier región del genoma viral.

Recientemente, Zaidi et al. (2016) han realizado una revisión, examinando los anteriores estudios sobre geminivirus, considerando que quizás la rotura del genoma de los geminivirus puede acelerar la aparición de cepas que sean capaces de evadir el sistema Cas9. Lo que en principio sería posible, por ejemplo, vía mutagénesis de la secuencia PAM. Estos autores expresan esta preocupación por los efectos de las modificaciones en zonas no especificas del genoma ("off-target"), a pesar de que Baltes et al. (2015) demostraron que una Cas9 catalíticamente inactiva (dCas9) es también útil para mediar la interferencia del virus y eliminar las actividades inespecíficas en el genoma de la planta. Según estos autores, CRISPR/Cas9 se podría usar para descubrir cómo ha evolucionado el genoma viral para contrarrestar la inmunidad de la planta, o descubrir los factores del huésped que determinan la resistencia y vulnerabilidad a la infección.

Resistencia a ipomovirus y potyvirus (Familia *Potyviridae*)

En este trabajo se demuestra el desarrollo de resistencia a los virus en pepino (*Cucumis sativus* L.) mediante la utilización de la tecnología Cas9/sgRNA, al interrumpir la función del gen eIF4E recesivo dirigiendo las construcciones Cas9/sgRNA a los extremos N' y C' de dicho gen. Los autores comentan que tras la aplicación de la tecnología Cas9/sgRNA, se observaron siempre pequeñas delecciones y SNPs ("single-nucleotide polymorphism") en las dianas de los genes eIF4E en la generación T1 de plantas transformadas de pepino, y nunca fuera de ellos. Por otra parte, seleccionaron plantas heterocigóticas mutantes en eIF4E no transgénicas para la producción de plantas de generación T3 homocigóticas. Estas plantas exhibieron inmunidad al ipomovirus *Cucumber vein yellowing virus* (CVYV) y a los potyvirus *Zucchini yellow mosaic virus* (ZYMV) and *Papaya ring spot mosaic virus-W* (PRSMV-W). Por el contrario, las plantas heterocigóticas mutantes y no mutantes fueron altamente susceptibles. Es, por tanto, por primera vez, a través de la tecnología CRISPR/Cas9, que se ha desarrollado resistencia a virus en el cultivo de pepino no transgénico, sin afectar visiblemente al desarrollo de las plantas, y sin retro-cruzamiento a largo plazo, lo que supone una nueva estrategia de control de virus fitopatógenos en una amplia gama de plantas de cultivo (**Figura 5**).

COMENTAROS FINALES

El volumen de información generado alrededor del sistema CRISPR-Cas en los últimos años es tal, que es difícil resumirlo en un artículo divulgativo como este. Si se quiere tener una idea global de su historia, repercusión e importancia en general, se aconseja la lectura del artículo de Landers (2016) titulado "The Heroes of CRISPR". Este autor cita el año 1989 como el año en el que se observaron las secuencias repetidas palindrómicas en el ADN de la archaea *Haloferax mediterranei*, adaptada al ambiente extremófilo de las salinas de Santa Pola (Alicante), por parte de un joven investigador, el microbiólogo alicantino Juan Francisco Mojica, actual profesor titular de la Universidad de Alicante. A partir de tal hallazgo se descubrió el sistema complejo utilizado por la bacteria *Streptococcus thermophilus* para defenderse

de las infecciones por fagos y que ahora la ciencia utiliza con diferentes versiones para modificar el genoma de plantas y animales (**Tabla 1**).

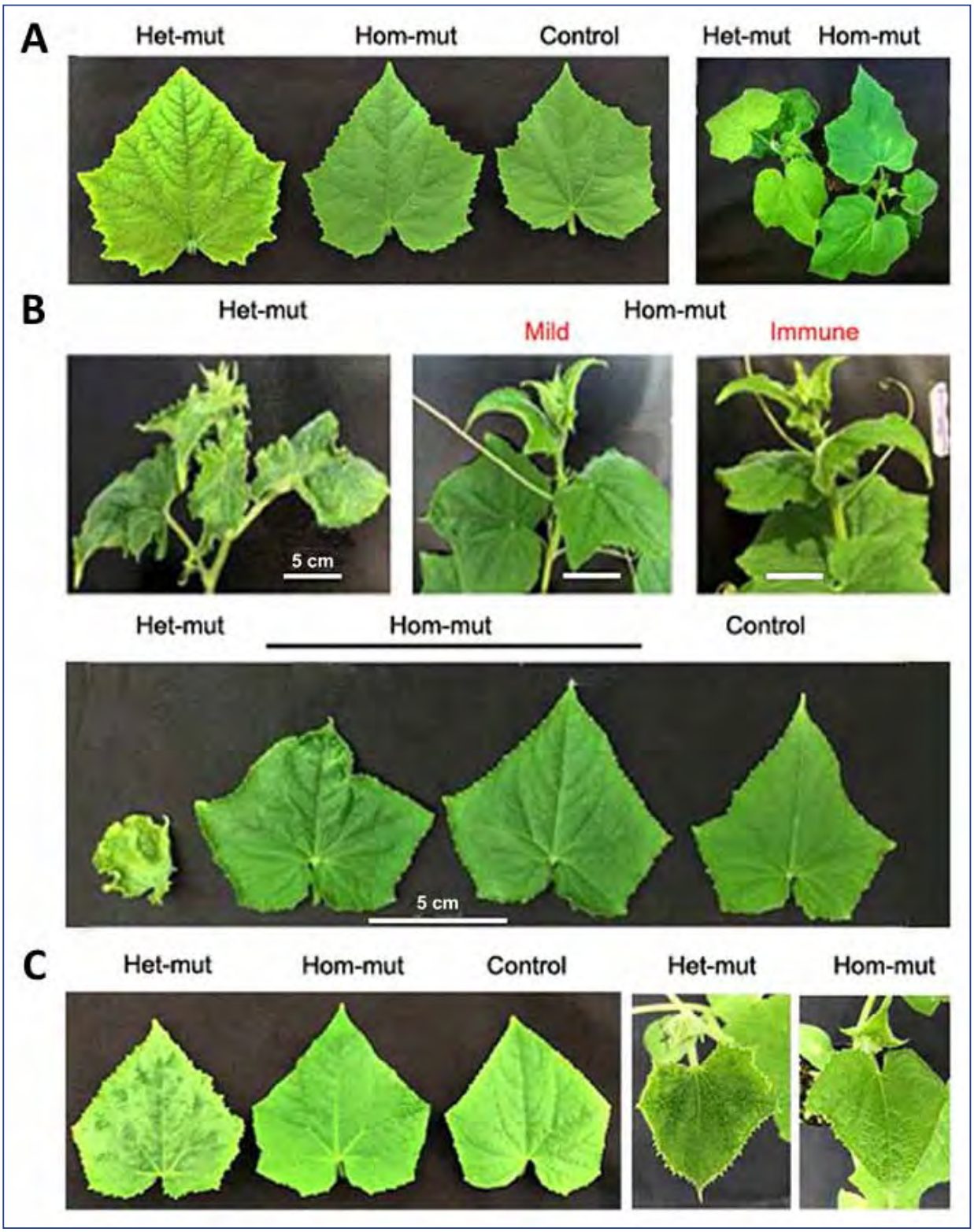

Figura 5. Mutantes eIF4E homocigóticos mostrando resistencia a la infección potyviral. **(A)** Síntomas inducidos por *Cucumber vein yellowing virus* (CVYV) en hojas y plantas de pepino mutantes heterocigóticas (Het-mut), mutantes homocigóticas (Hom-mut) y no inoculadas (control) de la generación T3, 10 dpi. **(b)** Síntomas inducidos por *Zucchini yellow mosaic virus* (ZYMV) en hojas y plantas de pepino mutantes heterocigóticas (Het-mut), mutantes homocigóticas (Hom-mut) y no inoculadas (control) de la generación T3, 25 dpi. **(C)** Síntomas inducidos por *Papaya ring spot mosaic virus*-W (PRSV-W) en hojas y plantas de pepino mutantes heterocigóticas (Het-mut), mutantes homocigóticas (Hom-mut) y no inoculadas (control) de la generación T3, 21 dpi. (adaptado de Chandrasekaran et al., 2016).

Tabla 1. Clasificación y ejemplos de sistemas CRISPR (Landers, 2016)

Clase	Tipo	Subtipo	Atributos	Efector ejemplo	Organismo ejemplo	Referencias bibliográficas
Clase 1	Tipo I		Complejo efector con multisubunidades; Cas3	Cascade	*E. coli*	Brouns *et al.*, 2008
	Tipo III	III-A	Complejo efector con multisubunidades; Csm modulo efector; dirigido a ADN	Cas10-Csm	*S. epidermidis*	Marraffini and Sontheimer, 2008
		II-B	Complejo efector con multisubunidades; dirigido a ADN	Cmr	*P. furiosus*	Hale *et al.*, 2009
Clase 2	Tipo II		Efector sencillo; tracrRNA	Cas9	*S. thermophilus*	Bolotin *et al.*, 2005; Barrangou *et al.*, 2007; Sapranauskas *et al.*, 2011; Gasiunas *et al.*, 2012
					S. pyogenes	Deltcheva *et al.*, 2011 Jinek *et al.*, 2012; Cong *et al.*, 2013 Mali *et al.*, 2013
	Tipo V		Efector sencillo; Guiado por un ARN	Cpf1	*F. novicida*	Zetsche *et al.*, 2015

Los sistemas CRISPR se organizan principalmente en dos Clases: Clase 1, contiene efectores con multi-subunidades, y Clase 2, que contiene efectores de proteínas sencillos. Estas clases se subdividen en 5 (Makarova et al., 2015), un tipo IV todavía es putativo y pertenece a la Clase 1. Aunque sólo la Clase 2 se ha podido usar en ingeniería genética, parece que hay diversos sistemas CRISPR (los sistemas tipo III-B se usan preferentemente para lograr mutaciones de ARN y no tanto de ADN [Hale et al., 2009]).

La tecnología CRISPR/Cas9 (Clase 2, Tipo II) en sus diferentes versiones nos permite actualmente: generar dobles roturas en el ADN ("double strand breaks, DSBs), romper sólo una de las cadenas del ADN ("Nick") (mediante una Cas9 mutada), interferir con la transcripción (mediante una Cas9 cataliticamente inactiva o dCas9, que puede incorporar o no un péptido represor), activar o incrementar la expresión de un gen (mediante una Cas9 que incorpore un péptido activador), co-expresar dos ARNs guías (gRNAs) homólogos (mediante una dCas9 fusionada con una nucleasa FokI), aislar segmentos genómicos de interés (mediante una dCas9 fusionada con un epitopo "tag"), visualizar regiones específicas del genoma (mediante una dCas9 fusionada con una proteína fluorescente), seleccionar genes involucrados en diferentes procesos biológicos usando "pools" de librerías CRISPR, pre-validar experimentalmente plásmidos gRNAs y seleccionar un plásmido gRNA basado en una variedad de factores, tales como la presencia o ausencia de Cas9 y el número de genes. Es decir, ofrece un abanico de posibilidades lo suficientemente amplio y sencillo como para competir con otras técnicas de edición del genoma (TALEN y "Zinc finger nucleases") algo más complicadas y de difícil ejecución.

Según Barrangou (2015), aunque la función principal de los sistemas establecidos CRISPR/Cas está en la defensa antiviral en las bacterias, un creciente grupo de evidencias indica que también desempeña papeles funcionales críticos más allá de la inmunidad, como pueda ser el control transcripcional endógeno. Además, los beneficios inherentes al mantenimiento de la homeostasis del genoma también vienen a costa de la reducción de la absorción de ADN beneficioso, y la prevención de adaptación estratégica para el medio ambiente. Esto abre nuevas vías para la investigación de los sistemas de CRISPR/Cas y su caracterización funcional más allá de la inmunidad adaptativa.

Para finalizar esta breve revisión, merece la pena repetir que el descubrimiento del sistema CRISPR, se debe al mencionado Juan Francisco Mojica, reivindicado por gran parte de la comunidad científica como su primer descubridor e incluso postulado como futuro premio Nobel español, aunque posiblemente comparta con otros científicos las primeras referencias (Bolotin et al., 2005; Mojica et al., 2005, 2009; Pourcel et al., 2005). Y que las científicas que ratificaron la nomenclatura "CRISPR" y describieron la tecnología CRISPR/Cas9, la bióloga estadounidense Jennifer A. Doudna, de la Universidad de California en Berkeley y la microbióloga francesa Emmanuelle Charpentier, actualmente

investigadora, entre otros centros, del centro Helmholtz para la Investigación de la Infección, dependiente del Max Plank Institute, recibieron el Premio Príncipe de Asturias en 2015, entre otros muchísimos galardones y menciones honoríficas.

No obstante, al igual que en muchos proyectos de colaboración que han evolucionado con el tiempo, no hay un "padre" claro del sistema CRISPR, al que se le asigne de manera irrevocable el descubrimiento, que está redefiniendo la tecnología de la mutación genética como un axioma común. La controversia latente en materia de propiedad intelectual relacionada con la patente de CRISPR/Cas no ayuda en ese sentido[7]. Además, como la ciencia que rodea a este descubrimiento sigue a un ritmo que sobrepasa la burocracia, todavía estamos sin una verdadera definición del proceso o producto a ojos de los organismos reguladores. Por tanto, el futuro derivado o asociado a esta tecnología va a ser muy emocionante, ya que con la tecnología de CRISPR/Cas se conocerán muchos de los detalles de los genoma de los organismos fitopatógenos en relación con sus plantas huéspedes y se establecerán probablemente nuevos métodos de control molecular de los mismos.

Agradecimientos

Los autores agradecen la revisión del escrito realizada por Paul Christou, Lucía Pérez y Can Baysal. Sarah B. Lade tiene una beca predoctoral de la Universidad de Lleida asociada al proyecto BIO2014-54426-P del MINECO.

bibliografía

Ali A., Abulfaraj A., Idris A., Ali S., Tashkandi M., Mahfouz M.M. 2015. CRISPR/Cas9-mediated viral interference in plants. Genome Biology 16:238. 11 páginas

Baltes N., Hummel A.W., Konecna E., Cegan R., Bruns A.N., Bisaro D. 2015. Conferring resistance to geminiviruses with the CRISPR–Cas prokaryotic immune system. Nature Plants 1(10): 15145.

Belhaj K., Chaparro-Garcia A., Kamoun S., Nekrasov V. 2013. Plant genome editing made easy: targeted mutagenesis in model and crop plants using the CRISPR/Cas system. Plant Methods 9:39.

Belhaj K., Chaparro-Garcia A., Kamoun S., Patron N.J., Nekrasov V. 2015. Editing plant genomes with CRISPR/Cas9. Current Opinion in Biotechnology 32:76-84.

Bolotin A., Quinquis B., Sorokin A., Ehrlich S.D. 2005. Clustered regularly interspaced short palindrome repeats (CRISPRs) have spacers of extrachromosomal origin. Microbiology 151:2551–2561.

Bortesi L., Fischer R. 2015. The CRISPR/Cas9 system for plant genome editing and beyond. Biotechnology Advances 33: 41-52.

Chandrasekaran J., Brumin M., Wolf D., LeibmanD., Klap C., Pearlsman M., Sherman A., Arazi T., Gal-On A. 2016. Development of broad virus resistance in non-transgenic cucumber using CRISPR/Cas9 technology. Molecular Plant Pathology, Early view, DOI: 10.1111/mpp.12375.

Doudna J.A., Charpentier E. 2014. The new frontier of genome engineering with CRISPR/Cas9. Science 346:1077-1086.

Elliott C., Zhou F., Spielmeyer W., Panstruga R., Schulze-Lefert P. 2002. Functional conservation of wheat and rice Mlo orthologs in defense modulation to the powdery mildew fungus. Molecular Plant Microbe Interactions 15: 1069–1077.

Endo M., Mikami M., Toki S. 2015. Multigene knockout utilizing off-target mutations of the CRISPR/Cas9 system in rice. Plant Cell Physiology 56: 41–47.

Fang Y., Tylere B.M. 2016. Efficient

[7] Dr. Zhang Feng, científico colaborador en el Instituto Broad del Instituto Tecnológico de Massachusetts (MIT) e investigador en el Instituto McGovern para la Investigación del Cerebro, que fue el primero en ganar una patente sobre la técnica después de la presentación de unos cuadernos de laboratorio suyos que parece demostraron que la inventó primero.

disruption and replacement of an effector gene in the oomycete *Phytophthora sojae* using CRISPR/Cas9. Molecular Plant Pathology 17(1): 127–139.

Hale C.R., Zhao P., Olson S., Duff M.O., Graveley B.R., Wells L., Terns R.M., Terns M.P.. 2009. RNA-Guided RNA Cleavage by a CRISPR RNA-Cas Protein Complex. Cell 139(5): 945-56.

Hsu P.D., Lander E.S., Zhang F. 2014. Development and applications of the CRISPR nuclease Cas9 for genome engineering. Cell 157(6):1262-1278.

Jain M. 2015. Function genomics of abiotic stress tolerance in plants; a CRISPR approach. Frontiers in Plant Science 6:375. DOI: 10.3389/fpls.2015.00375.

Ji X., Zhang H., Zhang Y., Wang Y., Gao C. 2015. Establishing a CRISPR–Cas-like immune system conferring DNA virus resistance in plants. Nature Plants 1: 1-4.

Jiang W., Zhou H., Bi H., Fromm M., Yang B., Weeks D.P. 2013. Demonstration of CRISPR/Cas9/sgRNA-mediated targeted gene modification in *Arabidopsis*, tobacco, sorghum and rice. Nucleic Acids Research, 41 (20): e188 12 páginas.

Jinek M., Chylinski K., Fonfara I., Hauer M., Doudna J.A., Charpentier E. 2012. A programmable dual-RNA-guided DNA endonuclease in adaptive bacterial immunity. Science 337:816–821.

Kim D., Bae S., Park J., Kim E., Kim S., Yu H-R., Hwang J., Kim J-II., Kim J-S. 2015. Nature Methods. DOI: 10.1038/nmeth.3284.

Kumar, V., Jain, M. 2015. The CRISPR-Cas system for plant genome editing: advances and opportunities. Journal of Experimental Botany 66: 47–57.

Landers E.S. 2016. The Heroes of CRISPR. Cell 164 (1–2):18–28.

Lei Y., Lu L., Liu H.Y., Li S., Xing F., Chen L.L. 2014. CRISPR-P: a web tool for synthetic single-guide RNA design of CRISPR-system in plants. Molecular Plant 7(9):1494–1496.

Liao H-K, Gu Y., Diaz A., Marlett J., Takahashi Y., Li M., Suzuki K., Xu R., Hishida T., Chang C-J., Rodriguez-Esteban C., Young J., Izpisua Belmonte J.C. 2015. Use of the CRISPR/Cas9 system as an intracellular defense against HIV-1 infection in human cells. Nature Communications. 6:6413 DOI: 10.1038/ncomms7413

Liu L., Fan X-D. 2014. CRISPR–Cas system: a powerful tool for genome engineering. Plant Molecular Biology 85:209-218.

Louwen R., Staals R.H.J., Endtz H.P., van Baarlen P., van der Oostb J. 2014. The Role of CRISPR-Cas Systems in Virulence of Pathogenic Bacteria. Microbiology and Molecular Biology Reviews 78 (1):74-88.

Makarova K.S., Wolf Y.I., Alkhnbashi O.S., Costa F., Shah S.A., Saunders S.J., Barrangou R., Brouns S.J.J., Charpentier E., Haft D.H., Horvath P., Moineau S., Mojica F.J.M., Terns R.M., Terns M.P., White M.F., Yakunin A.F., Garrett R.A., van der Oost J., Backofen R., Koonin E.V. 2015. An updated evolutionary classification of CRISPR-Cas systems. Nature Reviews Microbiology, 13: 722–736. DOI:10.1038/nrmicro3569.

Mojica FJ, Diez-Villasenor C, Garcia-Martinez J, Soria E. 2005. Intervening sequences of regularly spaced prokaryotic repeats derive from foreign genetic elements. Journal of Molecular Evolution 60:174–182.

Mojica, F. J. M.; Diez-Villasenor, C.; Garcia-Martinez, J.; Almendros, C. 2009. Short motif sequences determine the targets of the prokaryotic CRISPR defence system. Microbiology 155 (3): 733–740.

Pourcel C, Salvignol G, Vergnaud G. 2005. CRISPR elements in Yersinia pestis acquire new repeats by preferential uptake of bacteriophage DNA, and provide additional tools for evolutionary studies. Microbiology 151:653–663.

Rezzonico F, Smits TH, Duffy B. 2011. Diversity, evolution, and functionality of clustered regularly interspaced short palindromic repeat (CRISPR) regions in the fire blight pathogen *Erwinia amylovora*. Applied Environmental Microbiology 77:3819 –3829.

Schiml S., Fauser F., Puchta H. 2014. The CRISPR/Cas system can be used as nuclease for in planta gene targeting and as paired nickases for directed mutagenesis in *Arabidopsis* resulting in heritable progeny. The Plant Journal 80: 1139–1150.

Shan Q., Wang Y., Li J., Zhang Y., Chen K., Liang Z., Zhang K., Liu J., Xi J.J., Qiu J-L, Gao C. 2013. Targeted genome modification of crop plants using a CRISPR-Cas system. Nature Biotechnology 31 (8):686-688.

Van der Oost J., Westra E.R., Jackson R.N., Wiedenheft B. 2014. Unraveling the Structural and Mechanistic Basis of CRISPR-Cas Systems. Nature Reviews Microbiology 12(7): 479-492.

Wang Y., Cheng X., Shan Q., Zhang Y., Liu J., Gao C., Jin-Long Q.. 2014. Simultaneous editing of three homoeoalleles in hexaploid bread wheat confers heritable resistance to powdery mildew. Nature Biotechnology 32 (9):947-952.

Xing H-L., Dong L., Wang Z-P., Zhang H-Y., Han C-Y., Liu B., Wang X-C., Chen Q-J. 2014. A CRISPR/Cas9 toolkit for multiplex genome editing in plants. BMC Plant Biology 14:327 (12 páginas)

Zaidi S.S., Mansoor S., Ali Z., Tashkandi M., Mahfouz M.M. 2016. Engineering plants for geminivirus resistance with CRISPR/Cas9 System. Trends in Plant Science 21(4):279-281.

bOLETÍN DE LA SEF
Publicación trimestral **ISSN: 1998-513X**
Juan A. Navas-Cortés, IAS-CSIC (Córdoba), j.navas@csic.es
Inmaculada Viñas Almenar, UdL (Lleida) ivinas@tecal.udl.cat